2011

# A rapid in situ test device to evaluate the compaction effort of aggregate piers

Rachel Goldsmith
*Iowa State University*

**A rapid in situ test device to evaluate the compaction effort of aggregate piers**

by

**Rachel Marie Goldsmith**

A thesis submitted to the graduate faculty

In partial fulfillment of the requirements for the degree of

MASTER OF SCIENCE

Major: Civil Engineering (Geotechnical Engineering)

Program of Study Committee:
David J. White, Major Professor
Greg R. Luecke
Jeramy C. Ashlock

Iowa State University

Ames, Iowa

2011

**(DEDICATION)**

For
My parents, Jeff and Diane Goldsmith

## TABLE OF CONTENTS

TABLE OF CONTENTS ..... iii
ABSTRACT ..... vi
ACKNOWLEGEMENTS ..... vii
LIST OF TABLES ..... viii
LIST OF FIGURES ..... x
LIST OF EQUATIONS ..... xxi
CHAPTER 1. INTRODUCTION ..... 1
Industry problem ..... 1
Industry concerns ..... 1
Impact on industry ..... 1
Technical problem ..... 2
Goals of the research ..... 2
Objectives ..... 2
Significance of the research ..... 3
Organization of the document ..... 3
CHAPTER 2. BACKGROUND ..... 4
Literature review ..... 4
Plate load testing ..... 4
Measures of stiffness ..... 5
Accelerometers ..... 6
Load cells ..... 8
Summary of present practices ..... 9
Geopier Rammed Aggregate Piers® ..... 9
Pier load test ..... 9
Foundation QA/QC tests ..... 10
Preliminary Work ..... 10
CHAPTER 3. METHODS ..... 12
Research design ..... 12
The RAM Test ..... 12
Set-up the RAM Test ..... 14
Verify the RAM Test ..... 23
In situ testing ..... 24
Perform in situ RAM Tests ..... 24
RAM Test displacement verification ..... 32
Data analysis ..... 36
Calculate the load parameters ..... 36
Calculate the acceleration parameters ..... 37
Stiffness parameters ..... 38
Determine the permanent deformation values ..... 38
Calculate the stiffness values ..... 41

Compare stiffness values ..... 42
Laboratory analysis ..... 42

CHAPTER 4. MATERIALS ..... 43
Material La Port City ..... 43
Laboratory test results ..... 43
Material Fairfield ..... 46
Laboratory test results ..... 46
Material Council Bluffs ..... 47
Laboratory test results ..... 47
Material Oskaloosa ..... 48
Laboratory test results ..... 49

CHAPTER 5. RESULTS AND DISCUSSION ..... 50
Load ..... 50
Hampton load results ..... 52
La Port City load results ..... 56
Fairfield load results ..... 63
Council Bluffs load results ..... 70
Oskaloosa load results ..... 76
Acceleration ..... 89
Hampton acceleration results ..... 91
La Port City acceleration results ..... 93
Fairfield acceleration results ..... 95
Council Bluffs acceleration results ..... 100
Oskaloosa acceleration results ..... 106
Stiffness ..... 118
Hampton stiffness results ..... 118
La Port City stiffness results ..... 118
Fairfield stiffness results ..... 120
Council Bluffs stiffness results ..... 121
Oskaloosa stiffness results ..... 123
Verification ..... 125
La Port City verification results ..... 125
Fairfield verification results ..... 130
Council Bluffs verification results ..... 130
Oskaloosa verification results ..... 132

CHAPTER 6. CONCLUSIONS AND RECOMMENDATIONS ..... 137
Conclusions ..... 137
Recommendations for future research ..... 138
Recommendations for future practices ..... 139

APPENDIX ..... 140
Hampton ..... 145
La Port City ..... 150
Fairfield ..... 218

Council Bluffs ..... 233
Oskaloosa ..... 266
REFERENCES ..... 325

## ABSTRACT

A current in situ test exists to evaluate a load–deformation relationship of aggregate piers. However, the test is lengthy, evaluates only non-production aggregate piers, and does not provide a record of compaction. It would be beneficial to evaluate production piers as they are installed. A new in situ device was developed to provide knowledge about the compaction effort of aggregate piers. The device is referred to as the RAM Test. The device evaluates production piers and obtains a compaction record.

The report includes a detailed description of the device, the research methods involved to analyze the data, and results of the analyses. Last, the report includes conclusions and recommendations based on the objectives of the research; (1) test the RAM Test device, (2) use the device to observe, and collect load and acceleration data on aggregate piers during installation, (3) establish a relationship between acceleration and permanent deformation, (4) calculate load characteristics, and (5) determine stiffness values.

**ACKNOWLEGEMENTS**

I want to make a moment to thank everyone that helped me succeed during this process; My family, who are always there for me, and encourage and support my dreams. My boyfriend, Chad Holy, who is always there, especially on the most stressful of days. Dr. David White, who gave me this opportunity and pushed me to do my best, and my committee members, Dr. Greg Luecke and Dr. Jeramy Ashlock whose guidance I have appreciated during this process. Dr. Christianna White, who I owe a great deal, she has helped me to become the writer I am today and I appreciate her and all that she has done for me knows. Heath Gieselman, who always helped me with the heavy duty aspect of this research, lifting the 250 lb device, and made the field trips a little more exciting. Dr. Vennapusa, who has taught me a great deal about teaching and learning. I thank him for the opportunity to be his teaching assistant. Don Eichner, who was always there to answer my questions, whether they were silly or not, and helped me on more than a numerous occasions to figure out the RAM Test glitches. The Geopier Foundation Company®™, Peterson Contractors, Inc., Max Produkin, and Nate Meisgeier who helped in the field, without their generosity and hard work, testing would have been a lot more difficult. And last, my friends who were good stress relievers when the tough got tougher.

## LIST OF TABLES

Table 1. Summary of the initial field studies ..... 11
Table 2. Inventory of RAM Test parts ..... 13
Table 3. A summary of where each section's value originates within the time-history ..... 37
Table 4. Particle size summary for La Port City pier 1 aggregate ..... 43
Table 5. Particle size summary for La Port City pier 2 aggregate ..... 44
Table 6. Particle size summary for La Port City pier 3 aggregate ..... 45
Table 7. Particle size summary for Fairfield pier aggregate ..... 46
Table 8. Particle size summary for Council Bluffs pier aggregate ..... 48
Table 9. Particle size summary for Oskaloosa pier aggregate ..... 49
Table 10. Field study location, date, project, pier type, and verification summary ..... 50
Table 11. Hampton RAM Test field study summary ..... 52
Table 12. Load analysis A summary for Hampton ..... 56
Table 13. La Port City RAM Test field summary ..... 57
Table 14. Load analysis A summary for La Port City ..... 62
Table 15. RAM field summary for Fairfield ..... 63
Table 16. Load analysis A summary for Fairfield ..... 69
Table 17. RAM field summary for Council Bluffs ..... 70
Table 18. Load analysis A summary for Council Bluffs ..... 75
Table 19. RAM field summary for Oskaloosa ..... 76
Table 20. Load analysis A summary for Oskaloosa ..... 80
Table 21. Load analysis B summary for Oskaloosa ..... 87
Table 22. La Port City acceleration analysis A deformation results ..... 94
Table 23. Fairfield acceleration analysis A deformation results ..... 98
Table 24. Results of deformation by analysis A from Council Bluffs, with BST as a means for comparison ..... 104
Table 25. Results for deformation by analysis B for Council Bluffs ..... 105
Table 26. Comparison of deformation values for acceleration values greater than 5, 7.5, and 10 g ..... 107
Table 27. Summary of deformations (in.) from segments 1 to 4 for tests 2 to 5 and the resultant average and sum ..... 108
Table 28. Results of analysis A deformation from Oskaloosa ..... 108
Table 29. Results of acceleration analysis B deformation from Oskaloosa ..... 109
Table 30. Test 2 summary of Oskaloosa analysis C deformations (in.) ..... 111
Table 31. Differences in the deformation at the end of the time-history, and at minimum deformation within the time-history ..... 112
Table 32. Summary of Oskaloosa analysis D deformations (in.) ..... 115
Table 33. Comparison of deformation from all analyses for Oskaloosa ..... 118
Table 34. Summary of stiffness' (pci) based on acceleration analysis A and modulus load test deformations for La Port City ..... 119
Table 35. Summary of stiffness (pci) based on acceleration analysis A for Fairfield ..... 120
Table 36. Council Bluffs summary of stress (psf) and deformations (in.) of BST, acceleration analysis A and acceleration analysis B, and modulus load test ..... 122

Table 37. Council Bluffs summary of stiffness parameters for BST, acceleration analysis A and B, and modulus load test ..... 122
Table 38. Summary of plate size, stress, and BST, analysis A, B, C, D, and modulus load test deformations for Oskaloosa..... 124
Table 39. Summary of BST, acceleration analysis A, B, C, D, and modulus load test stiffness for Oskaloosa..... 124
Table 40. FWD load, deformation, stress, and stiffness results..... 126
Table 41. Comparison of FWD and RAM Test load and deformation results ..... 126
Table 42. Council Bluffs' BST results..... 131
Table 43. Oskaloosa's BST results ..... 133
Table 44. The acceleration analysis software code to determine permanent deformation ... 143

## LIST OF FIGURES

Figure 1. RAM Test device configuration, the gold colored plate represents plate 3 where the three loads sit in machined cavities ..... 14
Figure 2. The RAM Test collects data on a pier with the 9 in. plate ..... 14
Figure 3. “How to set up the data acquisition software test files” Step 1 ..... 15
Figure 4. “How to set up the data acquisition software test files” Step 2-a ..... 16
Figure 5. “How to set up the data acquisition software test files” Step 2-b ..... 16
Figure 6. “How to set up the data acquisition software test files” Step 2-c ..... 17
Figure 7. “How to set up the data acquisition software test files” Step 2-d ..... 17
Figure 8. “How to set up the data acquisition software test files” Step 2-e ..... 18
Figure 9. “How to set up the data acquisition software test files” Step 3 ..... 18
Figure 10. “How to set up the data acquisition software test files” Step 4-a, 4-b ..... 19
Figure 11. “How to set up the data acquisition software test files” Step 4-c ..... 19
Figure 12. “How to set up the data acquisition software test files” Step 4-e ..... 20
Figure 13. “How to set up the data acquisition software test files” Step 4-f ..... 21
Figure 14. “How to set up the data acquisition software test files” Step 4-h ..... 22
Figure 15. “How to set up the data acquisition software test files” Step 5 ..... 23
Figure 16. Load verification on February 4, 2010 ..... 23
Figure 17. Load verification on January 26, 2011 ..... 24
Figure 18. The back view of the data acquisition system before wires are plugged in, general procedure to prepare RAM Test step 1 ..... 25
Figure 19. The back view of the data acquisition system after RAM Test wires are plugged in, general procedure to prepare RAM Test step 1 ..... 25
Figure 20. Each load cell wire is numbered which corresponds to the channel number, general procedure to prepare RAM Test step 2 ..... 26
Figure 21. Front view of the data acquisition system, general procedure to prepare RAM Test steps 3 and 4 ..... 27
Figure 22. Front view of the data acquisition system, general procedure to prepare RAM Test step 5 ..... 27
Figure 23. The RAM Test in the field with the 9 in. steel plate in the upper right corner, and the 18 in. and 24 in. plates attached to the device ..... 28
Figure 24. View of the data acquisition software and the green play button ..... 29
Figure 25. The plot and display boxes where real-time data is viewed in the data acquisition software ..... 30
Figure 26. View of the data acquisition software and the red stop button ..... 31
Figure 27. Bottom stabilization test procedure step 3 ..... 32
Figure 28. FWD and RAM Test verification step 2 ..... 33
Figure 29. FWD and RAM Test verification step 3-b ..... 34
Figure 30. FWD and RAM Test verification step 3-d ..... 34
Figure 31. The camera verification set up ..... 35
Figure 32. Comparison of load analyses A and B, where analysis A includes the majority of the compaction impacts, while analysis B includes 5 sections of 5 compaction impacts. ..... 37

Figure 33. Analyses A–D for processing the acceleration in the acceleration analysis software ..... 39
Figure 34. The acceleration analysis software deformation (m) vs. time (sec.) example of analysis A for Oskaloosa test 2 segment 3 ..... 40
Figure 35. The acceleration analysis software deformation (m) vs. time (sec.) example of analysis B of Oskaloosa test 2 segment 3 ..... 40
Figure 36. The acceleration analysis software deformation (m) vs. time (sec.) example of analysis C for Oskaloosa test 2 segment 3 ..... 41
Figure 37. The acceleration analysis software deformation (m) vs. time (sec.) example of analysis D for Oskaloosa test 2 segment 3 ..... 41
Figure 38. Grain size distribution for La Port City pier 1 aggregate ..... 44
Figure 39. Grain size distribution for La Port City pier 2 aggregate ..... 45
Figure 40. Grain size distribution for La Port City pier 3 aggregate ..... 46
Figure 41. Grain size distribution for Fairfield pier aggregate ..... 47
Figure 42. Grain size distribution for Council Bluffs pier aggregate ..... 48
Figure 43. Grain size distribution for Oskaloosa pier aggregate ..... 49
Figure 44. The representative portions used for load analyses A and B. The 5 sections of 5 impacts marked by vertical lines and numbered 1–5 represent the impacts used to calculate each average dynamic load and ramming frequency for load analysis B ..... 51
Figure 45. Hampton field study conditions ..... 53
Figure 46. Example of the double impact behavior of Hampton test 1 ..... 54
Figure 47. Hampton test 1 exhibits an amplitude decrease over the duration of the test ..... 54
Figure 48. Hampton test 3 exhibits steady amplitude over the duration of the test ..... 54
Figure 49. Hampton test 6 ..... 55
Figure 50. Hampton test 9, data recorded on the matrix soil ..... 56
Figure 51. La Port City field conditions ..... 58
Figure 52. La Port City test 3 ..... 59
Figure 53. La Port City test 4 ..... 59
Figure 54. La Port City test 12 ..... 60
Figure 55. La Port City test 34 ..... 60
Figure 56. La Port City test 33 ..... 61
Figure 57. La Port City test 39 ..... 62
Figure 58. Fairfield field study conditions ..... 64
Figure 59. Fairfield test 1 ..... 65
Figure 60. Fairfield test 2 ..... 65
Figure 61. Example of the double impact behavior of Fairfield test 3 ..... 66
Figure 62. Fairfield test 5, pre compacted lift ..... 67
Figure 63. Fairfield test 6, post compacted lift ..... 67
Figure 64. Fairfield test 18 ..... 68
Figure 65. Fairfield test 21 ..... 69
Figure 66. Example of the double impact behavior of Fairfield test 21 ..... 69
Figure 67. Council Bluffs field study conditions ..... 71
Figure 68. Example of larger amplitudes of Council Bluffs test 8 ..... 72
Figure 69. Example of smaller amplitudes of Council Bluffs test 9 ..... 72
Figure 70. Council Bluffs test 9, 5 seconds of compaction ..... 73

Figure 71. Council Bluffs test 16.1, the amplitudes emphasized the maximum loads ..... 74
Figure 72. Council Bluffs test 18.1, double sinusoidal behavior ..... 75
Figure 73. Oskaloosa field study conditions ..... 77
Figure 74. Oskaloosa test 4.2, smallest amplitude ..... 78
Figure 75. Oskaloosa test 2.1, largest amplitude ..... 78
Figure 76. Oskaloosa test 6.1, smallest amplitude ..... 79
Figure 77. Oskaloosa test 7.1, largest amplitude ..... 79
Figure 78. Oskaloosa test 13.3, smallest amplitude ..... 80
Figure 79. Oskaloosa test 12.2, smallest amplitude ..... 80
Figure 80. Oskaloosa test 1 load analysis B results ..... 83
Figure 81. Oskaloosa test 2 load analysis B results ..... 84
Figure 82. Oskaloosa test 3 load analysis B results ..... 85
Figure 83. Oskaloosa test 4 load analysis B results ..... 86
Figure 84. Oskaloosa test 5 load analysis B results ..... 87
Figure 85. Acceleration analyses A to D for processing the acceleration ..... 91
Figure 86. Hampton test 12 deformation time-history ..... 92
Figure 87. The RAM Test plate buried during testing ..... 92
Figure 88. La Port City test 12, example of the maximum acceleration values at the start of the test ..... 93
Figure 89. La Port City test 36, example of the positive acceleration values ..... 94
Figure 90. La Port City test 5 deformation plot ..... 95
Figure 91. La Port City test 9 deformation plot ..... 95
Figure 92. Fairfield test 1 without the buffer pad ..... 96
Figure 93. Fairfield test 2 with the buffer pad ..... 96
Figure 94. Fairfield test 12 pre compacted lift ..... 97
Figure 95. Fairfield test 13 post compacted lift ..... 97
Figure 96. Fairfield test 19 ..... 98
Figure 97. Fairfield test 14, expected time-history ..... 99
Figure 98. Fairfield test 21, high deformation time-history ..... 99
Figure 99. Council Bluffs test 6, first test on pier 1 ..... 100
Figure 100. Council Bluffs test 11, last test on pier 1 ..... 101
Figure 101. Council Bluffs test 16.3 ..... 101
Figure 102. Council Bluffs test 17 segment 1 ..... 102
Figure 103. Council Bluffs test 17 segment 2 ..... 102
Figure 104. Council Bluffs test 17 segment 3 ..... 103
Figure 105. Council Bluffs test 17 segment 4 ..... 103
Figure 106. Council Bluffs test 6 acceleration analysis A deformation time-history ..... 104
Figure 107. Council Bluffs acceleration analysis B deformation time-histories ..... 105
Figure 108. Oskaloosa test 5.1 on 9 in. steel plate ..... 106
Figure 109. Oskaloosa test 7 erratic accelerations ..... 107
Figure 110. Oskaloosa pier 1 acceleration analysis B time-histories ..... 110
Figure 111. Oskaloosa pier 2 acceleration analysis B time-histories ..... 110
Figure 112. Oskaloosa pier 3 acceleration analysis B time-histories ..... 111
Figure 113. Oskaloosa test 2 segment 1 acceleration analysis C ..... 112
Figure 114. Oskaloosa test 2 segment 2 acceleration analysis C ..... 113

Figure 115. Oskaloosa test 2 segment 3 acceleration analysis C ..... 113
Figure 116. Oskaloosa test 3 segment 3 acceleration analysis C ..... 114
Figure 117. Oskaloosa test 4 segment 4 acceleration analysis C ..... 114
Figure 118. Oskaloosa test 5 segment 4 acceleration analysis C ..... 115
Figure 119. Oskaloosa test 2 segment 3 acceleration analysis D ..... 116
Figure 120. Oskaloosa test 3 segment 3 acceleration analysis D ..... 116
Figure 121. Oskaloosa test 4 segment 4 acceleration analysis D ..... 117
Figure 122. Oskaloosa test 5 segment 4 acceleration analysis D ..... 117
Figure 123. La Port City pier 1 stress (psf) vs. deformation (in.) plot ..... 119
Figure 124. Fairfield pier 1 stress (psf) vs. deformation (in.) plot ..... 120
Figure 125. Fairfield pier 2 stress (psf) vs. deformation (in.) plot ..... 121
Figure 126. Council Bluffs pier 1 stress (psf) vs. deformation (in.) plot ..... 123
Figure 127. Oskaloosa pier 1 to 3 stress (psf) vs. deformation (in.) plots ..... 125
Figure 128. Deformation time-history for La Port City test 53, recorded on pier 1 with the 18 in. plate, and the FWD dropping load at height 2. ..... 128
Figure 129. Modulus load test results for pier 1 at La Port City ..... 129
Figure 130. Modulus load test results for pier 2 at La Port City ..... 129
Figure 131. Modulus load test results for pier 3 at La Port City ..... 130
Figure 132. BST deformation vs. time for Council Bluffs pier 2 (tests 12 and 16) and pier 3 (tests 17–21) ..... 131
Figure 133. Modulus load test results for Council Bluffs ..... 132
Figure 134. BST deformation vs. time for pier 1 ..... 134
Figure 135. BST deformation vs. time for pier 2 ..... 135
Figure 136. BST deformation vs. time for pier 3 ..... 135
Figure 137. Modulus load test results for Oskaloosa ..... 136
Figure 138. Calibration certificate for accelerometer 1 on August 3, 2007 ..... 140
Figure 139. Calibration certificate for accelerometer 1 on February 21, 2011 ..... 141
Figure 140. Calibration certificate for accelerometer 2 on December 3, 2010 ..... 142
Figure 141. Hampton test 1 ..... 145
Figure 142. Hampton test 2 ..... 145
Figure 143. Hampton test 3 ..... 146
Figure 144. Hampton test 4 ..... 146
Figure 145. Hampton test 5 ..... 147
Figure 146. Hampton test 6 ..... 147
Figure 147. Hampton test 9 ..... 148
Figure 148. Hampton test 10 ..... 148
Figure 149. Hampton test 11 ..... 149
Figure 150. Hampton test 12 ..... 149
Figure 151. Hampton test 12 ..... 150
Figure 152. La Port City test 1 ..... 150
Figure 153. La Port City test 2 ..... 151
Figure 154. La Port City test 3 ..... 151
Figure 155. La Port City test 4 ..... 152
Figure 156. La Port City test 5 ..... 152
Figure 157. La Port City test 6 ..... 153

Figure 158. La Port City test 7 ..... 153
Figure 159. La Port City test 8 ..... 154
Figure 160. La Port City test 9 ..... 154
Figure 161. La Port City test 10 ..... 155
Figure 162. La Port City test 11 ..... 155
Figure 163. La Port City test 12 ..... 156
Figure 164. La Port City test 13 ..... 156
Figure 165. La Port City test 14 ..... 157
Figure 166. La Port City test 15 ..... 157
Figure 167. La Port City test 16 ..... 158
Figure 168. La Port City test 17 ..... 158
Figure 169. La Port City test 18 ..... 159
Figure 170. La Port City test 19 ..... 159
Figure 171. La Port City test 22 ..... 160
Figure 172. La Port City test 23 ..... 160
Figure 173. La Port City test 24 ..... 161
Figure 174. La Port City test 27 ..... 161
Figure 175. La Port City test 28 ..... 162
Figure 176. La Port City test 29 ..... 162
Figure 177. La Port City test 30 ..... 163
Figure 178. La Port City test 31 ..... 163
Figure 179. La Port City test 32 ..... 164
Figure 180. La Port City test 33 ..... 164
Figure 181. La Port City test 34 ..... 165
Figure 182. La Port City test 35 ..... 165
Figure 183. La Port City test 36 ..... 166
Figure 184. La Port City test 37 ..... 166
Figure 185. La Port City test 38 ..... 167
Figure 186. La Port City test 39 ..... 167
Figure 187. La Port City test 40 ..... 168
Figure 188. La Port City test 41 ..... 168
Figure 189. La Port City test 46 ..... 169
Figure 190. La Port City test 47 ..... 170
Figure 191. La Port City test 48 ..... 171
Figure 192. La Port City test 50 ..... 172
Figure 193. La Port City test 53 ..... 173
Figure 194. La Port City test 54 ..... 174
Figure 195. La Port City test 55 ..... 175
Figure 196. La Port City test 56 ..... 176
Figure 197. La Port City test 58 ..... 177
Figure 198. La Port City test 58 ..... 178
Figure 199. La Port City test 59 ..... 179
Figure 200. La Port City test 60 ..... 180
Figure 201. La Port City test 61 ..... 181
Figure 202. La Port City test 62 ..... 182

Figure 203. La Port City test 65 ..... 183
Figure 204. La Port City test 66 ..... 184
Figure 205. La Port City test 67 ..... 185
Figure 206. La Port City test 68 ..... 186
Figure 207. La Port City test 69 ..... 187
Figure 208. La Port City test 71 ..... 188
Figure 209. La Port City test 74 ..... 189
Figure 210. La Port City test 75 ..... 190
Figure 211. La Port City test 77 ..... 191
Figure 212. La Port City test 78 ..... 192
Figure 213. La Port City test 80 ..... 193
Figure 214. La Port City test 81 ..... 194
Figure 215. La Port City test 82 ..... 195
Figure 216. La Port City test 83 ..... 196
Figure 217. La Port City test 84 ..... 197
Figure 218. La Port City test 87 ..... 198
Figure 219. La Port City test 88 ..... 199
Figure 220. La Port City test 89 ..... 200
Figure 221. La Port City test 90 ..... 201
Figure 222. La Port City test 91 ..... 202
Figure 223. La Port City test 93 ..... 203
Figure 224. La Port City test 94 ..... 204
Figure 225. La Port City test 95 ..... 205
Figure 226. La Port City test 96 ..... 206
Figure 227. La Port City test 97 ..... 207
Figure 228. La Port City test 99 ..... 208
Figure 229. La Port City test 100 ..... 209
Figure 230. La Port City test 101 ..... 210
Figure 231. La Port City test 102 ..... 211
Figure 232. La Port City test 103 ..... 212
Figure 233. La Port City test 1 ..... 213
Figure 234. La Port City test 2 ..... 213
Figure 235. La Port City test 3 ..... 214
Figure 236. La Port City test 4 ..... 214
Figure 237. La Port City test 5 ..... 215
Figure 238. La Port City test 6 ..... 215
Figure 239. La Port City test 7 ..... 216
Figure 240. La Port City test 8 ..... 216
Figure 241. La Port City test 9 ..... 217
Figure 242. La Port City test 10 ..... 217
Figure 243. Fairfield test 1 ..... 218
Figure 244. Fairfield test 2 ..... 218
Figure 245. Fairfield test 3 ..... 219
Figure 246. Fairfield test 4 ..... 219
Figure 247. Fairfield test 5 ..... 220

Figure 248. Fairfield test 6 ..... 220
Figure 249. Fairfield test 8 ..... 221
Figure 250. Fairfield test 9 ..... 221
Figure 251. Fairfield test 10 ..... 222
Figure 252. Fairfield test 11 ..... 222
Figure 253. Fairfield test 12 ..... 223
Figure 254. Fairfield test 13 ..... 223
Figure 255. Fairfield test 14 ..... 224
Figure 256. Fairfield test 15 ..... 224
Figure 257. Fairfield test 16 ..... 225
Figure 258. Fairfield test 17 ..... 225
Figure 259. Fairfield test 18 ..... 226
Figure 260. Fairfield test 19 ..... 226
Figure 261. Fairfield test 20 ..... 227
Figure 262. Fairfield test 21 ..... 227
Figure 263. Fairfield test 22 ..... 228
Figure 264. Fairfield test 23 ..... 228
Figure 265. Fairfield test 24 ..... 229
Figure 266. Fairfield test 13 ..... 229
Figure 267. Fairfield test 14 ..... 230
Figure 268. Fairfield test 15 ..... 230
Figure 269. Fairfield test 20 ..... 231
Figure 270. Fairfield test 21 ..... 231
Figure 271. Fairfield test 22 ..... 232
Figure 272. Fairfield test 23 ..... 232
Figure 273. Fairfield test 23 ..... 233
Figure 274. Council Bluffs test 6 ..... 233
Figure 275. Council Bluffs test 7 ..... 234
Figure 276. Council Bluffs test 8 ..... 234
Figure 277. Council Bluffs test 9 ..... 235
Figure 278. Council Bluffs test 10 ..... 235
Figure 279. Council Bluffs test 11 ..... 236
Figure 280. Council Bluffs test 12 segment 1 ..... 236
Figure 281. Council Bluffs test 12 segment 2 ..... 237
Figure 282. Council Bluffs test 12 segment 3 ..... 237
Figure 283. Council Bluffs test 12 segment 4 ..... 238
Figure 284. Council Bluffs test 16 segment 1 ..... 238
Figure 285. Council Bluffs test 16 segment 2 ..... 239
Figure 286. Council Bluffs test 16 segment 3 ..... 239
Figure 287. Council Bluffs test 17 segment 1 ..... 240
Figure 288. Council Bluffs test 17 segment 2 ..... 240
Figure 289. Council Bluffs test 17 segment 3 ..... 241
Figure 290. Council Bluffs test 17 segment 4 ..... 241
Figure 291. Council Bluffs test 18 segment 1 ..... 242
Figure 292. Council Bluffs test 18 segment 2 ..... 242

Figure 293. Council Bluffs test 18 segment 3 ..... 243
Figure 294. Council Bluffs test 18 segment 4 ..... 243
Figure 295. Council Bluffs test 18 segment 5 ..... 244
Figure 296. Council Bluffs test 19 segment 1 ..... 244
Figure 297. Council Bluffs test 19 segment 2 ..... 245
Figure 298. Council Bluffs test 19 segment 3 ..... 245
Figure 299. Council Bluffs test 19 segment 4 ..... 246
Figure 300. Council Bluffs test 21 segment 1 ..... 246
Figure 301. Council Bluffs test 21 segment 2 ..... 247
Figure 302. Council Bluffs test 21 segment 3 ..... 247
Figure 303. Council Bluffs test 21 segment 4 ..... 248
Figure 304. Council Bluffs test 21 segment 5 ..... 248
Figure 305. Council Bluffs test 6 acceleration analysis A ..... 249
Figure 306. Council Bluffs test 7 acceleration analysis A ..... 249
Figure 307. Council Bluffs test 8 acceleration analysis A ..... 250
Figure 308. Council Bluffs test 9 acceleration analysis A ..... 250
Figure 309. Council Bluffs test 10 acceleration analysis A ..... 251
Figure 310. Council Bluffs test 11 acceleration analysis A ..... 251
Figure 311. Council Bluffs test 12 segment 1 acceleration analysis A ..... 252
Figure 312. Council Bluffs test 12 segment 2 acceleration analysis A ..... 252
Figure 313. Council Bluffs test 12 segment 3 acceleration analysis A ..... 253
Figure 314. Council Bluffs test 12 segment 4 acceleration analysis A ..... 253
Figure 315. Council Bluffs test 16 segment 1 acceleration analysis A ..... 254
Figure 316. Council Bluffs test 16 segment 2 acceleration analysis A ..... 254
Figure 317. Council Bluffs test 16 segment 3 acceleration analysis A ..... 255
Figure 318. Council Bluffs test 16 segment 4 acceleration analysis A ..... 255
Figure 319. Council Bluffs test 17 segment 1 acceleration analysis A ..... 256
Figure 320. Council Bluffs test 17 segment 2 acceleration analysis A ..... 256
Figure 321. Council Bluffs test 17 segment 3 acceleration analysis A ..... 257
Figure 322. Council Bluffs test 17 segment 4 acceleration analysis A ..... 257
Figure 323. Council Bluffs test 18 segment 1 acceleration analysis A ..... 258
Figure 324. Council Bluffs test 18 segment 2 acceleration analysis A ..... 258
Figure 325. Council Bluffs test 18 segment 3 acceleration analysis A ..... 259
Figure 326. Council Bluffs test 18 segment 4 acceleration analysis A ..... 259
Figure 327. Council Bluffs test 18 segment 5 acceleration analysis A ..... 260
Figure 328. Council Bluffs test 19 segment 1 acceleration analysis A ..... 260
Figure 329. Council Bluffs test 19 segment 2 acceleration analysis A ..... 261
Figure 330. Council Bluffs test 19 segment 3 acceleration analysis A ..... 261
Figure 331. Council Bluffs test 19 segment 4 acceleration analysis A ..... 262
Figure 332. Council Bluffs test 21 segment 1 acceleration analysis A ..... 262
Figure 333. Council Bluffs test 21 segment 2 acceleration analysis A ..... 263
Figure 334. Council Bluffs test 21 segment 3 acceleration analysis A ..... 263
Figure 335. Council Bluffs test 21 segment 4 acceleration analysis A ..... 264
Figure 336. Council Bluffs test 21 segment 5 acceleration analysis A ..... 264
Figure 337. Council Bluffs tests 6–21 acceleration analysis B ..... 265

Figure 338. Oskaloosa test 1 segment 1..... 266
Figure 339. Oskaloosa test 1 segment 2..... 266
Figure 340. Oskaloosa test 1 segment 3..... 267
Figure 341. Oskaloosa test 2 segment 1..... 267
Figure 342. Oskaloosa test 2 segment 2..... 268
Figure 343. Oskaloosa test 2 segment 3..... 268
Figure 344. Oskaloosa test 3 segment 1..... 269
Figure 345. Oskaloosa test 3 segment 2..... 269
Figure 346. Oskaloosa test 3 segment 3..... 270
Figure 347. Oskaloosa test 4 segment 1..... 270
Figure 348. Oskaloosa test 4 segment 2..... 271
Figure 349. Oskaloosa test 4 segment 3..... 271
Figure 350. Oskaloosa test 4 segment 4..... 272
Figure 351. Oskaloosa test 5 segment 1..... 272
Figure 352. Oskaloosa test 5 segment 2..... 273
Figure 353. Oskaloosa test 5 segment 3..... 273
Figure 354. Oskaloosa test 5 segment 4..... 274
Figure 355. Oskaloosa test 6 segment 1..... 274
Figure 356. Oskaloosa test 6 segment 2..... 275
Figure 357. Oskaloosa test 6 segment 3..... 275
Figure 358. Oskaloosa test 7 segment 1..... 276
Figure 359. Oskaloosa test 7 segment 2..... 276
Figure 360. Oskaloosa test 7 segment 3..... 277
Figure 361. Oskaloosa test 8 segment 1..... 277
Figure 362. Oskaloosa test 8 segment 2..... 278
Figure 363. Oskaloosa test 8 segment 3..... 278
Figure 364. Oskaloosa test 8 segment 4..... 279
Figure 365. Oskaloosa test 9 segment 1..... 279
Figure 366. Oskaloosa test 9 segment 2..... 280
Figure 367. Oskaloosa test 9 segment 3..... 280
Figure 368. Oskaloosa test 9 segment 4..... 281
Figure 369. Oskaloosa test 10 segment 1..... 281
Figure 370. Oskaloosa test 10 segment 2..... 282
Figure 371. Oskaloosa test 10 segment 3..... 282
Figure 372. Oskaloosa test 10 segment 4..... 283
Figure 373. Oskaloosa test 11 segment 1..... 283
Figure 374. Oskaloosa test 11 segment 2..... 284
Figure 375. Oskaloosa test 11 segment 3..... 284
Figure 376. Oskaloosa test 11 segment 4..... 285
Figure 377. Oskaloosa test 12 segment 1..... 285
Figure 378. Oskaloosa test 12 segment 2..... 286
Figure 379. Oskaloosa test 12 segment 3..... 286
Figure 380. Oskaloosa test 13 segment 1..... 287
Figure 381. Oskaloosa test 13 segment 2..... 287
Figure 382. Oskaloosa test 13 segment 3..... 288

Figure 383. Oskaloosa test 13 segment 4..... 288
Figure 384. Oskaloosa test 14 segment 1..... 289
Figure 385. Oskaloosa test 14 segment 2..... 289
Figure 386. Oskaloosa test 14 segment 3..... 290
Figure 387. Oskaloosa test 15 segment 1..... 290
Figure 388. Oskaloosa test 15 segment 2..... 291
Figure 389. Oskaloosa test 15 segment 3..... 291
Figure 390. Oskaloosa test 15 segment 4..... 292
Figure 391. Oskaloosa test 1 segment 1, 18 in. plate, acceleration analysis A..... 292
Figure 392. Oskaloosa test 1 segment 2, 18 in. plate, acceleration analysis A..... 293
Figure 393. Oskaloosa test 1 segment 3, 18 in. plate, acceleration analysis A..... 293
Figure 394. Oskaloosa test 2 segment 1, 24 in. plate, acceleration analysis A..... 294
Figure 395. Oskaloosa test 2 segment 2, 24 in. plate, acceleration analysis A..... 294
Figure 396. Oskaloosa test 2 segment 3, 24 in. plate, acceleration analysis A..... 295
Figure 397. Oskaloosa test 3 segment 1, 18 in. plate, acceleration analysis A..... 295
Figure 398. Oskaloosa test 3 segment 2, 18 in. plate, acceleration analysis A..... 296
Figure 399. Oskaloosa test 3 segment 3, 18 in. plate, acceleration analysis A..... 296
Figure 400. Oskaloosa test 4 segment 1, 12 in. plate, acceleration analysis A..... 297
Figure 401. Oskaloosa test 4 segment 2, 12 in. plate, acceleration analysis A..... 297
Figure 402. Oskaloosa test 4 segment 3, 12 in. plate, acceleration analysis A..... 298
Figure 403. Oskaloosa test 4 segment 4, 12 in. plate, acceleration analysis A..... 298
Figure 404. Oskaloosa test 5 segment 1, 9 in. plate, acceleration analysis A..... 299
Figure 405. Oskaloosa test 5 segment 2, 9 in. plate, acceleration analysis A..... 299
Figure 406. Oskaloosa test 5 segment 3, 9 in. plate, acceleration analysis A..... 300
Figure 407. Oskaloosa test 5 segment 4, 9 in. plate, acceleration analysis A..... 300
Figure 408. Oskaloosa test 6 segment 1, 18 in. plate, acceleration analysis A..... 301
Figure 409. Oskaloosa test 6 Segment 2, 18 in. plate, acceleration analysis A..... 301
Figure 410. Oskaloosa test 6 segment 3, 18 in. plate, acceleration analysis A..... 302
Figure 411. Oskaloosa test 7 segment 1, 24 in. plate, acceleration analysis A..... 302
Figure 412. Oskaloosa test 7 segment 2, 24 in. plate, acceleration analysis A..... 303
Figure 413. Oskaloosa test 7 segment 3, 24 in. plate, acceleration analysis A..... 303
Figure 414. Oskaloosa test 8 segment 1, 18 in. plate, acceleration analysis A..... 304
Figure 415. Oskaloosa test 8 segment 2, 18 in. plate, acceleration analysis A..... 304
Figure 416. Oskaloosa test 8 segment 3, 18 in. plate, acceleration analysis A..... 305
Figure 417. Oskaloosa test 8 segment 4, 18 in. plate, acceleration analysis A..... 305
Figure 418. Oskaloosa test 9 segment 1, 12 in. plate, acceleration analysis A..... 306
Figure 419. Oskaloosa test 9 segment 2, 12 in. plate, acceleration analysis A..... 306
Figure 420. Oskaloosa test 9 segment 3, 12 in. plate, acceleration analysis A..... 307
Figure 421. Oskaloosa test 9 segment 4, 12 in. plate, acceleration analysis A..... 307
Figure 422. Oskaloosa test 10 segment 1, 9 in. plate, acceleration analysis A..... 308
Figure 423. Oskaloosa test 10 segment 2, 9 in. plate, acceleration analysis A..... 308
Figure 424. Oskaloosa test 10 segment 3, 9 in. plate, acceleration analysis A..... 309
Figure 425. Oskaloosa test 10 segment 4, 9 in. plate, acceleration analysis A..... 309
Figure 426. Oskaloosa test 11 segment 1, 18 in. plate, acceleration analysis A..... 310
Figure 427. Oskaloosa test 11 segment 2, 18 in. plate, acceleration analysis A..... 310

Figure 428. Oskaloosa test 11 segment 3, 18 in. plate, acceleration analysis A..... 311
Figure 429. Oskaloosa test 12 segment 1, 24 in. plate, acceleration analysis A..... 311
Figure 430. Oskaloosa test 12 segment 2, 24 in. plate, acceleration analysis A..... 312
Figure 431. Oskaloosa test 12 segment 3, 24 in. plate, acceleration analysis A..... 312
Figure 432. Oskaloosa test 13 segment 1, 18 in. plate, acceleration analysis A..... 313
Figure 433. Oskaloosa test 13 segment 2, 18 in. plate, acceleration analysis A..... 313
Figure 434. Oskaloosa test 13 segment 3, 18 in. plate, acceleration analysis A..... 314
Figure 435. Oskaloosa test 13 segment 4, 18 in. plate, acceleration analysis A..... 314
Figure 436. Oskaloosa test 14 segment 1, 12 in. plate, acceleration analysis A..... 315
Figure 437. Oskaloosa test 14 segment 2, 12 in. plate, acceleration analysis A..... 315
Figure 438. Oskaloosa test 14 segment 3, 12 in. plate, acceleration analysis A..... 316
Figure 439. Oskaloosa test 15 segment 1, 9 in. plate, acceleration analysis A..... 316
Figure 440. Oskaloosa test 15 segment 2, 9 in. plate, acceleration analysis A..... 317
Figure 441. Oskaloosa test 15 segment 3, 9 in. plate, acceleration analysis A..... 317
Figure 442. Oskaloosa test 15 segment 4, 9 in. plate, acceleration analysis A..... 318
Figure 443. Oskaloosa pier 1 acceleration analysis B ..... 318
Figure 444. Oskaloosa pier 2 acceleration analysis B ..... 319
Figure 445. Oskaloosa pier 3 acceleration analysis B ..... 319
Figure 446. Oskaloosa test 2 segment 1, 24 in. plate, acceleration analysis C..... 320
Figure 447. Oskaloosa test 2 segment 2, 24 in. plate, acceleration analysis C..... 320
Figure 448. Oskaloosa test 2 segment 3, 24 in. plate, acceleration analysis C..... 321
Figure 449. Oskaloosa test 3 segment 3, 18 in. plate, acceleration analysis C..... 321
Figure 450. Oskaloosa test 4 segment 4, 12 in. plate, acceleration analysis C..... 322
Figure 451. Oskaloosa test 5 segment 4, 9 in. plate, acceleration analysis C..... 322
Figure 452. Oskaloosa test 2 segment 3, 24 in. plate, acceleration analysis D..... 323
Figure 453. Oskaloosa test 3 segment 3, 18 in. plate, acceleration analysis D..... 323
Figure 454. Oskaloosa test 4 segment 4, 12 in. plate, acceleration analysis D..... 324
Figure 455. Oskaloosa test 5 segment 4, 9 in. plate, acceleration analysis D..... 324

## LIST OF EQUATIONS

$E_{vd} = 1.5\ r\ (\Delta\sigma / \Delta s)$ (1) ..... 5
$F_d = A_1 M_1 + A_2 M_2$ (2) ..... 7
*Acceleration= (geophone output* x *calibration factor* x *i* x *2* x *pi* x *f)/(9.81)* (3) ..... 7
*9.81 / (DACF (2* x *pi* x $f)^2$*))* (4) ..... 7

# CHAPTER 1. INTRODUCTION

This chapter introduces the industry and technical problems in the research, the goal of the research, the objectives to reach the goal, and the significance of the research. The chapter will conclude with a discussion on the organization of the thesis.

## Industry problem

In situ measurement devices used in the geotechnical engineering and construction industries exist to evaluate quality characteristics of parameters to ensure installed components meet design specifications. However, obstacles exist that prevent measurement devices to be used at a high enough test frequency to ensure uniformity and to parameter values that are only surrogates to performances. Therefore, uncertainty exists in the quality of final products of construction. This research examined the quality testing methods for compacted aggregate piers and developed a new in situ test device to assess pier compaction efforts and stiffness parameters.

### Industry concerns

In situ measurement devices to ensure that aggregate piers meet design specifications need to be rugged because of the environment in which they are used and the compaction forces used for installation. Testing systems exist to assess the stiffness parameters, however, no current technologies exist to observe the compaction effort or to rapidly measure stiffness parameters as piers are installed. In practice, typically only a non–production pier is evaluated to measure the load–displacement relationship. For quality control and quality assurance (QC/QA) purposes it would be advantageous to test as many production piers as possible.

### Impact on industry

One pier cannot necessarily represent a whole site, and, as a result, foundation piers may not meet design specifications. Or, the design may be over conservative to account for unknown variability. Measuring the stiffness values of production foundation piers as they are installed would ensure that they meet the specifications, improve the design efficiency, and provide information to optimize the pier compaction effort. If they do not meet

specifications while being measured, immediate action can be taken to modify the construction process to ensure the design specifications are met.

## Technical problem

The technical issue is that there are currently no technologies that exist to observe and document the compaction effort or measure the stiffness as piers are installed. Because of the environment and the compaction forces used to install aggregate piers, an in situ device needs to be rugged but also easily accessible and easy to use. By integrating measurement technologies, a record of the compaction load and acceleration values can be obtained. By double integrating acceleration values, deformation can be obtained under the dynamic loading. Deformation is determined from the assumption of a rigid plate on an elastic half space with an inverse parabolic to uniform stress distribution. Then, the stiffness can be determined from the stress (calculated as the load divided by the plate size), and the deformation. The combination of technologies is herein referred to as the RAM Test and includes the device, data acquisition system, and software to record and to display the data.

No other solutions or devices to rapidly assess the compaction and stiffness of an aggregate pier as it is installed are known.

## Goals of the research

The overall goals of the research are to describe the RAM Test device development and components, demonstrate field measurements of load and acceleration, and show calculation results of pier stiffness using time-domain integration with filtering of the acceleration data in combination with loads from several plate diameters.

## Objectives

The objectives of the research are to

- test the RAM Test device;
- use the device to observe, and collect load and acceleration data on aggregate piers during installation,
- establish a relationship between acceleration and permanent deformation,
- calculate load characteristics, and
- determine stiffness values.

## Significance of the research

The manner that an aggregate pier is evaluated to find its stiffness can take up to 12 hours, and typically only one non–production aggregate pier is evaluated. It would be beneficial to rapidly test production. If piers are evaluated as they are installed, this will ensure the piers across the site meet design specifications. If the piers do not meet the desired design specifications, immediate action can be taken during the construction process. Currently, individual lifts of one pier are compacted for a set amount of time. If a pier reaches design specifications before that set amount of time, compaction can stop, and a new lift can be added and compaction started again. This has the potential to save time, resources, and therefore money.

Furthermore, no record of the installation loads and accelerations is kept. With the research, there is a potential to generate a compaction record for every pier tested. This has the potential to help gain more knowledge of the compaction record. This has the potential to serve as a tool to gain more knowledge about the site variability, lift thickness, and compaction effort.

## Organization of the document

The thesis will be organized into five chapters; background, methods, materials, results and discussion, and conclusions and recommendations. The background includes a review of relevant literature, a summary of present practices, and a discussion of preliminary work. The methods chapter describes conducting in situ testing, evaluating field data, determining the stiffness parameters, and describes the material used for the piers. The results and discussion will contain the analysis for the load, acceleration, stiffness, and verification. The conclusion and recommendations chapter will show the outcomes and benefits of the analysis, and will discuss the outcomes and future research.

# CHAPTER 2. BACKGROUND

This chapter presents two kinds of background for this project, a review of relevant literature and a summary of present practices. The purpose of this chapter is to provide an overview that shows how this research fits in theory and practice.

## Literature review

This section will present relevant literature as it pertains to the research, and includes a discussion on the following topics; plate load testing, measures of stiffness, accelerometers, load cells, and determination of shear modulus.

### Plate load testing

Plate load tests are performed on soils to interpolate the performance of the foundation structures. The tests consist of a loading device, a hydraulic jack assembly, bearing plates, dial gages, and a deflection beam (Johnson and Kavanagh, 1968). A loading device is normally a truck or trailer, or a structure with sufficient weight to produce the desired reaction on the surface. A hydraulic jack assembly has the capability to apply and release loads in increments and includes a gage to read the load. Steel bearing plates, at least 1 in. in thickness, range from 6 to 30 in. and are arranged in a pyramid manner. Dial gages are used to measure the maximum deflection. These dial gages are mounted on the deflection beam, which is 2 ½-in. standard black pipe or 3 by 3 by ¼ in. steel angle. The beam is at least 18 ft. long and rest on supports at least 8 ft. from the bearing plate. There are two types of plate load tests, repetitive and non repetitive.

The repetitive test involves a load that is applied, released, and then repeated again with increased applied loads. A load is applied giving a deflection of 0.04 in. and maintained until the rate of deflection is 0.001 in. per minute or less for three consecutive minutes and then the load is released. The rebound is observed until the rate of recovery is 0.001 in. per minute or less for three consecutive minutes. The same load is applied and released six times in this same manner. Next, a second and third load is applied to reach deflections of 0.2 in., and 0.4 in., respectively. In each case, the deflection is recorded at the end of each minute. The results include a plot of the deflection at exactly 0.001 in. per minute versus the number of repetitions of each corrected load (ASTM D1195).

The non repetitive test involves an applied load that is never released during the procedure (ASTM D1196). The loads are applied rapidly and uniformly, but small enough to record load-deflection points. A load is held until a rate of deflection of 0.001 in. per minute is maintained for three consecutive minutes. The load increments continue until the desired deflection is reached or the capacity of the assembly is reached. Next, release the load to the zero-setting load and maintain until the rate of recovery is less than 0.001 in. for three minutes. The results include a plot of the unit load for each increment versus the equivalent deflection.

**Measures of stiffness**

The light weight deflectometer (LWD) test is used for evaluating road construction materials like the subgrade, subsoil and granular base layers, and quality control. It was initially developed because the current tools were burdensome and time-consuming to use (Fleming et. al, 2006). The LWD allows for a fast evaluation of a dynamic deflection modulus, $E_{vd}$, and is intended to be an alternative to the static plate bearing test. The static plate bearing test is discussed in the plate load testing section. The device consists of a drop weight, 2, 3 or 4 buffers, a load cell, a deflection sensor, also called a velocity transducer or geophone, a bearing plate, and a geophone foot. The settlement, s, is measured from the deflection sensor. The $E_{vd}$ is calculated from s and displayed within the time of the test. The calculation of $E_{vd}$ is based from the theory "half space model" and the formula is

$$E_{vd} = 1.5\, r\, (\Delta\sigma / \Delta s) \quad (1)$$

where $r$ is the radius of the plate;

$\Delta\sigma$ is the stress below the plate; and

$\Delta s$ is the settlement (Zorn, 2003). The buffers located above the load cell and below the drop weight affect the loading rate. A lower stiffness buffer provides more efficient load transfer and behaves like a static plate load, while a higher stiffness buffer shortens the time-history and can increase the LWD stiffness value on asphalt pavements (Vennapusa and White, 2009)

The falling weight deflectometer (FWD) test is one of the most versatile tools to measure the stiffness of pavement systems. The test consists of 8 deflectometers and a load plate. The deflectometers are placed 0, 8, 12, 24, 36, 48, and 60 inches from the center of the load plate

(Uddin and McCullough, 1989). A predetermined load is dropped on the load plate, which causes a stress and 8 deflections. The output is a modulus and a time history for each load drop.

Research had been conducted at Iowa State University on an in situ device that used sound to record compaction. The device was named the noise dosimeter and collected decibels (dB) and GPS measurements to document compaction energy, lift thicknesses, pier locations, and production rates. An output of the device is a plot of dB verse time, where the dB for each lift can be determined. GPS allows for the lift depth and the compacted lift thickness to be determined. The production rate for each pier can ultimately be determined.

**Accelerometers**

This section discusses the history and the uses related to the research.

*History*

Instrumentation designer Patrick Walter is well versed in accelerometers and discussed their history in a journal article which is summarized in this section.

The accelerometer has existed since the early 1920s. The earliest record of an accelerometer is a quartz and tourmaline piezoelectric pressure transducers, which dates to 1919. In the beginning, private industry pushed the evolution of the accelerometer. McCollum and Peters developed the first accelerometer. It weighed approximately one pound, and the dimensions were 0.75 in. x 1.875 in. x 8.5 in. It consisted of 20 to 55 carbon rings in tension–compression. Initial applications for the accelerometer included bridges, dynamometers, and aircraft. Within ten years, applications included aeronautics, passenger elevators, and vibration recording of steam turbines, underground pipes, and explosions.

Large-scale commercialization did not begin until bonded resistance strain gages were developed. However, the accelerometers, which used strain gages, were limited to low frequency responses and were very fragile. The introduction of piezoelectric accelerometers helped with the strain gage accelerometer issues because piezoelectric materials had higher moduli and could produce a wider signal range. The piezoelectric materials were ferrous (barium titanate) and nonferrous (quartz). During the 1950s, 1960s and 1970s, further advances in piezoelectric materials improved sensitivity, compression accelerometers were introduced, and calibration techniques for shock and vibration were explored in the

government sector. In the past 20 years, Transducer Electronic Data Sheets (TEDS), a memory device, has been developed, and Micro-Electro-Mechanical-Systems (MEMS) has grown due to the advances in silicon technology.

Although accelerometers were originally produced for the test and evaluation community, today, they are used in a wide range of fields such as crash tests in the automotive industry, and in electronic and phone applications. In the future, consumers will see advances in computer devices, hand-held navigation products, game controllers, camcorders, and robots because of accelerometers. Other applications include military (unmanned vehicles) and biomedical. Historically, the push for accelerometer technology was the test and evaluation market, but in the future, the push will be the consumer MEMS market (Walter, 2007).

*Uses*

The rolling dynamic deflectometers (RDD) is a non destructive test method for the evaluation of pavements developed at the Center for Transportation Research, at the University of Texas at Austin. It consists of a truck, a servo-hydraulic vibrator, and three accelerometers. Two accelerometers measure dynamic force, and one measures the pavement motion. The accelerometers are used to calibrate the dynamic force with following equation.

$$F_d = A_1 M_1 + A_2 M_2 \quad (2)$$

The accelerometer output divided by the dynamic load is measured at different frequencies to produce a calibration curve, dynamic force calibration factor (DFCF). A dynamic acceleration calibration factor (DACF) is found by the outputs of a geophone and accelerometer. The geophone output is converted to acceleration by the equation,

$$Acceleration = (geophone\ output \times calibration\ factor \times i \times 2 \times pi \times f)/(9.81) \quad (3)$$

The acceleration from the geophone is divided by the acceleration from the accelerometer is determine the DACF. To analyze the pavement motion, the accelerometer output is processed with fast Fourier transform (FFT). The accelerometer output is volts verses time. The output is multiplied by the Hanning Weighting function which results in a weighted acceleration output in the time domain. This output is processed with FFT and results in an accelerometer output in the frequency domain. The following equation,

$$9.81 / (DACF\ (2 \times pi \times f)^2)) \quad (4)$$

is applied to the frequency domain to transform the units to peak-to-peak displacement. The same procedure is used to process the data from the load cells to determine peak-to-peak force (Stokoe and Bay, 2005).

Accelerometers are used in intelligent compaction to measure vertical and horizontal displacement reaction between the drum and the ground. When the ground is soft, the energy goes to the soil surface and not back into the equipment. When the material is compacted or denser, less energy goes to the soil surface and more energy is felt by the compaction system (Wilson, 2004).

**Load cells**

A load cell transforms force into a measurable electrical output. Load cells vary, but most commonly use strain gages (Noori et. al, 2005). Load cells come in different forms and each type has different purposes.

An Osterberg Cell (O Cell) is named after its inventor Dr. Jorj Osterberg. (Loadtest, 2011). The O Cell is a sacrificial tool to measure load using hydraulics as the loading mechanism. The cell is composed of a large diameter pressure cell filled with pressurized water or oil. The main use for the load cell is for drilled shaft foundations. The O cell is embedded in the shaft, at one or multiple levels to perform load tests (Fugro, 2011). The advantages include the ability to use on high capacity drilled shafts, realistic conditions are seen, data is measured that is too expensive to obtain other ways, design load are validated, and conservative guessing is reduced. The disadvantage is the shaft is load from the bottom to the top, where a structure will load the shaft from the top to the bottom (Paikowsky, 2006).

As stated before, calibration of the RDD uses weigh in motion (WIM) load cells. A comparison of the pressure in hydraulics to the force from the WIM load cells produces a calibration curve for the static force (Stokoe and Bay, 2005). Liu and group quoted American Society of Testing and Materials Standard Specification E 1318-94 that WIM technology is "the process of measuring the dynamic tire forces of a moving vehicle and estimating the corresponding tire loads of the static vehicle". WIM load cells are used in scale mechanisms for weighing trucks. The load is transferred to the load cells through load transfer tubes. The

advantages of the WIM load cells are that they are the most accurate load cell of all WIM sensors. The disadvantages are their cost and their complexity to install (Liu et. al, 2005).

The load cell is used in many applications, such as in situ measurement devices like the FWD, laboratory devices to measure pressure and load, such as direct shear tests, consolidation tests, and compression machines. One application is the use of load cells to measure the forces between a retaining wall and back fill to learn more about the interaction between the wall and soil. The analysis applies to cells on a rigid plate connected to a transducer to observe deflections (Carder, 1976). Although the load cell is commonly found in civil engineering applications, it is found in any engineering application where an applied or measured force is needed, like in the automotive industry and measuring forces in crash tests.

## Summary of present practices

This section will discuss present practices as it pertains to the research, and includes a discussion on the following topics; rammed aggregate piers, pier load test, and foundation QA/QC tests.

### Geopier Rammed Aggregate Piers®

Aggregate pier elements are installed by (1) drilling a cavity into the ground, (2) placing aggregate at the bottom of the cavity, (3) compacting a bottom bulb to densify and vertically pre-stress the matrix soil, and (4) installing an undulated-side shaft with 12 in. thick lifts of aggregate (Fox and Cowell, 1998). A beveled tamper is used for the installation of piers. The tamper uses an impact ramming energy with limited amplitudes of 10 mm and frequencies between 300-600 cycles per minute (Fox and Lien, 2001).

Impact® piersare similar to Geopier elements but instead of drilling a cavity in the ground, aggregate is placed in a hopper at the top of the mandrel. A high crowd load forces the mandrel through the soil and when the mandrel is raised, aggregate fills the cavity and is rammed to densify and stiffen the matrix soil. The mandrel is raised 3–4 ft. and compacts 2–3 ft. for each lift. This continues until the design elevation is reached (Farrell, 2010).

### Pier load test

Load testing is a method to determine the modulus of a pier. The modulus of a pier element is determined by applying pressure on the top of the pier by load increments. The

increments are determined from design stress calculations. The load is applied by a hydraulic jack and frame and held until the deflection rate is less than 0.01 in. per hour or the maximum duration for that load increment is met. The deflection is measured and recorded and the next load increment is added. The deflection value and stress for each load increment is plotted and the modulus is equal to the design stress divided by the corresponding deflection. The duration of the test is at least 2 hours and 45 minutes and at most 11 hours (Fox and Cowell, 1998).

**Foundation QA/QC tests**

The current quality control program for Geopier elements focuses on verifying correct pier installation. According to the 1998 Geopier Foundation and Soil Reinforcement Manual the program includes

- coordinating the footing layout,
- observing soil,
- measuring drill depths and top elevations,
- controlling moisture content,
- recording the type and number of lifts of aggregate,
- performing qualitative tests on production piers,
- implementing corrective measures if necessary, and
- writing a construction activities report (Fox and Cowell, 1998).

The quality assurance program includes

- observing installation of modulus load test piers,
- supervising load tests, and
- monitoring pier installation (Fox and Cowell, 1998).

QA/QC tests performed can include the bottom stabilization test (BST). The BST is a verification method to determine overall stabilization of the pier before installation is complete. It is also completed to check that the pier is comparable to the load test pier. The dynamic cone penetrometer test (DPT) is performed to verify that the top few feet of a pier have reached densification after installation is complete (Fox and Cowell, 1998).

## Preliminary Work

The Earthworks Engineering Research Center (EERC) began the development of the RAM Test along with Don Eichner of Eichner Engineering. Eichner designed and machined the device and wrote the data acquisition software program for collecting data. The RAM Test went to Newton, Iowa and Grand Junction, Iowa in 2007 and went to Canada twice in 2008 for preliminary tests. Table 1 summarizes the field study location, date, project, and pier type for the initial field studies.

**Table 1. Summary of the initial field studies**

| Field Study Location | Date | Project | Pier Type |
|---|---|---|---|
| Grand Junction, IA | November 6, 2007 | Phase II ethanol plant | RAPs |
| Newton, IA | November 29, 2007 | | RAPs |
| Toronto, Canada | January 10, and May 7, 2008 | Temperature research | RAPs |

These sites allowed for problems to be fixed, to have confidence in the input parameters, and to justify design decisions. The sample rate was 1,000 Hz and from these sites it was decided to change the rate to 10,000 Hz for future sites.

Greg Luecke, a professor in the mechanical engineering department and his student, Don Kieu, developed the code to analyze the acceleration–time data. Initially, they studied the device and its construction to understand how to best write the code. The code consists of integration equations and filters on the load and acceleration data. The code filters the acceleration values smaller than 5 g due to noise. The code at the end filters the data a second time. The filters exclude noise due to the surrounding environment and not from the pier installation process. An output of deformation verse time is produced. And, an output plot of filtered load verse deformation is also produced to show how the deformation changes with load. The deformation at peak load can be determined, and vice versa, the load at peak deformation can be determined.

# CHAPTER 3. METHODS

The methods used in this study were selected to address these objectives: to conduct in situ testing; to evaluate the data; and to determine load, acceleration, and stiffness parameters.

## Research design

The research objectives are to:

- test the RAM Test in situ;
- observe and collect load and acceleration data;
- use acceleration analysis code to establish the relationship between acceleration and permanent deformation;
- calculate stiffness parameters from load and permanent deformation data; and
- plot stress verse deformation against pier depth, plate size, and time.

To address these objectives 231 RAM Tests were conducted at 9 field studies. Gradation analyses were conducted from material from 4 field studies in the laboratory at Iowa State University. Data processing software was used to analyze the load data from the last 5 field studies, 167 tests in total. Acceleration analysis software was used to analyze the acceleration data from the last 5 field studies, 97 tests in total, while 27 of the 97 tests were processed by multiple analyses.

## The RAM Test

The RAM Test is composed of four stacked 12 in. diameter steel plates (referred to from the top of the device as plates 1 to 4), with a 12 in. diameter buffer pad between plates 1 and 2. Three load cells each with a 45,000 lb capacity and one accelerometer are positioned in machined cavities in the top surface of plate 3. Additional steel plates of 9 in., 18 in., and 24 in. diameter can be attached to the bottom of plate 4. Figure 1 shows a design drawing of the RAM Test, while Figure 2 shows the RAM Test with the 9 in. plate attached to the bottom.

Accelerometer 1 has a +/– 500 g range and was originally installed in the device in 2007. When reviewing the acceleration data from Hampton to Oskaloosa, a peak value of 391.29 g was observed at every site. The specifications showed the accelerometer had a +/– 500 g range. On January 13, 2011, accelerometer 1 was replaced with accelerometer 2.

Accelerometer 1 was shipped back to the manufacturer to be recalibrated and to ensure it is working properly. Accelerometer 2 has a +/– 5,000 g range, and will ensure the correct acceleration values are recorded. On April 29, 2011, the RAM Test with accelerometer 2 was taken in the field.

**Table 2. Inventory of RAM Test parts**

| Part | Size/Capacity | Quantity |
|---|---|---|
| Steel plate | 12 in. diameter | 4 |
| Rubber buffer pad | 12 in. diameter | 1 |
| Load cell | 45,000 lb | 3 |
| Accelerometer | 5,000 g | 1 |
| Bolt | machined to 4 in. x ¾ in. | 9 |
| Bolt | $^{3}/_{8}$-16 x 1 ½ | 9 |
| Bolt | ½ -13 x 2 ½ | 9 |
| Bolt | ½ -13 x 2 ¼ | 9 |
| 1/6 in. Washer | ¾ in. diameter | >36 |
| 1/8 in. Washer | ¾ in. diameter | >18 |
| Nuts | ¾, $^{3}/_{8}$, ½ in. | >50 |
| Handle | | 2 |
| Steel plate | 9 in. diameter | 1 |
| Steel plate | 18 in. diameter | 1 |
| Steel plate | 24 in. diameter | 1 |
| AST-Lock 42 MS | | 1 |
| Anti-seize and lubrication compound | | 1 |
| Duct tape | Heavy duty | 1 |
| Data acquisition system | | 1 |
| Data acquisition software | | 1 |
| Laptop | | 1 |

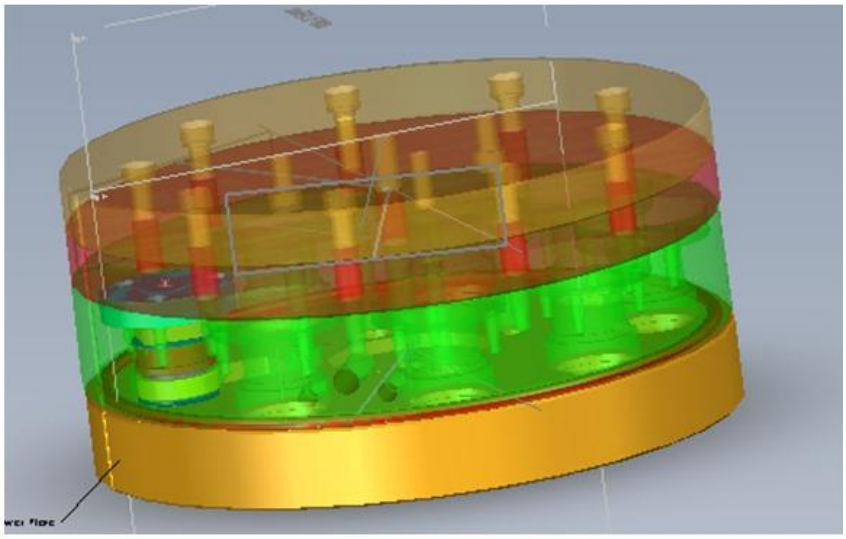

**Figure 1. RAM Test device configuration, the gold colored plate represents plate 3 where the three loads sit in machined cavities**

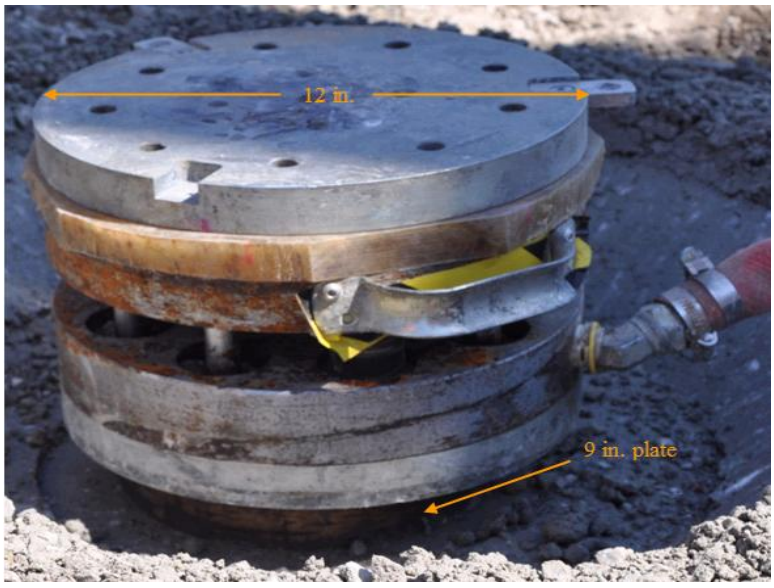


**Figure 2. The RAM Test collects data on a pier with the 9 in. plate**

**Set-up the RAM Test**

The purpose of setting up the RAM Test before going to a field site is to ensure that the connections between the RAM Test, the data acquisition system, and the laptop are working together, and that the data acquisition system and data acquisition software are working correctly and without problems.

A recurring issue is the data acquisition software not finding a connection to the data acquisition system. This occurs when the Ethernet cord which connects the data acquisition system to the laptop, and the wires which connect the RAM Test device to the acquisition system are not plugged in and turned on in a specific order. This issue is resolved by connecting the RAM Test to the data acquisition system first, then, connecting the Ethernet cord from the data acquisition system to the laptop second, and turning on the laptop last.

The data acquisition software writes an ASC file and a DDF file for the three load cells and the accelerometer data when the program is recorded in the field, and saves the files in a corresponding file of the user's choice. The following steps are how to set up the data acquisition software test files:

1) Open the data acquisition software

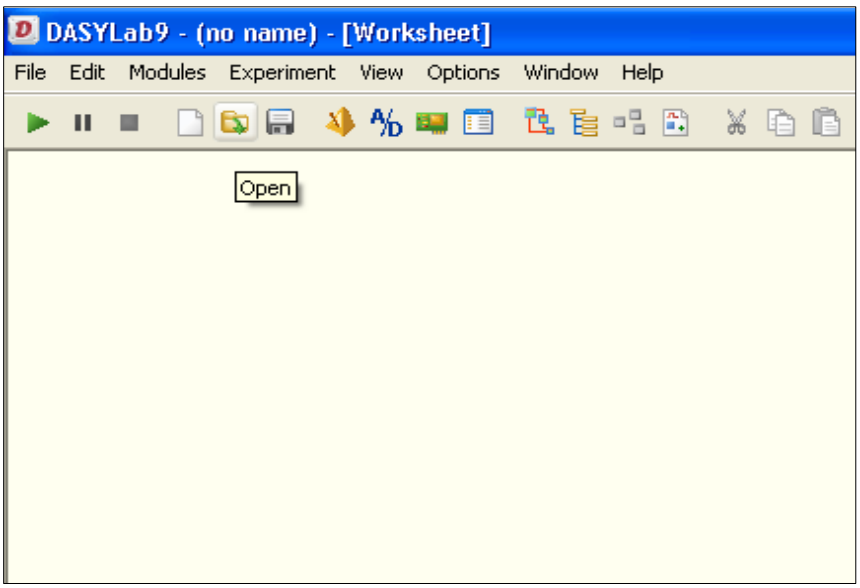


**Figure 3. "How to set up the data acquisition software test files" Step 1**

2) Open previous test site worksheet
   a) File: Open

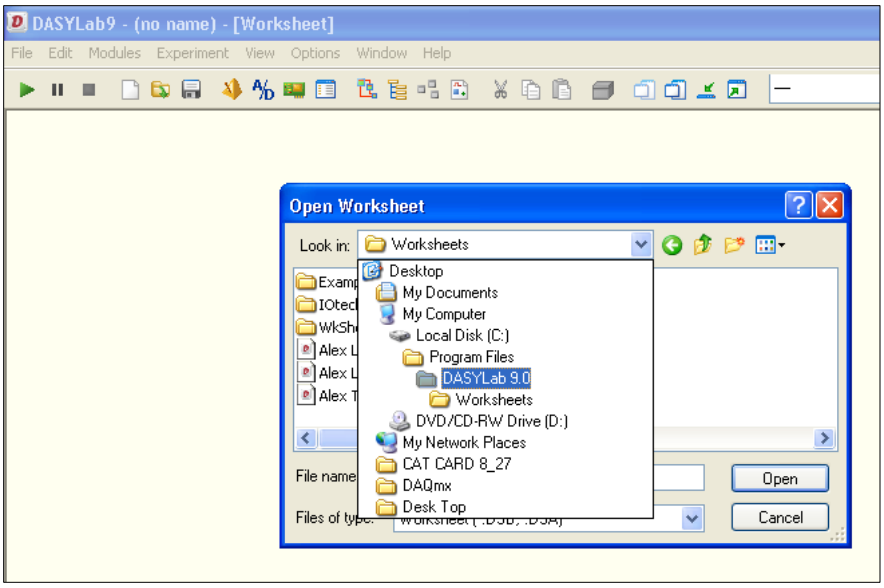


**Figure 4. "How to set up the data acquisition software test files" Step 2-a**

b) Open folder "Devices"

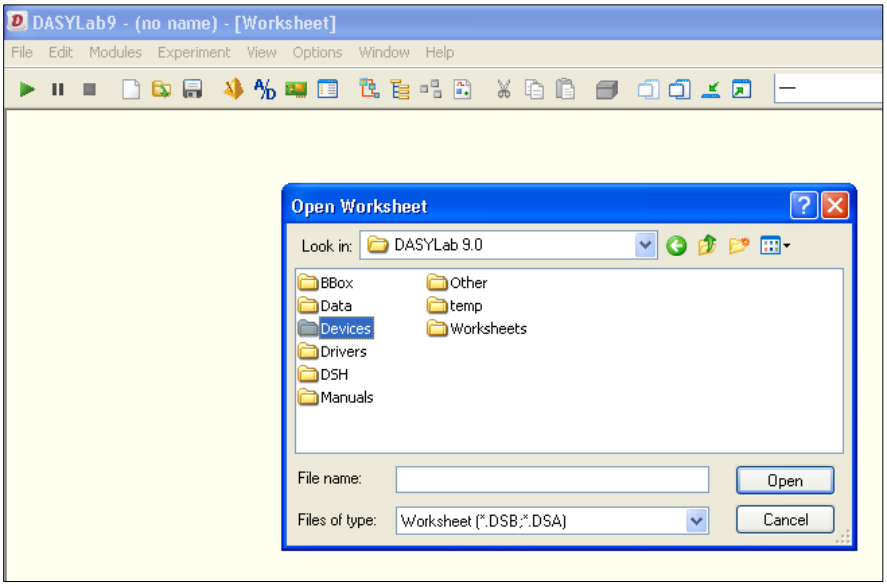


**Figure 5. "How to set up the data acquisition software test files" Step 2-b**

c) Open folder "Worksheets"

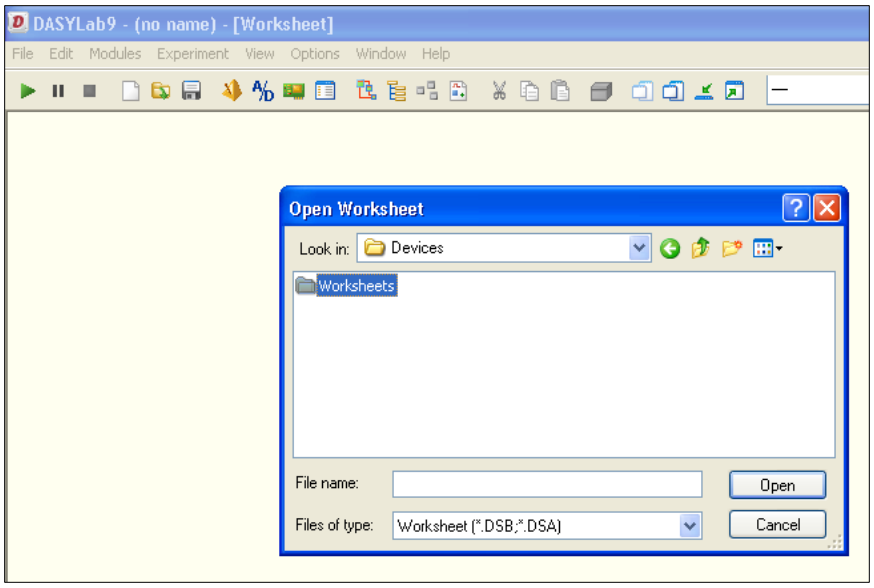


**Figure 6. "How to set up the data acquisition software test files" Step 2-c**

d) Open folder "WkSheet-Thumper"

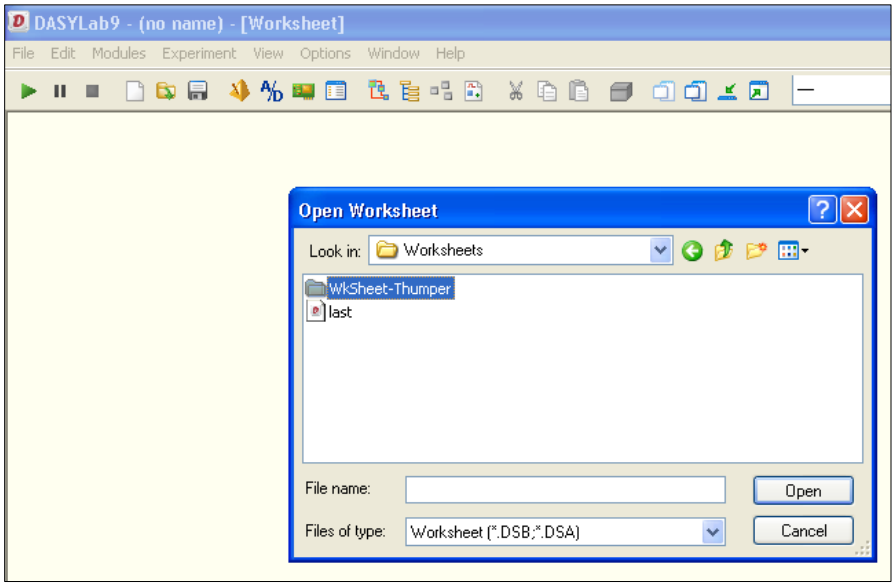


**Figure 7. "How to set up the data acquisition software test files" Step 2-d**

e) Double click on previous test file

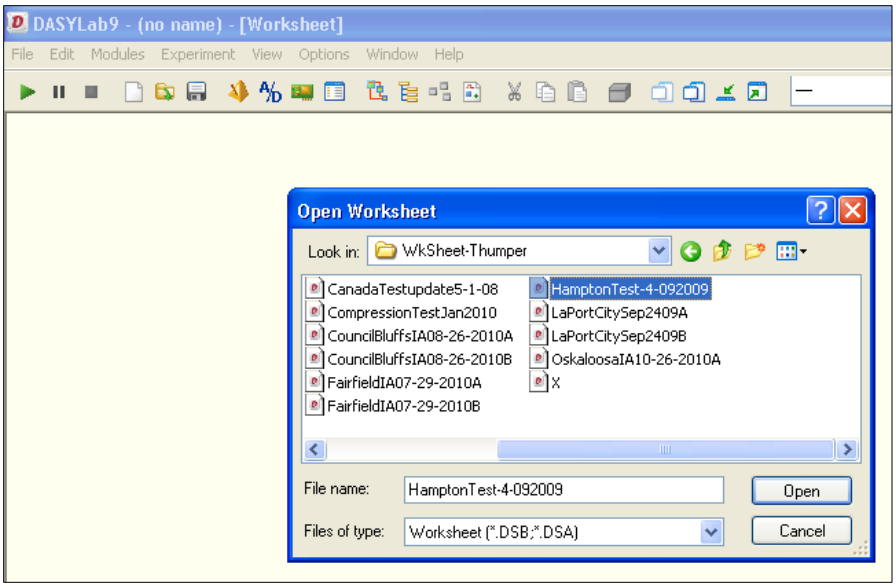


**Figure 8. "How to set up the data acquisition software test files" Step 2-e**

3) Save as and name after field study (for example: *CityState*Data*MonthDayYear)* in "WkSheet-Thumper" folder

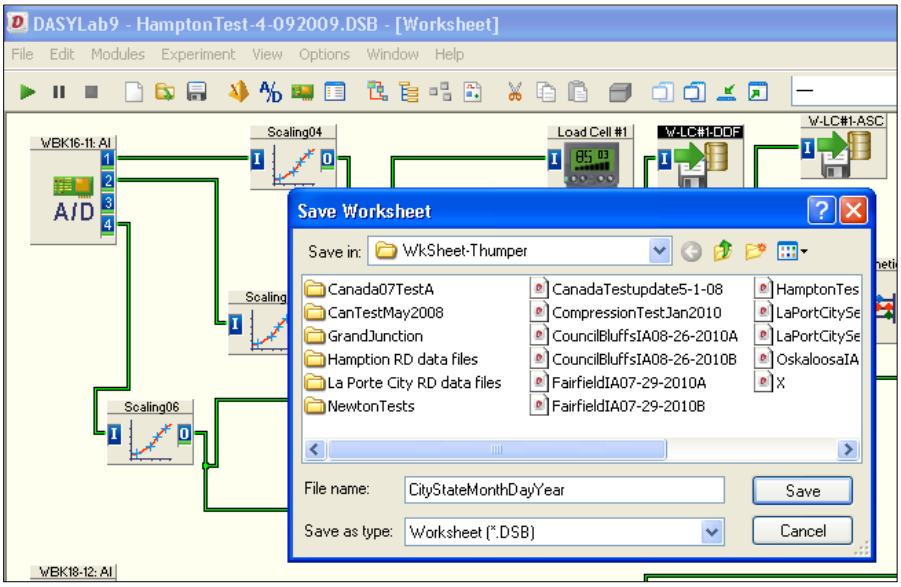


**Figure 9. "How to set up the data acquisition software test files" Step 3**

4) Change directory of where files are saved and the file name for each load cell, total load cell and accelerometer

   a) Right click on desired module

b) Click “Properties”

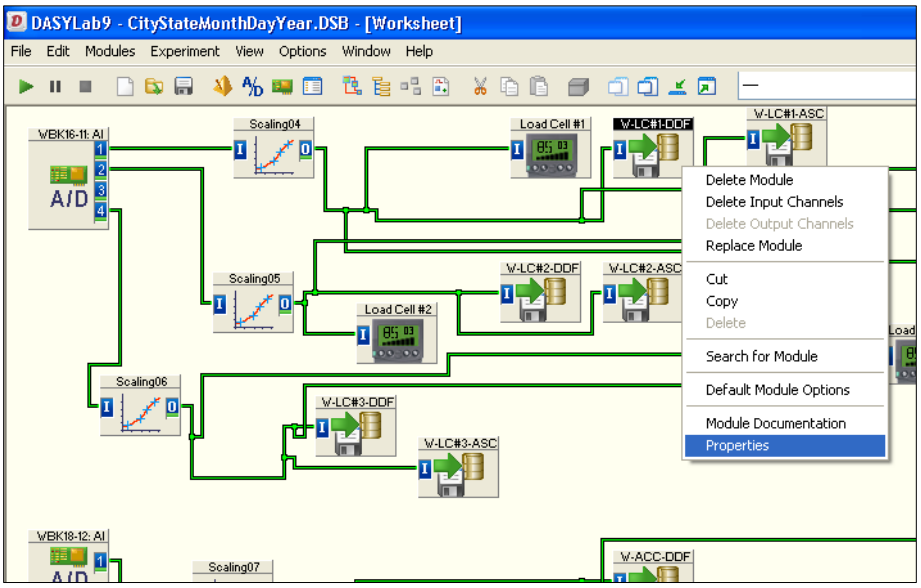


**Figure 10. “How to set up the data acquisition software test files” Step 4-a, 4-b**

c) Click “Filename…” on right side of pop up screen

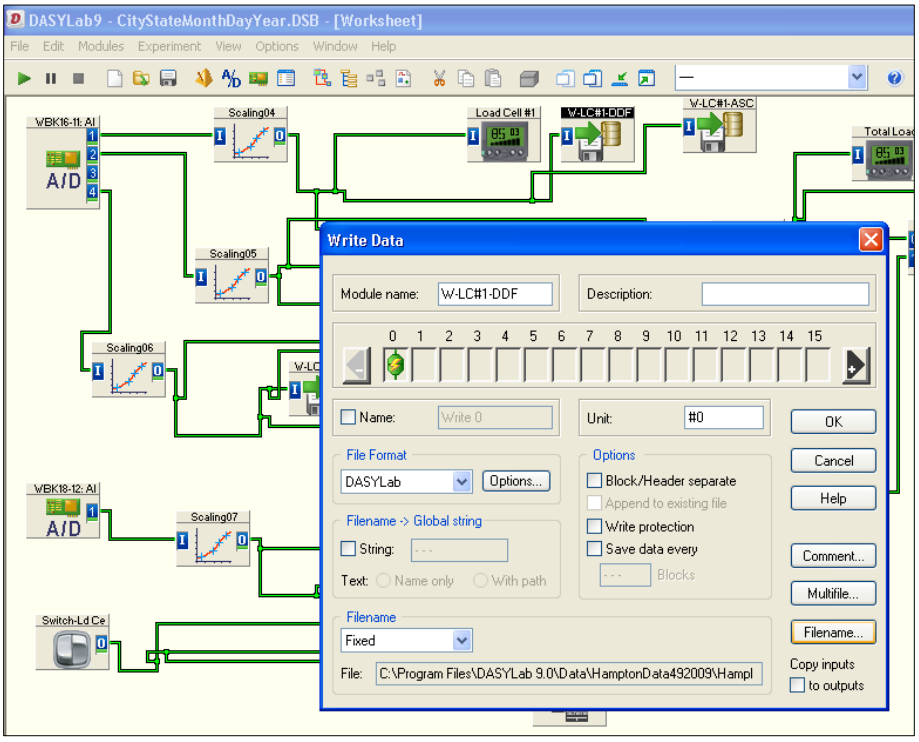


**Figure 11. “How to set up the data acquisition software test files” Step 4-c**

d) Choose new directory

e) Open folder “Data”

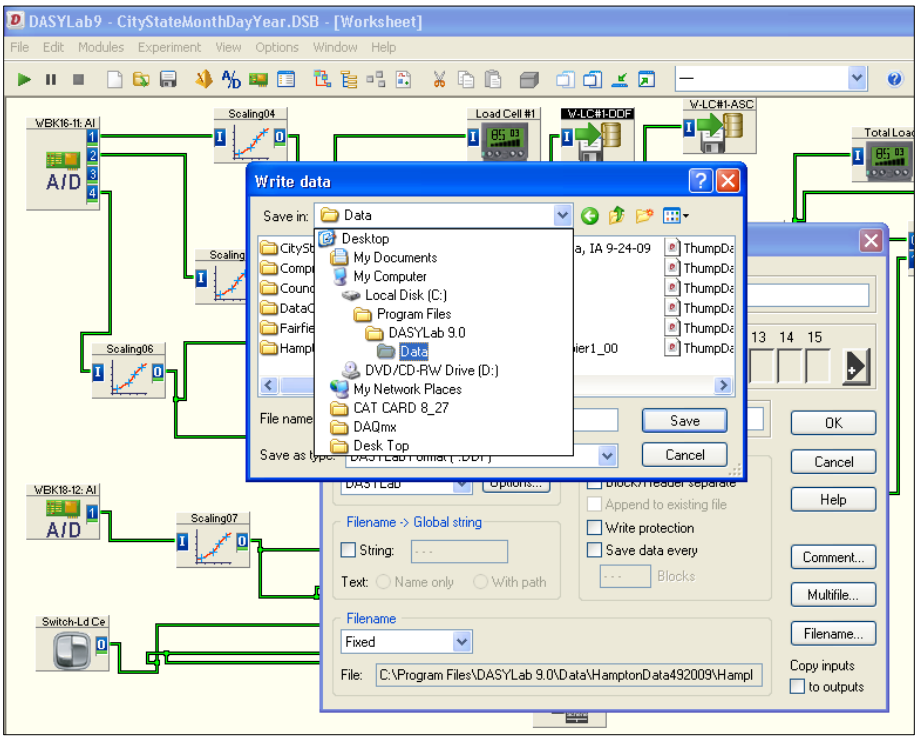


**Figure 12. “How to set up the data acquisition software test files” Step 4-e**

f) Create new folder “CityStateMonthDayYear”

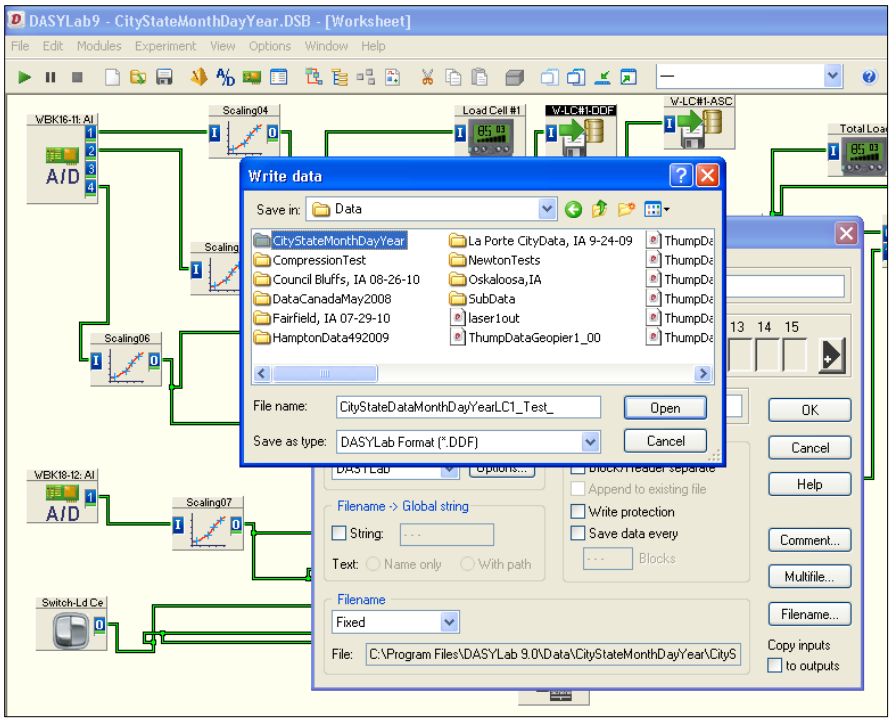


**Figure 13. "How to set up the data acquisition software test files" Step 4-f**

g) Open the created folder

h) Create new filename *(*for example: *CityState*Data*MonthDayYear*LC1_Test_XX, or LaPortDataSep242009ACC_Test_XX)

   i) The data acquisition software automatically numbers the tests when "XX" is in the name

   ii) The file will start with "01" and can record up to "99"

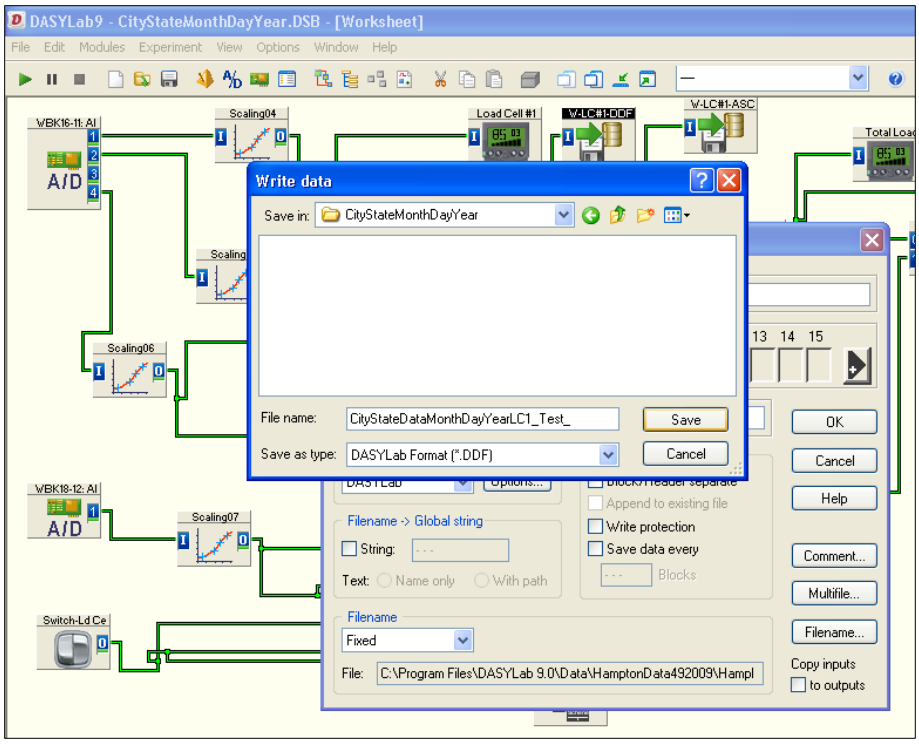


**Figure 14. "How to set up the data acquisition software test files" Step 4-h**

5) Repeat step 4 for both ASC and DDF file format for each load cell, total load cell, and accelerometer

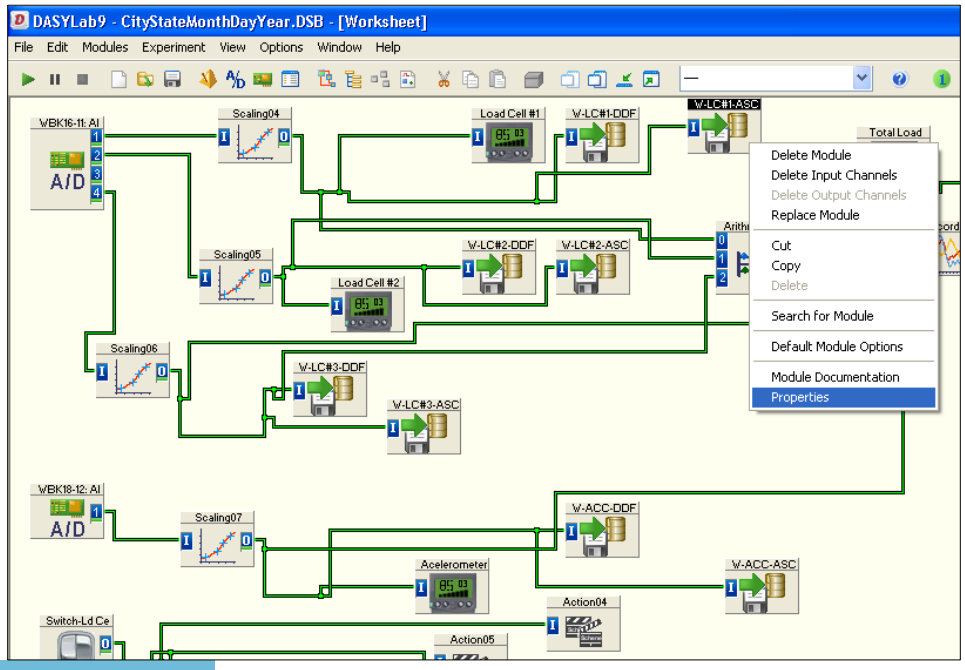

**Figure 15. "How to set up the data acquisition software test files" Step 5**

**Verify the RAM Test**

The purpose of verifying the RAM Test is to ensure that when the accelerometer and the load cells record and save data, they are recording accurate values. To calibrate the load cells, a compression machine was used to apply static load, up to 100,000 lbs, in increments to the device. As the load is applied, the data acquisition software is running and recording the loads from the RAM Test. The loads are then compared to the values from the compression machine to ensure the RAM Test is recording accurate values. The load has been calibrated twice, on February 4, 2010 and January 26, 2011. The calibration on January 26, 2011 was performed after accelerometer 2 was installed to replace accelerometer 1. The results from the calibration are found in Figure 16 and Figure 17.

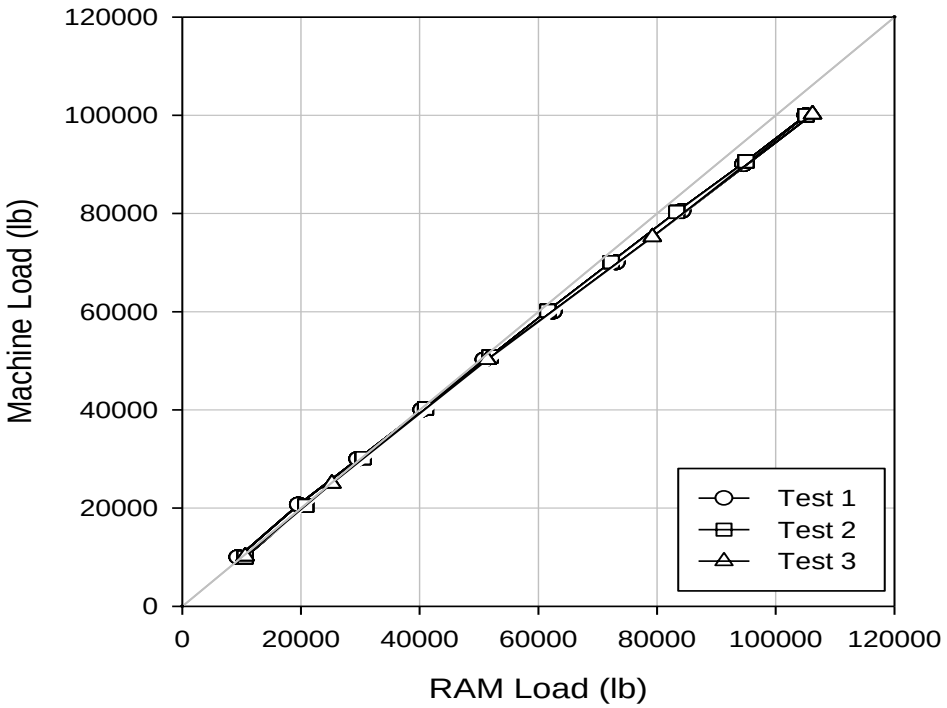


**Figure 16. Load verification on February 4, 2010**

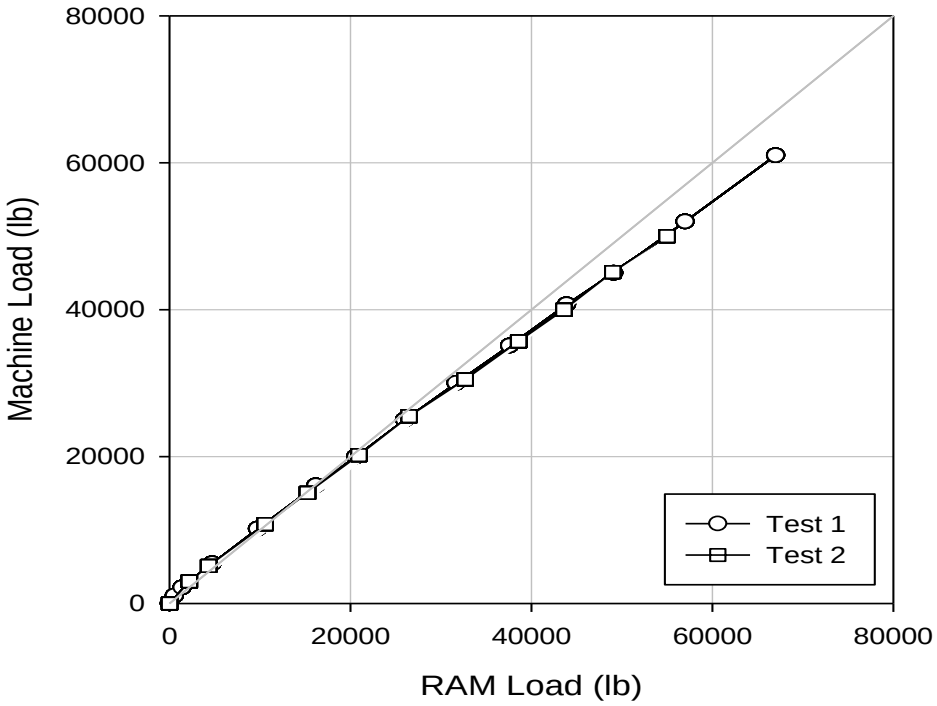


**Figure 17. Load verification on January 26, 2011**

Accelerometer 1 was calibrated by the manufacturer before installed in the RAM Test on August 3, 2007. After nine field studies accelerometer 1 was calibrated and inspected on February 21, 2011. Accelerometer 2 was calibrated by the manufacturer before installed in the RAM Test on December 3, 2010. The calibration and specification sheets from the manufacturer are shown in the appendix.

## In situ testing

The methods to conduct in situ testing consist of recording RAM Tests and verification tests on aggregate piers.

### Perform in situ RAM Tests

The purpose of recording RAM Tests on aggregate piers is to document load and acceleration time-history to quantify the crowd load, the dynamic load, the ramming frequency, the maximum absolute acceleration, and the deformation of the pier. The following is the steps to the general procedure to prepare the RAM Test before piers are tested:

1) Plug wires coming out of the RAM Test device into the back of the data acquisition system


**Figure 18. The back view of the data acquisition system before wires are plugged in, general procedure to prepare RAM Test step 1**

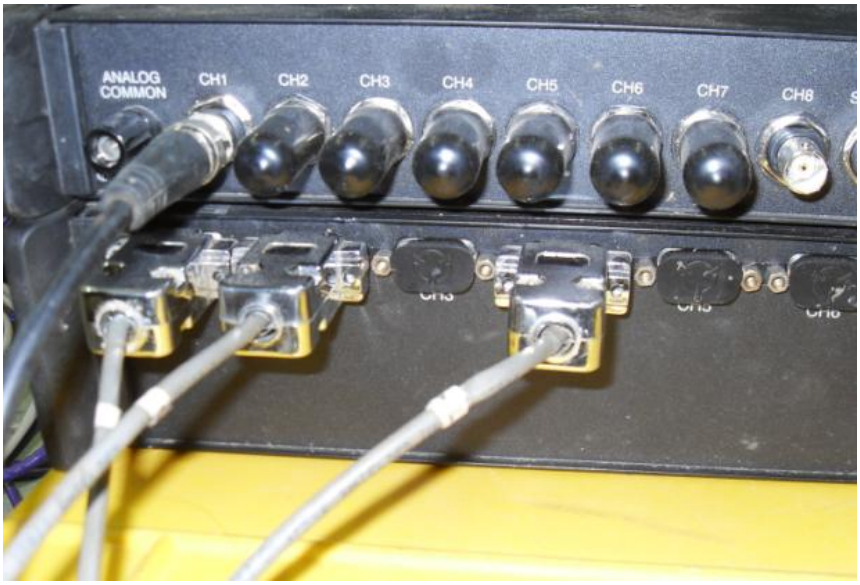


**Figure 19. The back view of the data acquisition system after RAM Test wires are plugged in, general procedure to prepare RAM Test step 1**

2)

a) The load cell wires are numbered 1, 2 and 4 which plug into CH1,CH2, and CH4
b) The accelerometer wire connects into the connection labeled CH1

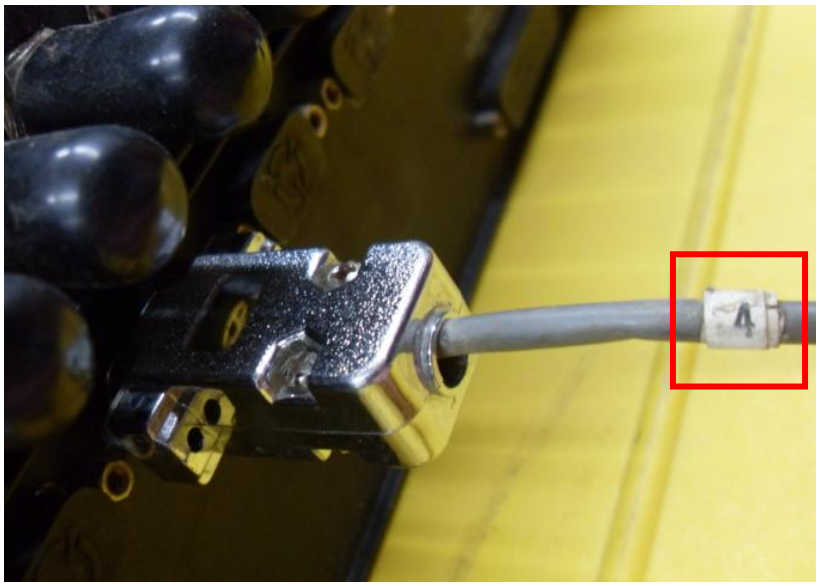


**Figure 20. Each load cell wire is numbered which corresponds to the channel number, general procedure to prepare RAM Test step 2**

3) Plug the ethernet cord into the computer (right side) and the other end into the data acquisition system
4) Plug the two power cords bungeed together into the "power in" slots on the back of the data acquisition system. Note: need a power source to run RAM Test because it does not include a battery system

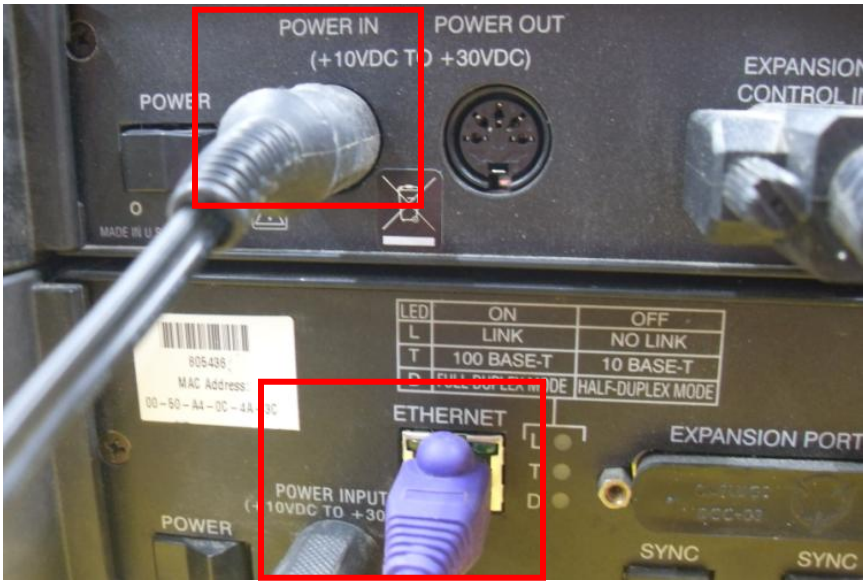


**Figure 21. Front view of the data acquisition system, general procedure to prepare RAM Test steps 3 and 4**

5) Turn on the data acquisition system by the two "on" switches


**Figure 22. Front view of the data acquisition system, general procedure to prepare RAM Test step 5**

6) Plug the laptop into a power source

7) Turn on Laptop
8) Log into the laptop(takes ~5mins)
9) Open the data acquisition software
    a) Click open file
    b) Click up one level
    c) Double click “Devices”
    d) Double click “Worksheets”
    e) Double click “WkSheet-Thumper”
    f) Open desired “set up” file (ex. LaPortCitySep2409A or HamptonTest-4-092009)

Once the RAM Test is prepared, there are two procedures to record a test on the pier. The following steps describe the general procedure:

1) Level the surface of the lift to be tested with hand or shovel
2) Optional: place an additional plate on the pier
    a) To test with the 9 in. steel plate, place the 9 in. steel plate on the pier and then place the RAM Test device on top of the steel plate (nothing holds the steel plate to the RAM Test device)
    b) To test with the 18 in. steel plate, place the 18 in. steel plate on the pier and place the RAM Test device on the within screws on the 18 in. steel plate
    c) To test with the 24 in. steel plate, attach the 24 in. steel plate to the 18 in. steel plate by screwing down the washers on the 18 in. steel plate and place the RAM Test device the same way when using the 18 in. steel plate alone

**Figure 23. The RAM Test in the field with the 9 in. steel plate in the upper right corner, and the 18 in. and 24 in. plates attached to the device**

3) Place the RAM Test device on an pre compacted and/or post compacted lift
   a) If a pre compacted lift is tested, the post compacted lift is also tested
   b) Or only the post compacted lift is tested
4) Ensure the RAM Test device is level
5) Instruct the tamper operator to move the tamper head above, but not touching the RAM Test device
6) Click green play button to start recording

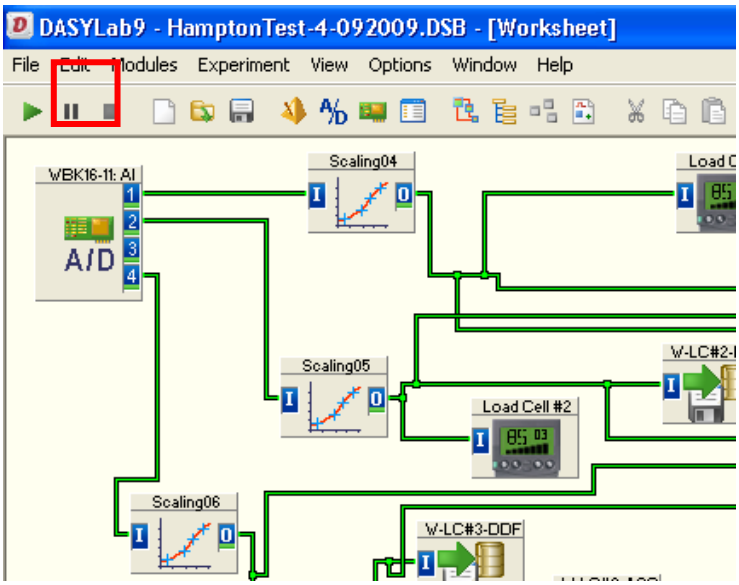


**Figure 24. View of the data acquisition software and the green play button**

   a) A graph of the real-time load and acceleration values is plotted
   b) Load cell 1, 2, and 3, total load, and acceleration values are shown in display box

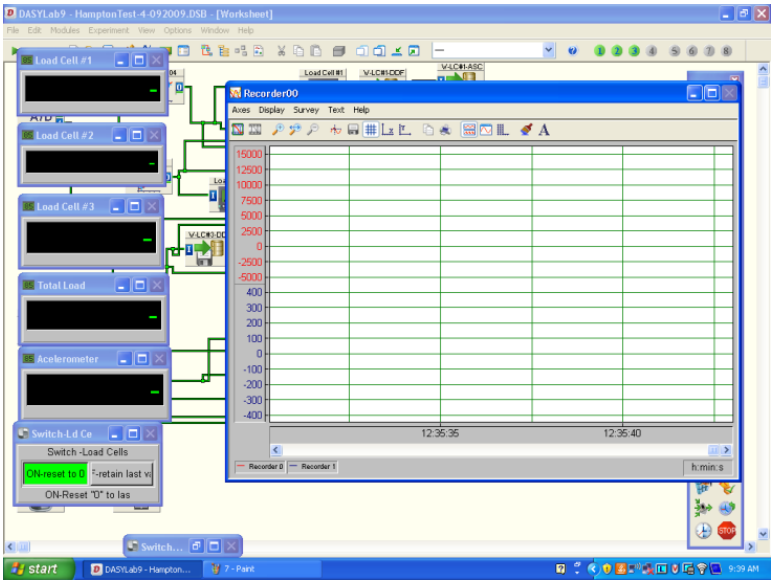


**Figure 25. The plot and display boxes where real-time data is viewed in the data acquisition software**

7) Instruct the tamper operator to move the tamper head while someone guides the tamper shaft by hand to place it evenly on the RAM Test device
8) Instruct the tamper operator to
   a) Apply the crowd load
   b) Apply ramming energy for 3 to 20 seconds
   c) Stop ramming energy
   d) Release applied load
   e) Move tamper shaft off of the RAM Test device
9) Click the red circle button to stop recording

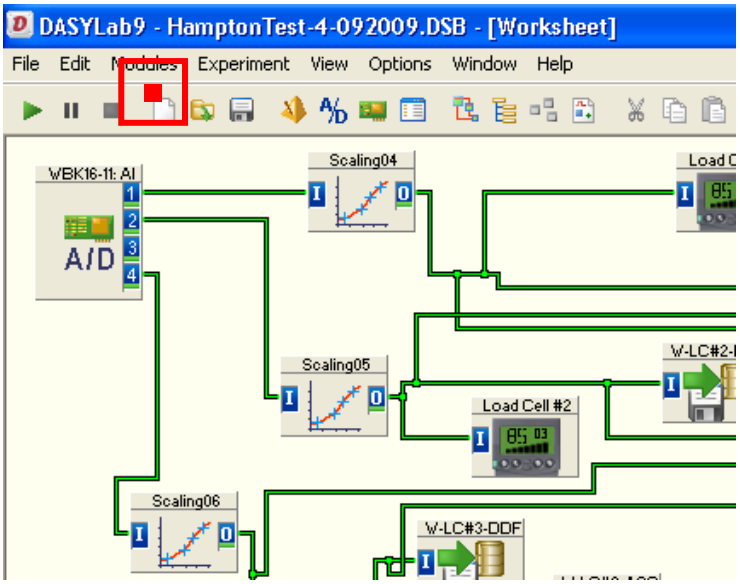


**Figure 26. View of the data acquisition software and the red stop button**

10) Click green play button to start a new test when desired.

The next procedure describes the process of recording a test on the pier with the bottom stabilization test (the test is described in more detail in the next section):

1) Follow steps 1–6 of the general procedure
2) Instruct the tamper operator to apply the crowd load
3) Mark the tamper shaft for the initial deformation

**Figure 27. Bottom stabilization test procedure step 3**

4) Instruct the tamper operator to apply ramming energy for 5 seconds
5) Instruct the tamper operator to stop the applied ramming energy
6) Mark the tamper shaft for segment 1 deformation
7) Instruct the tamper operator to apply ramming energy again for 5 seconds
8) Repeat steps 4–6 three to five times until there is no more visual deformation
9) Click the red circle button to stop recording
10) Click green play button to start a new test when desired

Multiple lifts of three to four piers are tested at a field study. All the RAM Test data is saved using the data acquisition system at a selected sampling rate and then post processed at the office. Field studies typically involve two to seven hours of testing.

**RAM Test displacement verification**

The purpose of verifying RAM Test displacement values recorded in the data acquisition software is to confirm that the values recorded are accurate. Verification has been completed three ways by means of; a falling weight deflectometer (FWD), a camera, and a bottom stabilization test (BST).

*FWD*

The FWD drops different loads at different heights which produces a stress on the load plate. In addition to the eight deflectometers, a modulus value is recorded with time. At the field site, the following procedure was used:

1) Tested the pier with the RAM Test as explained in the perform in situ RAM tests section
2) Tested the pier with the FWD
    a) Leveled a surface on the completed pier
    b) Drove the FWD over the pier and centered the load plate with the pier
    c) Recorded tests with five different load drops, approximately 9,000 lb, 14,000 lb, 19,000 lb, 28, 000 lb, and 31,000 lb

**Figure 28. FWD and RAM Test verification step 2**

3) Tested the pier with the FWD placed on the RAM Test
    a) Dug and leveled a surface several inches from ground level to allow space for both the RAM Test and the FWD
    b) When necessary, built a ramp using wood to bring FWD further from ground surface (can include picture) to allow more space for the deflectometers

**Figure 29. FWD and RAM Test verification step 3-b**

c) Placed the RAM Test device on the pier (to test with the 18 in. and 24 in. steel plates, followed steps 2-b and 2-c in the procedure to test a pier in the Perform in situ Ram tests section)

d) Drove the FWD over the pier and centered the load plate on the RAM Test device

**Figure 30. FWD and RAM Test verification step 3-d**

e) Recorded tests with five different load drops, approximately 9,000 lb, 14,000 lb, 19,000 lb, 28,000 lb, and 31,000 lb

A time-history of load (lb) and deflection (mils) from the FWD and a time-history of load (lb) and acceleration (g) from the RAM were successfully recorded; however, the procedure was time-consuming and difficult to repeat. The FWD verification was not used again.

*Camera*

The second method to verify RAM Test data was through a ruler and a high resolution camera. The camera was set in line with the ruler attached to the tamper shaft. Line reel was pulled in tension as a reference point. The camera was recorded during tamper compaction. Then, the camera was played back to obtain deformation values. However, when the camera was played back, values could not be read from the ruler and this verification was not used again.

**Figure 31. The camera verification set up**

*BST*

The third method involves a version of the bottom stabilization test (BST). A plastic rod is used to mark the tamper shaft, and a 2 in. by 4 in. piece of wood is used as the pivot point. A mark is made on the tamper shaft with the edge of the plastic rod before the test begins, and then tamper compaction is stopped and marked between 3 to 5 times throughout one test.

This allows for deformation readings to be recorded throughout one test and compared to the RAM Test data processed at the office to confirm the accuracy of the values.

## Data analysis

To evaluate the data, load and acceleration parameters are calculated from the time-history data.

### Calculate the load parameters

Two load analyses are used in evaluating the data. Load analysis A focuses on the whole time-history of compaction. A representative portion of each test is chosen in order to keep calculations consistent between tests. The representative portion starts when the load amplitude becomes steady as compared to the entire time-history (1 to 10 impacts from the start of compaction), and ends 1 to 2 impacts before the compaction stops. Figure 32 demonstrates the representative portion from the first vertical line on the left to the last vertical line on the right. From the representative portion, an average dynamic load, a load range and a ramming frequency are calculated, and the duration and the crowd load are determined. The average dynamic load is calculated by taking the average load of the representative portion and the average load range is calculated from five minimum and five maximum load values. The calculations result in an average load plus a maximum load and minus a minimum load (i.e., 12458 lb +1258/–967 lb). The ramming frequency is calculated by dividing the number of impacts in the representative portion by the time length of the portion. Last, the crowd load is observed right before compaction starts.

Load analysis B focuses on how the average dynamic load, and the ramming frequency change value within the representative portion of load analysis A. The average dynamic load, and the ramming frequency are calculated 5 times to obtain 5 values, while each value is based on five sequential impacts, as shown in Figure 32.

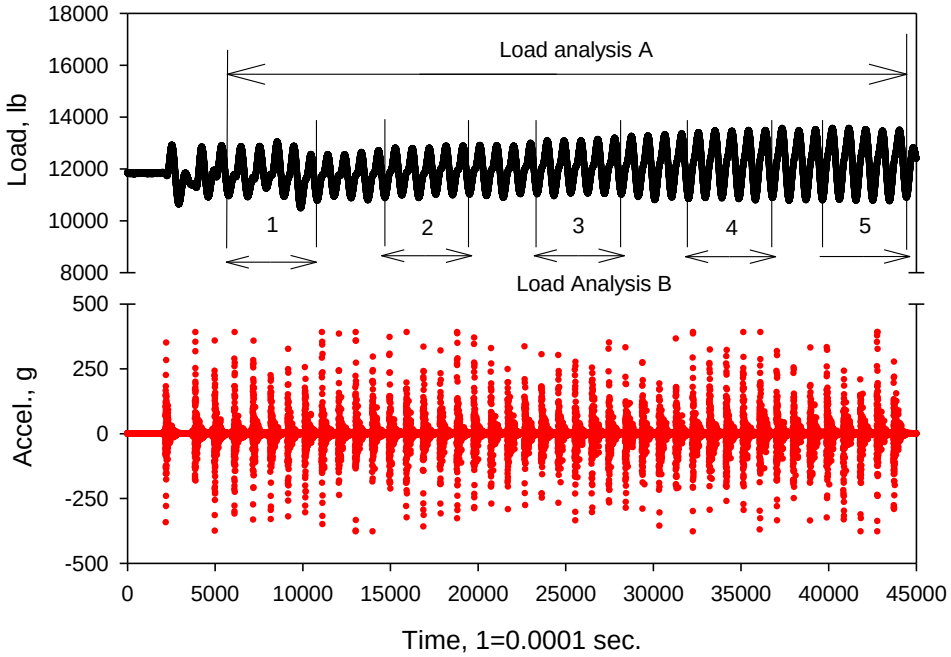


**Figure 32. Comparison of load analyses A and B, where analysis A includes the majority of the compaction impacts, while analysis B includes 5 sections of 5 compaction impacts.**

To decide how each section is chosen, Table 3 approximates where each section originates its value within the time-history.

**Table 3. A summary of where each section's value originates within the time-history**

| Section | Distribution of analysis A |
|---|---|
| 1 | First 5 impact |
| 2 | 2/5 of the way |
| 3 | Middle 5 impacts |
| 4 | 4/5 of the way |
| 5 | Last 5 impacts |

**Calculate the acceleration parameters**

The acceleration parameter determined is the maximum absolute acceleration. It is determined five times, based on the same five sections that the average dynamic load and ramming frequency are calculated in the second load analysis. Each determined value is based on five sequential ramming impacts. This characteristic is determined to evaluate if and how the acceleration changes as a pier becomes stiffer.

## Stiffness parameters

To determine the stiffness parameters of a pier, the acceleration time-history produced from the accelerometer is integrated twice to determine deformation. The code developed in the acceleration analysis software to process the acceleration time-history accounts for background noise and filters the acceleration and the velocity to obtain the actual deformation of the pier. The result of the process is a deformation time-history.

### Determine the permanent deformation values

The first step to determine stiffness is to determine the permanent deformation time-history. Once processed through the acceleration analysis software, the permanent deformation is compared to verification data.

Acceleration time-history is processed through the acceleration analysis software by acceleration analysis A, B, C, and D. Acceleration analysis A is processing the data from when the acceleration of the first compaction impact starts to when the acceleration of the last compaction impact stops. When one test consists of several segments, each segment is processed individually. Once the single test or all segments have been processed, the deformations are summed to obtain total deformation for analysis A.

Acceleration analysis B is processing the data from when the acceleration of the last compaction impact starts to when the acceleration of the last compaction impact stops. If a test consists of several segments, the last compaction impact is from the last segment.

Acceleration analysis C is processing the data from when the acceleration of the sixth compaction impact (impact 6) to the acceleration of the tenth compaction impact (impact 10). The first 5 compaction impacts are assumed as seating impacts. The compaction impacts 6–10 are processed individually, and the average of the deformations is taken as analysis C deformation. Analysis started with Oskaloosa test 2 and processed impacts 6–10 for each segment, then decided to go with the last segment for future data processing. The last segments were consistently negative deformation, while the first several segments were consistently positive deformation.

Acceleration analysis D is processing the data from the acceleration of the fifth to last compaction impact (impact 5) to the acceleration of the last compaction impact (impact 1).

The compaction impacts are processed individually, and the average of the deformations is taken as analysis D deformation. Figure 33 shows the data included in each analyses.

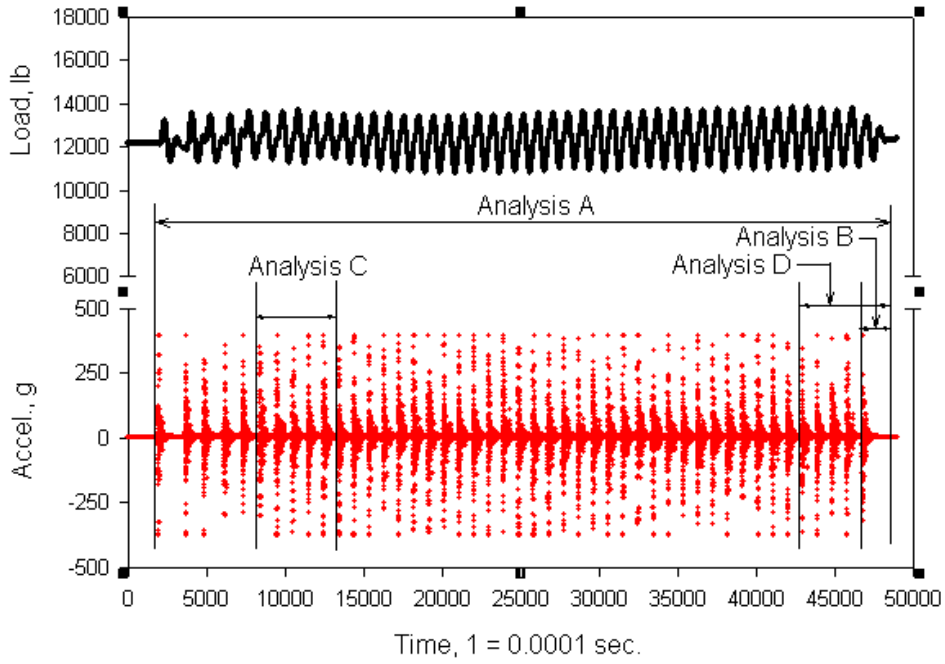


**Figure 33. Analyses A–D for processing the acceleration in the acceleration analysis software**

The acceleration analysis software output for all methods is a time-history of permanent deformation. Examples of the outputs are shown in Figure 34 through Figure 37 for Oskaloosa test 2. From the time-history, the maximum permanent deformation can be determined. The verification values are then compared to the RAM Test deformation values from analysis A.

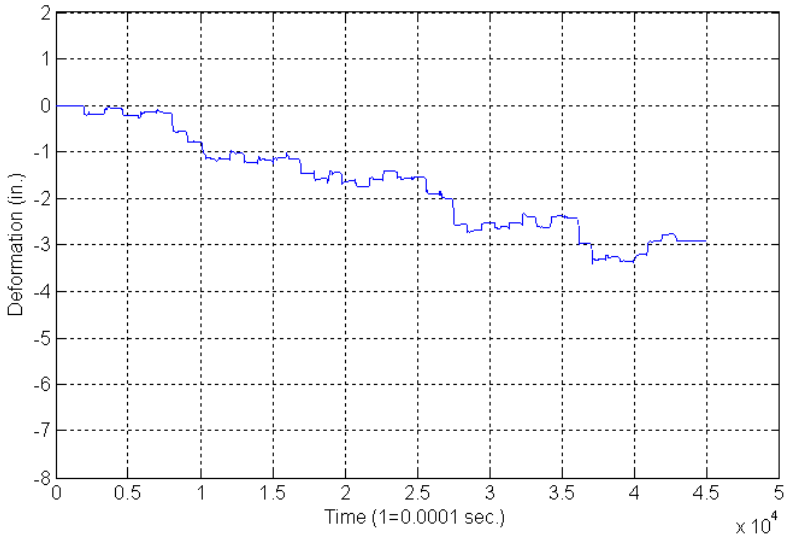


**Figure 34. The acceleration analysis software deformation (m) vs. time (sec.) example of analysis A for Oskaloosa test 2 segment 3**

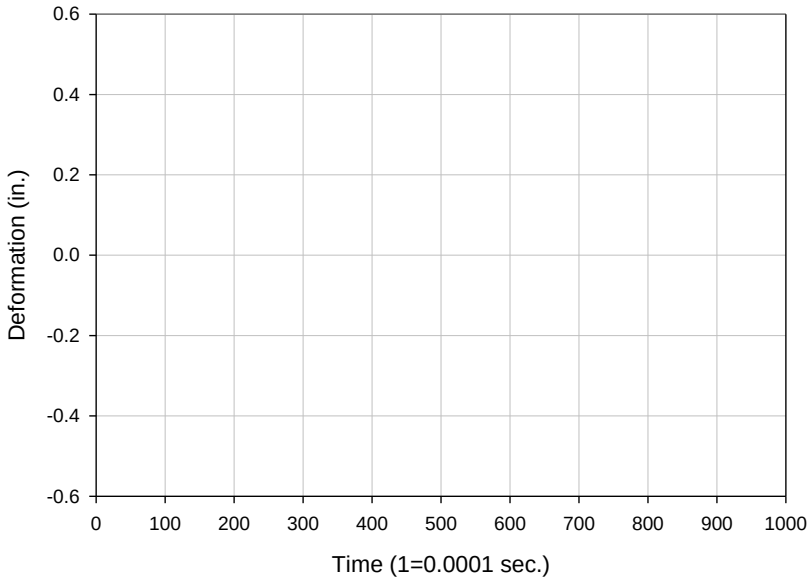


**Figure 35. The acceleration analysis software deformation (m) vs. time (sec.) example of analysis B of Oskaloosa test 2 segment 3**

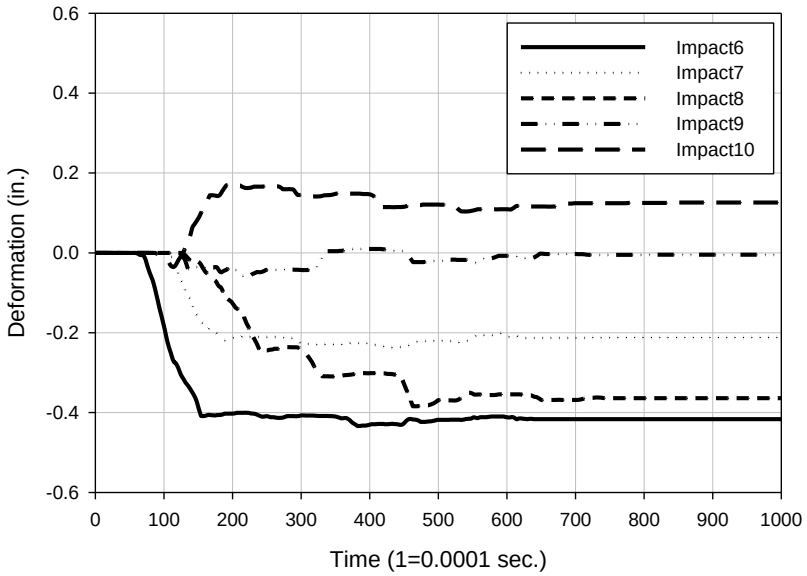


**Figure 36. The acceleration analysis software deformation (m) vs. time (sec.) example of analysis C for Oskaloosa test 2 segment 3**

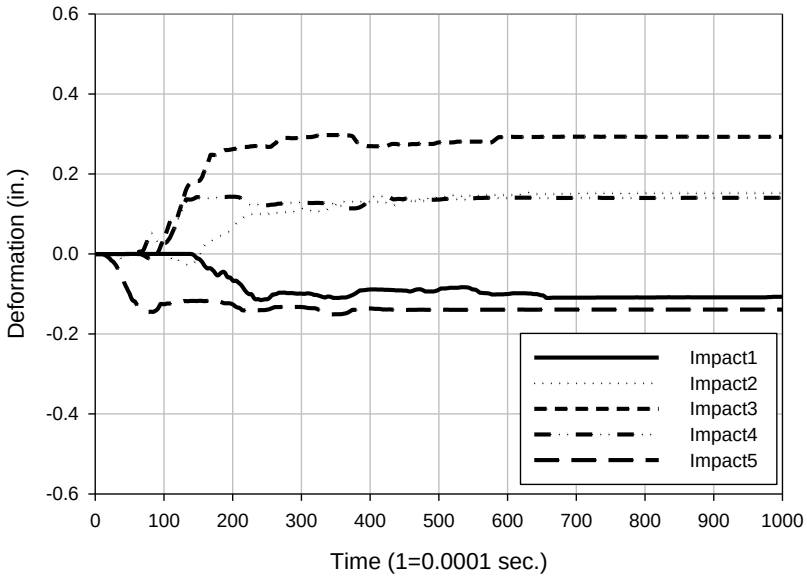


**Figure 37. The acceleration analysis software deformation (m) vs. time (sec.) example of analysis D for Oskaloosa test 2 segment 3**

**Calculate the stiffness values**

The stiffness characteristics are based on the calculated permanent deformation from the acceleration analysis software and the BST, and the average dynamic load.

*The acceleration analysis software*

The deformation values determined from the acceleration analysis software were plotted against stress. The stress was calculated from the RAM Test average dynamic load and the RAM Test plate size. A stiffness value is calculated for each method of deformation.

*BST*

The deformation values determined from the BST were plotted against stress. The stress was calculated from the RAM Test average dynamic load and the RAM Test plate size.

**Compare stiffness values**

The stiffness values determined from the RAM Test are compared to the BST values, and modulus load test values. When possible, the same portion of time was compared. However, it was not always feasible to compare the same portion of time, for example, analysis A of analyzing deformation involves all the compaction impacts and the number can vary. From the comparison, appropriate action can be taken to adjust the RAM Test analysis.

## Laboratory analysis

Pier aggregate and matrix material collected at La Port City, Fairfield, Council Bluffs, and Oskaloosa were analyzed in the laboratory by following the ASTM D 422-63 Standard Test Method for Particle-Size Analysis of Soils. The results of the analysis are presented in chapter 4.

# CHAPTER 4. MATERIALS

This chapter provides laboratory index properties for the aggregate used to install the pier elements. Aggregate collected at La Port City, Fairfield, Council Bluffs, and Oskaloosa was tested. Material was placed into buckets at the site and brought to the laboratory at Iowa State University for investigation using ASTM D 422-63 Standard Test Method for Particle-Size Analysis of Soils.

## Material La Port City

Three materials were collected in La Port City, road gravel, sand, and clean aggregate. A particle size analysis was completed on each material.

### Laboratory test results

This section will present the laboratory results and characterizations for the three materials used to install piers 1 through 3.

*Pier 1 aggregate*

The material used to install pier 1 is characterized as a coarse grained sand, but there is no $D_{10}$ to fully classify the material. Table 4 summarizes the particle size, and the grain size distribution is shown in Figure 38.

**Table 4. Particle size summary for La Port City pier 1 aggregate**

| Particle Size Summary | |
|---|---|
| Gravel | 37.8 % |
| Sand | 48.3 % |
| Silt and Clay | 13.9 % |
| $D_{10}$ | n/a |
| $D_{30}$ | 1.3 mm |
| $D_{60}$ | 4.4 mm |
| $C_u$ | n/a |
| $C_c$ | n/a |

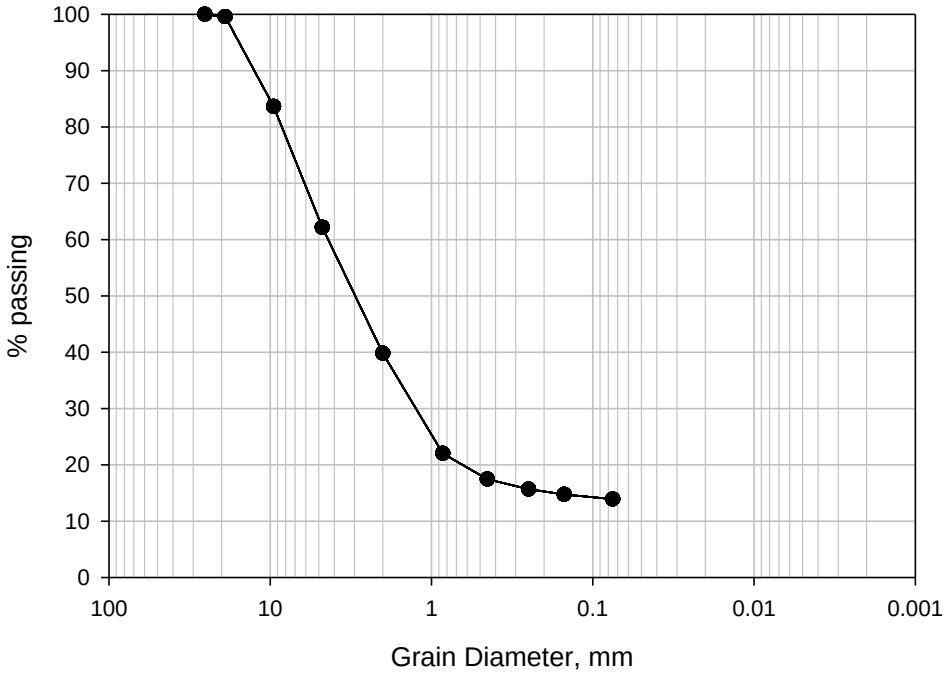


**Figure 38. Grain size distribution for La Port City pier 1 aggregate**

*Pier 2 aggregate*

The material used to install pier 2 is characterized as a poorly graded sand, SP. Table 5 summarizes the particle size, and the grain size distribution is shown Figure 39.

**Table 5. Particle size summary for La Port City pier 2 aggregate**

| **Particle Size Classes** | |
|---|---|
| Gravel | 3.4 % |
| Sand | 94.5 % |
| Silt and Clay | 2.1% |
| $D_{10}$ | 0.26 mm |
| $D_{30}$ | 0.46 mm |
| $D_{60}$ | 0.75 mm |
| $C_u$ | 2.9 |
| $C_c$ | 1.8 |

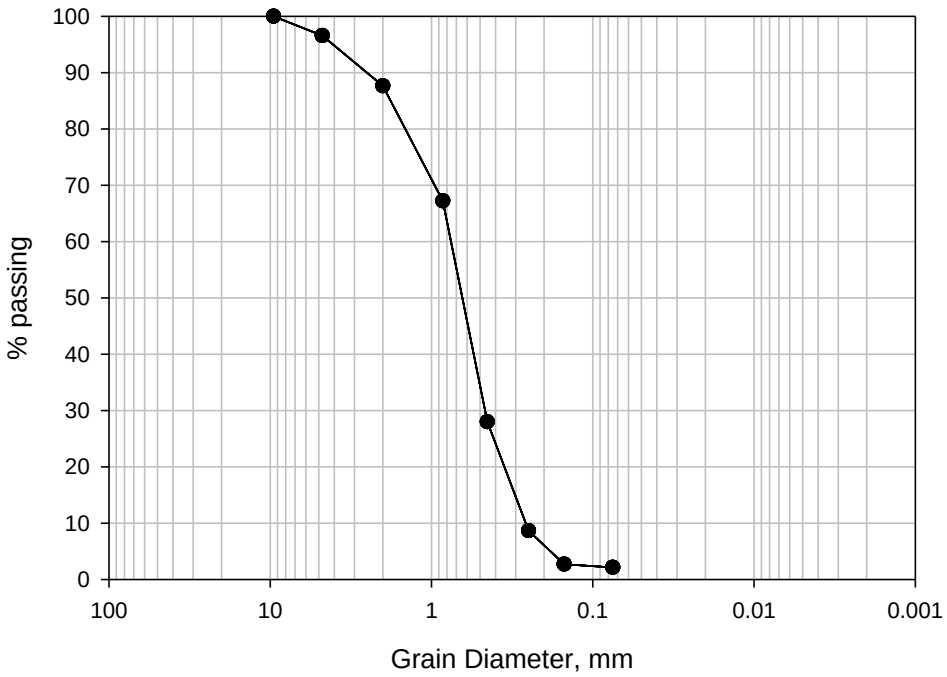


**Figure 39. Grain size distribution for La Port City pier 2 aggregate**

*Pier 3 aggregate*

The material used to install pier 3 is characterized as a poorly graded gravel, GP. Table 6 summarizes the particle size, and the grain size distribution is shown in Figure 40.

**Table 6. Particle size summary for La Port City pier 3 aggregate**

| **Particle Size Summary** | |
|---|---|
| Gravel | 95.4 % |
| Sand | 4.6 % |
| Silt and Clay | 0 % |
| $D_{10}$ | 21.5 mm |
| $D_{30}$ | 27.0 mm |
| $D_{60}$ | 31.6 mm |
| $C_u$ | 1.5 |
| $C_c$ | 1.1 |

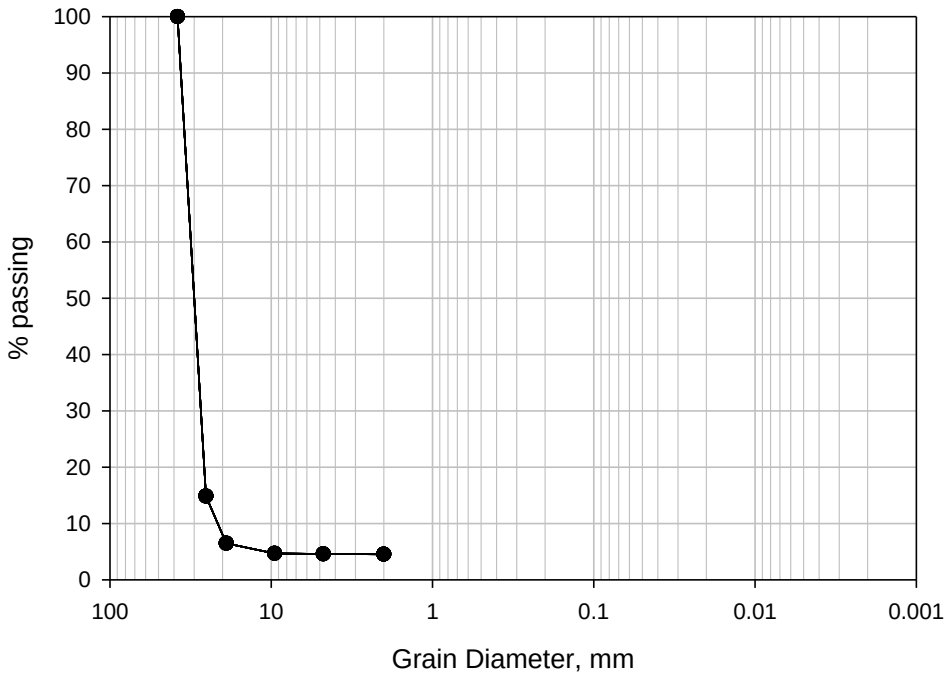


**Figure 40. Grain size distribution for La Port City pier 3 aggregate**

### Material Fairfield

Material from Fairfield, IA was collected into buckets and brought to the laboratory at Iowa State University for investigation. Only one type of aggregate was used at this site, and a particle size analysis was completed.

#### Laboratory test results

The material used to install all the piers is characterized as a gravel material, but there is no $D_{10}$ or $D_{30}$ to fully classify the material. Table 7 summarizes the particle size class, and the grain size distribution is shown in Figure 41.

**Table 7. Particle size summary for Fairfield pier aggregate**

| Particle Size Classes | |
|---|---|
| Gravel | 47.8 |
| Sand | 20.3 |
| Silt and Clay | 31.9 |
| $D_{10}$ | n/a |
| $D_{30}$ | n/a |

| Particle Size Classes | |
|---|---|
| $D_{60}$ | 6.2 mm |
| $C_u$ | n/a |
| $C_c$ | n/a |

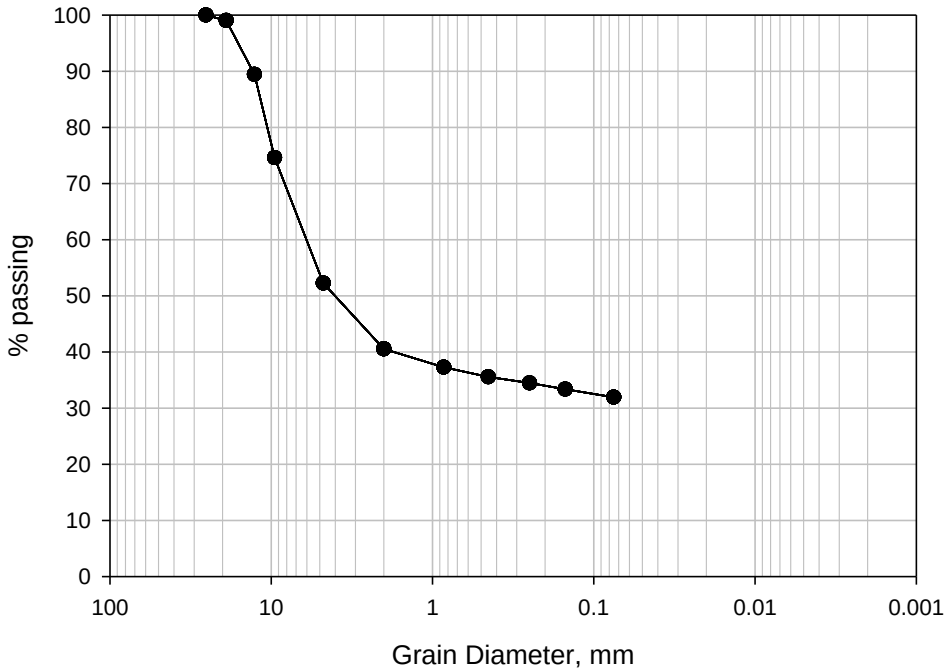


**Figure 41. Grain size distribution for Fairfield pier aggregate**

## Material Council Bluffs

Material from Council Bluffs, IA was collected into buckets and brought to the laboratory at Iowa State University for investigation. Only one type of aggregate was used at this site, and a particle size analysis was completed.

### Laboratory test results

The material used to install all the piers is characterized as a poorly graded gravel, GP. Table 8 summarizes the particle size class, and the grain size distribution is shown in Figure 42.

**Table 8. Particle size summary for Council Bluffs pier aggregate**

| Particle Size Classes | |
|---|---|
| Gravel | 100 % |
| Sand | 0 % |
| Silt and Clay | 0 % |
| $D_{10}$ | 32.4 mm |
| $D_{30}$ | 41.6 mm |
| $D_{60}$ | 48.6 mm |
| $C_u$ | 1.5 |
| $C_c$ | 1.1 |

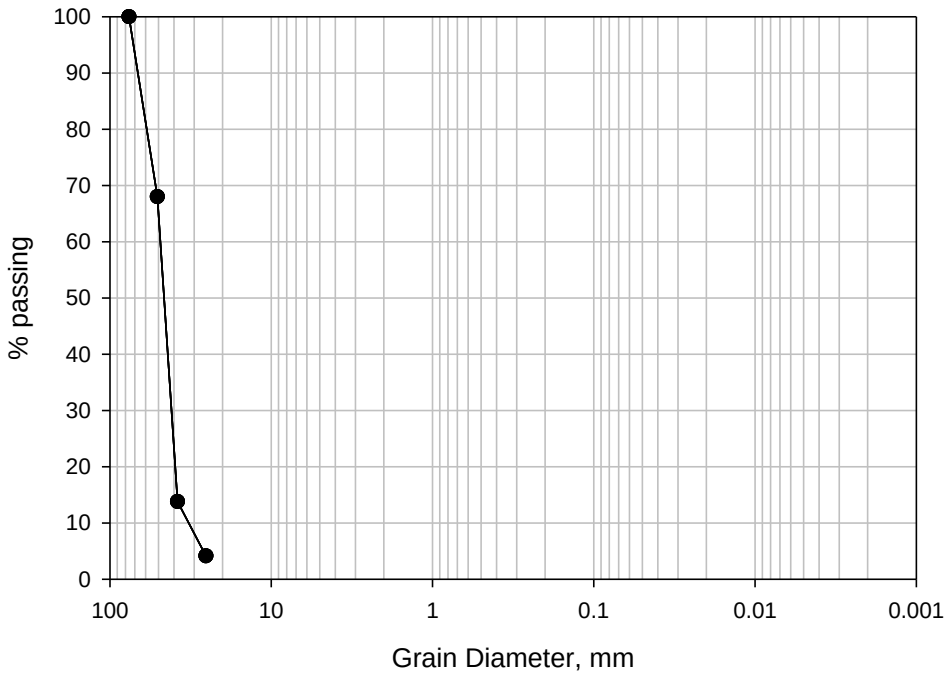


**Figure 42. Grain size distribution for Council Bluffs pier aggregate**

### Material Oskaloosa

Material from Oskaloosa, IA was collected into buckets and brought to the laboratory at Iowa State University for investigation. Only one type of aggregate was used at this site, and a particle size analysis was completed.

**Laboratory test results**

The material used to install all the piers is characterized as a well-graded gravel, GW. Table 9 summarizes the particle size class, and the grain size distribution is shown in Figure 43.

**Table 9. Particle size summary for Oskaloosa pier aggregate**

| Particle Size Summary | |
|---|---|
| Gravel | 83.6 % |
| Sand | 9.2 % |
| Silt and Clay | 7.2 % |
| $D_{10}$ | 1.0 mm |
| $D_{30}$ | 8.6 mm |
| $D_{60}$ | 60 mm |
| $C_u$ | 60 |
| $C_c$ | 1.2 |

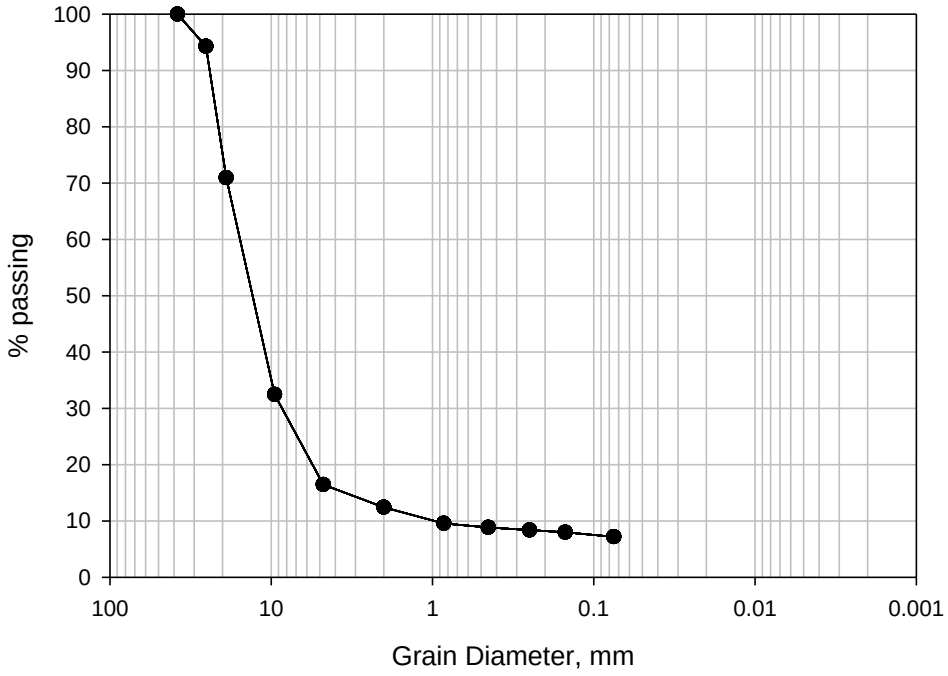


**Figure 43. Grain size distribution for Oskaloosa pier aggregate**

# CHAPTER 5. RESULTS AND DISCUSSION

This chapter includes the results and discussions from five field studies and is organized by load, acceleration, stiffness, and verification. Verification is mentioned in stiffness but is fully explained in the verification section. The field studies are presented in chronological order within each section. All load and acceleration time-histories, and deformation time-histories are shown in the appendix while representative tests are shown in the main section. Table 10 summarizes the location, date, project, pier type, verification, and conditions of each field study.

**Table 10. Field study location, date, project, pier type, and verification summary**

| Field Study Location | Date | Project | Pier Type | Verification | Conditions |
|---|---|---|---|---|---|
| Hampton, IA | April 9, 2009 | Wind farm | Aggregate piers with two different installation equipement | None | Windy, cloudy, 50°F |
| La Port City, IA | September 24, 2009 | Research area | Aggregate piers | FWD | Rain in morning, sun in afternoon, 60°–70°F |
| Fairfield, IA | July 28, 2010 | Hy-Vee | Aggregate piers | Recorder/ruler | Sunny, 90°F |
| Council Bluffs, IA | August 26, 2010 | Bunge | Aggregate piers with 2 foot lifts | BST | Sunny, 85°F |
| Oskaloosa, IA | October 28, 2010 | Hospital | Aggregate piers with 2 foot lifts | BST | Windy, cloudy, 30 -40°F |

## Load

One of the goals of this research is to obtain a record of compaction that occurs during pier installation by analyzing the load data. These data are used to determine the crowd load before compaction and to calculate the dynamic compaction, and to calculate the compaction frequency. Two analyses are used to calculate the load parameters. Load analysis A focuses on the whole time-history of compaction. A representative portion of each test is chosen in order to keep calculations consistent between tests. The representative portion starts when the

load amplitude becomes steady as compared to the entire time-history (1 to 10 impacts from the start of compaction), and ends 1 to 2 impacts before the compaction stops. Figure 44 demonstrates the representative portion from the first vertical line on the left to the last vertical line on the right. From the representative portion, an average dynamic load, a load range and a ramming frequency are calculated, and the duration and the crowd load are determined. The average dynamic load is calculated by taking the average load of the representative portion and the average load range is calculated from five minimum and five maximum load values. The calculation results in an average load plus a maximum load and minus a minimum load (i.e., 12458 lb +1258/–967 lb). The ramming frequency is calculated by dividing the number of impacts in the representative portion by the time length of the portion. Last, the crowd load is observed right before compaction starts.

Load analysis B focuses on how the average dynamic load, and the ramming frequency change value within the representative portion of load analysis A. The average dynamic load and the ramming frequency are calculated 5 times to obtain 5 values with time. Each of the 5 values corresponds to section 1 through 5, while each section is based on five sequential impacts, as demonstrated in Figure 44.

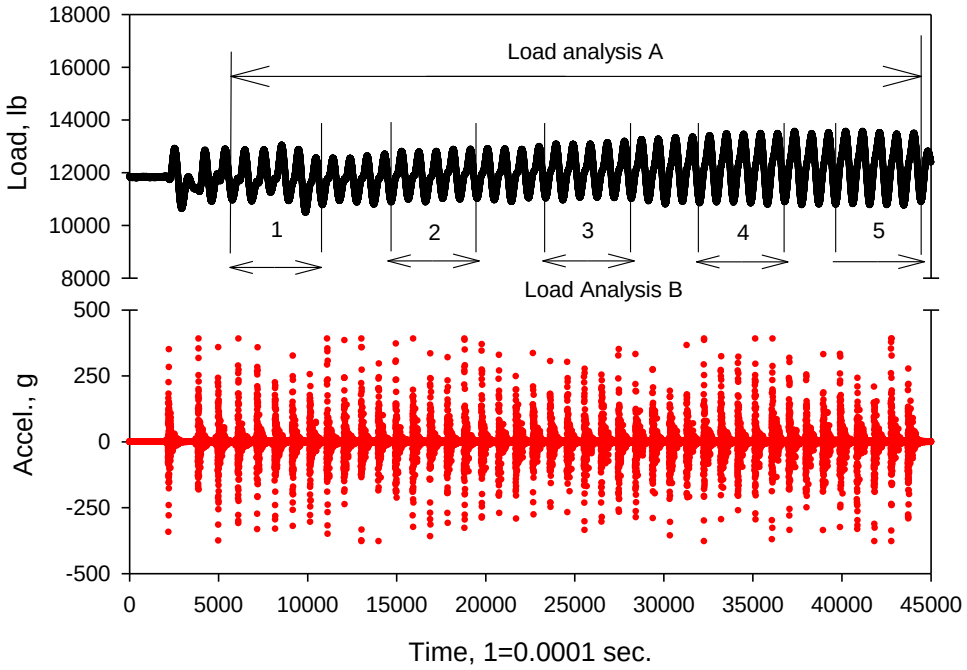


**Figure 44. The representative portions used for load analyses A and B. The 5 sections of**

**5 impacts marked by vertical lines and numbered 1–5 represent the impacts used to calculate each average dynamic load and ramming frequency for load analysis B**

**Hampton load results**

This section will present the load parameter results from the Hampton field study. Two types of piers were studied; cased aggregate elements and pier aggregate elements compacted with a hopper. This is the first site the 18 in. diameter steel plate was used. The pier elements were tested after a new lift was added, but before the piers were compacted by the tamper (pre compaction), and after the new lift was compacted by the tamper (post compaction) on the piers' top lift. To address the question of how the ramming energy affects the surrounding soil, tests were collected on the matrix soil 3 to 4 feet from the pier's center. Table 11. Hampton RAM Test field study summary summarizes the tests, while Figure 45. Hampton field study conditions.

**Table 11. Hampton RAM Test field study summary**

| RAM Test | Pier | Pier Type | Pier Conditions | Pier Lift | Buffer Pad | Plate Size |
|---|---|---|---|---|---|---|
| 1 | N/A | Cased aggregate pier | Matrix | N/A | Yes | 18 in. |
| 2 | 1 | | Pre compaction | Top | | |
| 3 | | | Post compaction | Top | | |
| 4 | 2 | | Pre compaction | Top | | |
| 5 | | | Post compaction | Top | | |
| 6 | 3 | Aggregate pier | Post compaction | Top | | |
| 9 | N/A | | Matrix | N/A | | |
| 10 | N/A | | Matrix | N/A | | |
| 11 | N/A | | Matrix | N/A | | |
| 12 | 4 | | Post compaction | Top | | |
| 13 | N/A | | Matrix | N/A | | |

**Figure 45. Hampton field study conditions**

Load time-histories were successfully collected on all piers. Load analysis A was used on Hampton tests. The cased elements show similar crowd loads, and relatively small dynamic amplitudes as compared to other field studies. The load time-history exhibits double sinusoidal behavior in one impact, as shown in Figure 46. This behavior occurs after the peak load, and appears to occur on the minimum side of the load values. Tests 1 and 2 exhibited a decrease in amplitude with time, while tests 3, 4 and 5 exhibited consistent amplitudes with time. The behavior was observed visual without the help of load analysis B.

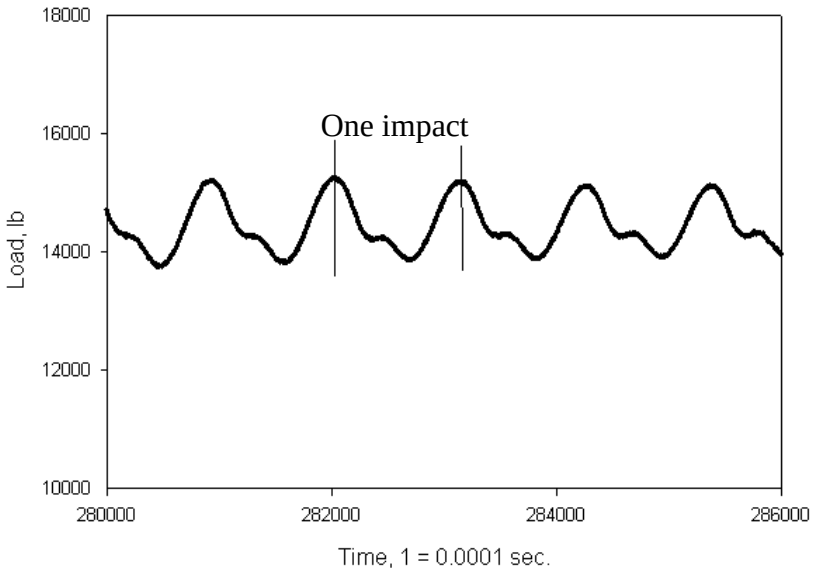

**Figure 46. Example of the double impact behavior of Hampton test 1**

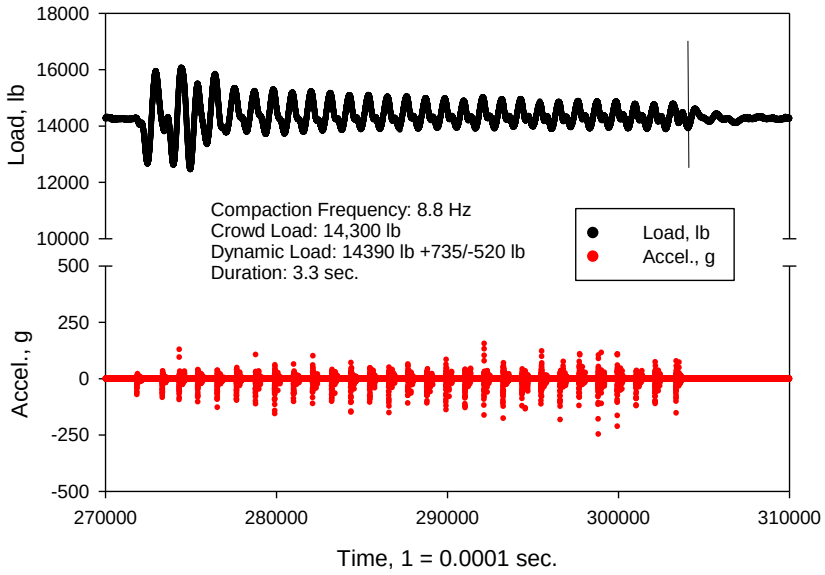


**Figure 47. Hampton test 1 exhibits an amplitude decrease over the duration of the test**

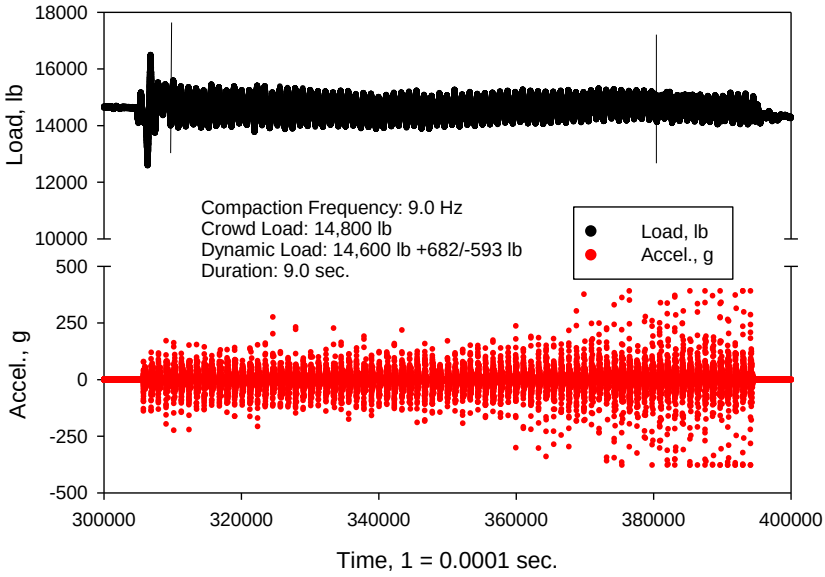


**Figure 48. Hampton test 3 exhibits steady amplitude over the duration of the test**

Loads from an aggregate pier installed with a hopper had not been collected on the RAM Test before Hampton. The RAM Test was able to withstand the loads, which are the highest loads applied to the RAM Test. Load values were seen as high as 56,000 lb. Crowd loads were recorded around 35,000 lb before compaction started and around 39,000 lb after

compaction stopped. The tests that recorded the compaction impacts (tests 6 and 12) exhibit larger amplitudes when the machine starts to compact, then decreases considerably during compaction impacts, then increases when the compaction stops, but then decreases to the end of the time-history while the machine is coming to a full stop, as shown in Figure 49. The tests recorded on the matrix soil while a pier was compacted showed load values between +/– 50 lb, and exhibited behavior that cannot be parameterized like the other data, as shown in Figure 50.

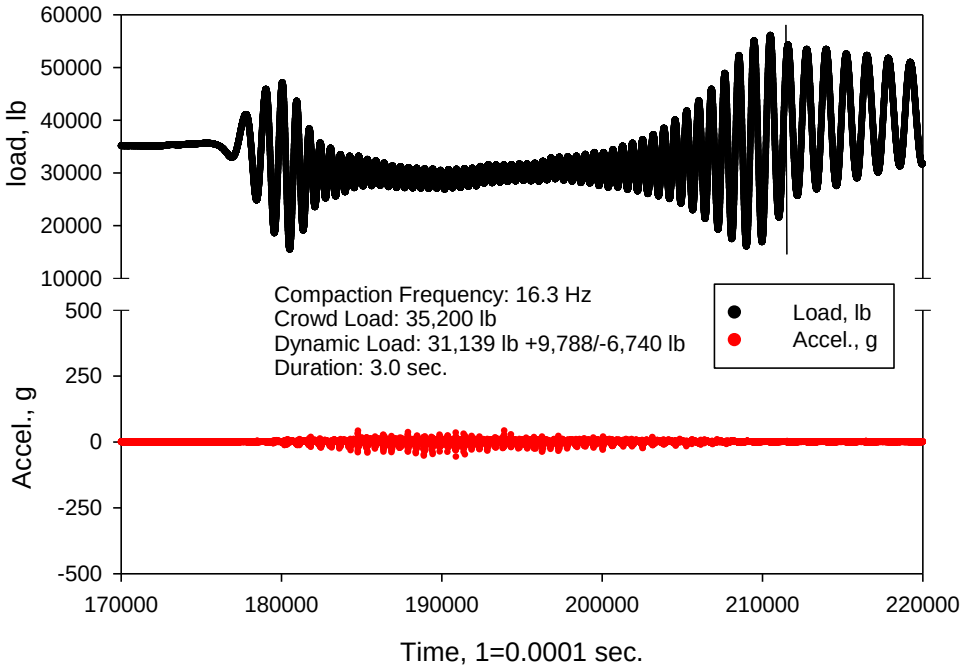


**Figure 49. Hampton test 6**

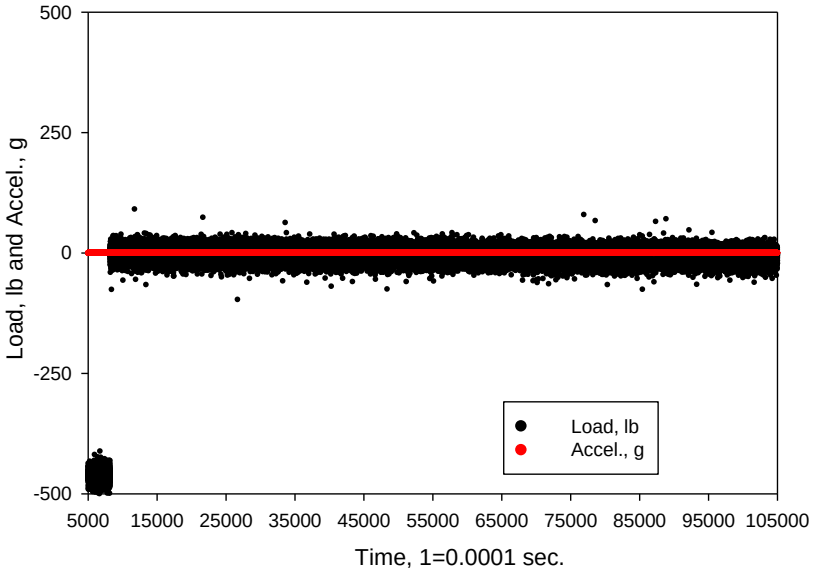


**Figure 50. Hampton test 9, data recorded on the matrix soil**

The load parameter results for ramming frequency, crowd load, dynamic load, and duration are summarized Table 12.

**Table 12. Load analysis A summary for Hampton**

| Test | Frequency (Hz) | Crowd Load (lb) | Dynamic Load (lb) | | | Duration (Sec.) |
|---|---|---|---|---|---|---|
| | | | Average | + | – | |
| 1 | 8.8 | 14,300 | 14,390 | 735 | 520 | 3.3 |
| 2 | 9.2 | 15,000 | 14,513 | 1,015 | 659 | 4.6 |
| 3 | 9.0 | 14,800 | 14,600 | 682 | 593 | 9.0 |
| 4 | 11.3 | 14,500 | 14,637 | 1,366 | 1,484 | 4.1 |
| 5 | 8.9 | 14,200 | 14,708 | 746 | 942 | 8.7 |
| 6 | 16.3 | 35,200 | 31,139 | 9,788 | 6,740 | 3.0 |
| 7–8[1] | – | – | – | – | – | – |
| 9–11[2] | – | – | – | – | – | – |
| 12 | 13.4 | 36,900 | 33,306 | 10,474 | 9,840 | 4.6 |
| 13[3] | – | 33,400 | – | – | – | – |

[1] Tests 7 and 8 were used to test connections between RAM and computer
[2] Tests 9–11 were tests on the matrix soil, and load analysis could not be completed
[3] Test 13 is a crowd load test, and load analysis could not be completed

**La Port City load results**

This section will present the load parameter results from the La Port City field study. Three different materials were used to install the aggregate piers, dirty road gravel (pier 1), sand (pier 2), and clean gravel (pier 3). And a completed pier with a concrete cap (pier 4) was

also tested. This is the only study where multiple materials were used to install the piers. This study included tests with the 24 in. plate, the 18 in. plate, and the 12 in plate. Tests were recorded on 4 to 5 pre compacted and post compacted lifts for the first three piers, and on top of the concrete cap for the pier 4. Table 13 summarizes the field study, while Figure 51 shows the field conditions.

**Table 13. La Port City RAM Test field summary**

| Test | Pier | Pier Type | Pier Condition | Test Layer | Buffer Pad | Plate Size(in.) |
|---|---|---|---|---|---|---|
| 1 | 1 | Dirty road gravel | Pre compaction | 1 | Yes | 12 |
| 2 | | | Post compaction | 1 | | 12 |
| 3 | | | Pre compaction | 2 | | 12 |
| 4 | | | Post compaction | 2 | | 12 |
| 5 | | | Pre compaction | 3 | | 12 |
| 6 | | | Post compaction | 3 | | 12 |
| 7 | | | Pre compaction | 4 | | 12 |
| 8 | | | Post compaction | 4 | | 24 |
| 9 | | | Post compaction | 4 | | 18 |
| 10 | | | Post compaction | 4 | | 12 |
| 11 | 2 | Sand | Pre compaction | 1 | | 12 |
| 12 | | | Post compaction | 1 | | 12 |
| 13 | | | Pre compaction | 2 | | 12 |
| 14 | | | Post compaction | 2 | | 12 |
| 15 | | | Pre compaction | 3 | | 12 |
| 16 | | | Post compaction | 3 | | 12 |
| 17 | | | Pre compaction | 4 | | 12 |
| 18 | | | Post compaction | 4 | | 12 |
| 19 | | | Pre compaction | 5 | | 12 |
| 20 | | | | | | |
| 21 | | | | | | |
| 22 | | | Post compaction | 5 | | 24 |
| 23 | | | Post compaction | 5 | | 18 |
| 24 | | | Post compaction | 5 | | 12 |
| 25 | 3 | Clean aggregate | | | | 12 |
| 26 | | | | | | 12 |
| 27 | | | Pre compaction | 1 | | 12 |
| 28 | | | Post compaction | 1 | | 12 |
| 29 | | | Pre compaction | 2 | | 12 |
| 30 | | | Post compaction | 2 | | 12 |
| 31 | | | Pre compaction | 3 | | 12 |
| 32 | | | Post compaction | 3 | | 12 |
| 33 | | | Pre compaction | 4 | | 12 |

| Test | Pier | Pier Type | Pier Condition | Test Layer | Buffer Pad | Plate Size(in.) |
|---|---|---|---|---|---|---|
| 34 | | | Post compaction | 4 | | 24 |
| 35 | | | Post compaction | 4 | | 18 |
| 36 | | | Post compaction | 4 | | 12 |
| 37 | 4 | Finished pier with concrete cap | Completed | - | No | 18 |
| 38 | | | Completed | - | | 18 |
| 39 | | | Completed | - | | 18 |
| 40 | | | Completed | - | | 18 |
| 41 | | | Completed | - | | 18 |


**Figure 51. La Port City field conditions**

Load time-histories were successfully collected on all piers. Load analysis A was used on the La Port City tests. Pier 1 exhibited consistent crowd loads, and average dynamic loads with relatively high amplitudes. The amplitudes were higher towards the maximum loads than they were towards the minimum loads. Test 3, 5, and 7 exhibited larger amplitudes at the beginning of the test, but decreased with time as shown in Figure 52. These tests were recorded on a pre compacted lift. The tests recorded on a post compacted lift exhibited consistent amplitudes with time, as shown in Figure 53. The frequencies also stayed consistent, and are consistent with aggregate pier elements from other field studies.

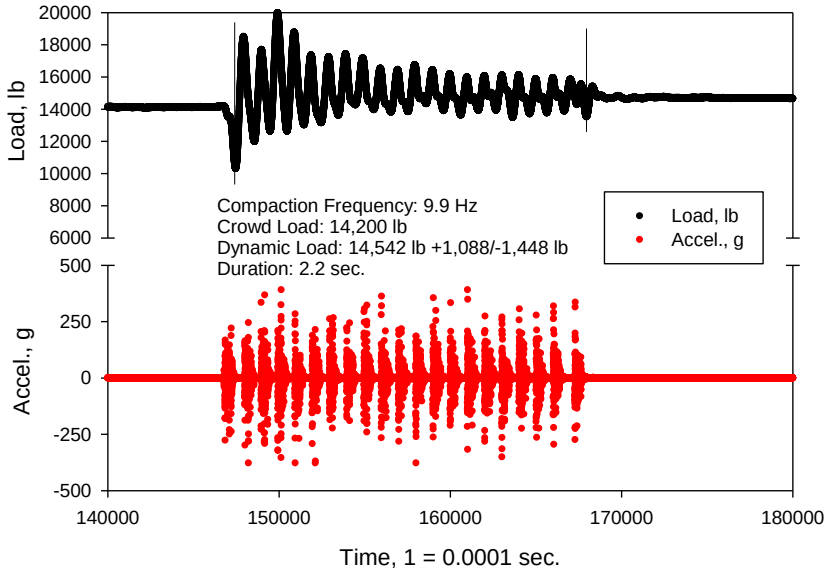


**Figure 52. La Port City test 3**

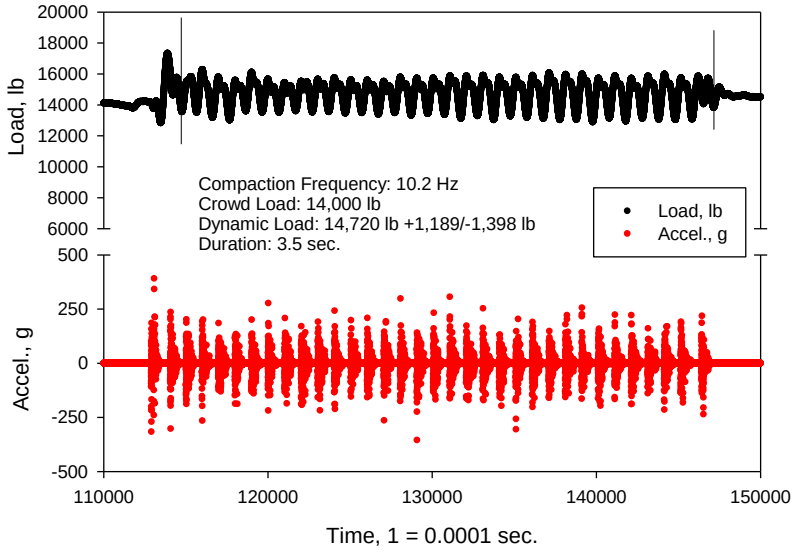


**Figure 53. La Port City test 4**

Pier 2 exhibited varying crowd loads, but relatively consistent average dynamic loads with balanced amplitudes, for example, test 12 shown in Figure 54. However, the amplitudes varied between tests, with some small (less than 1,000 lb) and some large (over 4,000 lb) with no distinguishable difference between pre or post compacted lifts. A frequency range of 1.1 Hz on pier 2 is the highest among the piers at La Port City.

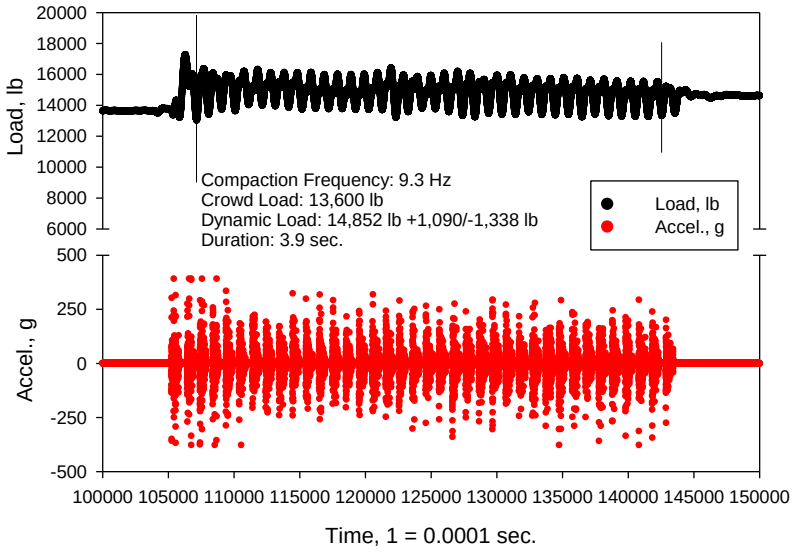


**Figure 54. La Port City test 12**

Pier 3 exhibited consistent crowd loads, and average dynamic loads that had a range of 2,493 lb with balanced amplitudes. The amplitudes are the highest for this field study; for example, test 34 shown in Figure 55 had an amplitude of 3,544 lb. Of all pier 3 tests, the highest frequency of 10.5 Hz was seen from test 33 shown in Figure 56. Test 33 was a pre compacted lift and also the shortest duration of time.

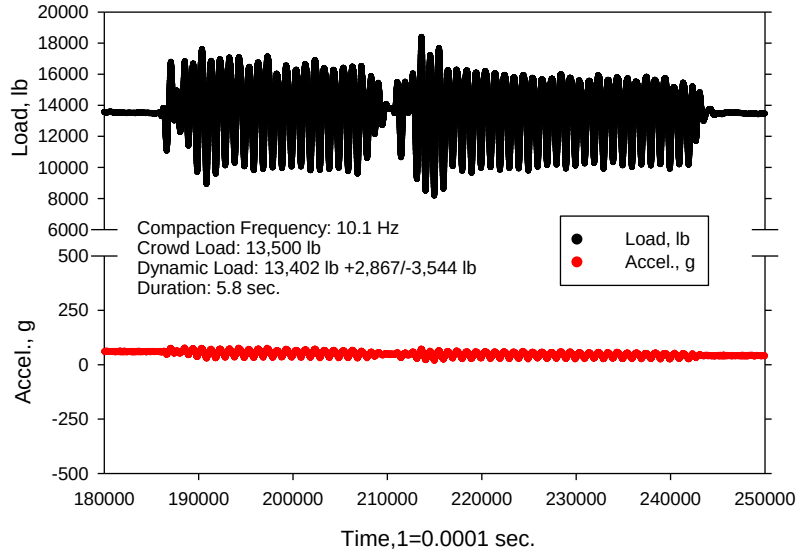


**Figure 55. La Port City test 34**

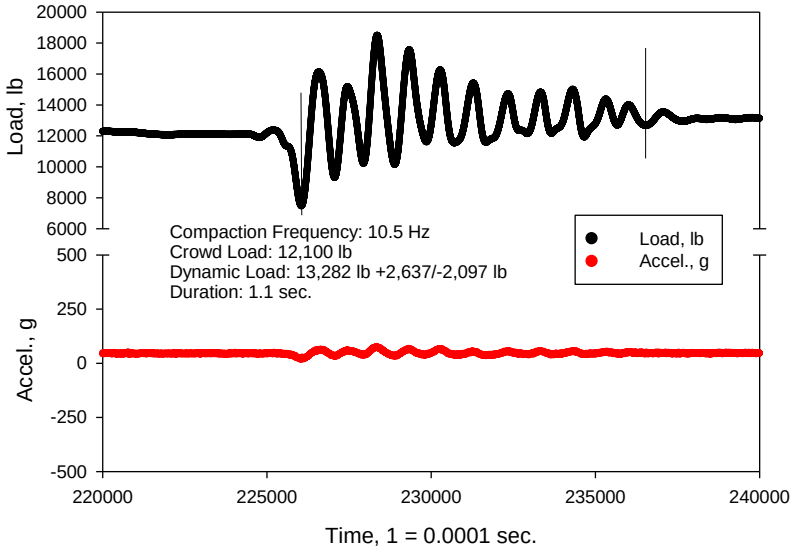


**Figure 56. La Port City test 33**

Pier 4 exhibited consistent crowd loads, and average dynamic loads that had a range of 1,258 lb with unbalanced amplitudes. The amplitudes were higher on the minimum side of loads, while the values were similar to those of pier 3. An example that represents the tests of pier 4 is shown in Figure 57. The crowd loads were consistently higher when compaction stopped, than right before compaction started. The frequencies were consistent, with a range of 0.2 Hz. All of the load parameters results for ramming frequency, crowd load, dynamic load, and duration are summarized in Table 14.

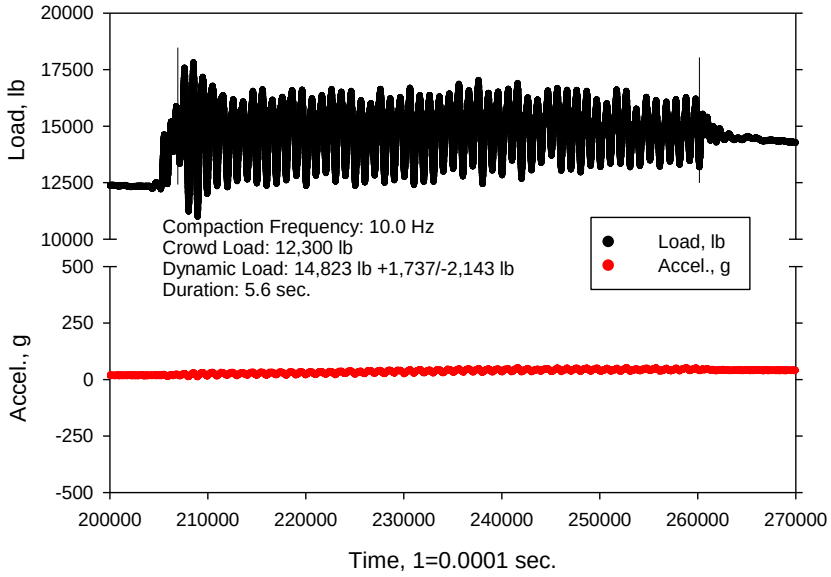


**Figure 57. La Port City test 39**

**Table 14. Load analysis A summary for La Port City**

| Test | Frequency (Hz) | Crowd Load (lb) | Dynamic Load (lb) | | | Duration (sec.) |
|---|---|---|---|---|---|---|
| | | | Average | + | – | |
| 1 | 10.2 | 12,500 | 13,911 | 3,040 | 3,802 | 1.5 |
| 2 | 9.9 | 14,000 | 15,583 | 1,756 | 2,726 | 3.1 |
| 3 | 9.9 | 14,200 | 14,542 | 1,088 | 1,448 | 2.2 |
| 4 | 10.2 | 14,000 | 14,720 | 1,189 | 1,398 | 3.5 |
| 5 | 10.0 | 14,400 | 14,991 | 1,482 | 1,101 | 2.3 |
| 6 | 9.9 | 14,300 | 14,771 | 702 | 1,095 | 4.4 |
| 7 | 10.1 | 13,800 | 14,356 | 1,943 | 1,870 | 1.8 |
| 8 | 10.0 | 14,600 | 15,326 | 259 | 873 | 6.2 |
| 9 | 10.0 | 14,800 | 15,200 | 989 | 869 | 6.7 |
| 10 | 9.9 | 14,000 | 14,542 | 983 | 1,518 | 5.7 |
| 11 | 9.9 | 12,800 | 13,545 | 931 | 959 | 3.0 |
| 12 | 9.3 | 13,600 | 14,852 | 1,090 | 1,338 | 3.9 |
| 13 | 9.8 | 10,900 | 11,795 | 1,263 | 1,198 | 2.5 |
| 14 | 9.9 | 12,800 | 13,301 | 853 | 737 | 4.0 |
| 15 | 10.4 | 12,100 | 13,349 | 2,589 | 2,369 | 1.2 |
| 16 | 9.9 | 14,000 | 14,879 | 1,173 | 1,184 | 3.8 |
| 17 | 10.3 | 12,000 | 13,621 | 2,342 | 2,213 | 1.1 |
| 18 | 9.9 | 14,000 | 14,916 | 936 | 1,262 | 2.5 |
| 19 | 10.3 | 11,200 | 12,908 | 2,363 | 1,850 | 1.0 |
| 20–21[1] | – | – | – | – | – | – |
| 22 | 9.9 | 13,700 | 14,833 | 1,292 | 861 | 8.6 |
| 23 | 9.9 | 14,400 | 14,367 | 1,231 | 1,067 | 4.4 |

| Test | Frequency (Hz) | Crowd Load (lb) | Dynamic Load (lb) | | | Duration (sec.) |
|---|---|---|---|---|---|---|
| | | | Average | + | – | |
| 24 | 9.8 | 13,100 | 14,360 | 918 | 876 | 3.2 |
| 25–26 | – | – | – | – | – | – |
| 27 | 9.9 | 13,200 | 14,117 | 1,751 | 1,503 | 3.4 |
| 28 | 10.0 | 13,600 | 15,271 | 1,173 | 1,200 | 3.5 |
| 29 | 10.0 | 13,800 | 15,775 | 1,950 | 2,127 | 1.6 |
| 30 | 10.0 | 12,800 | 15,304 | 1,387 | 890 | 4.2 |
| 31 | 9.9 | 13,200 | 14,343 | 1,160 | 1,760 | 1.7 |
| 32 | 9.9 | 15,000 | 15,131 | 1,132 | 835 | 4.4 |
| 33 | 10.5 | 12,100 | 13,282 | 2,637 | 2,097 | 1.1 |
| 34 | 10.1 | 13,500 | 13,402 | 2,867 | 3,544 | 5.8 |
| 35 | 9.9 | 13,800 | 14,558 | 997 | 791 | 5.7 |
| 36 | 9.9 | 13,200 | 15,057 | 1,020 | 797 | 5.2 |
| 37 | 9.9 | 12,100 | 13,564 | 1,094 | 1,741 | 6.4 |
| 38 | 9.9 | 13,500 | 14,732 | 965 | 1,183 | 7.3 |
| 39 | 10.0 | 12,300 | 14,823 | 1,737 | 2,143 | 5.6 |
| 40 | 10.0 | 12,500 | 14,022 | 2,112 | 2,943 | 12.5 |
| 41 | 9.8 | 12,300 | 14,234 | 1,693 | 2,317 | 11.7 |

[1] Tests 20 and 21 are bad files, pushed record by mistake
[2] Test 25 and 26 are files used to test connections between RAM and computer

**Fairfield load results**

This section will present the load parameter results from the Fairfield field study. Tests were recorded on three piers—at the surface of two fully compacted piers (pier 1 and 3) and on multiple lifts starting 5 ft below ground level for one pier (pier 2). Once pier 2 was fully compacted, tests were performed directly on the matrix soil about 2 feet from the center of that pier. In addition to the 24 in., 18 in. and 12 in. plates, this is the first site the 9 in. diameter steel plate was used attached to the RAM Test. The same material was used to install each pier. Table 15 summarizes the field study, and Figure 58 shows the field study conditions.

**Table 15. RAM field summary for Fairfield**

| Test | Pier | Pier Type | Pier Condition | Test Layer | Buffer Pad | Plate Size (in.) |
|---|---|---|---|---|---|---|
| 1 | 1 | Aggregate pier | Finished | Top | No | 18 |
| 2 | | | Finished | Top | Yes | 18 |
| 3 | | | Finished | Top | Yes | 9 |
| 4 | 2 | | Post compaction | 1 | Yes | 18 |
| 5 | | | Pre compaction | 2 | Yes | 18 |

| Test | Pier | Pier Type | Pier Condition | Test Layer | Buffer Pad | Plate Size (in.) |
|---|---|---|---|---|---|---|
| 6 | | | Post compaction | 2 | Yes | 18 |
| 7 | | | Pre compaction | 3 | Yes | 18 |
| 8 | | | Pre compaction | 3 | Yes | 18 |
| 9 | | | Post compaction | 3 | Yes | 18 |
| 10 | | | Pre compaction | 4 | Yes | 24 |
| 11 | | | Post compaction | 4 | Yes | 18 |
| 12 | | | Pre compaction | 5 | Yes | 18 |
| 13 | | | Post compaction | 5 | Yes | 18 |
| 14 | | | Post compaction | 5 | Yes | 12 |
| 15 | | | Post compaction | 5 | Yes | 9 |
| 20 | | | Post compaction | 5 | Yes | 24 |
| 16 | 3 | | | Matrix | Yes | 24 |
| 17 | | | | Matrix | Yes | 18 |
| 18 | | | | Matrix | Yes | 12 |
| 19 | | | | Matrix | Yes | 9 |
| 21 | 4 | | Post compaction | Top | Yes | 24 |
| 22 | | | Post compaction | Top | Yes | 18 |
| 23 | | | Post compaction | Top | Yes | 12 |
| 24 | | | Post compaction | Top | Yes | 9 |

**Figure 58. Fairfield field study conditions**

Load time-histories were successfully collected on all piers. Load analysis A was used for Fairfield tests. Pier 1 exhibited consistent crowd loads, and varying dynamic loads. The amplitudes were not consistent; test 1 and 3 demonstrated higher values towards the

maximum loads, and test 2 demonstrated higher values towards the lower loads, as shown in Figure 59 and Figure 60. The behavior may be explained by the double sinusoidal behavior as shown in Figure 61. The frequencies for test 1 and 3 were the same value, 9.7 Hz, and were higher than the frequency of 9.4 Hz calculated for test 2.

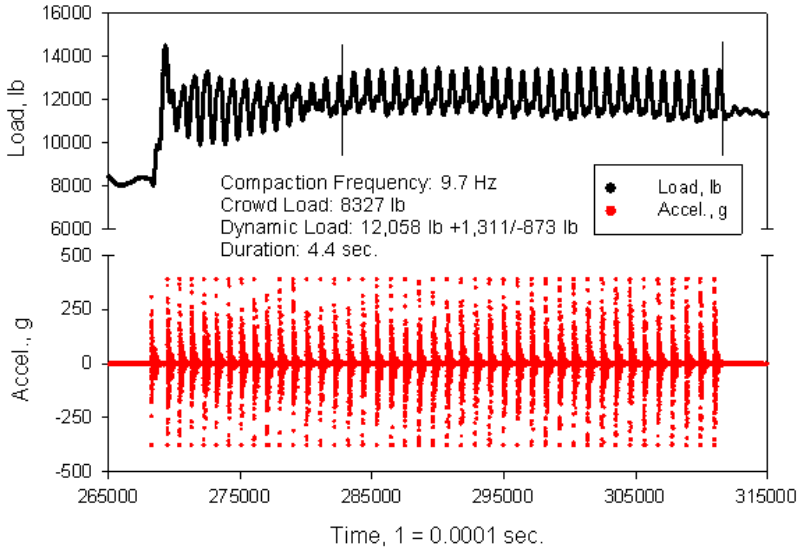


**Figure 59. Fairfield test 1**

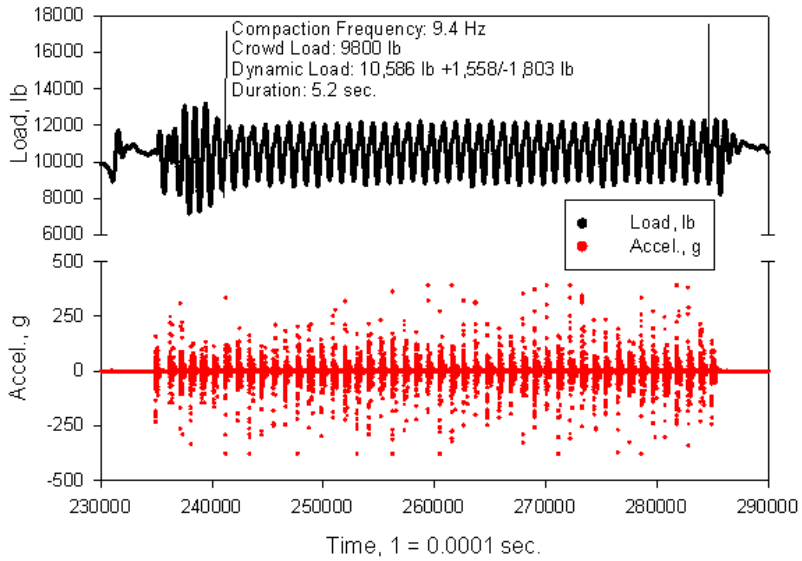


**Figure 60. Fairfield test 2**

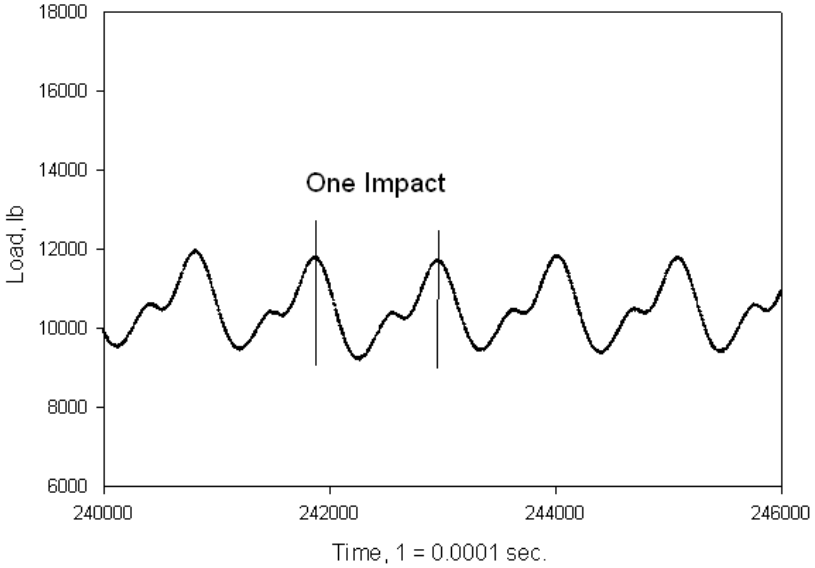


**Figure 61. Example of the double impact behavior of Fairfield test 3**

Pier 2 exhibited variation between crowd loads, dynamic loads, and frequencies. The tests on the pre compacted lifts showed lower crowd loads than the tests on post compacted lifts, almost half the value. For example, test 5 had a crowd load of 6,100 lb and test 6 had a crowd load of 11,800 lb. Both plots are shown in Figure 62 and Figure 63. The dynamic loads exhibited similar behavior; test layers 1 through 3 demonstrated post compacted lifts with higher average dynamic loads, but smaller amplitudes than pre compacted lifts. Even though the amplitudes were smaller, the values for all the tests were still large, between 2,051 lb and 8,803 lb. Test layer 5 was the top lift for pier 2 and showed consistent crowd loads, and dynamic loads with lower amplitudes compared to the other piers, and had frequencies that ranged from 9.6 to 11 Hz. The tests from layer 5 exhibited the same double sinusoidal behavior as pier 1.

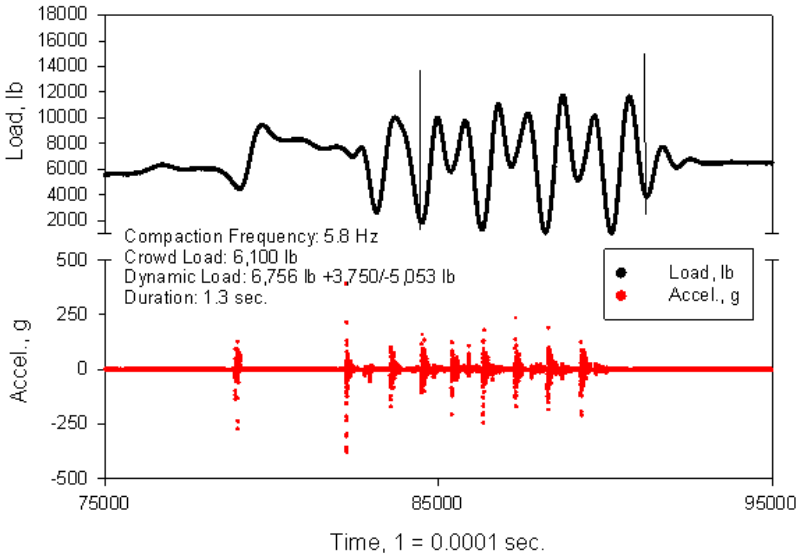


**Figure 62. Fairfield test 5, pre compacted lift**

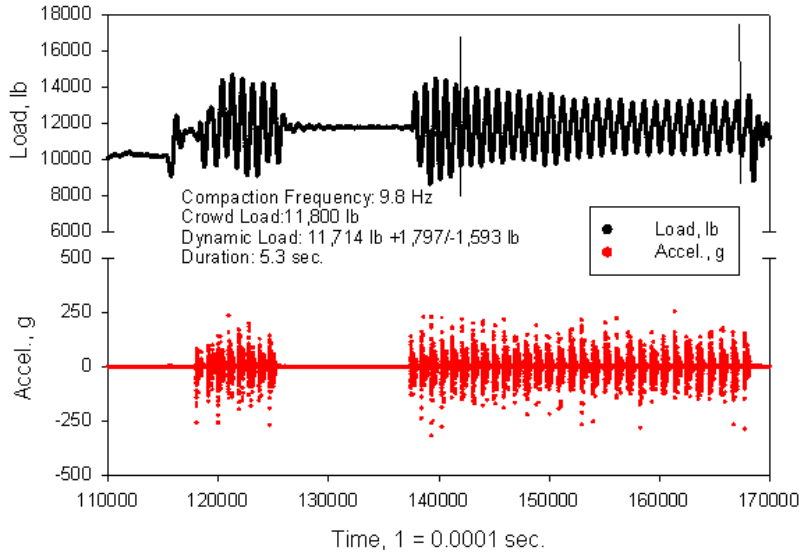


**Figure 63. Fairfield test 6, post compacted lift**

Pier 3 exhibited consistent crowd load and dynamic load values but are lower as compared to the other piers. Pier 3 was not an aggregate pier element, but was matrix soil. Pier 3 tests recorded the tamper on the RAM Test on the matrix soil 2 feet from the pier aggregate. A representative example is test 18 shown in Figure 64.

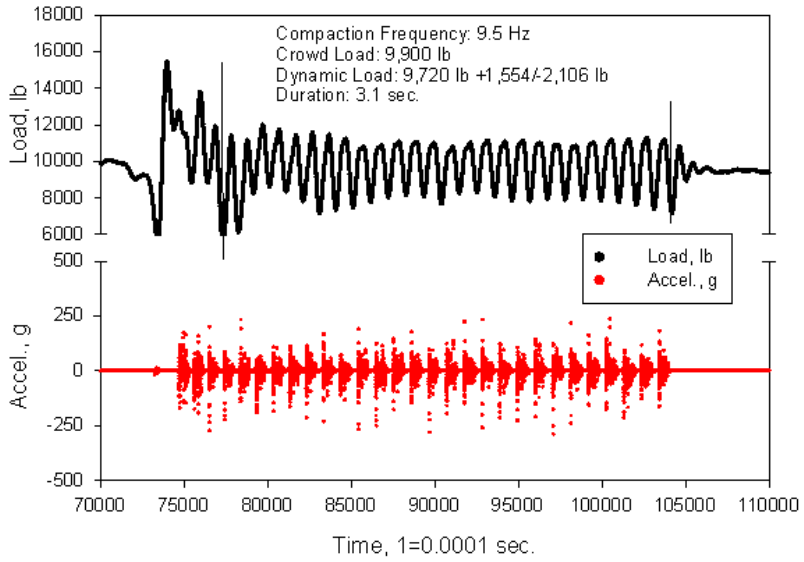


**Figure 64. Fairfield test 18**

Pier 4 exhibited consistent crowd loads, dynamic loads, and frequencies, except for test 21. The amplitude range of test 21 was uneven, emphasized the maximum loads, and demonstrated the double sinusoidal behavior. Test 21 shown in Figure 65, and 0.6 seconds of test 21 is shown in Figure 66 to demonstrate the double sinusoidal behavior in Figure 66. This behavior appears to happen before peak load is reached. Tests 22 through 24 demonstrated the same double impact behavior but not to the degree of test 21. The load parameters results for ramming frequency, crowd load, dynamic load, and duration are summarized in Table 16.

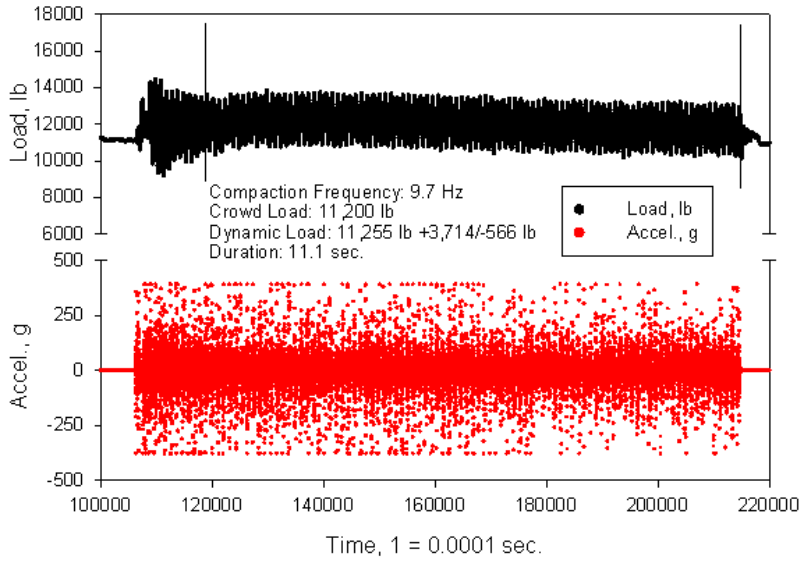


**Figure 65. Fairfield test 21**

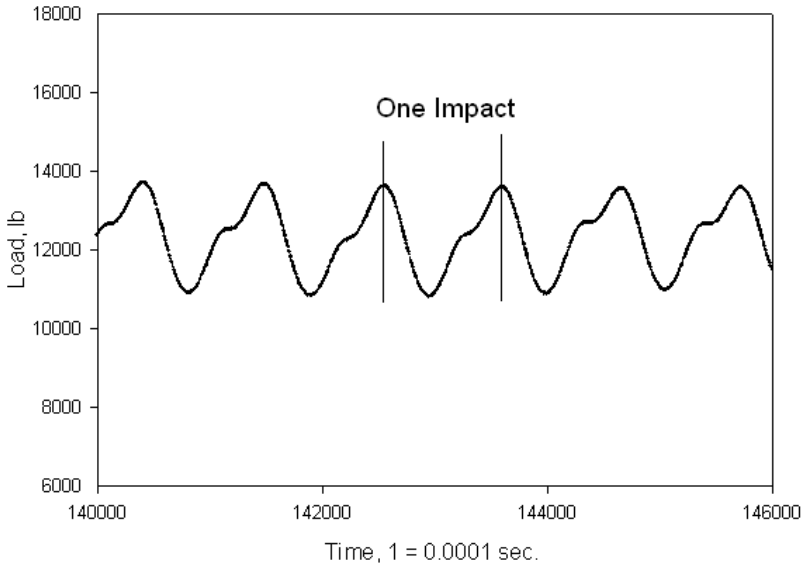


**Figure 66. Example of the double impact behavior of Fairfield test 21**

**Table 16. Load analysis A summary for Fairfield**

| Test | Frequency (Hz) | Crowd Load (lb) | Dynamic Load (lb) | | | Duration (Hz) |
|---|---|---|---|---|---|---|
| | | | Average | + | – | |
| 1 | 9.7 | 8,327 | 12,058 | 1,311 | 873 | 4.4 |
| 2 | 9.4 | 9,800 | 10,586 | 1,558 | 1,803 | 5.2 |
| 3 | 9.7 | 9,400 | 10,516 | 1,382 | 1,190 | 3.5 |
| 4 | 9.6 | 11,100 | 11,904 | 2,293 | 2,463 | 3.1 |

| Test | Frequency (Hz) | Crowd Load (lb) | Dynamic Load (lb) | | | Duration (Hz) |
|---|---|---|---|---|---|---|
| | | | Average | + | – | |
| 5 | 5.8 | 6,100 | 6,756 | 3,750 | 5,053 | 1.3 |
| 6 | 9.8 | 11,800 | 11,714 | 1,797 | 1,593 | 5.3 |
| 8 | 6.3 | 5,600 | 5,534 | 3,718 | 4,131 | 1.0 |
| 9 | 9.6 | 11,300 | 12,969 | 1,374 | 1,174 | 4.9 |
| 10 | 10.9 | 9,800 | 11,202 | 1,686 | 1,696 | 0.6 |
| 11 | 9.4 | 11,000 | 12,447 | 1,527 | 1,231 | 5.4 |
| 12 | 11.0 | 9,900 | 11,202 | 1,688 | 1,844 | 0.8 |
| 13 | 10.0 | 11,150 | 11,985 | 1,742 | 1,249 | 4.0 |
| 14 | 9.6 | 10,900 | 12,470 | 1,406 | 1,043 | 3.6 |
| 15 | 10.0 | 10,300 | 10,781 | 1,172 | 879 | 3.3 |
| 16 | 9.4 | 9,000 | 10,508 | 1,840 | 1,440 | 3.6 |
| 17 | 9.8 | 8,900 | 9,204 | 1,969 | 1,565 | 2.4 |
| 18 | 9.5 | 9,900 | 9,720 | 1,554 | 2,106 | 3.1 |
| 19 | 10.4 | 10,600 | 11,851 | 1,573 | 1,937 | 2.0 |
| 20 | 9.9 | 13,200 | 12,216 | 1,683 | 1,373 | 3.6 |
| 21 | 9.7 | 11,200 | 11,255 | 3,714 | 566 | 11.1 |
| 22 | 9.4 | 11,100 | 11,624 | 1,170 | 1,173 | 9.2 |
| 23 | 9.4 | 11,000 | 11,298 | 1,141 | 1,082 | 9.3 |
| 24 | 9.7 | 10,600 | 10,916 | 1,127 | 1,063 | 5.0 |

**Council Bluffs load results**

This section will present the load results from the Council Bluffs field study. Tests were performed on three aggregate piers—at the surface of one post compacted pier (pier 1), on two post compacted lifts for one pier (pier 2), and on multiple post compacted lifts starting 6 ft. below ground level for one pier (pier 3). This is the first time 2 foot lifts were tested with the RAM Test. And, this is the only study where the material consisted of recycled concrete. Data was collected with the 24 in., 18 in., and 12 in. plates. Table 17 summarizes the field study and Figure 67 shows the field study conditions.

**Table 17. RAM field summary for Council Bluffs**

| Test | Pier | Pier Type | Pier Condition | Test Layer | Buffer Pad | Plate Size (in.) |
|---|---|---|---|---|---|---|
| 6 | 1 | Aggregate piers with 2 foot lifts | Post compaction | Top | Yes | 24 |
| 7 | | | | Top | | 24 |
| 8 | | | | Top | | 18 |
| 9 | | | | Top | | 24 |
| 10 | | | | Top | | 18 |
| 11 | | | | Top | | 12 |

| Test | Pier | Pier Type | Pier Condition | Test Layer | Buffer Pad | Plate Size (in.) |
|---|---|---|---|---|---|---|
| 12 | 2 | | | 1 | | 18 |
| 16 | | | | 2 | | 18 |
| 17 | 3 | | | 1 | | 18 |
| 18 | | | | 2 | | 18 |
| 19 | | | | 3 | | 18 |
| 21 | | | | 4 | | 18 |

**Figure 67. Council Bluffs field study conditions**

Load time-histories were successfully collected on all piers. Load analysis A was used for Council Bluff tests. Pier 1 exhibited consistent crowd loads, average dynamic loads, but varying amplitudes and frequencies. The amplitudes were consistent for tests 6– 8 with amplitudes between 2,905 lb and 3,500 lb. And, amplitudes were consistent for tests 9– 11 with amplitudes between 550 lb and 775 lb. This range of amplitudes was large over one pier, but the duration of the tests may explain the difference. Tests 6–8 were under 7 seconds while tests 9–11 were over 19 seconds, and tests 6–8 had already compacted the pier when tests 9–11 were recorded. The frequencies ranged from 9.4 Hz to 10.7 Hz, with no consistency. The differences are shown in Figure 68 and Figure 69. Figure 70 shows 5 seconds of compaction at the end of test 9, the small amplitudes may demonstrate stiff pier conditions. The crowd loads were higher after compaction stopped than when compaction started.

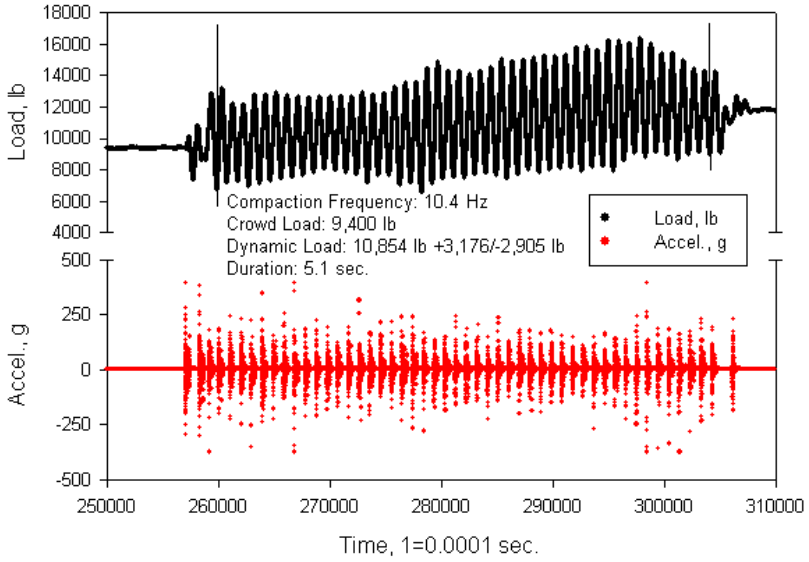


**Figure 68. Example of larger amplitudes of Council Bluffs test 8**

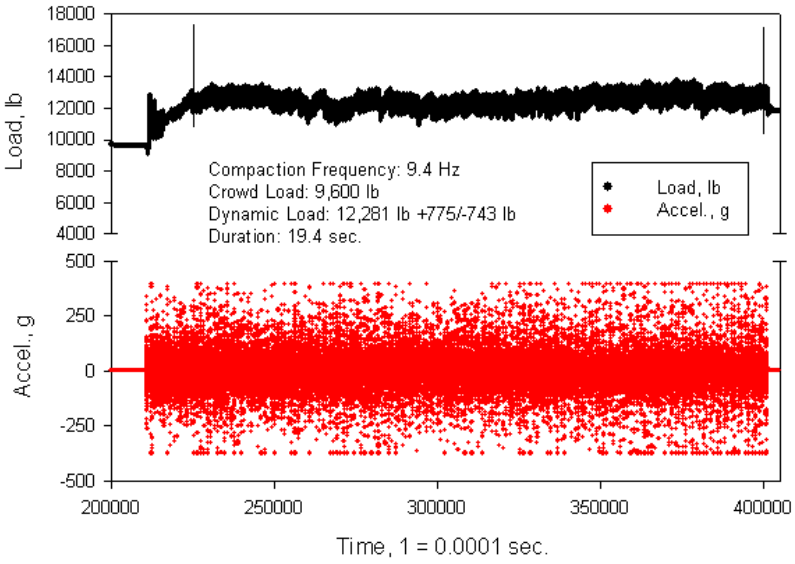


**Figure 69. Example of smaller amplitudes of Council Bluffs test 9**

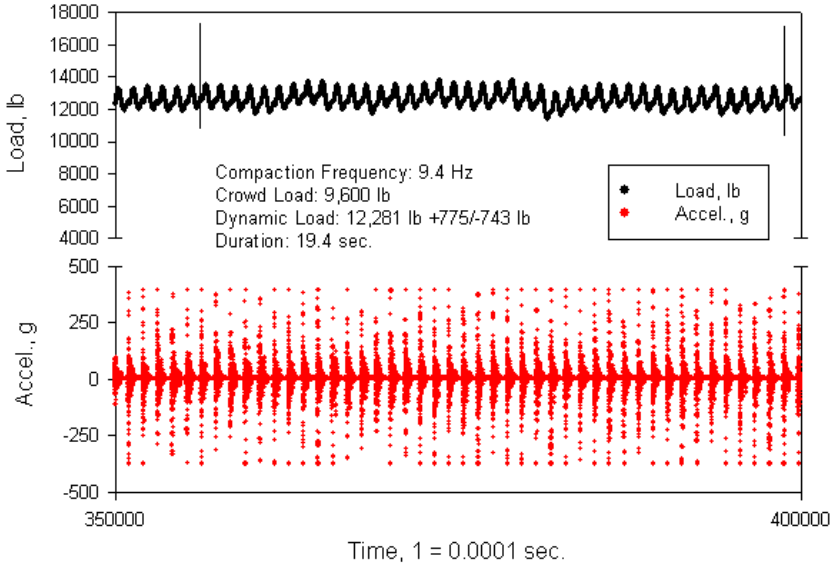


**Figure 70. Council Bluffs test 9, 5 seconds of compaction**

Pier 2 exhibited consistent crowd loads, but varying average dynamic loads, and frequencies. The amplitudes remained consistent except for test 16.1 (test 16 segment 1), where the amplitude emphasized the maximum loads over the minimum loads by a magnitude of 3.5. Figure 71 shows the load time-history and how variable the minimum and maximum loads were. The rest of the tests stayed relatively balanced between the maximum and minimum loads. The crowd loads generally increased with each segment, while the average dynamic loads generally decreased with each segment.

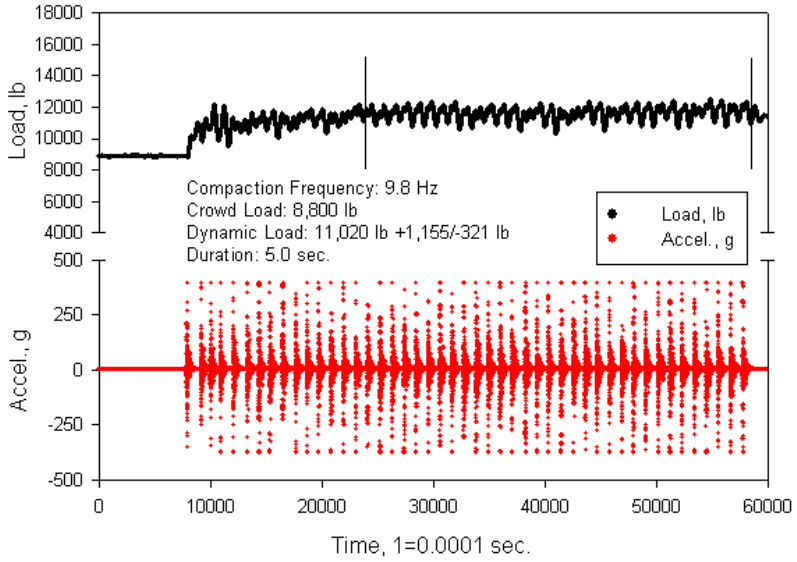


**Figure 71. Council Bluffs test 16.1, the amplitudes emphasized the maximum loads**

Pier 3 exhibited consistent frequencies (except for tests 19.1–19.3), but varying crowd loads, and dynamic loads. Test 19.1 had a frequency of 11.6 Hz which was higher than the average of 9.6 Hz. The crowd loads general decreased with each test (with the exception of tests 19.1–19.3). The average dynamic load decreased from layer 1 (test 17) to layer 2 (test 18), then increased from layer 2 (test 18) to layer 3 (test 19), then decreased from layer 3 (test 19) to the top layer, layer 4 (test 21). The amplitudes varied, the range was from 418 lb to 1,351 lb, and showed no distinguishable difference between tests. A similar version of the double sinusoidal behavior was seen from pier 3. The double behavior appears to occur right after the peak load is reached, shown in Figure 72. The load parameter results for ramming frequency, crowd load, dynamic load, and duration are summarized in Table 18.

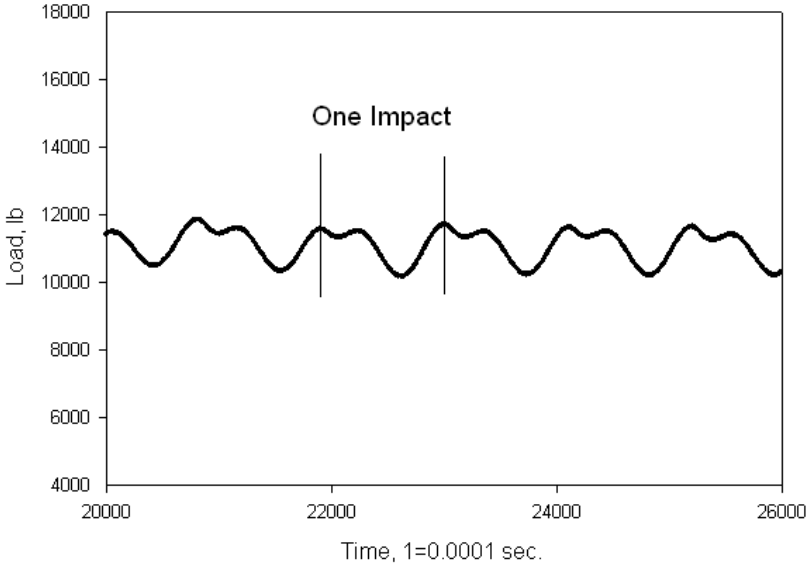


**Figure 72. Council Bluffs test 18.1, double sinusoidal behavior**

**Table 18. Load analysis A summary for Council Bluffs**

| Test | Frequency (Hz) | Crowd Load (lb) | Dynamic Load (lb) | | | Duration (Sec.) |
|---|---|---|---|---|---|---|
| | | | Average | + | – | |
| 6 | 10.4 | 10,900 | 10,139 | 3,211 | 2,752 | 6.6 |
| 7 | 10.4 | 9,900 | 11,155 | 3,500 | 3,031 | 6.5 |
| 8 | 10.4 | 9,400 | 10,854 | 3,176 | 2,905 | 5.1 |
| 9 | 9.4 | 9,600 | 12,281 | 775 | 743 | 19.4 |
| 10 | 9.4 | 10,500 | 11,804 | 756 | 550 | 19.0 |
| 11 | 10.7 | 9,500 | 11,952 | 771 | 556 | 28.8 |
| 12.1[1] | 9.2 | 6,500 | 9,900 | 730 | 770 | 3.6 |
| 12.2 | 9.4 | 9,400 | 9,381 | 879 | 853 | 5.1 |
| 12.3 | 9.3 | 8,700 | 8,517 | 806 | 1,114 | 5.9 |
| 12.4 | 9.3 | 8,000 | 7,821 | 853 | 1,151 | 4.2 |
| 16.1 | 9.8 | 8,800 | 11,020 | 1,155 | 321 | 5.0 |
| 16.2 | 9.3 | 11,100 | 11,332 | 732 | 900 | 5.4 |
| 16.3 | 9.3 | 11,000 | 10,943 | 885 | 1,049 | 4.9 |
| 16.4 | 9.2 | 10,600 | 10,704 | 834 | 966 | 5.3 |
| 17.1 | 9.1 | 11,600 | 11,775 | 951 | 496 | 3.7 |
| 17.2 | 9.5 | 11,600 | 11,732 | 934 | 975 | 4.2 |
| 17.3 | 9.2 | 11,500 | 11,791 | 1,021 | 1,064 | 4.3 |
| 17.4 | 9.2 | 11,600 | 11,668 | 938 | 1,103 | 3.6 |
| 18.1 | 9.4 | 10,000 | 11,021 | 816 | 668 | 4.0 |
| 18.2 | 9.8 | 11,100 | 10,676 | 596 | 780 | 3.5. |
| 18.3 | 9.9 | 10,700 | 10,602 | 741 | 838 | 3.7 |
| 18.4 | 9.3 | 10,300 | 10,410 | 689 | 1,068 | 4.2 |

| Test | Frequency (Hz) | Crowd Load (lb) | Dynamic Load (lb) | | | Duration (Sec.) |
|---|---|---|---|---|---|---|
| | | | Average | + | – | |
| 18.5 | 9.3 | 10,000 | 10,197 | 723 | 1,089 | 3.3 |
| 19.1 | 11.6 | 9,800 | 11,826 | 821 | 782 | 3.7 |
| 19.2 | 9.9 | 12,000 | 11,946 | 505 | 927 | 3.7 |
| 19.3 | 10.3 | 11,500 | 11,703 | 418 | 915 | 3.7 |
| 19.4 | 9.2 | 11,700 | 11,533 | 586 | 949 | 3.1 |
| 21.1 | 9.1 | 9,700 | 10,226 | 638 | 755 | 3.2 |
| 21.2 | 9.9 | 9,600 | 9,558 | 883 | 676 | 3.1 |
| 21.3 | 9.2 | 9,500 | 9,533 | 971 | 846 | 3.3 |
| 21.4 | 9.3 | 9,600 | 9,745 | 1,341 | 891 | 4.1 |
| 21.5 | 9.2 | 9,300 | 9,646 | 1,351 | 862 | 4.1 |

[1]There are 3 to 4 segments per one test to allow for deformation values to be read from verification system. The abbreviation 12.1 is test 12 segment 1

**Oskaloosa load results**

This section will present the load results from the Oskaloosa field study. Tests were performed on three piers: on the second to top post compacted lift with the 18 in. plate, and on the top post compacted lift with the 24 in., 18 in., 12 in., and 9 in. plates. This is the first study where all four plate sizes were able to be used. Table 10 summarizes the field study and Figure 73 shows the field study conditions. The Oskaloosa load results are organized by load analysis A and load analysis B.

**Table 19. RAM field summary for Oskaloosa**

| Test | Pier | Pier Type | Pier Conditions | Test Layer | Buffer Pad | Plate Size (in.) |
|---|---|---|---|---|---|---|
| 1 | 1 | Aggregate pier | Post compaction | 1 | Yes | 18 |
| 2 | | | | 2 | | 24 |
| 3 | | | | | | 18 |
| 4 | | | | | | 12 |
| 5 | | | | | | 9 |
| 6 | 2 | Aggregate pier | Post compaction | 1 | Yes | 18 |
| 7 | | | | 2 | | 24 |
| 8 | | | | | | 18 |
| 9 | | | | | | 12 |
| 10 | | | | | | 9 |
| 11 | 3 | Aggregate pier | Post compaction | 1 | Yes | 18 |
| 12 | | | | 2 | | 24 |

| Test | Pier | Pier Type | Pier Conditions | Test Layer | Buffer Pad | Plate Size (in.) |
|---|---|---|---|---|---|---|
| 13 | | | | | | 18 |
| 14 | | | | | | 12 |
| 15 | | | | | | 9 |

**Figure 73. Oskaloosa field study conditions**

*Load Analysis A*

Load time-histories were successfully collected on all piers. Load analysis A was first used for Oskaloosa tests. Pier 1 exhibited consistent frequencies, relatively consistent crowd loads, consistent average dynamic loads, and even dynamic amplitudes. However, the amplitudes varied greatly between tests and segments. The smallest dynamic amplitude was 621 lb (test 4.2, Figure 74) and the largest amplitude was 3,738 lb (test 2.1, Figure 75). There appears to be no significant differences between plate sizes.

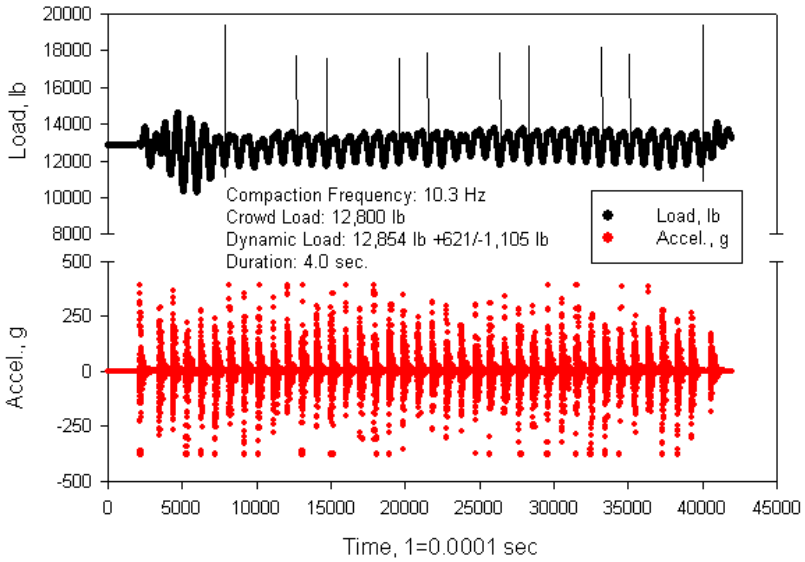


**Figure 74. Oskaloosa test 4.2, smallest amplitude**

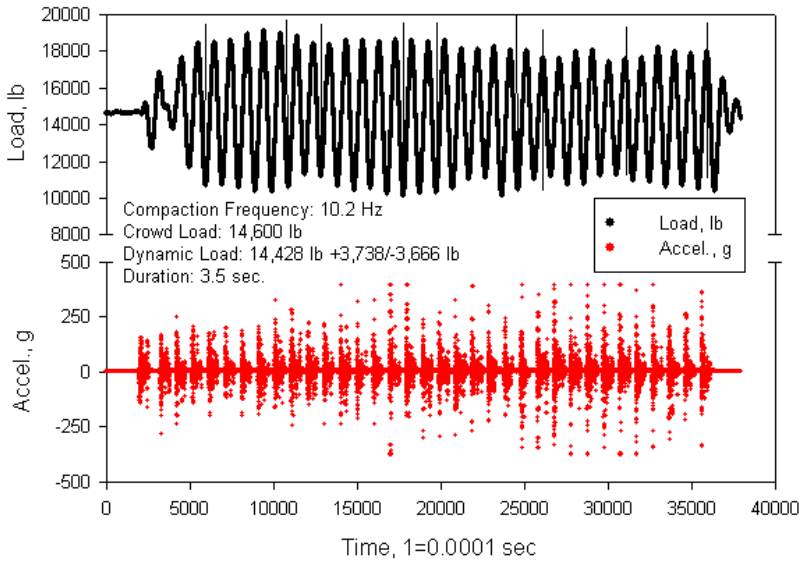


**Figure 75. Oskaloosa test 2.1, largest amplitude**

Pier 2 exhibited consistent frequencies, relatively consistent crowd loads, consistent average dynamic loads, and even dynamic amplitudes. The amplitudes varied, but the differences were not as great as pier 1. The smallest amplitude was 705 lb (test 6.1, Figure 76) and the largest amplitude was 2,456 lb (test 7.1, Figure 77). There appears to be no significant differences between plate sizes.

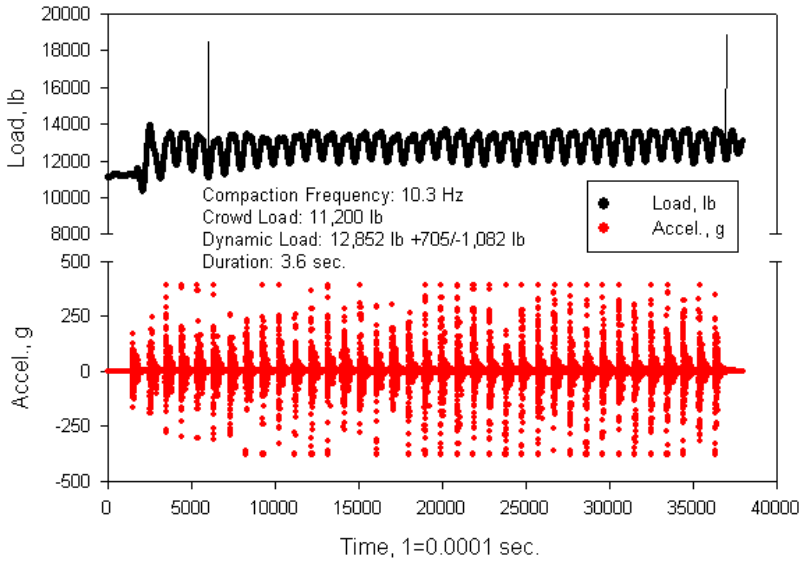


**Figure 76. Oskaloosa test 6.1, smallest amplitude**

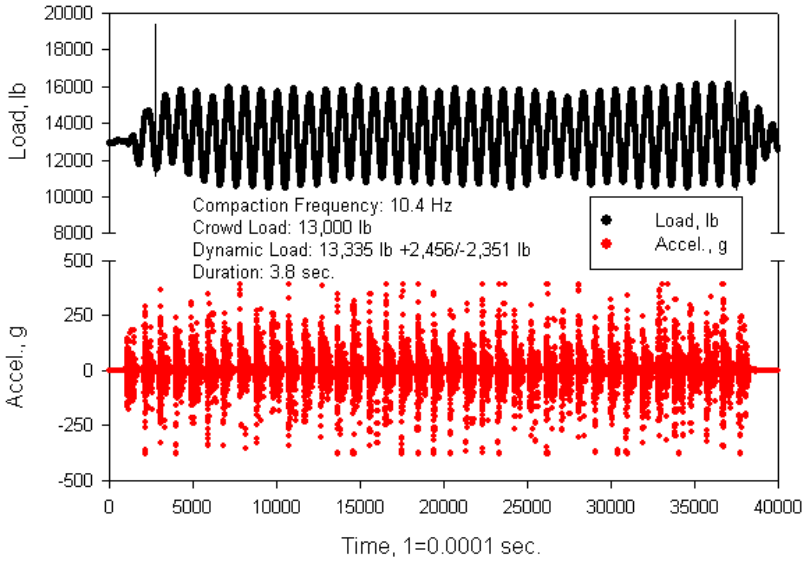


**Figure 77. Oskaloosa test 7.1, largest amplitude**

Pier 3 exhibited consistent frequencies, relatively consistent crowd loads, consistent average dynamic loads, and balanced dynamic amplitudes. The dynamic amplitudes stayed relatively consistent compared to pier 1 and pier 2. The smallest dynamic amplitude was 643 lb and 1,808 lb. There appears to be no significant differences between plate sizes. The load

parameter results for ramming frequency, crowd load, dynamic load, and duration are summarized in Table 20.

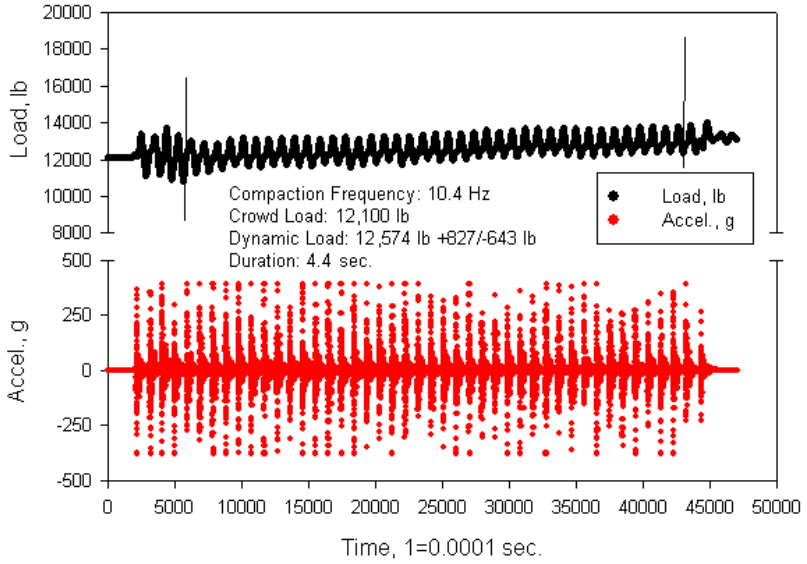


**Figure 78. Oskaloosa test 13.3, smallest amplitude**

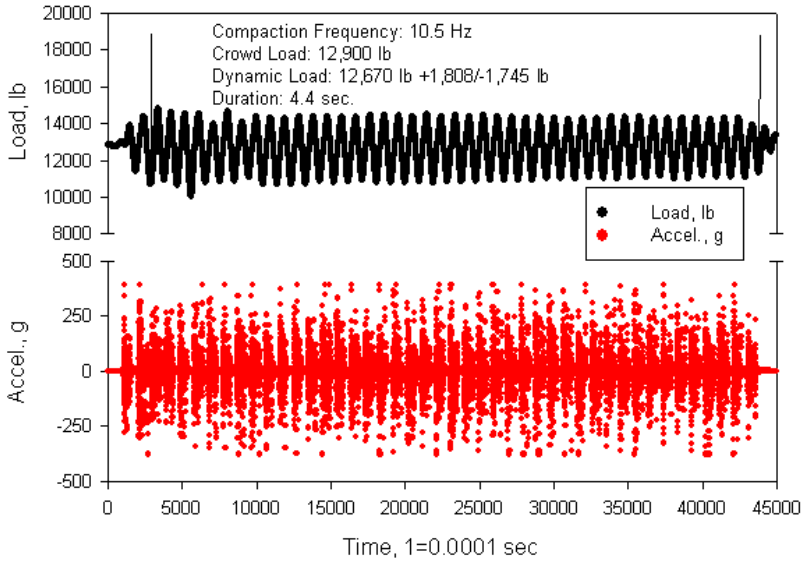


**Figure 79. Oskaloosa test 12.2, smallest amplitude**

**Table 20. Load analysis A summary for Oskaloosa**

| Test | Frequency (Hz) | Crowd Load (lb) | Dynamic Load (lb) | | | Duration (sec.) |
|---|---|---|---|---|---|---|
| | | | Average | + | – | |
| 1.1[1] | 10.2 | 11,200 | 11,641 | 777 | 856 | 3.6 |

| Test | Frequency (Hz) | Crowd Load (lb) | Dynamic Load (lb) | | | Duration (sec.) |
|---|---|---|---|---|---|---|
| | | | Average | + | – | |
| 1.2 | 10.3 | 11,800 | 12,003 | 1,140 | 1,145 | 4.3 |
| 1.3 | 10.2 | 12,100 | 12,294 | 1,272 | 1,268 | 4.3 |
| 2.1 | 10.2 | 14,600 | 14,428 | 3,738 | 3,666 | 3.5 |
| 2.2 | 10.3 | 14,400 | 13,975 | 3,407 | 3,568 | 3.6 |
| 2.3 | 10.4 | 14,100 | 13,664 | 3,144 | 3,230 | 4.2 |
| 3.1 | 10.2 | 11,300 | 12,925 | 964 | 1,292 | 3.7 |
| 3.2 | 10.4 | 13,300 | 12,942 | 1,081 | 1,148 | 4.5 |
| 3.3 | 10.5 | 13,400 | 12,849 | 1,272 | 1,399 | 4.6 |
| 4.1 | 10.2 | 12,000 | 12,700 | 962 | 1,375 | 3.1 |
| 4.2 | 10.3 | 12,800 | 12,854 | 621 | 1,105 | 4.0 |
| 4.3 | 10.3 | 13,200 | 12,922 | 1,028 | 1,325 | 3.7 |
| 4.4 | 10.5 | 13,200 | 12,997 | 1,254 | 1,606 | 3.5 |
| 5.1 | 10.2 | 11,800 | 12,409 | 733 | 1,077 | 3.5 |
| 5.2 | 10.4 | 12,700 | 12,789 | 945 | 1,369 | 4.1 |
| 5.3 | 10.5 | 12,900 | 12,986 | 1,339 | 1,600 | 4.0 |
| 5.4 | 10.5 | 13,200 | 12,898 | 1,991 | 2,364 | 3.7 |
| 6.1 | 10.3 | 11,200 | 12,852 | 705 | 1,082 | 3.6 |
| 6.2 | 10.4 | 11,800 | 12,450 | 1,264 | 1,089 | 3.9 |
| 6.3 | 10.4 | 11,900 | 12,527 | 1,133 | 1,155 | 3.9 |
| 7.1 | 10.4 | 13,000 | 13,335 | 2,456 | 2,351 | 3.8 |
| 7.2 | 10.5 | 13,000 | 13,067 | 2,369 | 2,316 | 3.8 |
| 7.3 | 10.5 | 13,100 | 12,913 | 2,068 | 2,099 | 4.3 |
| 8.1 | 10.2 | 12,300 | 14,247 | 1,175 | 1,438 | 3.7 |
| 8.2 | 10.5 | 14,200 | 13,781 | 1,274 | 1,565 | 3.9 |
| 8.3 | 10.6 | 13,800 | 14,092 | 1,300 | 1,479 | 4.0 |
| 8.4 | 10.2 | 12,300 | 14,247 | 1,175 | 1,438 | 3.6 |
| 9.1 | 10.3 | 11,200 | 12,436 | 1,473 | 1,772 | 3.3 |
| 9.2 | 10.5 | 11,900 | 12,685 | 1,499 | 1,783 | 3.1 |
| 9.3 | 10.5 | 12,800 | 12,934 | 1,345 | 1,510 | 3.2 |
| 9.4 | 10.5 | 12,900 | 12,925 | 1,592 | 1,711 | 3.5 |
| 10.1 | 10.3 | 10,900 | 12,598 | 1,277 | 1,518 | 3.1 |
| 10.2 | 10.5 | 12,700 | 12,462 | 1,482 | 1,651 | 3.4 |
| 10.3 | 10.5 | 12,400 | 12,505 | 1,388 | 1,592 | 3.4 |
| 10.4 | 10.6 | 12,600 | 12,484 | 1,514 | 1,608 | 3.1 |
| 11.1 | 10.3 | 12,800 | 12,555 | 963 | 1,035 | 4.3 |
| 11.2 | 10.3 | 12,800 | 12,789 | 891 | 844 | 3.6 |
| 11.3 | 10.4 | 12,700 | 12,670 | 1,009 | 1,250 | 3.7 |
| 11.4 | 10.5 | 13,100 | 13,398 | 1,244 | 1,359 | 3.5 |
| 12.1 | 10.3 | 10,800 | 12,528 | 1,682 | 1,682 | 3.5 |
| 12.2 | 10.5 | 12,900 | 12,670 | 1,808 | 1,745 | 4.4 |
| 12.3 | 10.3 | 12,900 | 12,723 | 1,580 | 1,710 | 4.3 |
| 13.1 | [2] | 11,100 | | | | 3.9 |

| Test | Frequency (Hz) | Crowd Load (lb) | Dynamic Load (lb) | | | Duration (sec.) |
|---|---|---|---|---|---|---|
| | | | Average | + | – | |
| 13.2 | 10.4 | 12,000 | 11,967 | 915 | 673 | 3.9 |
| 13.3 | 10.4 | 12,100 | 12,574 | 827 | 643 | 4.4 |
| 13.4 | 10.5 | 13,100 | 13,230 | 820 | 722 | 3.9 |
| 14.1 | 10.2 | 10,900 | 11,785 | 843 | 712 | 4.0 |
| 14.2 | 10.3 | 11,500 | 11,711 | 1,017 | 899 | 3.9 |
| 14.3 | 10.4 | 11,500 | 11,757 | 1,051 | 747 | 4.8 |
| 15.1 | 10.4 | 9,500 | 11,798 | 938 | 929 | 3.6 |
| 15.2 | 11.0 | 11,500 | 11,582 | 1,301 | 1,092 | 4.3 |
| 15.3 | 10.5 | 11,300 | 11,491 | 1,202 | 992 | 4.2 |
| 15.4 | 10.5 | 11,200 | 11,301 | 1,173 | 1,085 | 3.4 |

[1]There are 3 to 4 segments per one test to allow for deformation values to be read from verification system. The abbreviation 1.1 is test 1 segment 1
[2]The plot is illegible to characterize

*Load Analysis B*

Load analysis B was used for Oskaloosa tests to analyze how the parameters from load analysis A change with time. The output of load analysis B is a dynamic load range (the difference between the maximum and minimum load), a maximum absolute acceleration, and a frequency. The analysis was completed on tests 1 through 5.

Test 1 segment 1 exhibited no variation in the dynamic load range, the maximum absolute acceleration, or the frequency. Test 1 segment 2 exhibited an increase the dynamic load range, and some variation in the maximum absolute acceleration and frequency. Test 1 segment 3 exhibited an increase in the dynamic load range, no variation in the maximum absolute acceleration, and an initial increase in the frequency but no variation after section 1, the results are plotted in Figure 80.

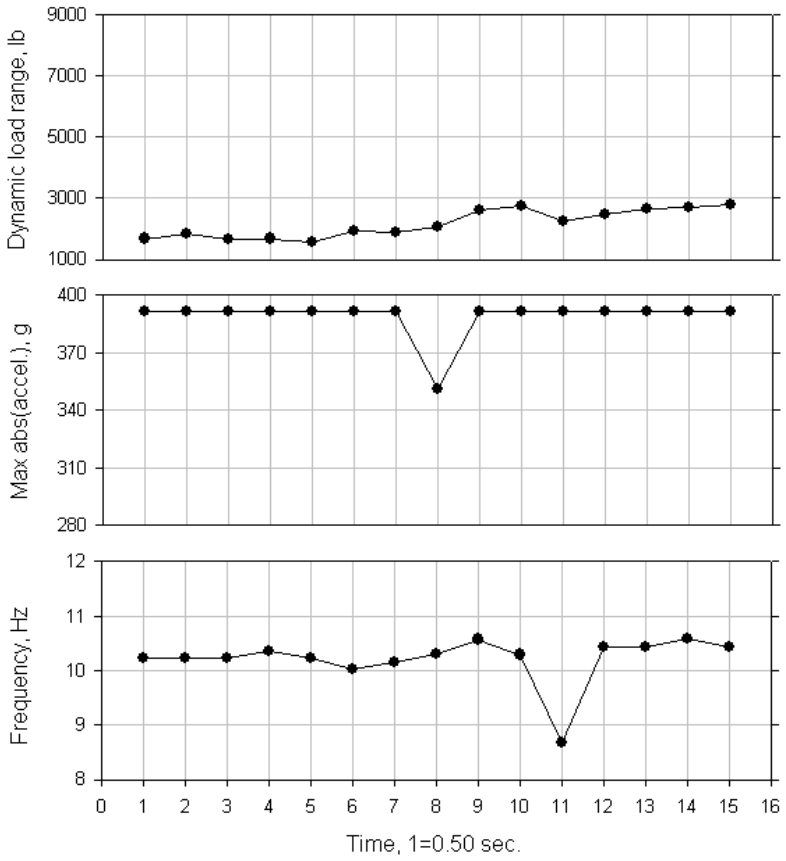


**Figure 80. Oskaloosa test 1 load analysis B results**

Test 2 segment 1 exhibited a decreased in the dynamic load range, initial increase in the maximum absolute acceleration but then did not vary, and a slight increase in the frequency. Test 2 segment 2 exhibited little variation in the dynamic load range and maximum absolute acceleration, and a slight increase in the frequency. Test 2 segment 3 exhibited a decrease in the dynamic load range, no variation in the maximum absolute acceleration, and a slight increase in the frequency. Overall, the dynamic load range decreased by 1,700 lb, the maximum absolute acceleration increased by 70 g, and the frequency increased by 0.70 Hz, the results are plotted in Figure 81.

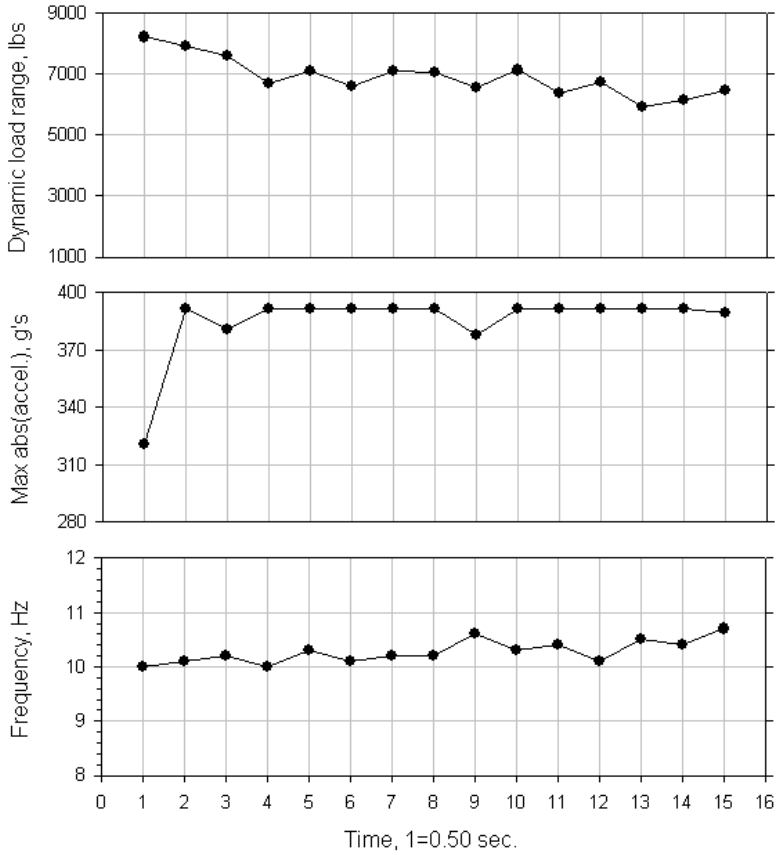


**Figure 81. Oskaloosa test 2 load analysis B results**

Test 3 segment 1 exhibited an increase in the dynamic load range, no variation in the maximum absolute acceleration, and an increase in the frequency. Test 3 segment 2 exhibited a decrease, then increase in the dynamic load range, a decrease in the maximum absolute acceleration at section 5, and variation in the frequency. Test 3 segment 3 exhibited little variation in the dynamic load range, variation in the maximum absolute acceleration, and an increase in the frequency. Overall, the dynamic load range increased by 700 lb, the maximum absolute acceleration varied within the test but did not show an overall difference, and the frequency increased by 0.60 Hz, the results are plotted in Figure 82.

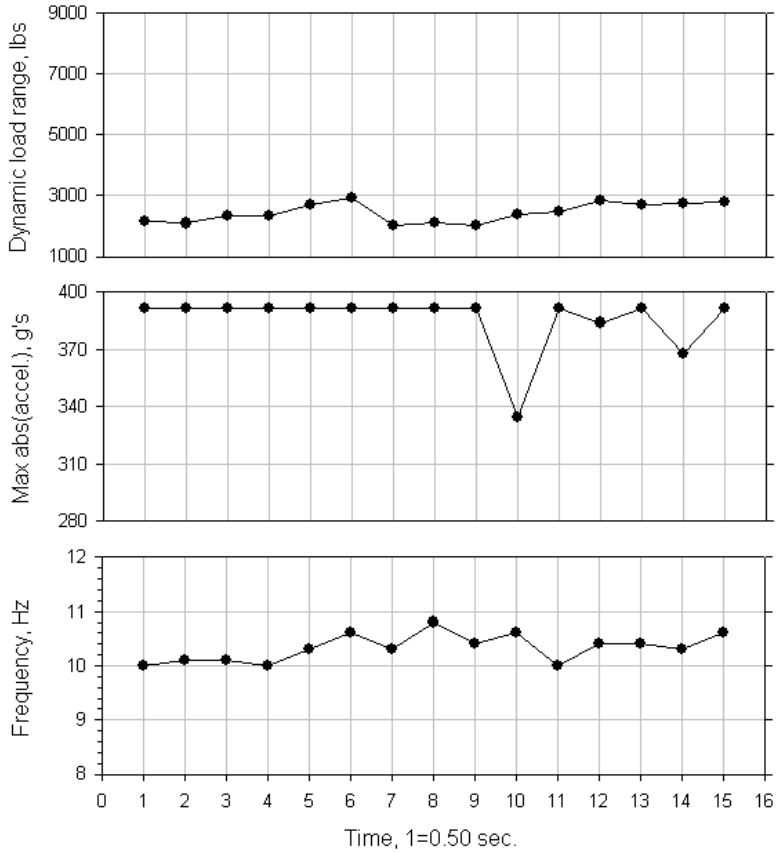


**Figure 82. Oskaloosa test 3 load analysis B results**

Test 4 segment 1 exhibited a decrease in the dynamic load range, no variation in the maximum absolute acceleration, and some variation in the frequency. Test 4 segment 2 exhibited an increase in the dynamic load range, some variation in the maximum absolute acceleration and frequency. Test 4 segment 3 exhibited an increase in the dynamic load range, a decrease in the maximum absolute acceleration, and variation in the frequency. Test 4 segment 4 exhibited an increase in the dynamic load range, a decrease in the maximum absolute acceleration in section 5, and variation in the frequency. Overall, the dynamic load range increased by 500 lb, the maximum absolute acceleration decreased by 14 g, and the frequency increased by 0.50 Hz, the results are plotted in Figure 83.

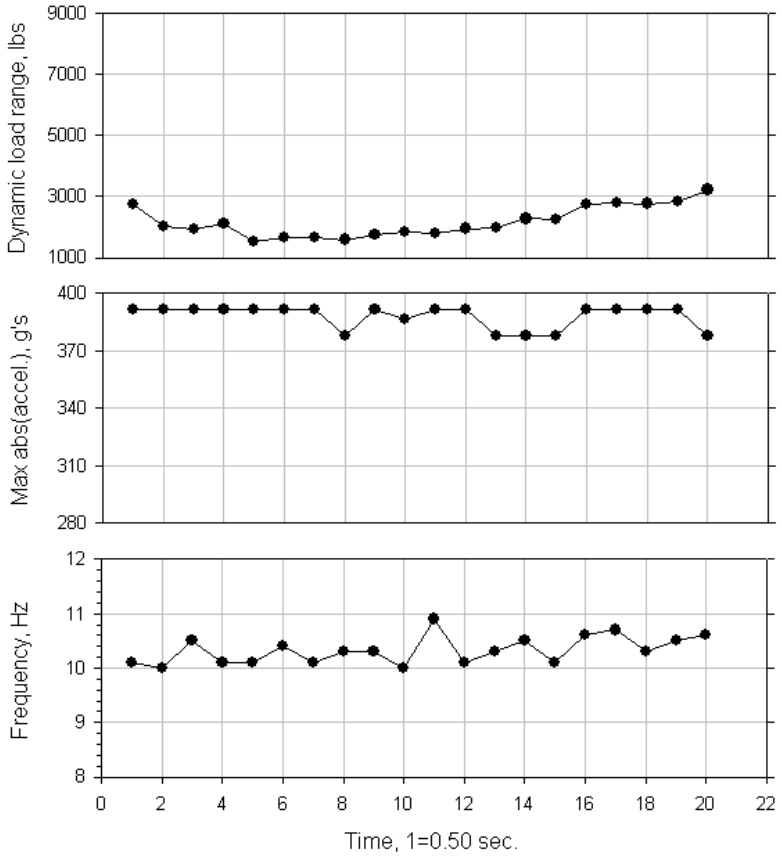


**Figure 83. Oskaloosa test 4 load analysis B results**

Test 5 segment 1 exhibited variation in the dynamic load range, no variation in the maximum absolute acceleration, and an increase in the frequency. Test 5 segment 2 exhibited some variation in the dynamic load range, a large variation in the maximum absolute acceleration, and no variation in the frequency. Test 5 segment 3 exhibited an increase in the dynamic load range, an increase in the maximum absolute acceleration, and some variation in the frequency. Test 5 segment 4 exhibited an increase in the dynamic load range, a large variation in the maximum absolute acceleration, and some variation in the frequency. Overall, the dynamic load range increased 2,400 lb, the maximum absolute acceleration varied a lot and showed a decrease of 14 g, and the frequency also varied and showed an overall increase of 0.10 Hz, the results are plotted in Figure 84.

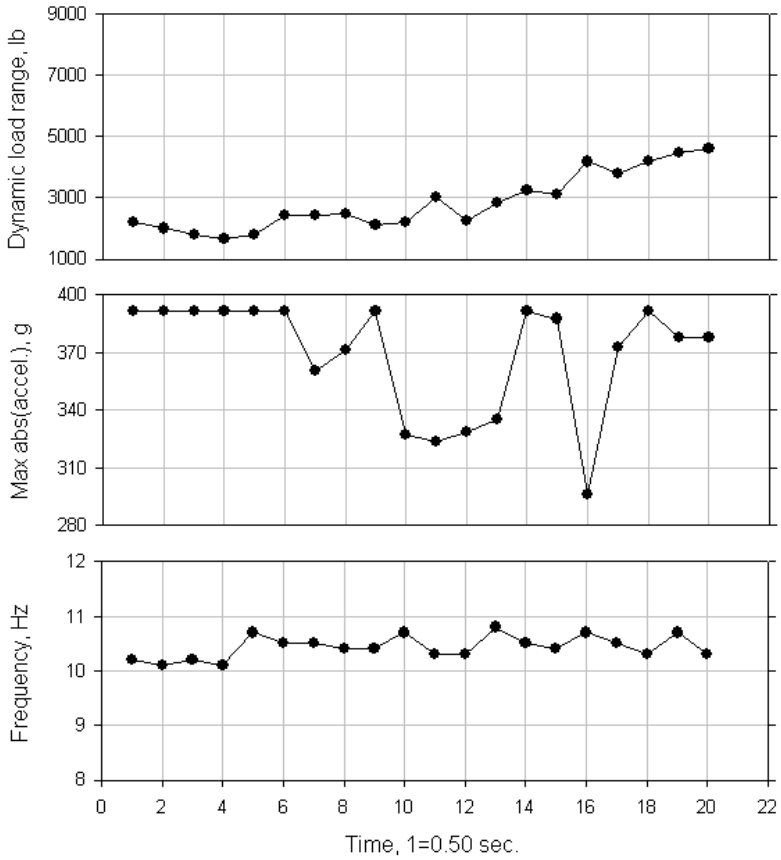


**Figure 84. Oskaloosa test 5 load analysis B results**

From test 1 to 5, there was a lot of variation in the dynamic load range, 1,517 lb to 8,196 lb, fairly consistent accelerations, and the frequencies varied between 10.0 and 11.0 Hz. The load parameter results for the dynamic load range, the maximum absolute acceleration, and the frequency are summarized in Table 21.

**Table 21. Load analysis B summary for Oskaloosa**

| Test | Segment | Section | Dynamic Load range, lb | Maximum Absolute Acceleration, g | Frequency, Hz |
|---|---|---|---|---|---|
| 1 | 1 | 1 | 1,680.4 | 391.29 | 10.23 |
| | | 2 | 1,823.2 | 391.29 | 10.23 |
| | | 3 | 1,668.6 | 391.29 | 10.23 |
| | | 4 | 1,680.4 | 391.29 | 10.35 |
| | | 5 | 1,584.0 | 391.29 | 10.23 |
| | 2 | 1 | 1,923.6 | 391.29 | 10.03 |
| | | 2 | 1,874.4 | 391.29 | 10.16 |

| Test | Segment | Section | Dynamic Load range, lb | Maximum Absolute Acceleration, g | Frequency, Hz |
|---|---|---|---|---|---|
| | | 3 | 2,062.2 | 351.15 | 10.31 |
| | | 4 | 2,596.4 | 391.29 | 10.57 |
| | | 5 | 2,732.3 | 391.29 | 10.29 |
| | 3 | 1 | 2,242.2 | 391.29 | 8.68 |
| | | 2 | 2,479.6 | 391.29 | 10.44 |
| | | 3 | 2,657.8 | 391.29 | 10.44 |
| | | 4 | 2,711.6 | 391.29 | 10.59 |
| | | 5 | 2,806.6 | 391.29 | 10.44 |
| 2 | 1 | 1 | 8,196.0 | 320.67 | 10.00 |
| | | 2 | 7,884.2 | 391.28 | 10.10 |
| | | 3 | 7,588.8 | 380.77 | 10.20 |
| | | 4 | 6,688.2 | 391.28 | 10.00 |
| | | 5 | 7,090.0 | 391.28 | 10.30 |
| | 2 | 1 | 6,575.6 | 391.28 | 10.10 |
| | | 2 | 7,078.4 | 391.28 | 10.20 |
| | | 3 | 7,048.4 | 391.28 | 10.20 |
| | | 4 | 6,551.0 | 377.50 | 10.60 |
| | | 5 | 7,107.6 | 391.28 | 10.30 |
| | 3 | 1 | 6,354.4 | 391.28 | 10.40 |
| | | 2 | 6,704.6 | 391.28 | 10.10 |
| | | 3 | 5,924.2 | 391.28 | 10.50 |
| | | 4 | 6,126.0 | 391.28 | 10.40 |
| | | 5 | 6,443.6 | 389.20 | 10.70 |
| 3 | 1 | 1 | 2,147.2 | 391.29 | 10.00 |
| | | 2 | 2,089.6 | 391.29 | 10.10 |
| | | 3 | 2,344.6 | 391.29 | 10.10 |
| | | 4 | 2,338.0 | 391.29 | 10.00 |
| | | 5 | 2,691.6 | 391.29 | 10.30 |
| | 2 | 1 | 2,938.6 | 391.29 | 10.60 |
| | | 2 | 2,020.6 | 391.29 | 10.30 |
| | | 3 | 2,125.8 | 391.29 | 10.80 |
| | | 4 | 2,038.4 | 391.29 | 10.40 |
| | | 5 | 2,397.4 | 334.53 | 10.60 |
| | 3 | 1 | 2,455.4 | 391.29 | 10.00 |
| | | 2 | 2,849.4 | 383.81 | 10.40 |
| | | 3 | 2,696.0 | 391.29 | 10.40 |
| | | 4 | 2,756.8 | 367.60 | 10.30 |
| | | 5 | 2,800.0 | 391.29 | 10.60 |
| 4 | 1 | 1 | 2,750.4 | 391.29 | 10.10 |
| | | 2 | 2,021.0 | 391.29 | 10.00 |
| | | 3 | 1,935.6 | 391.29 | 10.50 |

| Test | Segment | Section | Dynamic Load range, lb | Maximum Absolute Acceleration, g | Frequency, Hz |
|---|---|---|---|---|---|
| | | 4 | 2,104.8 | 391.29 | 10.10 |
| | | 5 | 1,517.6 | 391.29 | 10.10 |
| | 2 | 1 | 1,657.8 | 391.29 | 10.40 |
| | | 2 | 1,675.6 | 391.29 | 10.10 |
| | | 3 | 1,590.4 | 377.50 | 10.30 |
| | | 4 | 1,766.4 | 391.29 | 10.30 |
| | | 5 | 1,847.8 | 386.05 | 10.00 |
| | 3 | 1 | 1,794.4 | 391.29 | 10.90 |
| | | 2 | 1,952.0 | 391.29 | 10.10 |
| | | 3 | 1,970.0 | 377.50 | 10.30 |
| | | 4 | 2,273.0 | 377.50 | 10.50 |
| | | 5 | 2,267.4 | 377.50 | 10.10 |
| | 4 | 1 | 2,747.2 | 391.29 | 10.60 |
| | | 2 | 2,803.8 | 391.29 | 10.70 |
| | | 3 | 2,762.6 | 391.29 | 10.30 |
| | | 4 | 2,830.6 | 391.29 | 10.50 |
| | | 5 | 3,221.0 | 377.50 | 10.60 |
| 5 | 1 | 1 | 2,192.6 | 391.29 | 10.20 |
| | | 2 | 2,000.6 | 391.29 | 10.10 |
| | | 3 | 1,788.0 | 391.29 | 10.20 |
| | | 4 | 1,662.6 | 391.29 | 10.10 |
| | | 5 | 1,793.2 | 391.29 | 10.70 |
| | 2 | 1 | 2,416.2 | 391.29 | 10.50 |
| | | 2 | 2,414.0 | 360.50 | 10.50 |
| | | 3 | 2,461.4 | 371.10 | 10.40 |
| | | 4 | 2,124.4 | 391.29 | 10.40 |
| | | 5 | 2,189.6 | 326.93 | 10.70 |
| | 3 | 1 | 2,998.8 | 323.70 | 10.30 |
| | | 2 | 2,229.2 | 328.50 | 10.30 |
| | | 3 | 2,818.8 | 334.94 | 10.80 |
| | | 4 | 3,257.8 | 391.29 | 10.50 |
| | | 5 | 3,092.8 | 387.39 | 10.40 |
| | 4 | 1 | 4,170.2 | 295.80 | 10.70 |
| | | 2 | 3,769.0 | 372.36 | 10.50 |
| | | 3 | 4,184.2 | 391.29 | 10.30 |
| | | 4 | 4,448.8 | 377.50 | 10.70 |
| | | 5 | 4,588.4 | 377.50 | 10.30 |

**Acceleration**

Accelerometer 1 has a +/– 500 g range and was originally installed in the device in 2007. When reviewing the acceleration data from all five field studies, a peak value of 391.29 g

was observed at every site. The specifications showed the accelerometer has a +/– 500 g range. On January 13, 2011, accelerometer 1 was replaced with accelerometer 2. Accelerometer 1 was shipped back to the manufacturer to be recalibrated and to ensure it was working properly. Accelerometer 2 has a +/– 5000 g range, and will ensure the correct acceleration values are recorded.

Acceleration time-history is processed through the acceleration analysis software by acceleration analysis A, B, C, and D. The acceleration analysis software code is shown in the methods chapter. Acceleration analysis A is processing the data from when the acceleration of the first compaction impact starts to when the acceleration of the last compaction impact stops. When one test consists of several segments, each segment is processed individually. Once the single test or all segments have been processed, the deformations are summed to obtain total deformation for analysis A.

Acceleration analysis B is processing the data from when the acceleration of the last compaction impact starts to when the acceleration of the last compaction impact stops. If a test consists of several segments, the last compaction impact is from the last segment.

Acceleration analysis C is processing the data from when the acceleration of the sixth compaction impact (impact 6) to the acceleration of the tenth compaction impact (impact 10). The first 5 compaction impacts are assumed as seating impacts. The compaction impacts 6–10 are processed individually, and the average of the deformations is taken as analysis C deformation. Analysis started with Oskaloosa test 2 and processed impacts 6–10 for each segment, then decided to go with the last segment for future data processing. The last segments were consistently negative deformation, while the first several segments were consistently positive deformation.

Acceleration analysis D is processing the data from the acceleration of the fifth to last compaction impact (impact 5) to the acceleration of the last compaction impact (impact 1). The compaction impacts are processed individually, and the average of the deformations is taken as analysis D deformation. Figure 33 shows the data included in each analysis.

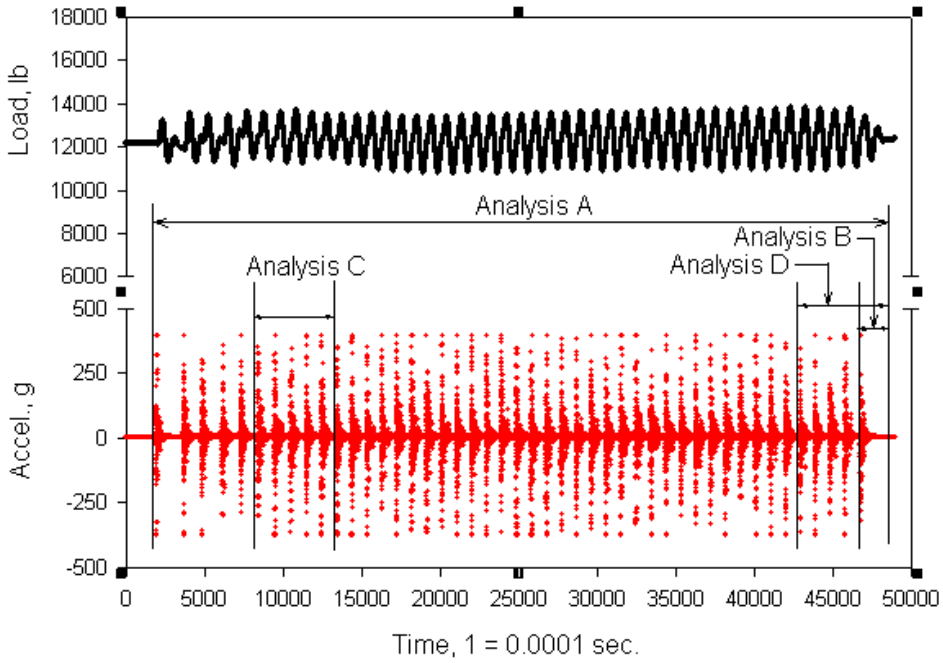


**Figure 85. Acceleration analyses A to D for processing the acceleration**

All data presented are from accelerometer 1. Negative values denote movement in to the ground, while positive values denote movement out of the ground. Results are presented in five sections; Hampton, La Port City, Fairfield, Council Bluffs, and Oskaloosa.

**Hampton acceleration results**

The cased aggregate pier elements exhibited increasing acceleration values as the tests progressed. Test 1 showed the smallest acceleration values with a range of –246 g to 156 g, while test 5 showed the largest acceleration values, with a range of –378 g to 391 g. Tests 1–5, with the exception of test 3, showed consistently the same range of values with time. Test 3 started consistent, but then within the last quarter of the test, acceleration values increased to around +/– 391 g.

The aggregate pier with 2 foot lift had very small acceleration values relative to all the tests from all field studies. Test 6 showed a range of –56 g to 42 g, while test 12 showed a range of –22 g to 20 g.

Test 12 was process by acceleration analysis A, as shown in Figure 86. The plot shows a minimum downward deformation of approximately 8 in., but a maximum upward deformation of over 50 in. However, this is physically impossible as the research team saw

the RAM Test move in to the ground at least a foot as it was buried by the aggregate as shown in Figure 87. The other Hampton tests were not processed because of the test 12 results and because this study included no verification data to compare values.

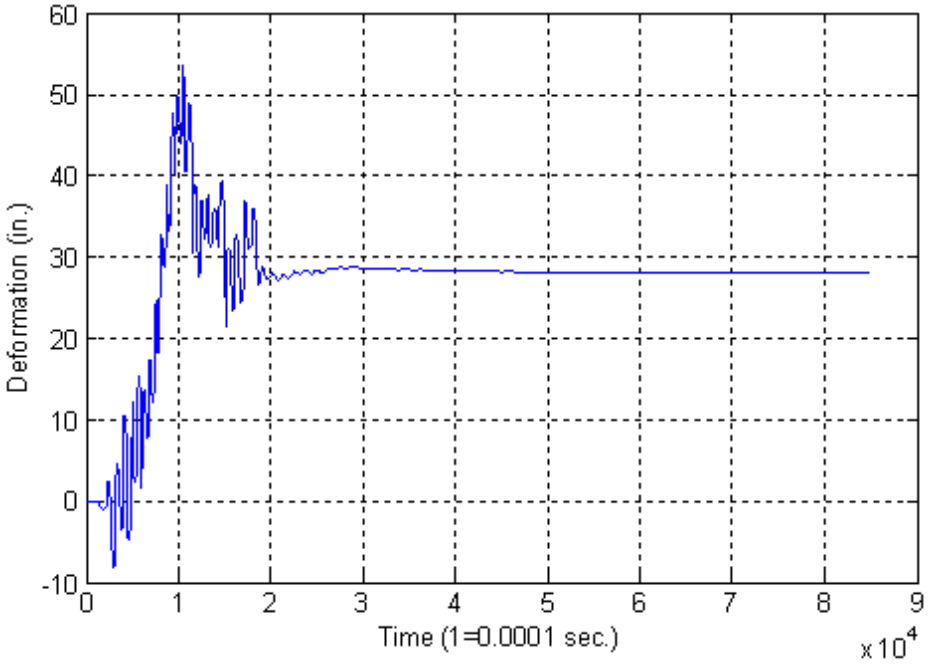


**Figure 86. Hampton test 12 deformation time-history**

**Figure 87. The RAM Test plate buried during testing**

**La Port City acceleration results**

The RAM Tests showed both consistent acceleration time-histories, and also inconsistent acceleration time-histories. The road gravel pier, pier 1 (tests 1–10) exhibited consistent behavior. The acceleration values did not appear to behave differently between test layers 1 to 3. Tests 12–14 on the sand pier, pier 2 exhibited peculiarly. The maximum acceleration values were high at the start of the test, and then decreased after the first 5 impacts, as shown in Figure 88. The behavior is peculiar because normally accelerations will either increase with time, or stay consistently the same value with time. All the tests from the clean aggregate pier, pier 3, and the pier with the concrete cap, pier 4, exhibited much different than what is typically seen. The accelerations showed only positive acceleration values, such as test 36, where the values were between 0 and 53 g, as shown in Figure 89. A sensor may have become disconnected but there is no proof of that occurring.

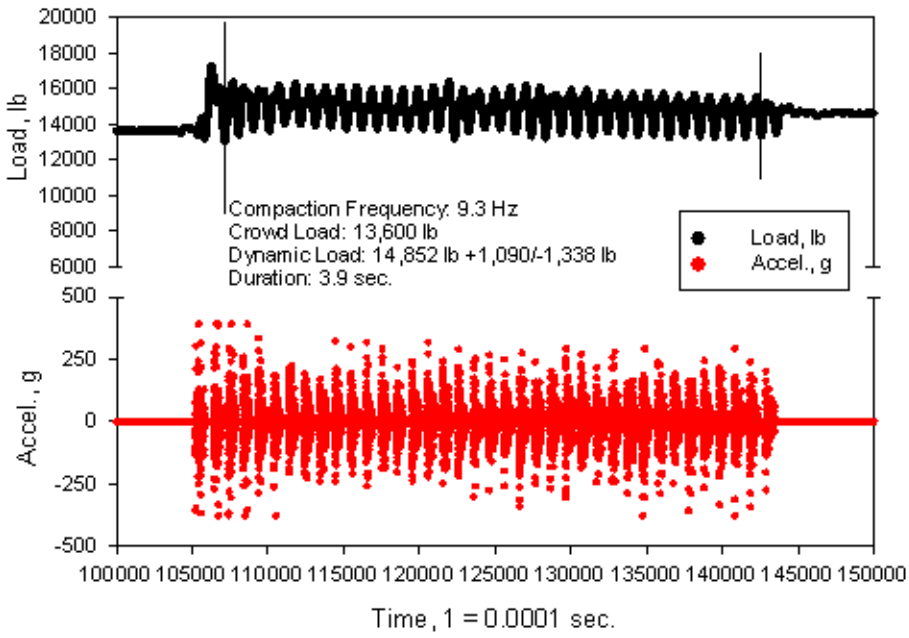


**Figure 88. La Port City test 12, example of the maximum acceleration values at the start of the test**

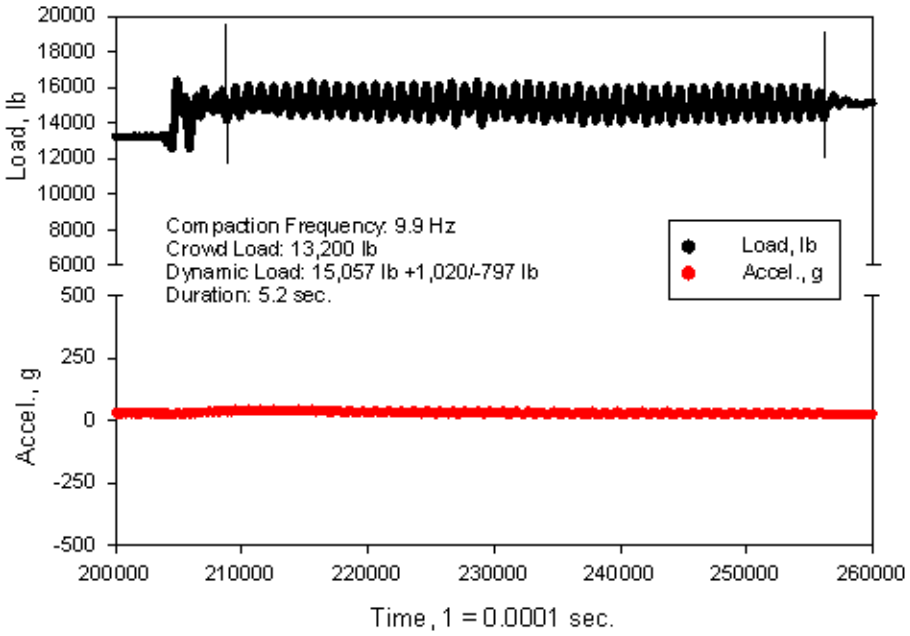


**Figure 89. La Port City test 36, example of the positive acceleration values**

Time-histories from pier 1 were analyzed by acceleration analysis A, and the results shown in

Table 22. Tests 1 through 7 showed similar results. The range stayed fairly consistent around –/+250 g. This is reflected by the deformation results being around or less than 2 in. Tests 8 through 10 reached the maximum acceleration value of +/–392 g, and those results are reflected by the deformations being relatively large, greater than 4 in. Figure 90 and Figure 91 demonstrate the typical deformation plots from pier 1. The deformations consistently decreased with time until the end of the test. The higher the acceleration values, the higher the resultant deformation.

**Table 22. La Port City acceleration analysis A deformation results**

| Test | Analysis A δ (in.) |
|---|---|
| 1 | -1.327 |
| 2 | -1.016 |
| 3 | -0.337 |
| 4 | -1.609 |
| 5 | -1.435 |
| 6 | -2.145 |
| 7 | -0.675 |

| Test | Analysis A δ (in.) |
|---|---|
| 8 | -8.089 |
| 9 | -5.537 |
| 10 | -4.446 |

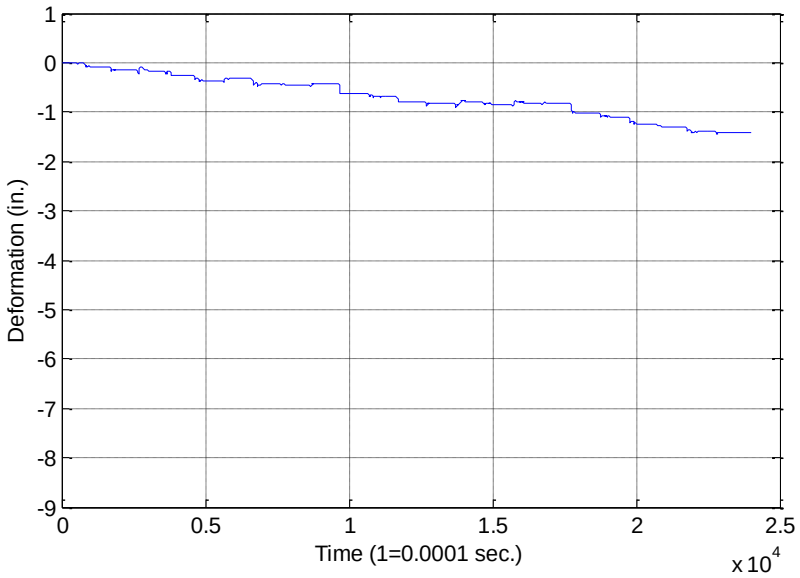


**Figure 90. La Port City test 5 deformation plot**

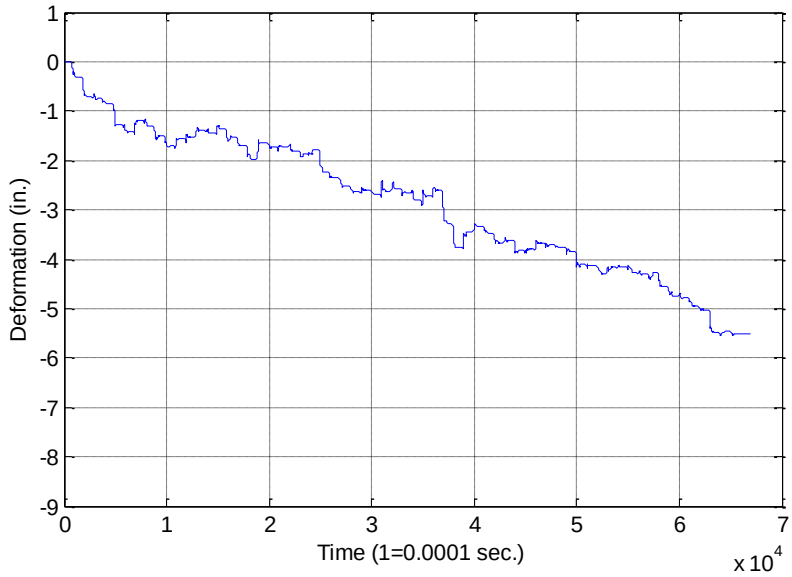


**Figure 91. La Port City test 9 deformation plot**

**Fairfield acceleration results**

The RAM Tests showed consistent acceleration time-histories. Pier 1 was a finished pier used to determine whether to conduct the rest of the tests with the rubber buffer pad or

without it. Test 1 (Figure 92) showed the acceleration values reach the peak value of 392 g across the whole time-history, while tests 2 (Figure 93) and 3 showed acceleration values vary with time and the values did not reach the peak value of 392 g consistently. The results of tests 1 through 3 were used to make the decision to leave the buffer pad on while conducting the rest of the tests.

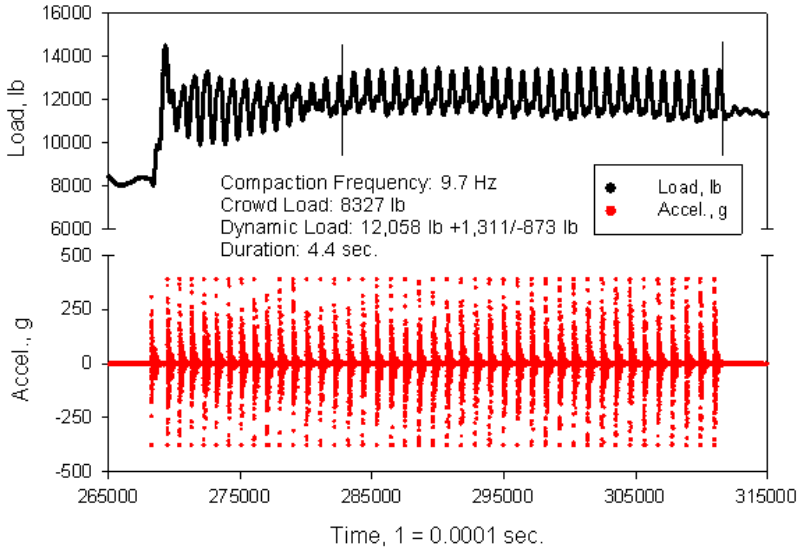


**Figure 92. Fairfield test 1 without the buffer pad**

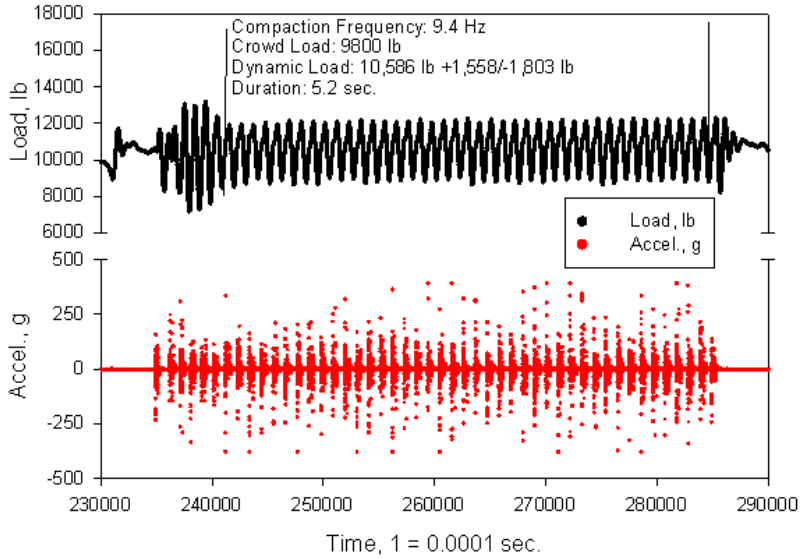


**Figure 93. Fairfield test 2 with the buffer pad**

Pier 2 exhibited consistent acceleration time-histories. The main difference was between the pre compacted lift and the post compacted lift. The pre compacted lift accelerations were more erratic but still showed similar ranges as shown in Figure 94 and Figure 95. However, the test layer did not appear to influence the behavior greatly.

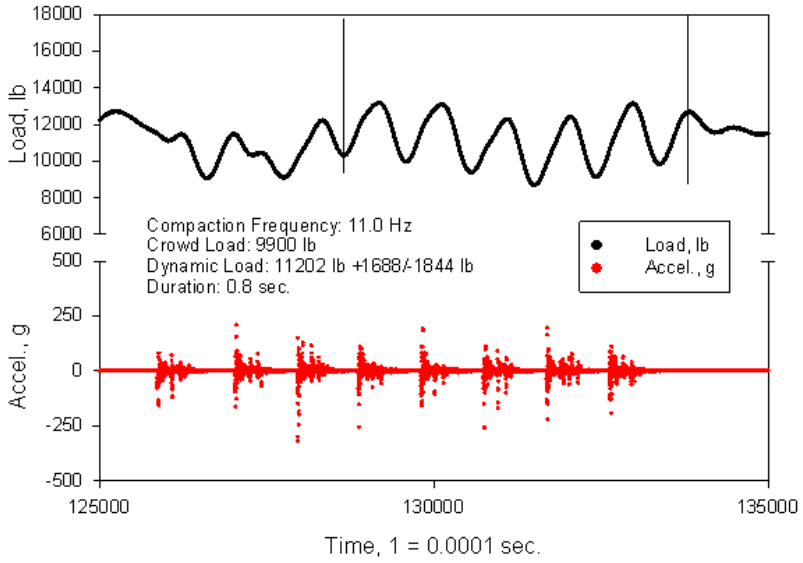


**Figure 94. Fairfield test 12 pre compacted lift**

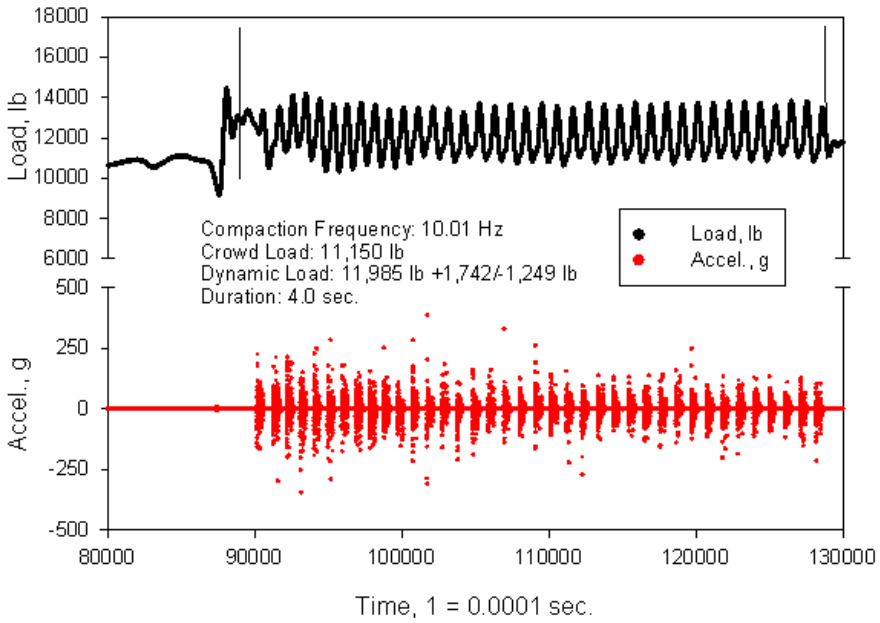


**Figure 95. Fairfield test 13 post compacted lift**

Pier 3 exhibited consistent acceleration time-histories. The tests were conducted on the matrix soil, and saw acceleration ranges similar to pier 1. The main difference of the accelerations is that it appears the length of the acceleration that one compaction impact influenced is longer. In test 19, accelerations last about 0.07 seconds per impact, while in test 13 accelerations last about 0.05 seconds per impact. This may be caused by the erratic behavior of test 19 as compared to test 13.

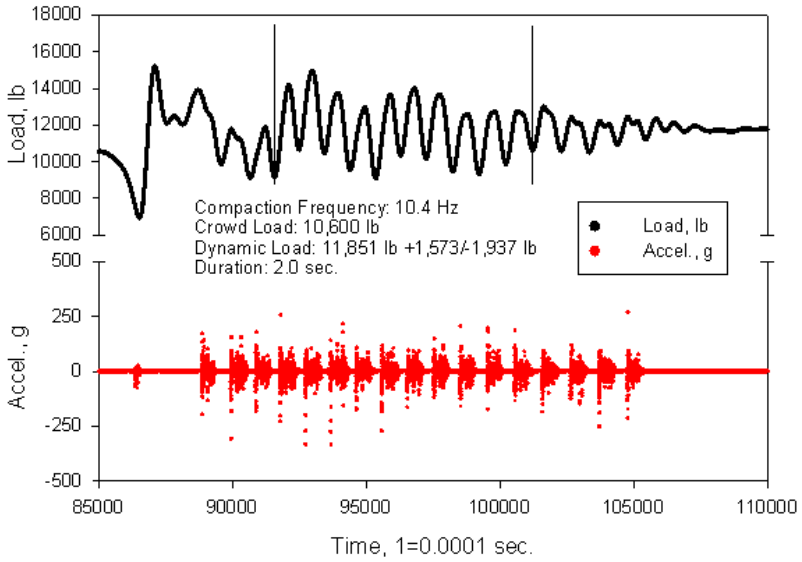


**Figure 96. Fairfield test 19**

Acceleration analysis A was used to process the Fairfield data. The deformation results are presented in Table 23. Fairfield acceleration analysis A deformation results The table shows the results for the top test layers of piers 2 and 4. Overall, they appear to be reasonable results with the exception of tests 21 to 23. Tests 21 and 23 seem high; however, verification did not work at Fairfield to confirm the results. Also, the accelerations reached +/ 392 consistently for the whole time-history which may suggest the acceleration maxed its capability.

**Table 23. Fairfield acceleration analysis A deformation results**

| Test | Analysis A δ (in.) |
|---|---|
| 13 | -2.058 |
| 14 | -0.8469 |
| 15 | -1.3837 |

| Test | Analysis A δ (in.) |
|---|---|
| 20 | -2.2094 |
| 21 | -9.0015 |
| 22 | -3.863 |
| 23 | -5.772 |
| 24 | -1.6830 |

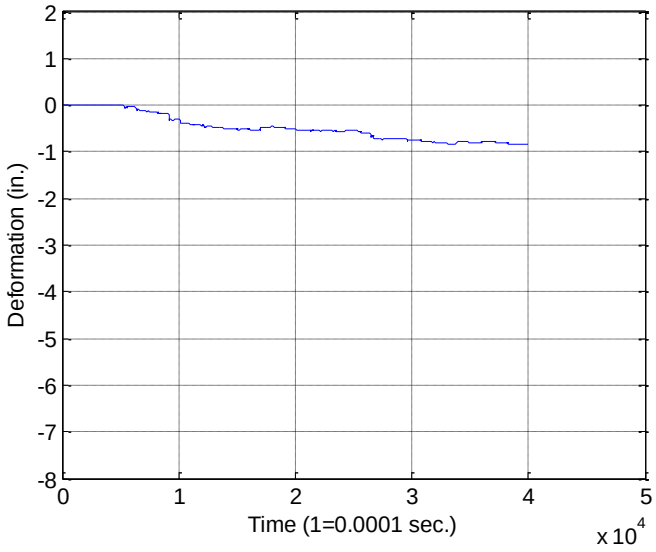


**Figure 97. Fairfield test 14, expected time-history**

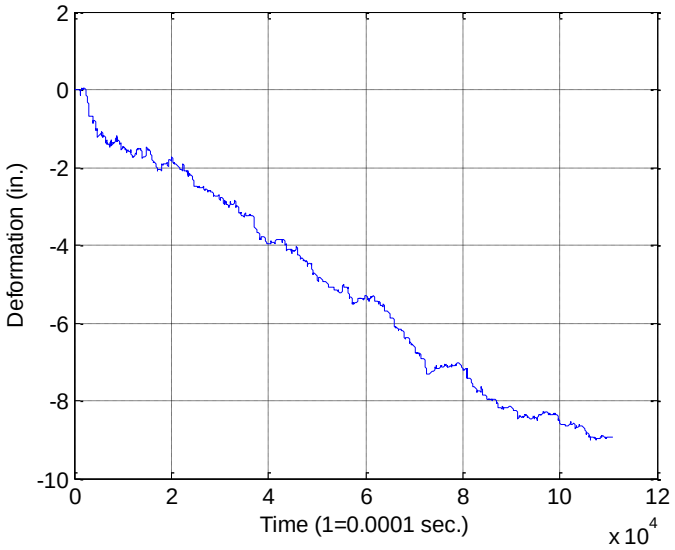


**Figure 98. Fairfield test 21, high deformation time-history**

**Council Bluffs acceleration results**

The RAM Tests showed consistent acceleration time-histories. Pier 1 tests (tests 611) were taken on the top test layer with the different plate sizes, and it was not until test 9 when the accelerations reached the peak value of +/ 392 g. It does not appear the plate size affects the behavior. The length of compaction time appears to affect the behavior more; test 9 was 19.4 seconds and was recorded after three tests already compacted the pier. The difference in the accelerations between the first test and last test on pier 1 is shown in Figure 99 and Figure 100. Test 6 does occasionally reached the peak value, however test 11 consistently reached the peak value.

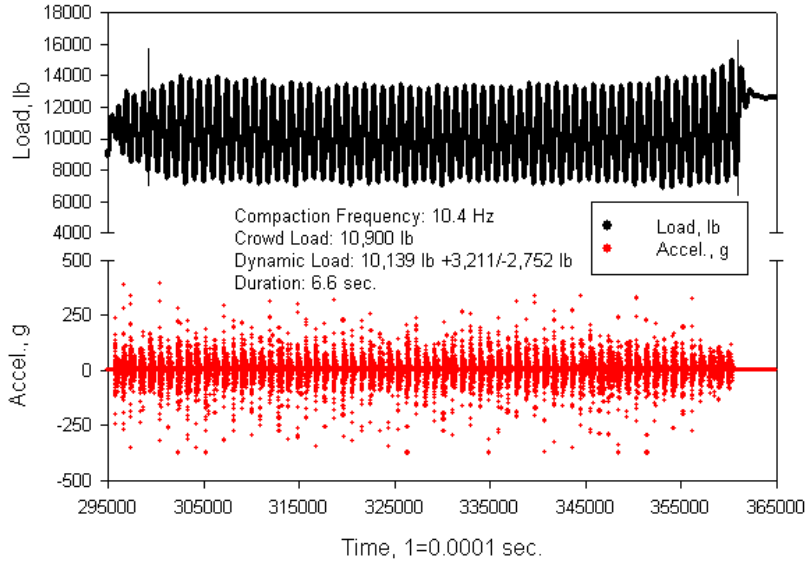


**Figure 99. Council Bluffs test 6, first test on pier 1**

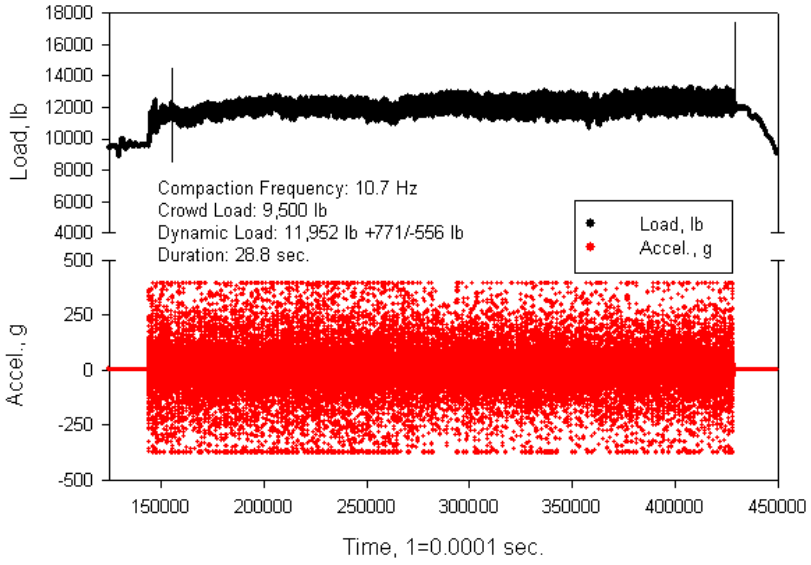


**Figure 100. Council Bluffs test 11, last test on pier 1**

Pier 2 (tests 12 and 16) consistently reached the peak value of +/ 392 g. Both tests were recorded on the 18 in. plate, but on two different test layers. The acceleration values reached the peak value, but more consistently in test 16. Figure 101 represents what the accelerations are in test 12 and 16.

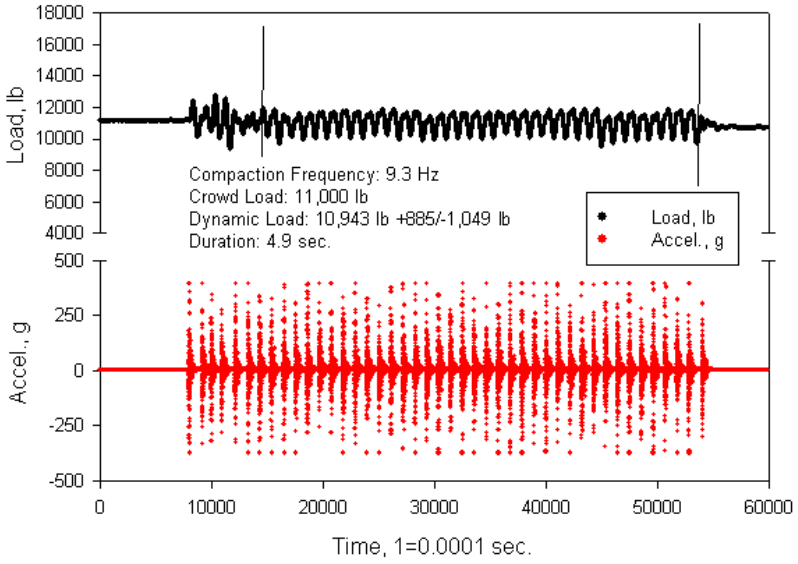


**Figure 101. Council Bluffs test 16.3**

Pier 3 (tests 17,19, 20) reached the peak value of +/–392 g, but not consistently. The tests were recorded on the 18 in. plate, but on four different test layers. Test 21 consistently

reached the peak value, but tests 17 and 19 did not. The maximum values increased with each segment for tests 17 and 18, but decreased with each segment for test 19. The acceleration changes for test 17 is shown in Figure 102 through Figure 105.

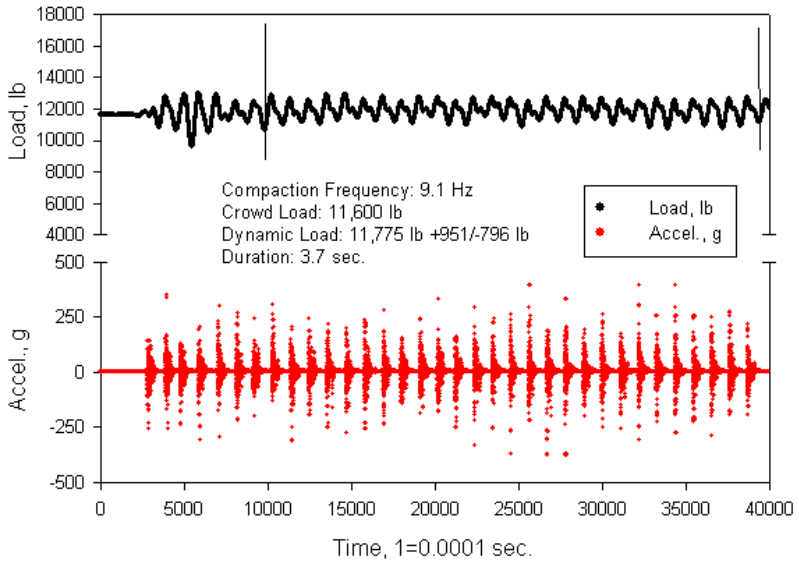


**Figure 102. Council Bluffs test 17 segment 1**

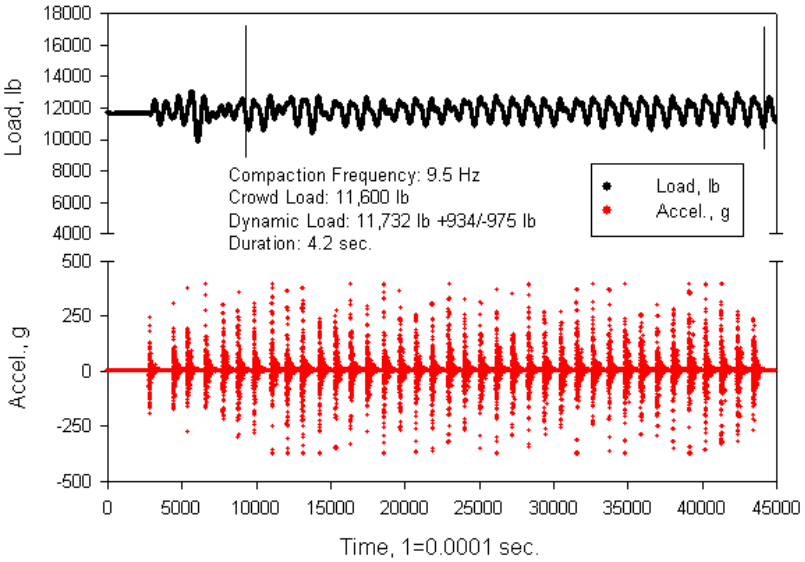


**Figure 103. Council Bluffs test 17 segment 2**

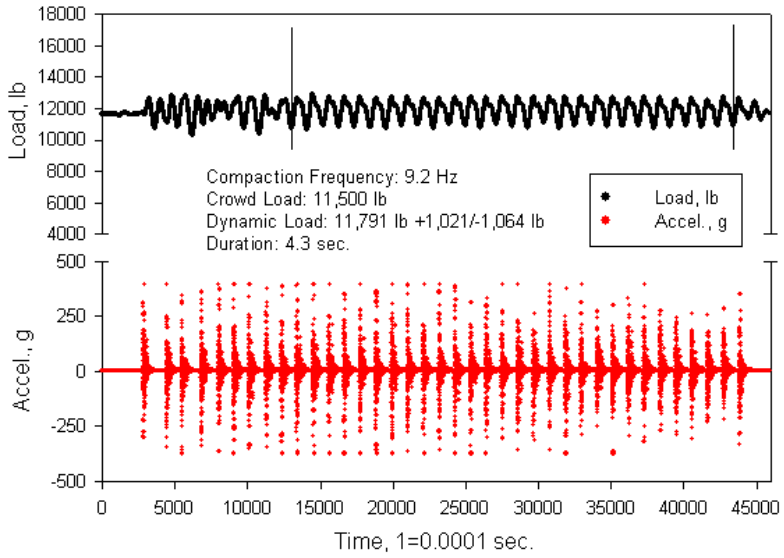


**Figure 104. Council Bluffs test 17 segment 3**

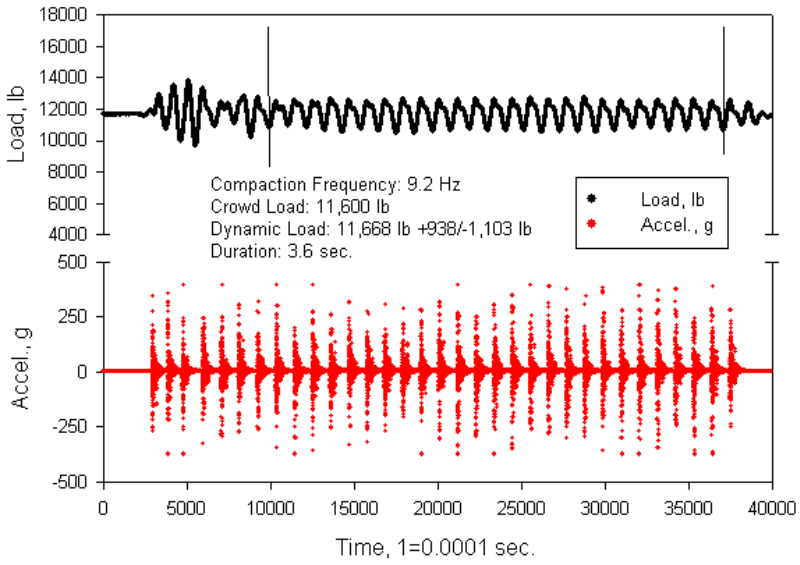


**Figure 105. Council Bluffs test 17 segment 4**

The acceleration data from Council Bluffs were processed by acceleration analysis A and B.

*Acceleration Analysis A*

All of the compaction impacts were processed for acceleration analysis A. The deformations obtained are summarized in Table 24. The deformation time-histories produced

appeared to be reasonable. There was continuous accumulation of deformation with time, for example, test 6 in Figure 106.

**Table 24. Results of deformation by analysis A from Council Bluffs, with BST as a means for comparison**

| Test | Analysis A δ (in.) |
|---|---|
| 6 | -2.8 |
| 7 | -3.2 |
| 8 | -2.6 |
| 9 | -6.89 |
| 10 | -5.23 |
| 11 | -7.17 |
| 12 | -1.31 |
| 16 | -2.12 |
| 17 | -0.72 |
| 18 | -0.66 |
| 19 | -1.86 |
| 21 | -2.21 |

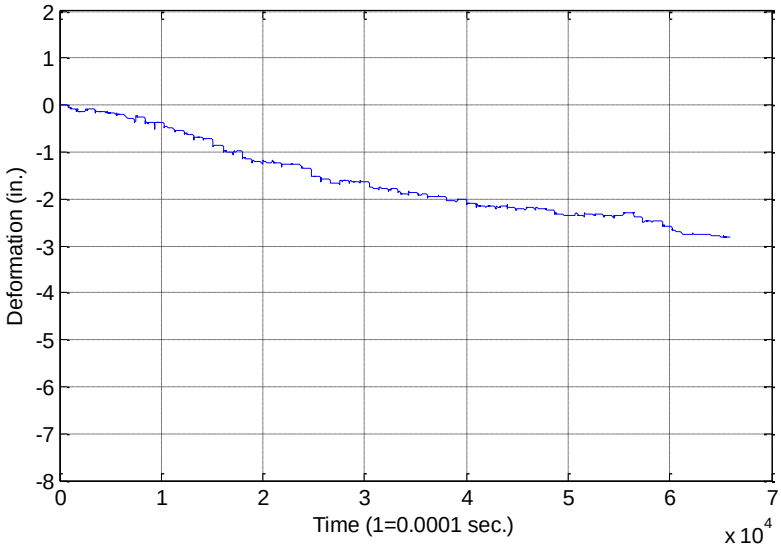


**Figure 106. Council Bluffs test 6 acceleration analysis A deformation time-history**

*Acceleration Analysis B*

Acceleration analysis B looks at just the last compaction impact. The deformations obtained are summarized in Table 25. The deformations obtained showed smaller values than the values from analysis A. This is expected since acceleration analysis B is the deformation

from one compaction impact, while acceleration analysis A can consist of up to 60 compaction impacts. Tests 7, 8, 9, 11, 16, and 19 exhibited behavior as expected, continuous downward movement with time. Tests 10, 12, and 18 did not exhibit behavior as expected, they moved upward with time. The tests that did behave as expected and the tests that did not behave as expected did not have any distinguishable differences. The deformation time-history plots are shown in Figure 107.

**Table 25. Results for deformation by analysis B for Council Bluffs**

| Test | Analysis B δ (in.) |
|---|---|
| 6 | -0.0253 |
| 7 | -0.0825 |
| 8 | -0.0720 |
| 9 | -0.0691 |
| 10 | 0.005732 |
| 11 | -0.2369 |
| 12 | -0.0100 |
| 16 | -0.1939 |
| 17 | -0.1145 |
| 18 | -0.00547 |
| 19 | -0.1427 |
| 21 | -0.00220 |

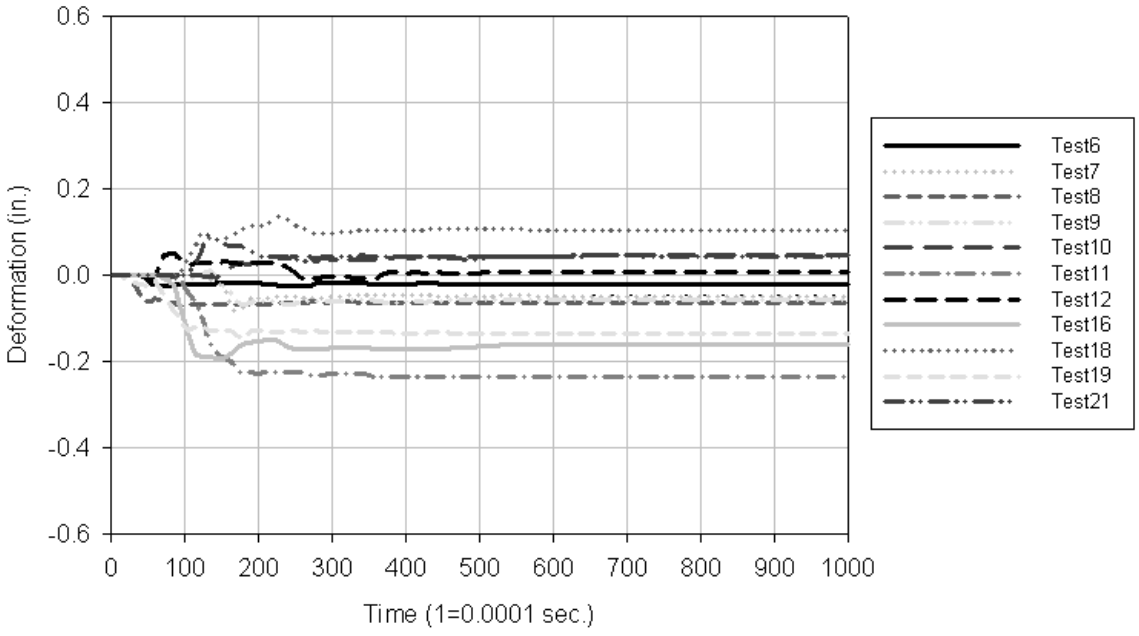


**Figure 107. Council Bluffs acceleration analysis B deformation time-histories**

**Oskaloosa acceleration results**

The RAM Tests showed consistent acceleration time-histories. Pier 1 consistently exhibited a large range of accelerations reaching +/–392 g. The differences in acceleration between plate sizes were not discernible. Test 5.1, in Figure 108, represents what typical accelerations were from pier 1.

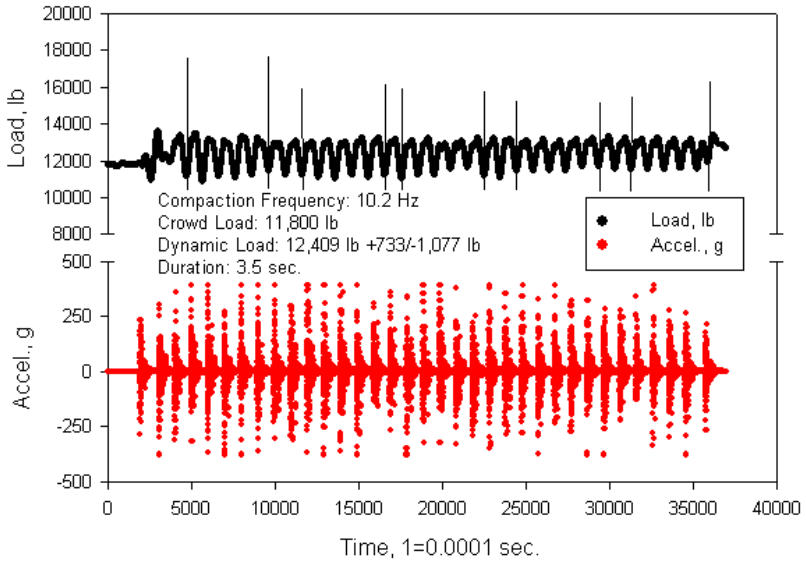


**Figure 108. Oskaloosa test 5.1 on 9 in. steel plate**

Pier 2 exhibited a large range of accelerations reaching +/–392 g, but not as consistent as pier 1. Test 7 appeared to have more erratic accelerations, as shown in Figure 109. The gap between acceleration peaks is not as distinguishable as the other tests.

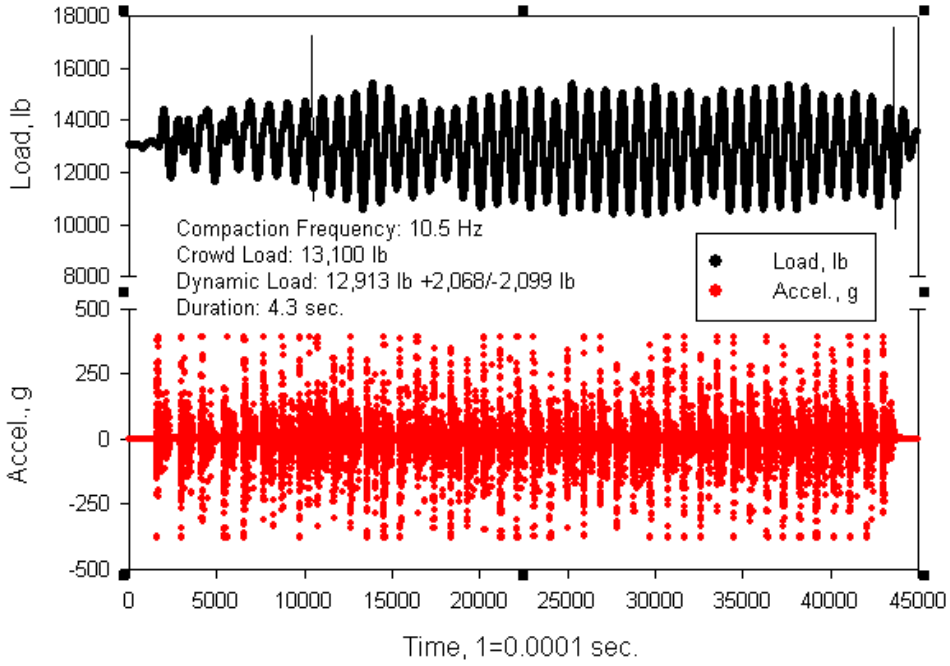


**Figure 109. Oskaloosa test 7 erratic accelerations**

Pier 3 exhibited ranges reaching +/–392 g, but not until the second test on the pier. Test11 reached the range of +/–392 g, but not consistently like tests 12 through 15.

The acceleration data from Oskaloosa was processed by analysis A, B, C, and D. The minimum deformation was recorded for each process, unless otherwise noted.

*Acceleration Analysis A*

Acceleration Analysis A was performed on all segments from each test. The deformations from all the segments were summed and also averaged to represent each test. The analysis started with an investigation into the effect of the arbitrary value of 5 g in the acceleration analysis software code. If an acceleration value is less than 5 g, it is excluded from further integration. The values of 7.5 g and 10 g were substituted for the value of 5 g, and the data was processed for the top test layer of pier 1and the results are shown in Table 26. Comparison of deformation values for acceleration values greater than 5, 7.5, and 10 g The results are from summing all the individual segments within the test. The effect of this value is as follows: all the deformations decreased from 5 g to 7.5 g, and then tests 2 and 4 increased from 7.5 g to 10 g, while tests 3 and 5 decreased from 7.5 g to 10 g.

**Table 26. Comparison of deformation values for acceleration values greater than 5, 7.5,**

**and 10 g**

| Test | Analysis A δ (in.) > 5 g | Analysis A δ (in.) > 7.5 g | Analysis A δ (in.) > 10 g |
|---|---|---|---|
| 2 | -4.168 | -1.263 | -1.328 |
| 3 | -8.171 | -6.354 | -5.485 |
| 4 | -4.331 | -1.072 | -1.67 |
| 5 | -4.701 | -2.914 | -2.084 |

After the investigation on the effect of the arbitrary value of 5 was complete, an investigation into summing or averaging the individual segments to represent a test was done on the same four tests. The results are shown in Table 27. A significant difference exists between the average and sum of the deformations. The purpose of acceleration analysis A is to see the deformation from all of the compaction impacts, therefore, summing the segments stayed as the primary practice.

**Table 27. Summary of deformations (in.) from segments 1 to 4 for tests 2 to 5 and the resultant average and sum**

| Test | Segment 1 | Segment 2 | Segment 3 | Segment 4 | Average | Sum |
|---|---|---|---|---|---|---|
| 2 | -0.10 | -0.66 | -3.41 | n/a | -1.389 | -4.168 |
| 3 | -3.57 | -1.91 | -2.69 | n/a | -2.724 | -8.171 |
| 4 | -0.34 | -1.51 | -1.68 | -0.79 | -1.083 | -4.331 |
| 5 | -2 | -0.8 | -0.1 | -1.8 | -1.175 | -4.701 |

The results for acceleration analysis A was completed with accelerations excluded under 5 g, and the segments summed to get the total deformation for each test. The results are shown in Table 28. The results are higher than expected, therefore, integration of all the compaction impacts may not be the best approach or the value of 5 in the code needs to be analyzed more.

**Table 28. Results of analysis A deformation from Oskaloosa**

| Test | Analysis A δ (in.) > 5 g |
|---|---|
| 1 | -3.428 |
| 2 | -4.168 |
| 3 | -8.171 |
| 4 | -4.331 |
| 5 | -4.701 |
| 6 | -4.17 |

| Test | Analysis A δ (in.) > 5 g |
|---|---|
| 7 | -10.9 |
| 8 | -1.87 |
| 9 | -3.78 |
| 10 | -3.71 |
| 11 | -8.76 |
| 12 | -8.72 |
| 13 | -8.02 |
| 14 | -3.35 |
| 15 | -4.96 |

*Acceleration Analysis B*

Acceleration analysis B evaluates the deformation of the last compaction impact of the last segment and the results are summarized in Table 29. The results are generally closer to what is expected. The time-histories for pier 1 through 3 are plotted in Figure 110 to Figure 112. Like Council Bluffs results, there are time-histories that show the pier moving out of the ground. Some of the positive deformations are minimal, but these results are not typical and are not what is expected. The time-histories that behaved as expected decrease with time and plateau by the end of the time. There does not appear to be any distinguishable behavior between the tests that did and did not behave as expected.

**Table 29. Results of acceleration analysis B deformation from Oskaloosa**

| Test | Analysis B δ (in.) |
|---|---|
| 1 | -0.25 |
| 2 | -0.15 |
| 3 | -0.051 |
| 4 | -0.10 |
| 5 | -0.021 |
| 6 | -0.047 |
| 7 | -0.3239 |
| 8 | -0.0910 |
| 9 | -0.0025 |
| 10 | -0.12 |
| 11 | -0.027 |
| 12 | -0.22 |
| 13 | -0.033 |
| 14 | -0.0092 |
| 15 | -0.10 |

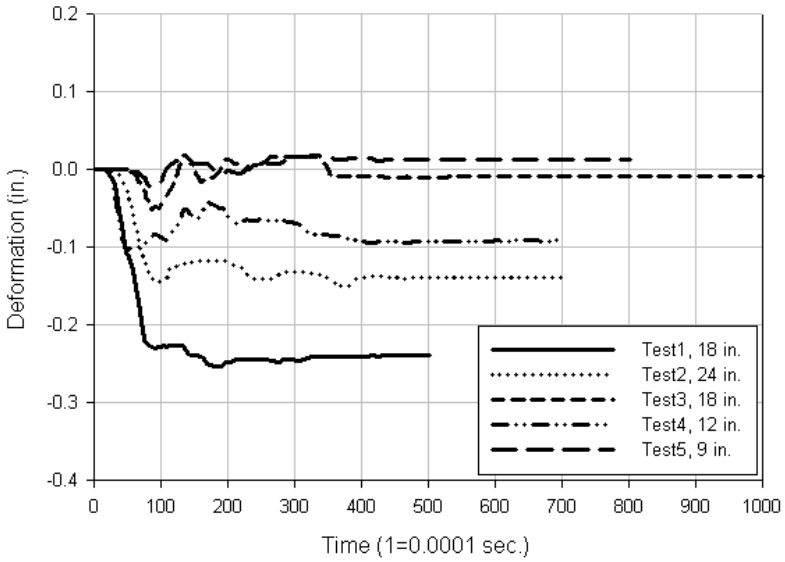


**Figure 110. Oskaloosa pier 1 acceleration analysis B time-histories**

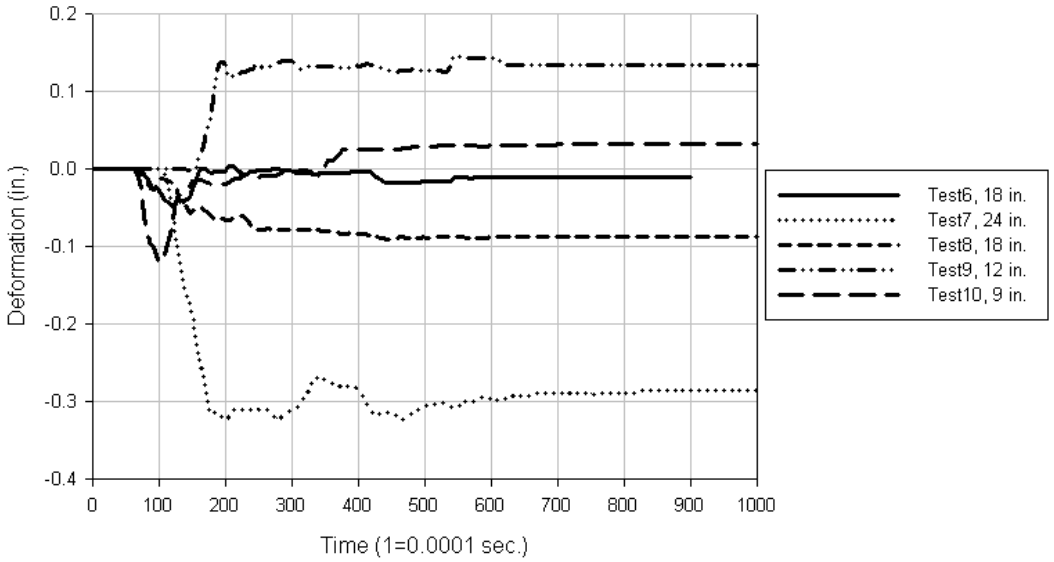


**Figure 111. Oskaloosa pier 2 acceleration analysis B time-histories**

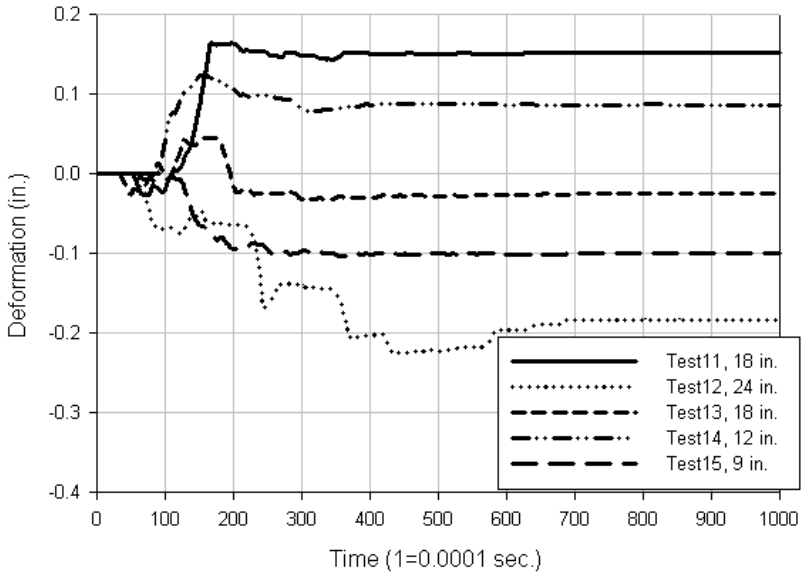


**Figure 112. Oskaloosa pier 3 acceleration analysis B time-histories**

*Acceleration Analysis C*

Acceleration analysis C deformations include the 6$^{th}$ to 10$^{th}$ compaction impacts of the last segment. To help decide on which segment to focus the analyses, test 2 segments 1 through 3 were processed and results compared, shown in Table 30. Test 2 summary of Oskaloosa analysis C deformations (in.) The results showed that as the segments progress as the deformation increases. The last segment deformation appeared to be most reasonable; therefore the last segment of a test was chosen to further analyze the tests.

**Table 30. Test 2 summary of Oskaloosa analysis C deformations (in.)**

| Test 2 Segment | Compaction Impact δ (in.) | | | | | Average |
|---|---|---|---|---|---|---|
| | 6 | 7 | 8 | 9 | 10 | δ (in.) |
| 1 | -0.0042 | -0.012 | -0.037 | -0.011 | -0.026 | -0.018 |
| 2 | -0.019 | -0.096 | -0.18 | -0.042 | -0.037 | -0.075 |
| 3 | -0.43 | -0.24 | -0.38 | -0.05 | -0.036 | -0.23 |

Deformations were noted three ways, the minimum deformation value, the deformation at the end of the time-history, and the deformation associated with the peak load. Within one test, the minimum value can be negative while the end deformation can be positive, such as test 4 in Table 31. Large discrepancies existed between deformations; however, the minimum deformation value was the focus of this research because the goal is evaluating how much the pier can deform. The time-histories of acceleration analysis C deformations are shown in

Figure 113 through Figure 118. All test 2 segments (24 in. steel plate) are plotted as these tests helped with the decision on which segment to process.

**Table 31. Differences in the deformation at the end of the time-history, and at minimum deformation within the time-history**

| Test | End δ (in.) | Min δ (in.) |
|---|---|---|
| 2 | -0.174 | -0.230 |
| 3 | -0.039 | -0.093 |
| 4 | 0.052 | -0.111 |
| 5 | -0.075 | -0.093 |

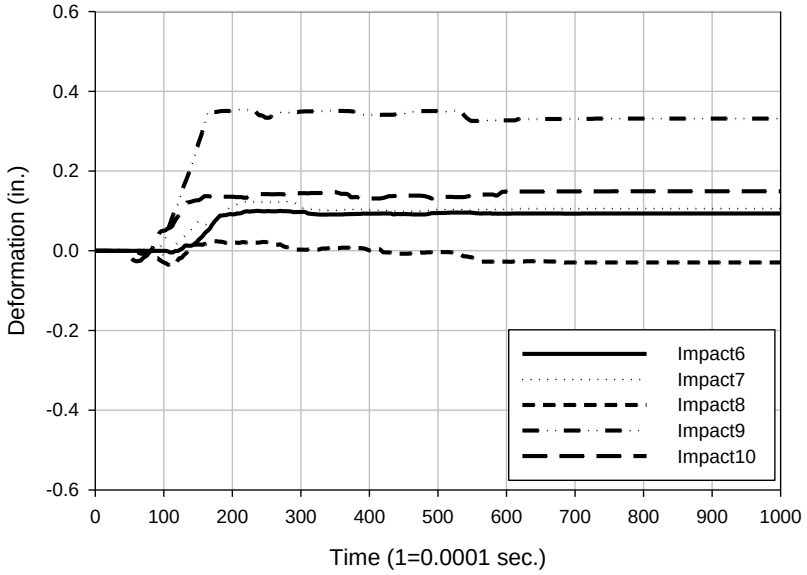


**Figure 113. Oskaloosa test 2 segment 1 acceleration analysis C**

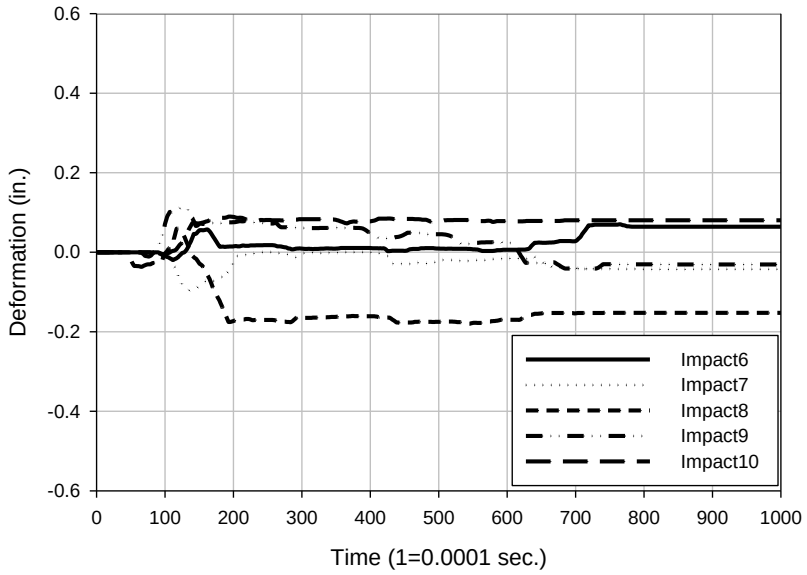


**Figure 114. Oskaloosa test 2 segment 2 acceleration analysis C**

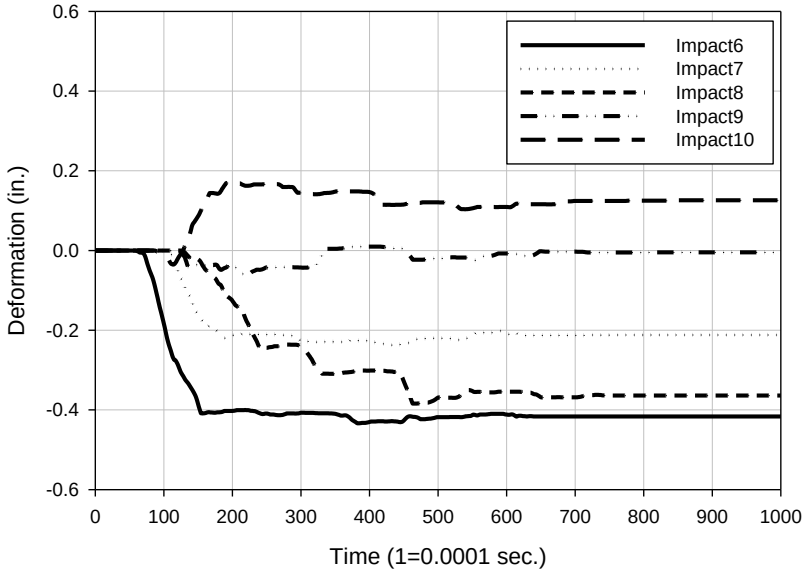


**Figure 115. Oskaloosa test 2 segment 3 acceleration analysis C**

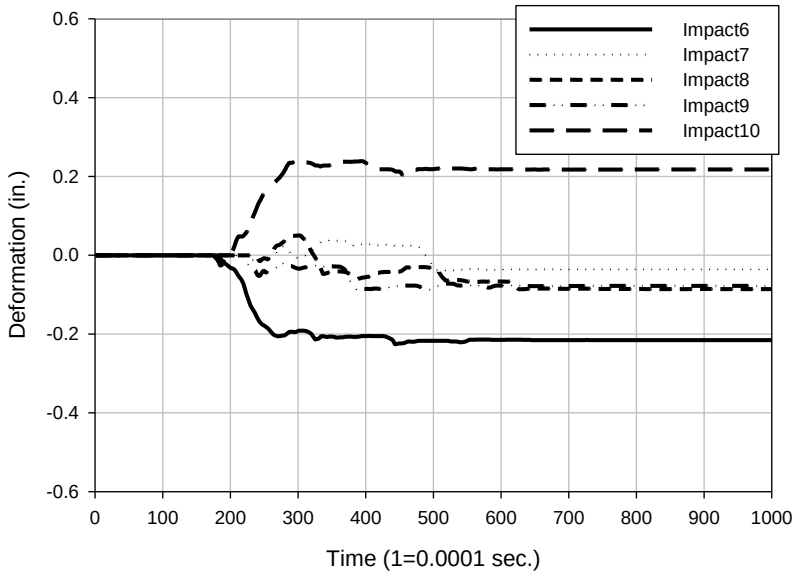


**Figure 116. Oskaloosa test 3 segment 3 acceleration analysis C**

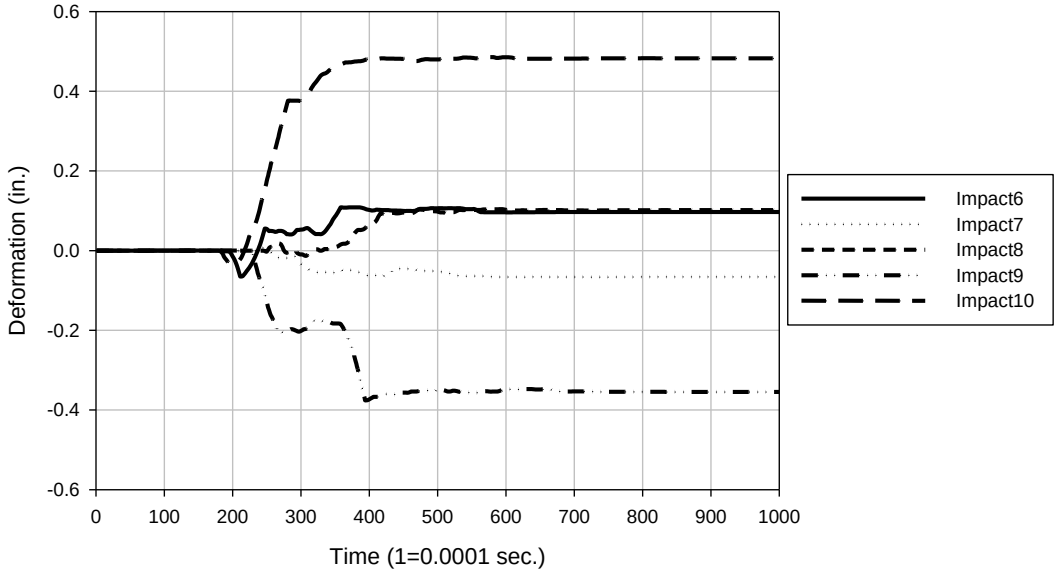


**Figure 117. Oskaloosa test 4 segment 4 acceleration analysis C**

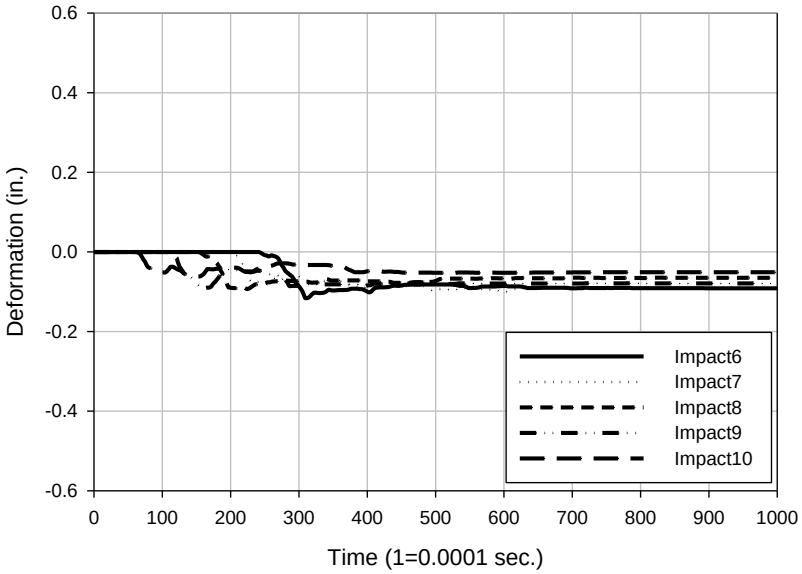


**Figure 118. Oskaloosa test 5 segment 4 acceleration analysis C**

*Acceleration Analysis D*

Acceleration analysis D evaluates the last five compaction impacts of the last segment. The results are summarized in Table 32. The results are relatively small. The time-histories of acceleration analysis D deformations are shown in Figure 119 through Figure 122. Like the other analyses, some time-histories show atypical upward movement, but the other tests show typical downward movement.

**Table 32. Summary of Oskaloosa analysis D deformations (in.)**

| Test | Analysis D δ (in.) |
|---|---|
| 2 | -0.064 |
| 3 | -0.112 |
| 4 | -0.059 |
| 5 | -0.095 |

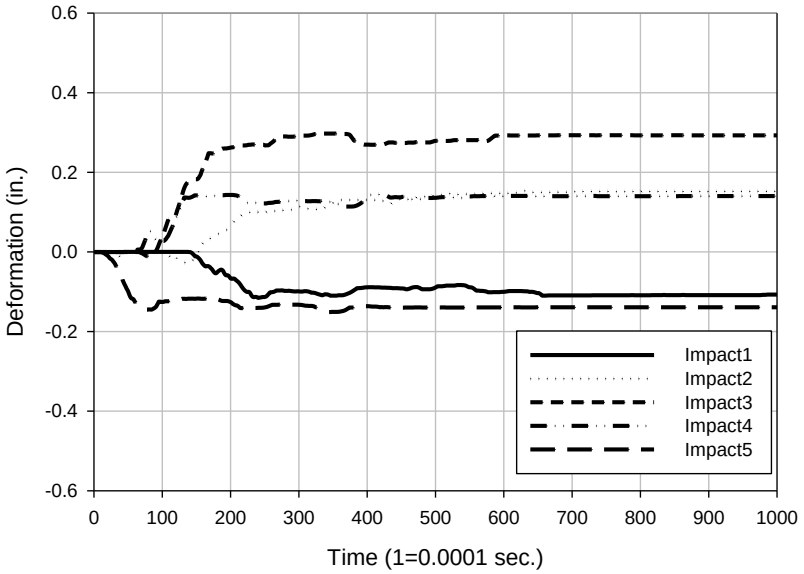


**Figure 119. Oskaloosa test 2 segment 3 acceleration analysis D**

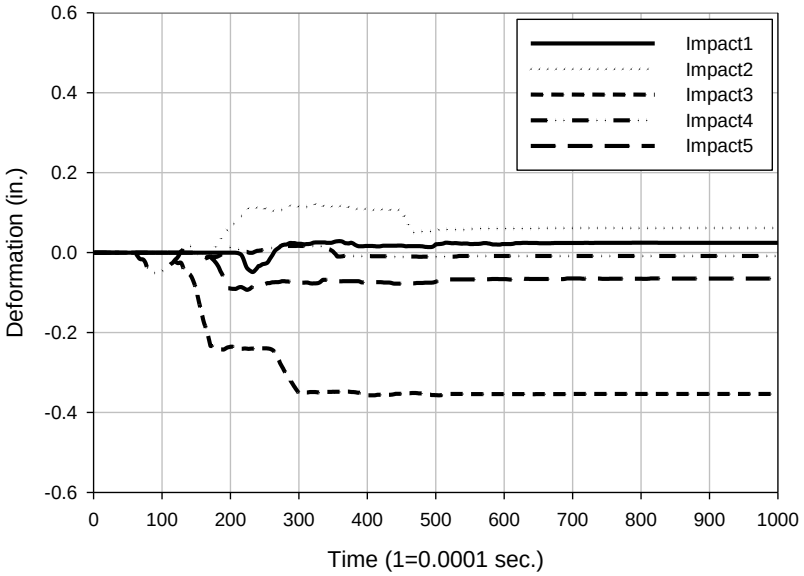


**Figure 120. Oskaloosa test 3 segment 3 acceleration analysis D**

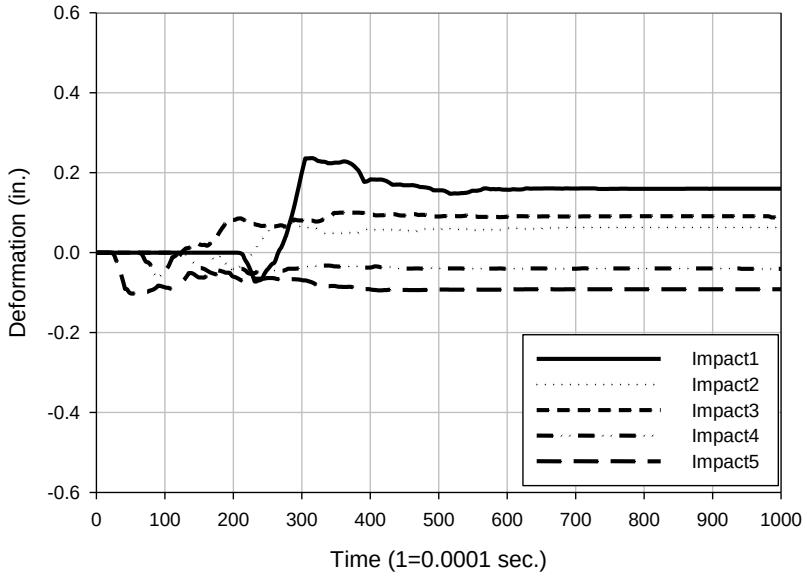


**Figure 121. Oskaloosa test 4 segment 4 acceleration analysis D**

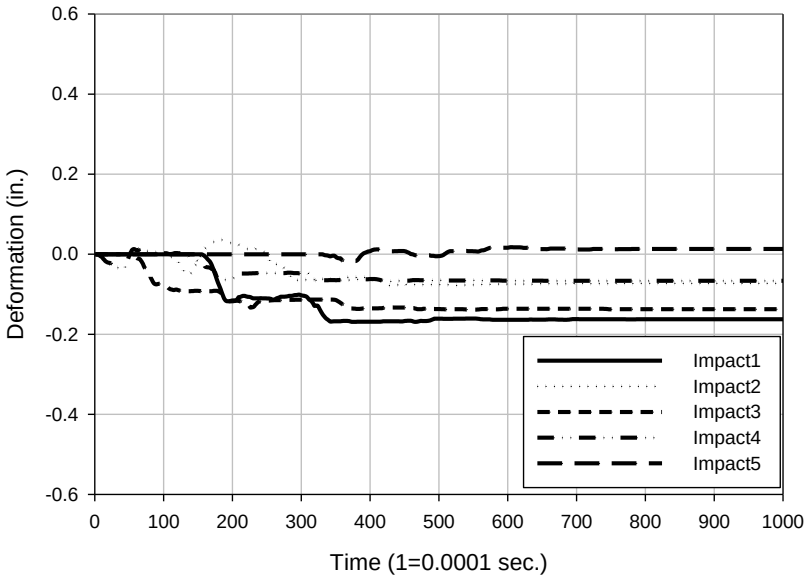


**Figure 122. Oskaloosa test 5 segment 4 acceleration analysis D**

A comparison of all the analyses along with verification, BST and modulus load test, results are shown in Table 33. The table shows a lot of discrepancies between deformation values. Some of the discrepancies in the analysis of acceleration may be explained by the:

- acceleration data consistently reached a maximum value of 391.29 g,
- acceleration analysis outcomes showed positive permanent deformation values, and

- The arbitrary value of 5 in the code that excludes the low acceleration values caused by background noise

Accelerometer 2 was installed to hopefully help solve issues with the same peak value recorded at multiple studies. And, the results will need to be discussed with the code developer in the future to determine the best changes to be made to produce more favorable results.

**Table 33. Comparison of deformation from all analyses for Oskaloosa**

| Test | Analysis A δ (in.) | Analysis B δ (in.) | Analysis C δ (in.) | Analysis D δ (in.) | BST δ (in.) | Modulus load test δ (in.) |
|---|---|---|---|---|---|---|
| 2 | -4.168 | -0.15 | -0.230 | -0.064 | -1.225 | -0.131 |
| 3 | -8.171 | -0.051 | -0.093 | -0.112 | -0.985 | -0.241 |
| 4 | -4.331 | -0.10 | -0.111 | -0.059 | -1.565 | -0.612 |
| 5 | -4.701 | -0.021 | -0.093 | -0.095 | -1.31 | – |

[1]The modulus load test did not reach an equivalent stress of test 5, therefore an equivalent deformation could not be evaluated

## Stiffness

The stiffness parameter is calculated by dividing the stress by the deformation found from the acceleration analysis software. The stress is calculated by taking the average load from the RAM Test divided by the area of the plate for each corresponding test.

### Hampton stiffness results

The stiffness parameters were not calculated at Hampton because there is no verification as a means for comparison, and the initial acceleration analysis resulted in physically impossible deformations.

### La Port City stiffness results

The stiffness parameters were calculated based on the RAM Test, and the modulus load test as a means for comparison. The plate sizes, average loads, stresses, acceleration analysis A deformations, acceleration analysis A stiffness, modulus load test deformations, and modulus load test stiffness are summarized for tests 8–10 in Table 34. Summary of stiffness' (pci) based on acceleration analysis A and modulus load test deformations for La Port CityThe deformations from the modulus load test were determined based on the RAM Test stress and the corresponding deformation from the modulus load test plot provided to the

research team. The acceleration analysis A stiffnesses are much smaller than the modulus load test stiffnesses. This is caused by the large deformations. Even when compared to the modulus load test stiffness at 100% design stress of 278 pci, the analysis A stiffness' are much smaller too. The plot of stress verses deformation is shown in Figure 123. The stress verse deformation exhibited the opposite behavior that is expected. With higher stress, higher deformation is expected; however, the plot shows higher deformations with lower stress. The order of the tests occurred from the smallest stress (24 in. plate) to the largest stress (9 in. plate) which is similar to the modulus load test where stresses increase during the duration of the test.

**Table 34. Summary of stiffness' (pci) based on acceleration analysis A and modulus load test deformations for La Port City**

| RAM test | Plate size (in.) | Average load (lb) | Stress (psf) | Analysis A Deformation (in.) | Analysis A Stiffness (pci) | Modulus load test deformation (in.) | Modulus load test Stiffness (pci) |
|---|---|---|---|---|---|---|---|
| 8 | 24 | 15,326 | 4,878 | -8.082 | 4 | -0.102 | 332 |
| 9 | 18 | 15,200 | 8,601 | -5.537 | 11 | -0.184 | 325 |
| 10 | 12 | 14,542 | 18,515 | -4.446 | 29 | -0.405 | 318 |

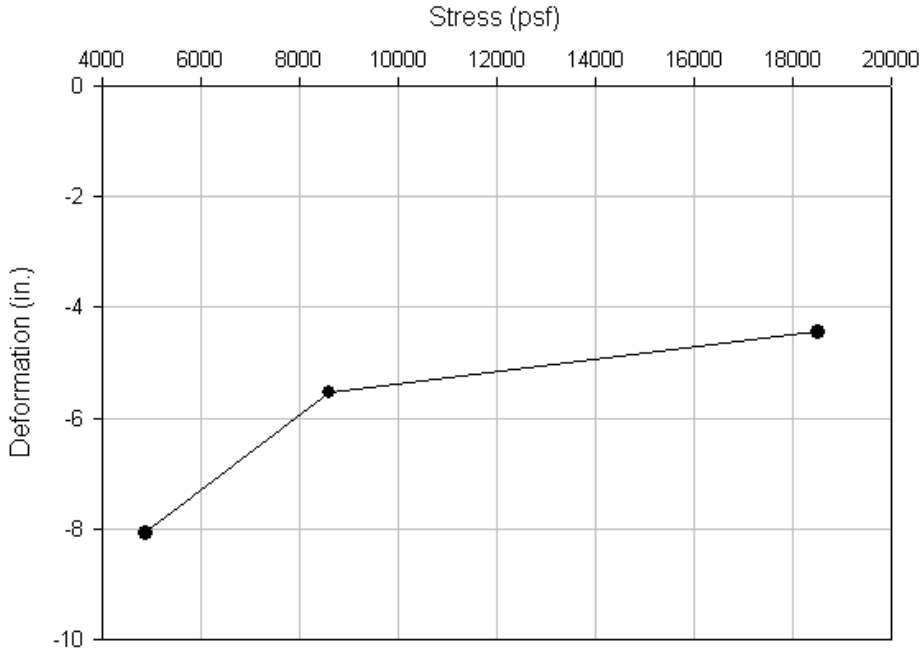


**Figure 123. La Port City pier 1 stress (psf) vs. deformation (in.) plot**

**Fairfield stiffness results**

The stiffness parameters were calculated based on the RAM Test. Verification did not work successfully, nor were modulus load test results provided as a means for comparison. The plate sizes, average loads, stresses, analysis A deformations, and analysis A stiffness parameters are summarized in Table 35. The plots of stress verses deformation for pier 1 and pier 2 are shown in Figure 124 and Figure 125. Like La Port City, Fairfield stress verses deformation plots exhibited opposite behavior as expected. The pier 1 plot increased then decreased with increasing stress. The pier 2 plot deformation decreased by 7.5 in. with an increase of stress. Without knowing the 100% design stress of the aggregate piers, it is difficult whether to comment if the stiffness parameters are reasonable.

**Table 35. Summary of stiffness (pci) based on acceleration analysis A for Fairfield**

| Test | Plate size (in.) | Average load (lb) | Stress (psf) | Analysis A δ (in.) | Analysis A Stiffness (pci) |
|---|---|---|---|---|---|
| 13 | 18 | 11,985 | 6782 | -2.058 | 23 |
| 14 | 12 | 12,470 | 15877 | -0.847 | 130 |
| 15 | 9 | 10,781 | 24403 | -1.384 | 122 |
| 20 | 24 | 13,200 | 3888 | -2.209 | 12 |
| 21 | 24 | 11,200 | 3565 | -9.002 | 3 |
| 22 | 18 | 11,100 | 6281 | -3.863 | 11 |
| 23 | 12 | 11,000 | 14006 | -5.772 | 17 |
| 24 | 9 | 10,600 | 23993 | -1.683 | 99 |

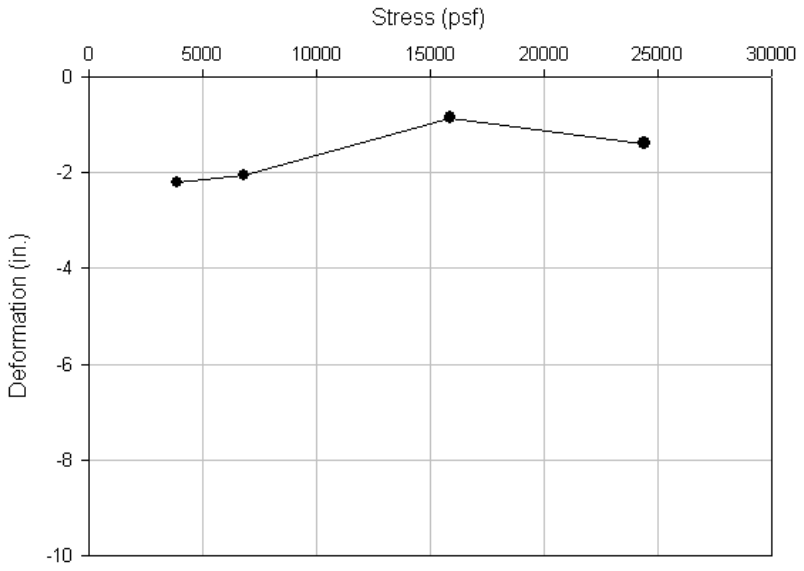


**Figure 124. Fairfield pier 1 stress (psf) vs. deformation (in.) plot**

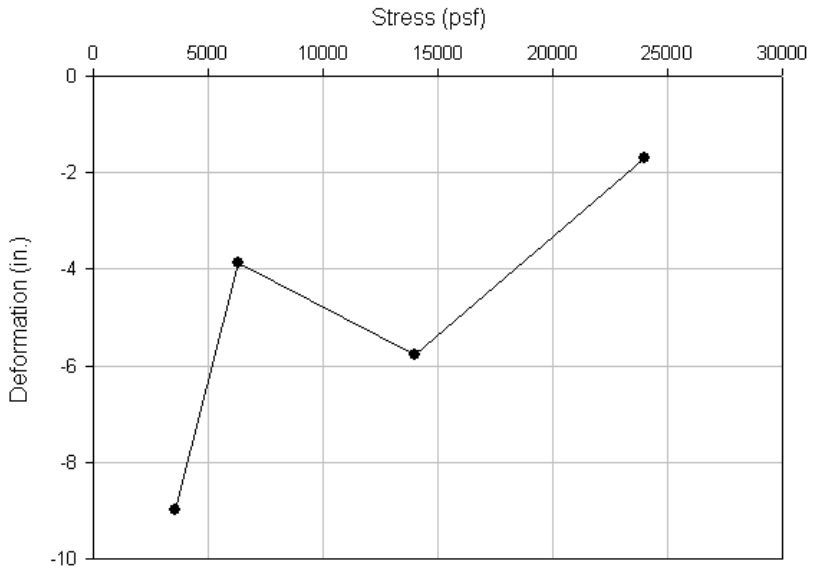


**Figure 125. Fairfield pier 2 stress (psf) vs. deformation (in.) plot**

**Council Bluffs stiffness results**

The stiffness parameters were calculated based on the RAM Test, and verification, BST and modulus load test, as a means for comparison. The plate sizes, stresses, BST, acceleration analysis A, acceleration analysis B, and modulus load test deformations are summarized in Table 36. The stress and deformations were then used to calculate the stiffness parameters. The deformations from the modulus load test were determined based on the RAM Test stress and the corresponding deformation from the modulus load test plot provided to the research team. The BST stiffness parameters were calculated based on the RAM Test stress. The results are summarized in Table 37. Pier 1 was the only pier with different plate sizes and is plotted in Figure 126. The deformations generally increase with increasing stress which is what is expected. However, the stiffness parameters for acceleration analysis A and B do not relate at all to the modulus load test stiffness parameters. The BST stiffness parameters are closer to the acceleration analysis A stiffness parameters but still exhibit differences.

**Table 36. Council Bluffs summary of stress (psf) and deformations (in.) of BST, acceleration analysis A and acceleration analysis B, and modulus load test**

| Test | Plate size (in.) | Stress (psf) | BST δ (in.) | Analysis A δ (in.) | Analysis B δ (in.) | Modulus load test δ (in.) |
|---|---|---|---|---|---|---|
| 6 | 24 | 3,909 | | -2.8 | -0.0253 | -0.036 |
| 7 | 24 | 6,625 | | -3.2 | -0.0825 | -0.099 |
| 8 | 18 | 15,139 | | -2.6 | -0.0720 | -0.443 |
| 9 | 24 | 5,039 | | -6.9 | -0.0691 | -0.062 |
| 10 | 18 | 6,225 | | -5.2 | 0.005732 | -0.089 |
| 11 | 12 | 15,139 | | -7.2 | -0.2369 | -0.443 |
| 12 | 18 | 5,039 | -3.64 | -5.3 | -0.0100 | -0.062 |
| 16 | 18 | 6,225 | -0.77 | -8.5 | -0.1939 | -0.089 |
| 17 | 18 | 6,644 | -2.43 | -2.9 | -0.1145 | -0.099 |
| 18 | 18 | 5,988 | -4.429 | -3.3 | -0.00547 | -0.084 |
| 19 | 18 | 6,650 | -2.715 | -7.4 | -0.1427 | -0.099 |
| 21 | 18 | 5,513 | -1.829 | -11.0 | -0.00220 | -0.073 |

**Table 37. Council Bluffs summary of stiffness parameters for BST, acceleration analysis A and B, and modulus load test**

| Test | BST stiffness (pci) | Analysis A stiffness (pci) | Analysis B stiffness (pci) | Modulus load test stiffness (pci) |
|---|---|---|---|---|
| 6 | – | 8 | 886 | 623 |
| 7 | – | 8 | 299 | 249 |
| 8 | – | 16 | 592 | 96 |
| 9 | – | 4 | 393 | 438 |
| 10 | – | 9 | 8,027 | 517 |
| 11 | – | 15 | 444 | 237 |
| 12 | 10 | 27 | 3,499 | 564 |
| 16 | 56 | 20 | 223 | 486 |
| 17 | 19 | 4 | 403 | 466 |
| 18 | 9 | 63 | 7,604 | 495 |
| 19 | 17 | 25 | 324 | 466 |
| 21 | 21 | 17 | 17,437 | 524 |

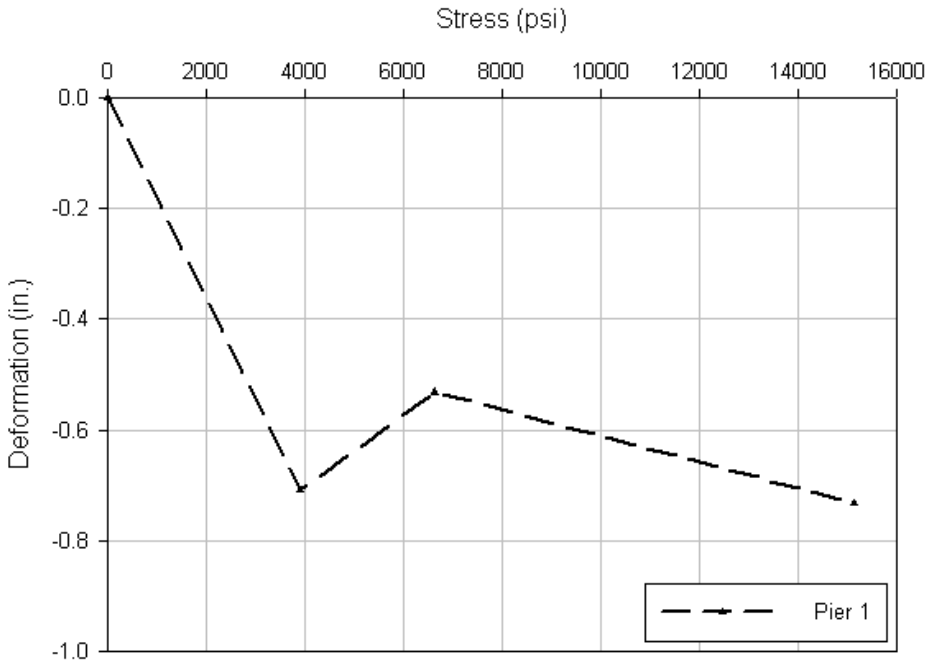


**Figure 126. Council Bluffs pier 1 stress (psf) vs. deformation (in.) plot**

**Oskaloosa stiffness results**

The stiffness parameters were calculated based on the RAM Test, and verification, BST and modulus load test, as a means for comparison. The deformations used to calculate the stiffness parameters are summarized in Table 39 The deformations from the modulus load test were determined based on the RAM Test stress and the corresponding deformation from the modulus load test plot provided to the research team. The stiffness parameters are summarized in Table 39. The values do not show a good correlation. Acceleration analysis A stiffness parameters are small, while acceleration analysis B stiff parameters are extremely high. Acceleration analysis C and D stiff parameters show better relation the modulus load test stiffness parameters but are still high as well. Figure 127 shows the stress verse deformation plot for piers 1 to 3. The plots increased, decreased, and then slightly increased in deformation as stress increased. The correlation between stress and deformation was better than the La Port City and Fairfield field studies but was still not what is expected.

**Table 38. Summary of plate size, stress, and BST, analysis A, B, C, D, and modulus load test deformations for Oskaloosa**

| Test | Plate size (in.) | Stress (psf) | BST δ (in.) | Analysis A δ (in.) | Analysis B δ (in.) | Analysis C δ (in.) | Analysis D δ (in.) | Modulus load test δ (in.) |
|---|---|---|---|---|---|---|---|---|
| 1 | 18 | 6764 | | -3.428 | -0.25 | | | -0.222 |
| 2 | 24 | 4463 | | -4.168 | -0.15 | -0.230 | -0.064 | -0.131 |
| 3 | 18 | 7303 | | -8.171 | -0.051 | -0.093 | -0.112 | -0.241 |
| 4 | 12 | 16384 | | -4.331 | -0.10 | -0.111 | -0.059 | -0.612 |
| 5 | 9 | 28908 | | -4.701 | -0.021 | -0.093 | -0.095 | – |
| 6 | 18 | 7136 | | -4.17 | -0.047 | Analysis not performed | | -0.235 |
| 7 | 24 | 4171 | | -10.9 | -0.3239 | | | -0.117 |
| 8 | 18 | 7974 | | -1.87 | -0.0910 | | | -0.262 |
| 9 | 12 | 16227 | | -3.78 | -0.0025 | | | -0.606 |
| 10 | 9 | 28321 | | -3.71 | -0.12 | | | – |
| 11 | 18 | 7273 | | -8.76 | -0.027 | | | -0.239 |
| 12 | 24 | 4023 | | -8.72 | -0.22 | | | -0.112 |
| 13 | 18 | 7124 | | -8.02 | -0.033 | | | -0.235 |
| 14 | 12 | 14975 | | -3.35 | -0.0092 | | | -0.540 |
| 15 | 9 | 26128 | | -4.96 | -0.10 | | | – |

**Table 39. Summary of BST, acceleration analysis A, B, C, D, and modulus load test stiffness for Oskaloosa**

| Test | BST stiffness (pci) | Analysis A stiffness (pci) | Analysis B stiffness (pci) | Analysis C stiffness (pci) | Analysis D stiffness (pci) | Modulus load test stiffness (pci) |
|---|---|---|---|---|---|---|
| 1 | 49 | 14 | 188 | | | 212 |
| 2 | 25 | 7 | 205 | 135 | 487 | 237 |
| 3 | 51 | 6 | 994 | 546 | 454 | 210 |
| 4 | 73 | 26 | 1,090 | 1,026 | 1,939 | 186 |
| 5 | 153 | 43 | 9,559 | 2,166 | 2,116 | –[1] |
| 6 | | 12 | 1,054 | Analysis not performed | | 211 |
| 7 | 33 | 3 | 89 | | | 248 |
| 8 | 126 | 30 | 609 | | | 211 |
| 9 | 228 | 30 | 45,040 | | | 186 |
| 10 | 163 | 53 | 1,628 | | | – |
| 11 | 33 | 6 | 1,840 | | | 211 |
| 12 | 133 | 3 | 124 | | | 249 |
| 13 | 330 | 6 | 1,516 | | | 211 |
| 14 | | 31 | 11,364 | | | 193 |

| Test | BST stiffness (pci) | Analysis A stiffness (pci) | Analysis B stiffness (pci) | Analysis C stiffness (pci) | Analysis D stiffness (pci) | Modulus load test stiffness (pci) |
|---|---|---|---|---|---|---|
| 15 | 825 | 37 | 1,762 | | | – |

[1]The modulus load test did not reach an equivalent stress of test 5

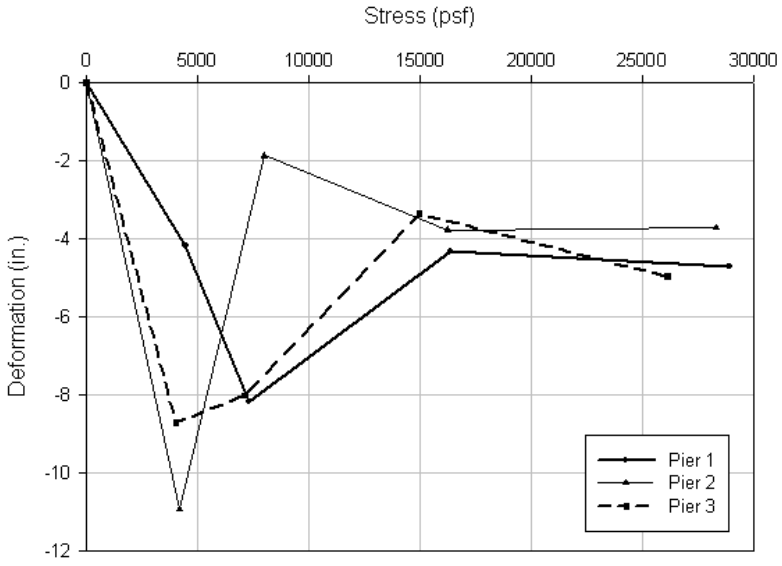


**Figure 127. Oskaloosa pier 1 to 3 stress (psf) vs. deformation (in.) plots**

## Verification

The verification data for La Port City, Fairfield, Council Bluffs, and Oskaloosa are presented in this section. The Hampton field study did not include any verification and is the reason no information is included from the study.

### La Port City verification results

Verification was conducted by the research team, and a contractor performed load tests and the results were available for analysis. Falling weight deflectometer (FWD) tests were performed for verification.

*FWD without the RAM Test*

FWD tests were performed without the RAM Test on all the piers. From the load results and plate area, a stress was calculated, and then a stiffness value was calculated from the deformation and stress values. The results of the FWD are shown in Table 40.

**Table 40. FWD load, deformation, stress, and stiffness results**

| Pier | Load (lb) | Deformation (mil) | Stress (psi) | Stiffness (pci) |
|---|---|---|---|---|
| 1 | 9,841 | 27.06 | 87.0 | 3,216 |
| | 10,078 | 17.28 | 89.1 | 5,157 |
| | 15,125 | 26.76 | 133.7 | 4,998 |
| | 20,590 | 37.76 | 182.1 | 4,821 |
| | 28,969 | 54.96 | 256.1 | 4,661 |
| | 27,565 | 50.59 | 243.7 | 4,818 |
| 2 | 8,689 | 8.84 | 76.8 | 8,691 |
| | 13,344 | 14.46 | 118.0 | 8,160 |
| | 17,999 | 20.36 | 159.1 | 7,817 |
| 3 | 8,561 | 40.24 | 75.7 | 1,881 |
| | 14,253 | 52.81 | 126.0 | 2,386 |
| | 19,594 | 72.45 | 173.2 | 2,391 |
| | 27,961 | 101.95 | 247.2 | 2,425 |
| | 27,859 | 116.4 | 246.3 | 2,116 |
| | 30,243 | 102.2 | 267.4 | 2,617 |
| 4 | 10,323 | 34.27 | 91.3 | 2,663 |
| | 15,603 | 51.08 | 138.0 | 2,701 |
| | 21,404 | 69.48 | 189.3 | 2,724 |
| | 31,347 | 96.71 | 277.2 | 2,866 |
| | 28,689 | 90.5 | 253.7 | 2,803 |

*FWD with the RAM Test*

When the FWD was used with the RAM Test, the RAM Test was set on the pier and the FWD load plate dropped on top of the RAM Test. Tests were recorded at the same time on the FWD and the RAM Test at five different loads. Table 41 shows the comparison between the FWD and the RAM Test values. The majority of the RAM Test accelerations showed only positive values (marked by the + in Table 41), which resulted in very high deformation values. Six tests did record negative and positive values but still resulted in high deformation values using acceleration analysis A to evaluate the data. For example, test 53 deformation increased until the end of the time-history and resulted in a positive 43.84 in., shown in Figure 128. From visual inspection, deformation of 44 in. out of the ground did not occur.

**Table 41. Comparison of FWD and RAM Test load and deformation results**

| Pier | RAM test | RAM Test diameter (in.) | Load (lb) | | Deformation (mil) | |
|---|---|---|---|---|---|---|
| | | | FWD | RAM | FWD | RAM |
| 1 | 46 | 24 | 8,745 | 8,567 | 126.33 | + |

| Pier | RAM test | RAM Test diameter (in.) | Load (lb) | | Deformation (mil) | |
|---|---|---|---|---|---|---|
| | | | FWD | RAM | FWD | RAM |
| | 47 | 24 | 13,037 | 10,771 | 225.34 | + |
| | 48 | 24 | 17,463 | 13,617 | 303.38 | 70,000 |
| | N/A | N/A | 24,507 | N/A | 276.82 | N/A |
| | 50 | 24 | 26,594 | 15,778 | 280.29 | + |
| | N/A | 24 | 8,888 | N/A | 150.31 | N/A |
| | 53 | 18 | 14,543 | 9,962 | 118.7 | 43,840 |
| | 54 | 18 | 20,128 | 11,636 | 131 | – |
| | 55 | 18 | 29,284 | 13,686 | 165.78 | – |
| | 56 | 18 | 27,532 | 13,821 | 135.47 | – |
| | 58 | 12 | 9,578 | 6,308 | 35.7 | – |
| | 59 | 12 | 14,349 | 8,803 | 56.62 | + |
| | 60 | 12 | 19,561 | 11,185 | 77.92 | + |
| | 61 | 12 | 27,983 | 13,995 | 112.34 | + |
| | 62 | 12 | 30,618 | 15,149 | 111.14 | – |
| 2 | 65 | 24 | 9,927 | 6,531 | 75.83 | + |
| | 66 | 24 | 14,716 | 10,147 | 109.05 | + |
| | 67 | 24 | 20,206 | 11,634 | 134.16 | + |
| | 68 | 24 | 29,341 | 14,980 | 172.87 | + |
| | 69 | 24 | 27,549 | 13,848 | 147.95 | + |
| | 71 | 18 | 9,526 | 6,032 | 51.44 | + |
| | 74 | 18 | 14,339 | 8,441 | 66.41 | + |
| | 75 | 18 | 19,603 | 10,838 | 87.67 | + |
| | 77 | 18 | 27,877 | 13,818 | 123.55 | + |
| | 78 | 18 | 30,458 | 14,991 | 127.47 | + |
| | 80 | 12 | 10,053 | 6,648 | 52.74 | + |
| | 81 | 12 | 14,881 | 9,166 | 83.82 | + |
| | 82 | 12 | 20,189 | 11,632 | 115.68 | + |
| | 83 | 12 | 28,312 | 14,536 | 178.37 | + |
| | 84 | 12 | 26,839 | 13,644 | 151.05 | + |
| 3 | 87 | 24 | 9,227 | 6,144 | 81.26 | + |
| | 88 | 24 | 13,458 | 8,471 | 123.95 | + |
| | 89 | 24 | 18,179 | 10,755 | 160.92 | + |
| | 90 | 24 | 25,506 | 13,796 | 210.08 | + |
| | 91 | 24 | 28,520 | 14,981 | 199.3 | + |
| | 93 | 18 | 10,008 | 6,565 | 61.64 | + |
| | 94 | 18 | 14,764 | 9,124 | 91.34 | + |
| | 95 | 18 | 20,051 | 11,601 | 125.57 | + |

| Pier | RAM test | RAM Test diameter (in.) | Load (lb) | | Deformation (mil) | |
|---|---|---|---|---|---|---|
| | | | FWD | RAM | FWD | RAM |
| | 96 | 18 | 28,554 | 14,778 | 123.53 | + |
| | 97 | 18 | 27,622 | 13,768 | 108.49 | + |
| | 99 | 12 | 9,538 | 6,135 | 40.05 | + |
| | 100 | 12 | 14,147 | 8,510 | 64.73 | + |
| | 101 | 12 | 19,123 | 10,930 | 87.35 | + |
| | 102 | 12 | 27,556 | 14,002 | 122.75 | + |
| | 103 | 12 | 30,538 | 14,198 | 113.5 | + |

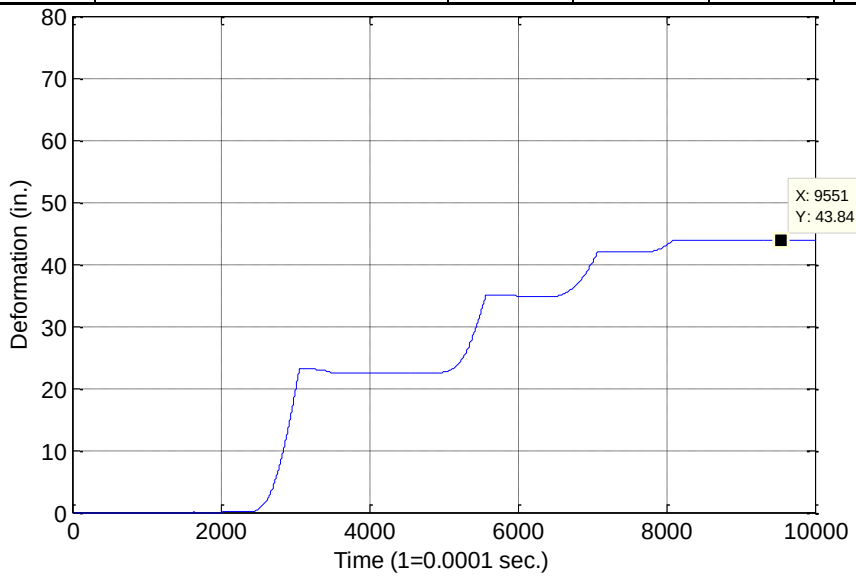


**Figure 128. Deformation time-history for La Port City test 53, recorded on pier 1 with the 18 in. plate, and the FWD dropping load at height 2.**

No more tests were processed as the results were unreasonable, and extremely higher than the maximum deformations recorded from the FWD tests. The high deformations may have resulted from the RAM Test recording a rebound effect from the FWD plate load dropping on top of the RAM Test. Overall; the FWD was difficult to maneuver across the site, timely to place accurately on the RAM Test, and performing the test distressed the other 7 deflectometers not used during testing. The FWD was not used again for verification.

*Load test*

Modulus load tests were completed on pier 1 through 3 at La Port City and the results are shown in Figure 129 through Figure 131. These data were collected from the Geopier

Foundation Company®™ (Minks, 2009). The 100% design stress is noted on the plots as well as the stiffness at that stress for each test.

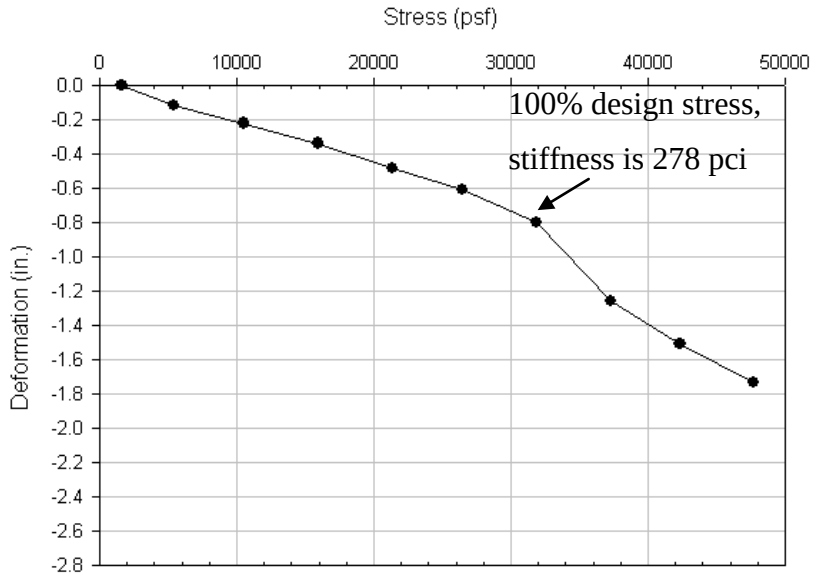


**Figure 129. Modulus load test results for pier 1 at La Port City**

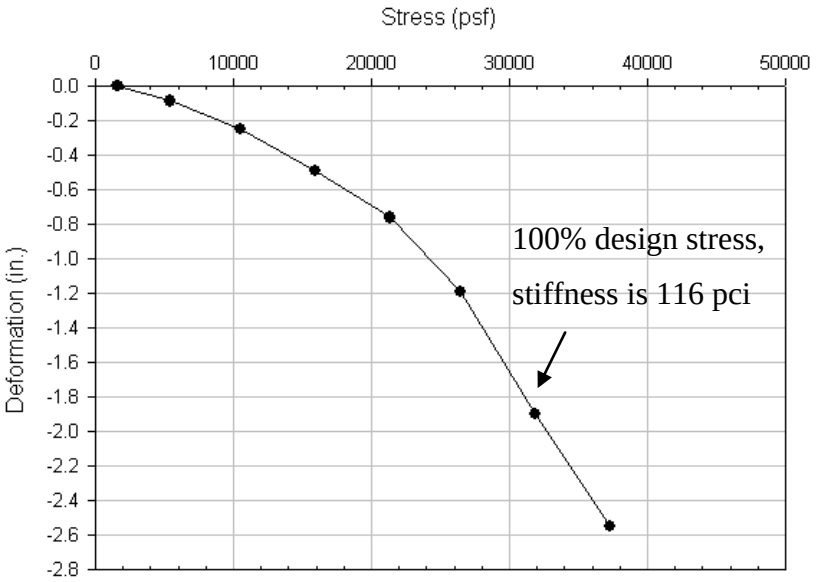


**Figure 130. Modulus load test results for pier 2 at La Port City**

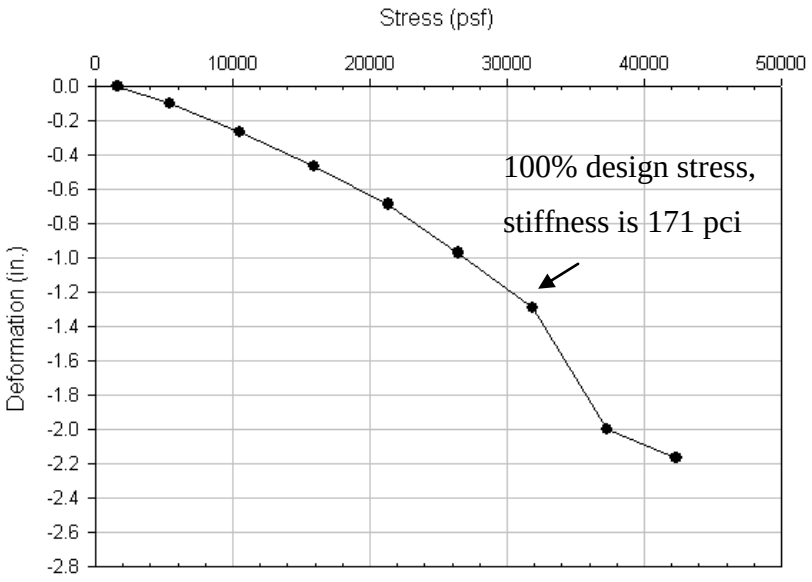


**Figure 131. Modulus load test results for pier 3 at La Port City**

**Fairfield verification results**

A high resolution video camera, two stakes with a string tied between and a 3 ft. ruler taped to the tamper shaft to verify the data from the RAM. Originally, independent measurements of deformation were going to be used to verify the RAM values, however, the set up did not provide reliable data due the lack of clarity in reading the ruler through the video camera back at the office. This set up was not used again. In the future, the ruler should not be attached to the tamper shaft.

**Council Bluffs verification results**

The research team performed verification, and a contractor performed load tests and the results were available for analysis. These data were collected from the Geopier Foundation Company®™.

*BST*

Bottom stabilization (BST) tests were performed to verify the data from the RAM Test. A plastic rod is used to mark the tamper shaft, and a 2 in. by 4 in. piece of wood is used as the pivot point. A mark is made on the tamper shaft with the edge of the plastic rod before the test begins, and then tamper compaction is stopped and marked between 3 to 5 times throughout one test. This allows for deformation readings to be recorded throughout one test and compared to the RAM Test data processed at the office to confirm the accuracy of the

values. BST verification was done for pier 2 and 3, and the deformation results are summarized in Table 42, and plotted in Figure 132. Overall, the BST was reliable, repeatable, and easy to maneuver from pier to pier.

**Table 42. Council Bluffs' BST results**

| Test | BST δ (in.) |
|---|---|
| 12 | -3.64 |
| 16 | -0.77 |
| 17 | -2.43 |
| 18 | -4.429 |
| 19 | -2.715 |
| 21 | -1.829 |

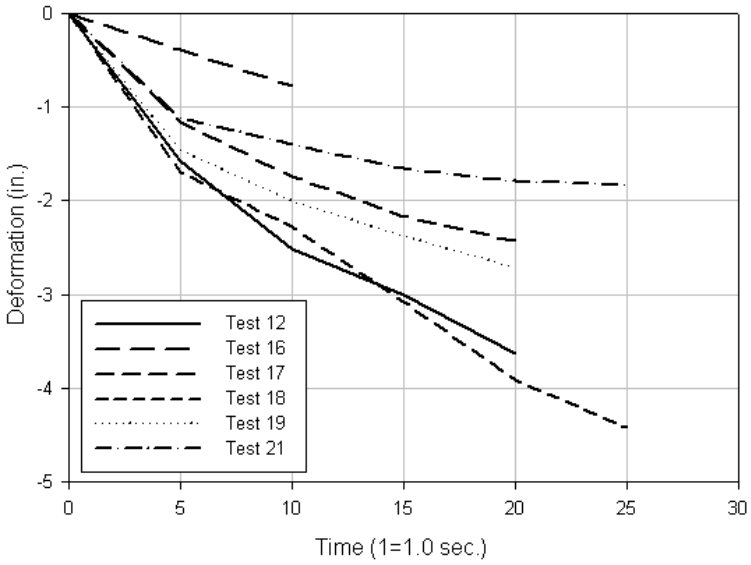


**Figure 132. BST deformation vs. time for Council Bluffs pier 2 (tests 12 and 16) and pier 3 (tests 17–21)**

*Load test*

One modulus load test was completed and the results were provided by the Geopier Foundation Company®™ (Plotkin, 2010). The 100% design stress is noted on the plot as well as the stiffness at that stress.

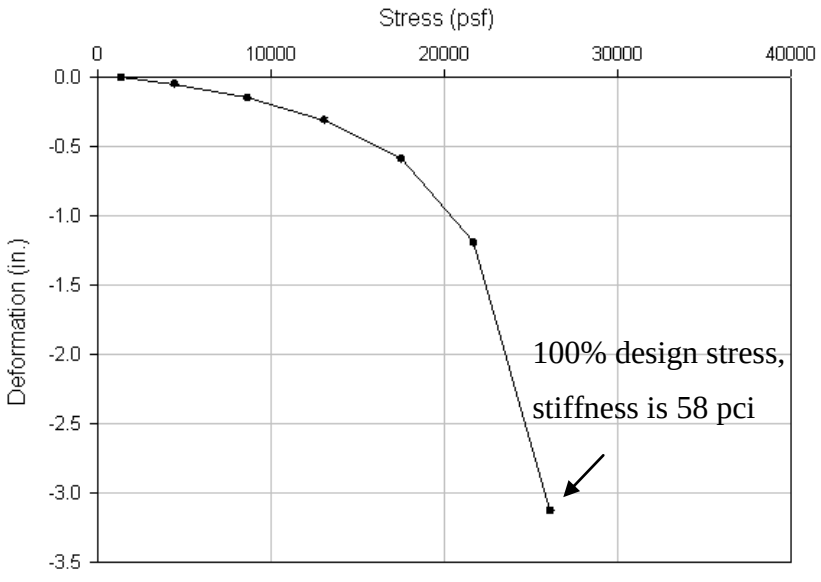


**Figure 133. Modulus load test results for Council Bluffs**

**Oskaloosa verification results**

The research team performed verification, and a contractor performed load tests and the results were available for analysis. These data were collected from the Geopier Foundation Company®™.

*BST*

Bottom stabilization (BST) tests were performed to verify the data from the RAM. A plastic rod is used to mark the tamper shaft, and a 2 in. by 4 in. piece of wood is used as the pivot point. A mark is made on the tamper shaft with the edge of the plastic rod before the test begins, and then tamper compaction is stopped and marked between 3 to 5 times throughout one test. This allows for deformation readings to be recorded throughout one test and compared to the RAM data processed at the office to confirm the accuracy of the values. The deformation results are summarized in

Table 43, and plotted in Figure 134 through Figure 136. Overall, the BST was reliable, repeatable, and easy to maneuver from pier to pier.

**Table 43. Oskaloosa's BST results**

| RAM test | Plate diameter (in.) | Test layer | Segment | Deformation (in.) | Cumulative deformation (in.) |
|---|---|---|---|---|---|
| 1 | 18 | 1 | 1 | -0.635 | -0.635 |
| | | | 2 | -0.210 | -0.845 |
| | | | 3 | -0.105 | -0.950 |
| | | | 4 | 0.000 | -0.950 |
| 2 | 24 | 2 | 1 | -1.050 | -1.050 |
| | | | 2 | -0.175 | -1.225 |
| | | | 3 | 0.000 | -1.225 |
| 3 | 18 | | 1 | -0.860 | -0.860 |
| | | | 2 | -0.125 | -0.985 |
| | | | 3 | 0.000 | -0.985 |
| 4 | 12 | | 1 | -0.865 | -0.865 |
| | | | 2 | -0.345 | -1.210 |
| | | | 3 | -0.200 | -1.410 |
| | | | 4 | -0.155 | -1.565 |
| 5 | 9 | | 1 | -0.620 | -0.620 |
| | | | 2 | -0.260 | -0.880 |
| | | | 3 | -0.260 | -1.140 |
| | | | 4 | -0.170 | -1.310 |
| 6[1] | 18 | 1 | – | – | – |
| 7 | 24 | 2 | 1 | -0.8750 | -0.875 |
| | | | 2 | 0.0000 | -0.875 |
| | | | 3 | 0.0000 | -0.875 |
| | | | 4 | 0.0000 | -0.875 |
| 8 | 18 | | 1 | -0.440 | -0.440 |
| | | | 2 | 0.000 | -0.440 |
| | | | 3 | 0.000 | -0.440 |
| | | | 4 | 0.000 | -0.440 |
| 9 | 12 | | 1 | -0.495 | -0.495 |
| | | | 2 | 0 | -0.495 |
| | | | 3 | 0 | -0.495 |
| | | | 4 | 0 | -0.495 |
| 10 | 9 | | 1 | -0.550 | -0.550 |
| | | | 2 | -0.255 | -0.805 |
| | | | 3 | -0.190 | -0.995 |
| | | | 4 | -0.215 | -1.210 |
| 11 | 18 | 1 | 1 | -0.800 | -0.800 |
| | | | 2 | -0.290 | -1.090 |
| | | | 3 | -0.250 | -1.340 |
| | | | 4 | -0.180 | -1.520 |

| RAM test | Plate diameter (in.) | Test layer | Segment | Deformation (in.) | Cumulative deformation (in.) |
|---|---|---|---|---|---|
| 12 | 24 | 2 | 1 | -0.210 | -0.210 |
| | | | 2 | 0.000 | -0.210 |
| | | | 3 | 0.000 | -0.210 |
| | | | 4 | 0.000 | -0.210 |
| 13 | 18 | | 1 | ? | ? (missed first) |
| | | | 2 | ? | -0.15 |
| | | | 3 | 0 | -0.15 |
| | | | 4 | 0 | -0.15 |
| 14[1] | 12 | | – | – | – |
| 15 | 9 | | 1 | ? | ? (missed first) |
| | | | 2 | -0.140 | -0.140 |
| | | | 3 | -0.080 | -0.220 |
| | | | 4 | 0.000 | -0.220 |

[1] The tamper shifted on test 6 and 14 and the values were unreliable

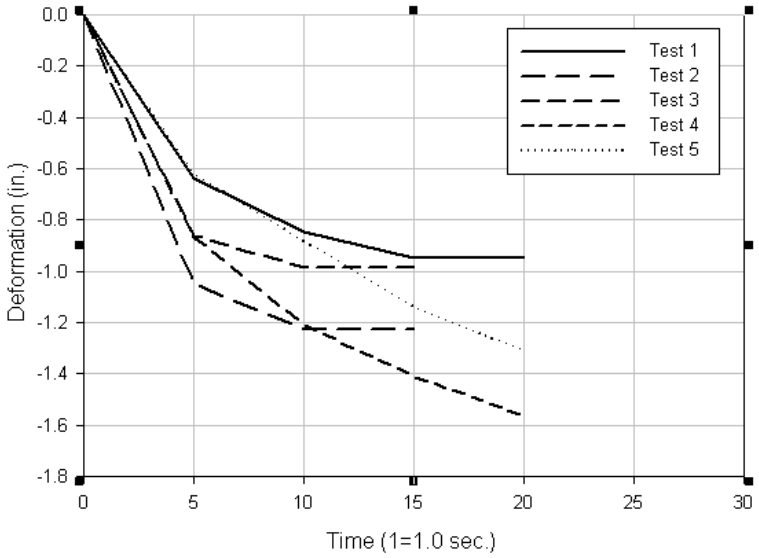


**Figure 134. BST deformation vs. time for pier 1**

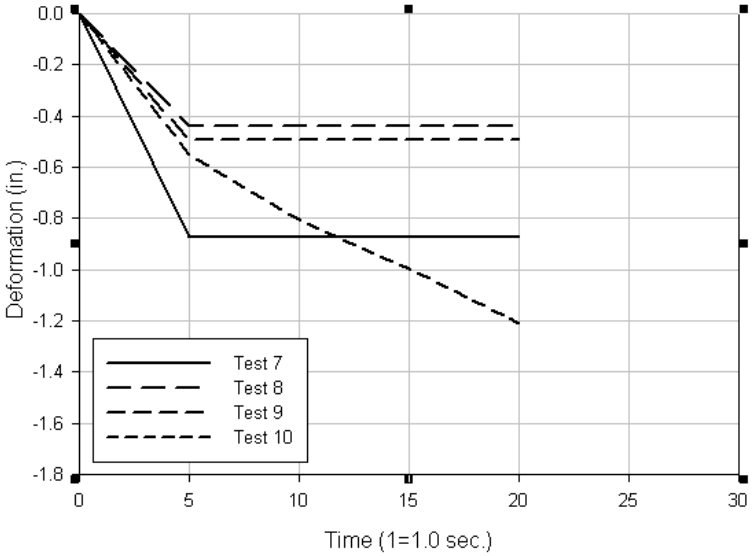


**Figure 135. BST deformation vs. time for pier 2**

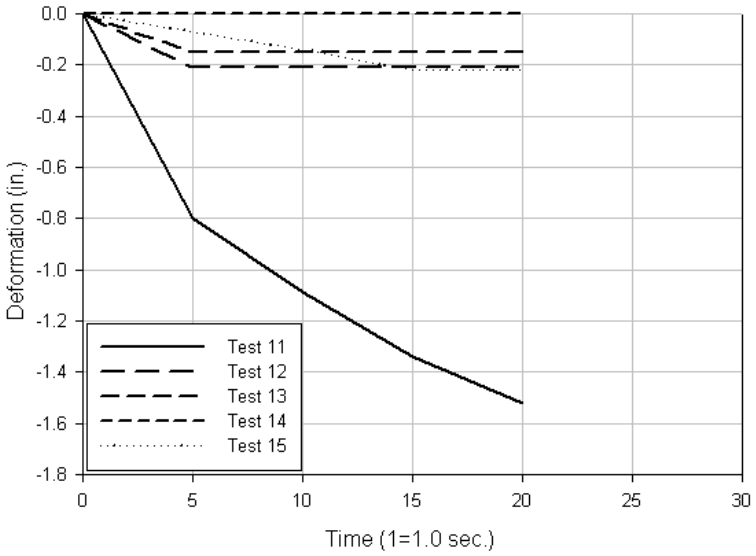


**Figure 136. BST deformation vs. time for pier 3**

*Load test*

A modulus load test was completed and the results were provided by Geopier Foundation Company®™ (Plotkin, 2011), and are shown in Figure 137. The 100% design stress is noted on the plot as well as the stiffness at that stress.

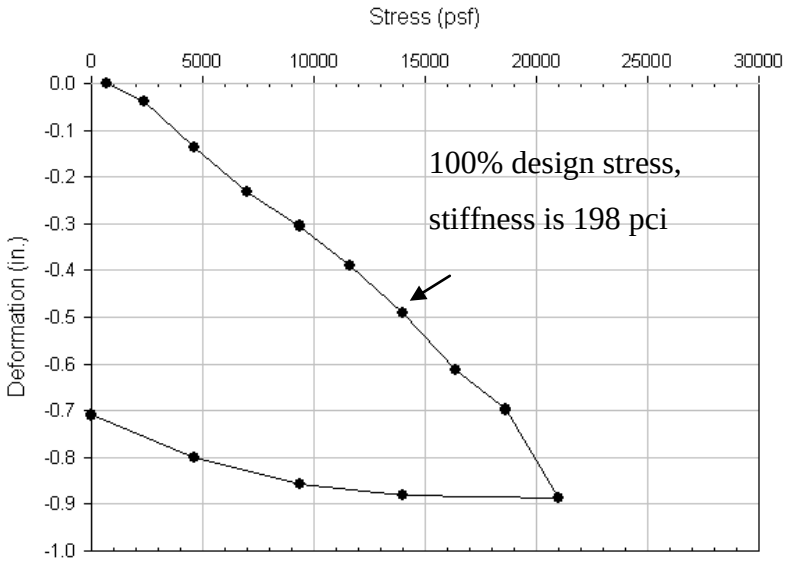


**Figure 137. Modulus load test results for Oskaloosa**

# CHAPTER 6. CONCLUSIONS AND RECOMMENDATIONS

This chapter presents an overview of the technical merit and/or scientific value gained from the study and an overview of the lessons learned. The conclusions are grouped into 3 categories (e.g., conclusions about load, acceleration, and stiffness) and associated with outcomes, benefits, and applications. The second part of this chapter associates the conclusions with the goal of the research. The last part of this chapter associates the recommendations for future research and future practices.

## Conclusions

The conclusions are separated by load, acceleration, and stiffness.

### *Load*

The ability to characterize the load and put values to what was occurring during compaction installation was an unexpected, yet a great outcome of this research. No one had done load analysis before now. Five conclusions are made from the load analysis;

- When the time-history exhibited smaller amplitudes, the pier was more compacted, and therefore stiffer,
- When the crowd load was higher, it did not necessarily mean the pier was more compacted,
- The crowd load was typically higher at the end of compaction than at the beginning of compaction,
- The double sinusoidal behavior was exhibited at all of the field studies, and appears to be a characteristic of the ramming compaction energy, and
- The use of the buffer pad is necessary for load transfer to the RAM Test.

### *Acceleration*

The ability to characterize the acceleration is important to understand how the pier deforms. Unfortunately, the outcome of using the acceleration analyses A to D to determine deformation did not always result in the best correlations to the verification. Four conclusions are made from the acceleration analysis;

- The more the negative acceleration values, the higher the resultant deformation,

- The negative valued accelerations could be high, but unless there are more negative accelerations, the deformation will be positive, or very minuscule,
- The arbitrary value of 5 in the software code does impact the deformation results,
- The RAM Test plate size did not affect the acceleration behavior, and
- It is difficult to conclude how the accelerations behave during stiff conditions, the accelerations from very stiff conditions (e.g., the concrete cap pier at La Port City) behaved differently as a pier was being installed and becoming stiffer.

*Stiffness*

The ability to characterize the stiffness parameters allows for comparison between verifications. The stiffness parameters were compared using the same RAM Test stress with each corresponding deformation. Unfortunately, little to no correlation was found between the RAM Test and verification. And last, the stress verse deformation plots exhibited atypical behavior.

Overall, the RAM Test performs well under tough environments and high installation loads. And, the RAM Test can be used on multiple types of aggregate piers.

**Recommendations for future research**

The next phase of this research should focus on the following;

- The value of 5 which excludes smaller acceleration values was chosen at arbitrary and because it does affect the results, a more extensive study should be done to verify the best value used in the analysis code,
- The RAM Test with accelerometer 2. This research was based on accelerometer 1 and because of the peak acceleration value seen at multiple studies, it would be beneficial test piers with a higher capacity accelerometer,
- Load analysis B. The results from the initial study completed from Oskaloosa were beneficial and helpful in gaining better knowledge on the load during compaction,
- The positive deformation results. Without guessing or speculating, the research team does not know why this is occurring, and
- The ability to attach the RAM Test to the tamper to ease the use of the RAM Test during production.

**Recommendations for future practices**

The RAM Test has provided beneficial knowledge during the installation of piers. A recommendation would be to evaluate production piers during the installation process.

# APPENDIX

**Dytran Instruments, Inc.**
21592 Marilla St. Chatsworth, CA 91311 Ph: 818-700-7818 Fax 818-700-7880
www.dytran.com email: info@dytran.com



## CALIBRATION CERTIFICATE
## VOLTAGE MODE ACCELEROMETER

| | | | | | |
|---|---|---|---|---|---|
| **CUSTOMER:** | *IOWA STATE UNOVERSITY* | | | **TEST REPORT #:** *5237* | *8/3/2007* |
| **PURCHASE ORDER #:** | *ONLINE 266/28332* | **SALES ORDER #:** | *127919* | **PROCEDURE:** | *TP3002* |
| **MODEL:** | *3220E* | **SERIAL #:** | *5237* | **RANGE, F.S. (g's):** | *+/- 500* |
| **NEW UNIT** | X | **RE-CALIBRATION [1]** | | **AS RECEIVED CODE** | **AS RETURNED CODE** |
| **REF. SENSITIVITY (mV/g) [2]:** | *10.10* | **TEMP (°C):** | *24* | **HUMIDITY (%):** | *35* |

***FREQUENCY RESPONSE [3]***

| FREQUENCY (Hz) | SENSITIVITY (mV/g) | FREQUENCY (Hz) | SENSITIVITY (mV/g) |
|---|---|---|---|
| 20 | *10.10* | 500 | *10.10* |
| 30 | *10.10* | 1000 | *10.10* |
| 50 | *10.10* | 2000 | *10.20* |
| 100 | *10.10* | 3000 | *10.30* |
| 300 | *10.10* | 4000 | *10.30* |
| **TRANSVERSE SENSITIVITY (%):** | *0.7* | 5000 | *10.50* |
| **DISCHARGE TIME CONSTANT (sec):** | *0.90* | **BIAS VOLTAGE (VDC):** | *10.4* |

**Amplitude Response**

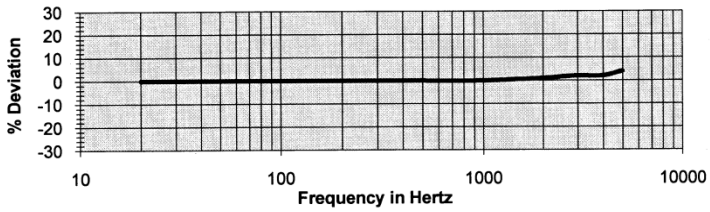


**REMARKS:**

***TEST EQUIPMENT LIST - CALIBRATION STATION # 9***

| DII # | MANUFACTURER | MODEL | SERIAL # | DESCRIPTION | CAL DATE | DUE DATE |
|---|---|---|---|---|---|---|
| *540* | *BERAN INSTRUMENTS* | *475* | *182448* | *VIBRATION CALIBRATOR* | *06/18/07* | *06/18/08* |
| *541* | *BERAN INSTRUMENTS* | *801A* | *A004* | *DUAL AMPLIFIER UNIT* | *06/18/07* | *06/18/08* |
| *045* | *HEWLETT PACKARD* | *3478A* | *2911A67811* | *MULTIMETER* | *01/12/07* | *01/12/08* |
| *017* | *NICOLET* | *310* | *IAQ9406710* | *DIGITAL OSCILLOSCOPE* | *08/30/06* | *08/30/07* |
| *054* | *DYTRAN INST.* | *3010M8* | *975* | *ACCELEROMETER* | *07/26/06* | *08/26/07* |

[1] AS RECEIVED / AS RETURNED CODES:
1 = IN TOLERANCE, NO ADJUSTMENTS
2 = IN TOLERANCE, BUT ADJUSTED
3 = OUT OF TOLERANCE < 5%
4 = OUT OF TOLERANCE > 5%
5 = REPAIR REQUIRED
6 = REPAIRED AND CALIBRATED
7 = UNIT NON-REPAIRABLE, RECOMMEND REPLACEMENT
8 = UNIT SERVICEABLE WITH CURRENT CALIBRATION DATA

[2] THE REFERENCE SENSITIVITY IS MEASURED AT 100 Hz, 1G RMS.

[3] THIS CALIBRATION WAS PERFORMED IN ACCORDANCE WITH MIL-STD-45662A, ANSI/NCSL Z540-1-1994, ISO 10012-1 USING THE BACK-TO-BACK COMPARISON METHOD PER ISA RP37.2 AND IS TRACEABLE TO THE NIST THROUGH TEST REPORT # 2622-130LHS DUE 08-26-07.
ESTIMATED UNCERTAINTY OF CALIBRATION: 2% FROM 5-50 Hz, 1% FROM 100-2000 Hz, 2% FROM 2.5-10 kHz.



**CALIBRATION TECHNICIAN:** _____
*PHUOC TRAN*

**TEST DATE:** *08/03/07*
**RECALL DATE:** *08/03/08*

**Figure 138. Calibration certificate for accelerometer 1 on August 3, 2007**

**Dytran Instruments, Inc.**
21592 Marilla St. Chatsworth, CA 91311 Ph: 818-700-7818 Fax 818-700-7880
www.dytran.com email: info@dytran.com

## CALIBRATION CERTIFICATE
## VOLTAGE MODE ACCELEROMETER

| | | | | | |
|---|---|---|---|---|---|
| **CUSTOMER:** | IOWA STATE UNIVERSITY | | | **TEST REPORT #:** | 5237 |
| **PURCHASE ORDER #:** | VISA/D.WAGNER | **SALES ORDER #:** | RMA#23532 | **PROCEDURE:** | TP3002 |
| **MODEL:** | 3220E | **SERIAL #:** | 5237 | **RANGE, F.S. (g's):** | +/- 500 |
| **NEW UNIT** | | **RE-CALIBRATION [1]** | X | **AS RECEIVED CODE** | 1 |
| **AS RETURNED CODE** | 1 | | | | |
| **REF. SENSITIVITY (mV/g) [2]:** | 10.09 | **TEMP (°C):** | 24 | **HUMIDITY (%):** | 41 |

*FREQUENCY RESPONSE [3]*

| FREQUENCY (Hz) | SENSITIVITY (mV/g) | FREQUENCY (Hz) | SENSITIVITY (mV/g) |
|---|---|---|---|
| 20 | 9.99 | 500 | 10.13 |
| 30 | 10.05 | 1000 | 10.16 |
| 50 | 10.09 | 2000 | 10.19 |
| 100 | 10.09 | 3000 | 10.22 |
| 300 | 9.90 | 4000 | 10.30 |
| **TRANSVERSE SENSITIVITY (%):** | 0.7 | 5000 | 10.37 |
| **DISCHARGE TIME CONSTANT (sec):** | 0.90 | **BIAS VOLTAGE (VDC):** | 10.4 |

**Amplitude Response**

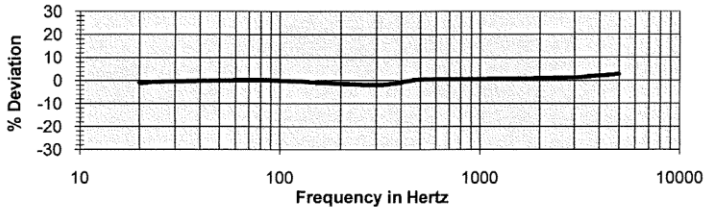


**REMARKS:**

*TEST EQUIPMENT LIST - CALIBRATION STATION # 10*

| DII # | MANUFACTURER | MODEL | SERIAL # | DESCRIPTION | CAL DATE | DUE DATE |
|---|---|---|---|---|---|---|
| 1281 | NATIONAL INST. | NI PCI-4461 | 15222A3 | DATA ACQUISTION CARD | 01/07/11 | 01/07/12 |
| 686 | DYTRAN INST. | 3010M14 | 1684 | ACCELEROMETER | 11/08/10 | 11/08/11 |
| 591 | KIETHLEY | 2000 | 0642889 | MULTIMETER | 04/14/10 | 04/14/11 |

[1] AS RECEIVED / AS RETURNED CODES:
1 = IN TOLERANCE, NO ADJUSTMENTS
2 = IN TOLERANCE, BUT ADJUSTED
3 = OUT OF TOLERANCE < 5%
4 = OUT OF TOLERANCE > 5%
5 = REPAIR REQUIRED
6 = REPAIRED AND CALIBRATED
7 = UNIT NON-REPAIRABLE, RECOMMEND REPLACEMENT
8 = UNIT SERVICEABLE WITH CURRENT CALIBRATION DATA

[2] THE REFERENCE SENSITIVITY IS MEASURED AT 100 Hz, 1G RMS.

[3] THIS CALIBRATION WAS PERFORMED IN ACCORDANCE WITH ANSI/NCSL Z540-1-1994, ISO 10012-1, ISO/IEC17025 USING THE BACK-TO-BACK COMPARISON METHOD PER ISA RP37.2 AND IS TRACEABLE TO THE NIST THROUGH TEST REPORT # 13339-120H DUE 11-08-11
ESTIMATED UNCERTAINTY OF CALIBRATION: 2% FROM 20-100 Hz, 1.5% FROM 100-2500 Hz, 2.8% FROM 2.5KHZ-10 kHz. APPLIES TO FREQUENCY RESPONSE ONLY.



**CALIBRATION TECHNICIAN:** VU LE **TEST DATE :** 02/21/11

**RECOMMENDED RECALL DATE :** 02/21/12

**Figure 139. Calibration certificate for accelerometer 1 on February 21, 2011**

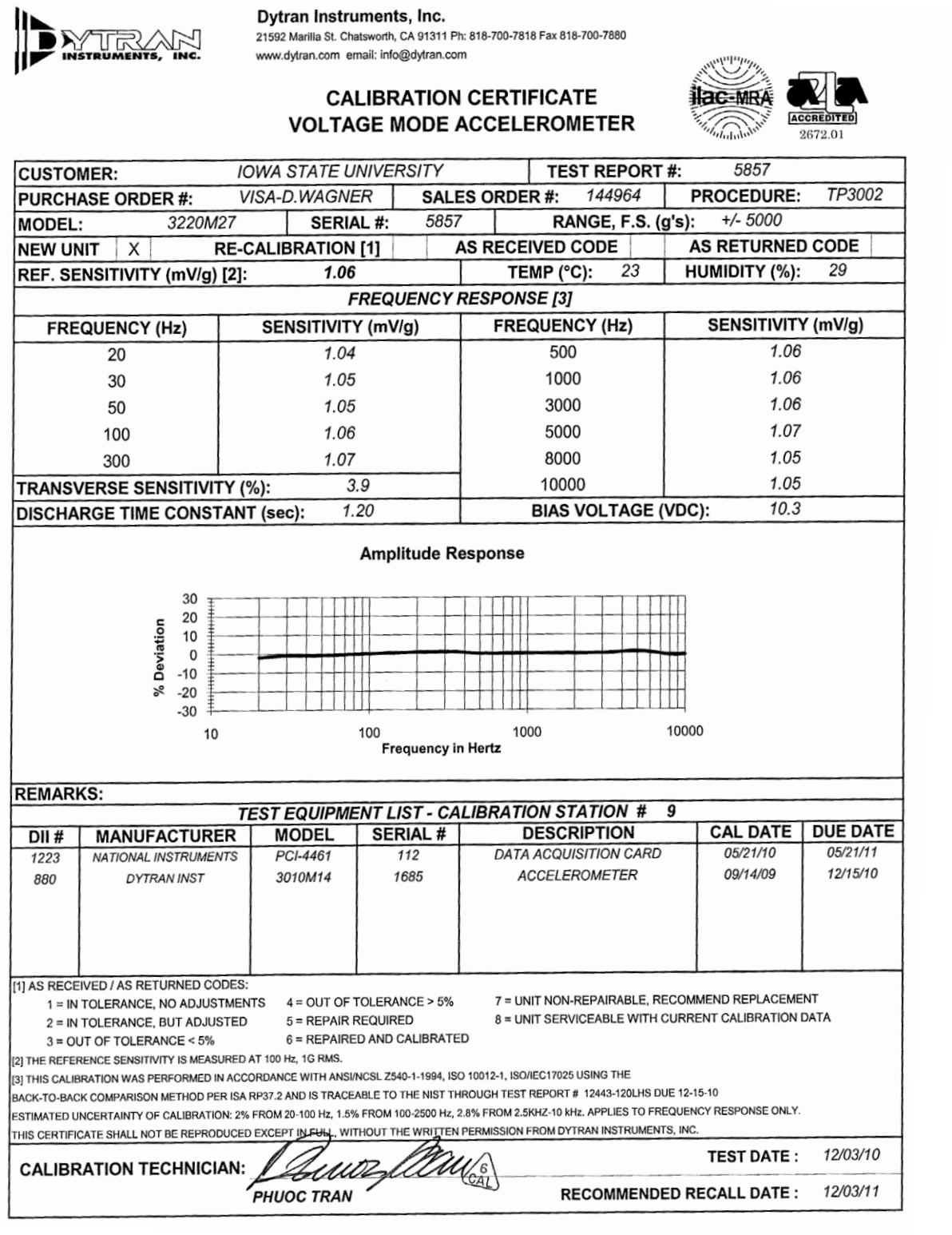

Dytran Instruments, Inc.
21592 Marilla St. Chatsworth, CA 91311 Ph: 818-700-7818 Fax 818-700-7880
www.dytran.com email: info@dytran.com

ACCREDITED 2672.01

**CALIBRATION CERTIFICATE**
**VOLTAGE MODE ACCELEROMETER**

| | | | | | |
|---|---|---|---|---|---|
| CUSTOMER: | IOWA STATE UNIVERSITY | | | TEST REPORT #: | 5857 |
| PURCHASE ORDER #: | VISA-D.WAGNER | SALES ORDER #: | 144964 | PROCEDURE: | TP3002 |
| MODEL: | 3220M27 | SERIAL #: | 5857 | RANGE, F.S. (g's): | +/- 5000 |
| NEW UNIT | X | RE-CALIBRATION [1] | | AS RECEIVED CODE | AS RETURNED CODE |
| REF. SENSITIVITY (mV/g) [2]: | 1.06 | TEMP (°C): | 23 | HUMIDITY (%): | 29 |

*FREQUENCY RESPONSE [3]*

| FREQUENCY (Hz) | SENSITIVITY (mV/g) | FREQUENCY (Hz) | SENSITIVITY (mV/g) |
|---|---|---|---|
| 20 | 1.04 | 500 | 1.06 |
| 30 | 1.05 | 1000 | 1.06 |
| 50 | 1.05 | 3000 | 1.06 |
| 100 | 1.06 | 5000 | 1.07 |
| 300 | 1.07 | 8000 | 1.05 |
| | | 10000 | 1.05 |

| | | | |
|---|---|---|---|
| TRANSVERSE SENSITIVITY (%): | 3.9 | | |
| DISCHARGE TIME CONSTANT (sec): | 1.20 | BIAS VOLTAGE (VDC): | 10.3 |

Amplitude Response



REMARKS:

*TEST EQUIPMENT LIST - CALIBRATION STATION # 9*

| DII # | MANUFACTURER | MODEL | SERIAL # | DESCRIPTION | CAL DATE | DUE DATE |
|---|---|---|---|---|---|---|
| 1223 | NATIONAL INSTRUMENTS | PCI-4461 | 112 | DATA ACQUISITION CARD | 05/21/10 | 05/21/11 |
| 880 | DYTRAN INST | 3010M14 | 1685 | ACCELEROMETER | 09/14/09 | 12/15/10 |

[1] AS RECEIVED / AS RETURNED CODES:
1 = IN TOLERANCE, NO ADJUSTMENTS
2 = IN TOLERANCE, BUT ADJUSTED
3 = OUT OF TOLERANCE < 5%
4 = OUT OF TOLERANCE > 5%
5 = REPAIR REQUIRED
6 = REPAIRED AND CALIBRATED
7 = UNIT NON-REPAIRABLE, RECOMMEND REPLACEMENT
8 = UNIT SERVICEABLE WITH CURRENT CALIBRATION DATA

[2] THE REFERENCE SENSITIVITY IS MEASURED AT 100 Hz, 1G RMS.
[3] THIS CALIBRATION WAS PERFORMED IN ACCORDANCE WITH ANSI/NCSL Z540-1-1994, ISO 10012-1, ISO/IEC17025 USING THE BACK-TO-BACK COMPARISON METHOD PER ISA RP37.2 AND IS TRACEABLE TO THE NIST THROUGH TEST REPORT # 12443-120LHS DUE 12-15-10
ESTIMATED UNCERTAINTY OF CALIBRATION: 2% FROM 20-100 Hz, 1.5% FROM 100-2500 Hz, 2.8% FROM 2.5KHZ-10 kHz. APPLIES TO FREQUENCY RESPONSE ONLY.


CALIBRATION TECHNICIAN: PHUOC TRAN 6 CAL

TEST DATE : 12/03/10
RECOMMENDED RECALL DATE : 12/03/11

**Figure 140. Calibration certificate for accelerometer 2 on December 3, 2010**

**Table 44. The acceleration analysis software code to determine permanent deformation**

```
%Test7RealTime.m
%run this file finds the deformation in "real time"

close all;
clear all;

load Oskaloosa_test15_1tamperhit.txt;

Accel=Oskaloosa_test15_1tamperhit(:,3);
Load=Oskaloosa_test15_1tamperhit(:,1);

clear Oskaloosa_test15_1tamperhit;
%time=[0:.0001:length(Accel)]

%Let's try to integrate the acceleration

dt=0.0001;
y(1)=0;
y2(1)=0;
v(1)=0;
vf(1)=0;
yfold=0;
yffold=0;
yfold2=0;
vfold=0;
Lfold=0;
Afold=0;

aL=10;
aA=50;
aA2=50;
aV=50;


for k=2:length(Accel);
    if abs(Accel(k-1)) > 1932;
    v(k)=v(k-1)+Accel(k-1)*dt;
    else;
        v(k)=0;
    end;

    y(k)=y(k-1)+v(k-1)*dt;
```

```
%add a high-pass filter to zero the velocity
    vf(k)=( vfold+v(k)-v(k-1) )/(1+aV*dt);
    y2(k)=y2(k-1)+vf(k-1)*dt;%y2 integrates the filtered velocity, vf
    DY(k)=( y(k)-y(k-1) )/dt;
    DVF(k)=( vf(k)-vf(k-1))/dt;%this is, actually, the acceleration

    vfold=vf(k);

    %add a high-pass filter to zero the position
    yf(k)=( yfold+y(k)-y(k-1) )/(1+aA*dt);%this filters the raw y-value
    yf2(k)=( yfold2+y2(k)-y2(k-1) )/(1+aA2*dt);%this filters the FILTERED (velocity) y-
      value

    DYF(k)=( yf(k)-yf(k-1) )/dt;
    DYF2(k)=( yf2(k)-yf2(k-1) )/dt;

    yfold2=yf2(k);
    yfold=yf(k);
    %add a high-pass filter to zero the load
   Lf(k)=( Lfold+Load(k)-Load(k-1) )/(1+aL*dt);
   DL(k)= ( Load(k)-Load(k-1) )/dt;
   Lfold=Lf(k);

   time(k)=k/10000;

end;

figure;
plot(y);
figure;
plot(yf,Lf);
```

**Hampton**

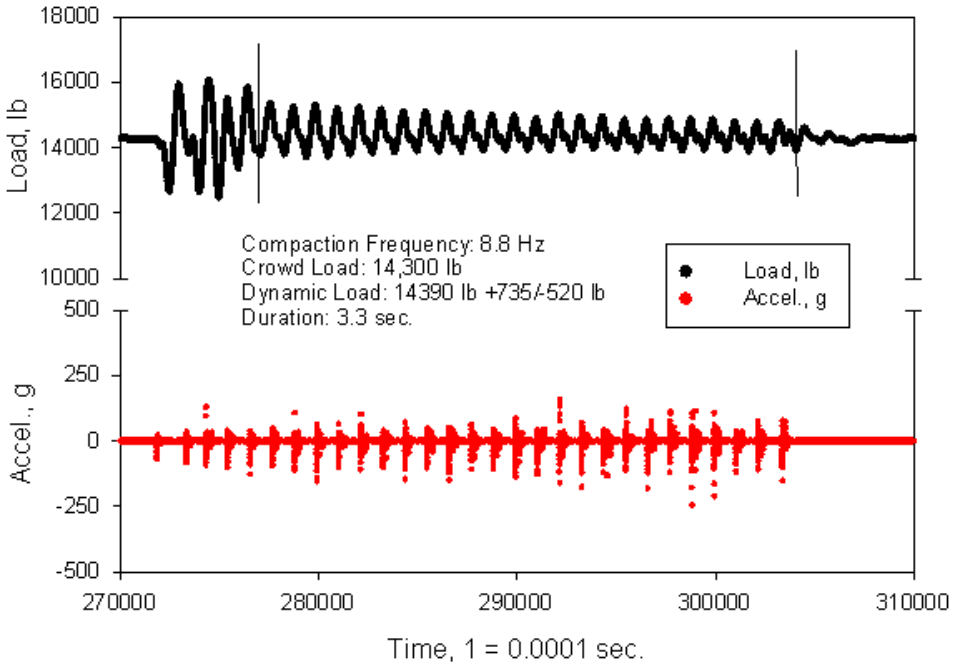


**Figure 141. Hampton test 1**

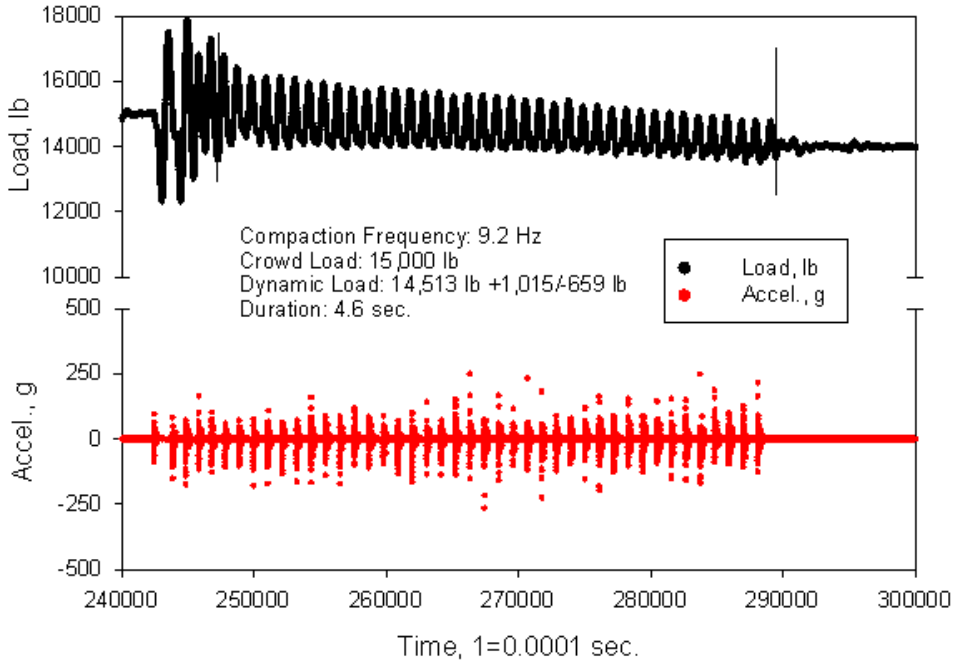


**Figure 142. Hampton test 2**

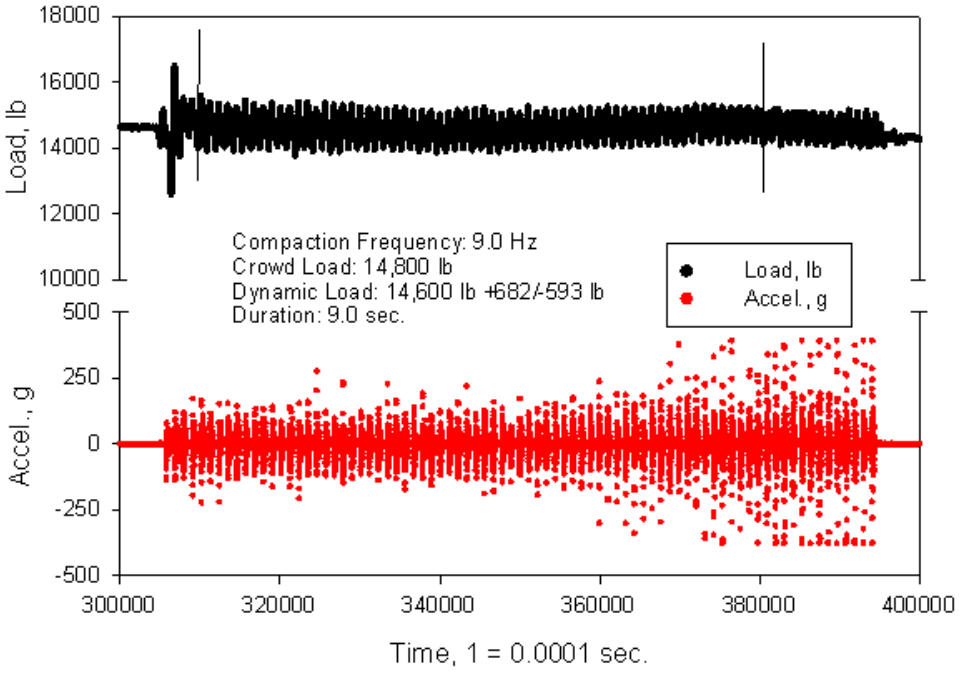


**Figure 143. Hampton test 3**

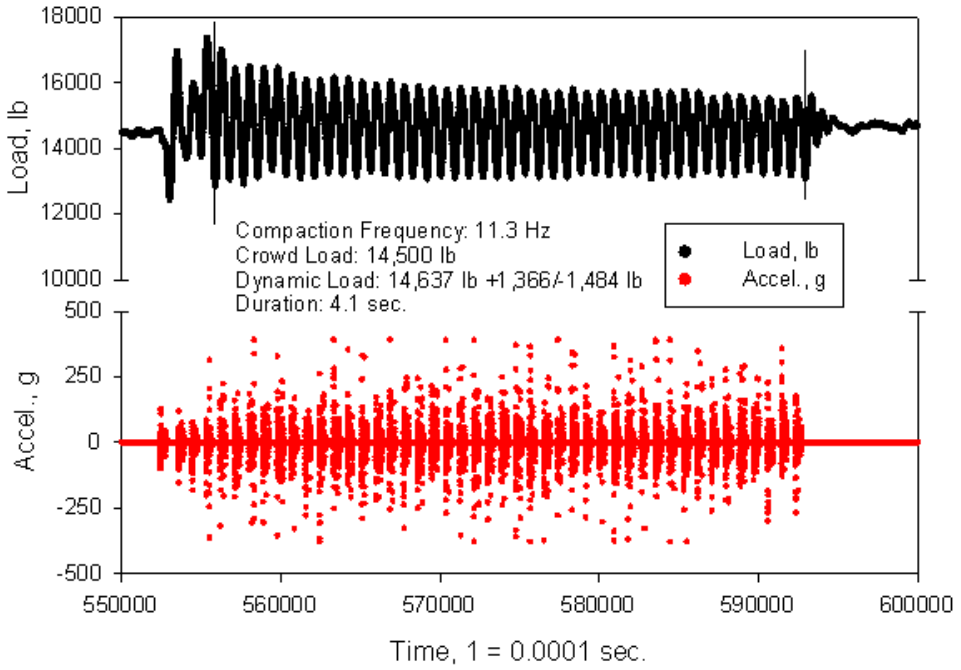


**Figure 144. Hampton test 4**

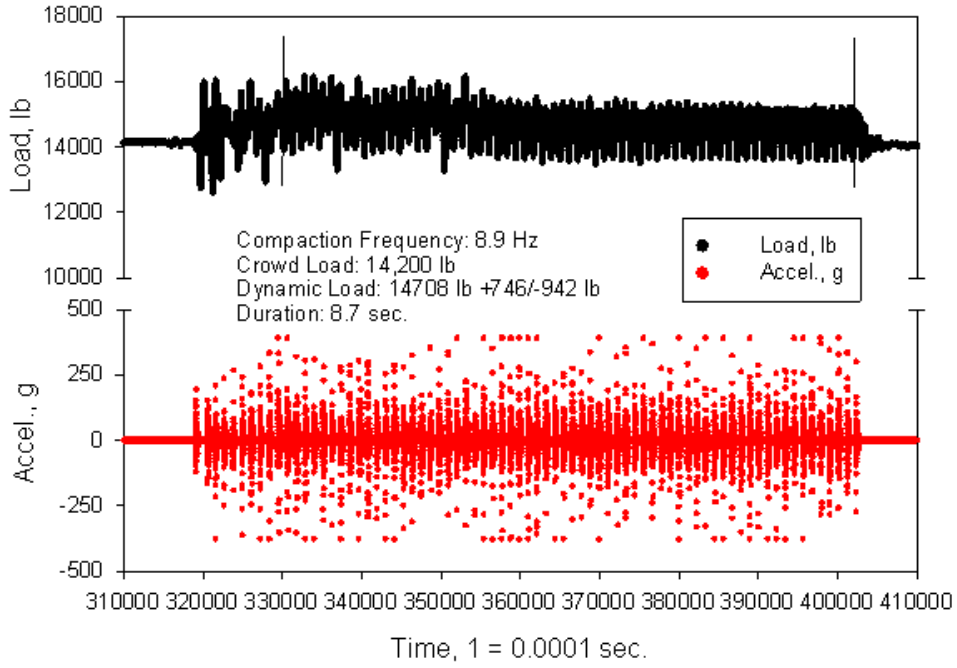


**Figure 145. Hampton test 5**

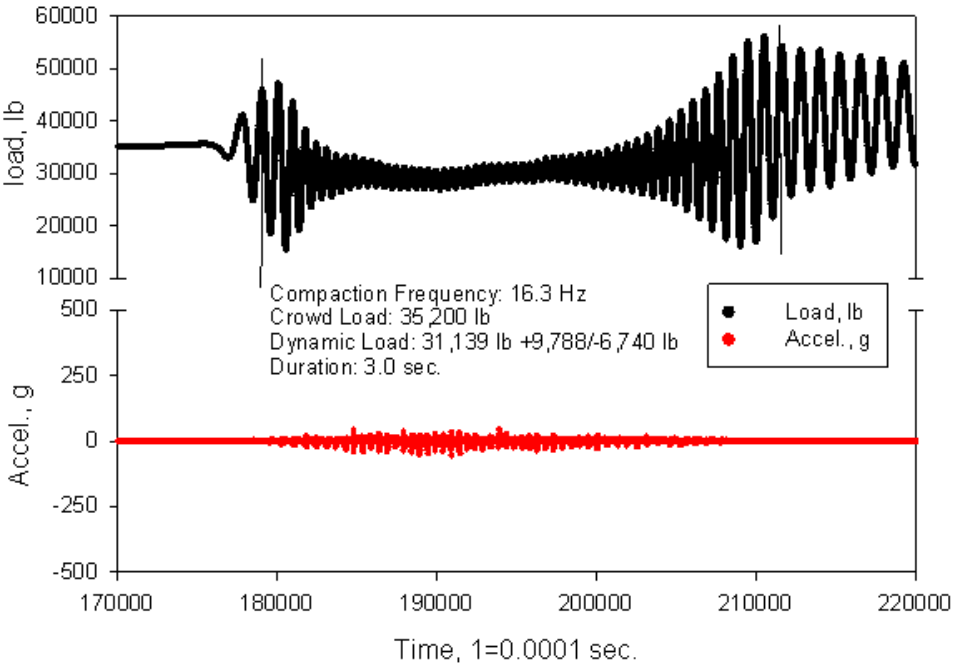


**Figure 146. Hampton test 6**

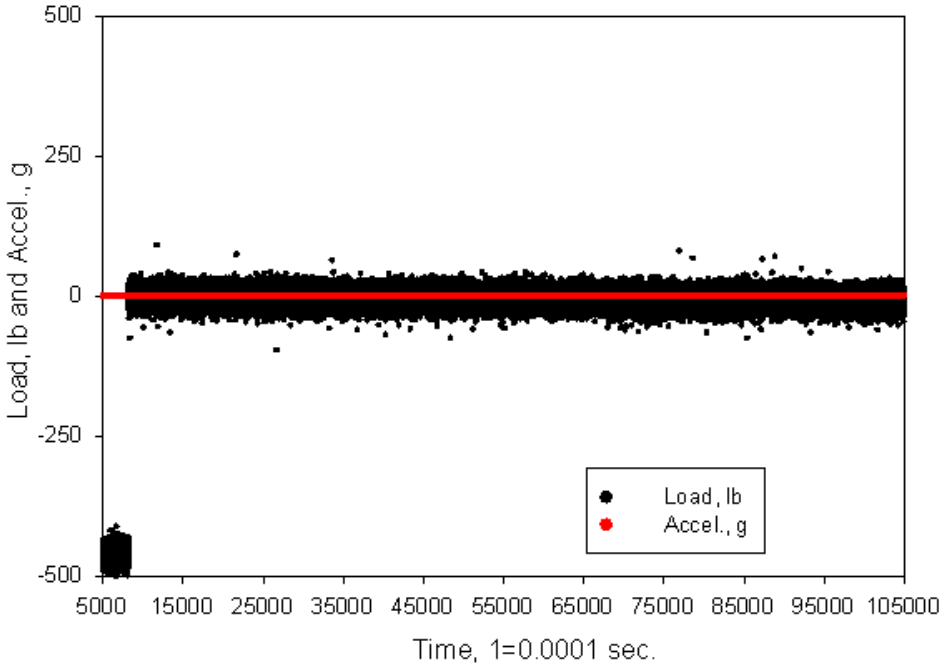


**Figure 147. Hampton test 9**

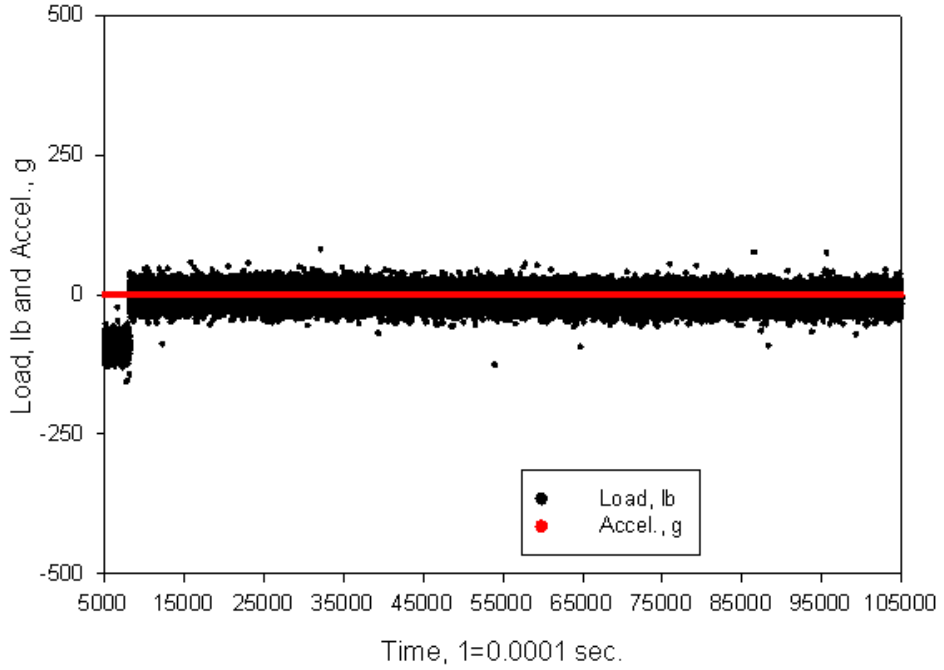


**Figure 148. Hampton test 10**

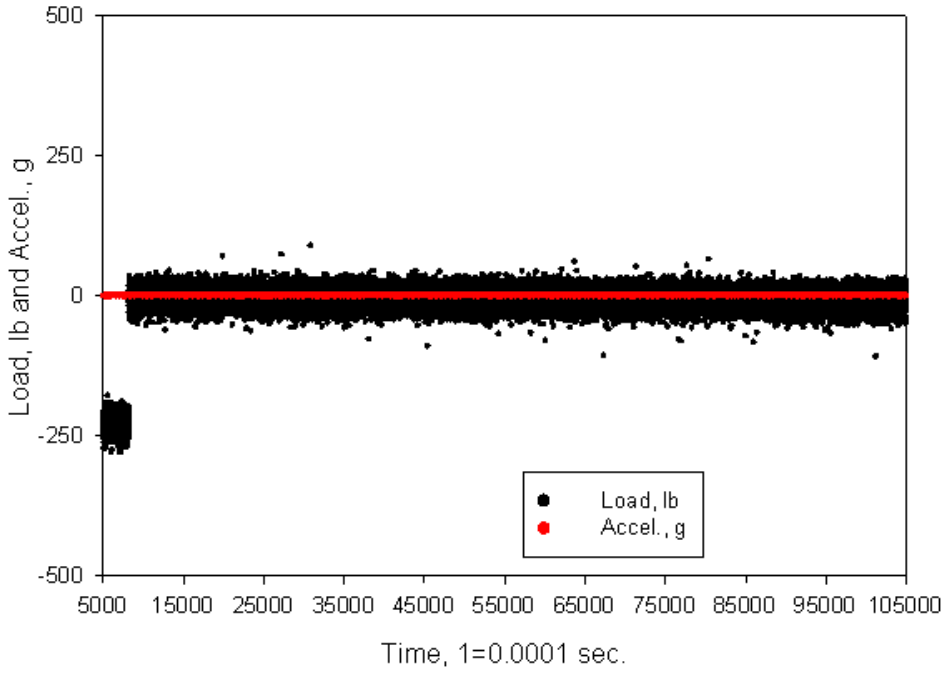


**Figure 149. Hampton test 11**

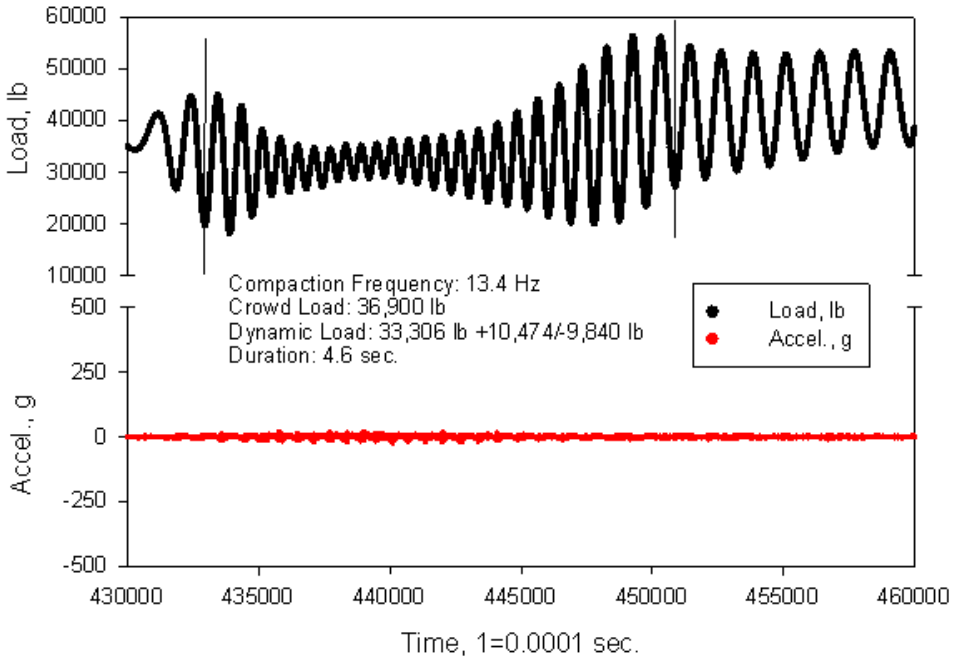


**Figure 150. Hampton test 12**

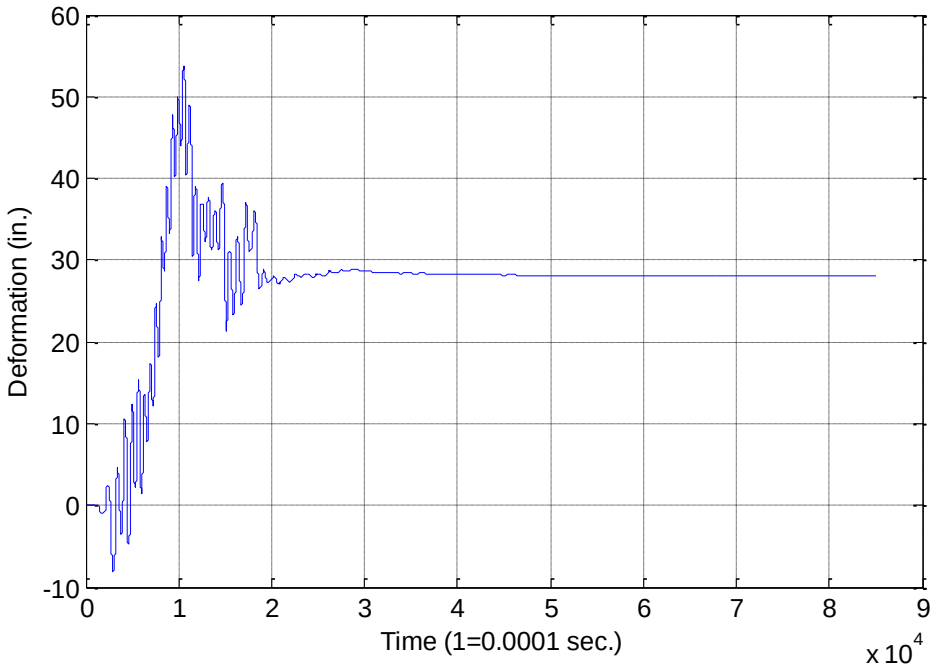


**Figure 151. Hampton test 12**

**La Port City**

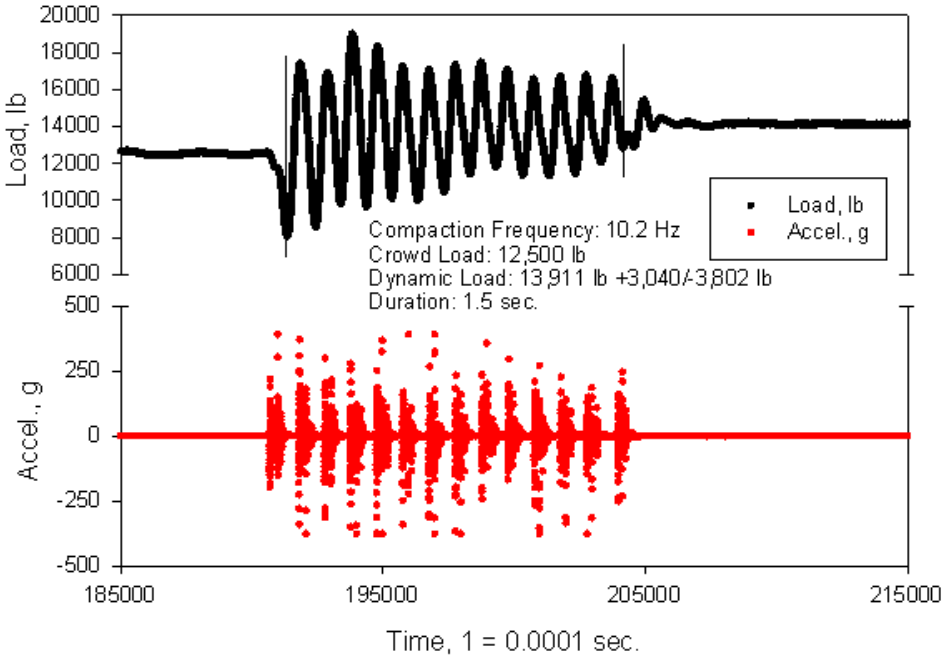


**Figure 152. La Port City test 1**

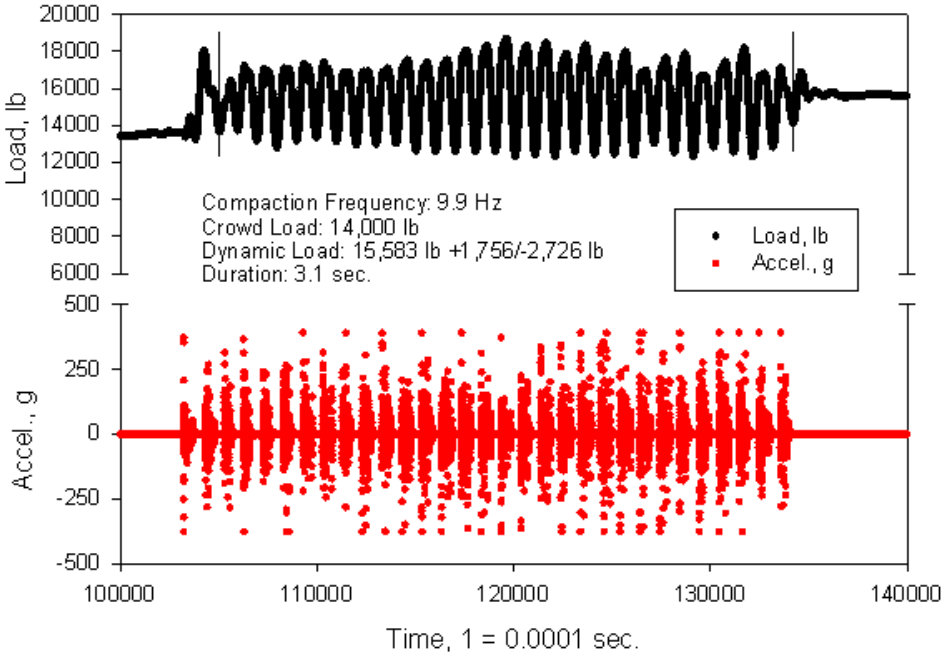


**Figure 153. La Port City test 2**

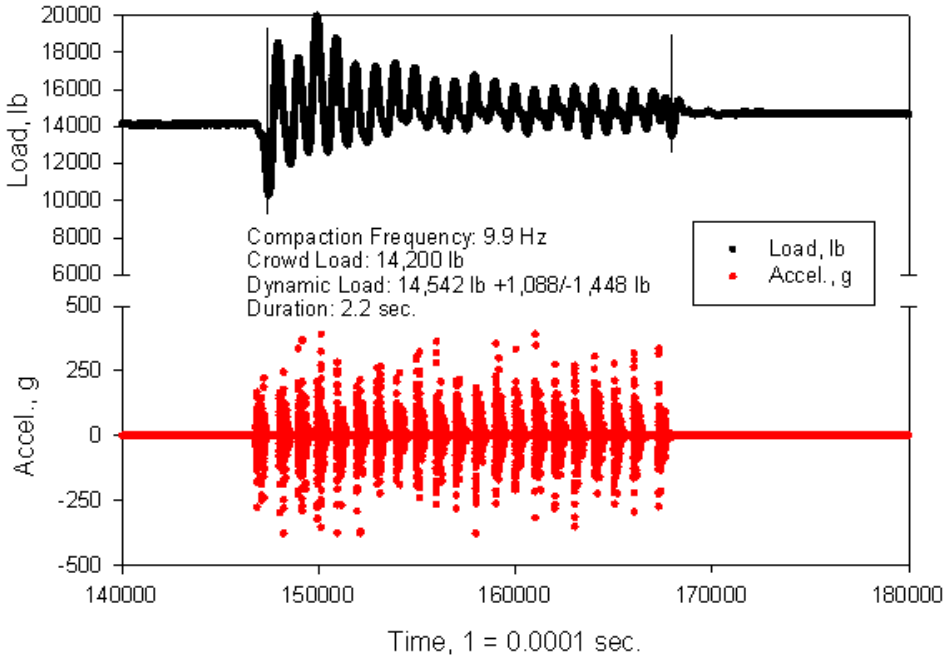


**Figure 154. La Port City test 3**

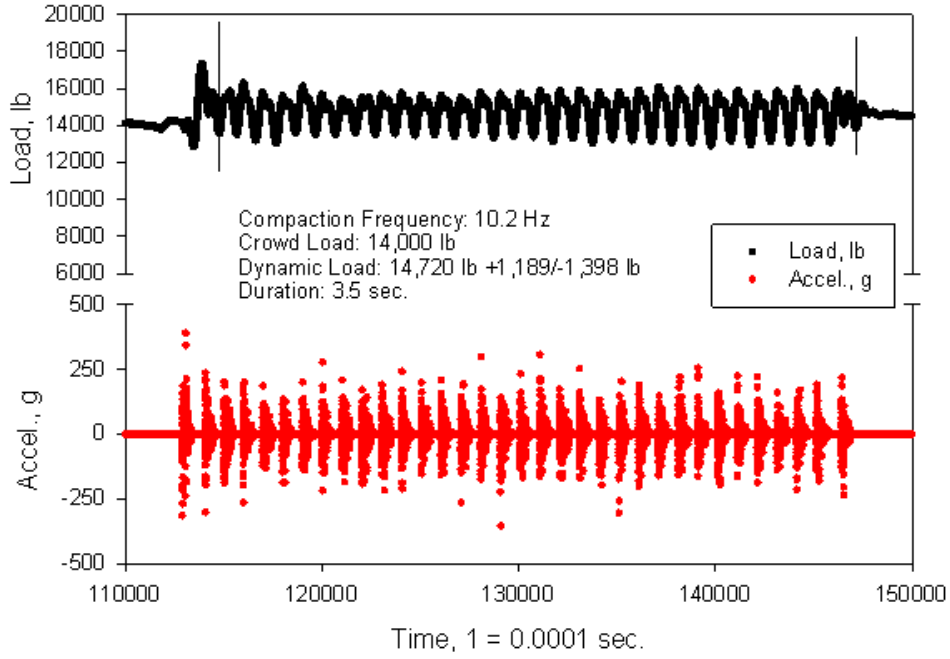


**Figure 155. La Port City test 4**

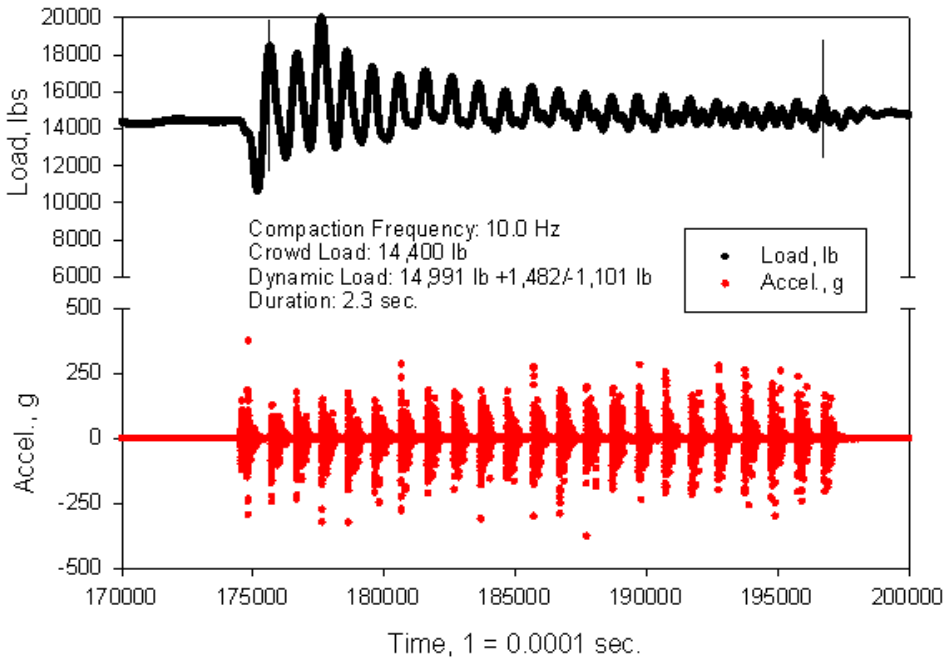


**Figure 156. La Port City test 5**

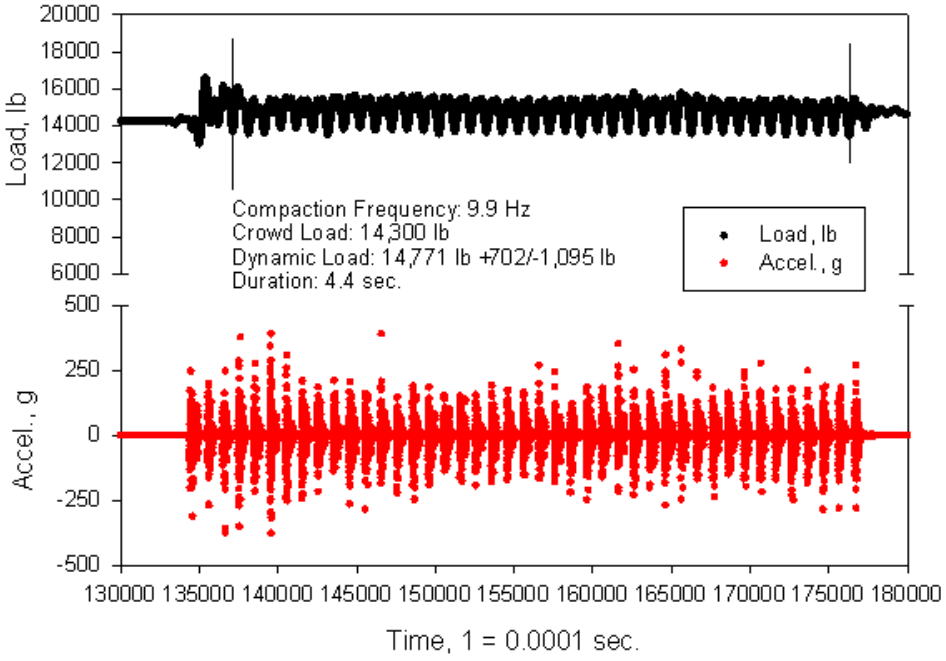


**Figure 157. La Port City test 6**

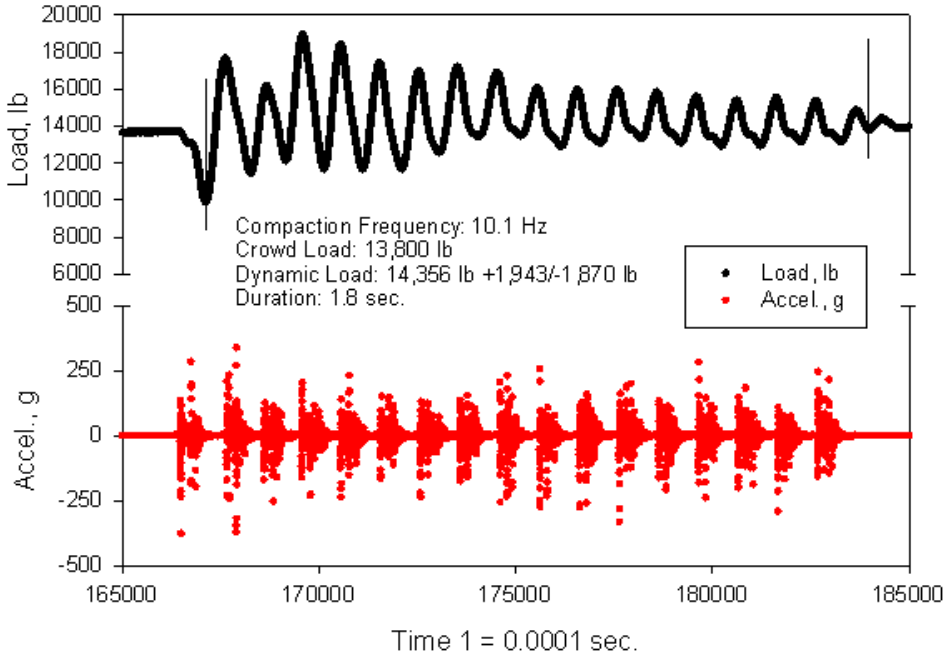


**Figure 158. La Port City test 7**

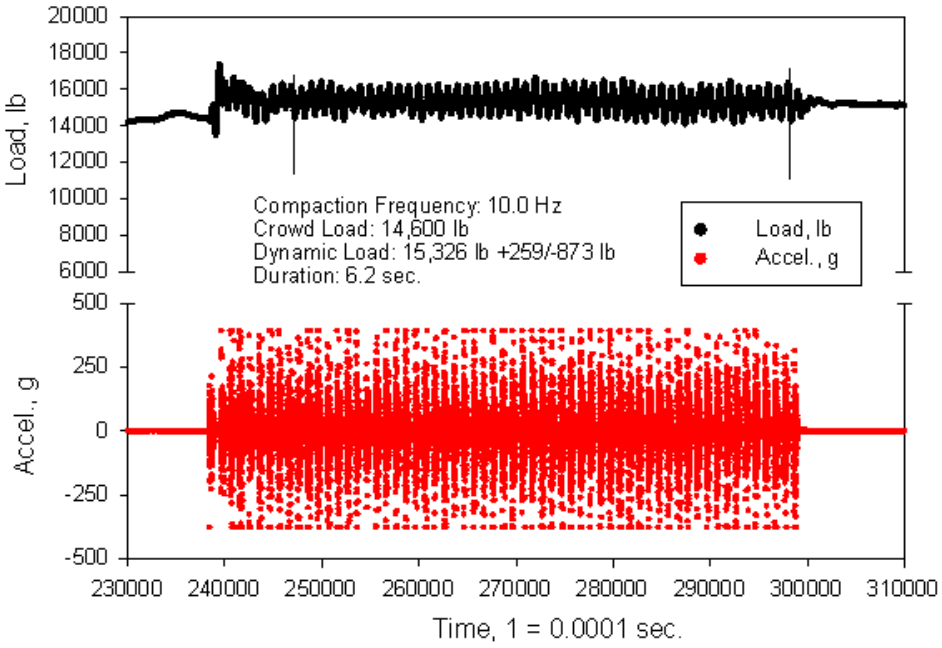


**Figure 159. La Port City test 8**

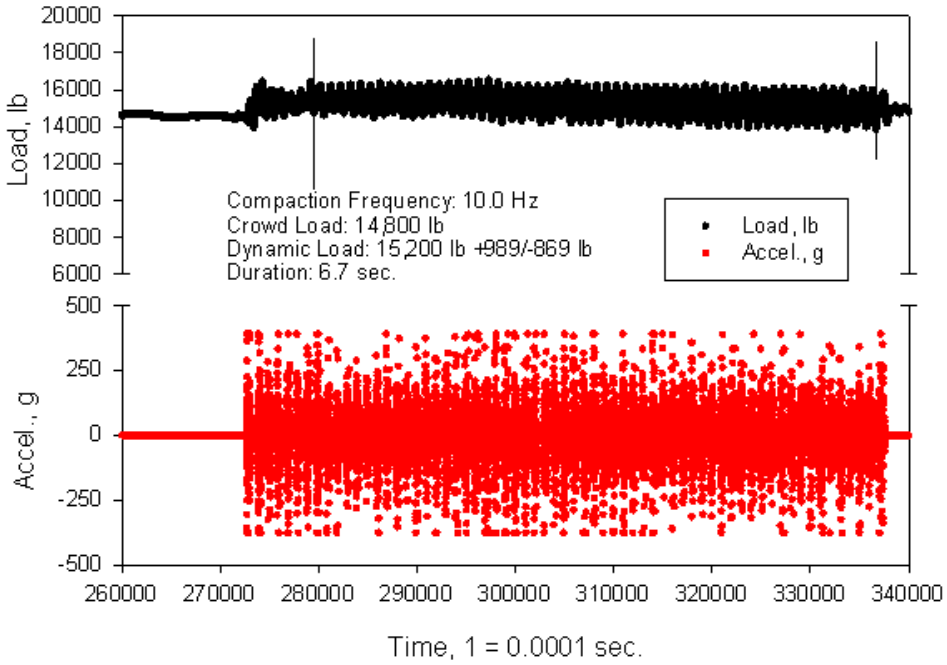


**Figure 160. La Port City test 9**

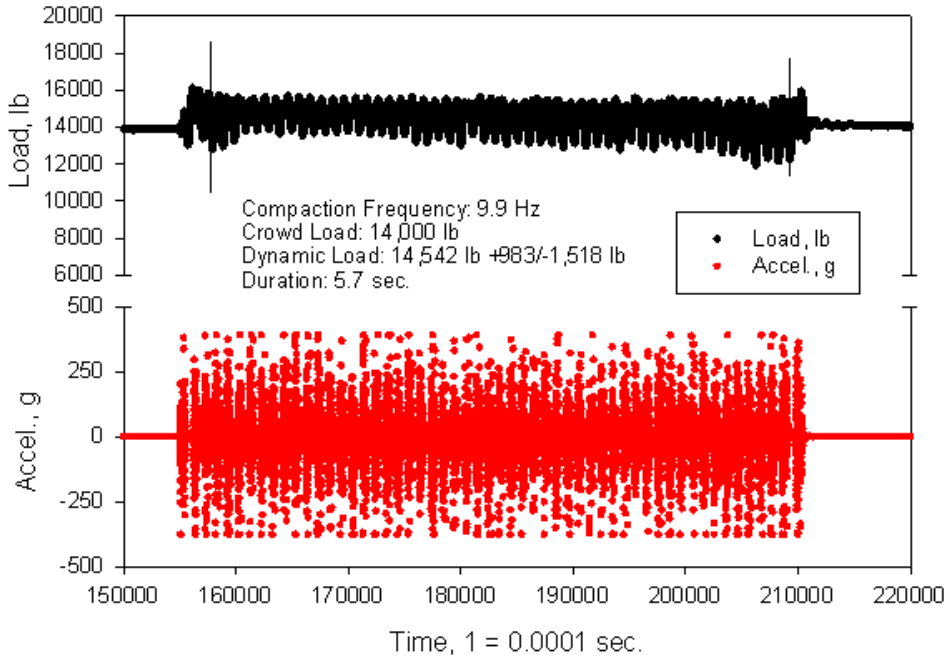


**Figure 161. La Port City test 10**

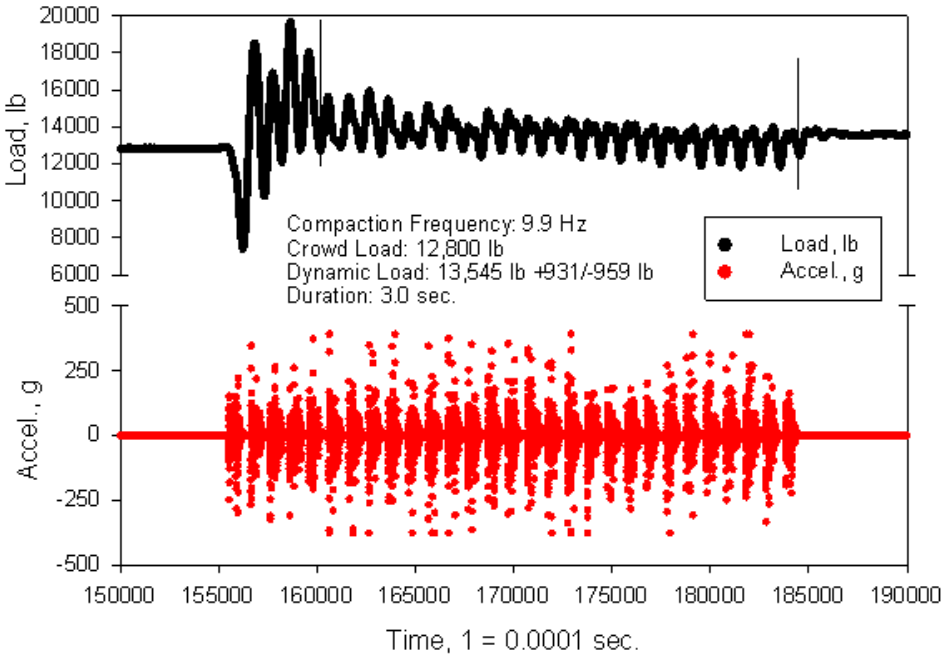


**Figure 162. La Port City test 11**

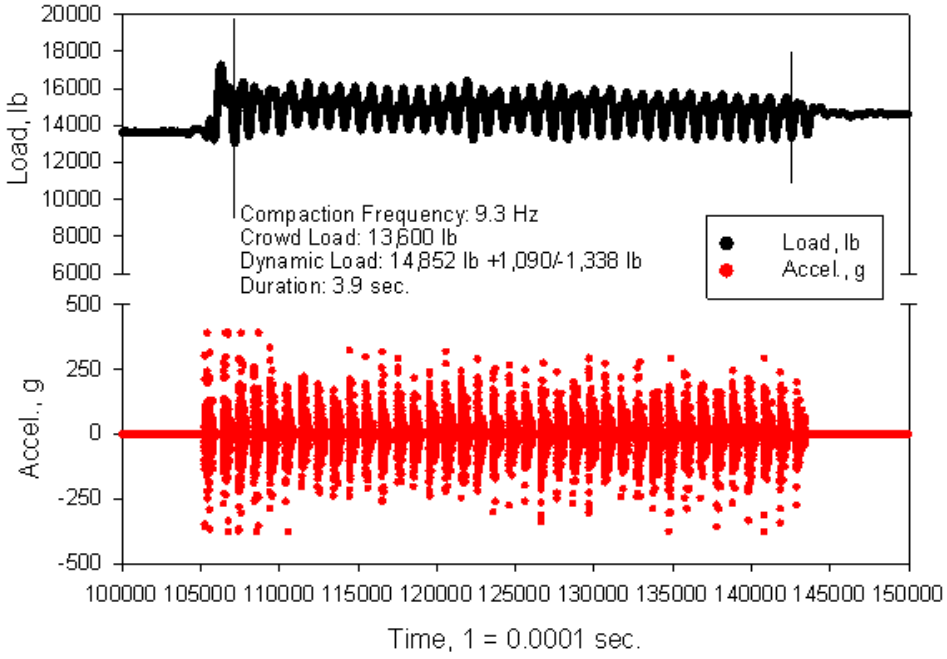


**Figure 163. La Port City test 12**

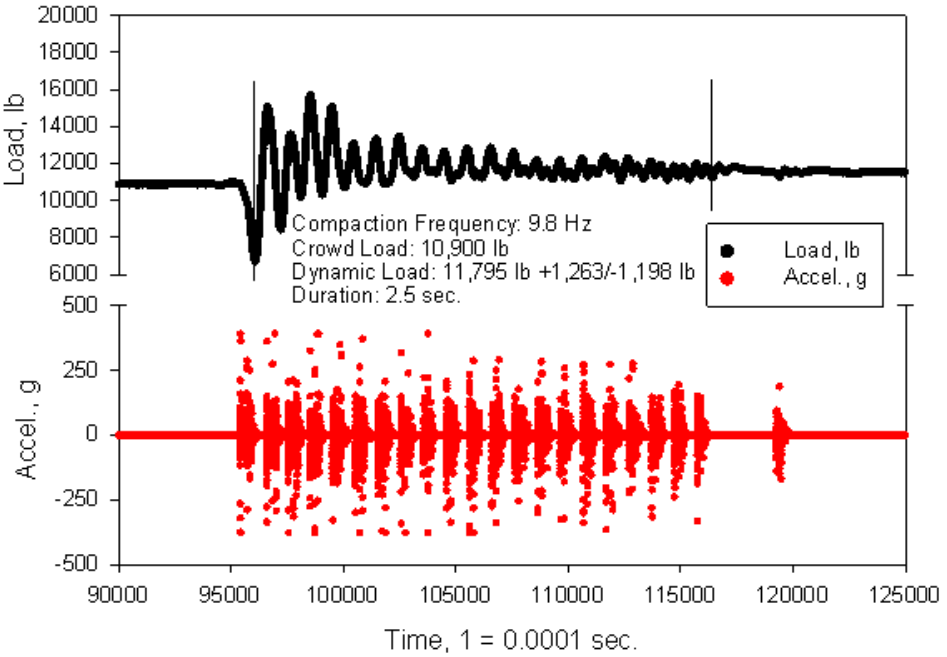


**Figure 164. La Port City test 13**

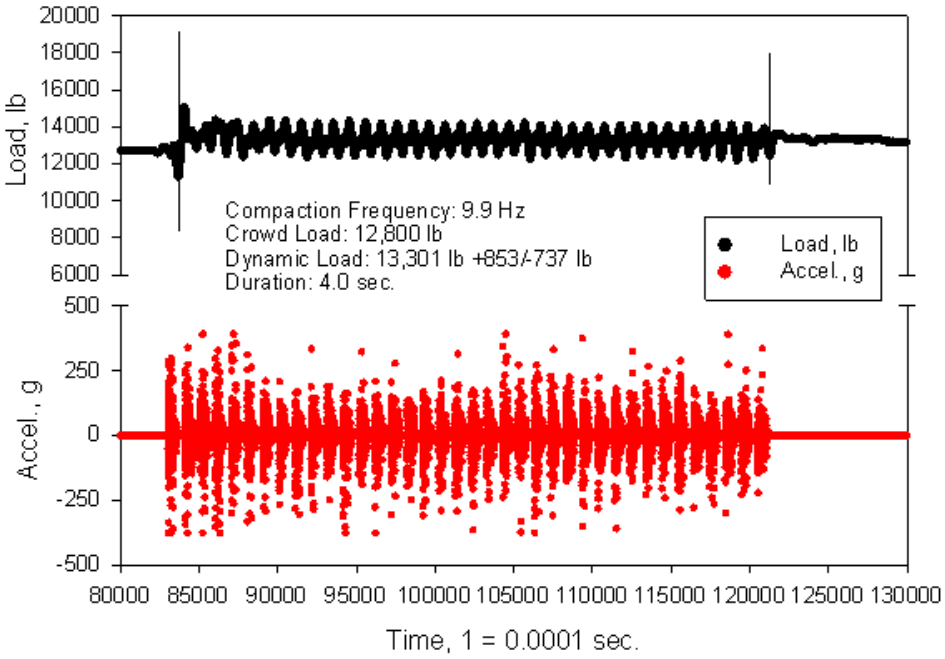


**Figure 165. La Port City test 14**

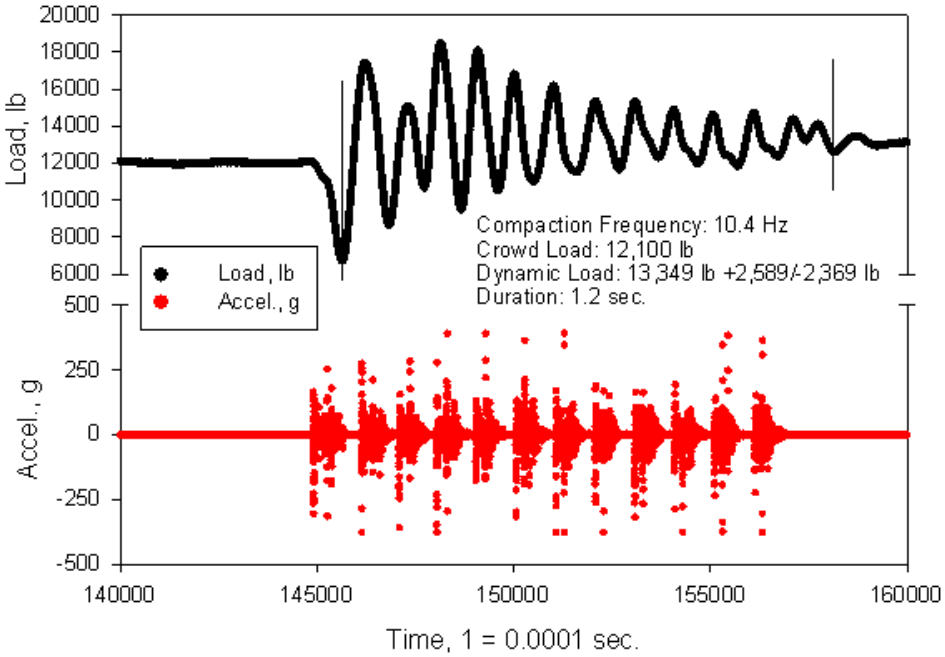


**Figure 166. La Port City test 15**

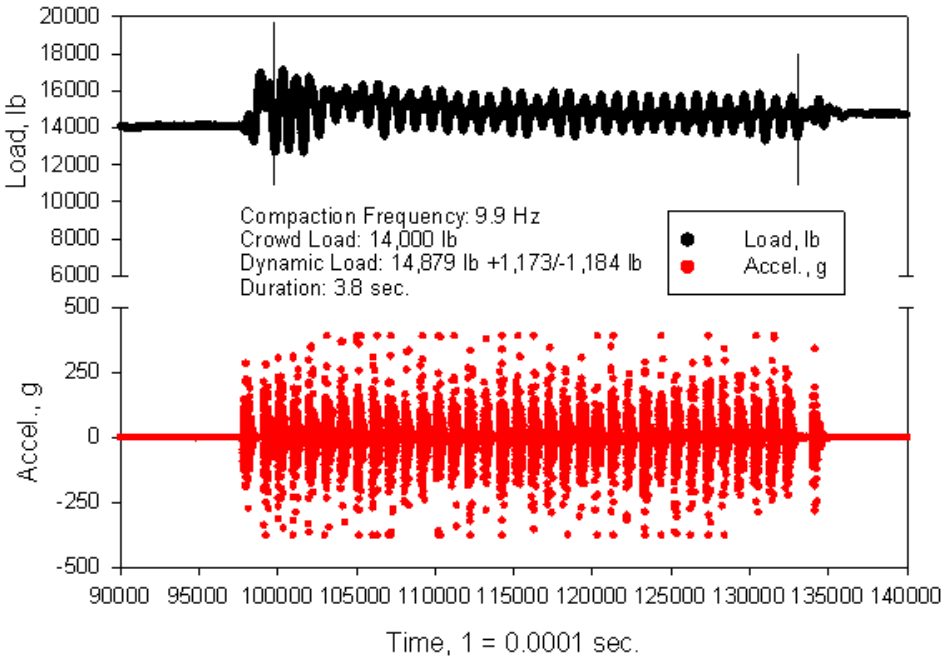


**Figure 167. La Port City test 16**

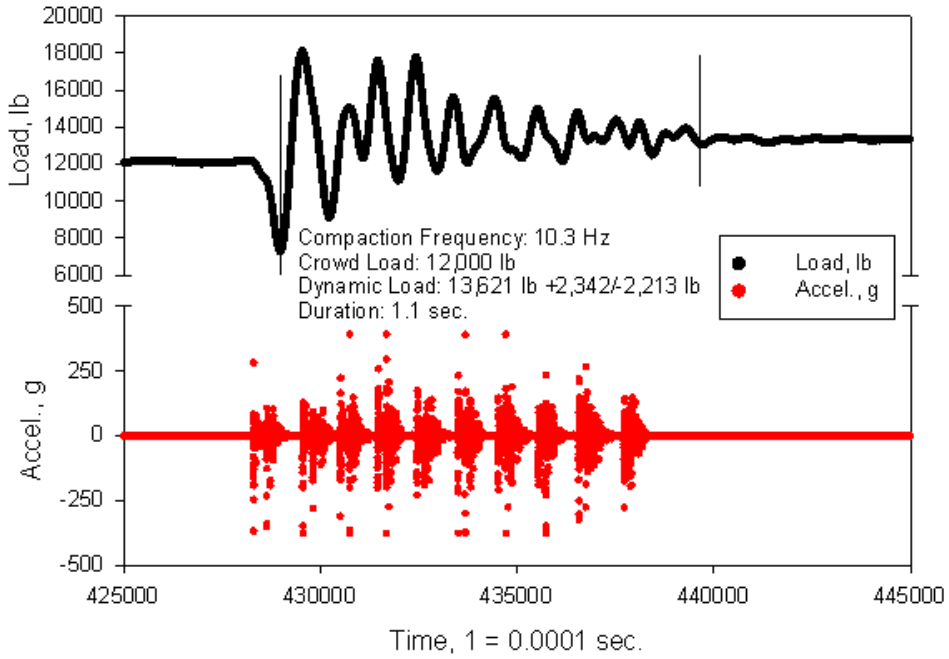


**Figure 168. La Port City test 17**

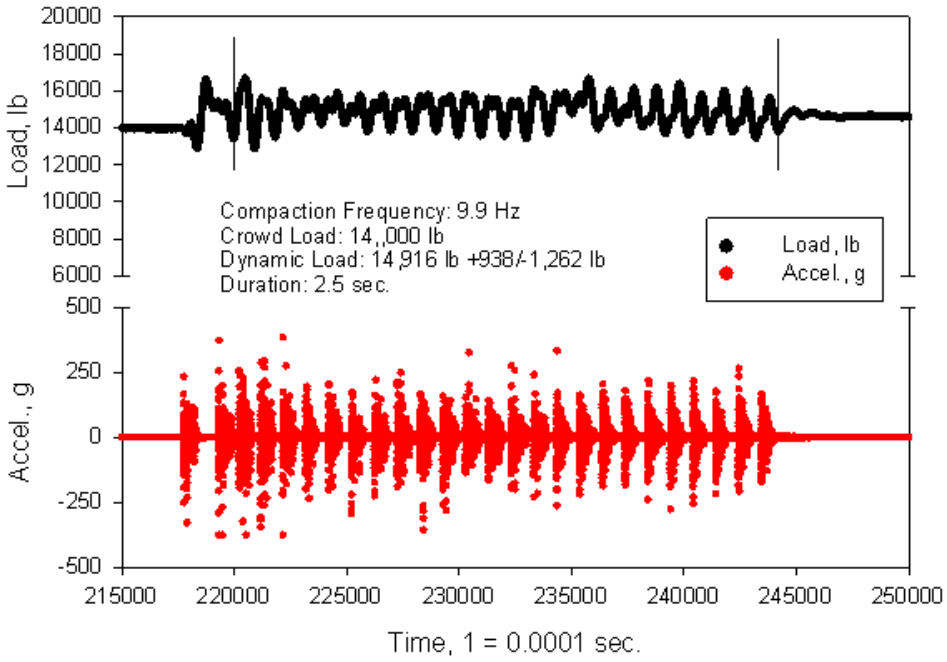


**Figure 169. La Port City test 18**

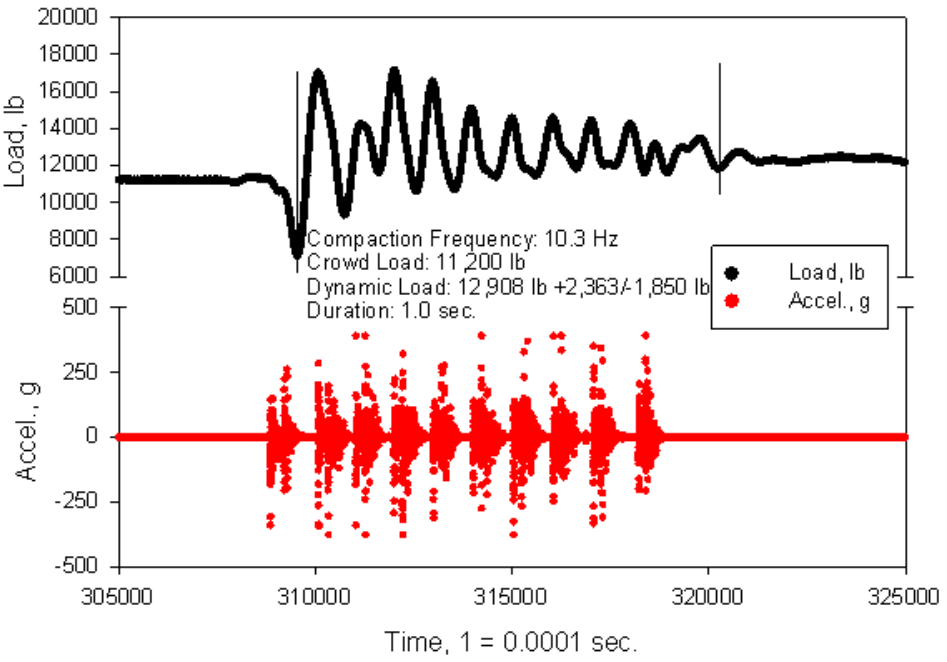


**Figure 170. La Port City test 19**

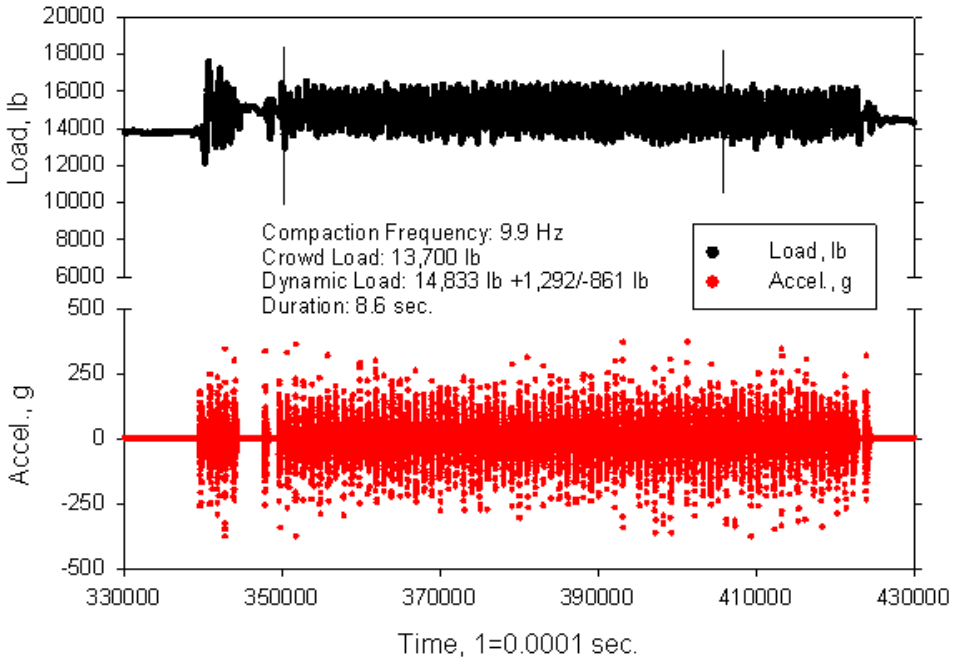


**Figure 171. La Port City test 22**

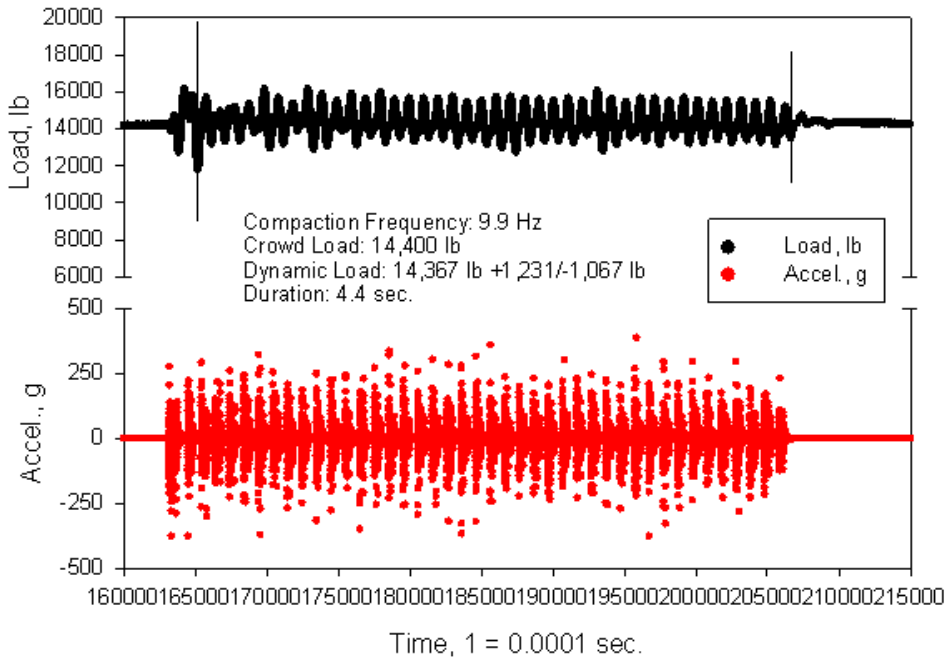


**Figure 172. La Port City test 23**

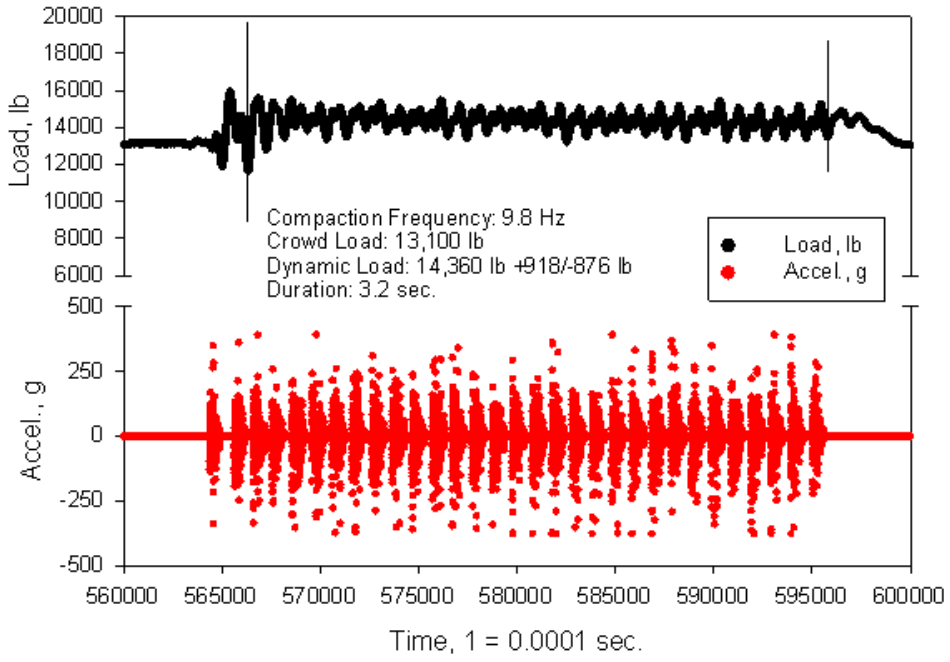


**Figure 173. La Port City test 24**

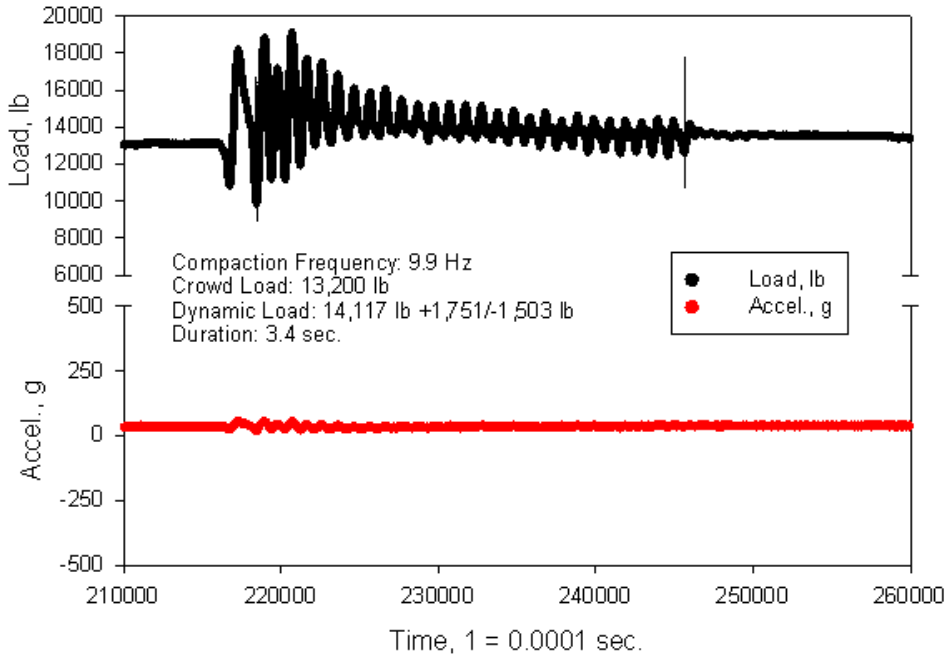


**Figure 174. La Port City test 27**

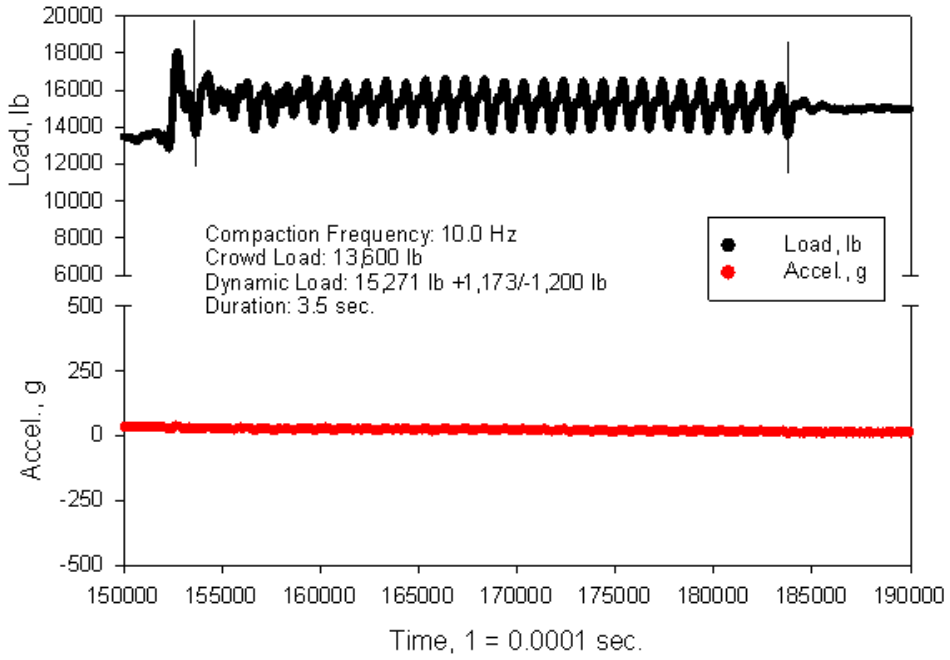


**Figure 175. La Port City test 28**

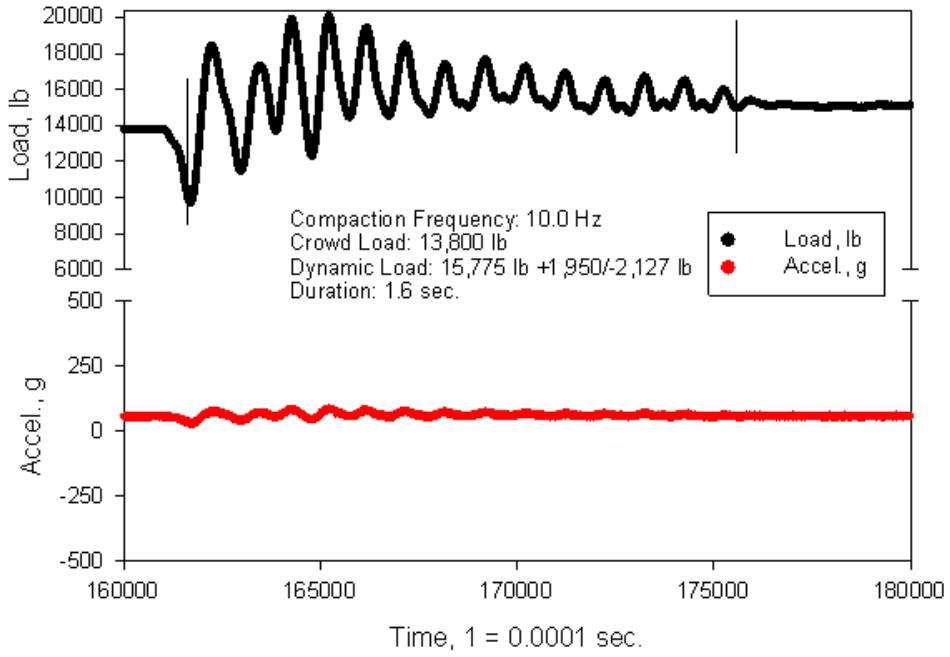


**Figure 176. La Port City test 29**

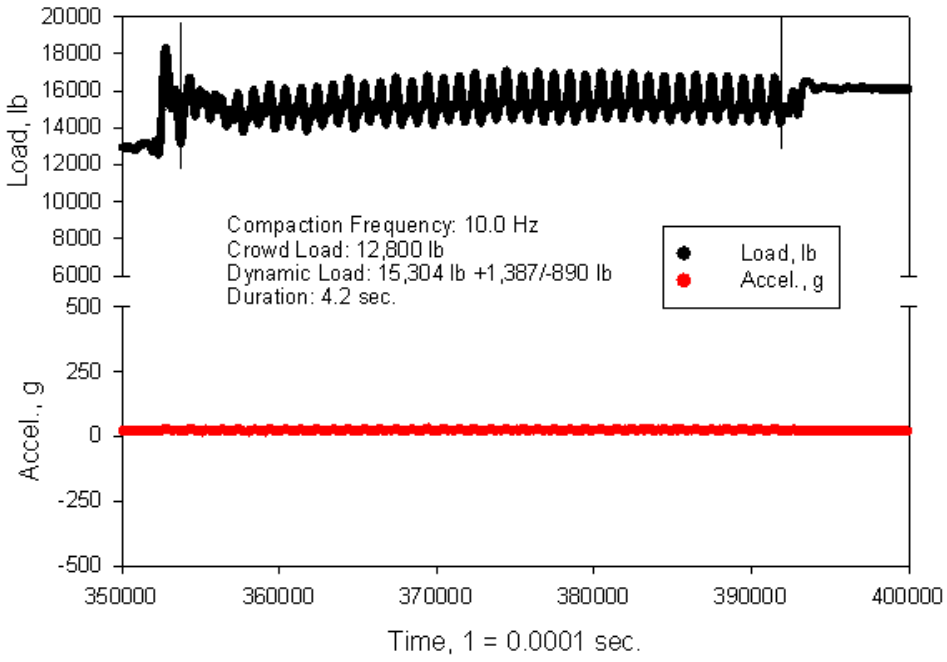


**Figure 177. La Port City test 30**

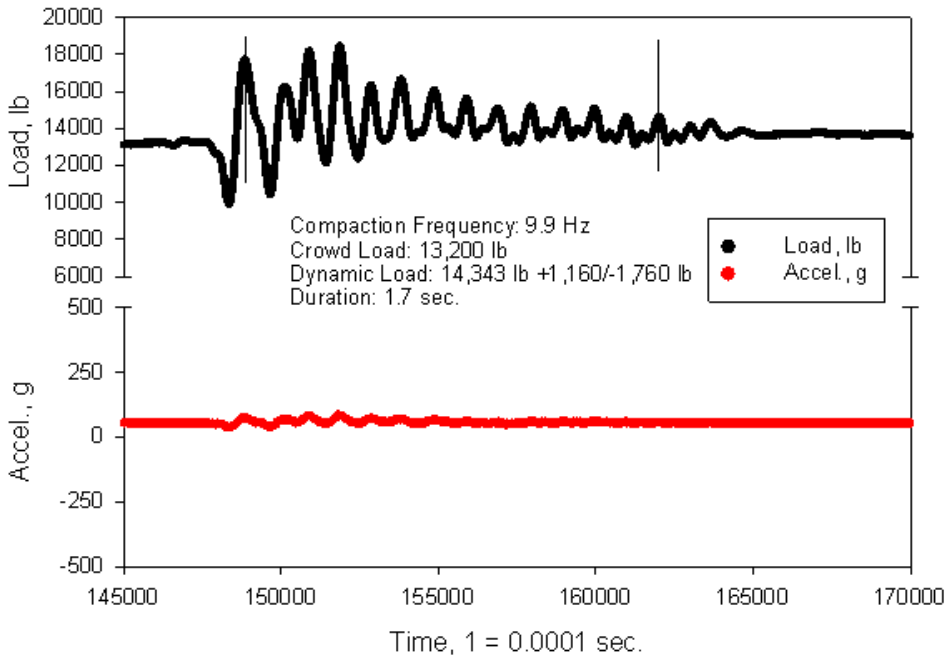


**Figure 178. La Port City test 31**

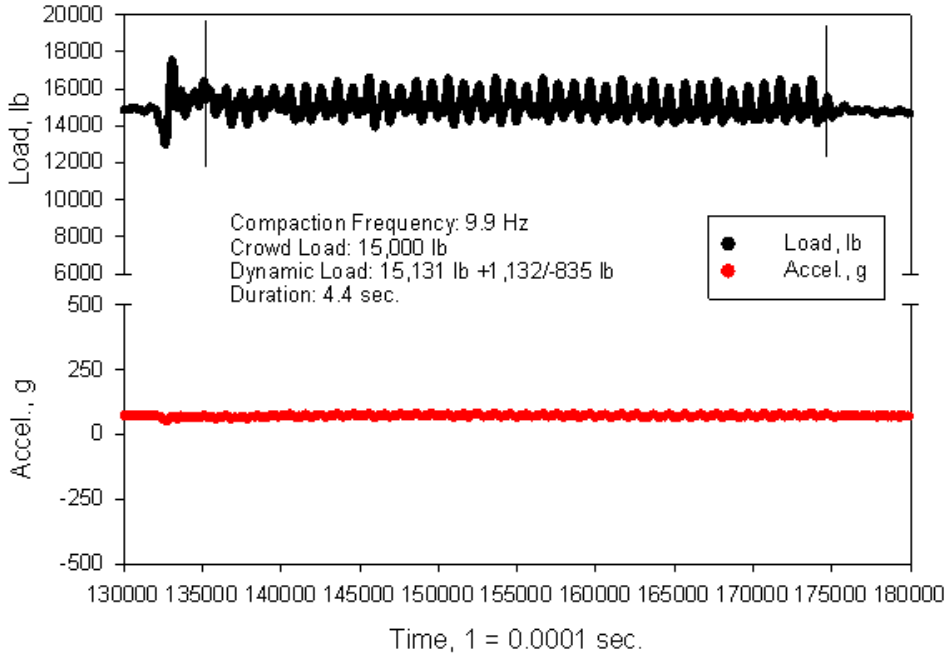


**Figure 179. La Port City test 32**

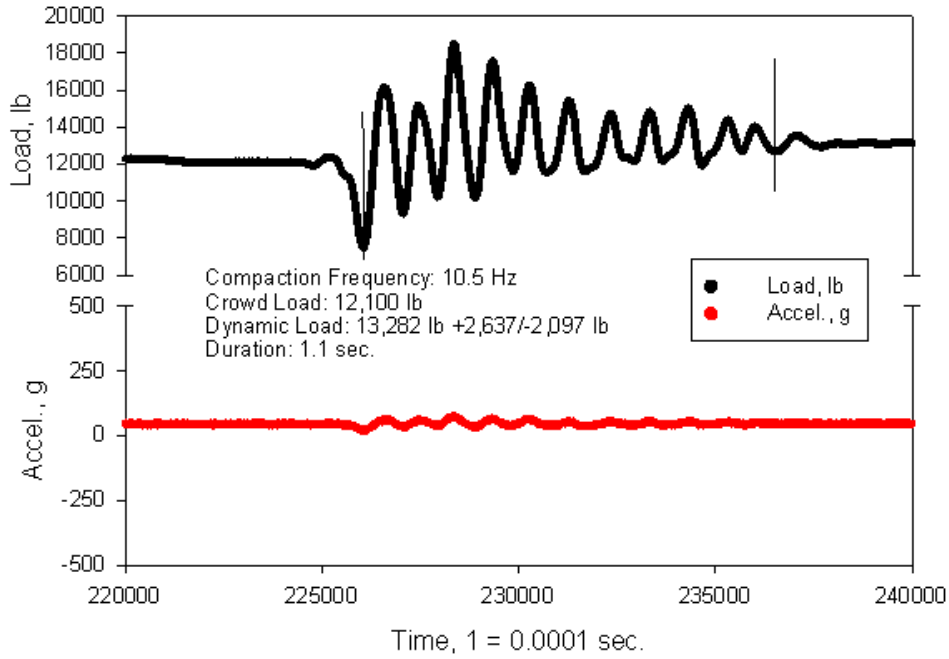


**Figure 180. La Port City test 33**

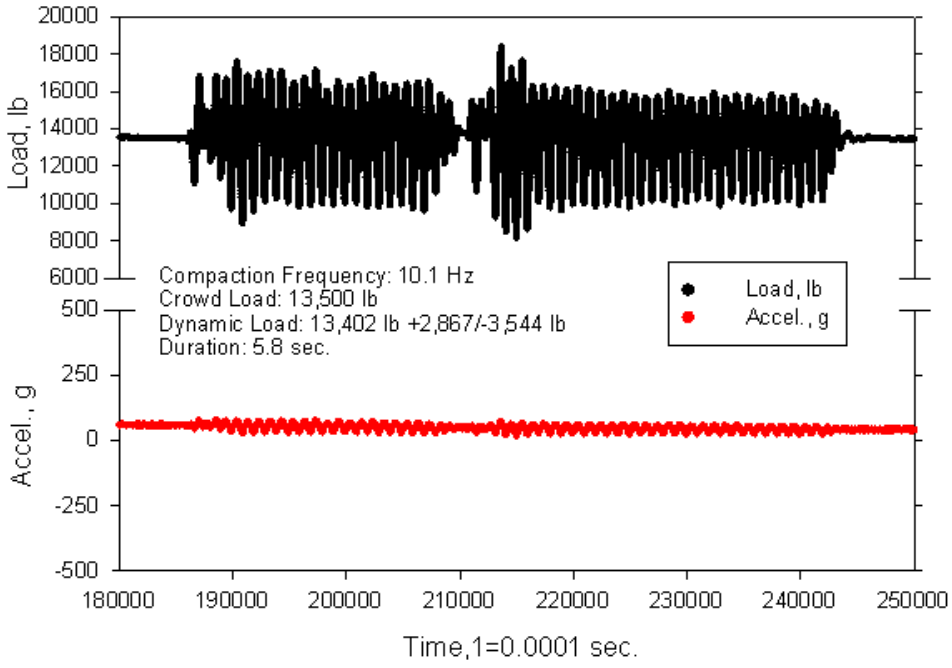


**Figure 181. La Port City test 34**

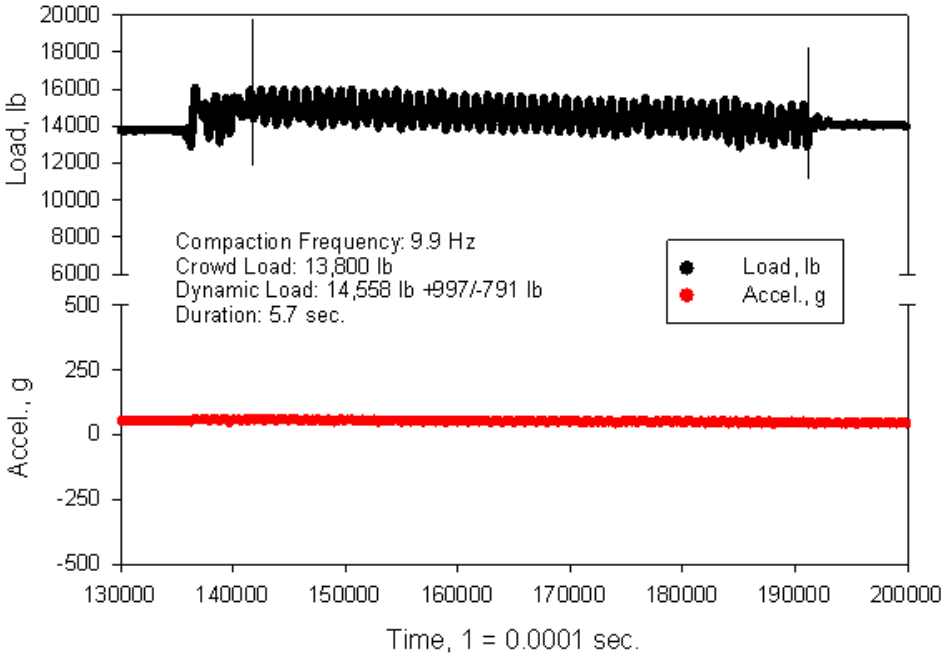


**Figure 182. La Port City test 35**

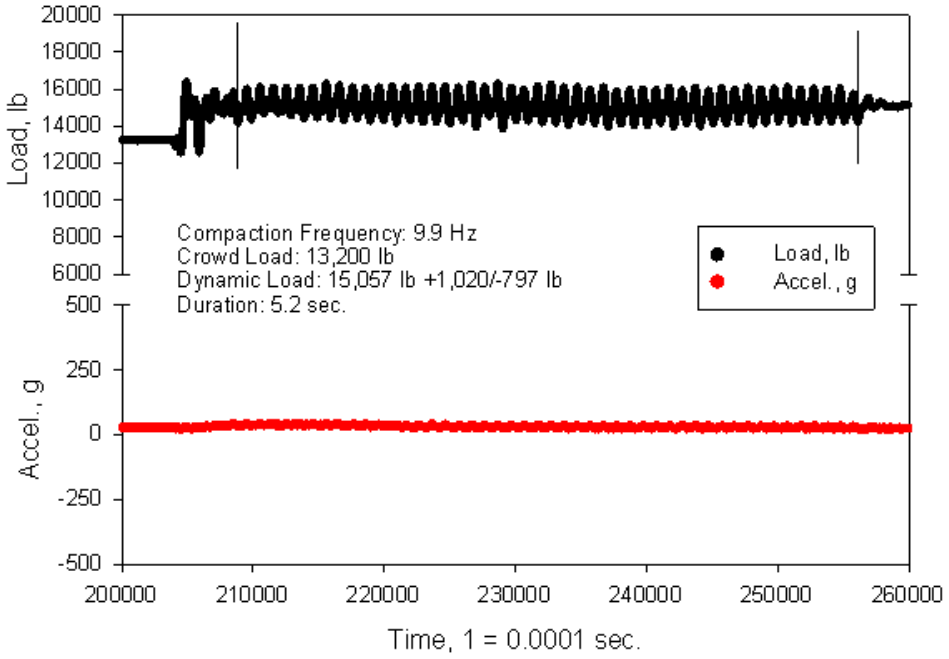


**Figure 183. La Port City test 36**

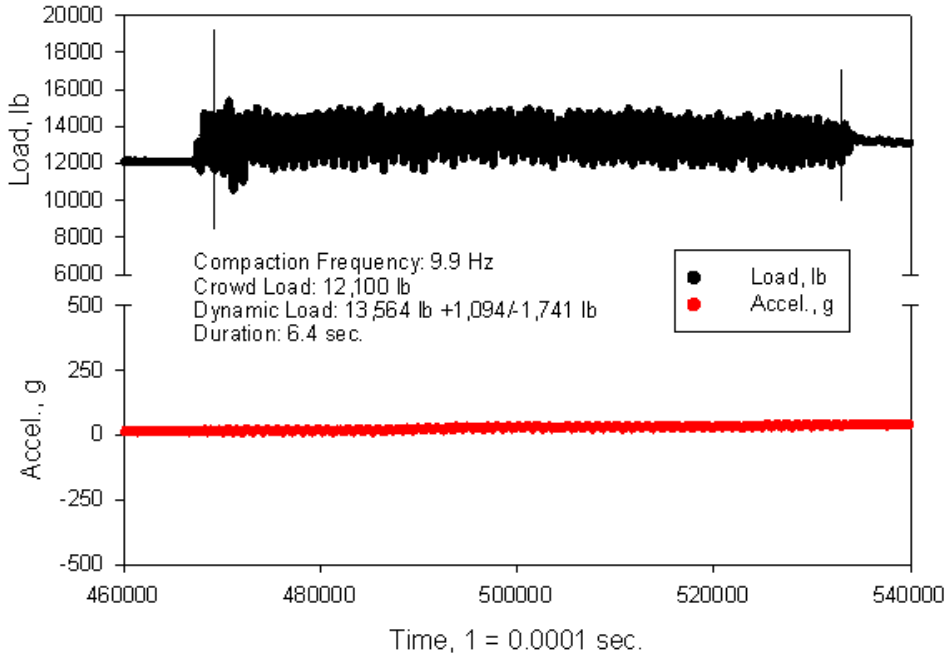


**Figure 184. La Port City test 37**

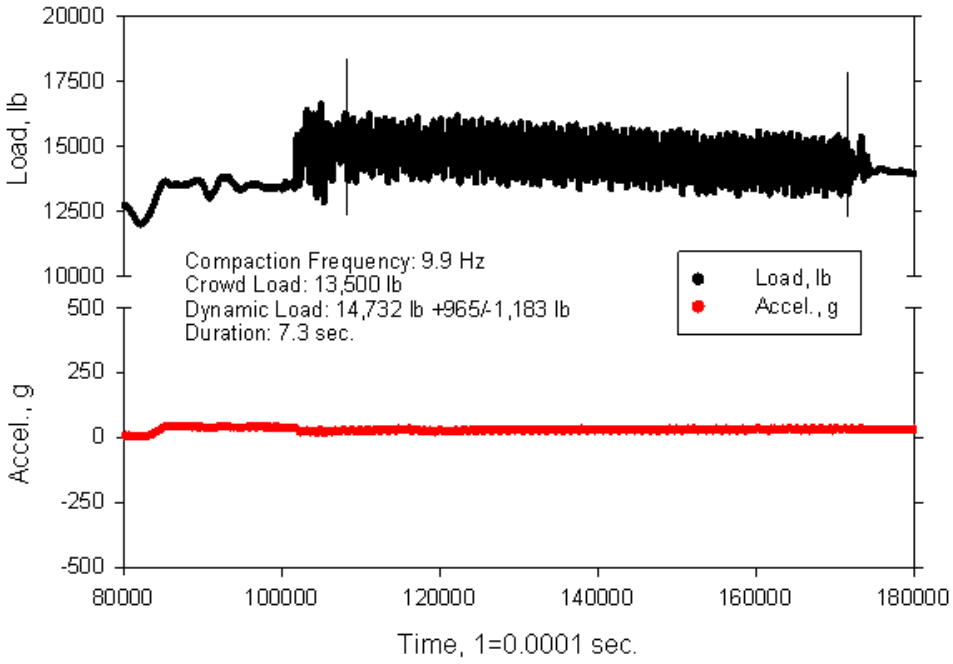


**Figure 185. La Port City test 38**

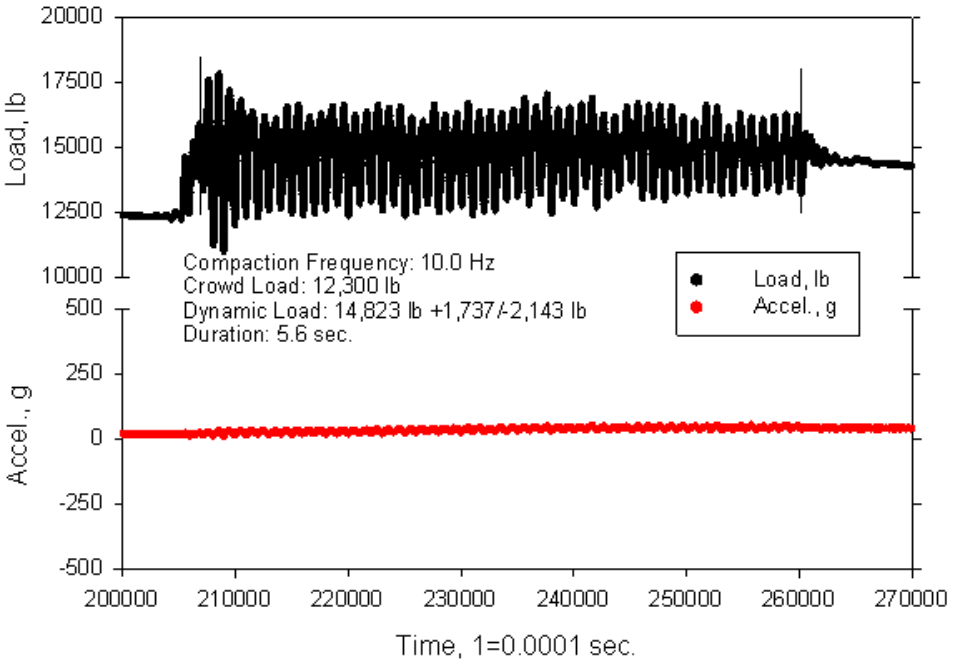


**Figure 186. La Port City test 39**

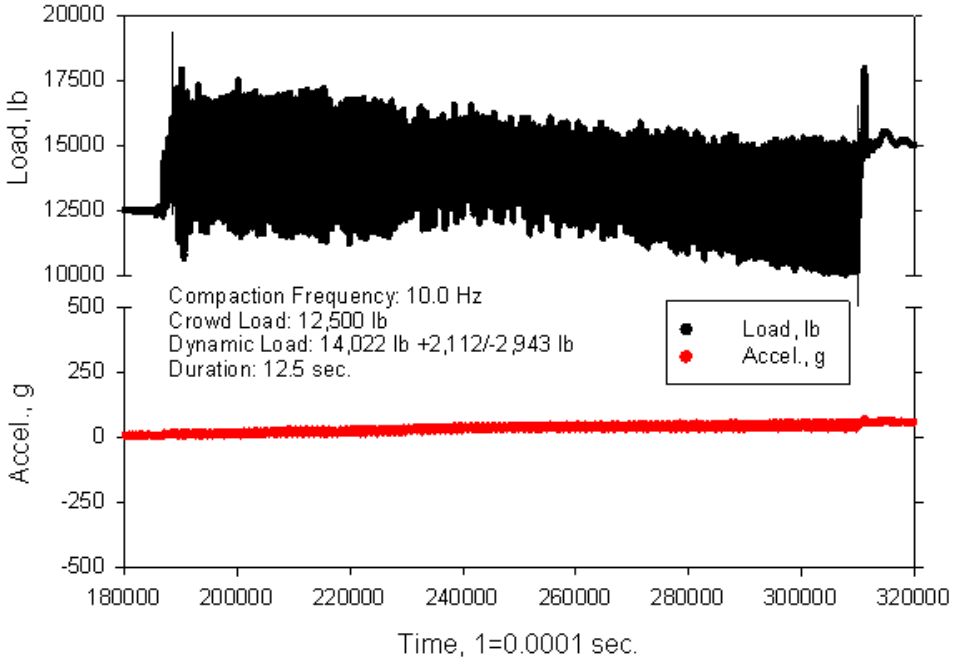


**Figure 187. La Port City test 40**

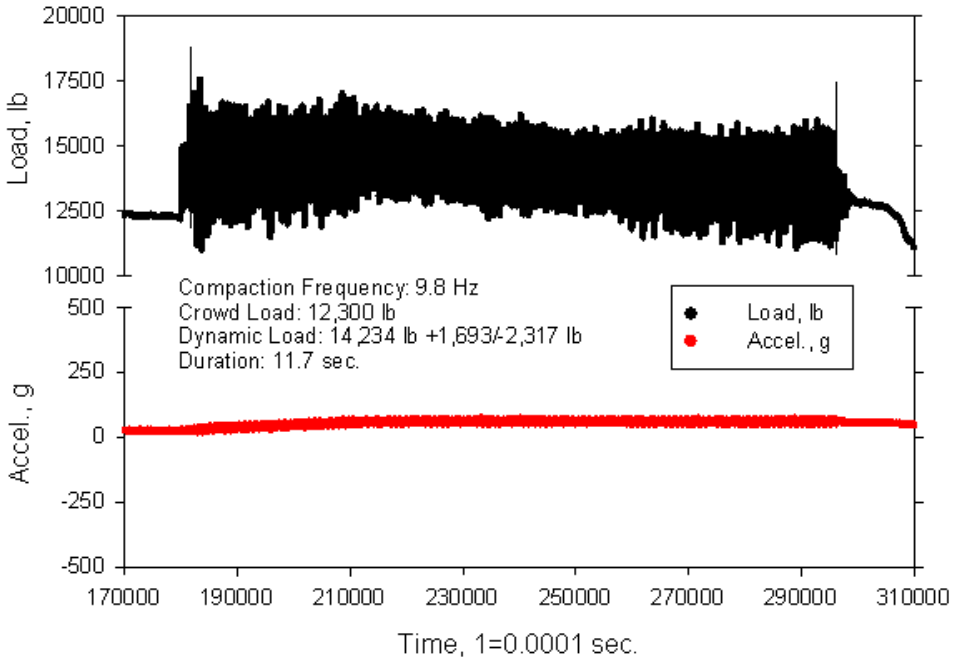


**Figure 188. La Port City test 41**

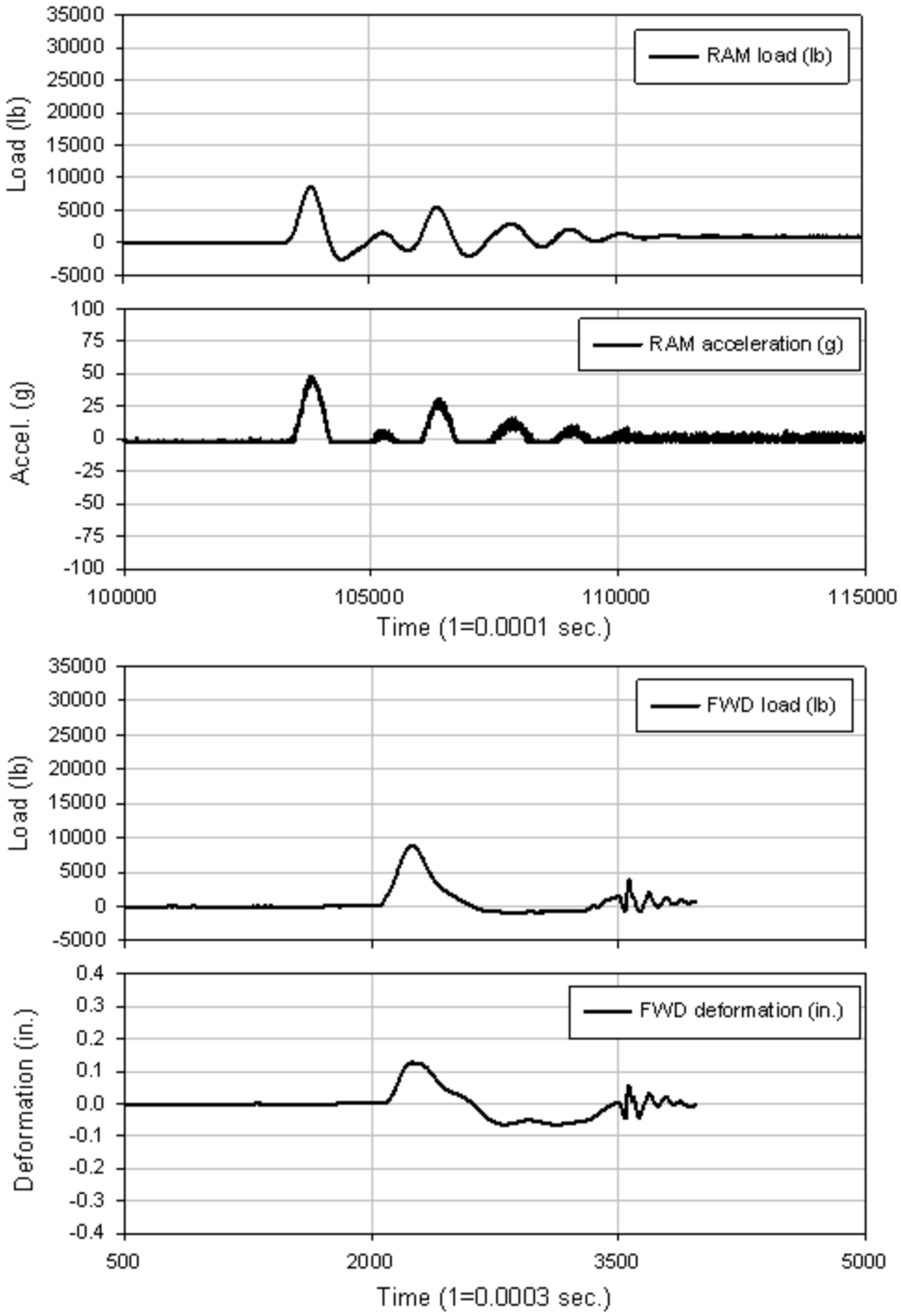


**Figure 189. La Port City test 46**

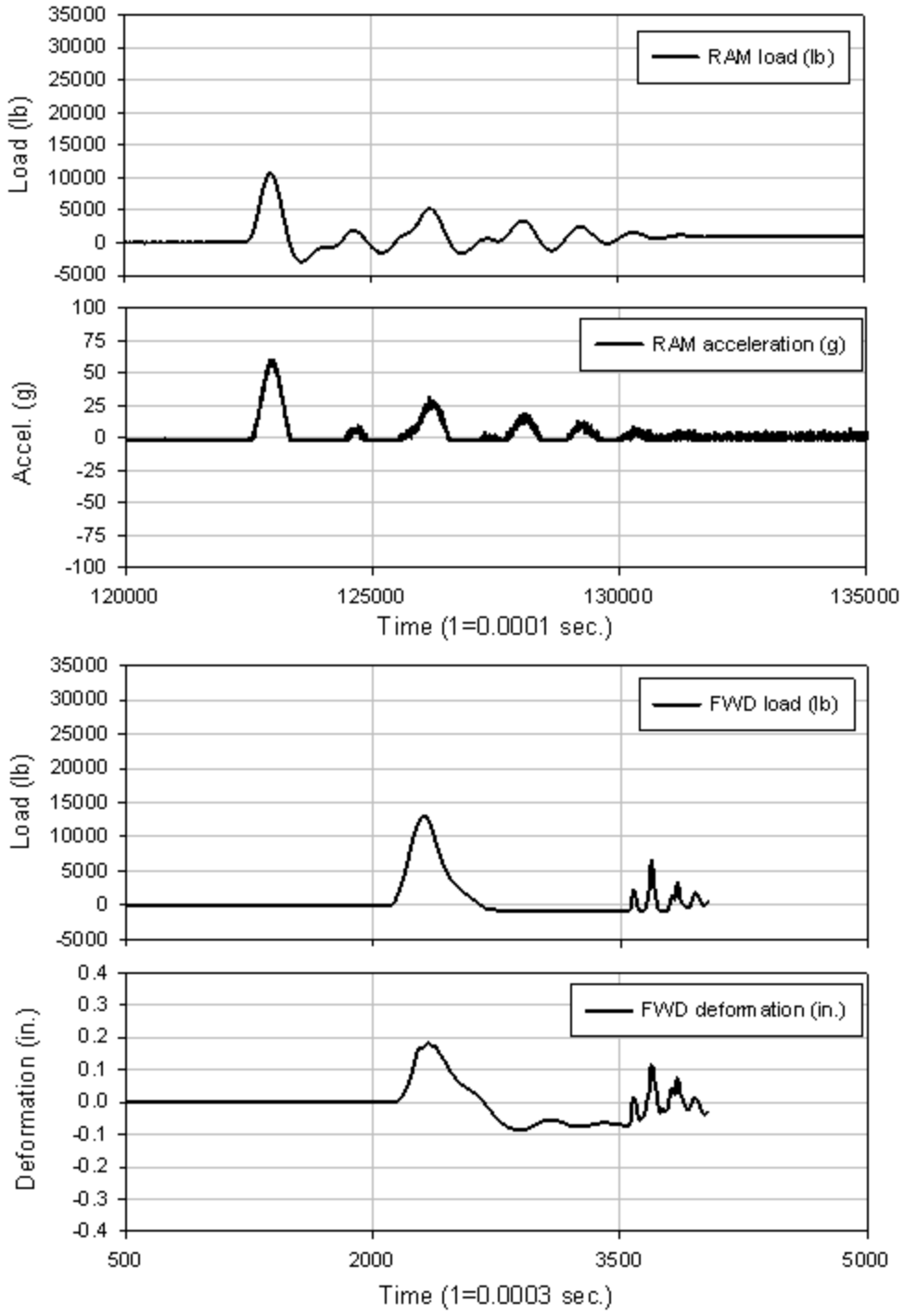


**Figure 190. La Port City test 47**

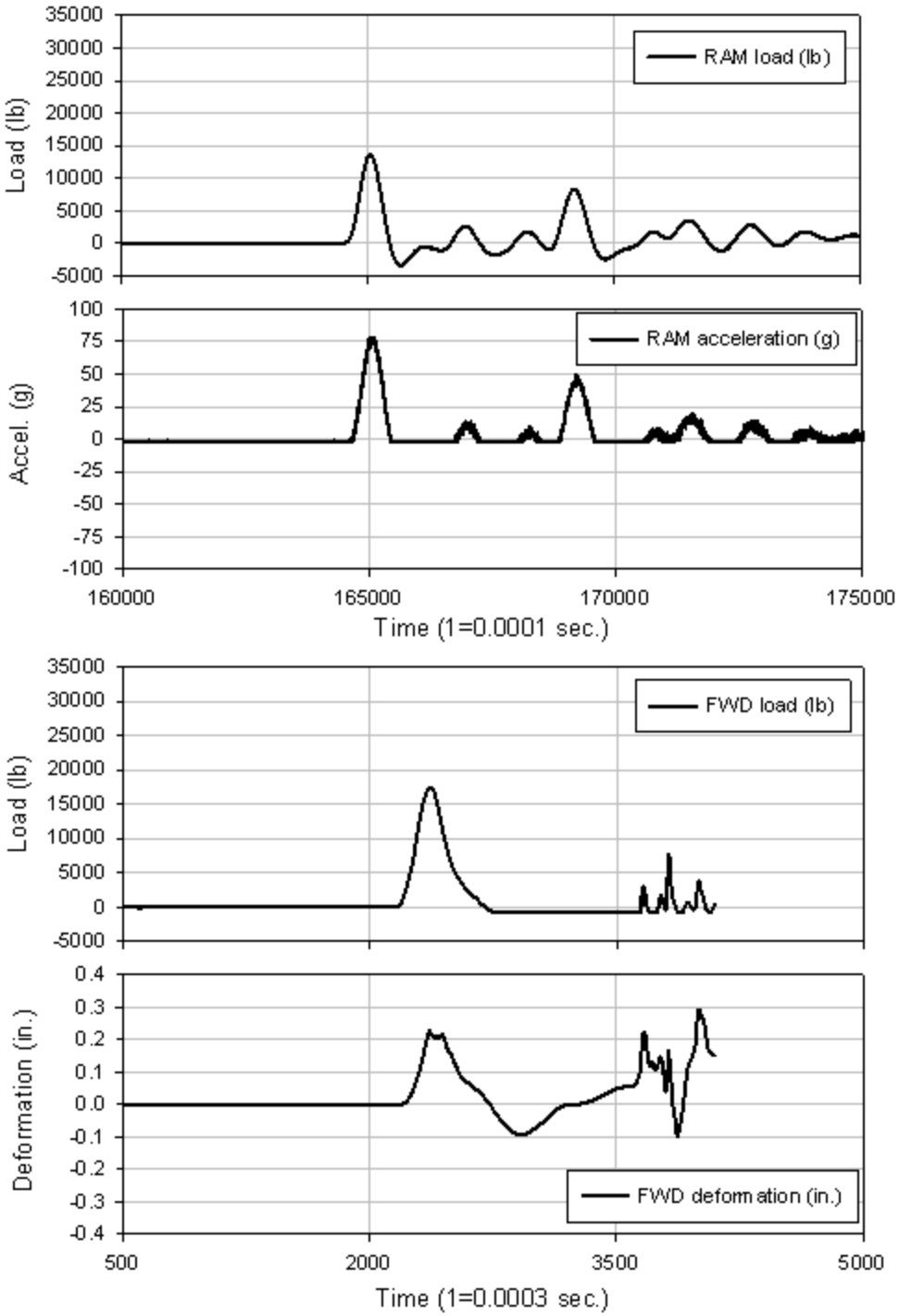


**Figure 191. La Port City test 48**

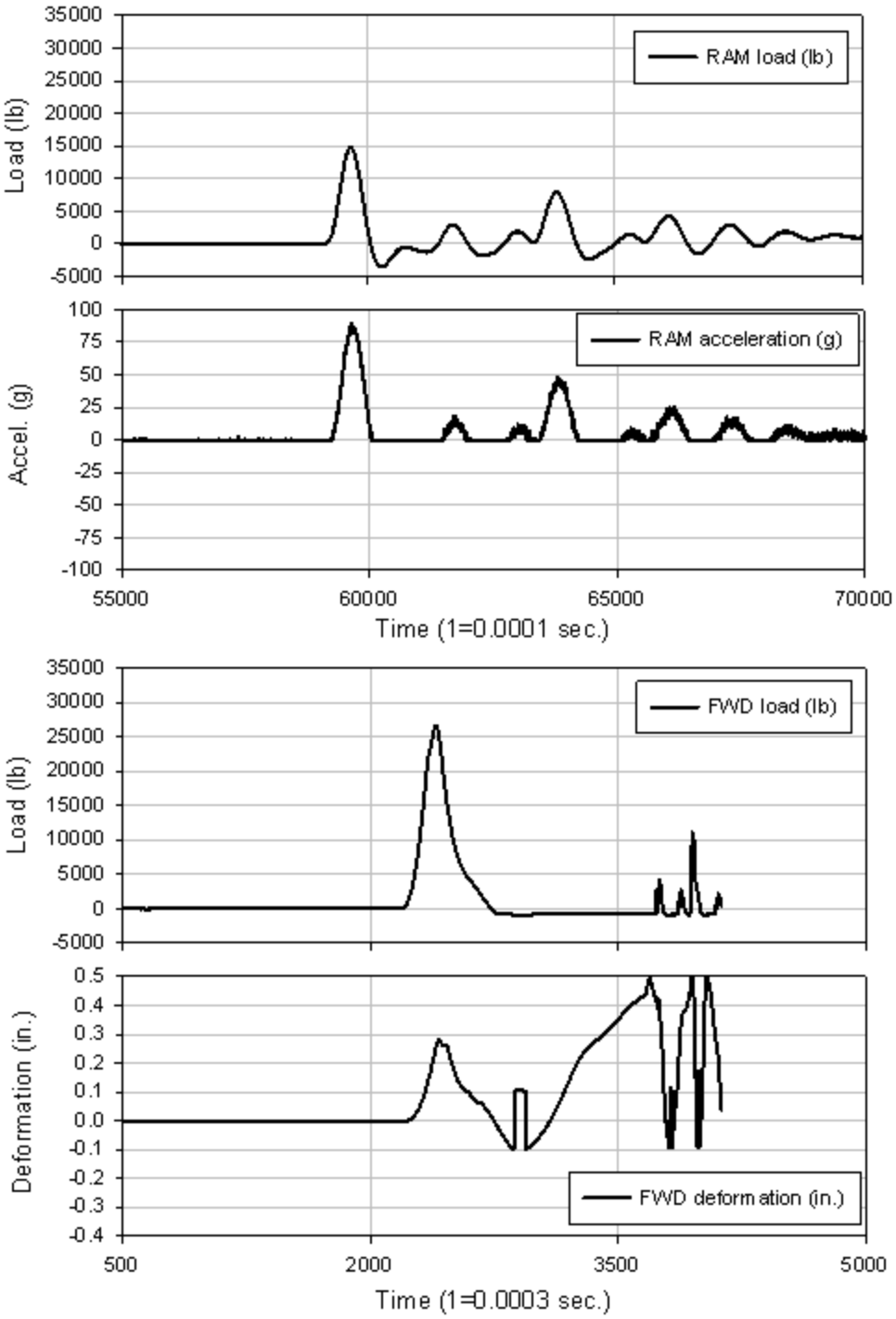


**Figure 192. La Port City test 50**

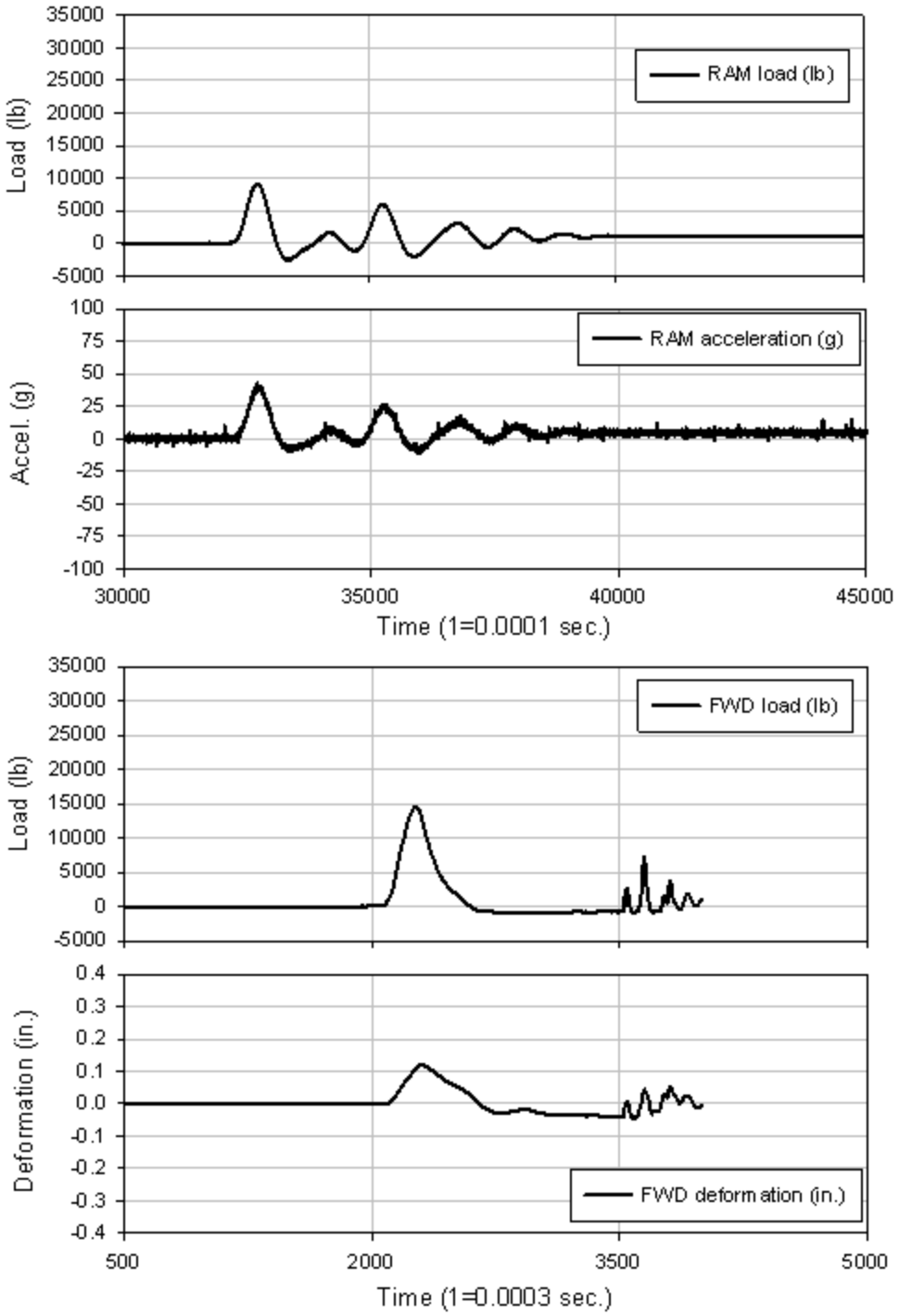


**Figure 193. La Port City test 53**

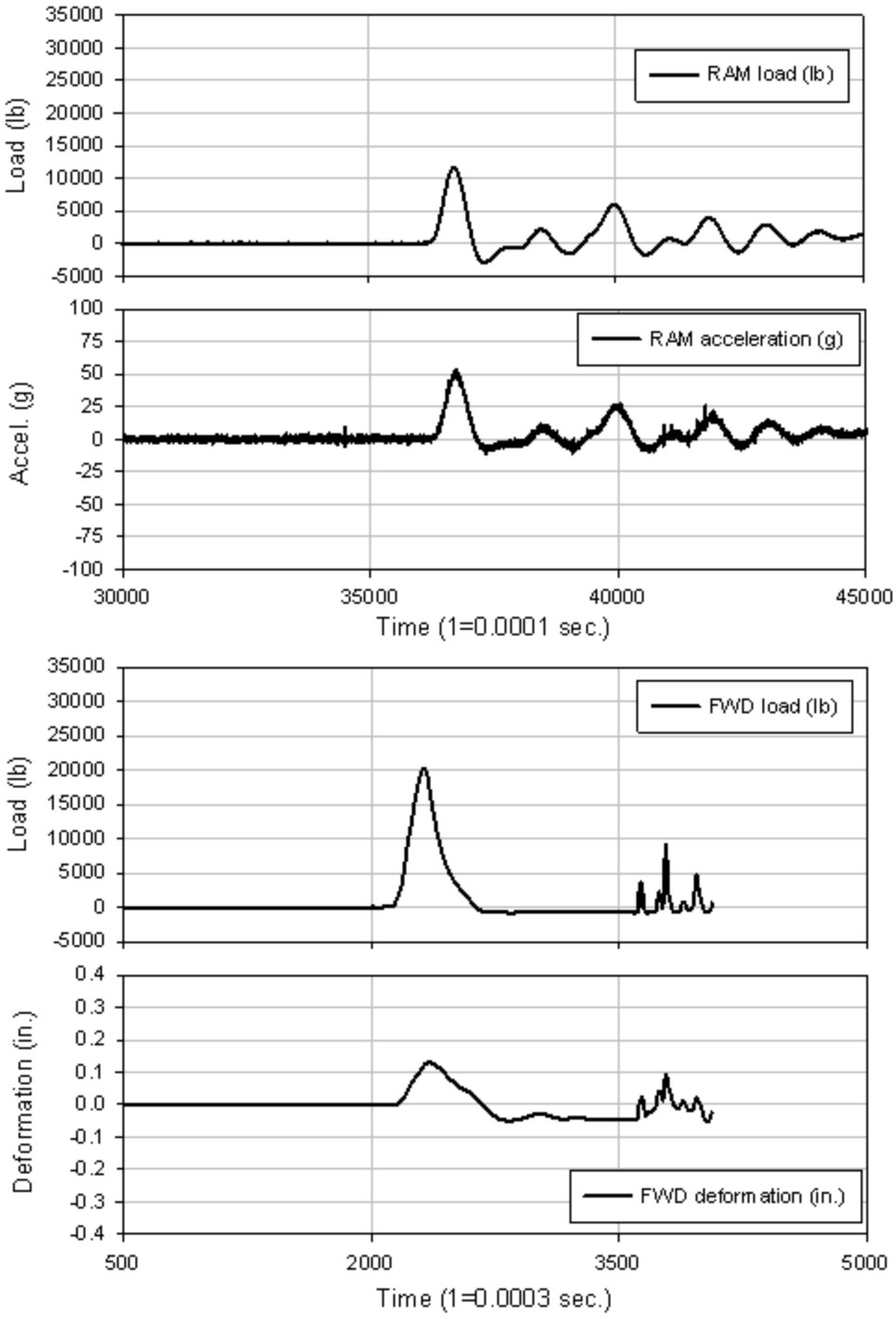


**Figure 194. La Port City test 54**

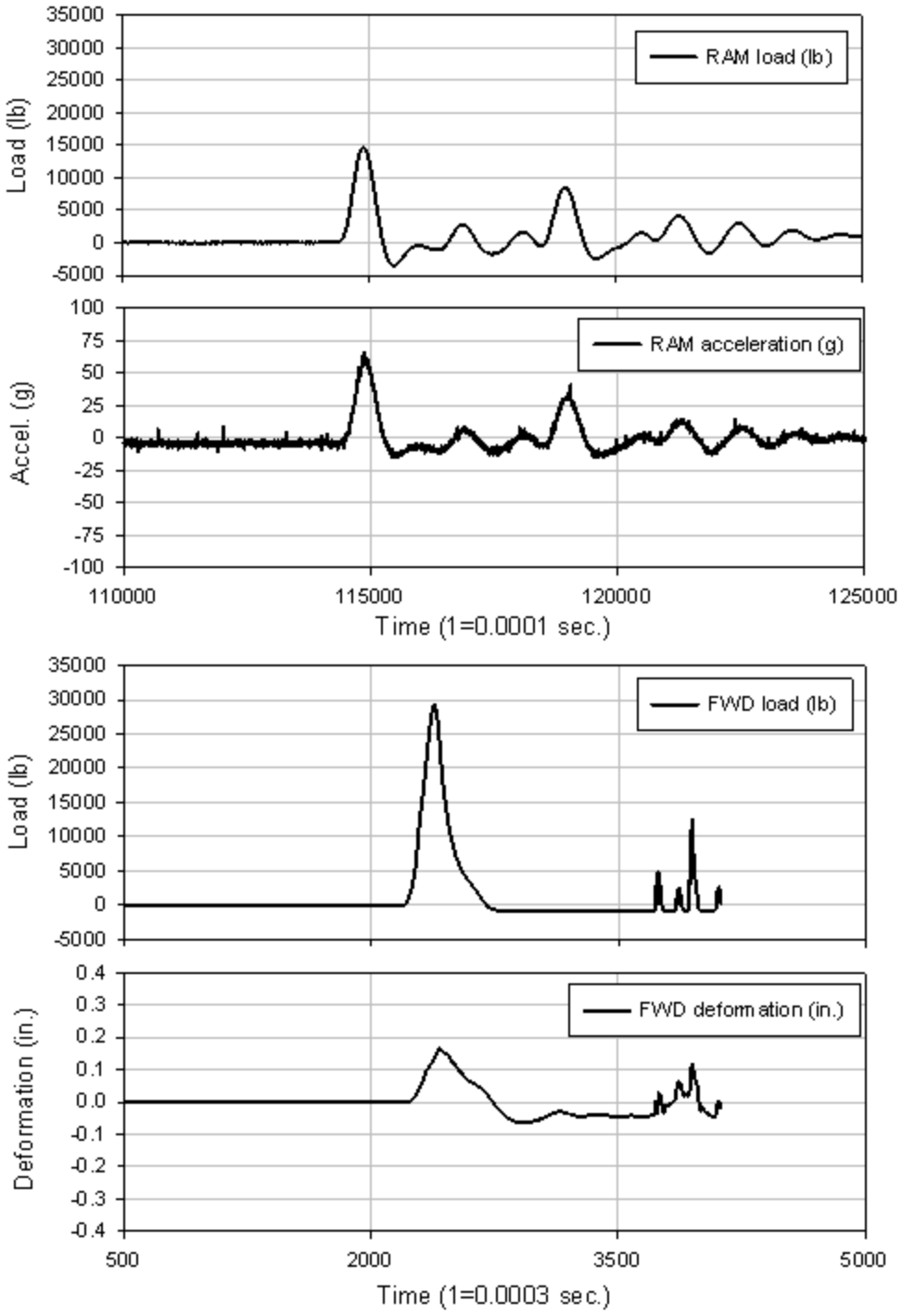


**Figure 195. La Port City test 55**

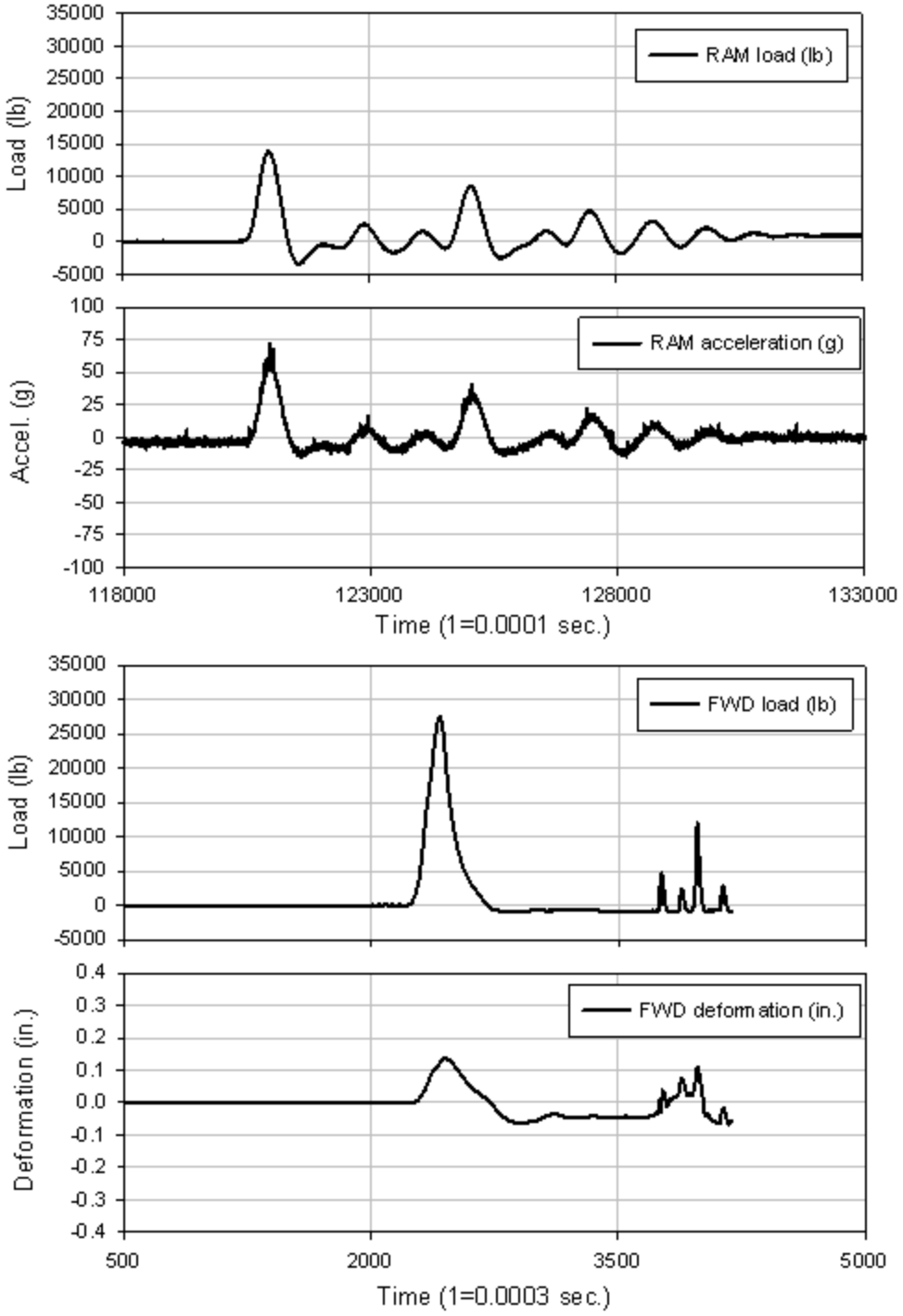


**Figure 196. La Port City test 56**

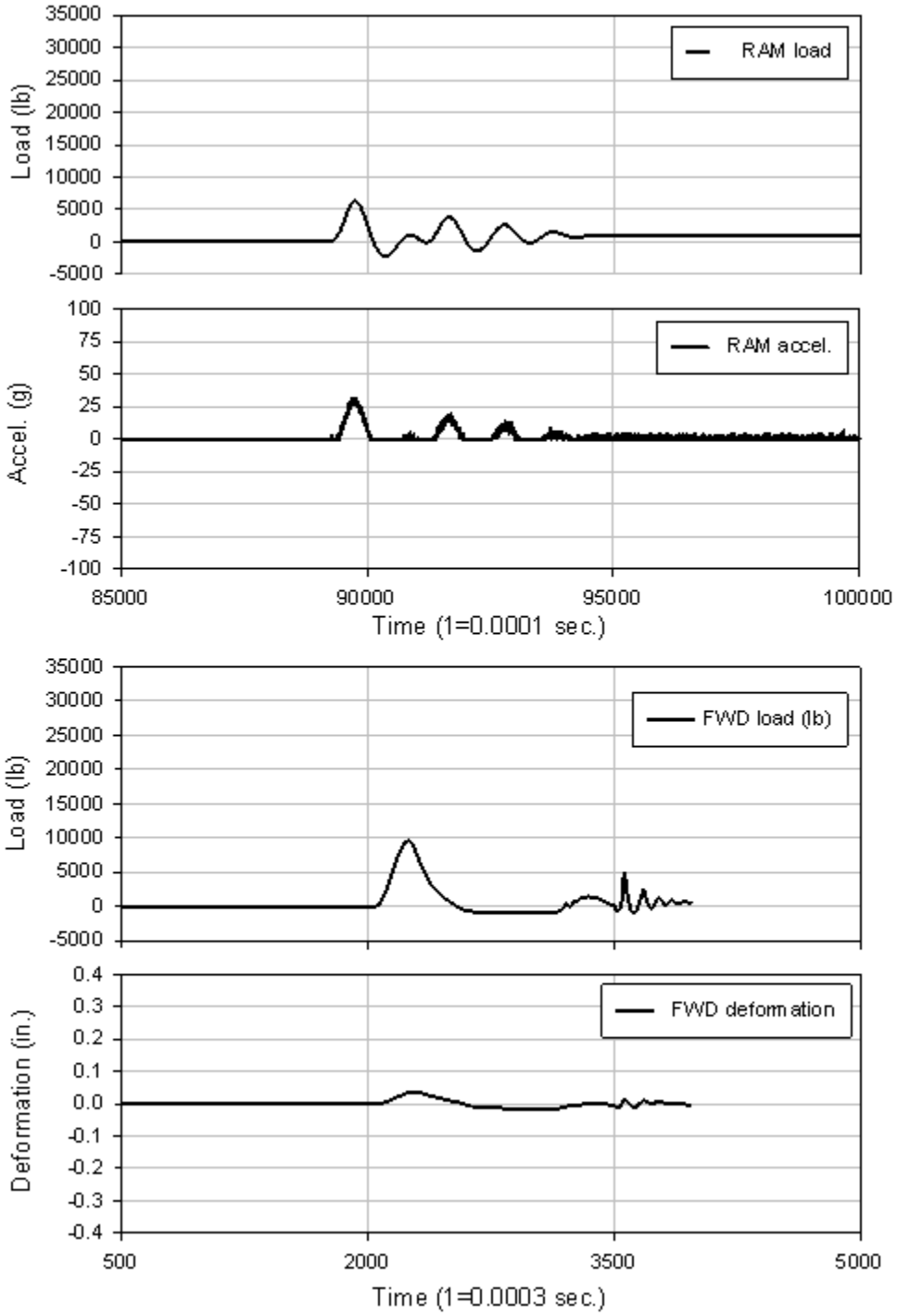


**Figure 197. La Port City test 58**

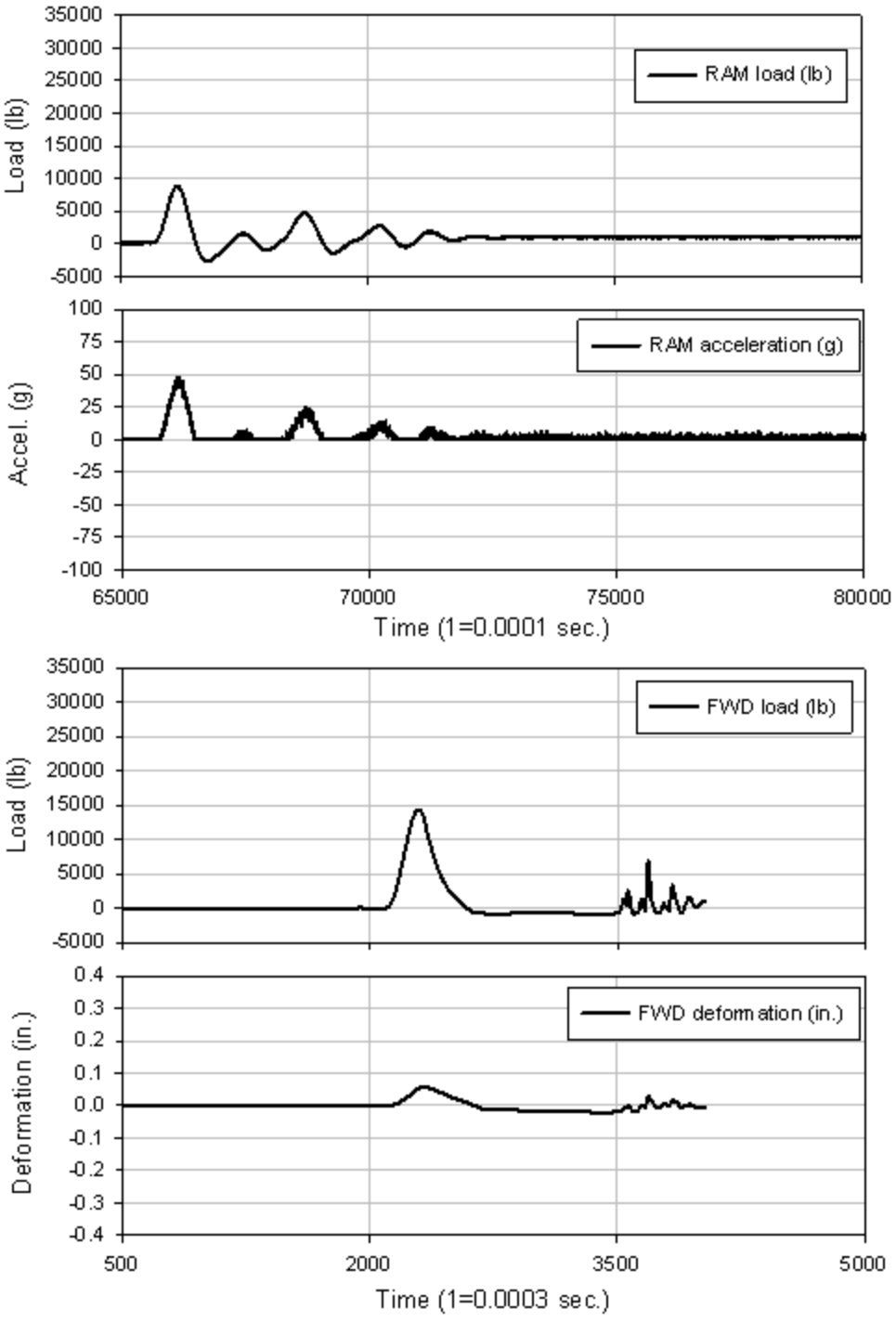


**Figure 198. La Port City test 58**

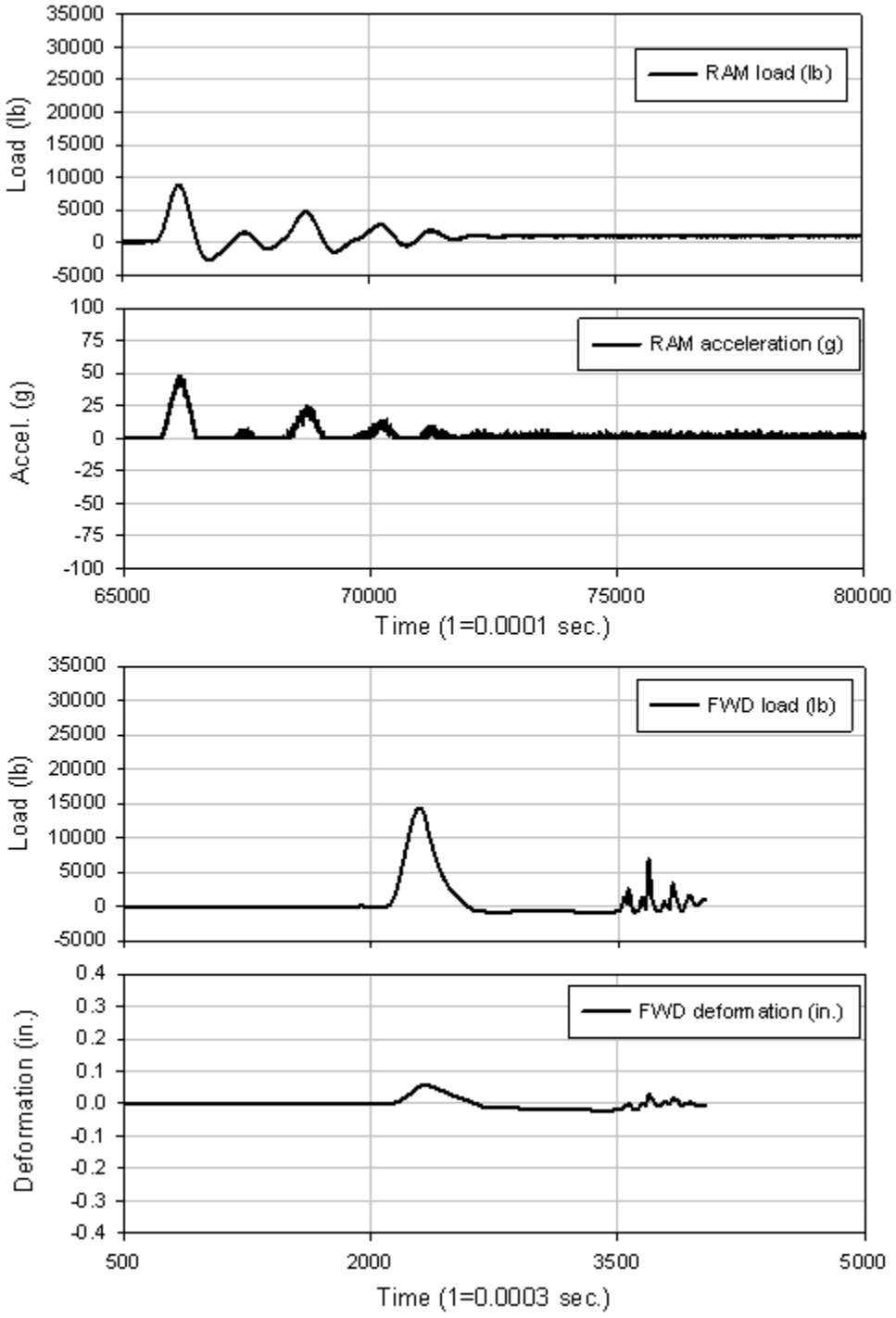


**Figure 199. La Port City test 59**

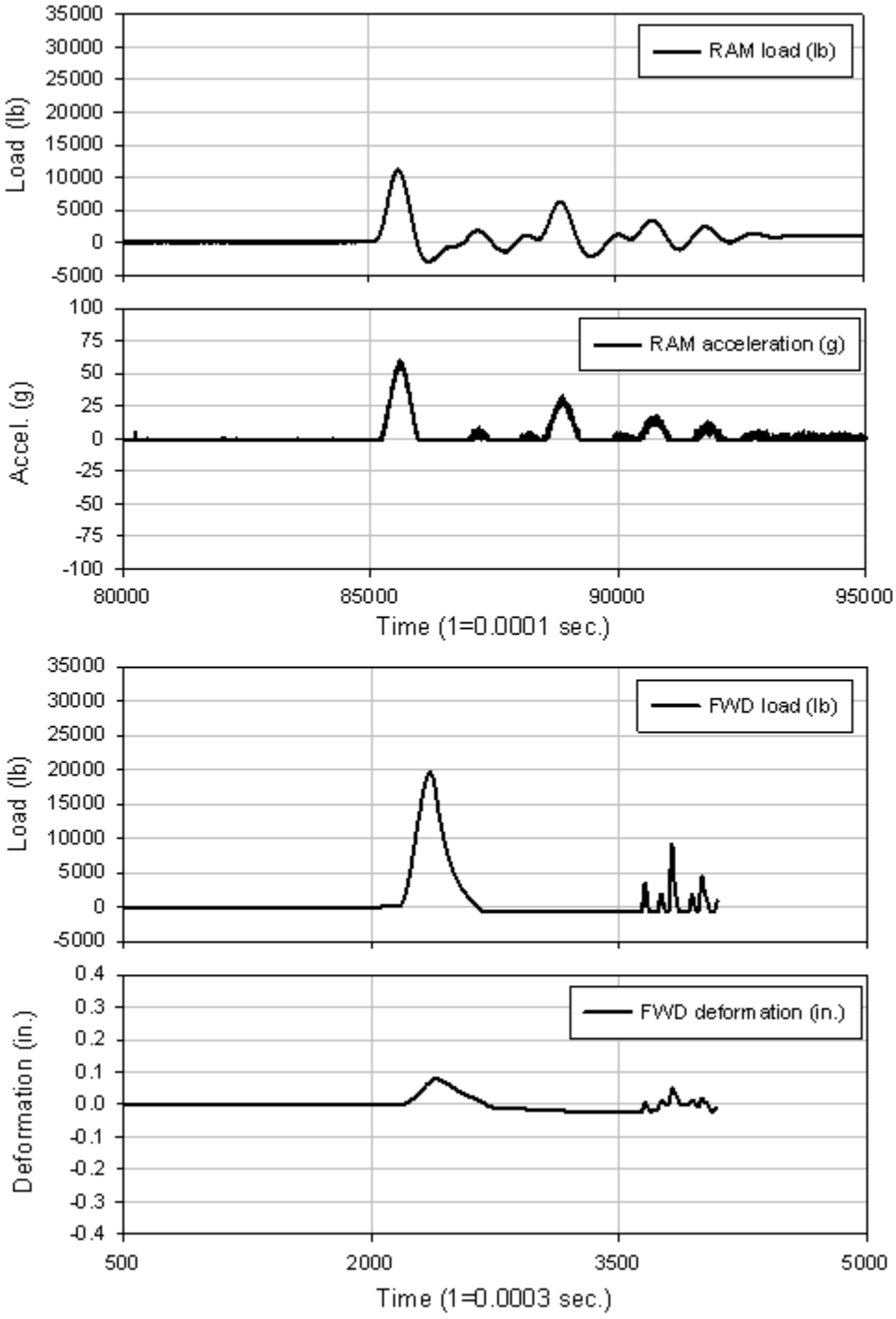


**Figure 200. La Port City test 60**

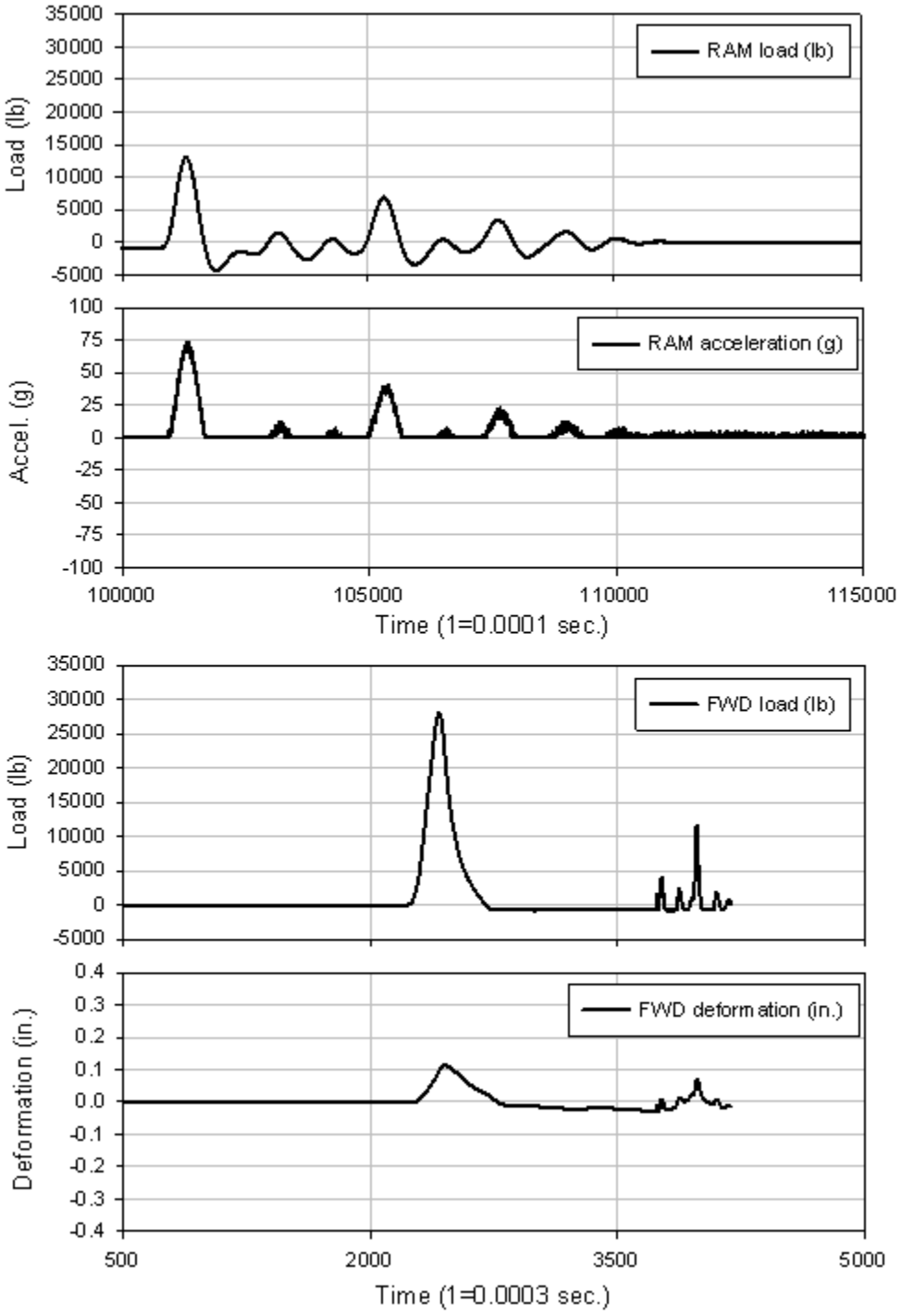


**Figure 201. La Port City test 61**

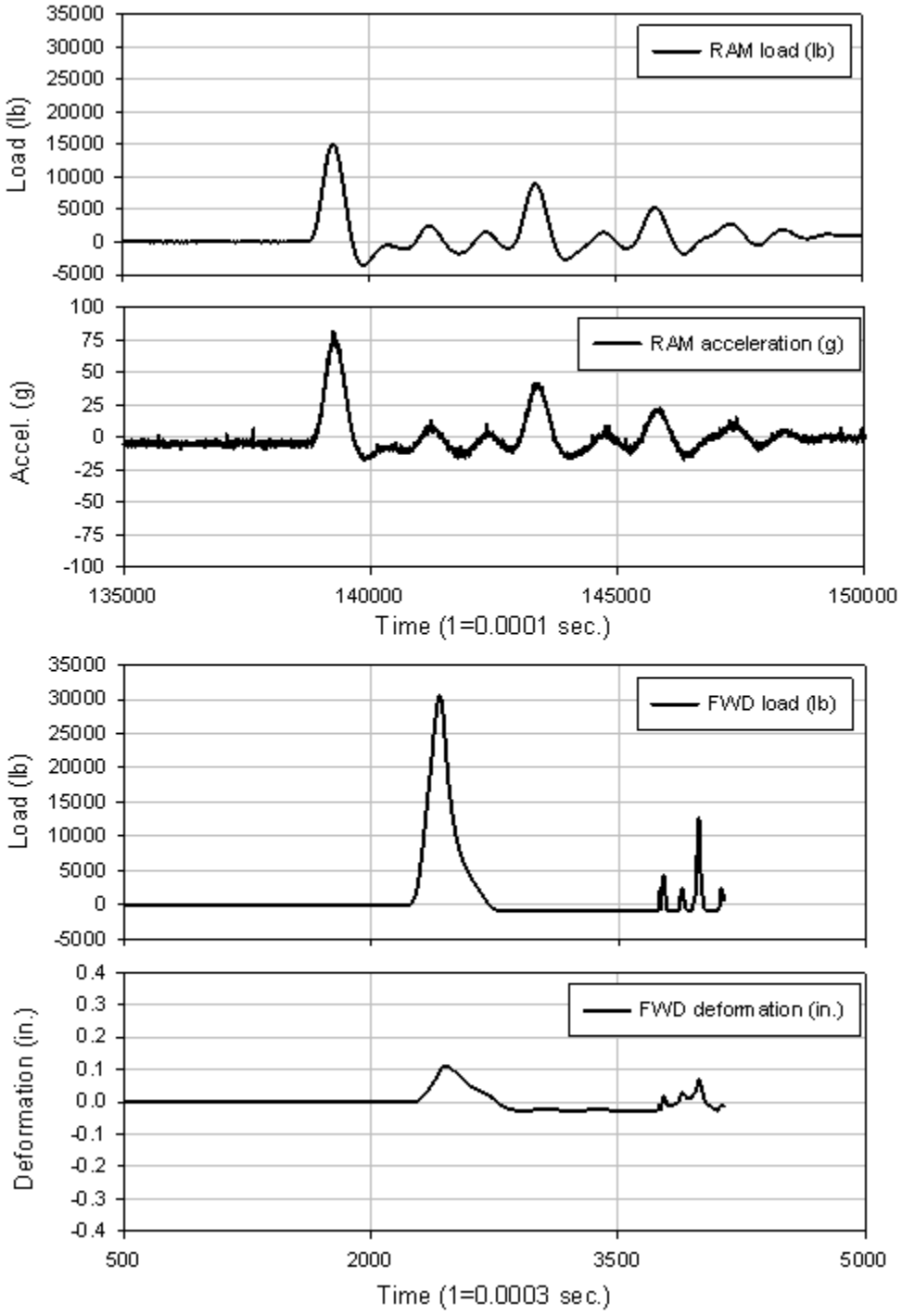


**Figure 202. La Port City test 62**

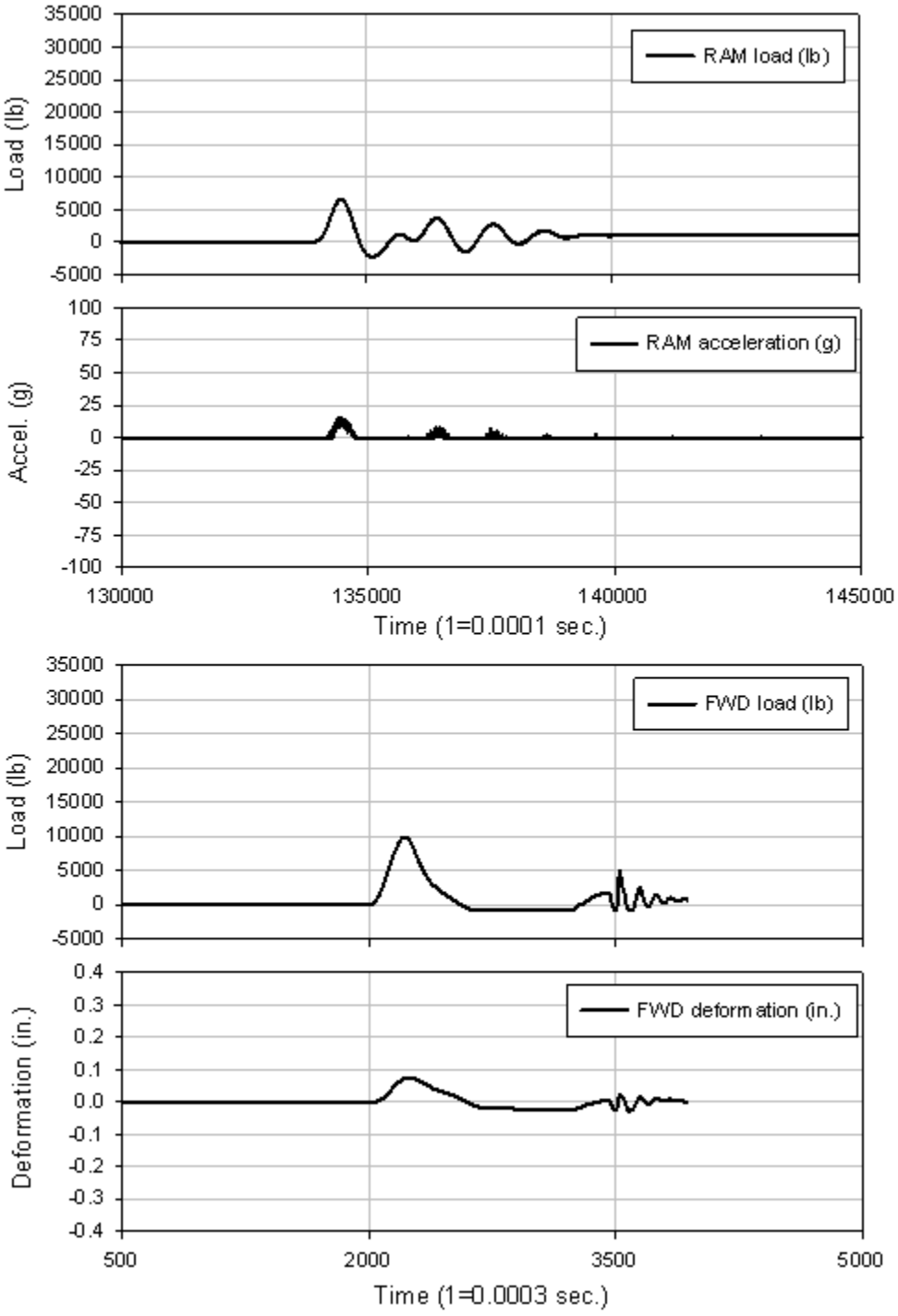


**Figure 203. La Port City test 65**

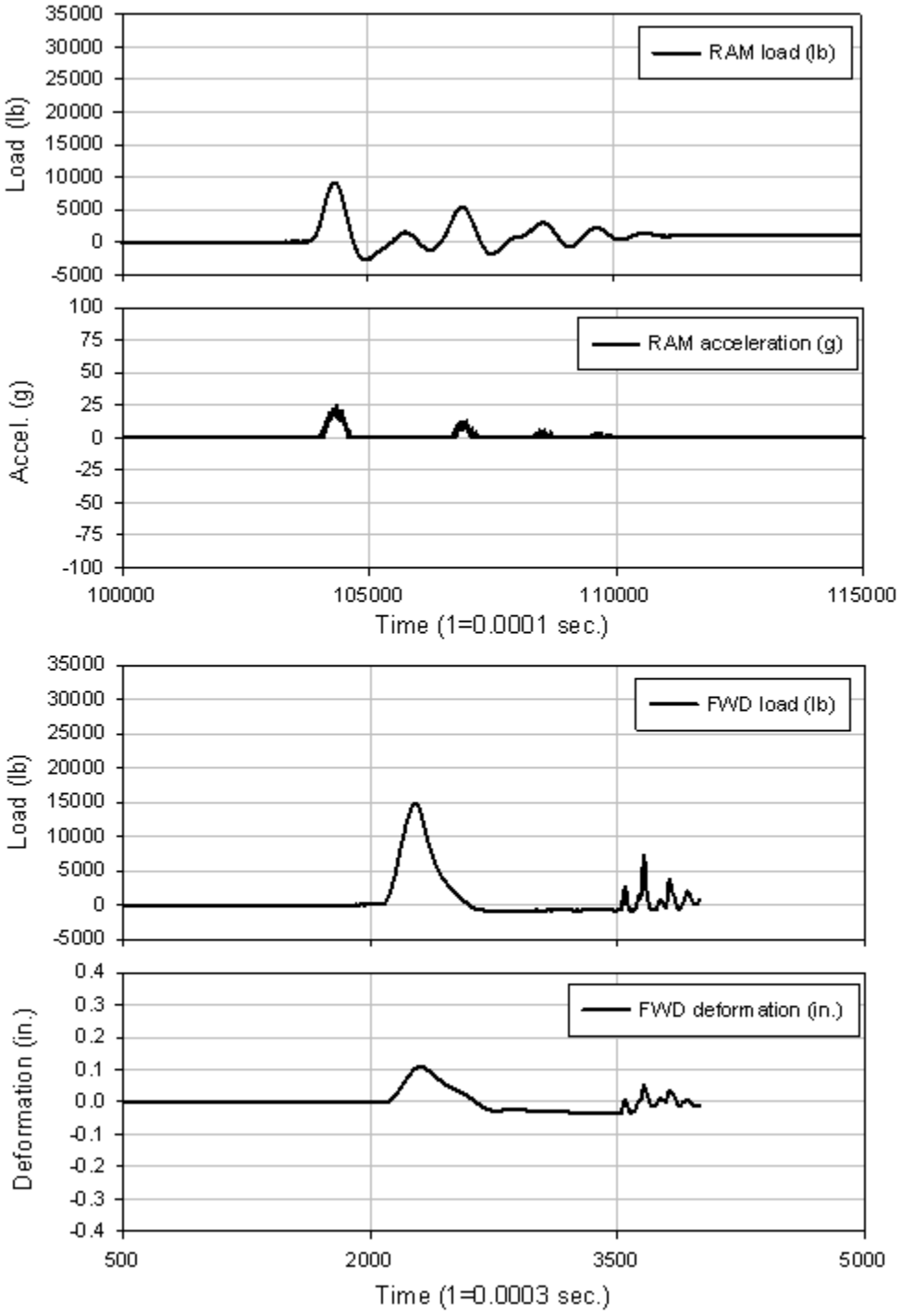


**Figure 204. La Port City test 66**

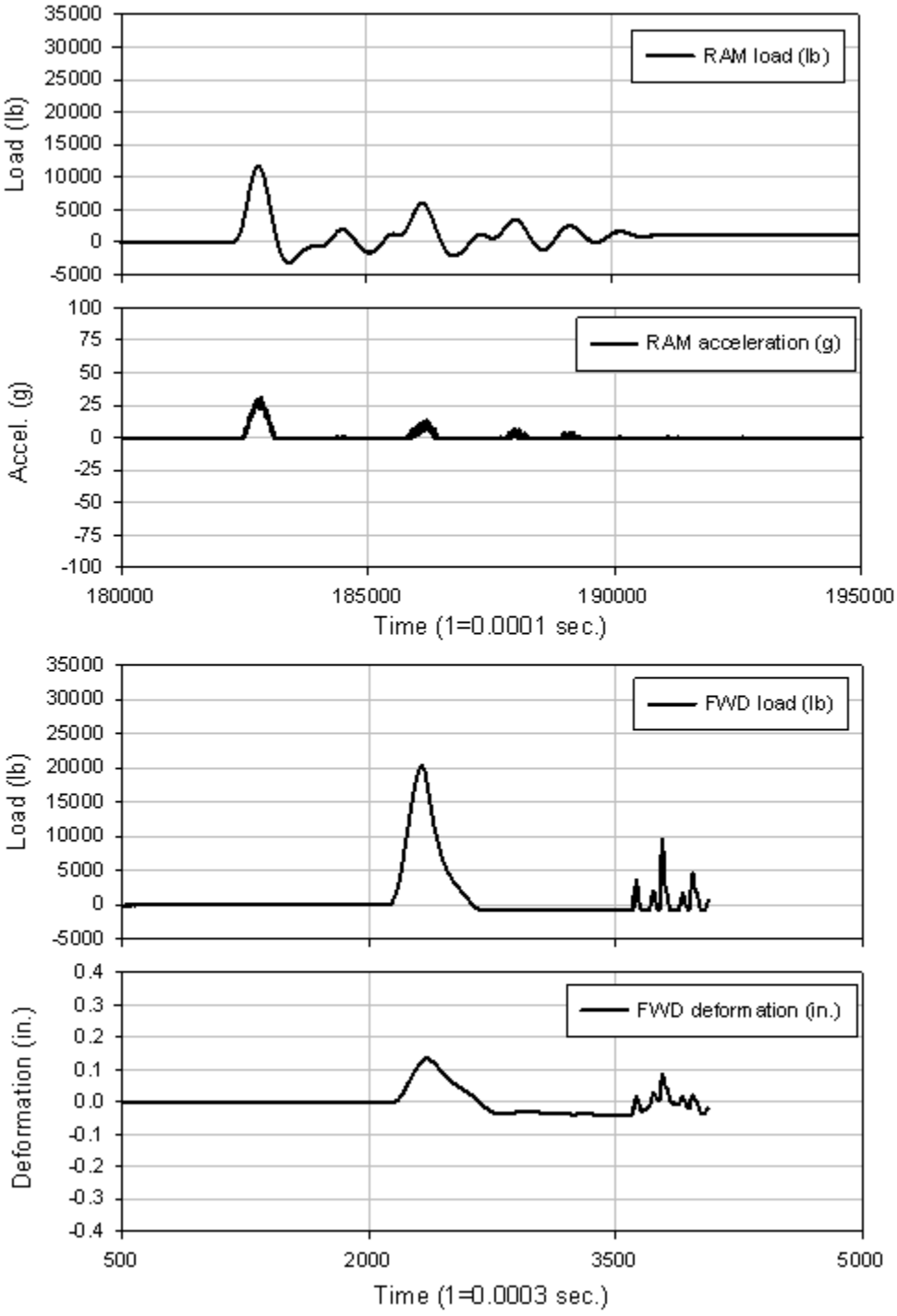


**Figure 205. La Port City test 67**

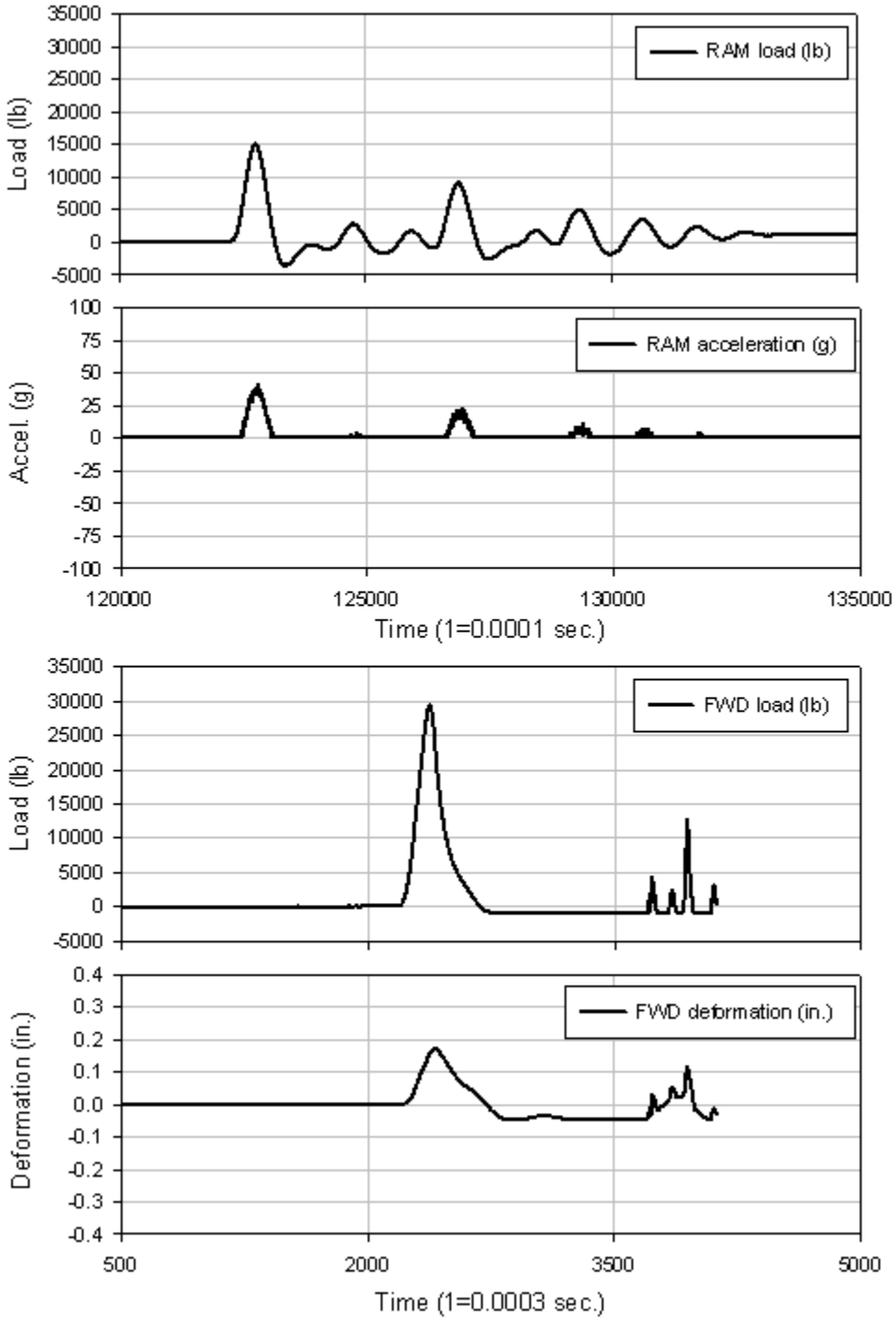


**Figure 206. La Port City test 68**

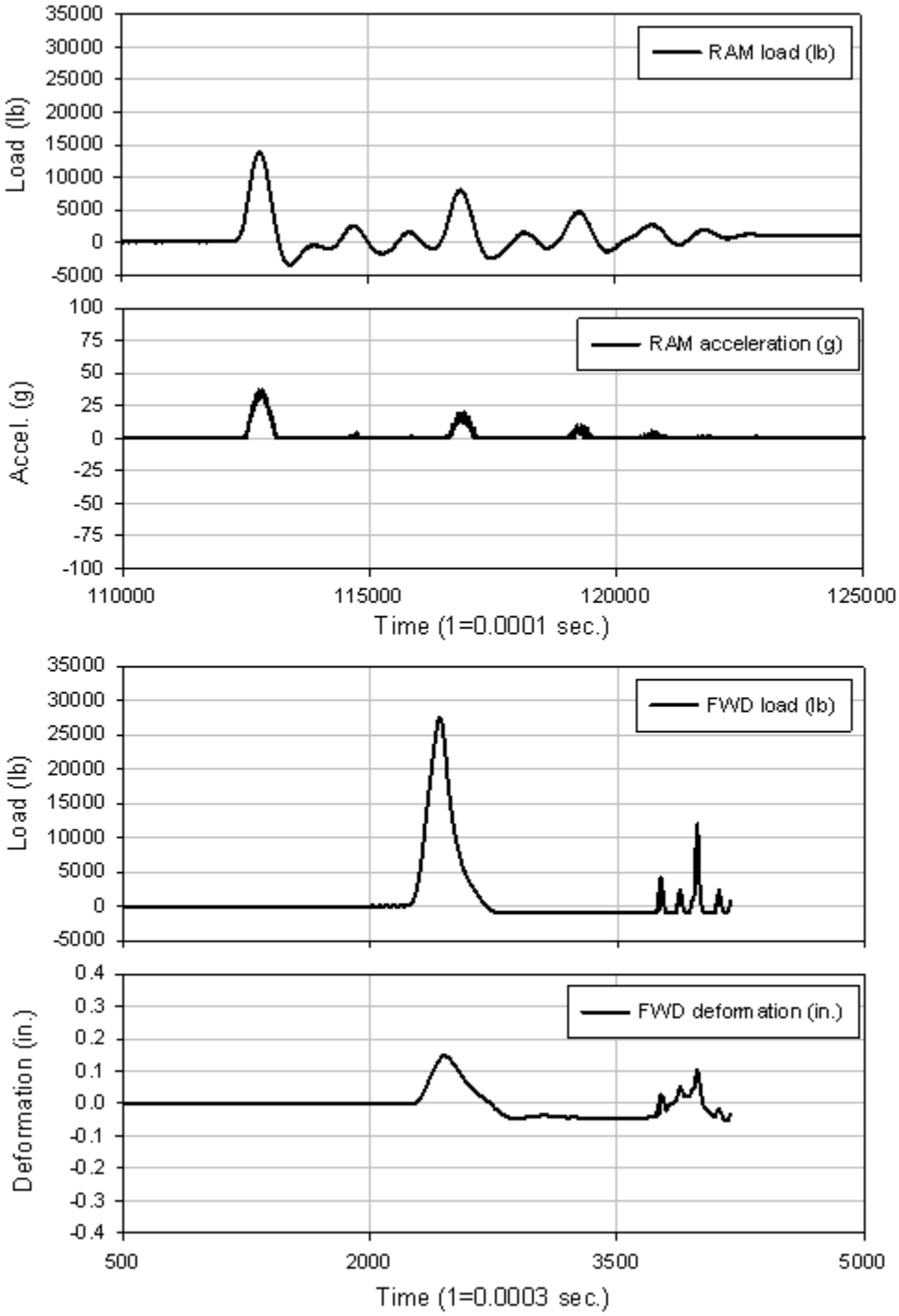


**Figure 207. La Port City test 69**

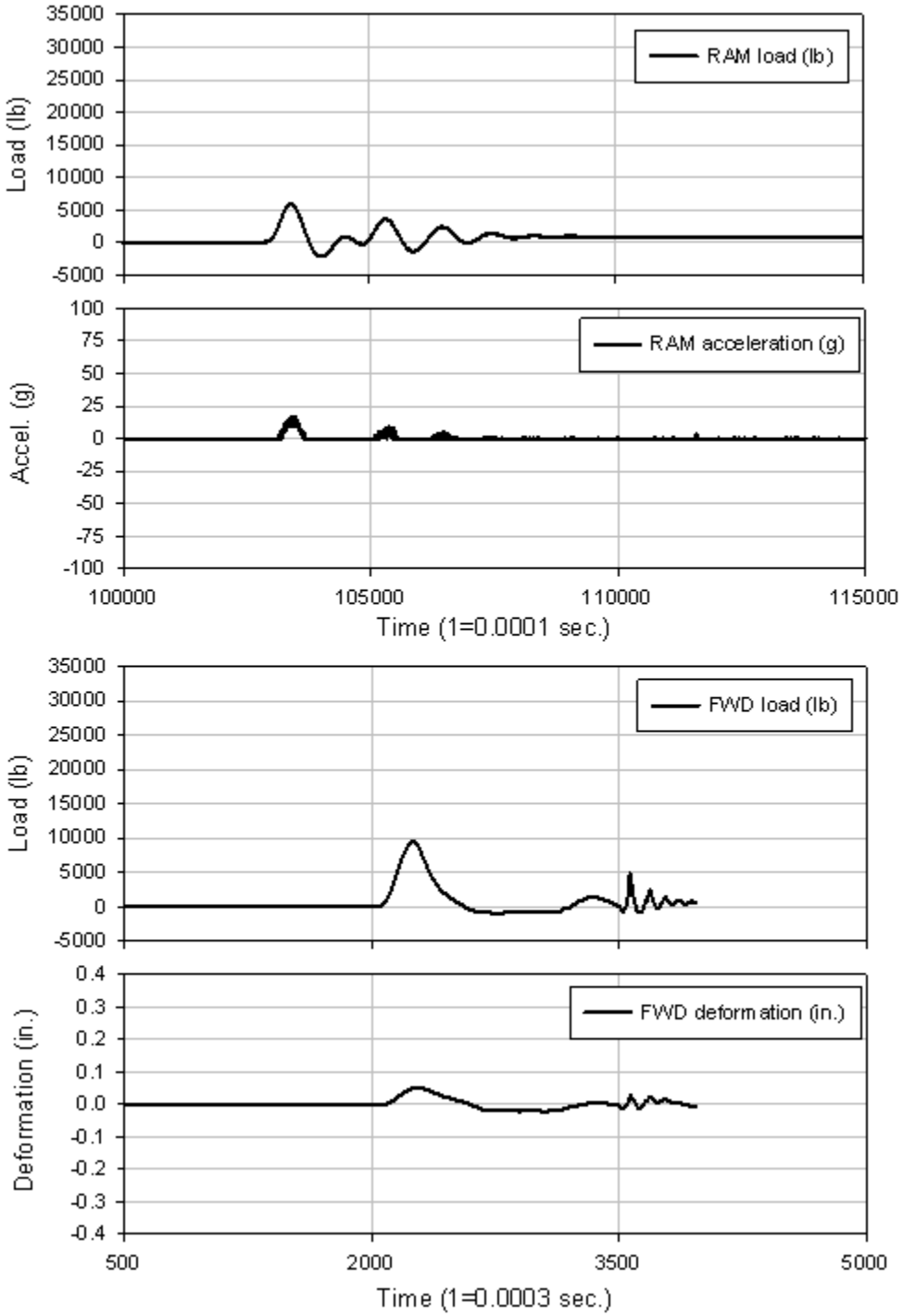


**Figure 208. La Port City test 71**

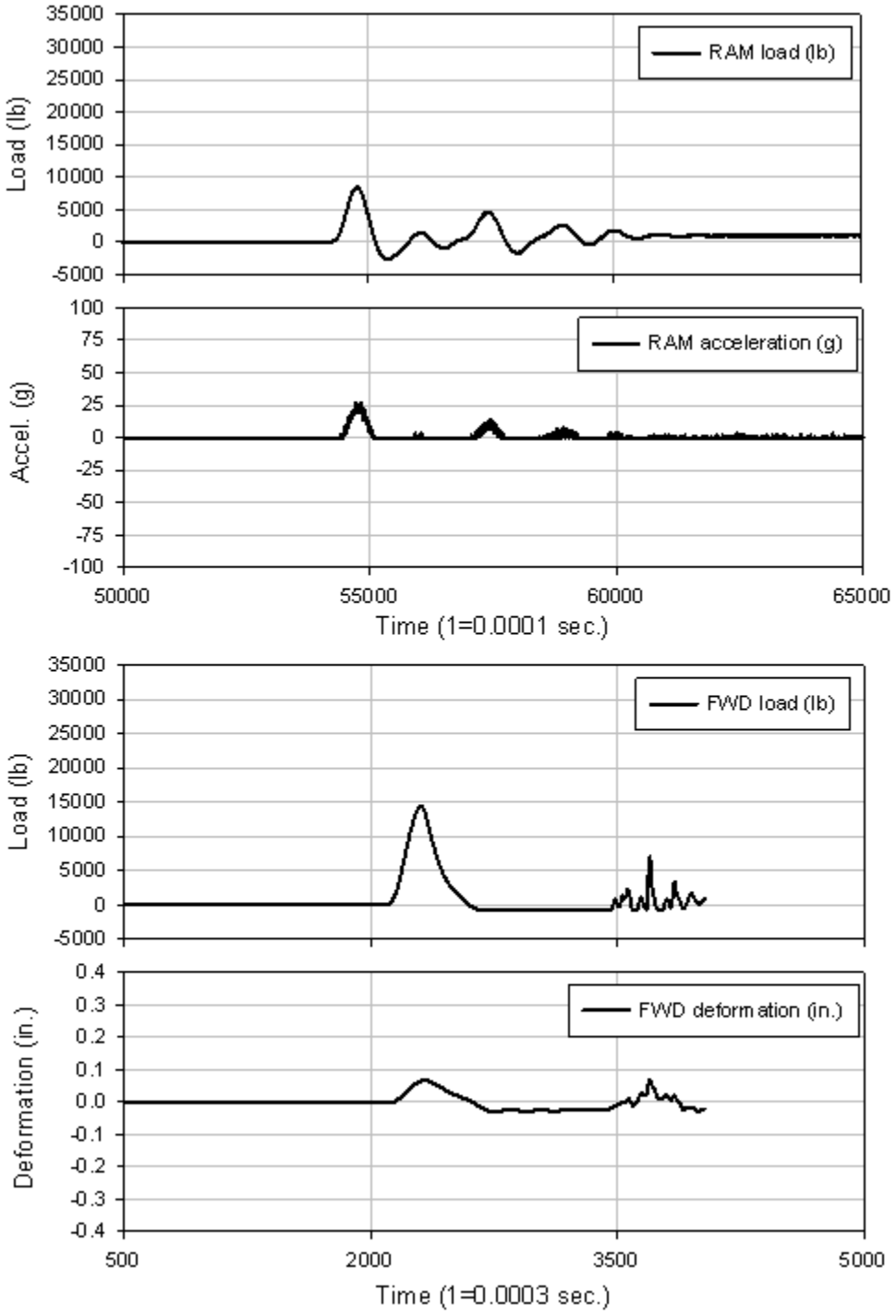


**Figure 209. La Port City test 74**

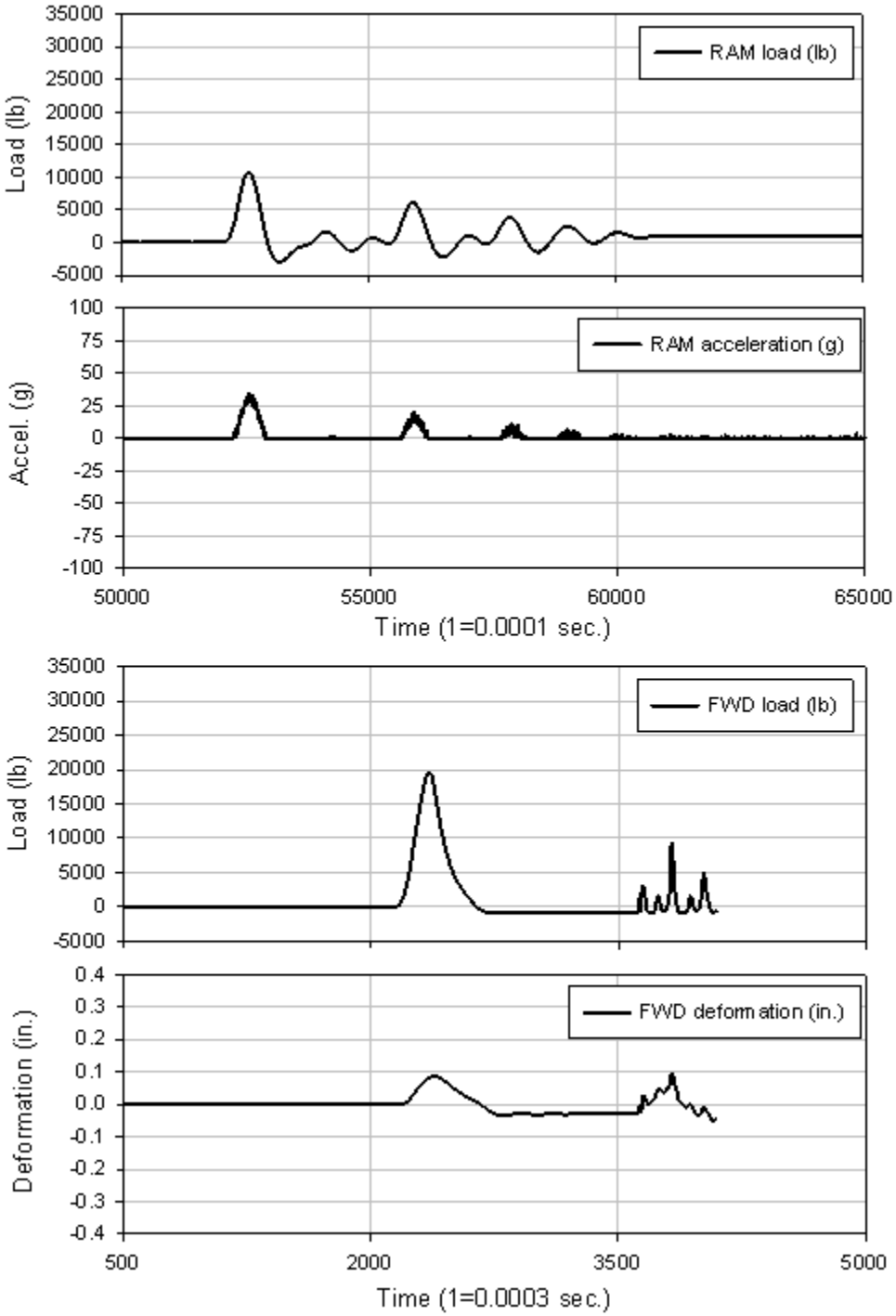


**Figure 210. La Port City test 75**

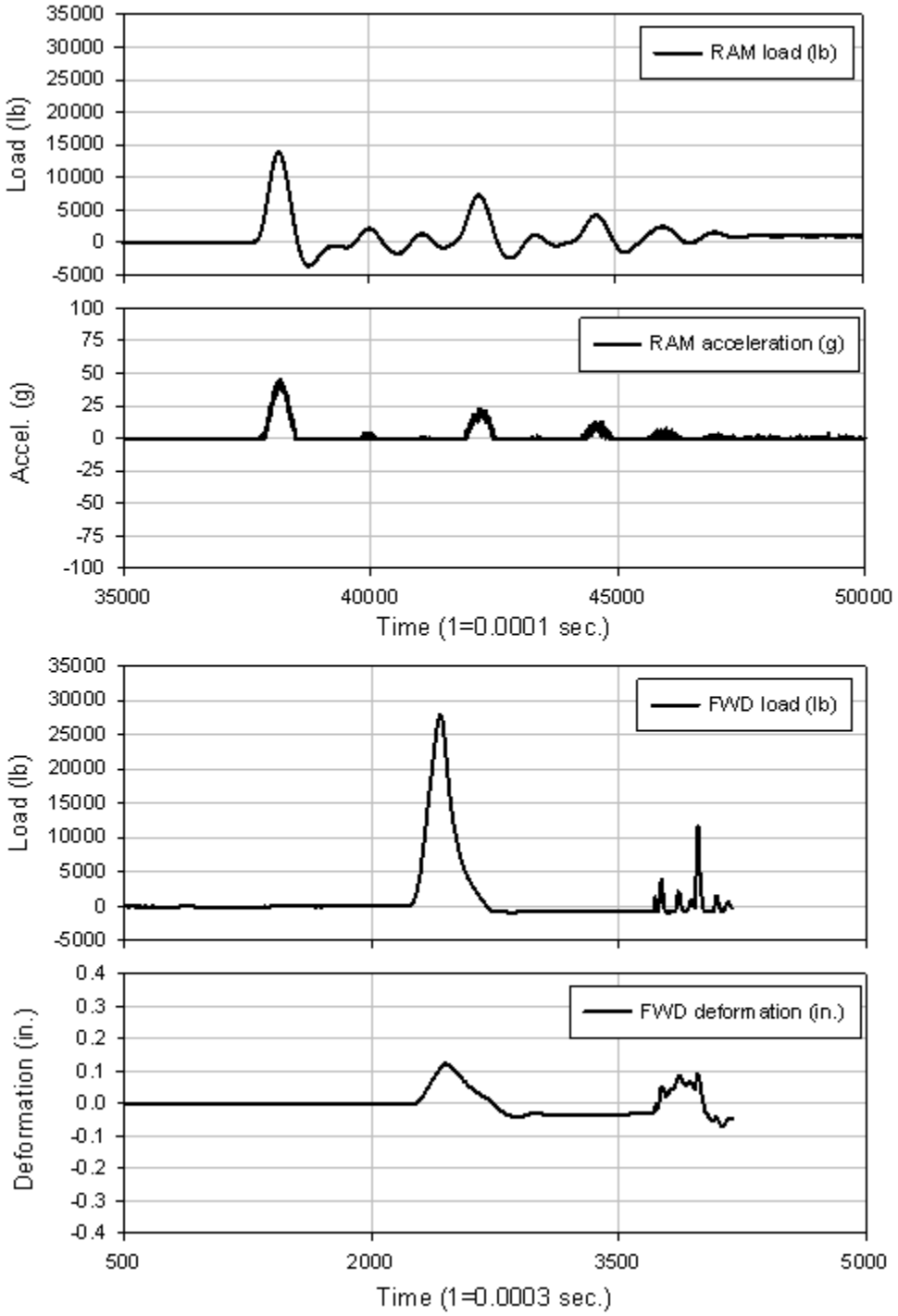


**Figure 211. La Port City test 77**

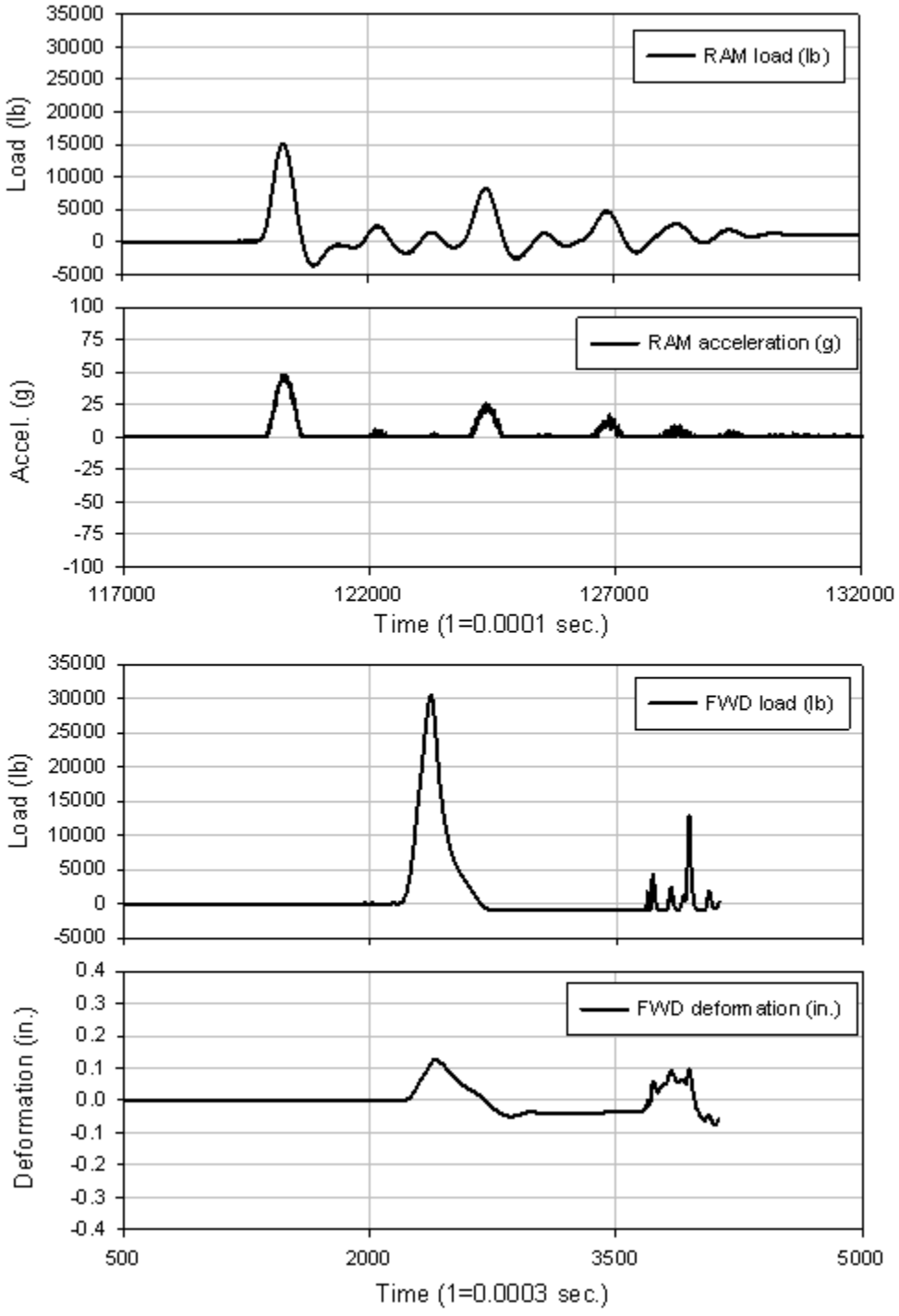


**Figure 212. La Port City test 78**

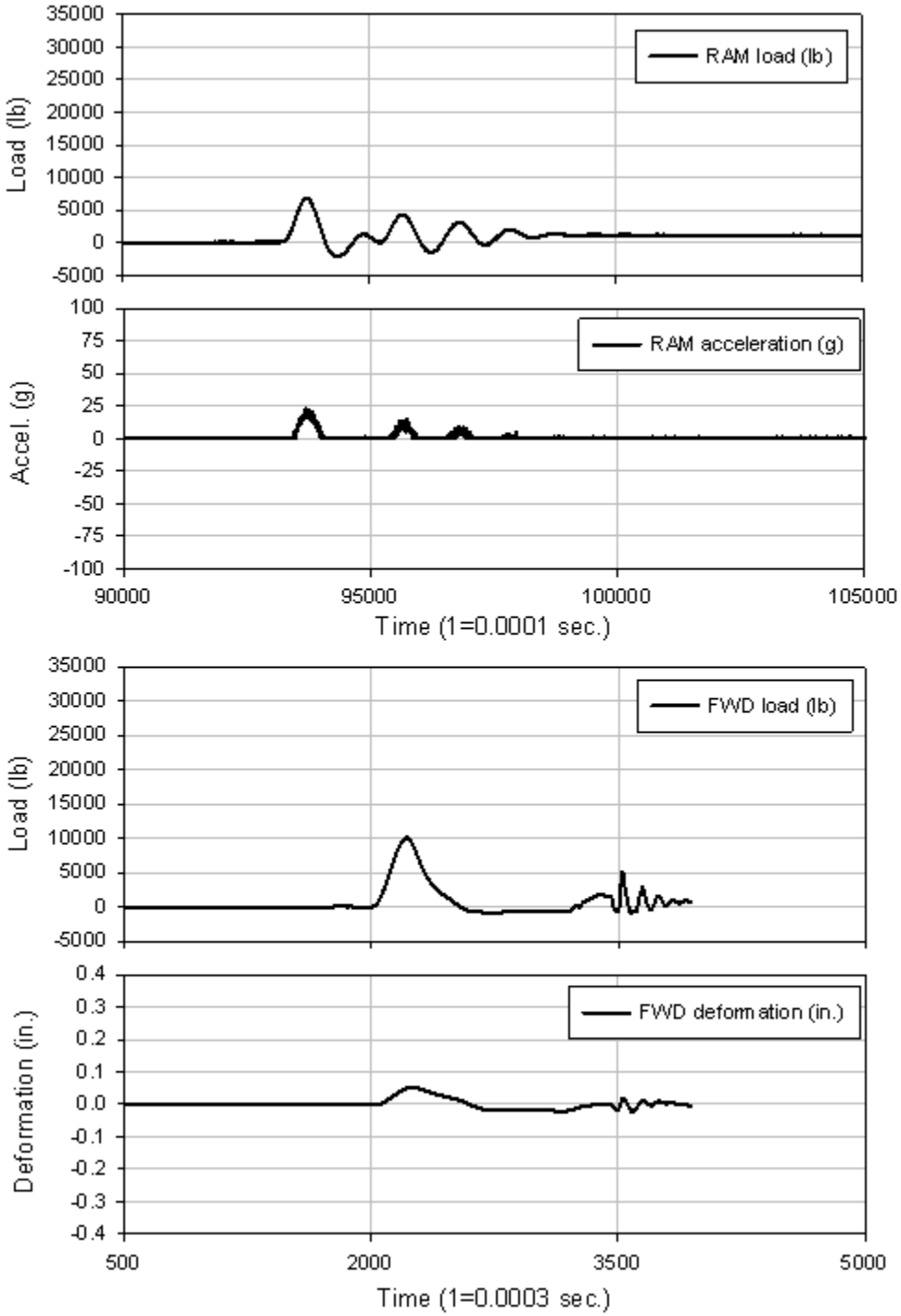


**Figure 213. La Port City test 80**

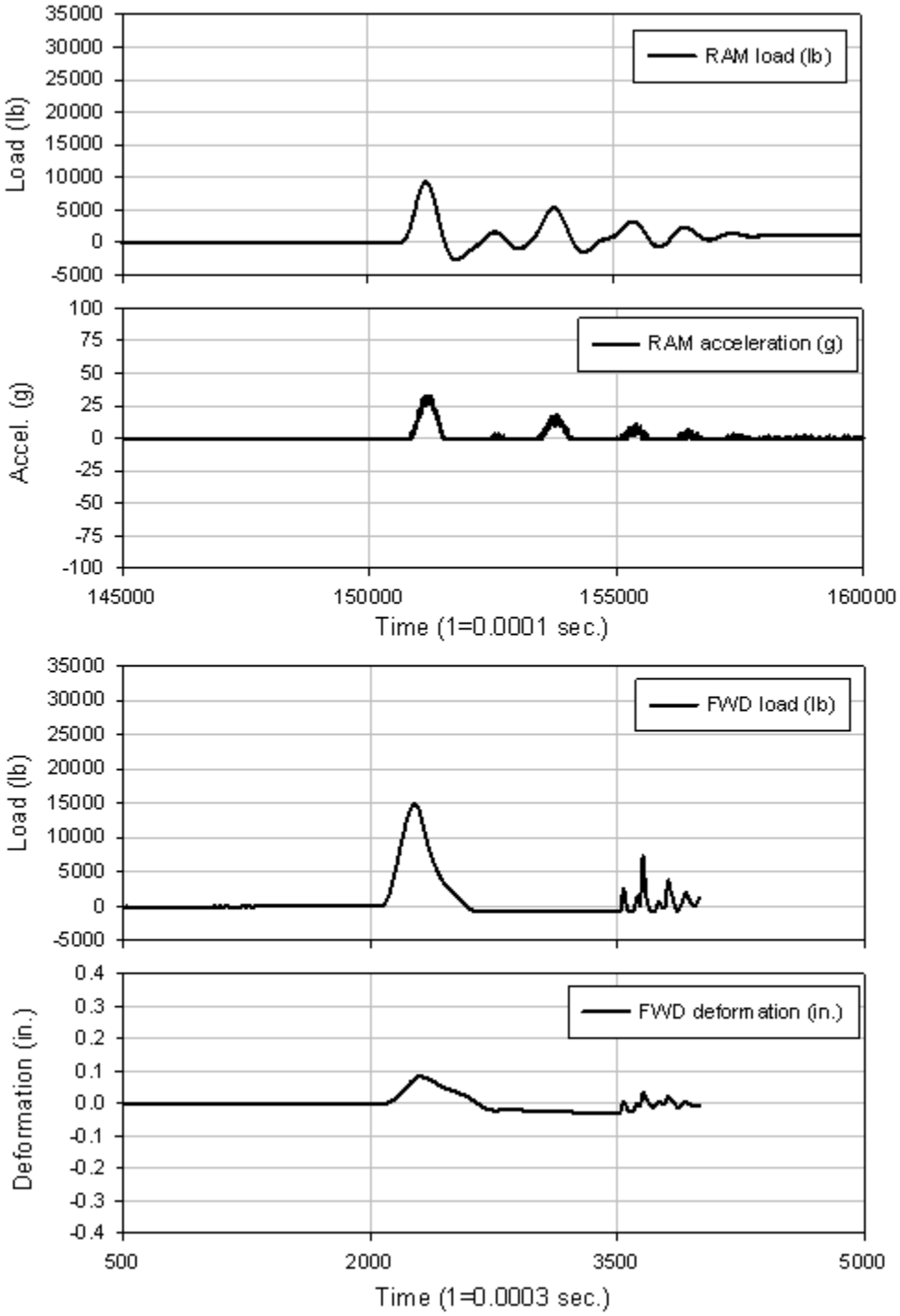


**Figure 214. La Port City test 81**

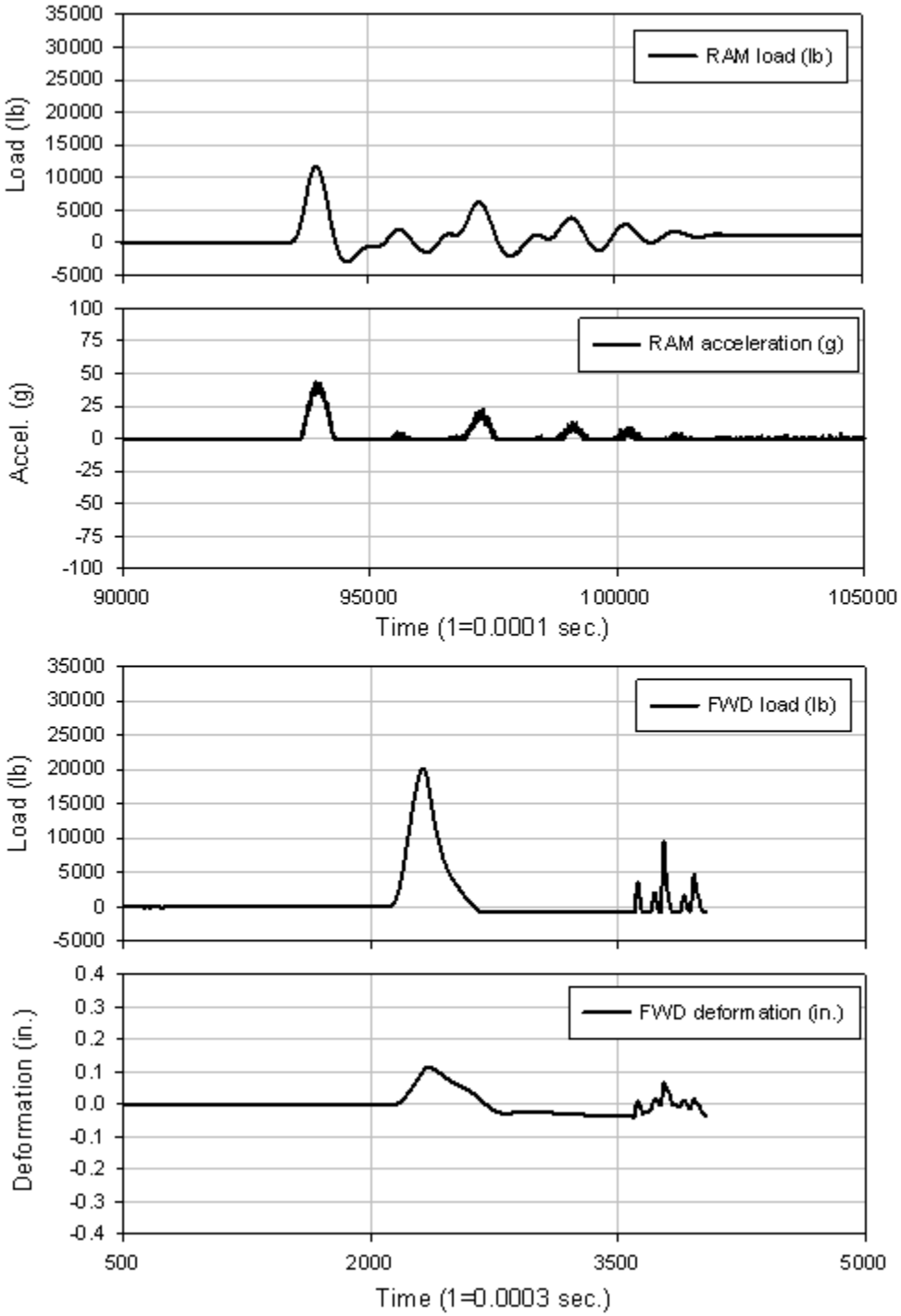


**Figure 215. La Port City test 82**

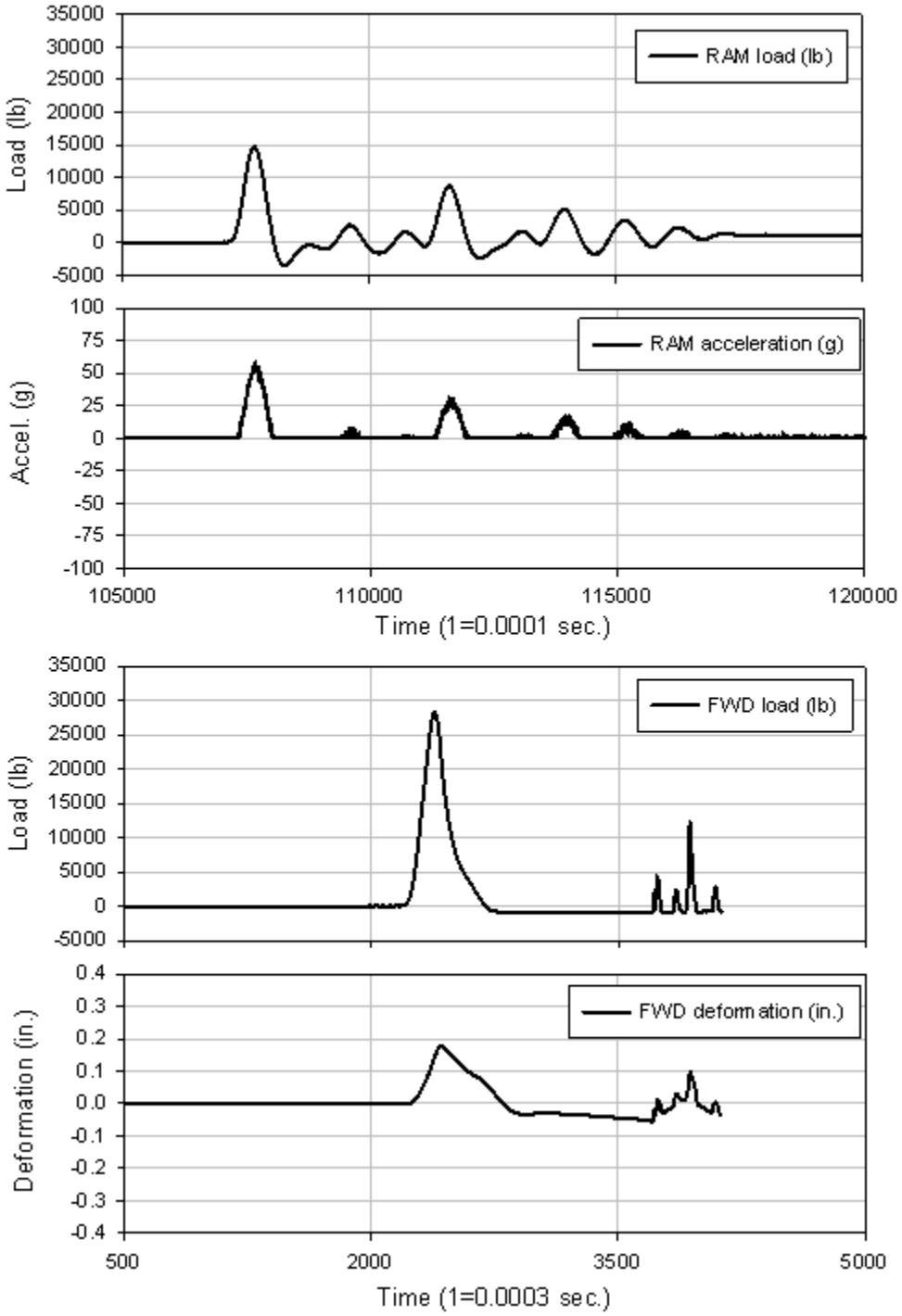


**Figure 216. La Port City test 83**

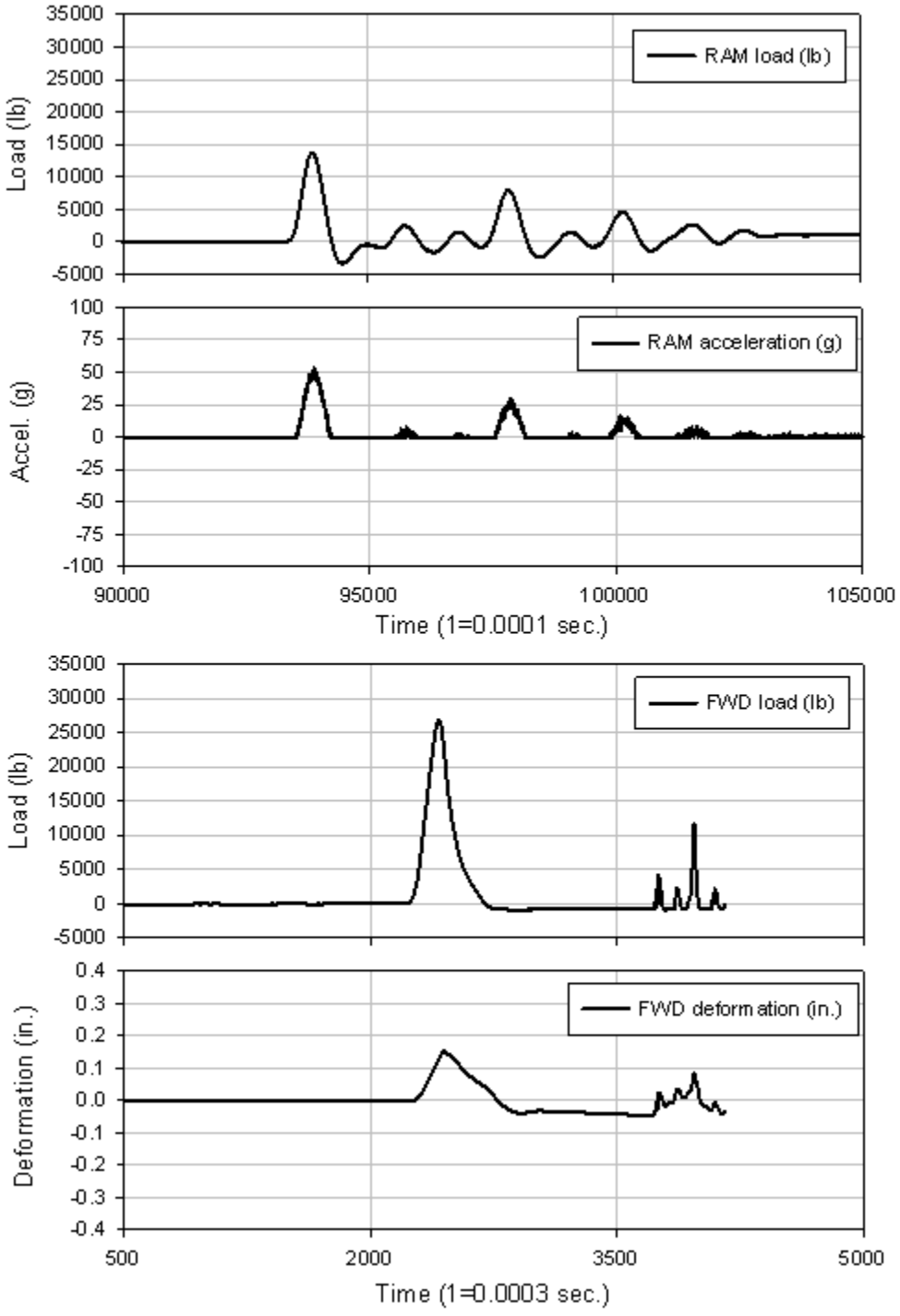


**Figure 217. La Port City test 84**

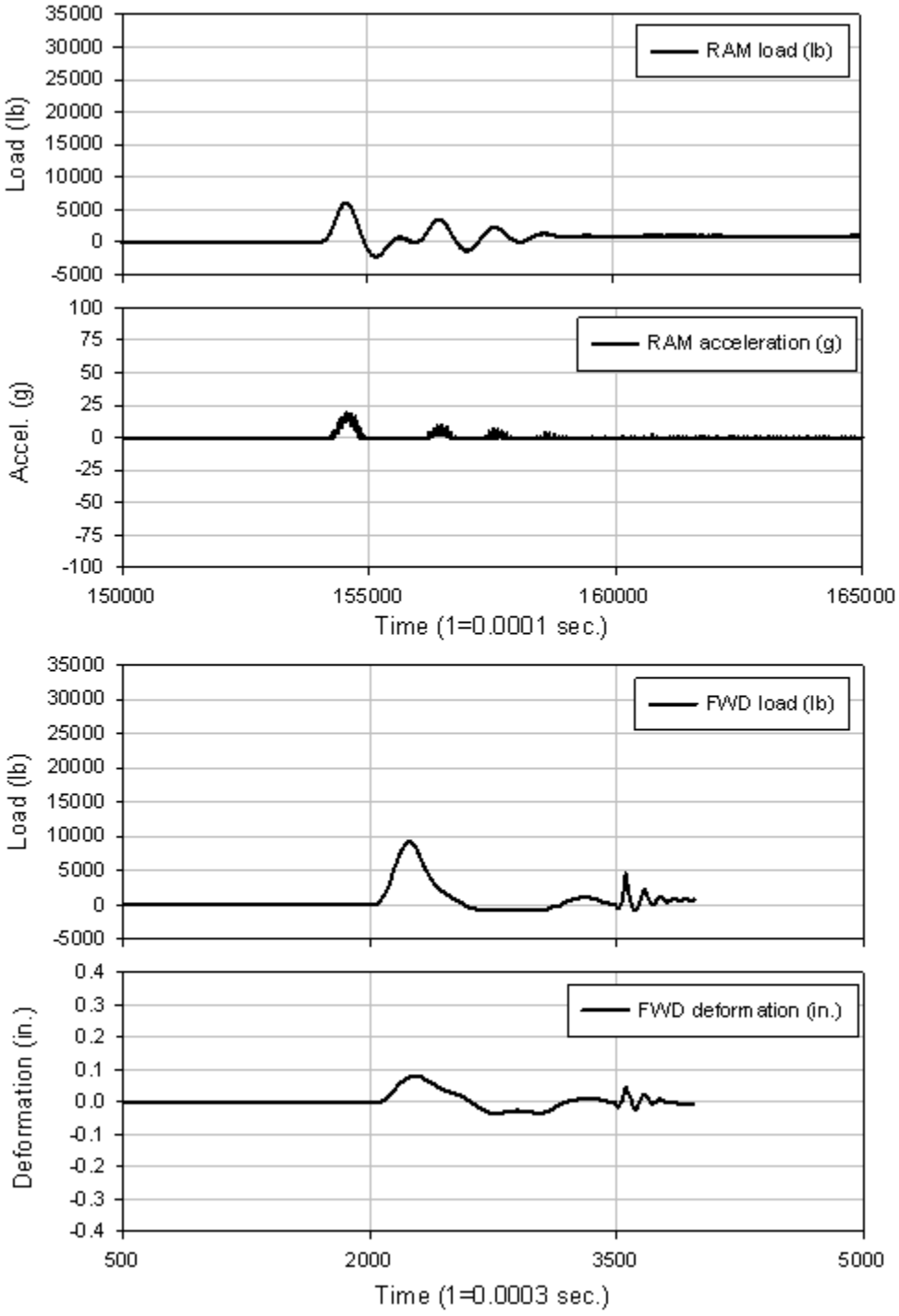


**Figure 218. La Port City test 87**

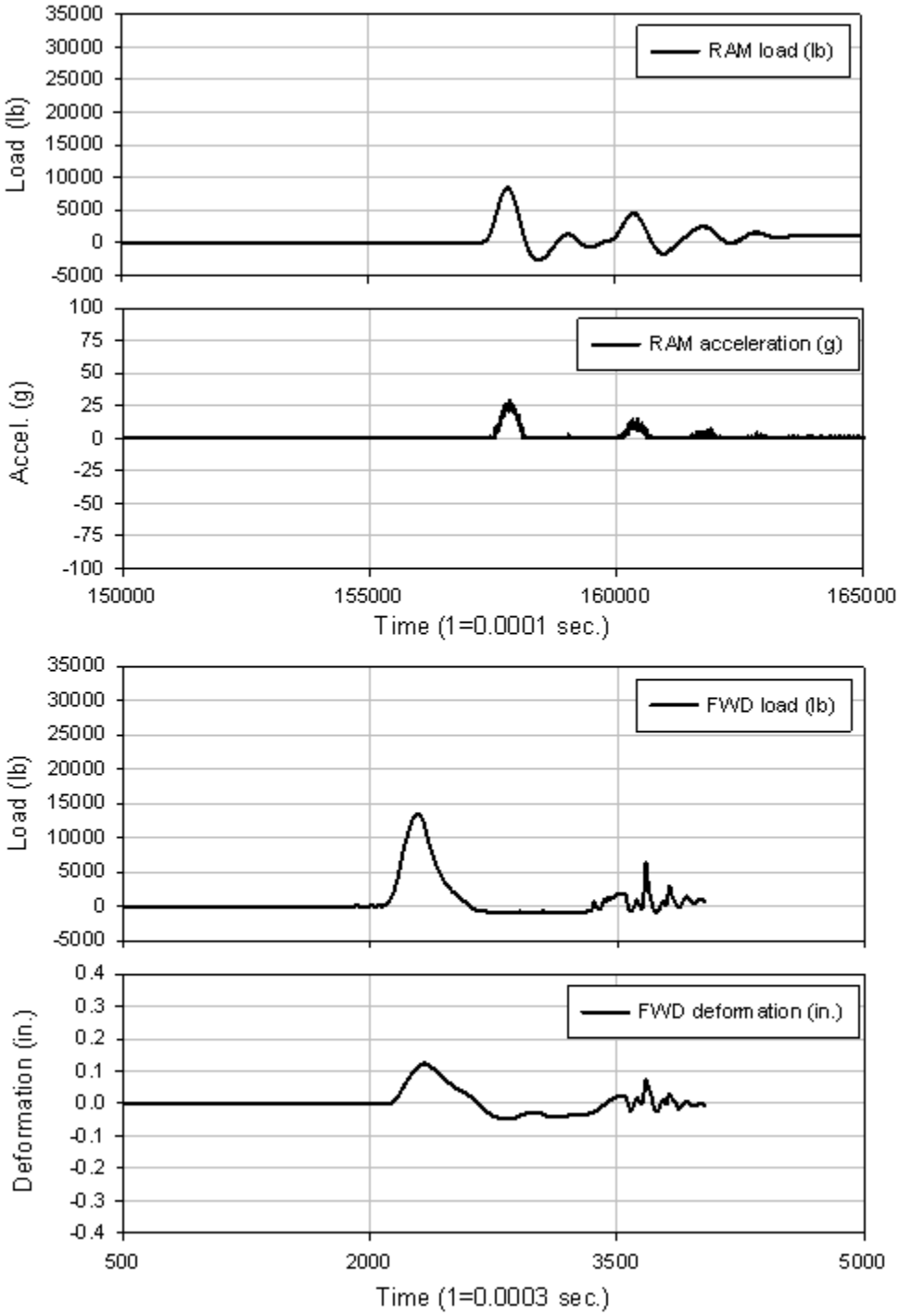


**Figure 219. La Port City test 88**

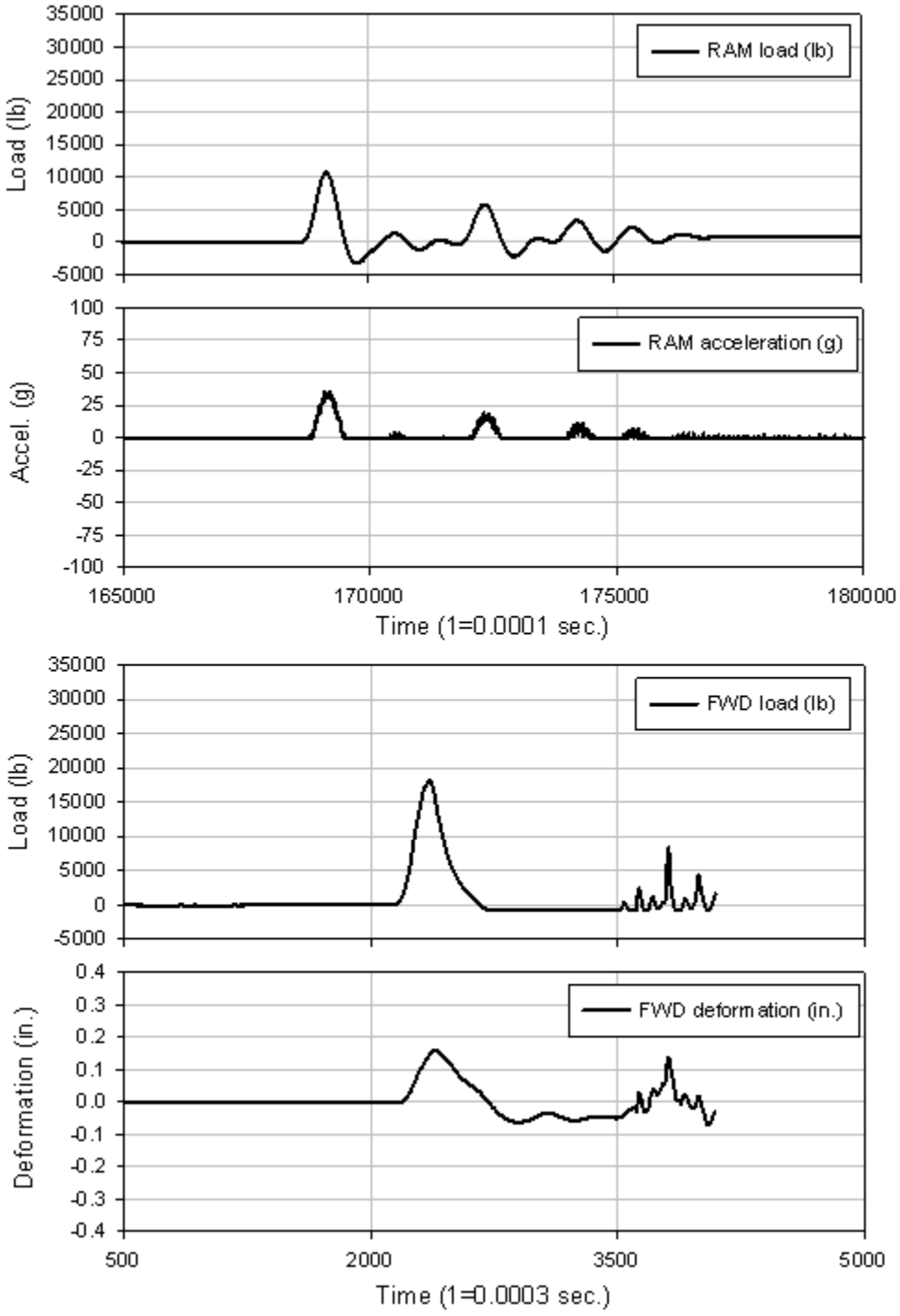


**Figure 220. La Port City test 89**

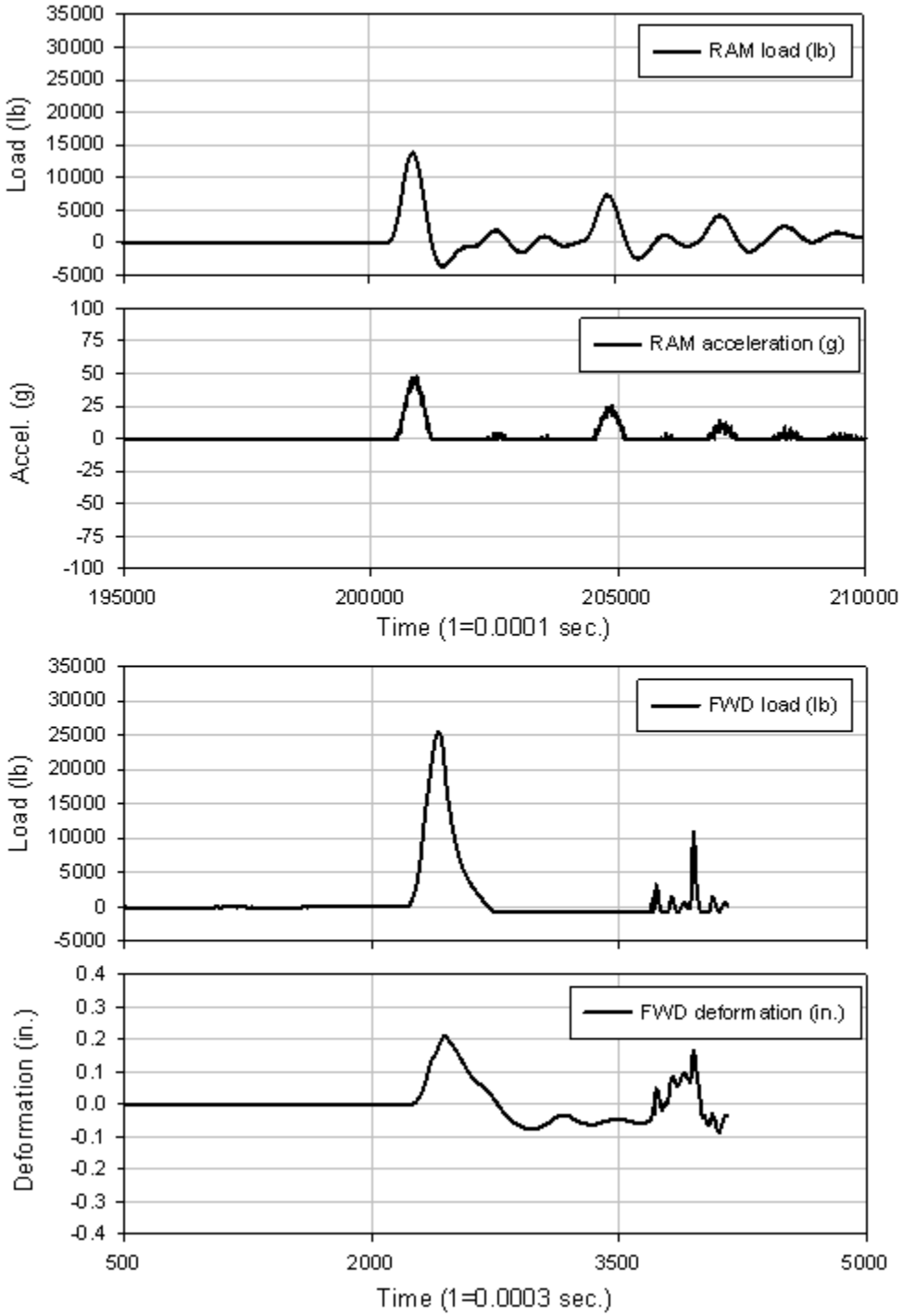


**Figure 221. La Port City test 90**

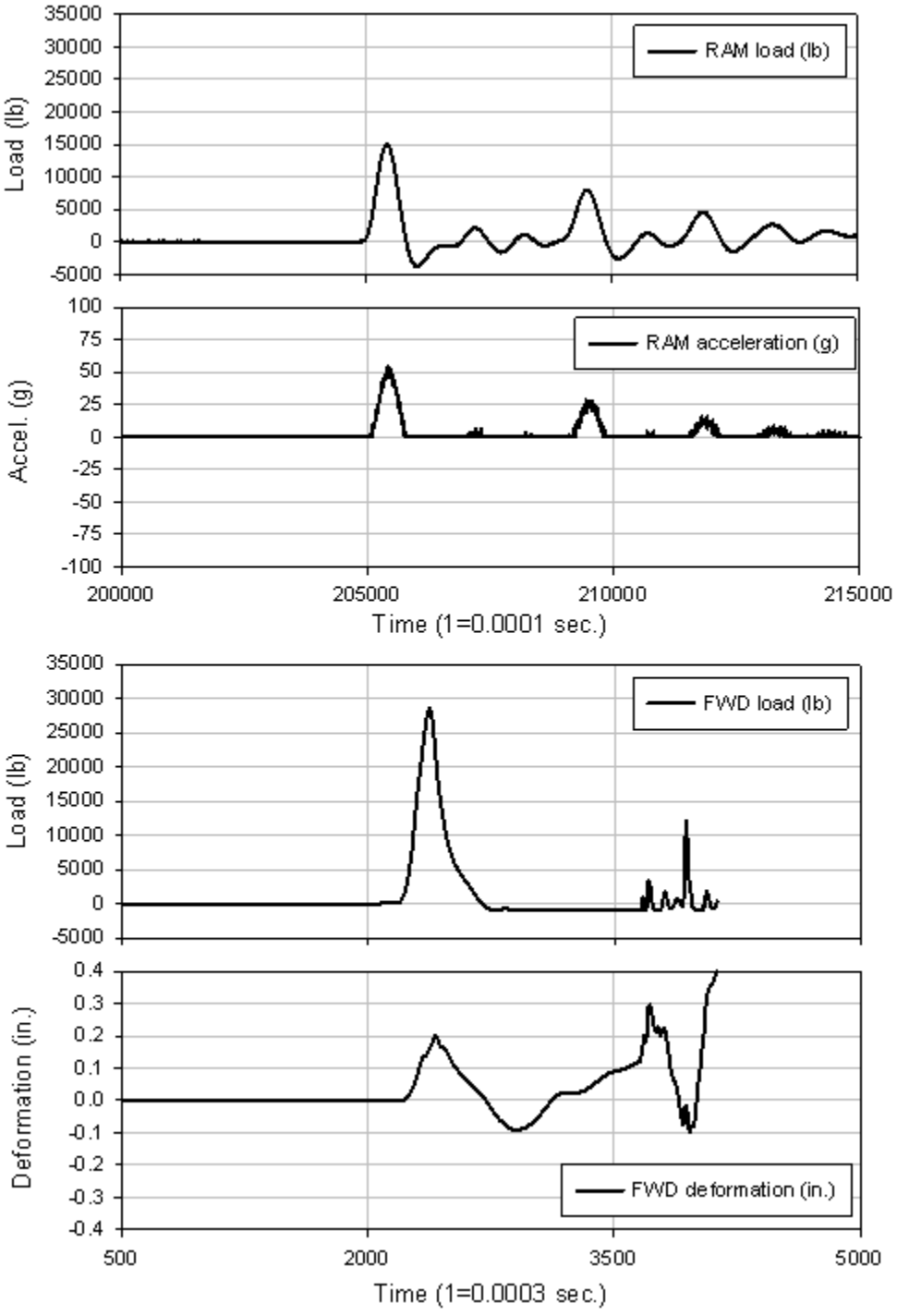


**Figure 222. La Port City test 91**

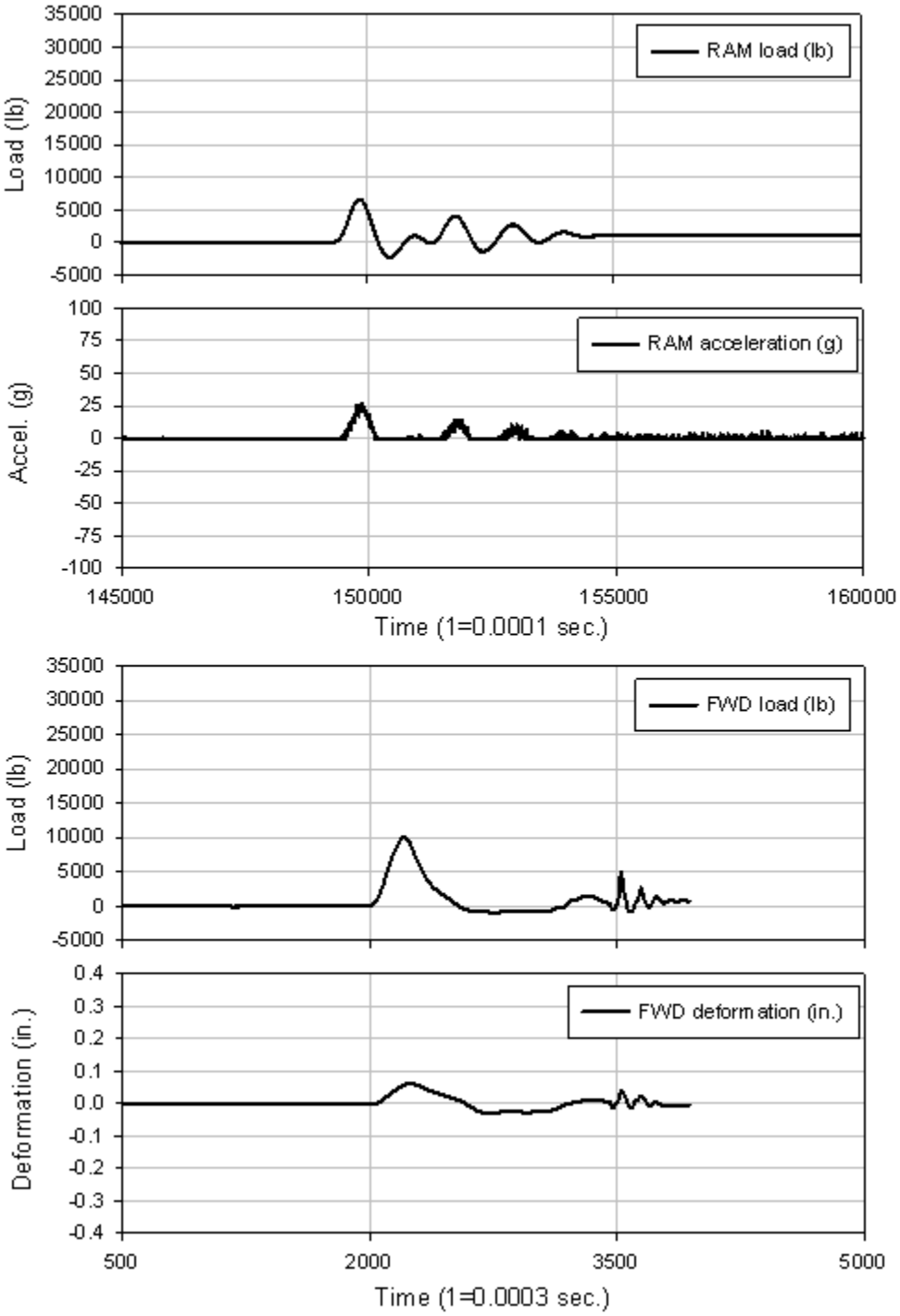


**Figure 223. La Port City test 93**

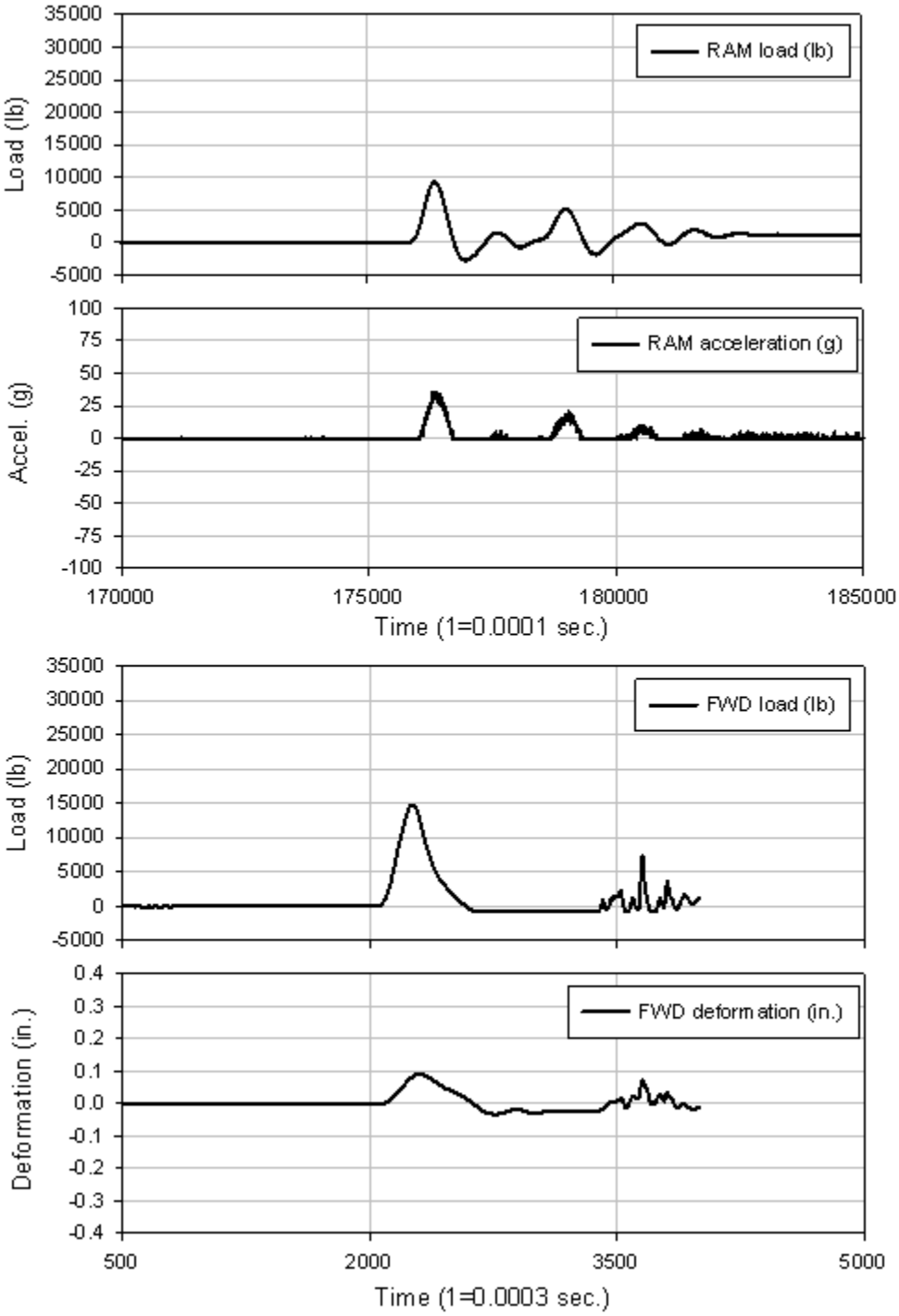


**Figure 224. La Port City test 94**

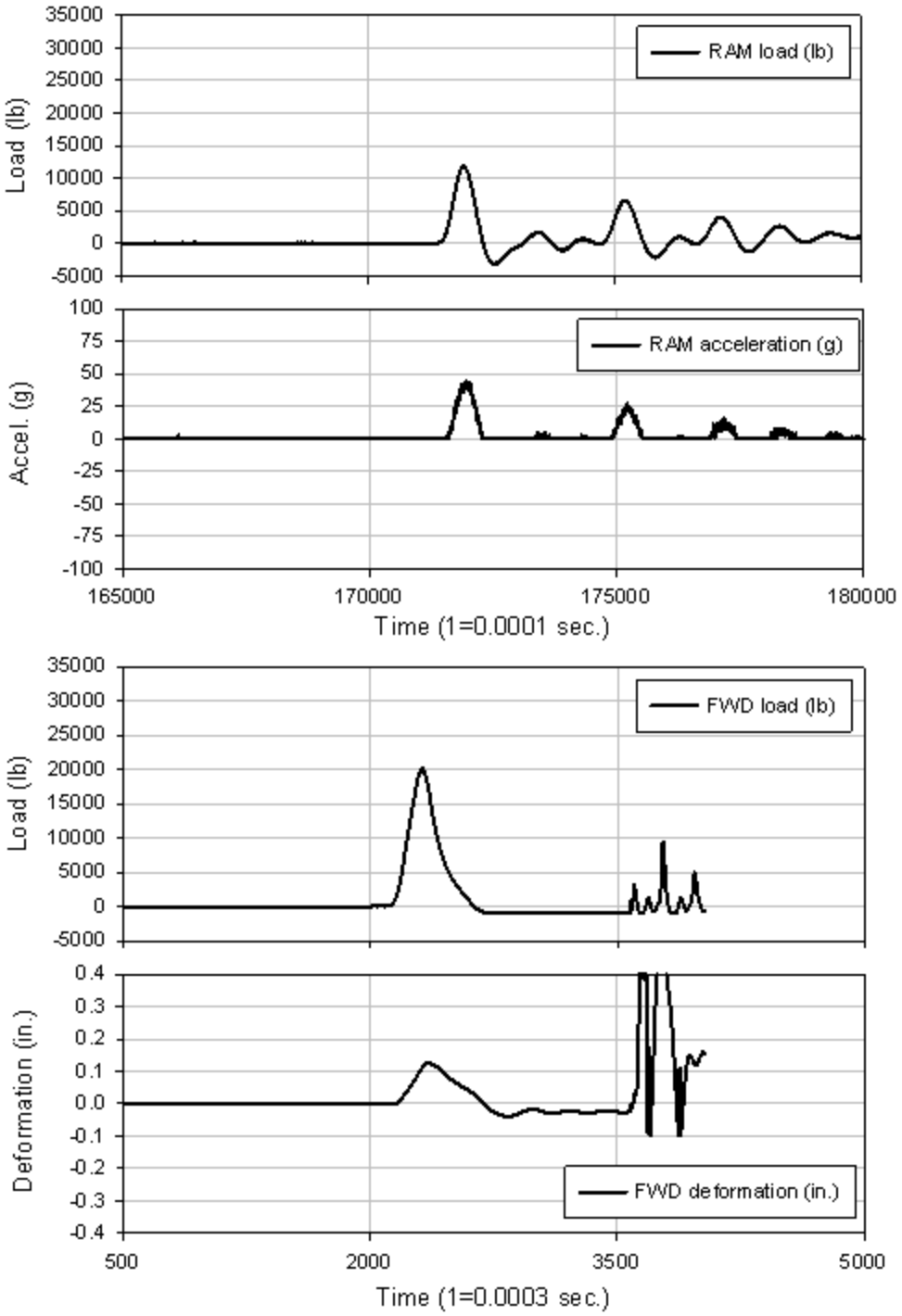


**Figure 225. La Port City test 95**

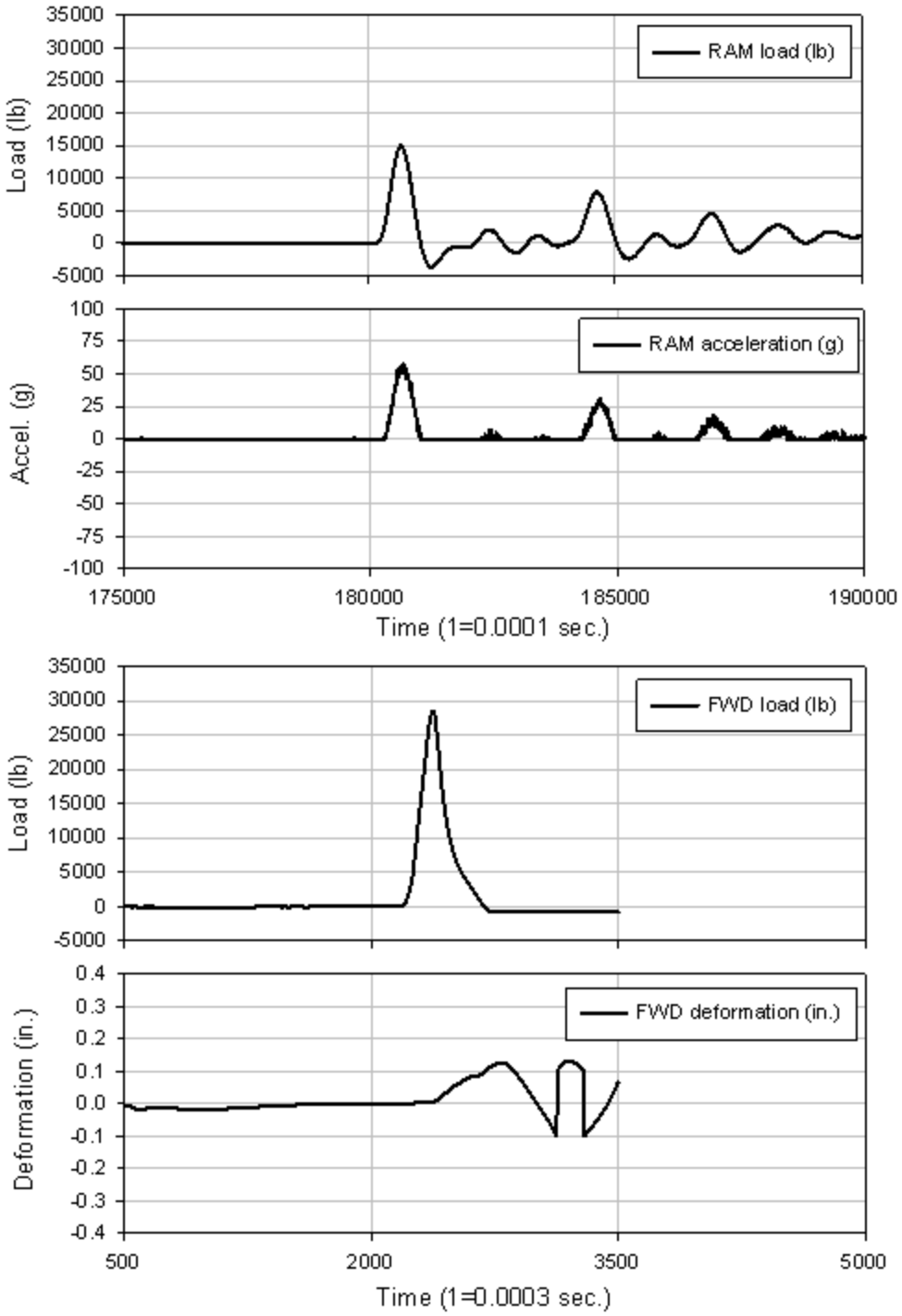


**Figure 226. La Port City test 96**

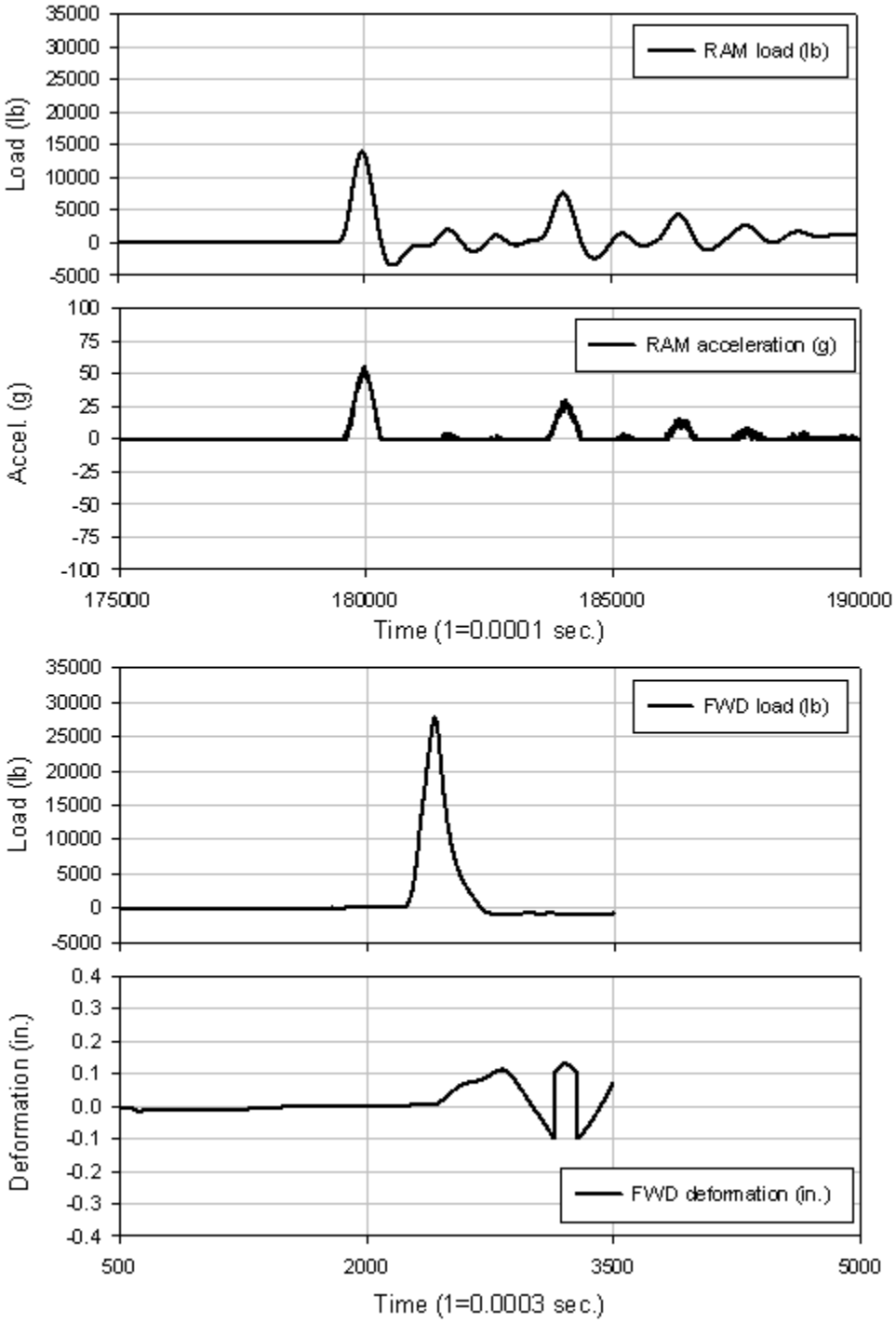


**Figure 227. La Port City test 97**

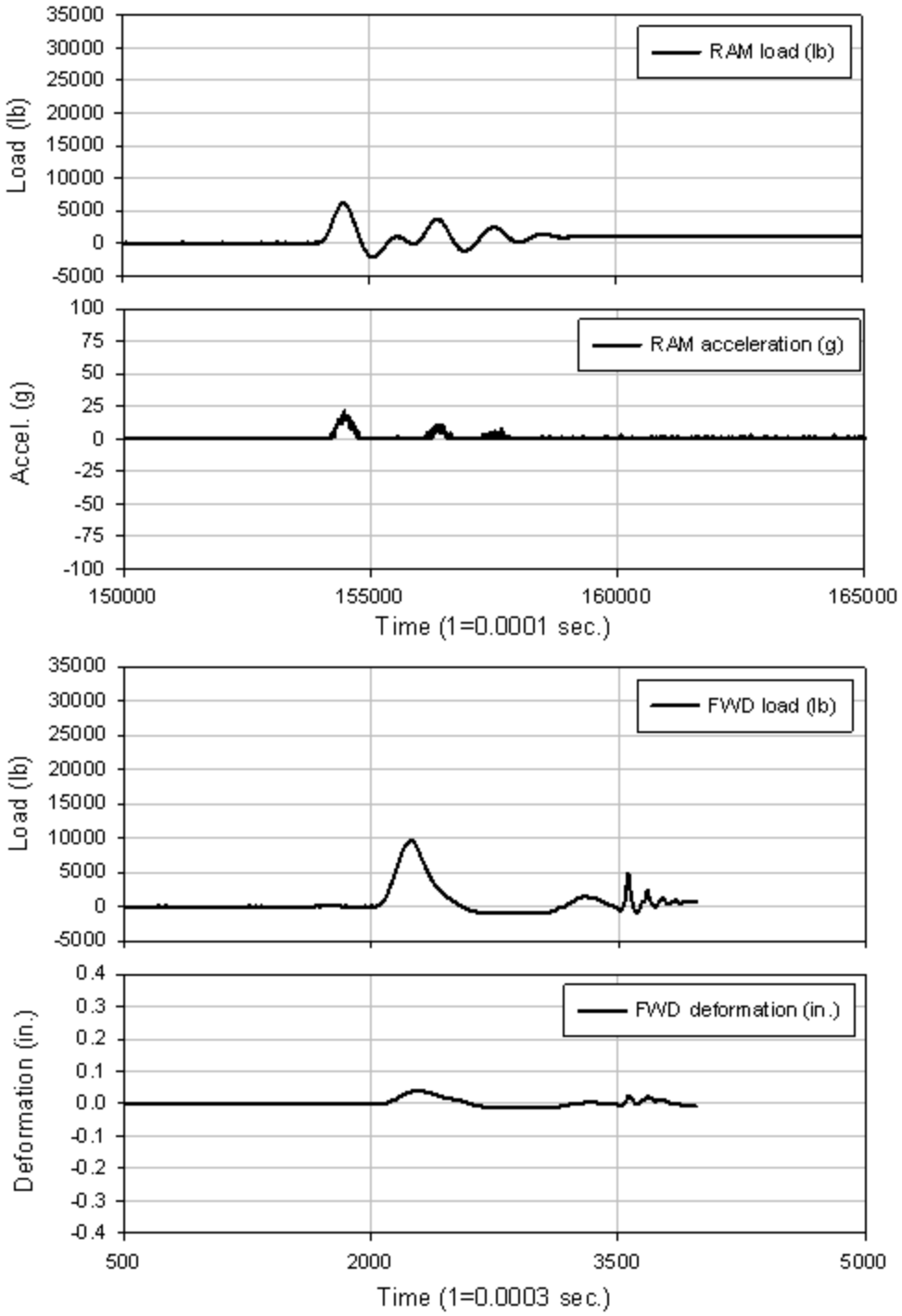


**Figure 228. La Port City test 99**

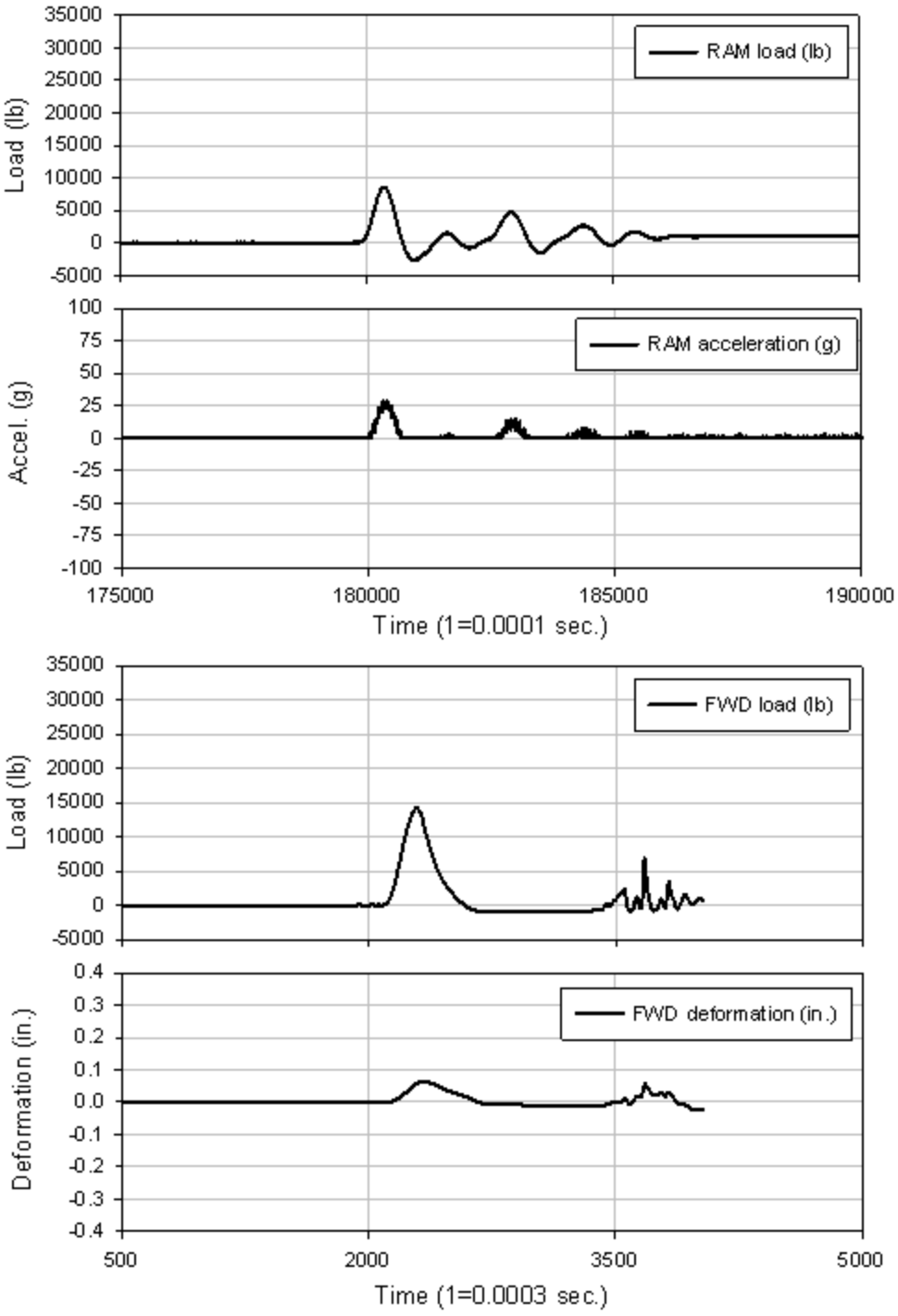


**Figure 229. La Port City test 100**

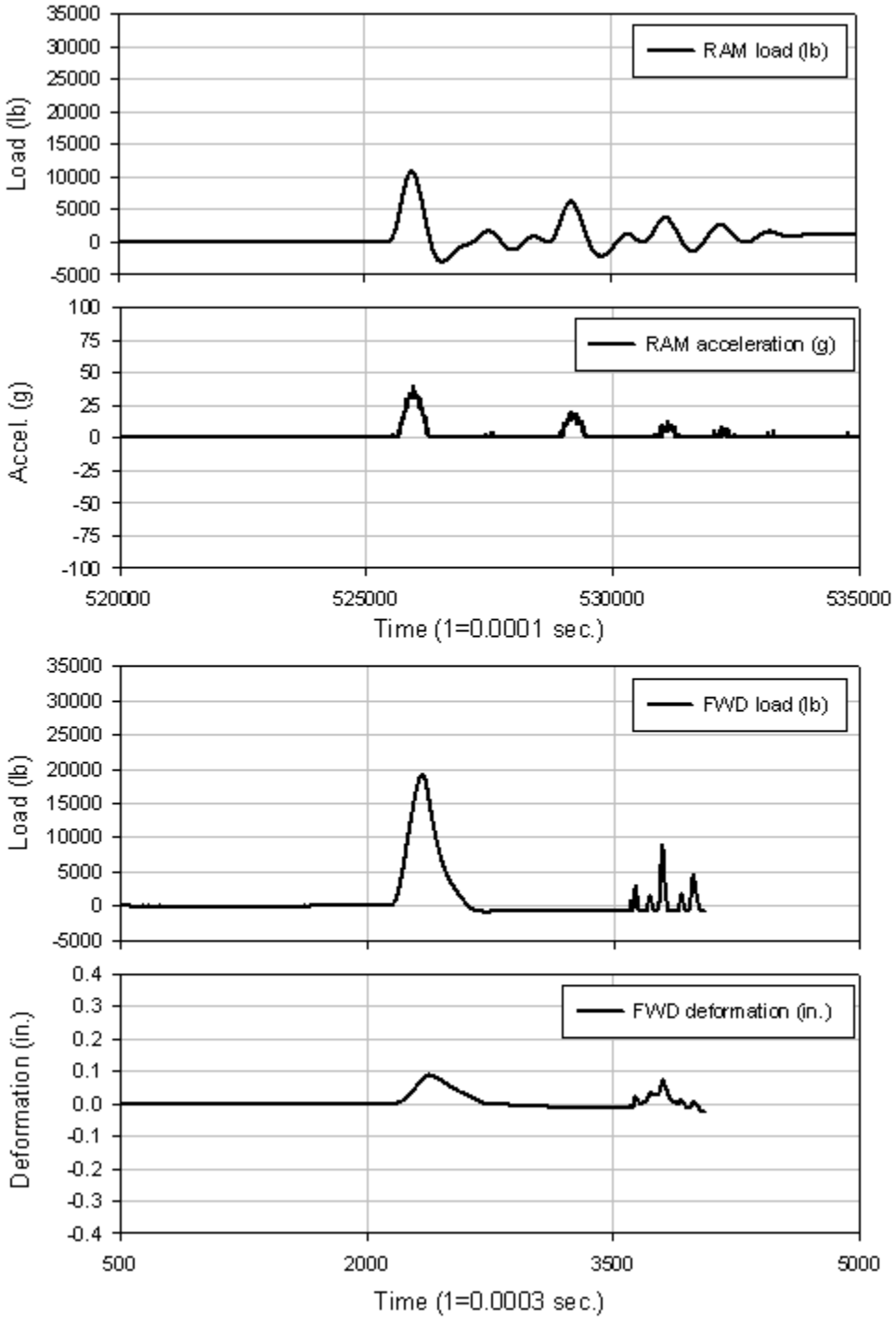


**Figure 230. La Port City test 101**

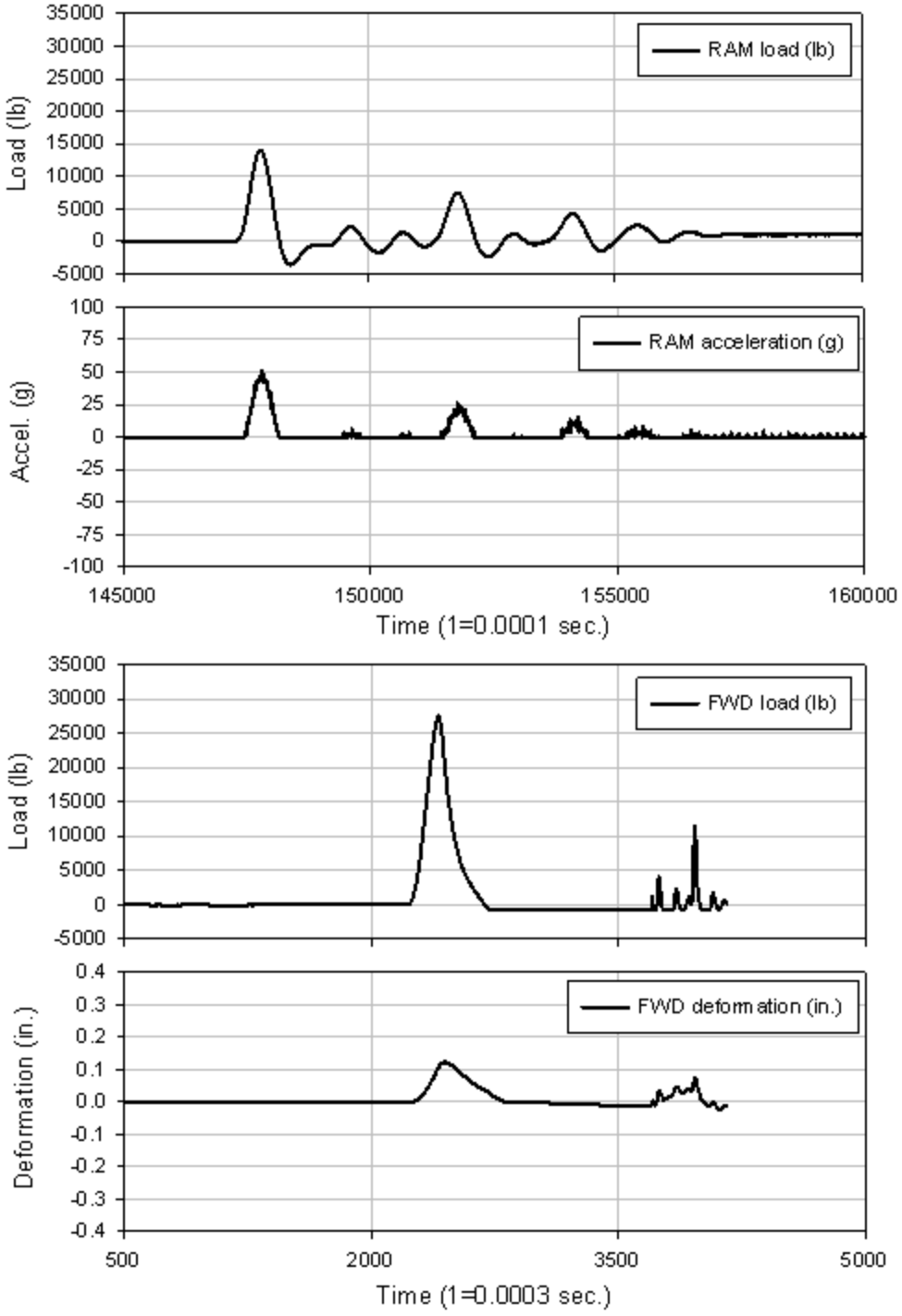


**Figure 231. La Port City test 102**

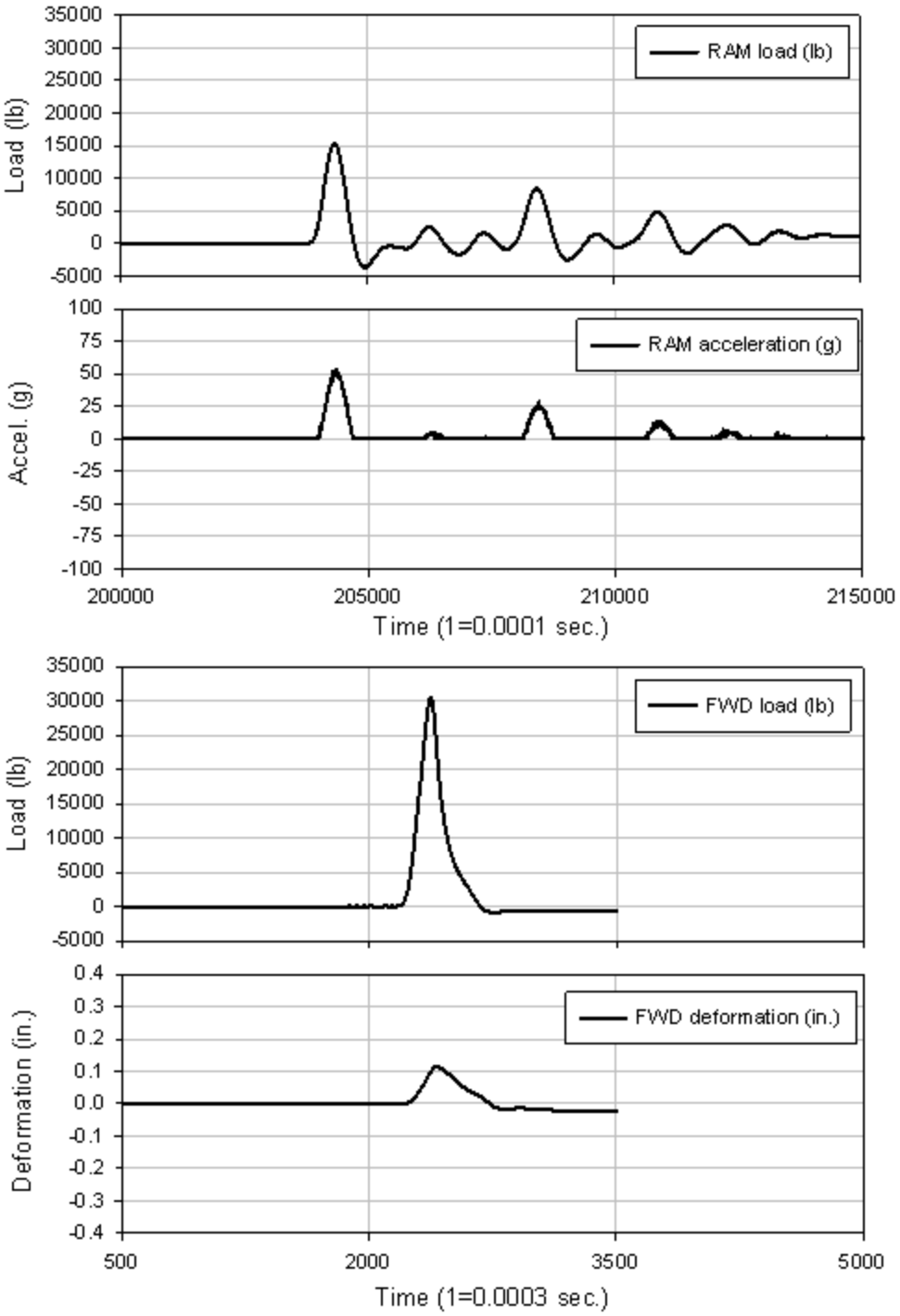


**Figure 232. La Port City test 103**

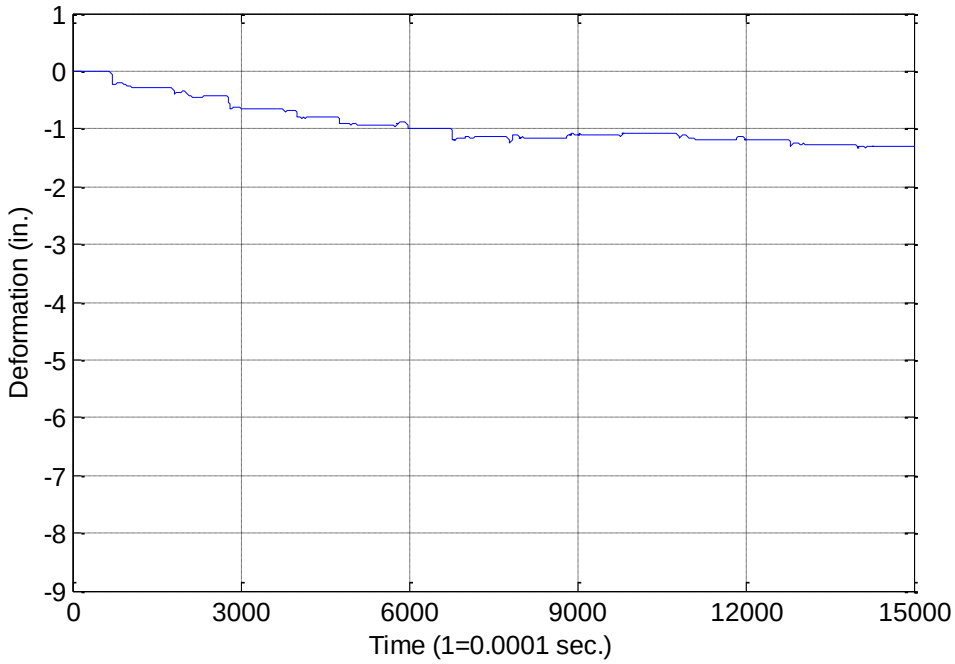


**Figure 233. La Port City test 1**

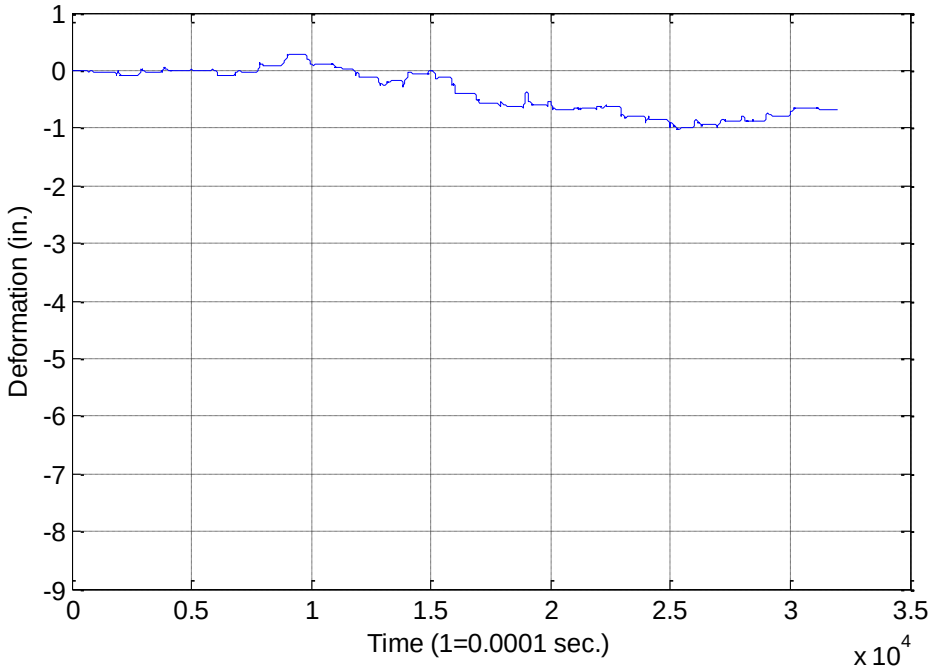


**Figure 234. La Port City test 2**

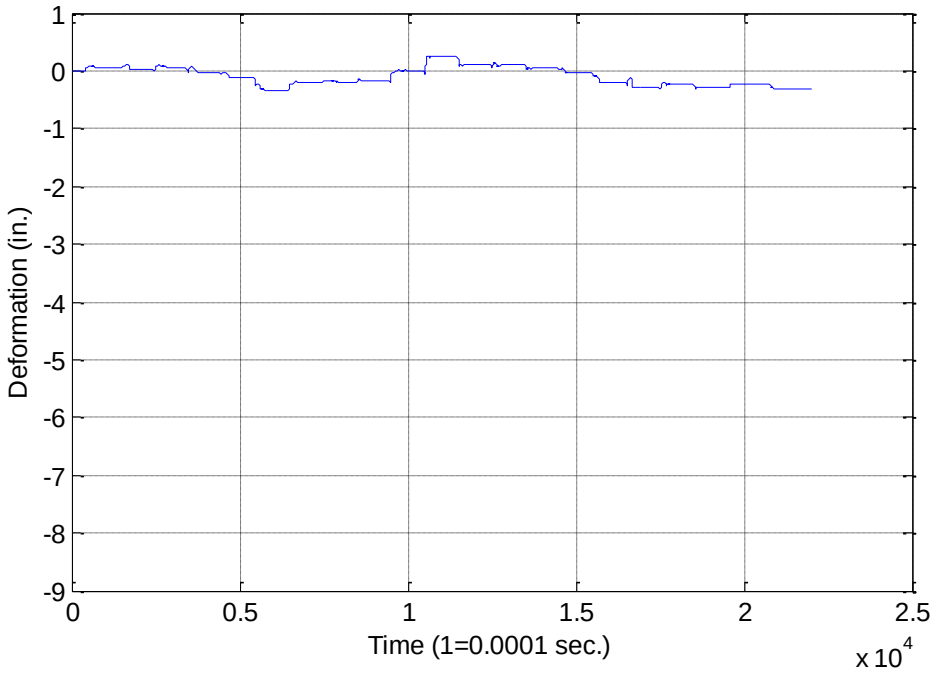


**Figure 235. La Port City test 3**

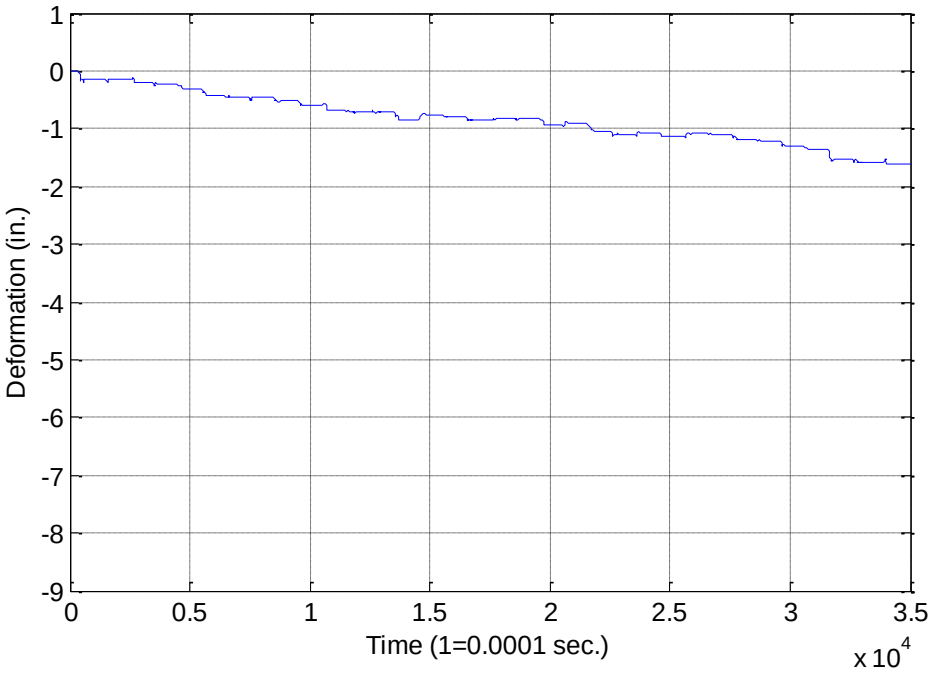


**Figure 236. La Port City test 4**

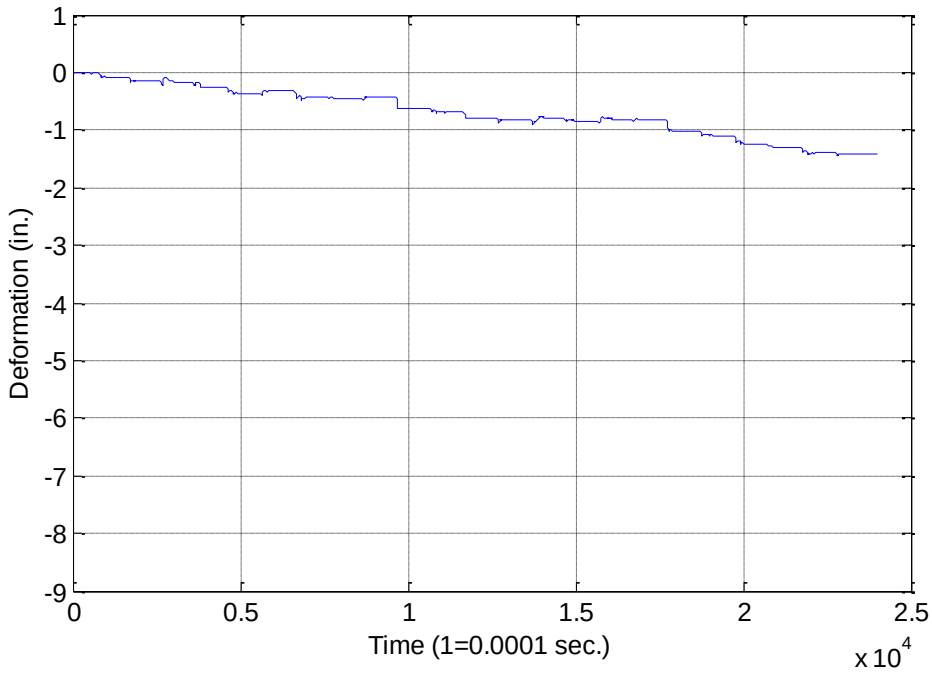


**Figure 237. La Port City test 5**

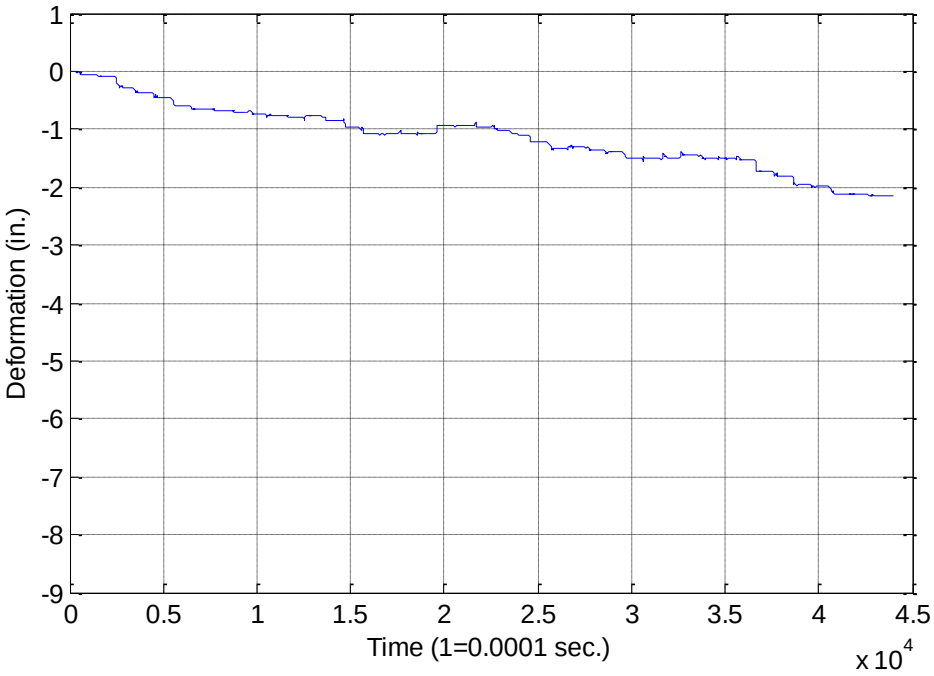


**Figure 238. La Port City test 6**

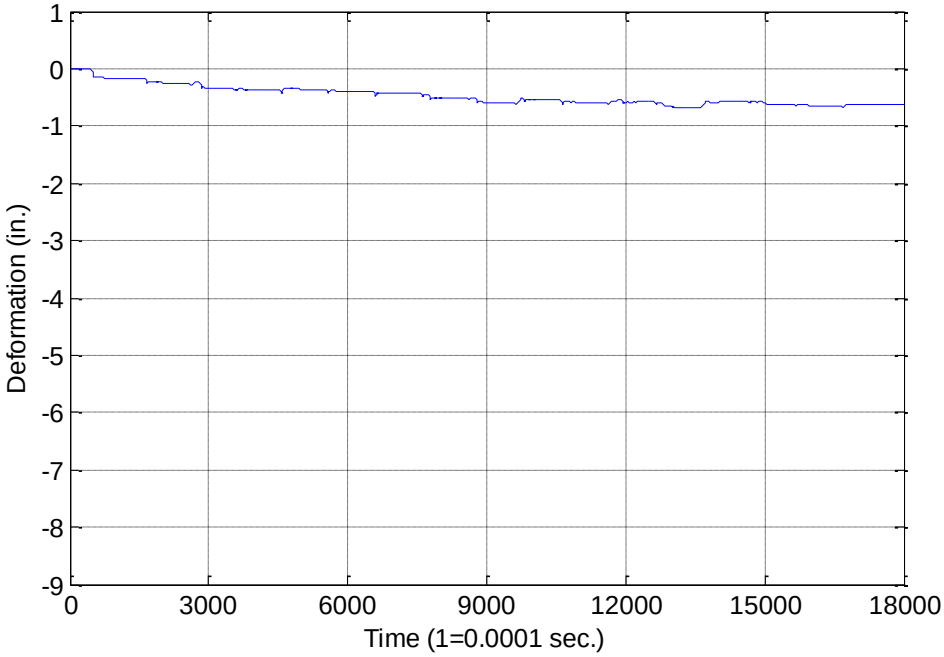


**Figure 239. La Port City test 7**

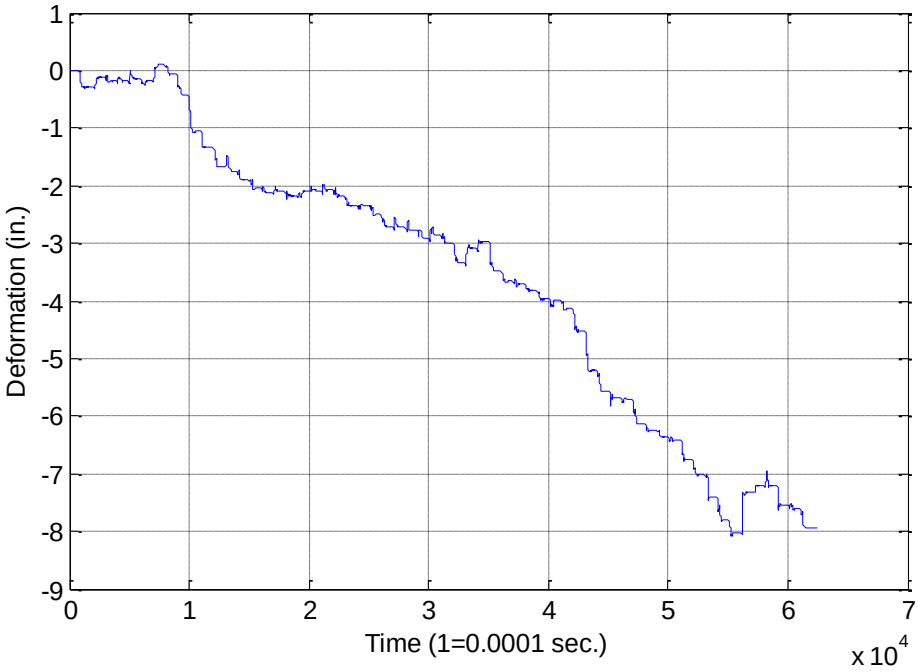


**Figure 240. La Port City test 8**

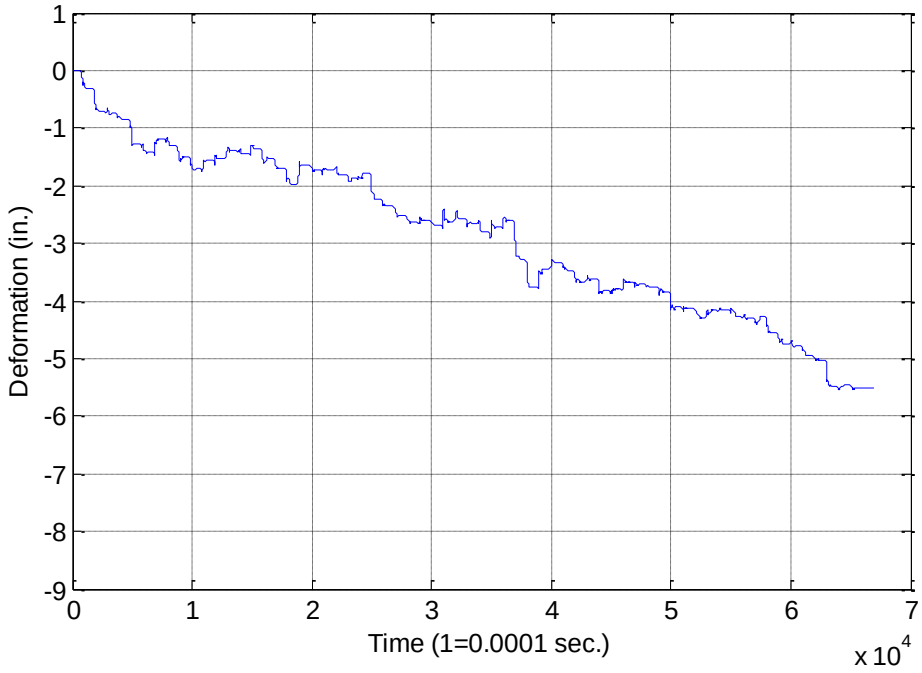


**Figure 241. La Port City test 9**

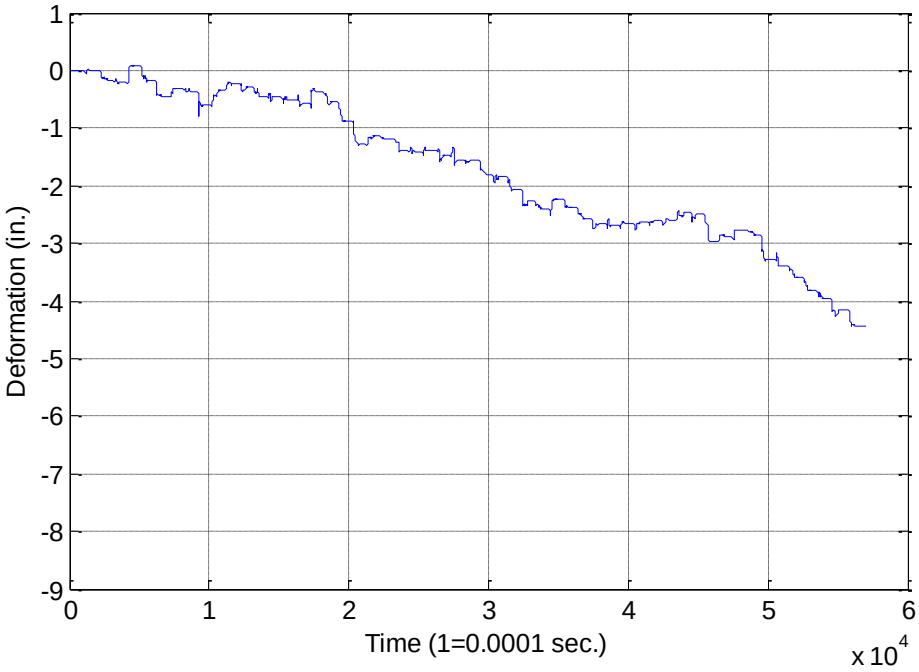


**Figure 242. La Port City test 10**

**Fairfield**

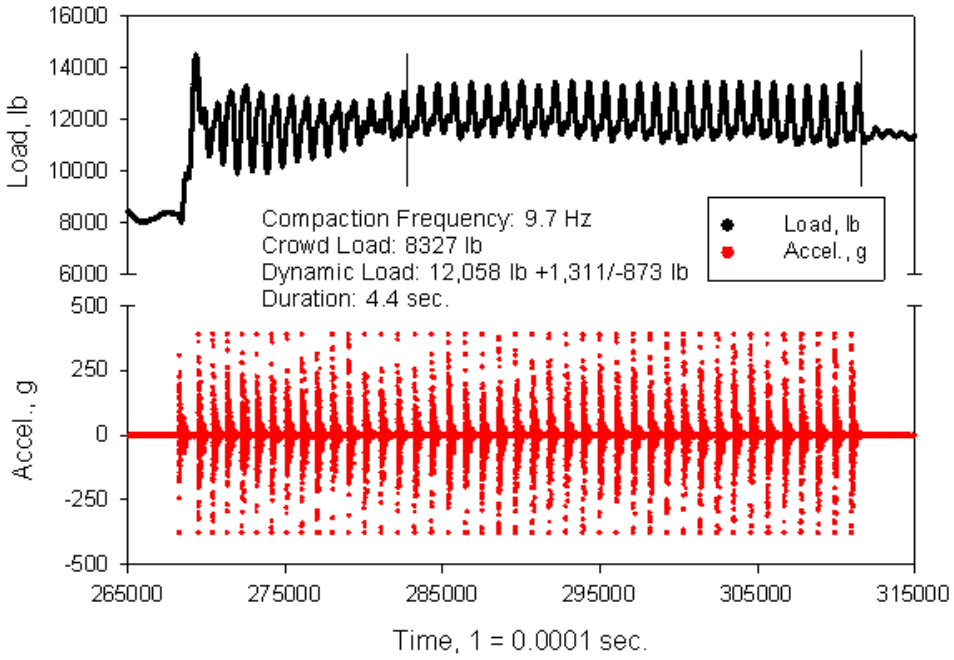


**Figure 243. Fairfield test 1**

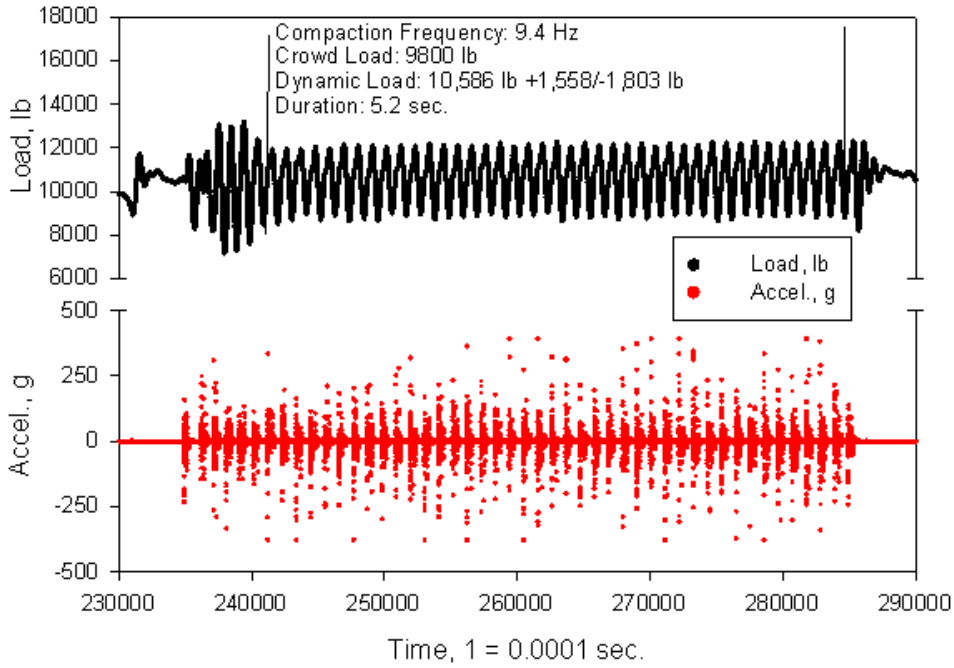


**Figure 244. Fairfield test 2**

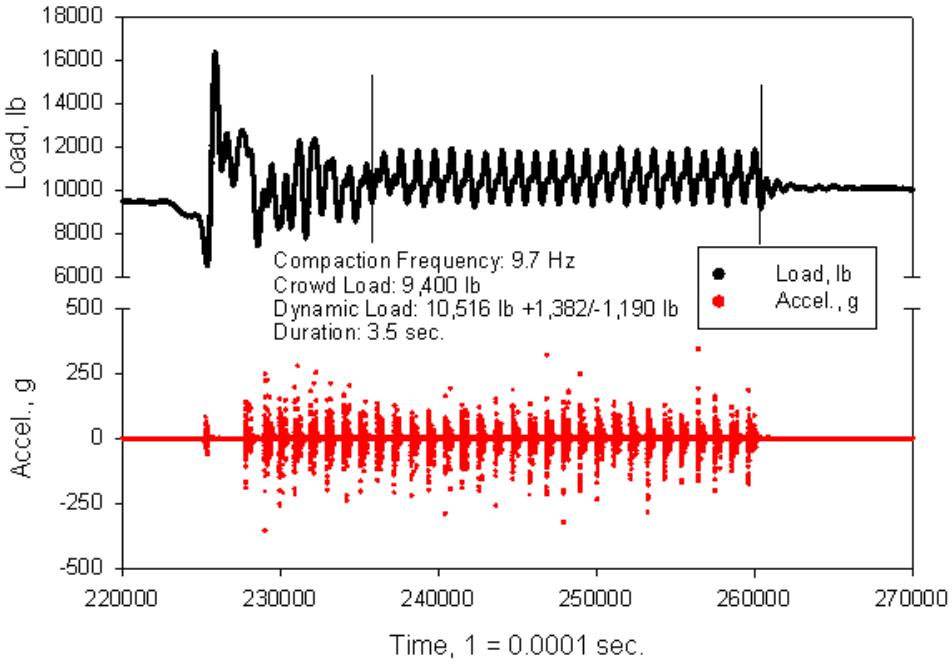


**Figure 245. Fairfield test 3**

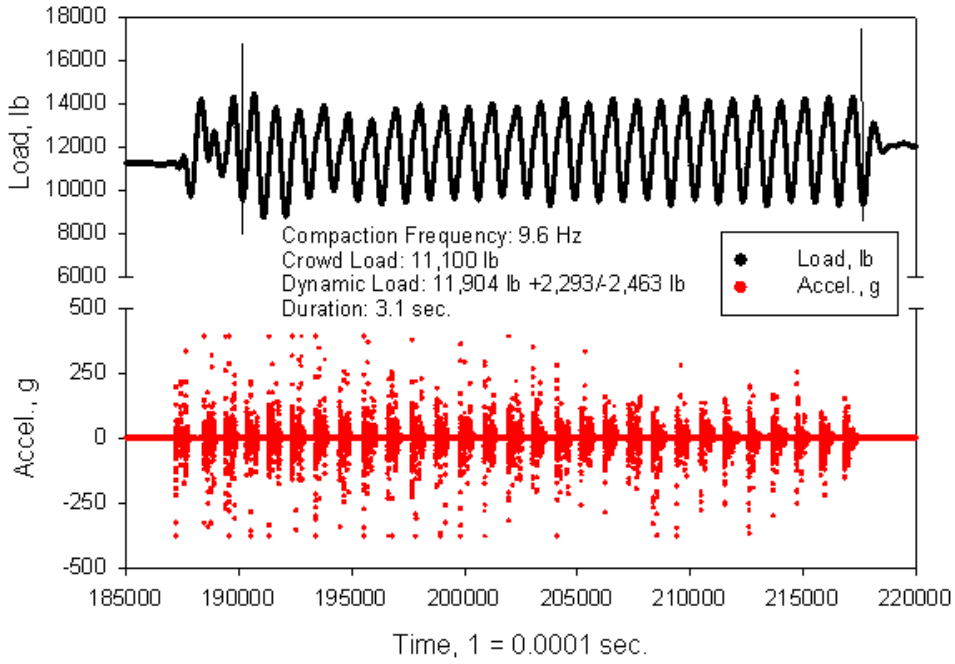


**Figure 246. Fairfield test 4**

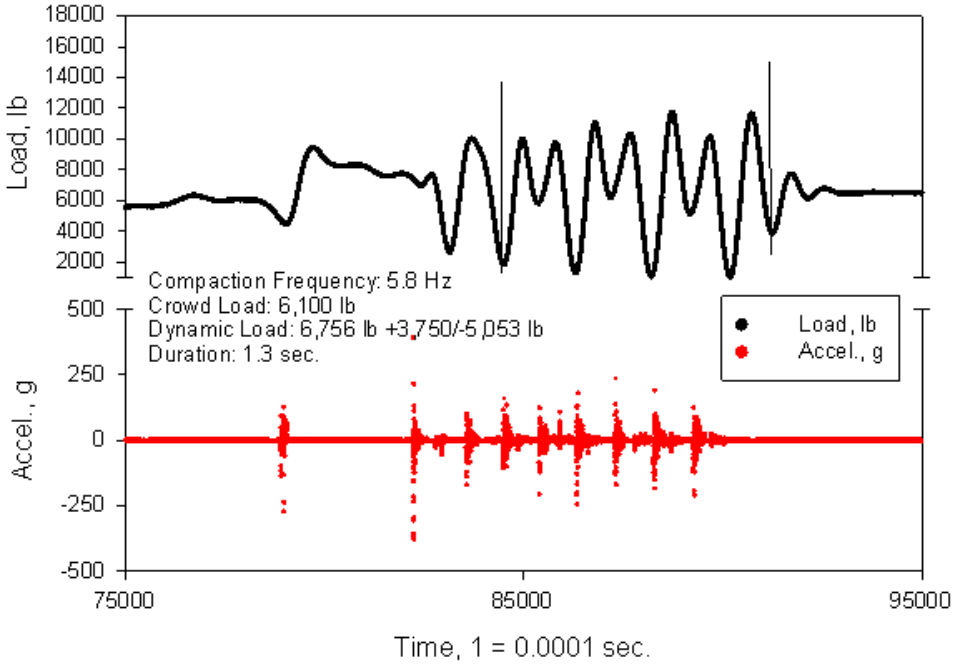


**Figure 247. Fairfield test 5**

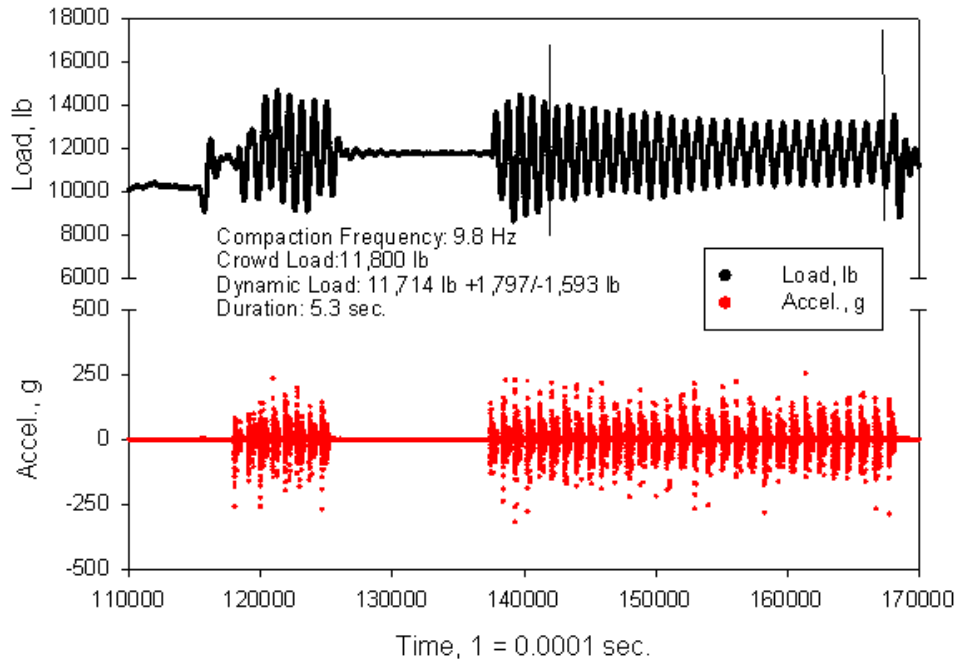


**Figure 248. Fairfield test 6**

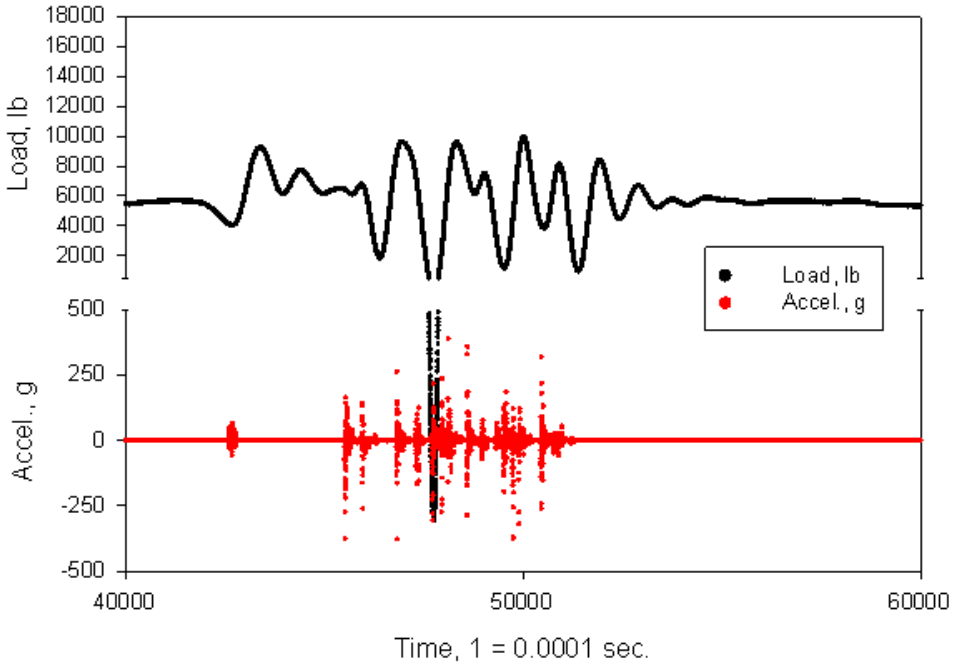


**Figure 249. Fairfield test 8**

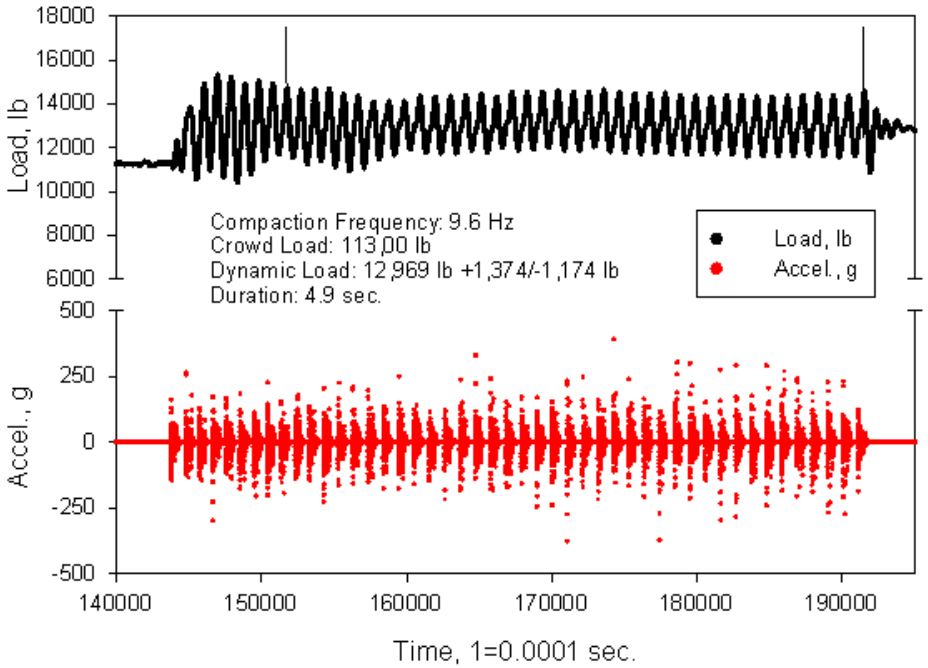


**Figure 250. Fairfield test 9**

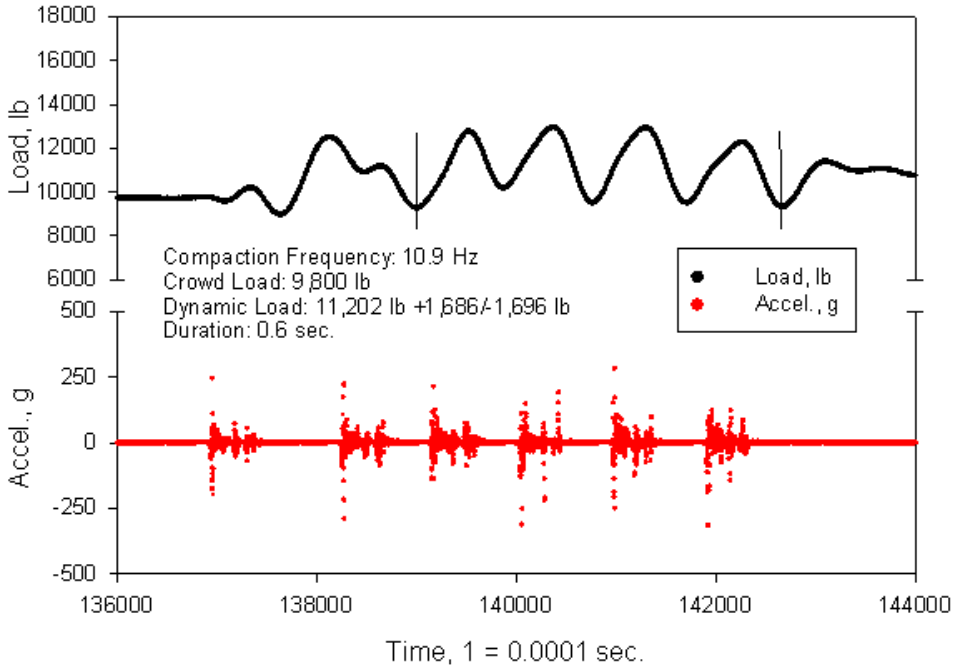


**Figure 251. Fairfield test 10**

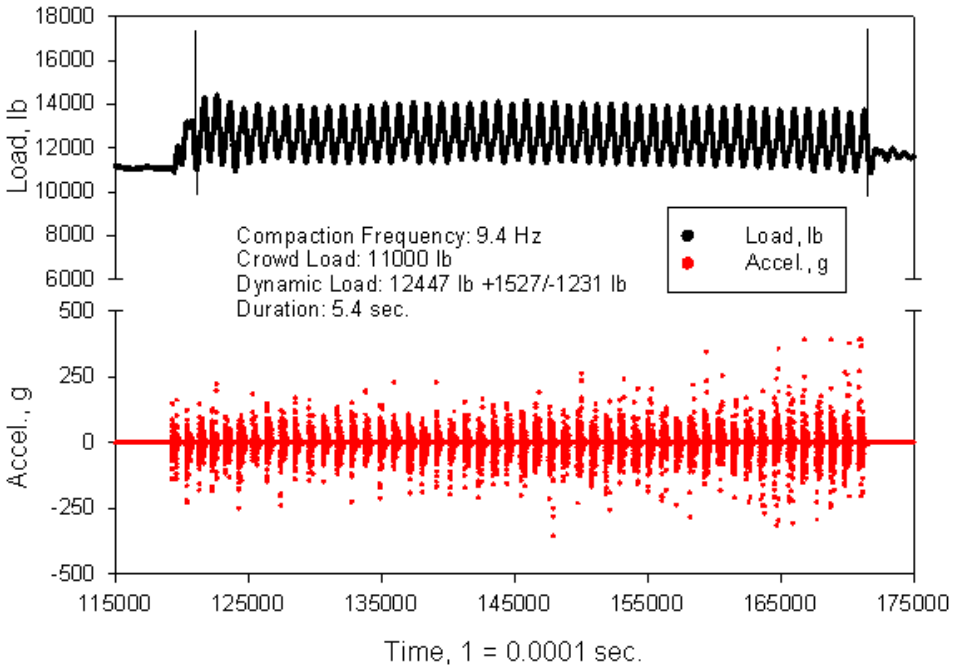


**Figure 252. Fairfield test 11**

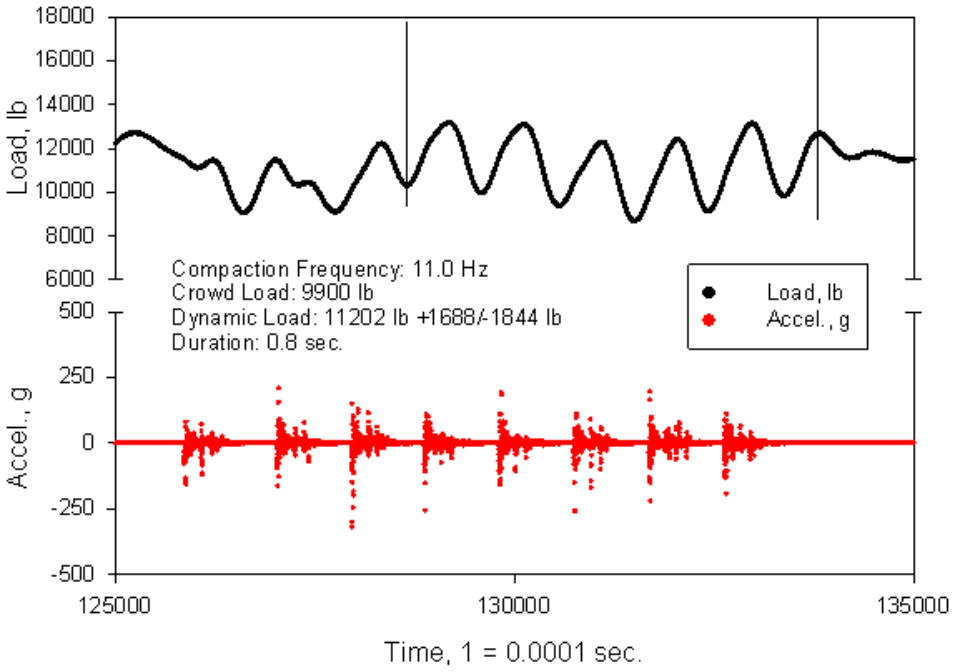


**Figure 253. Fairfield test 12**

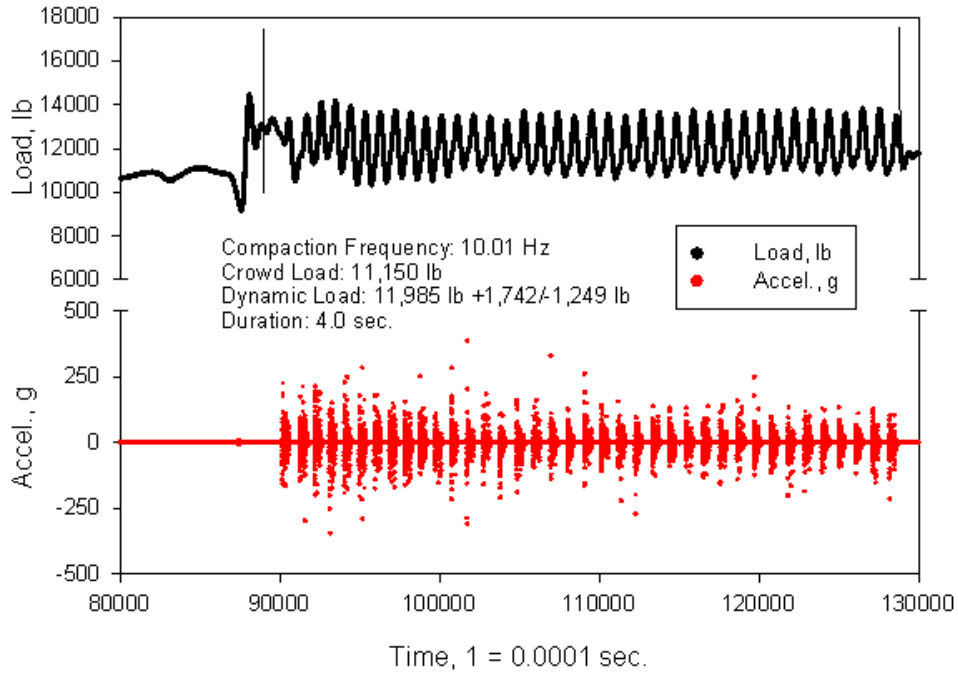


**Figure 254. Fairfield test 13**

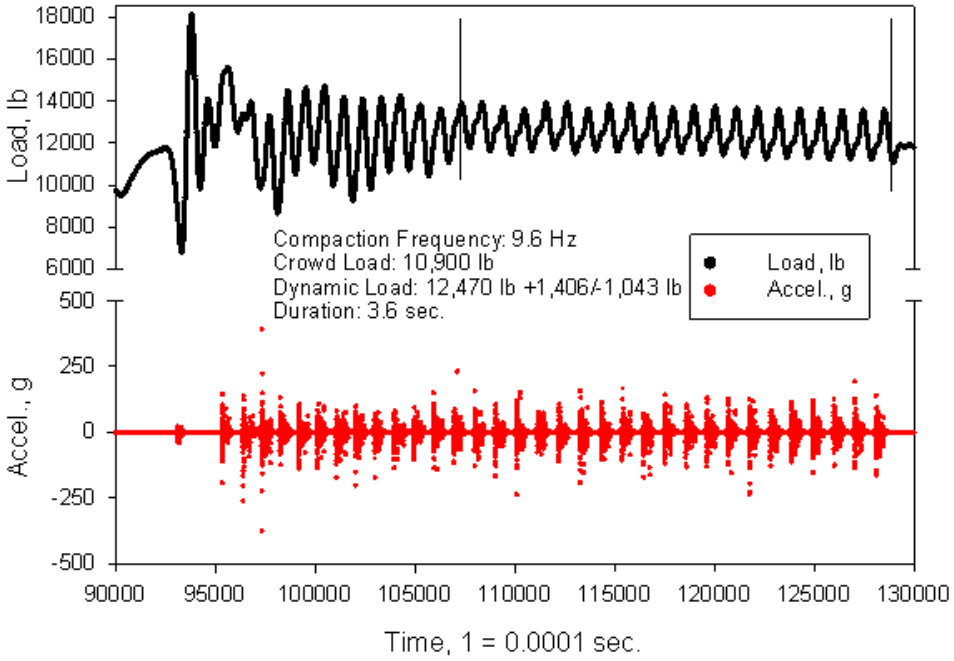


**Figure 255. Fairfield test 14**

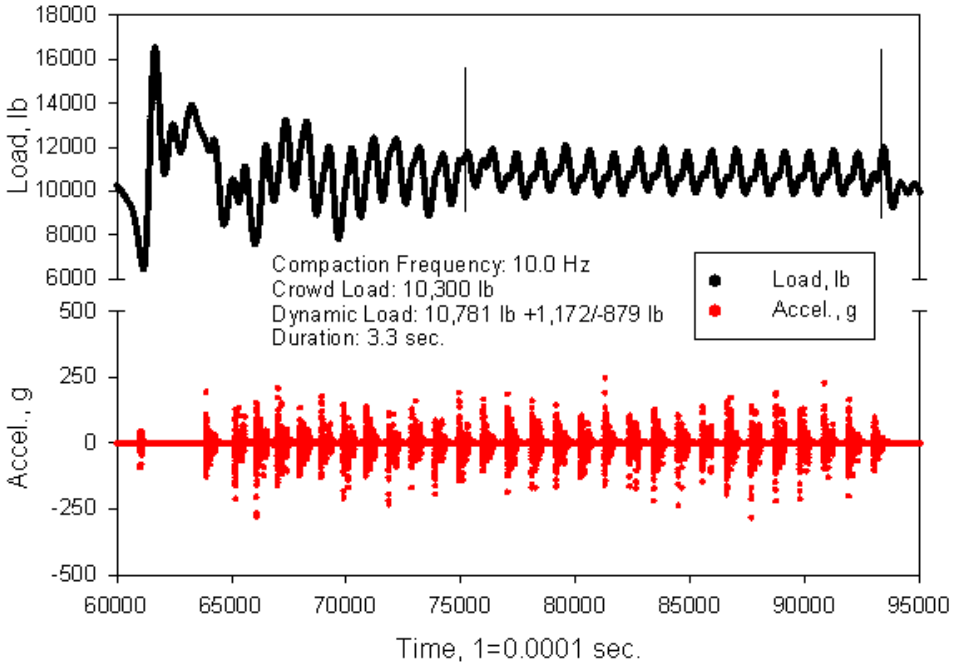


**Figure 256. Fairfield test 15**

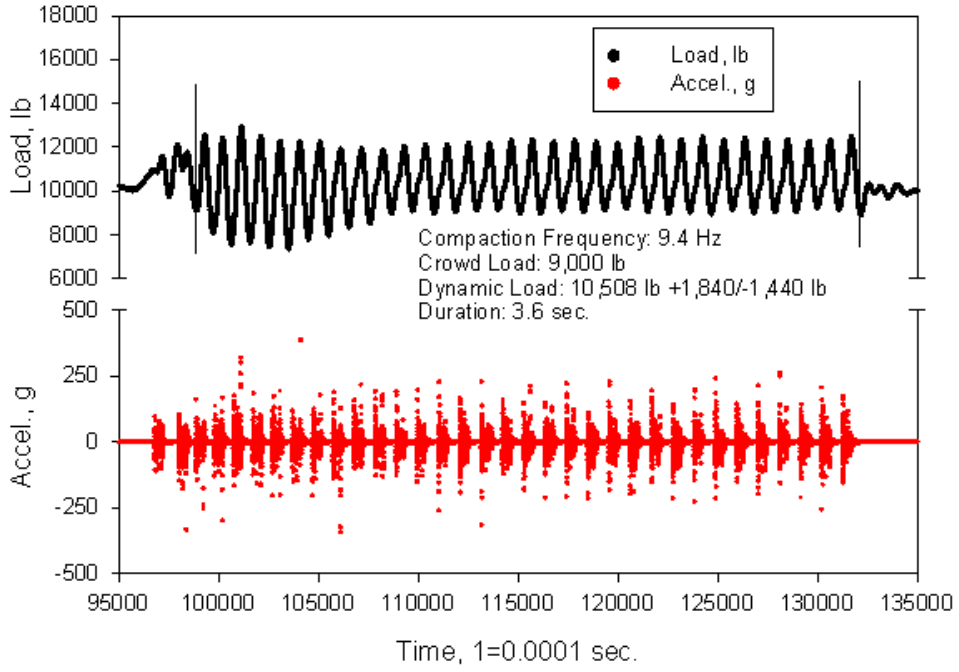


**Figure 257. Fairfield test 16**

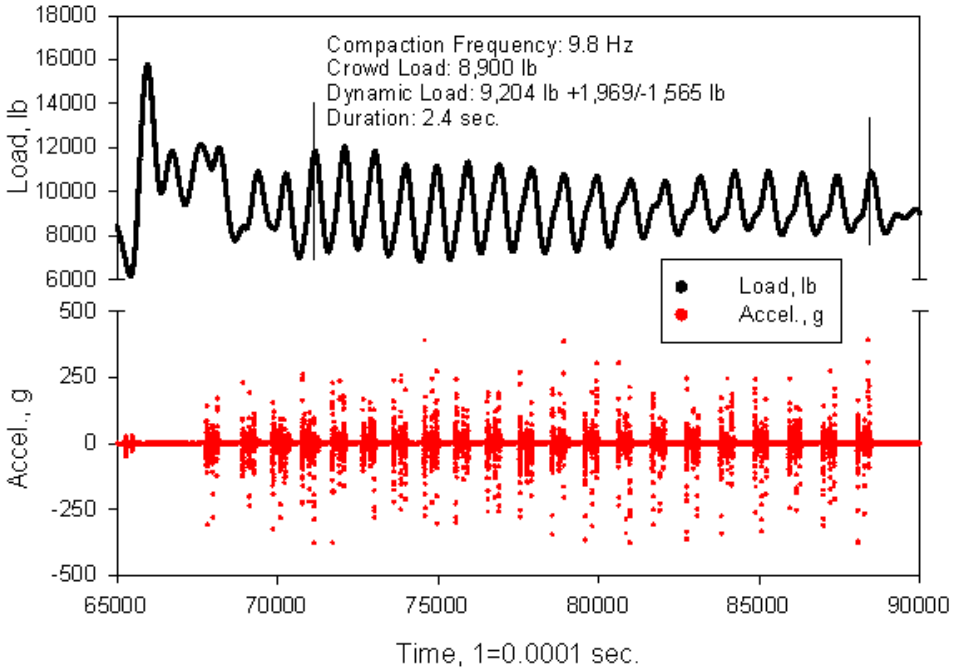


**Figure 258. Fairfield test 17**

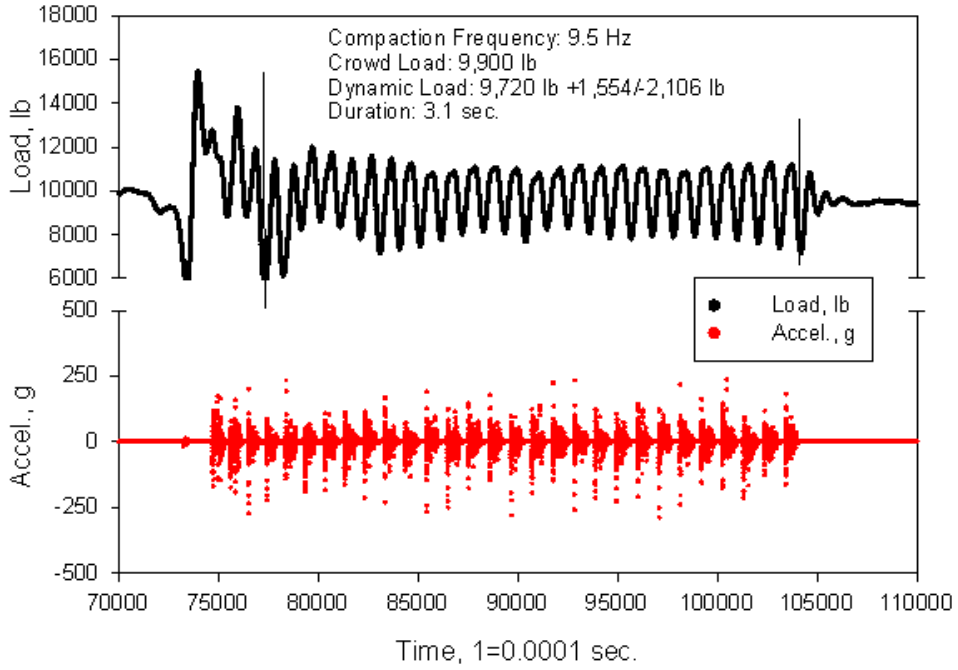


**Figure 259. Fairfield test 18**

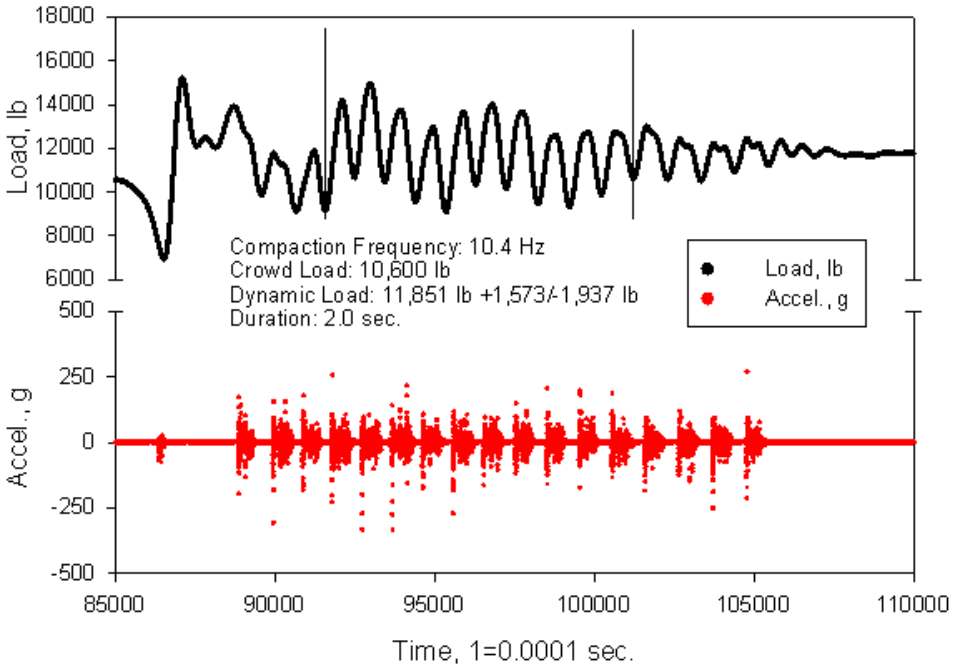


**Figure 260. Fairfield test 19**

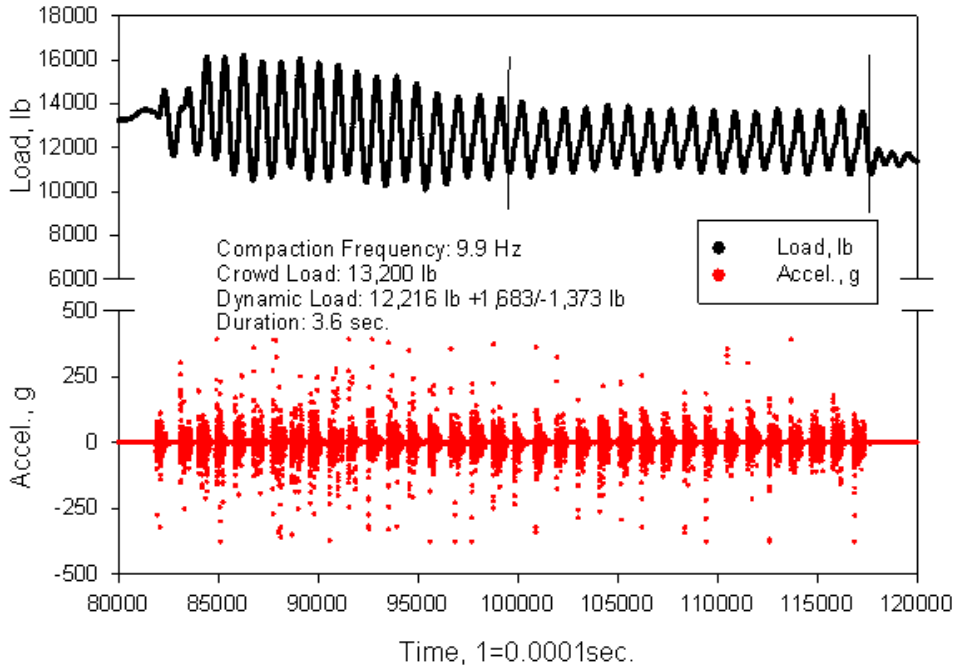


**Figure 261. Fairfield test 20**

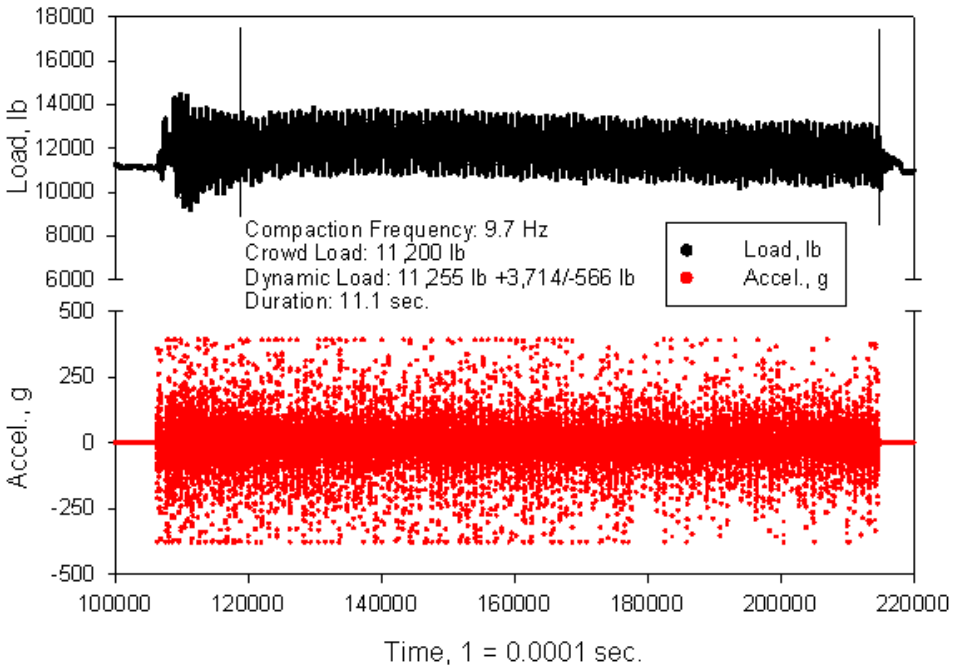


**Figure 262. Fairfield test 21**

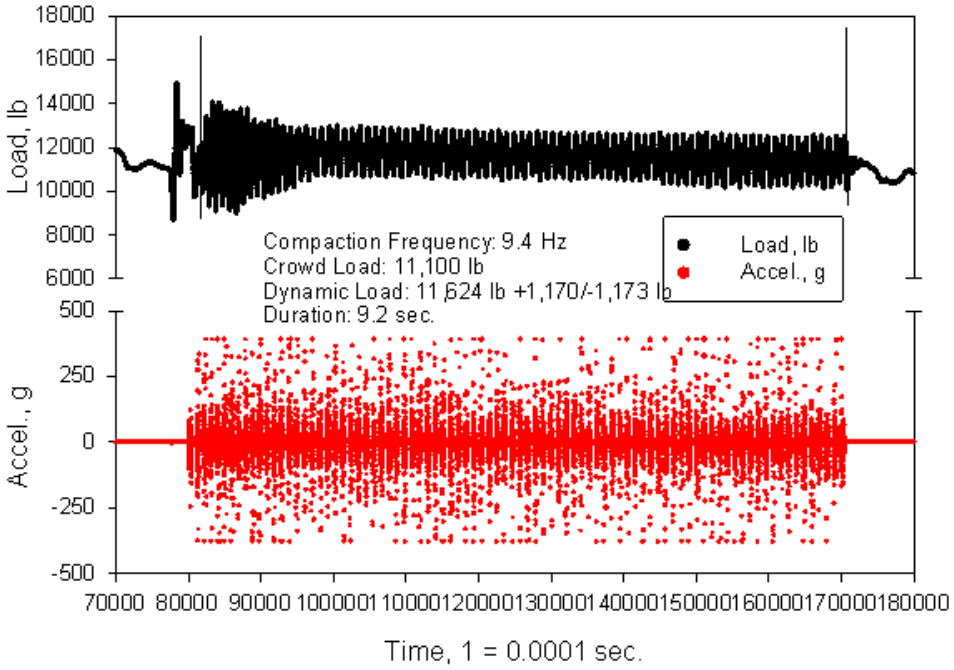


**Figure 263. Fairfield test 22**

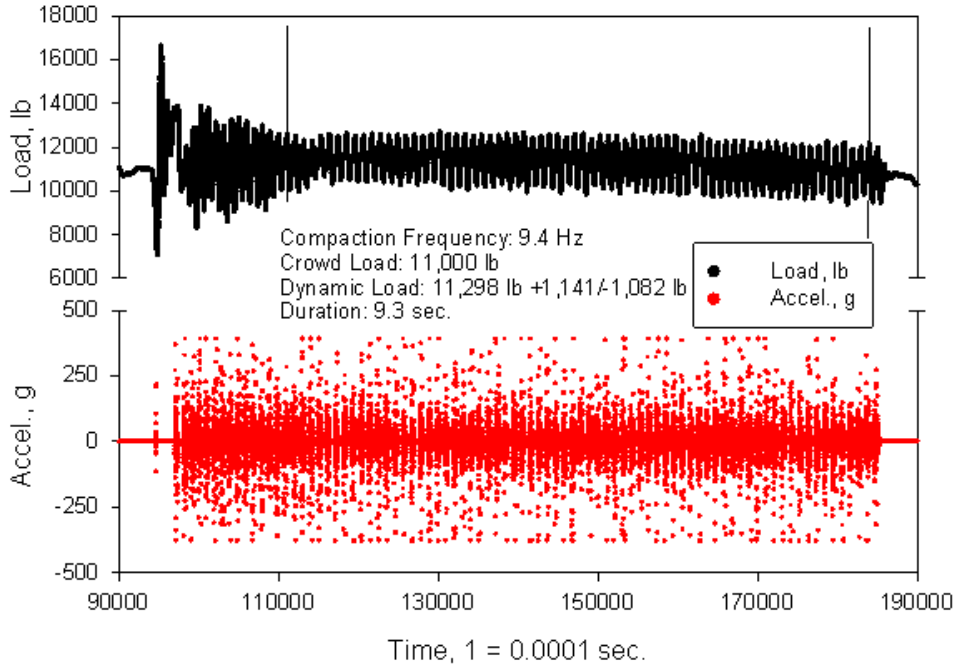


**Figure 264. Fairfield test 23**

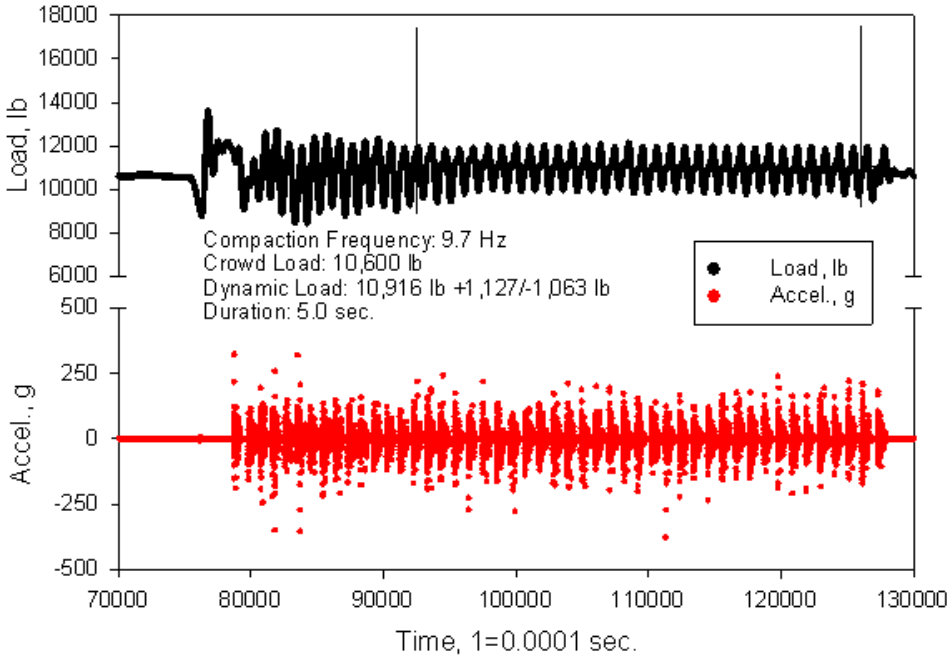


**Figure 265. Fairfield test 24**

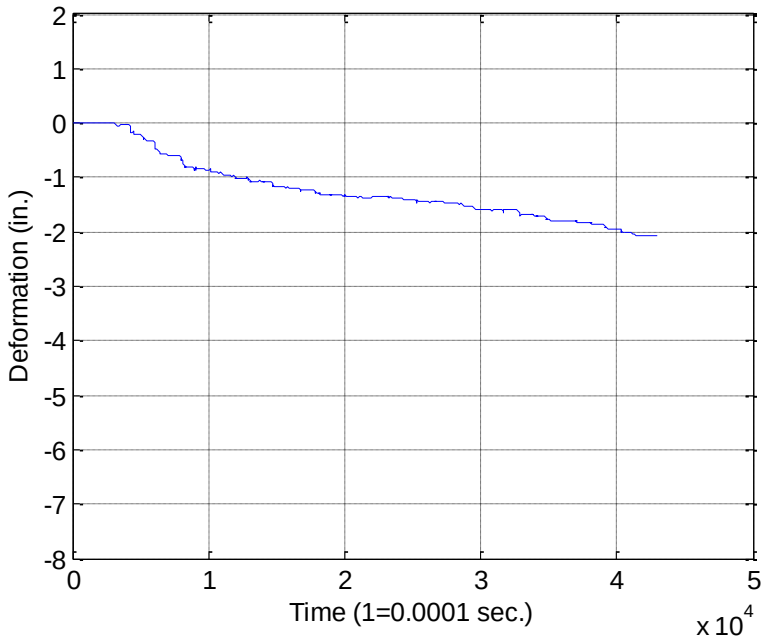


**Figure 266. Fairfield test 13**

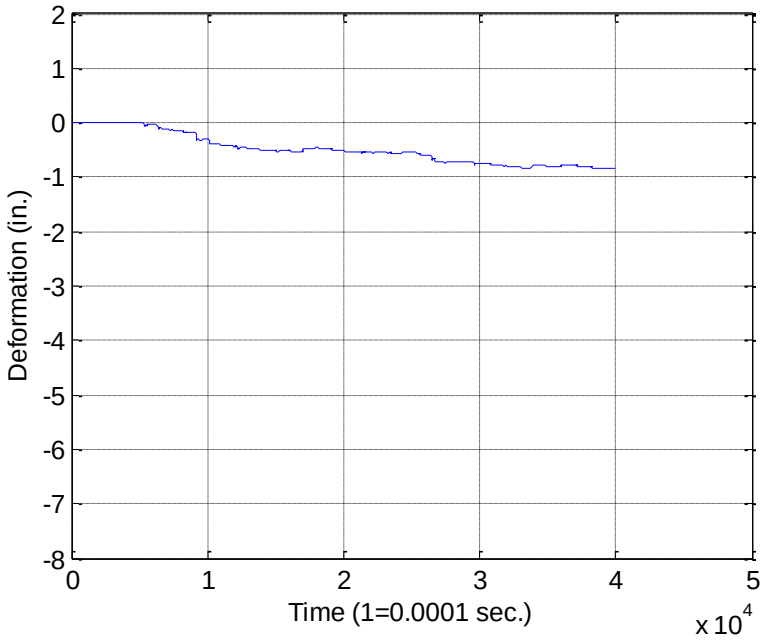


**Figure 267. Fairfield test 14**

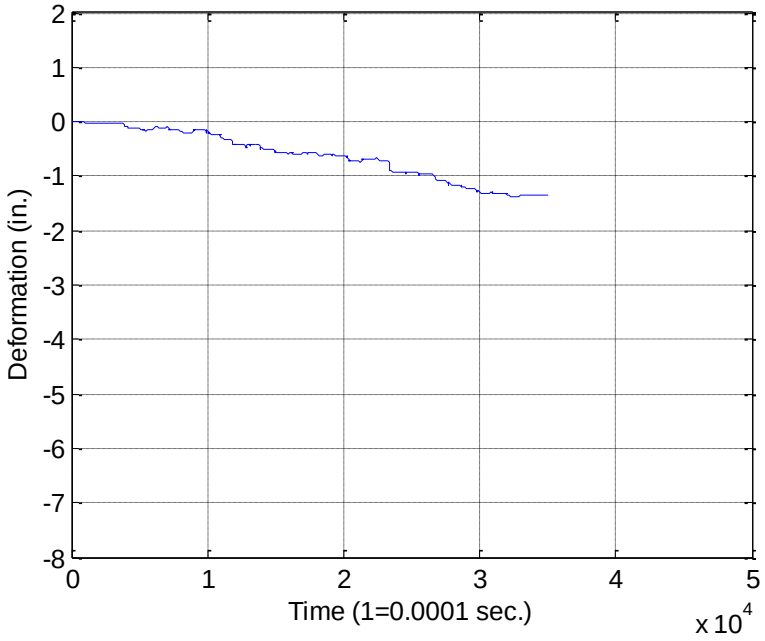


**Figure 268. Fairfield test 15**

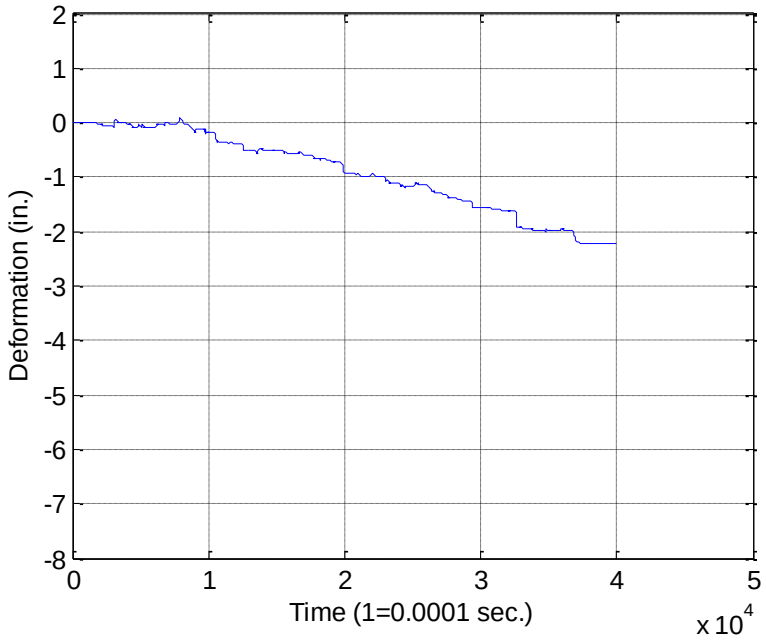


**Figure 269. Fairfield test 20**

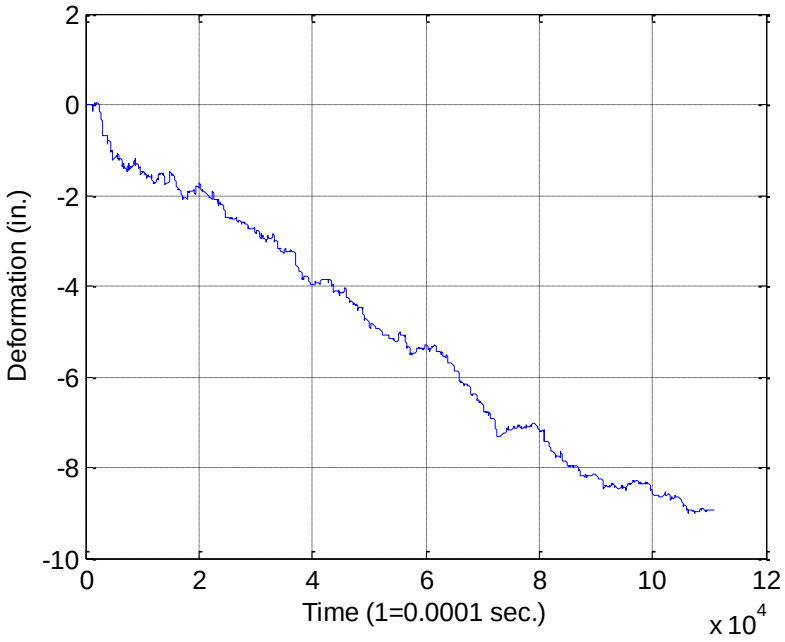


**Figure 270. Fairfield test 21**

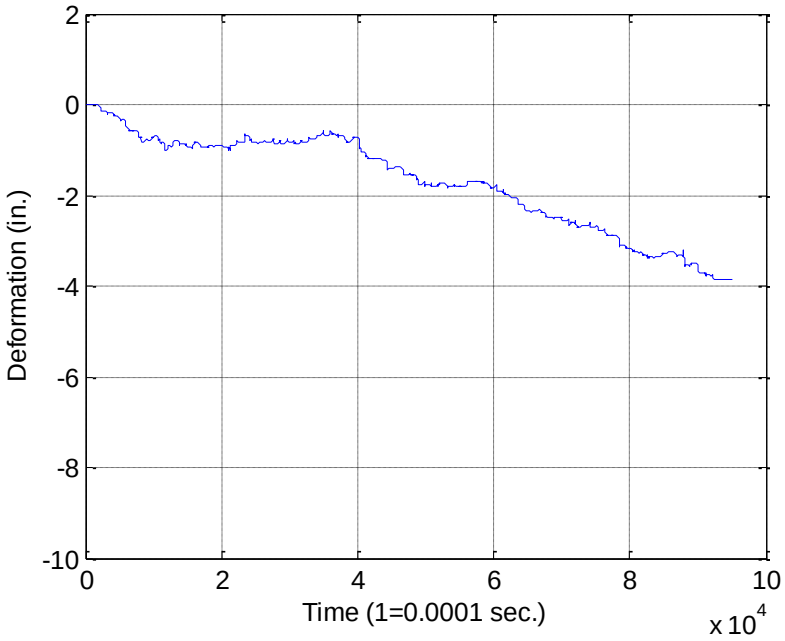


**Figure 271. Fairfield test 22**

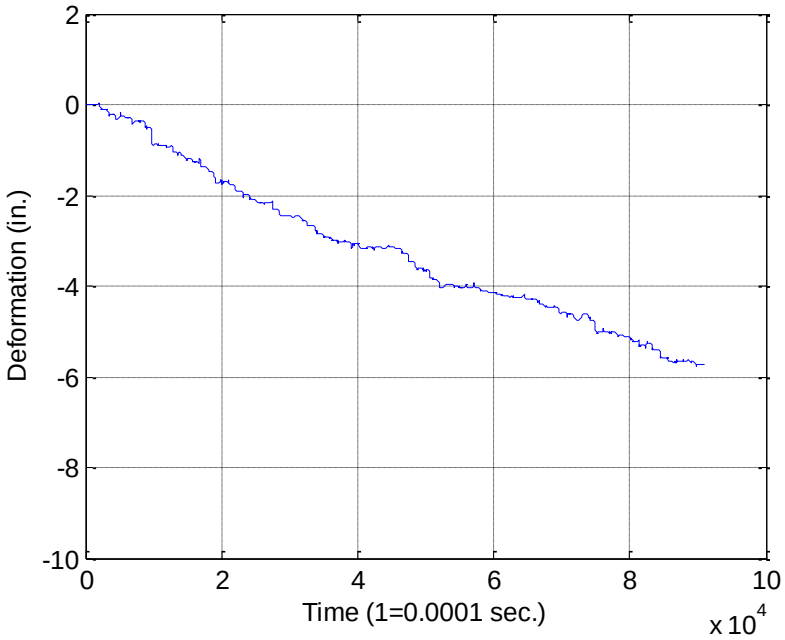


**Figure 272. Fairfield test 23**

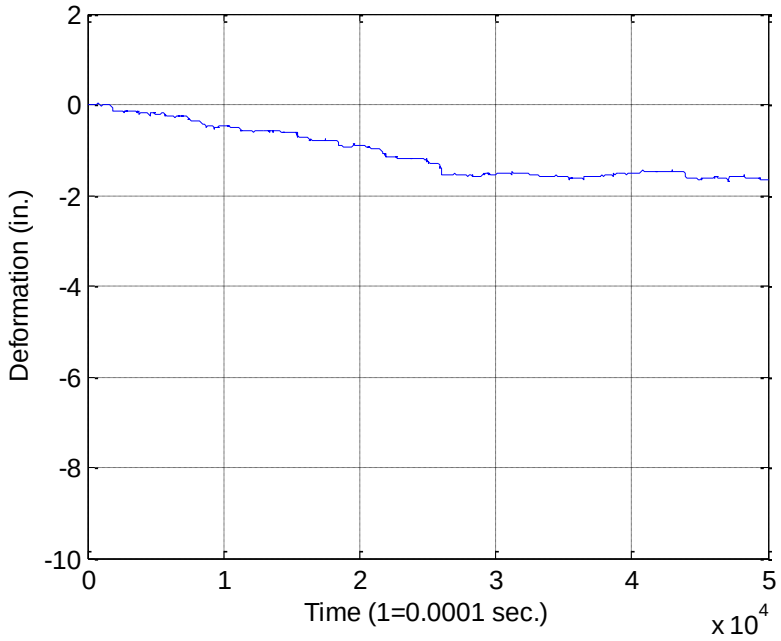


**Figure 273. Fairfield test 23**

**Council Bluffs**

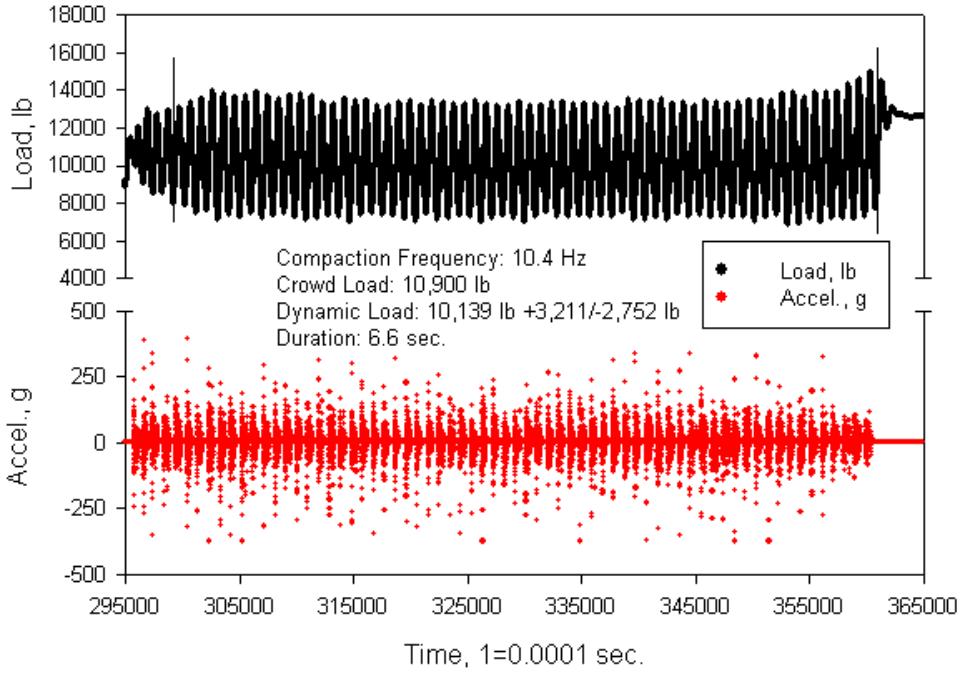


**Figure 274. Council Bluffs test 6**

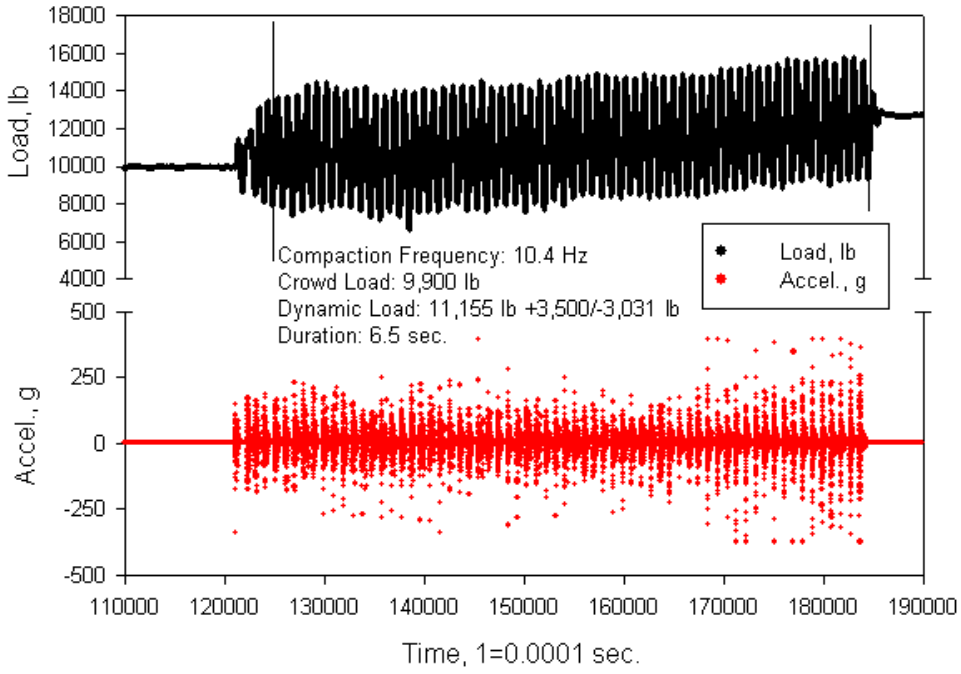


**Figure 275. Council Bluffs test 7**

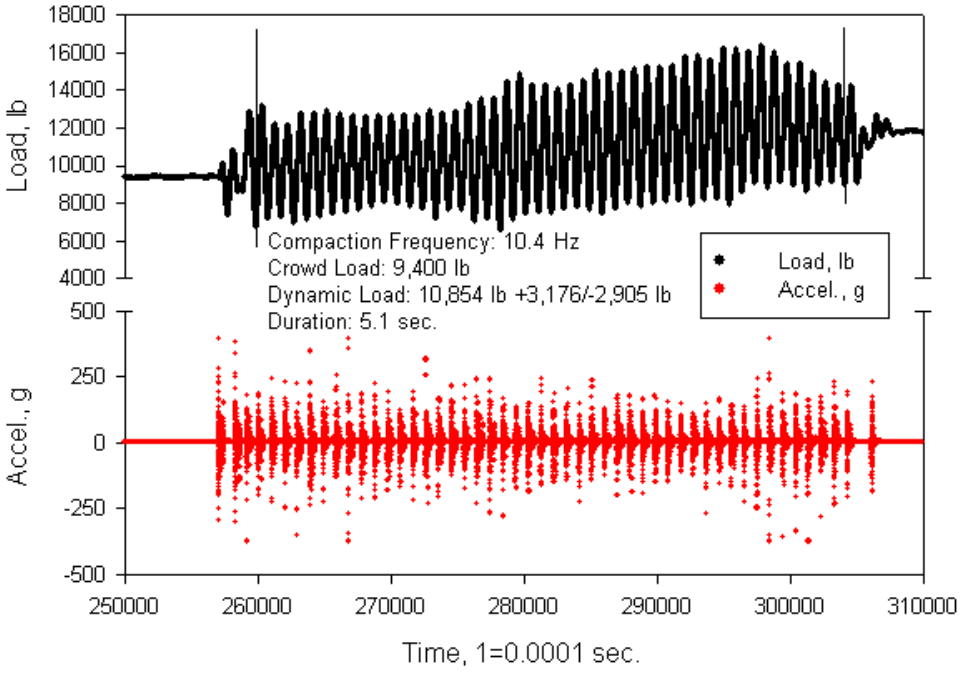


**Figure 276. Council Bluffs test 8**

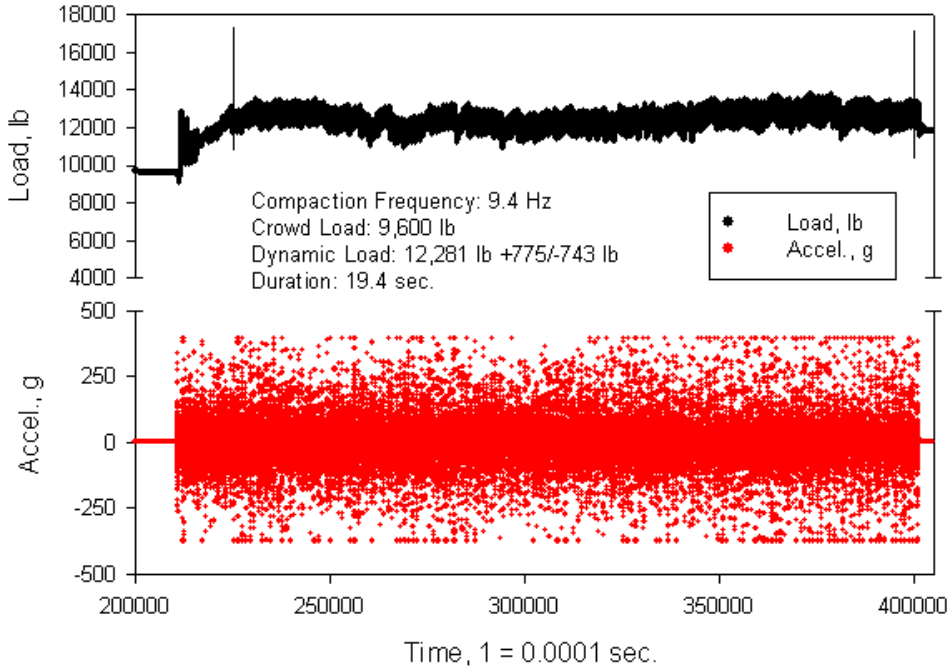


**Figure 277. Council Bluffs test 9**

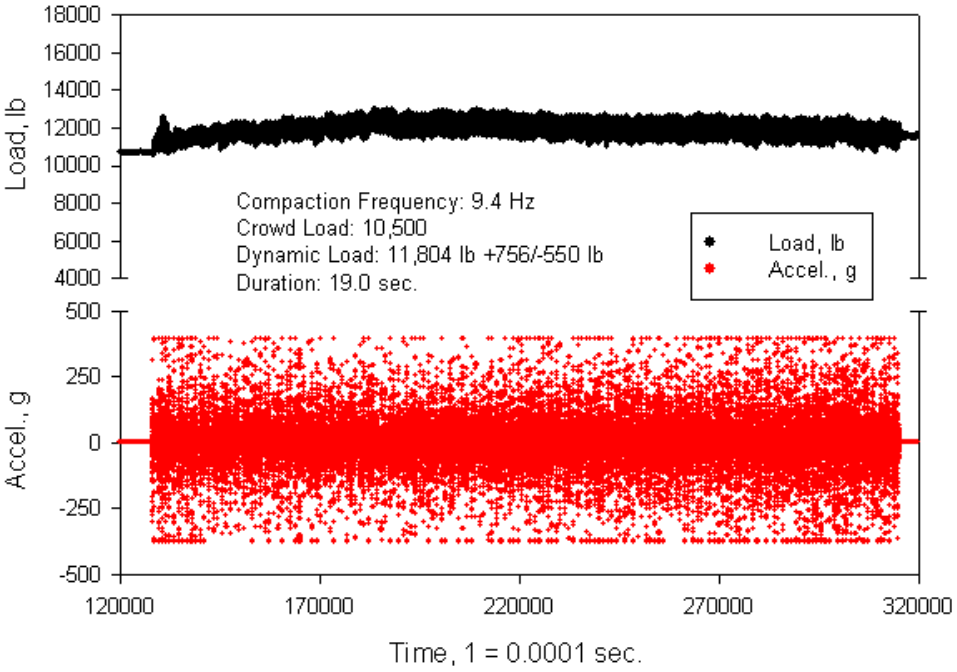


**Figure 278. Council Bluffs test 10**

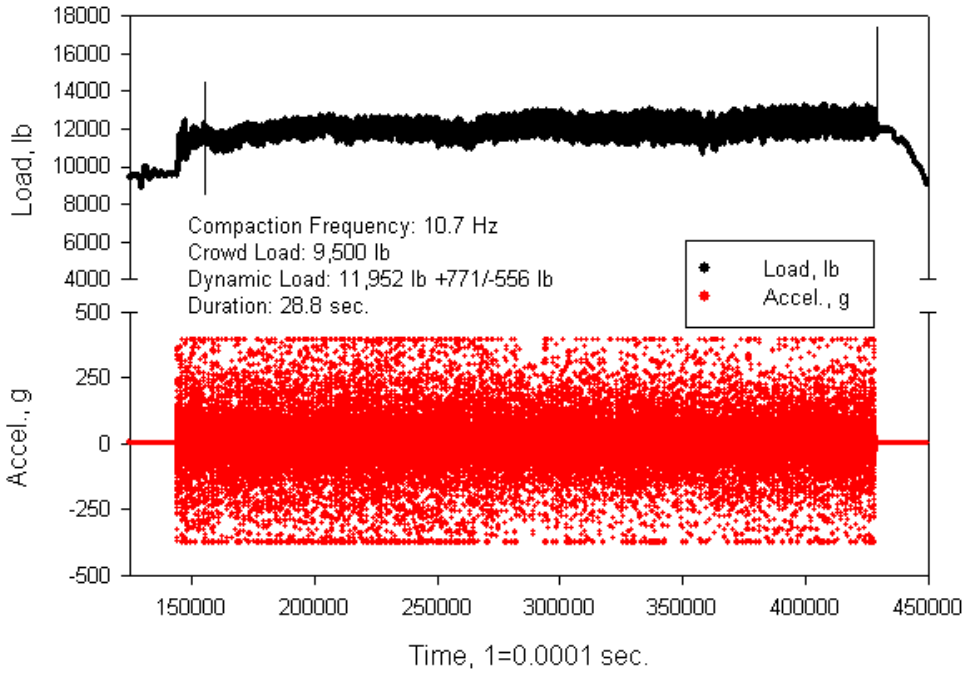


**Figure 279. Council Bluffs test 11**

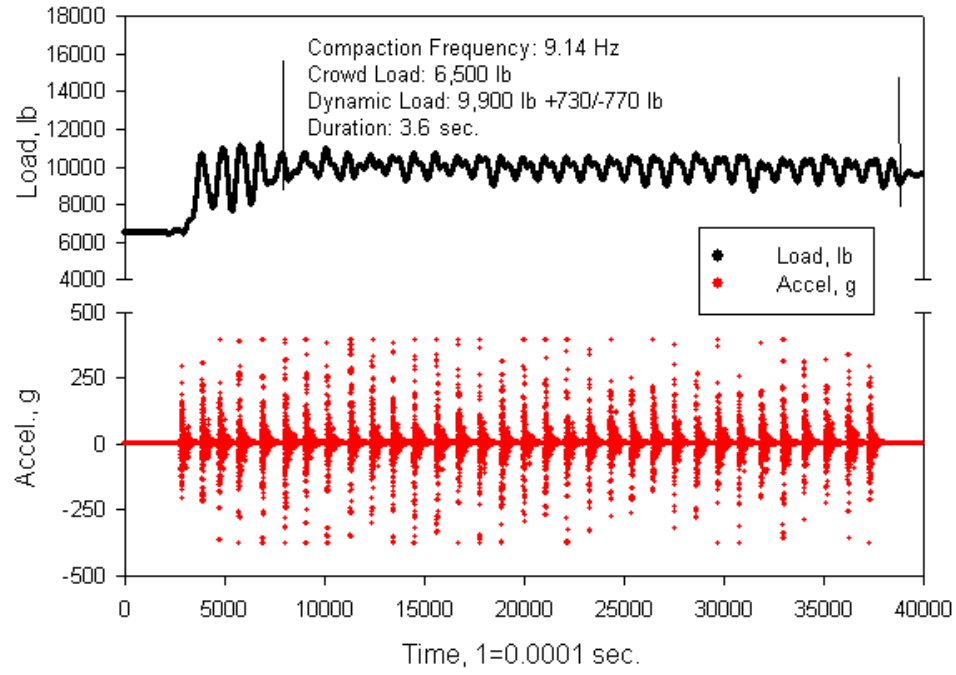


**Figure 280. Council Bluffs test 12 segment 1**

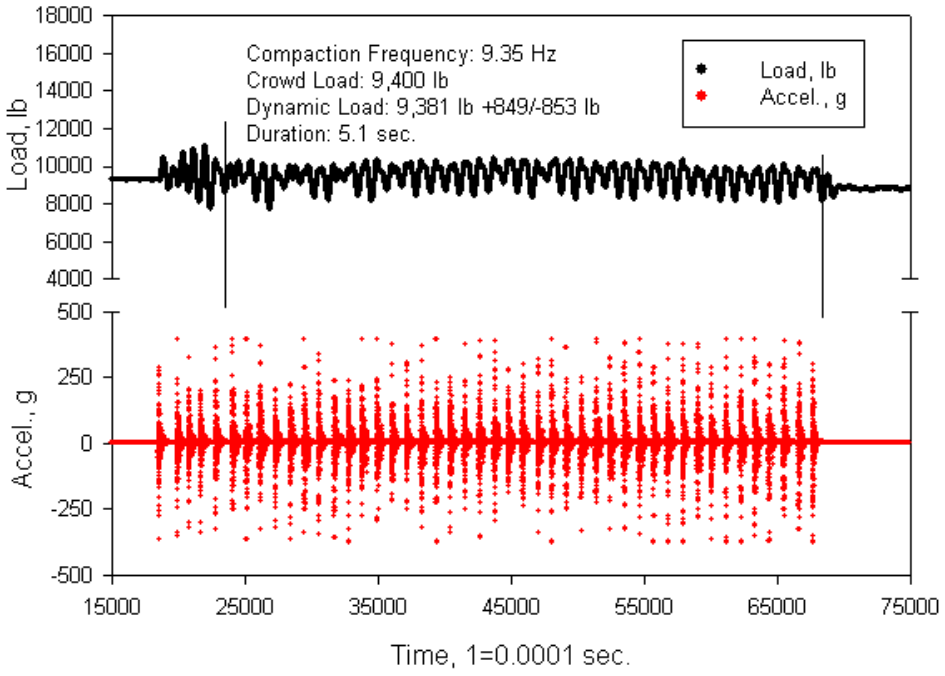


**Figure 281. Council Bluffs test 12 segment 2**

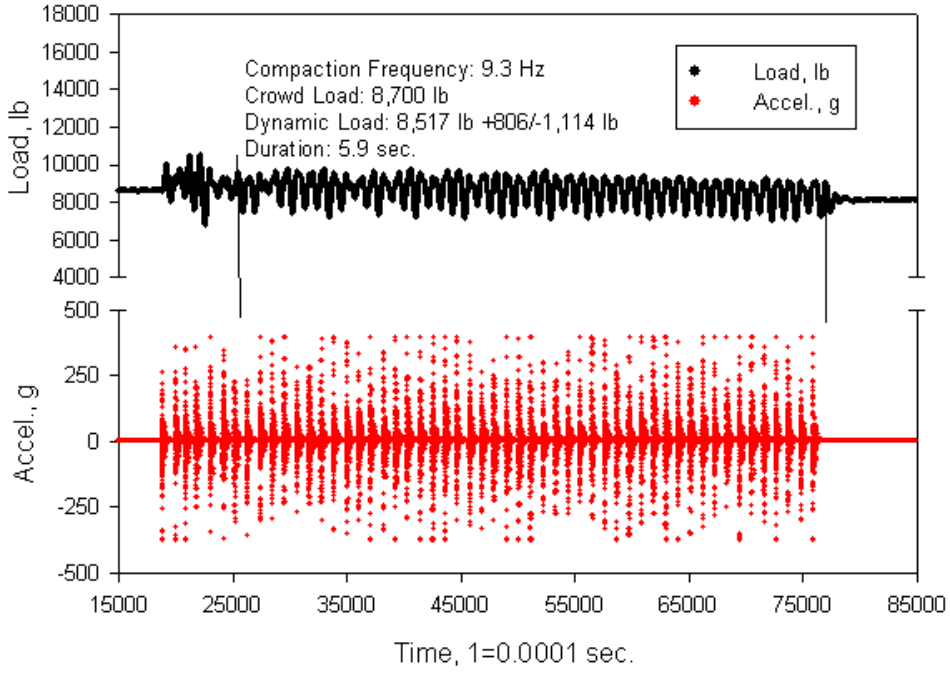


**Figure 282. Council Bluffs test 12 segment 3**

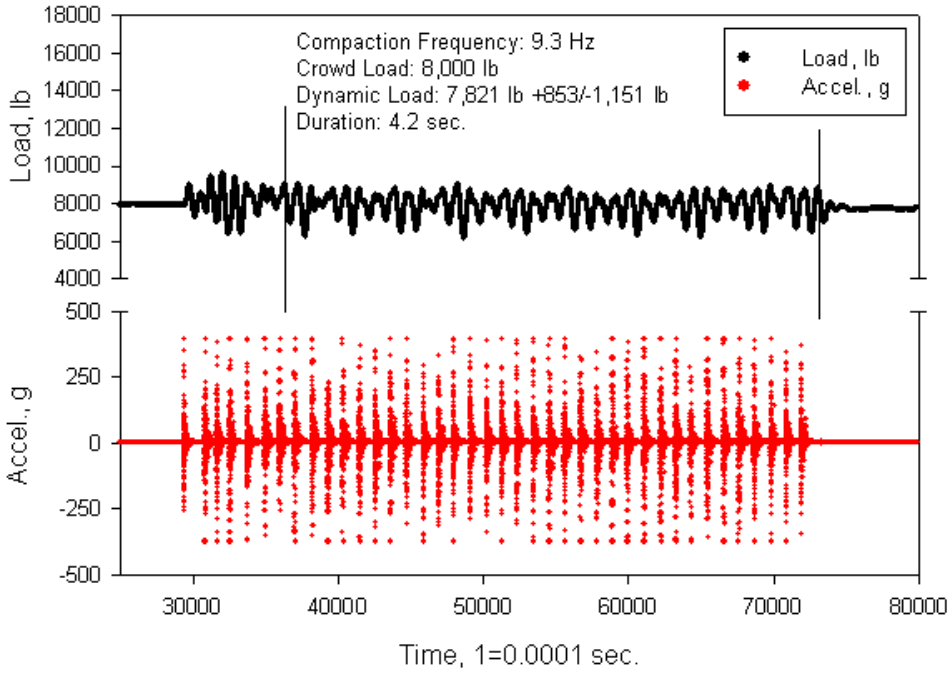


**Figure 283. Council Bluffs test 12 segment 4**

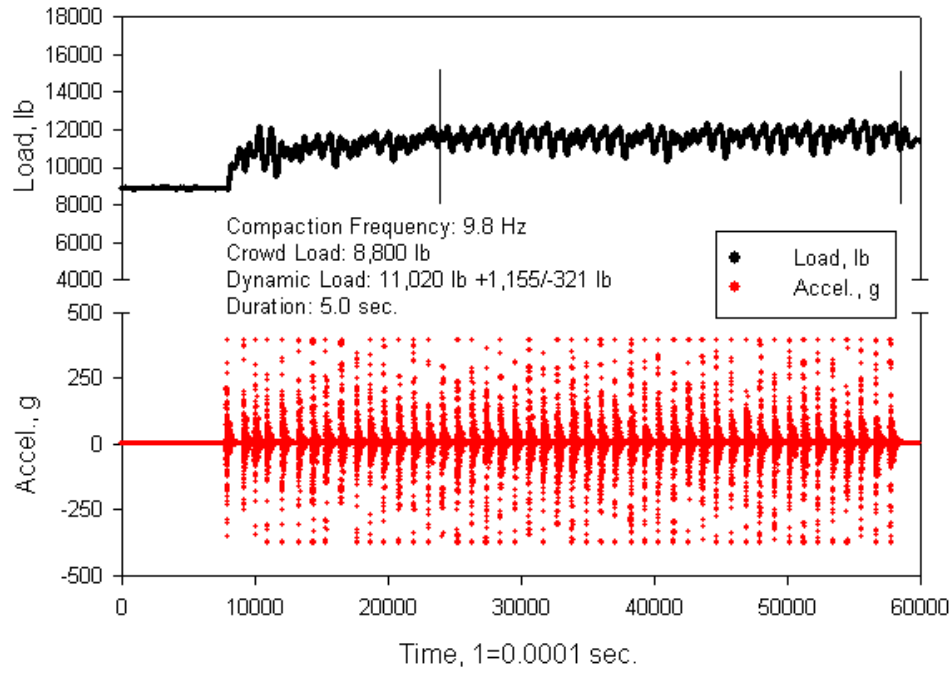


**Figure 284. Council Bluffs test 16 segment 1**

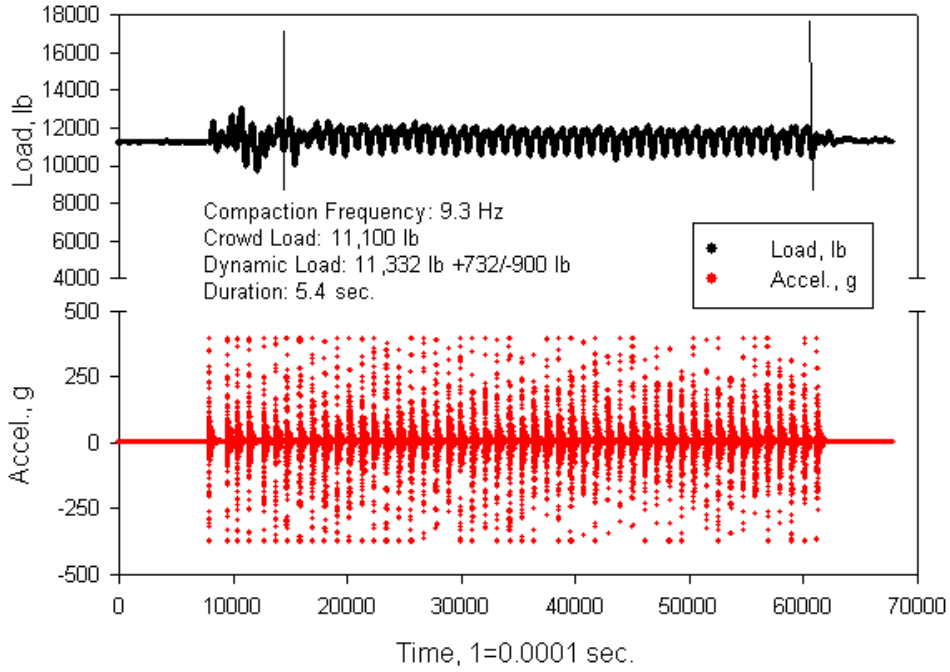


**Figure 285. Council Bluffs test 16 segment 2**

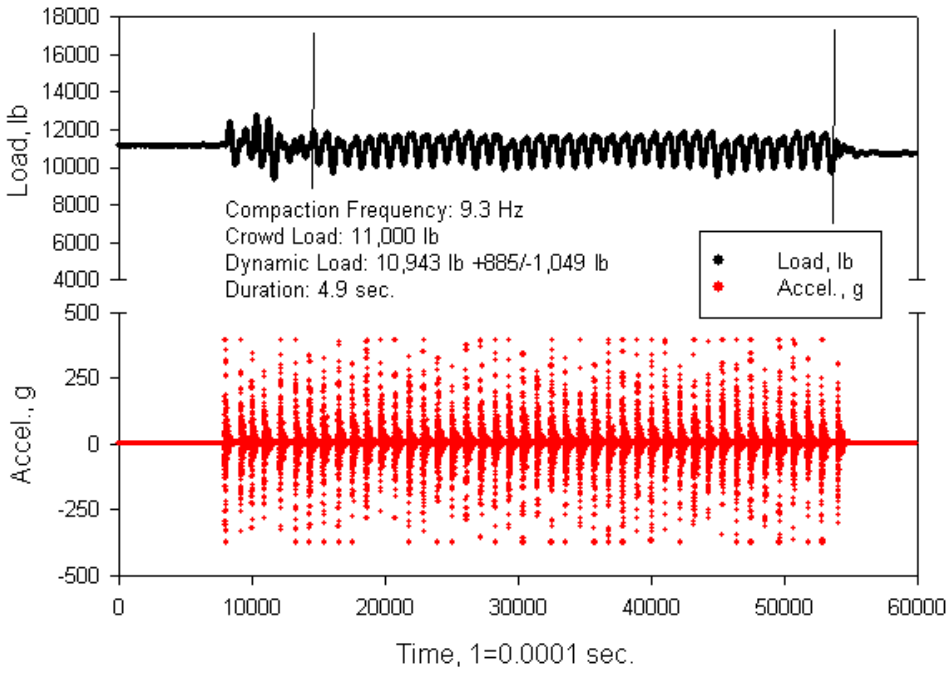


**Figure 286. Council Bluffs test 16 segment 3**

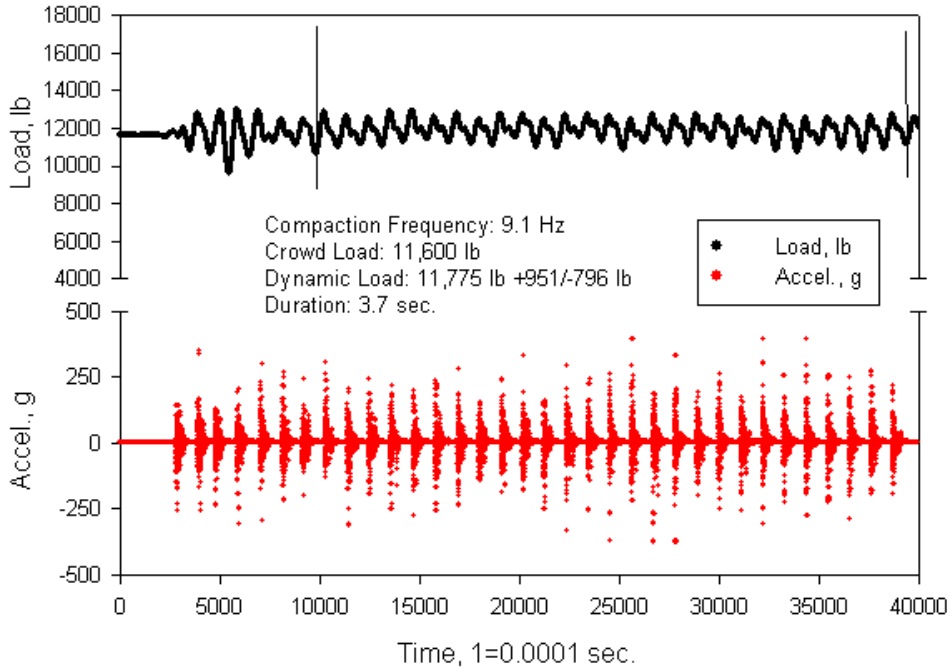


**Figure 287. Council Bluffs test 17 segment 1**

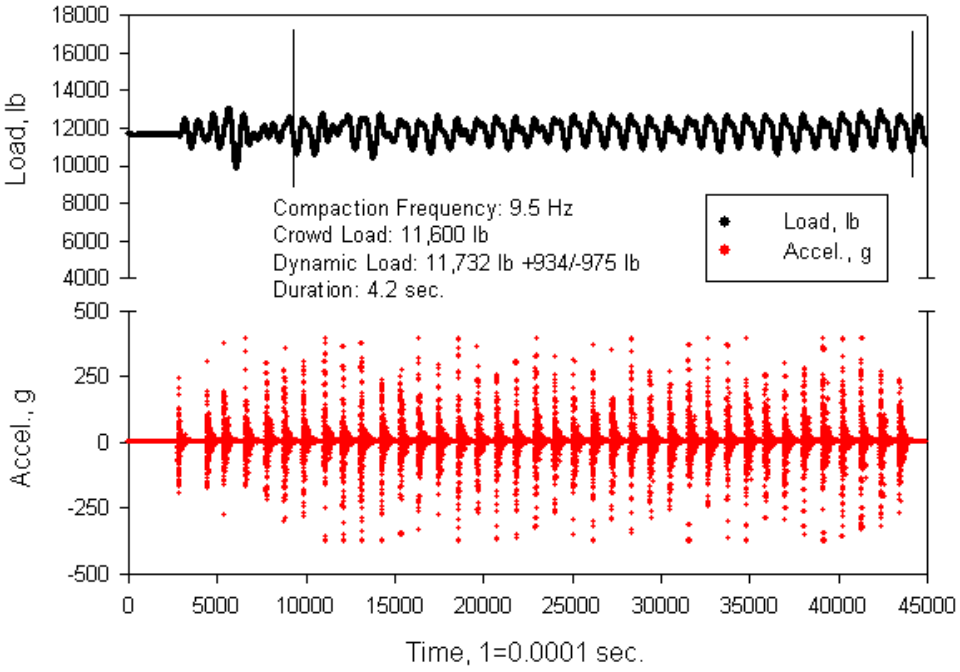


**Figure 288. Council Bluffs test 17 segment 2**

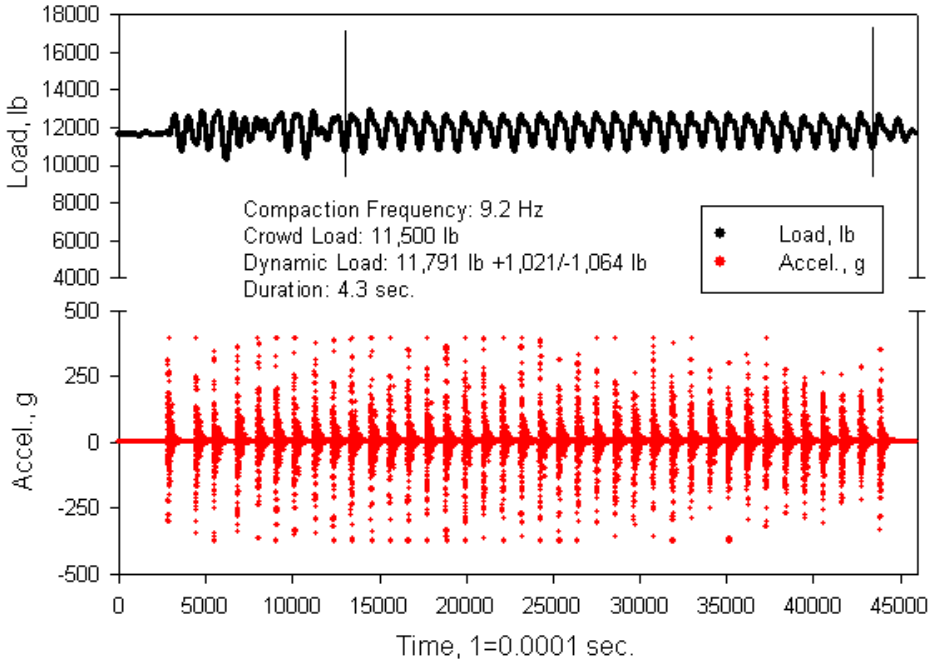


**Figure 289. Council Bluffs test 17 segment 3**

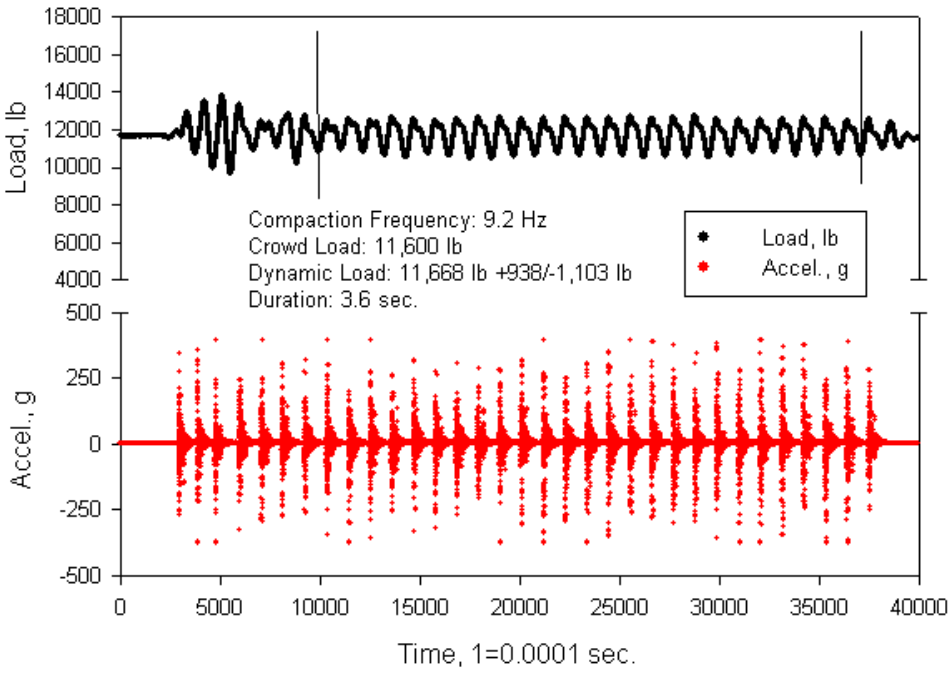


**Figure 290. Council Bluffs test 17 segment 4**

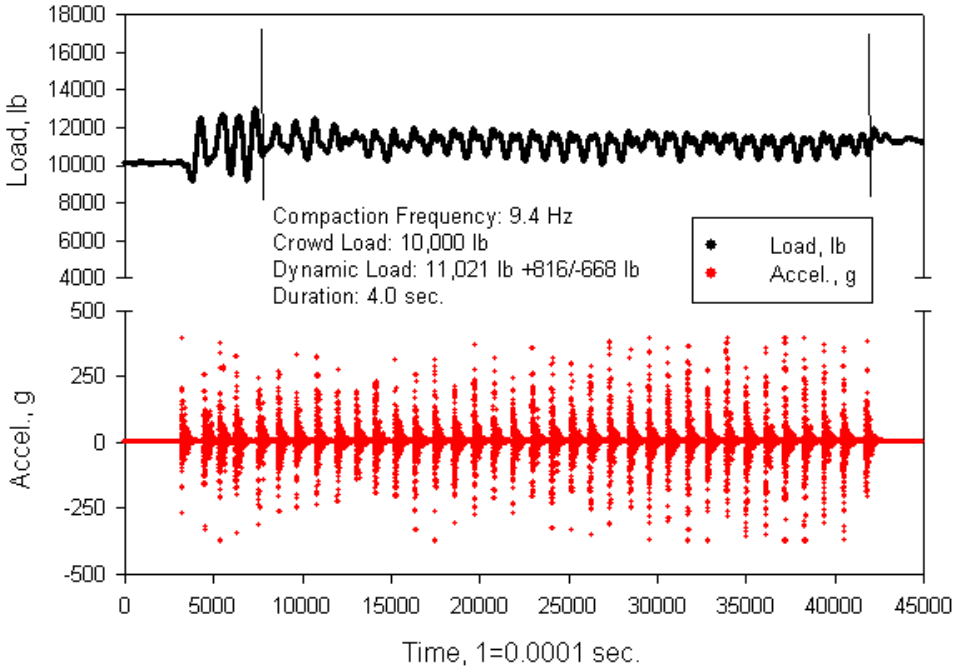


**Figure 291. Council Bluffs test 18 segment 1**

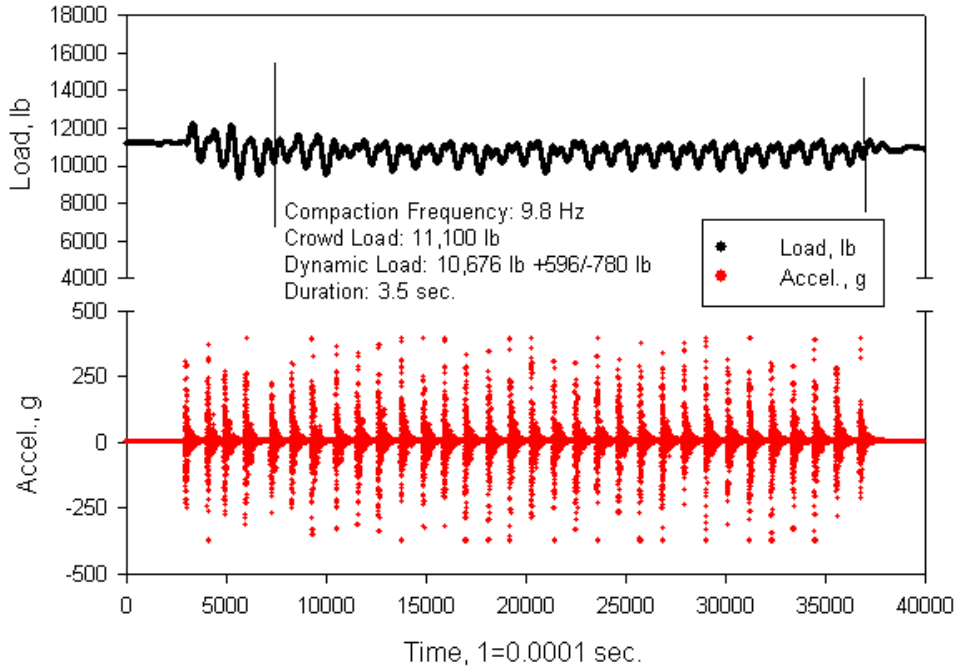


**Figure 292. Council Bluffs test 18 segment 2**

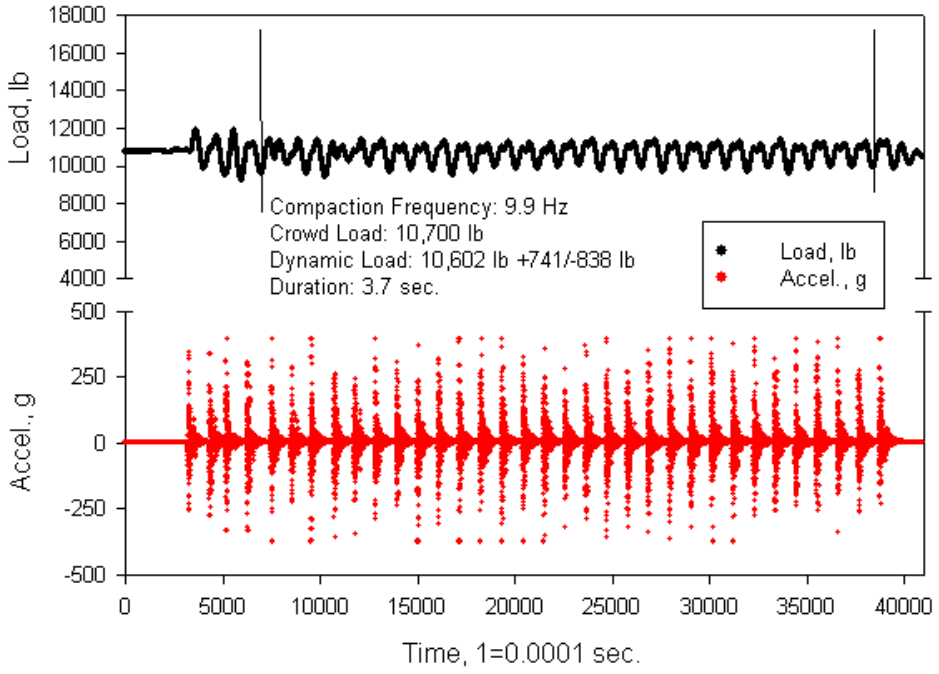


**Figure 293. Council Bluffs test 18 segment 3**

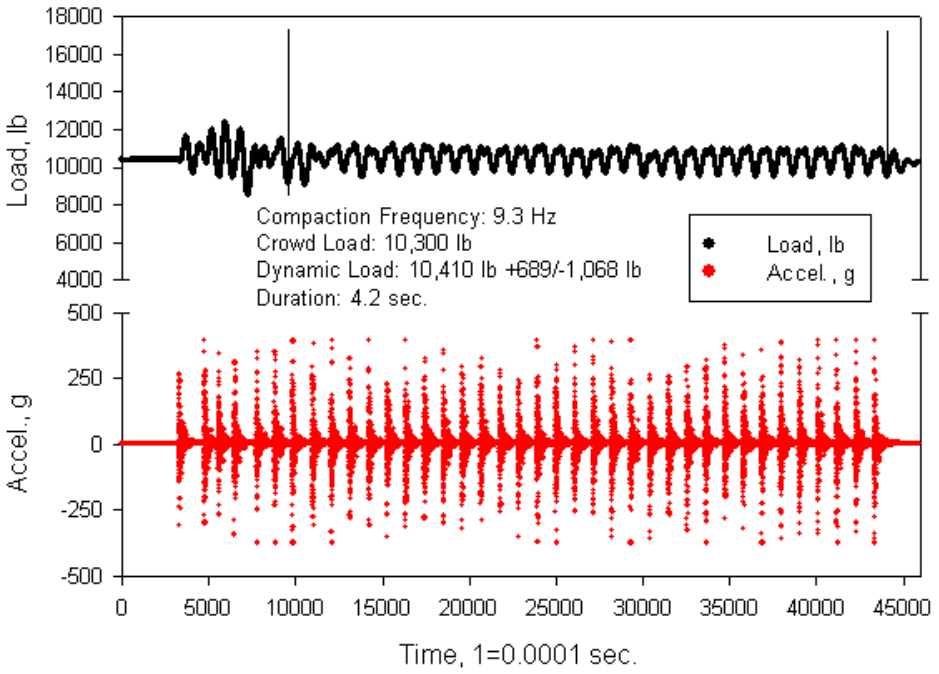


**Figure 294. Council Bluffs test 18 segment 4**

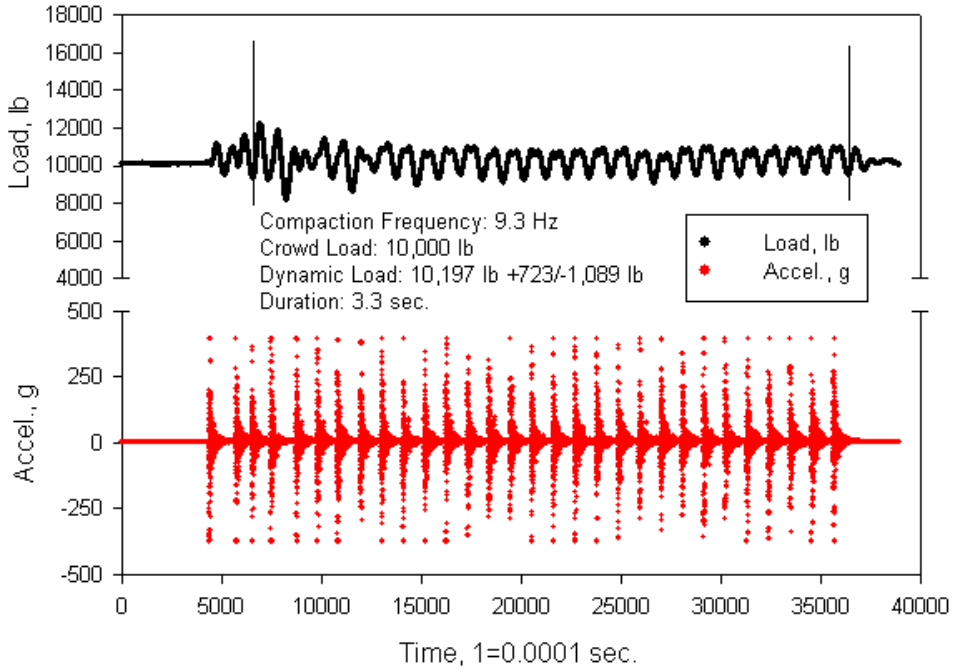


**Figure 295. Council Bluffs test 18 segment 5**

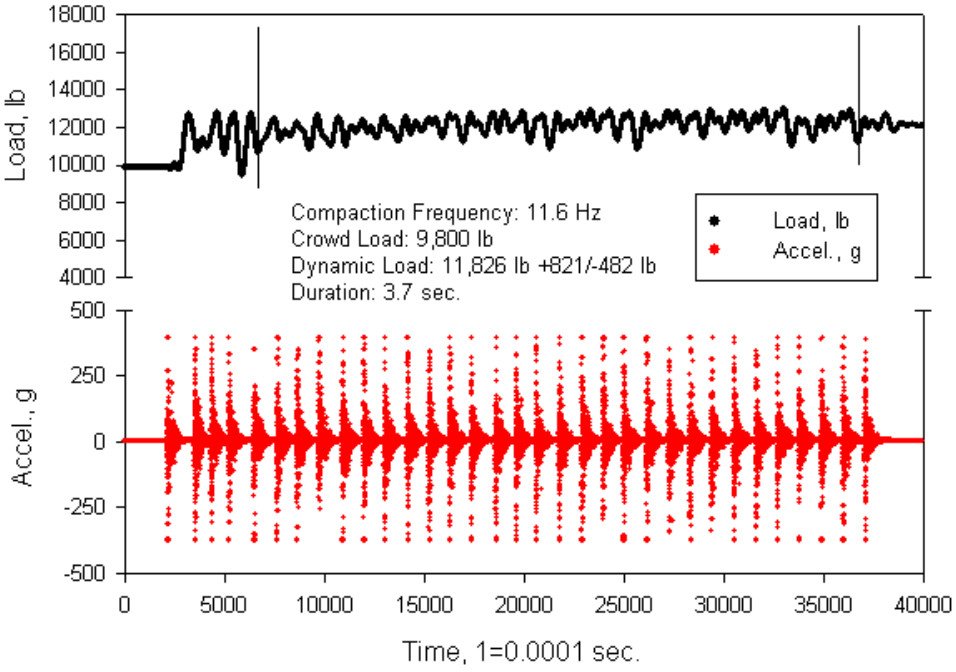


**Figure 296. Council Bluffs test 19 segment 1**

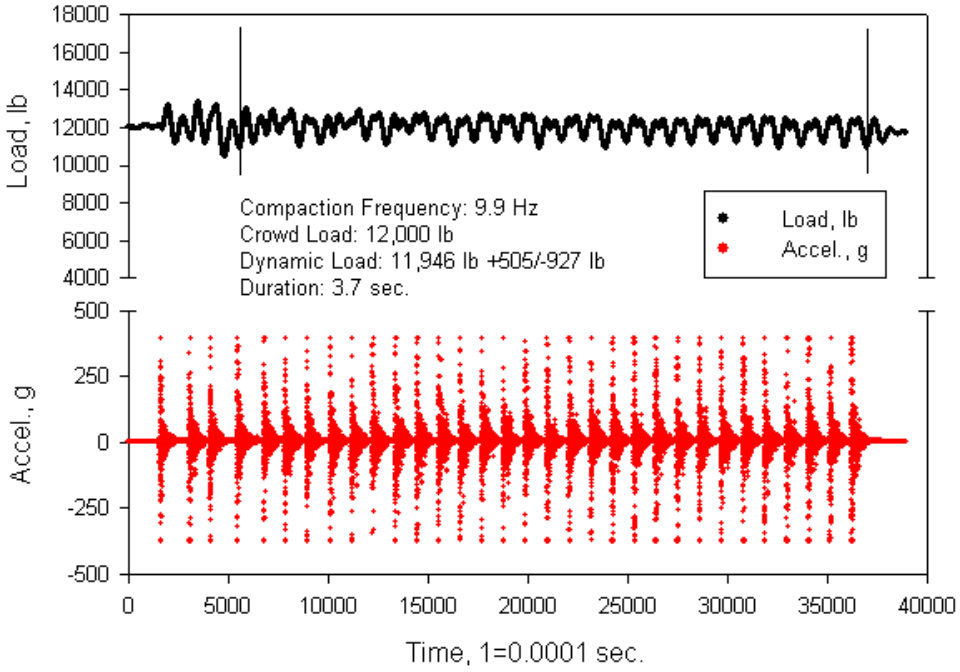


**Figure 297. Council Bluffs test 19 segment 2**

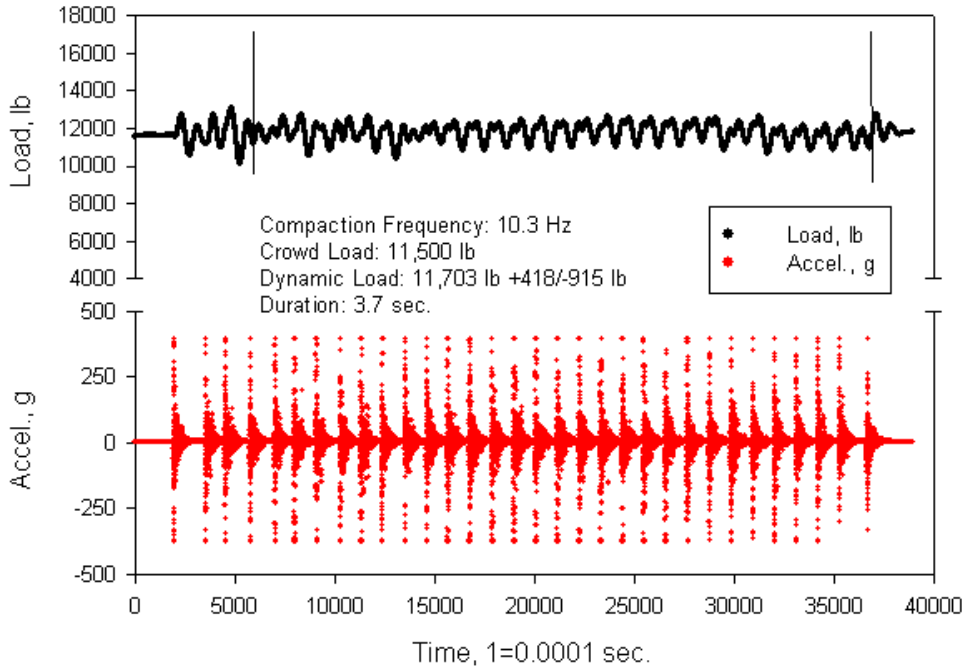


**Figure 298. Council Bluffs test 19 segment 3**

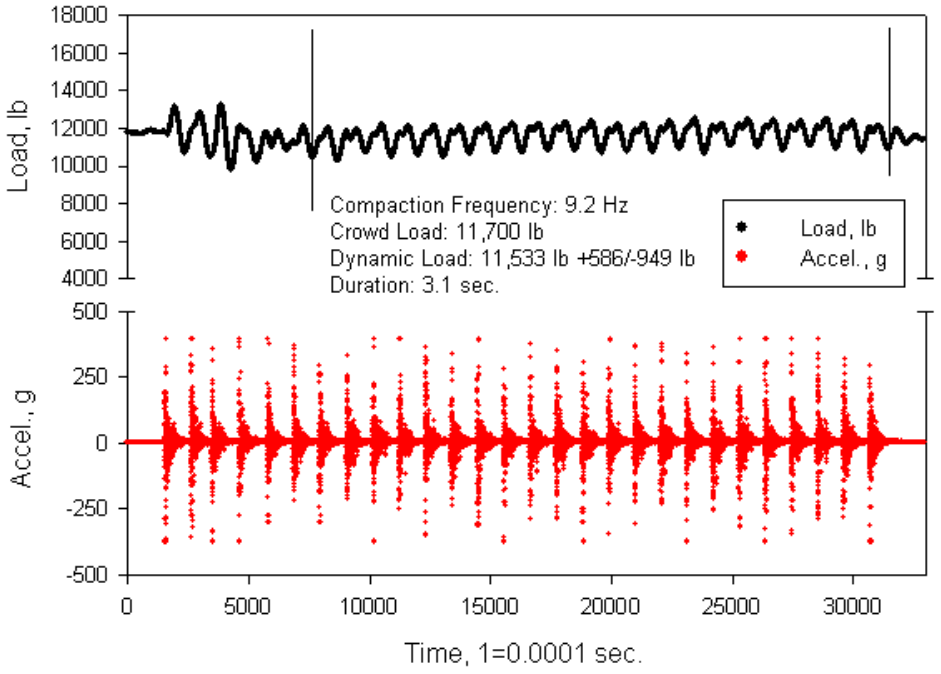


**Figure 299. Council Bluffs test 19 segment 4**

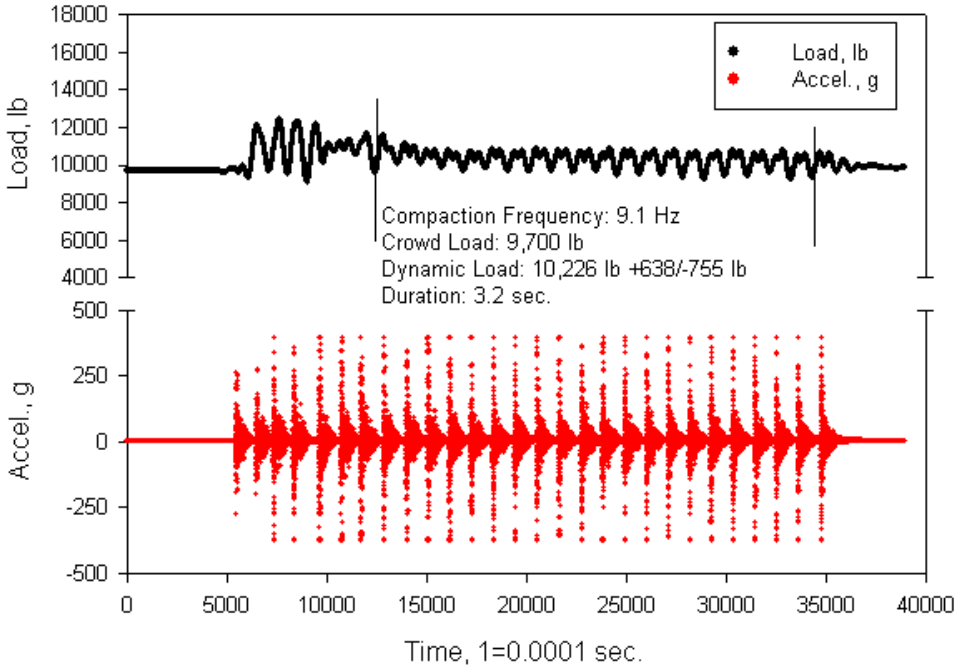


**Figure 300. Council Bluffs test 21 segment 1**

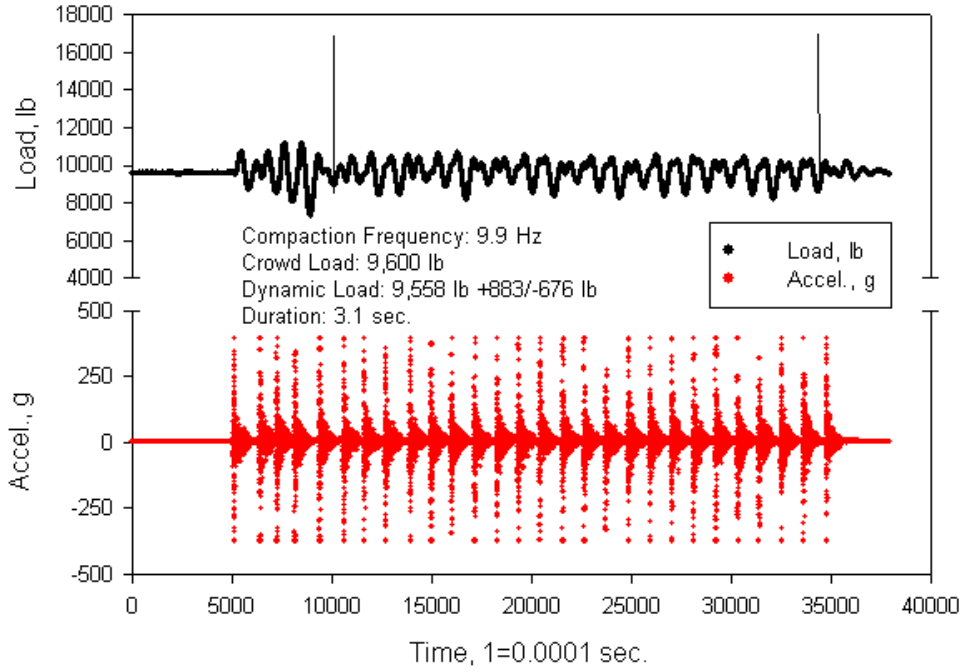


**Figure 301. Council Bluffs test 21 segment 2**

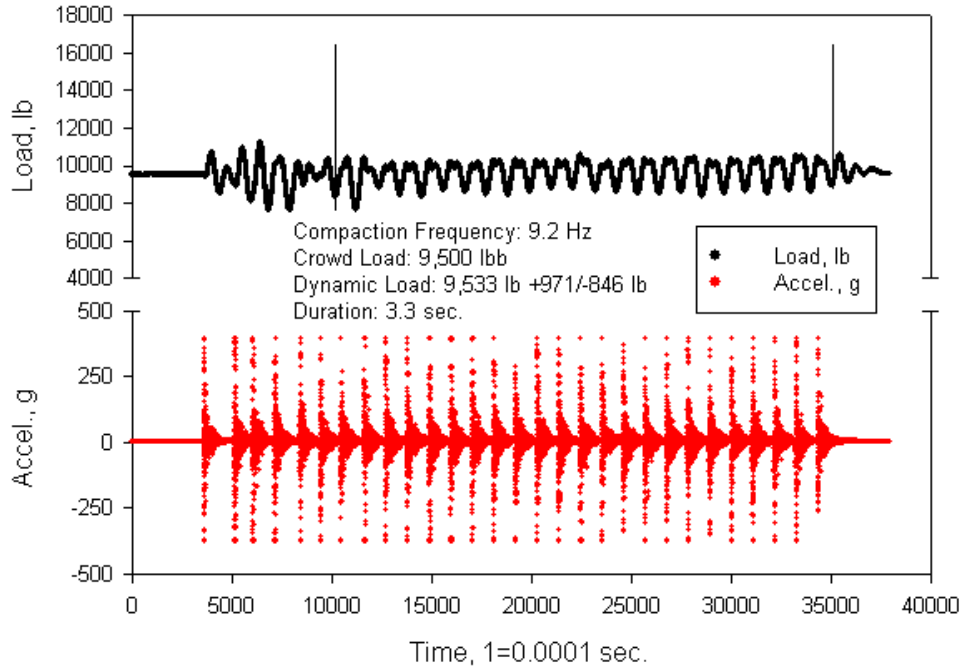


**Figure 302. Council Bluffs test 21 segment 3**

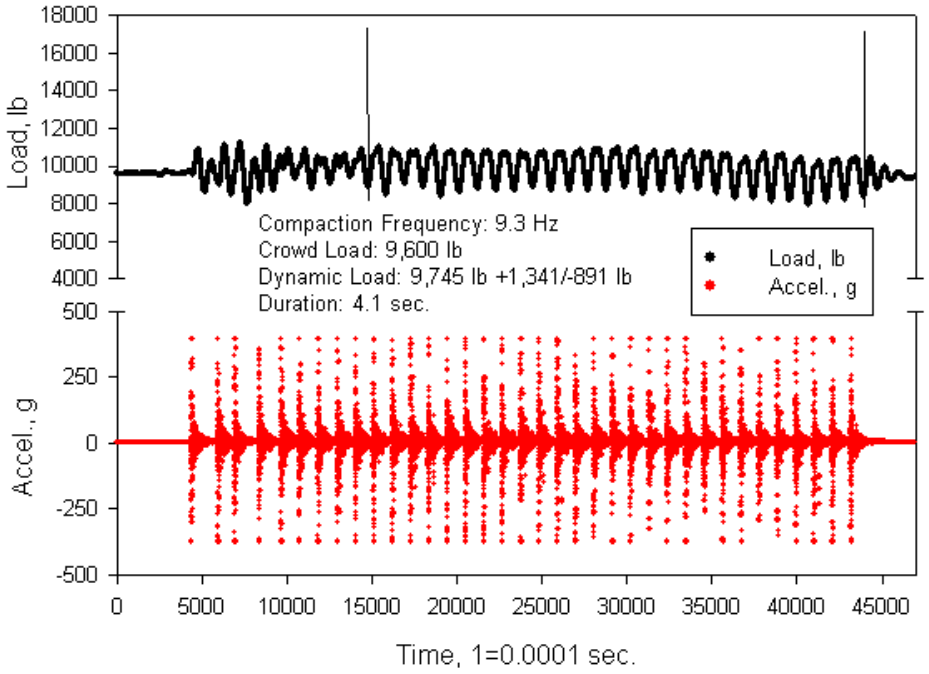


**Figure 303. Council Bluffs test 21 segment 4**

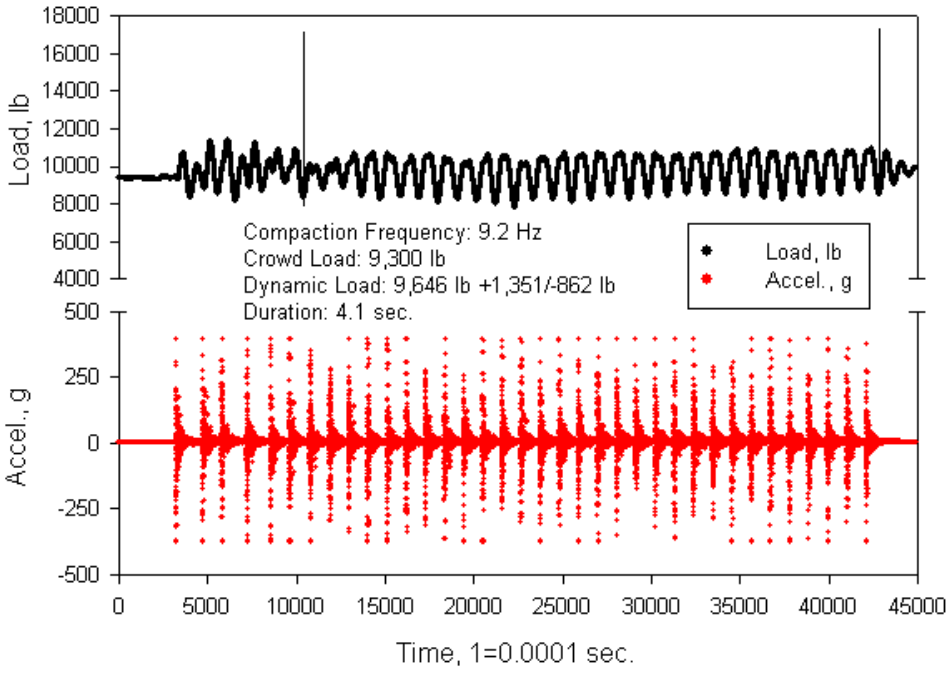


**Figure 304. Council Bluffs test 21 segment 5**

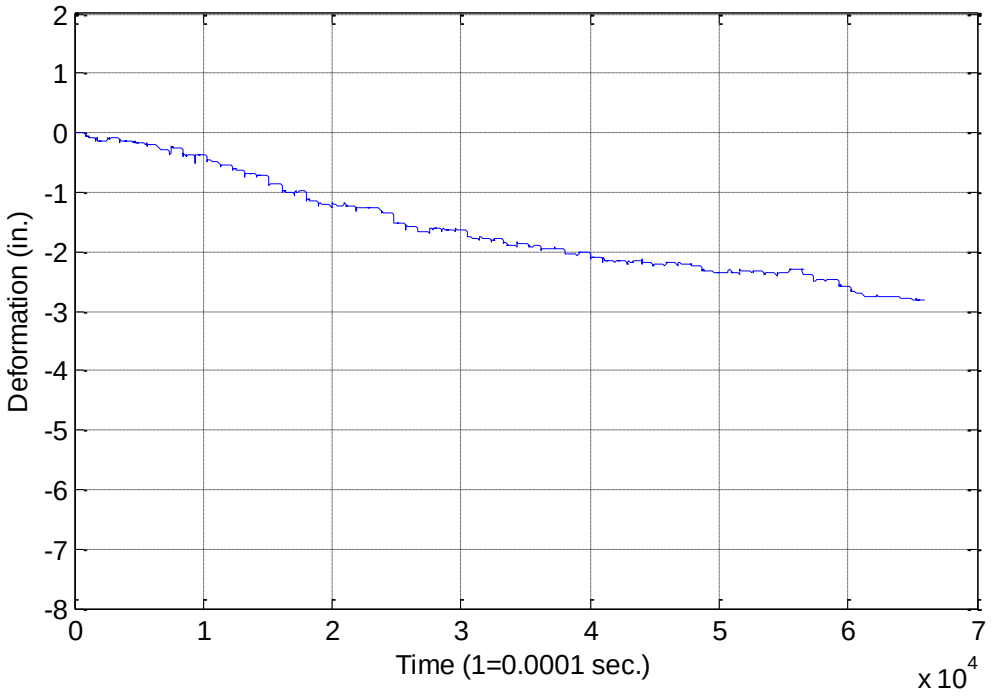


**Figure 305. Council Bluffs test 6 acceleration analysis A**

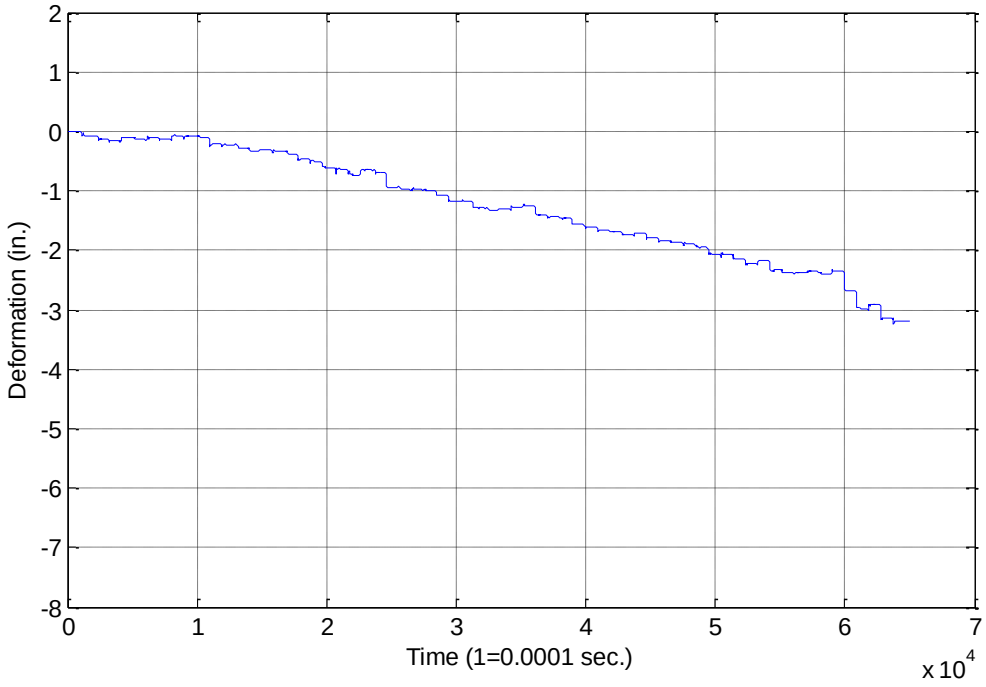


**Figure 306. Council Bluffs test 7 acceleration analysis A**

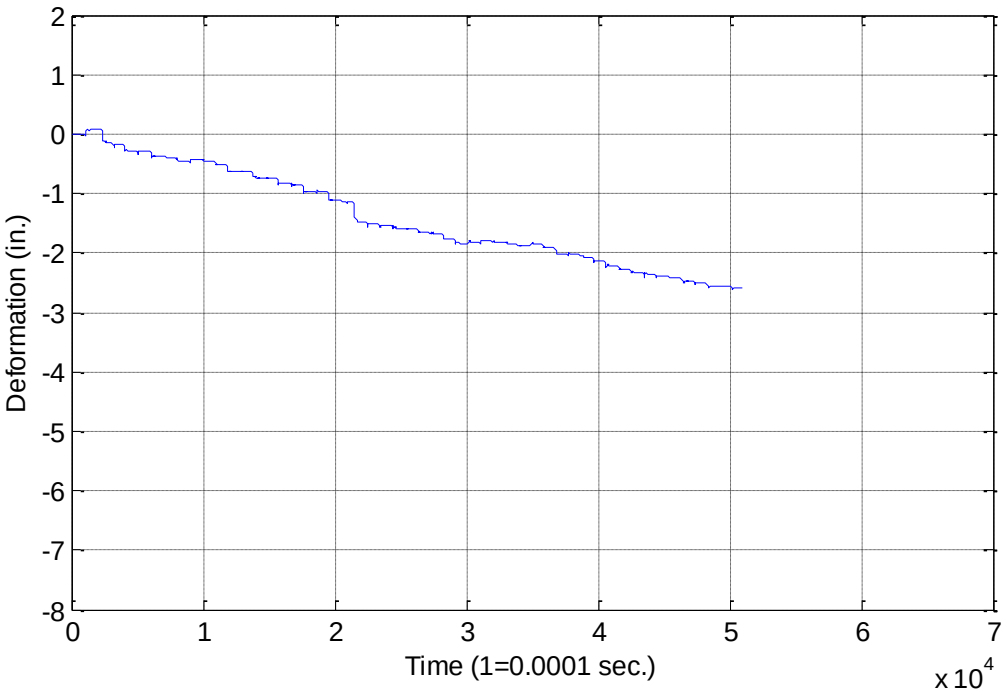


**Figure 307. Council Bluffs test 8 acceleration analysis A**

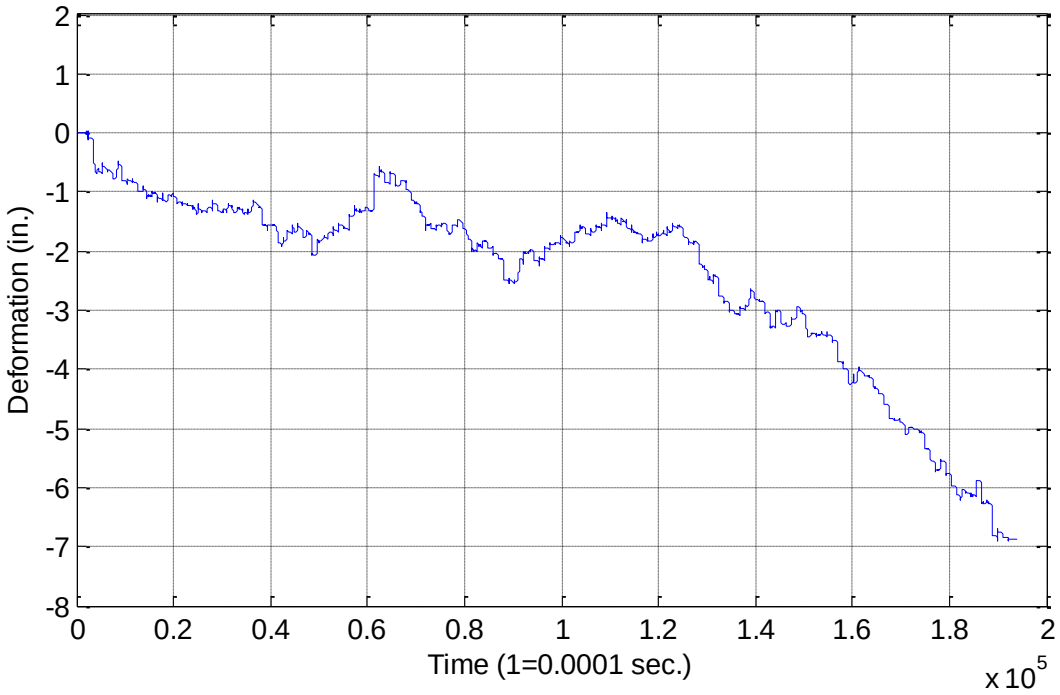


**Figure 308. Council Bluffs test 9 acceleration analysis A**

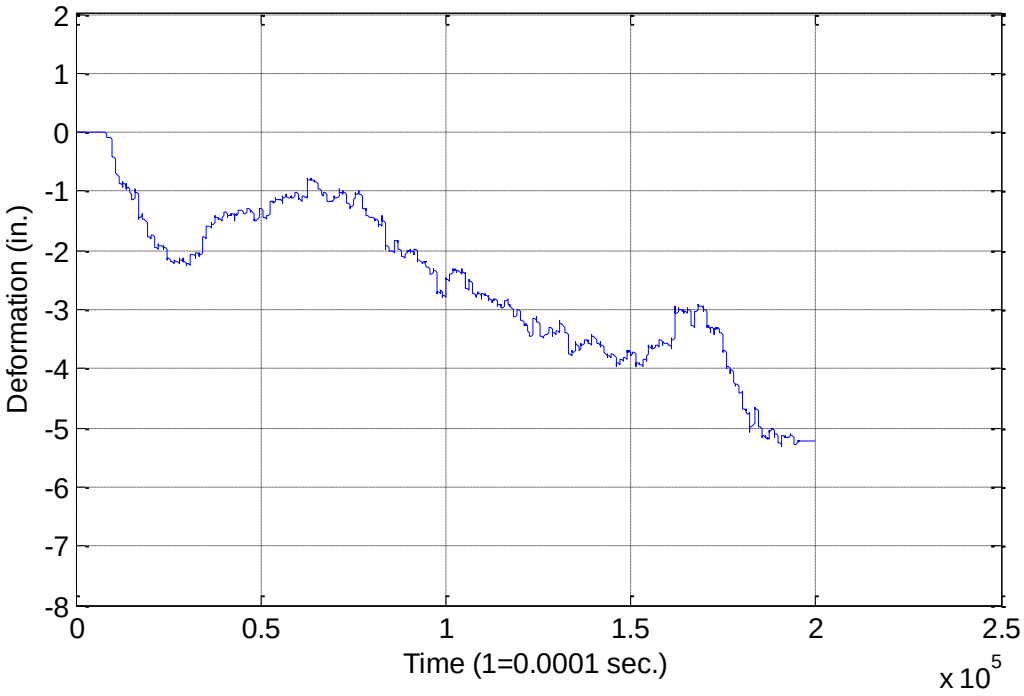


**Figure 309. Council Bluffs test 10 acceleration analysis A**

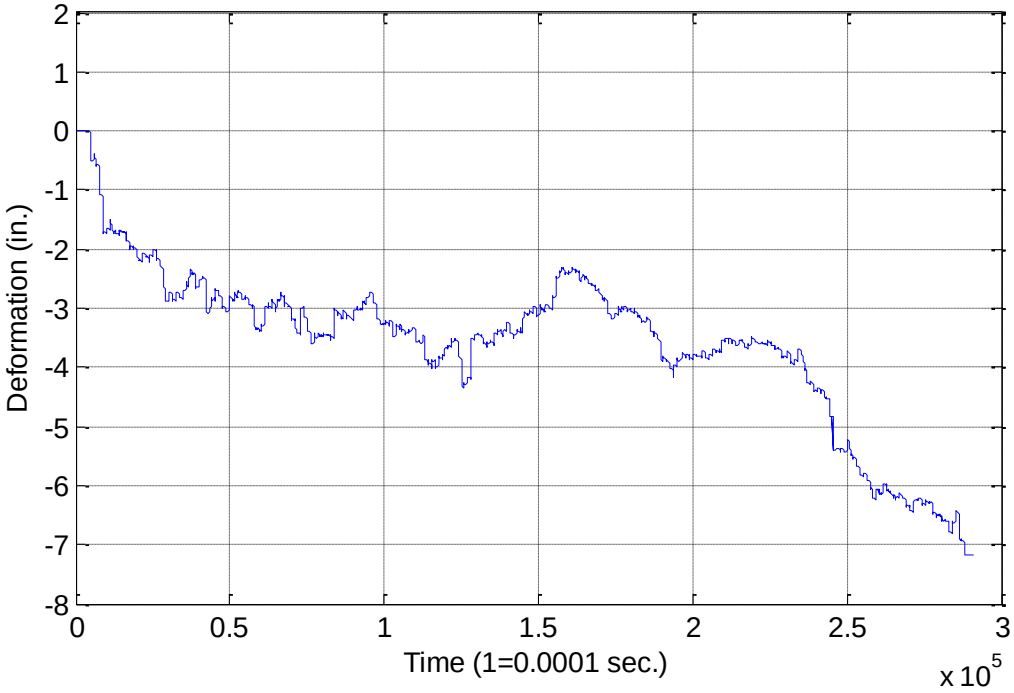


**Figure 310. Council Bluffs test 11 acceleration analysis A**

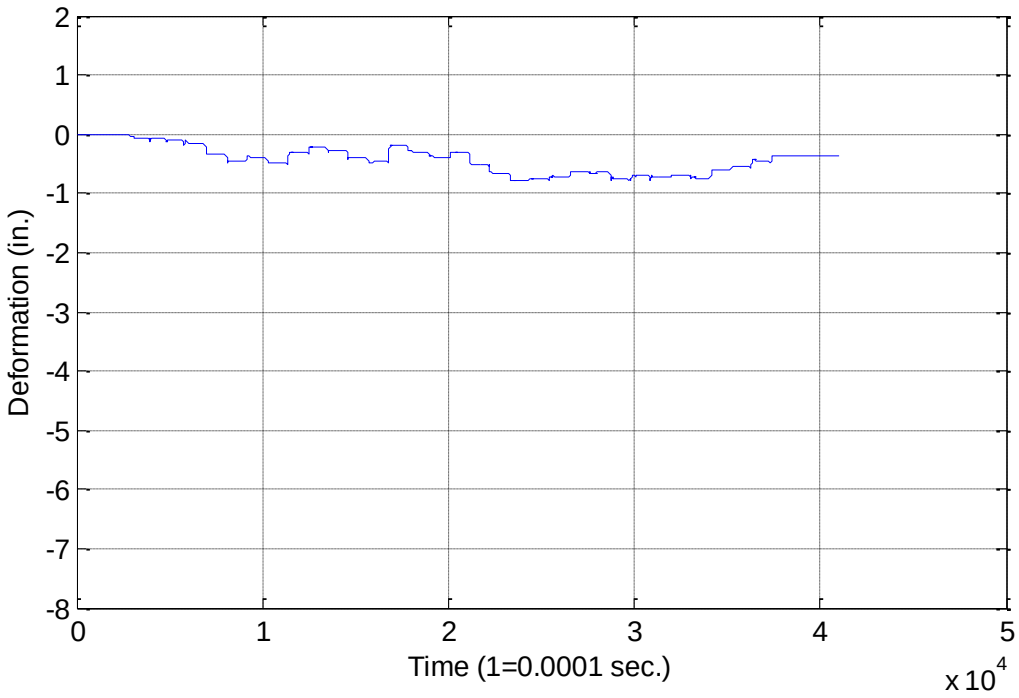


**Figure 311. Council Bluffs test 12 segment 1 acceleration analysis A**

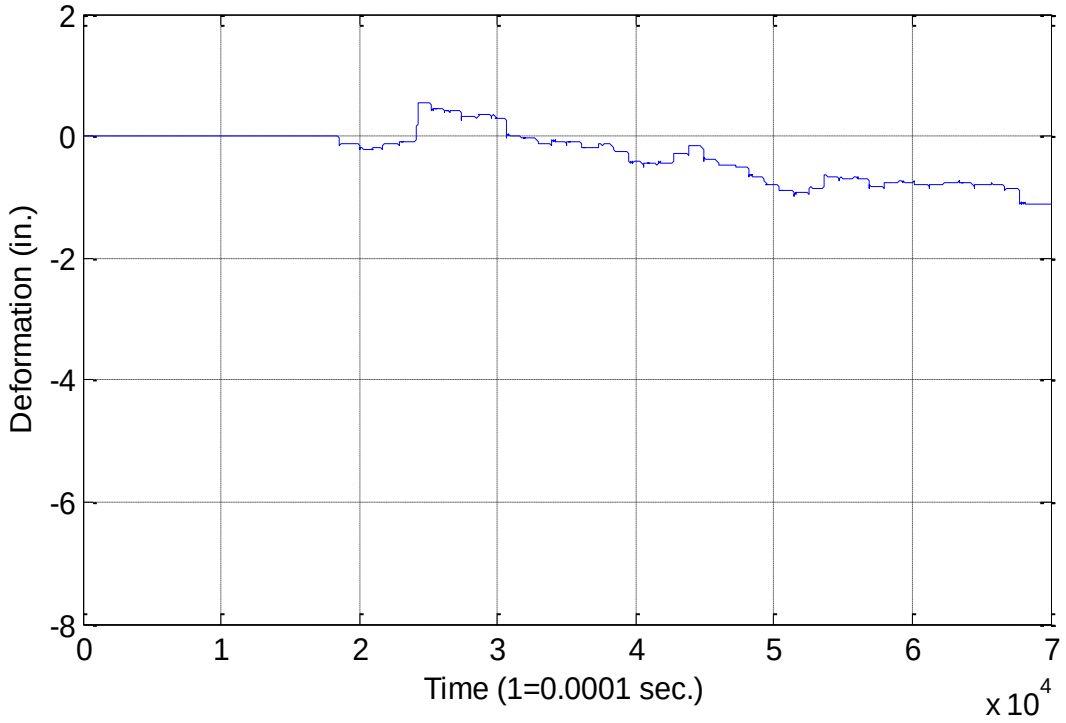


**Figure 312. Council Bluffs test 12 segment 2 acceleration analysis A**

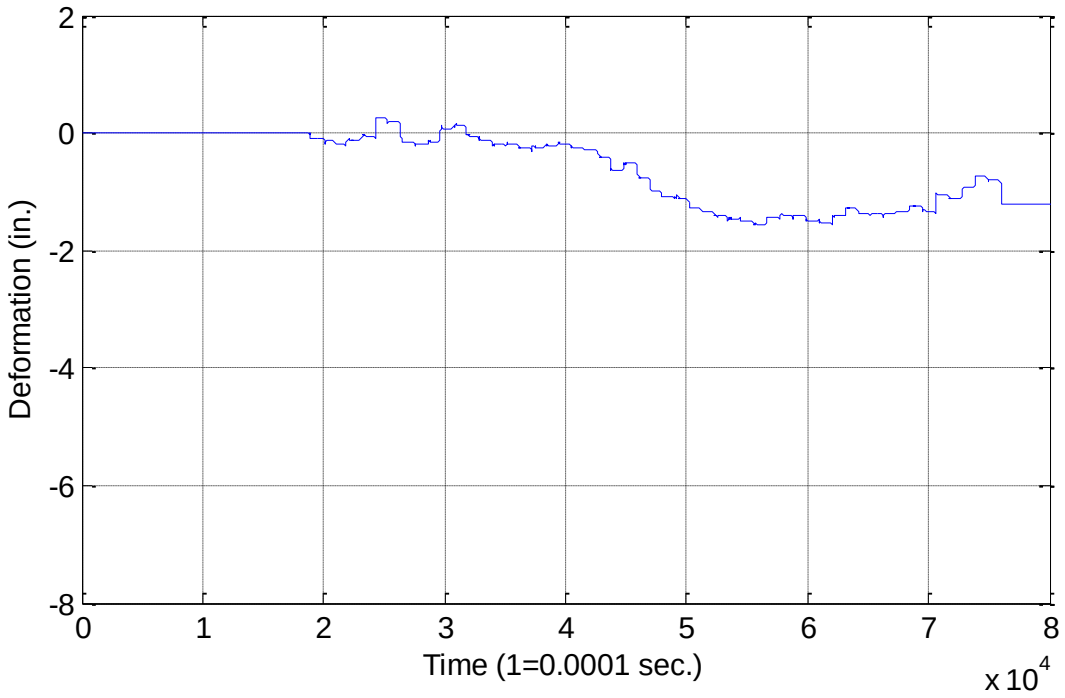


**Figure 313. Council Bluffs test 12 segment 3 acceleration analysis A**

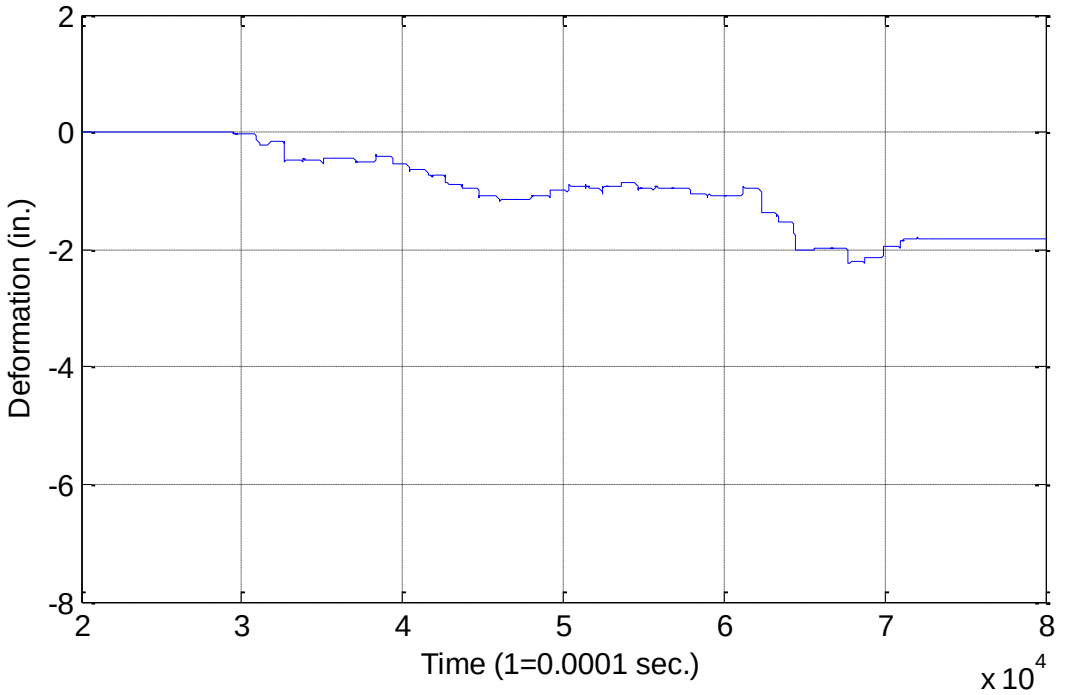


**Figure 314. Council Bluffs test 12 segment 4 acceleration analysis A**

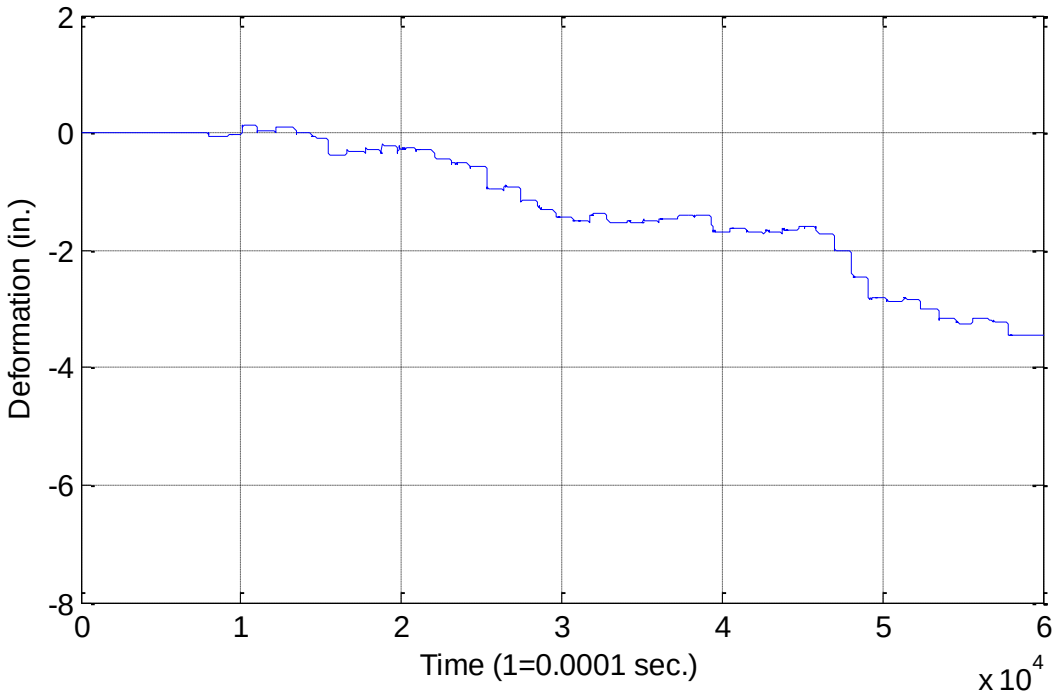


**Figure 315. Council Bluffs test 16 segment 1 acceleration analysis A**

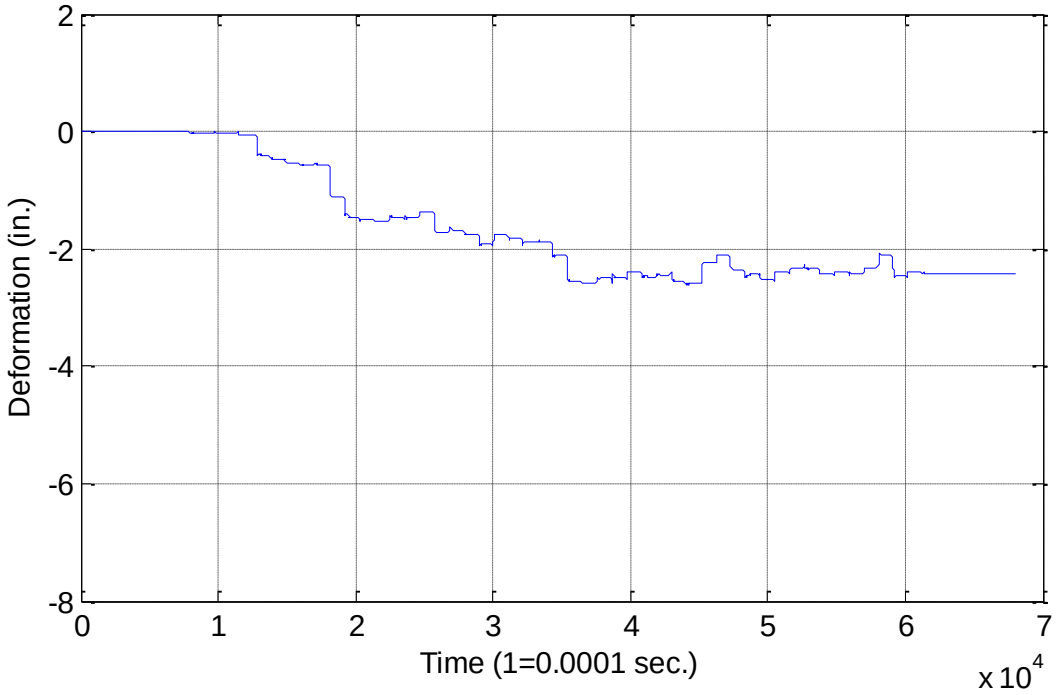


**Figure 316. Council Bluffs test 16 segment 2 acceleration analysis A**

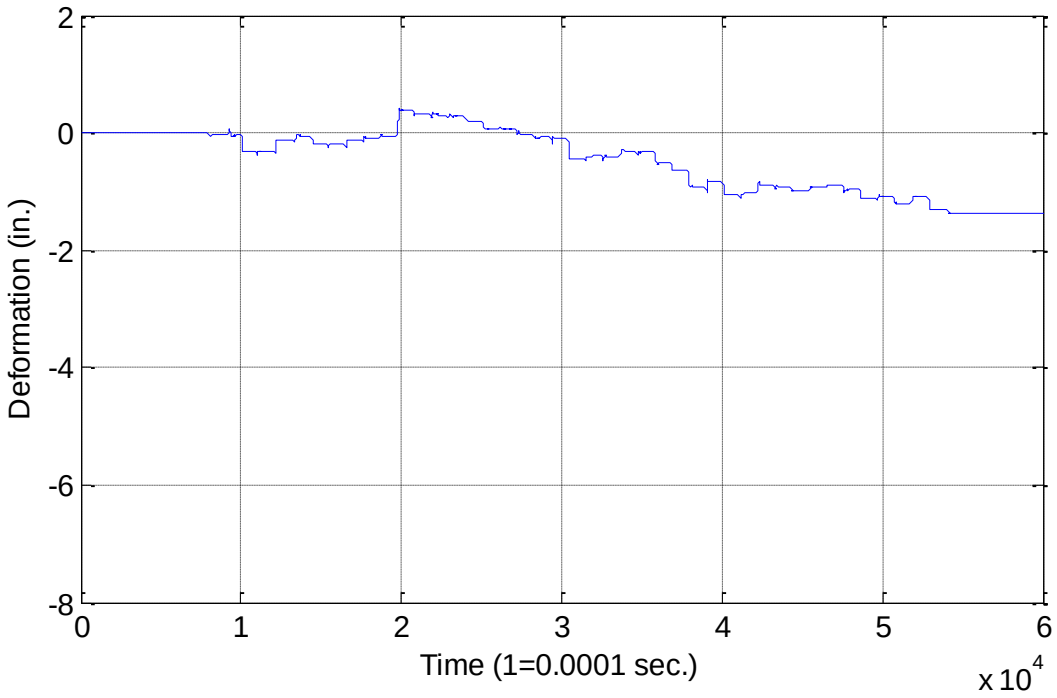


**Figure 317. Council Bluffs test 16 segment 3 acceleration analysis A**

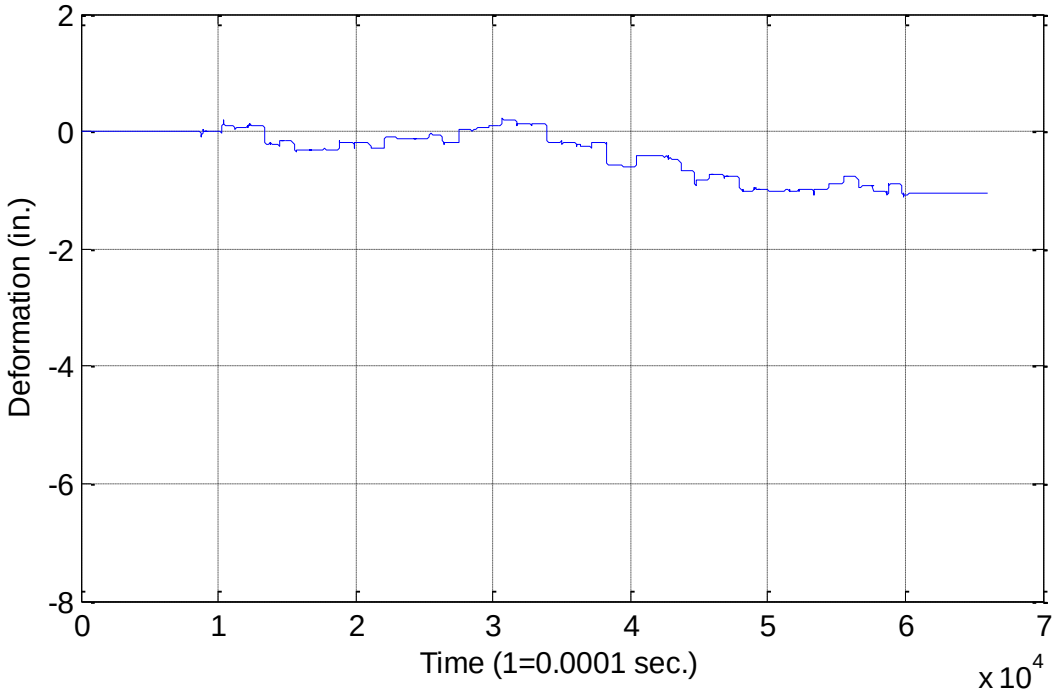


**Figure 318. Council Bluffs test 16 segment 4 acceleration analysis A**

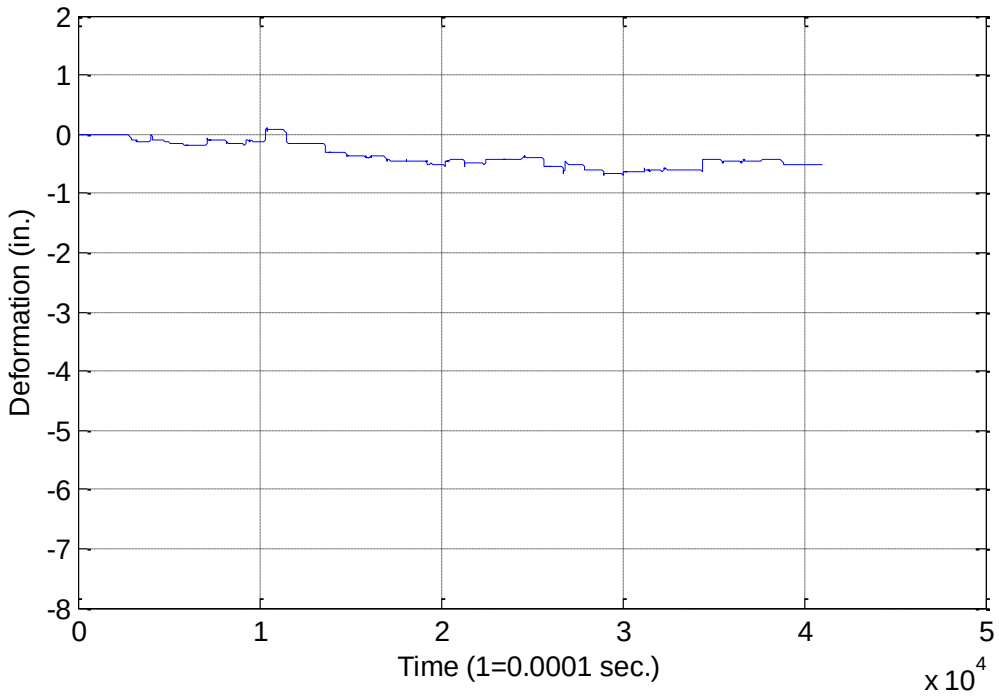


**Figure 319. Council Bluffs test 17 segment 1 acceleration analysis A**

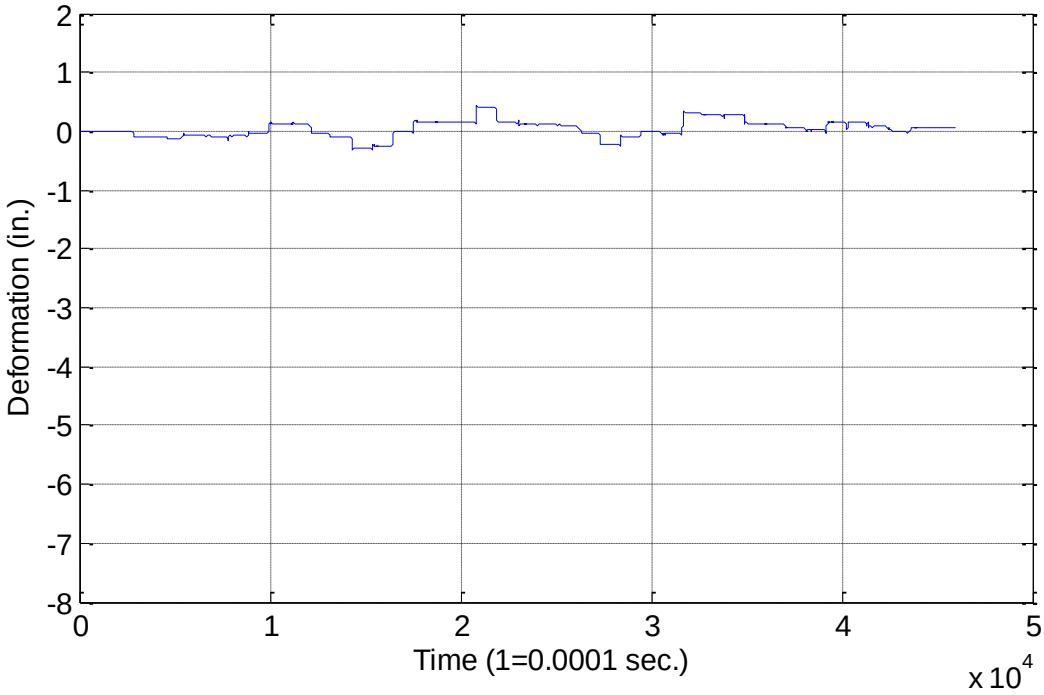


**Figure 320. Council Bluffs test 17 segment 2 acceleration analysis A**

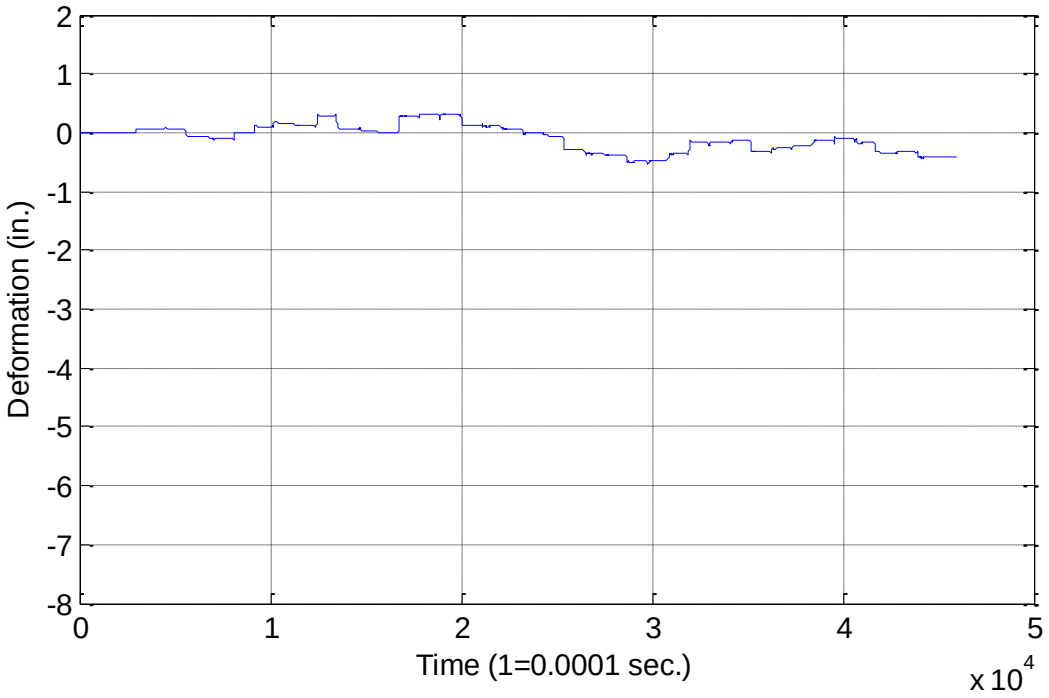


**Figure 321. Council Bluffs test 17 segment 3 acceleration analysis A**

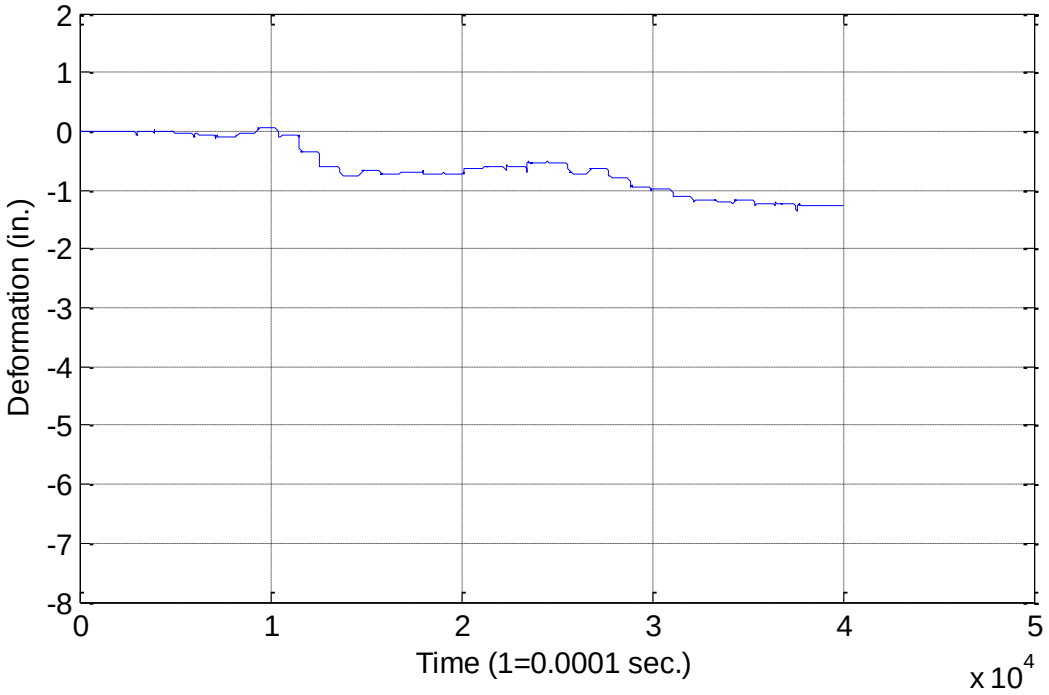


**Figure 322. Council Bluffs test 17 segment 4 acceleration analysis A**

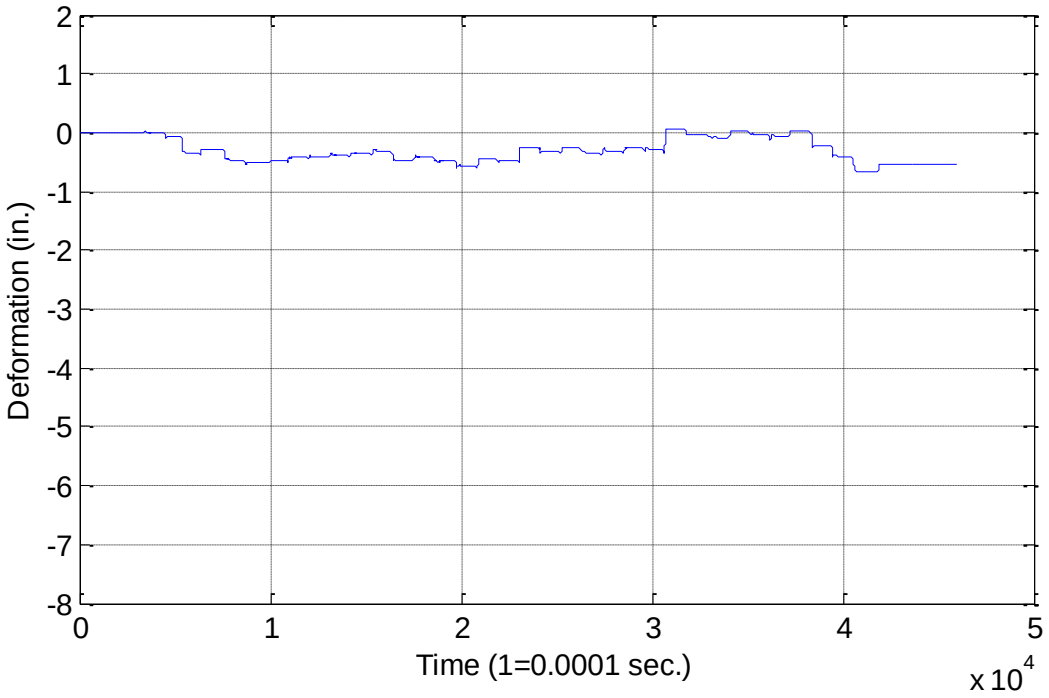


**Figure 323. Council Bluffs test 18 segment 1 acceleration analysis A**

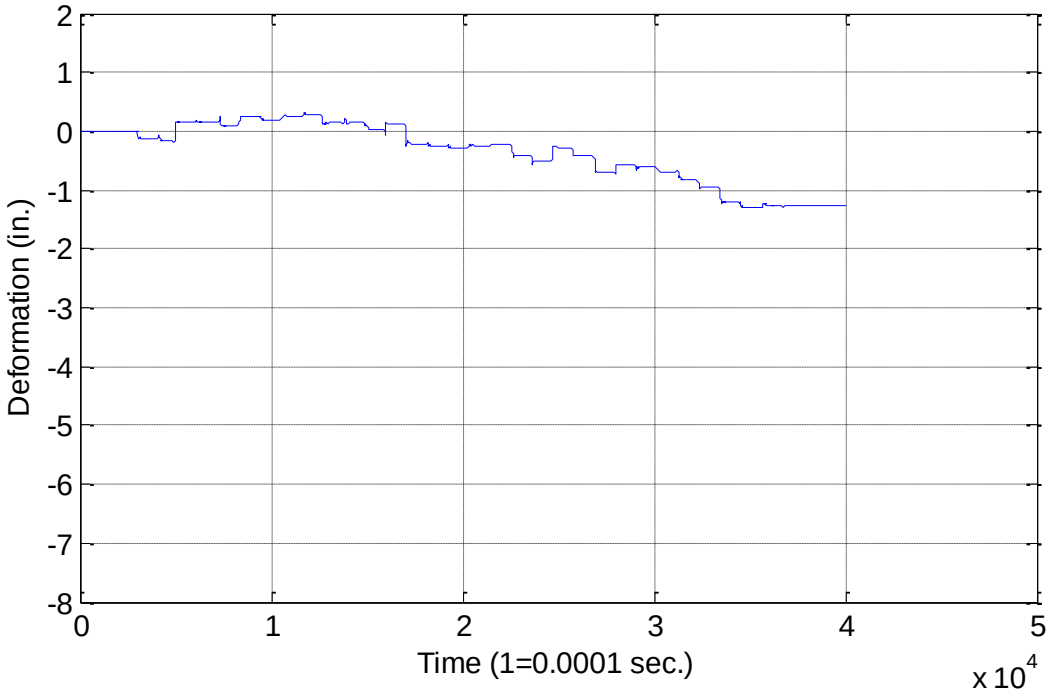


**Figure 324. Council Bluffs test 18 segment 2 acceleration analysis A**

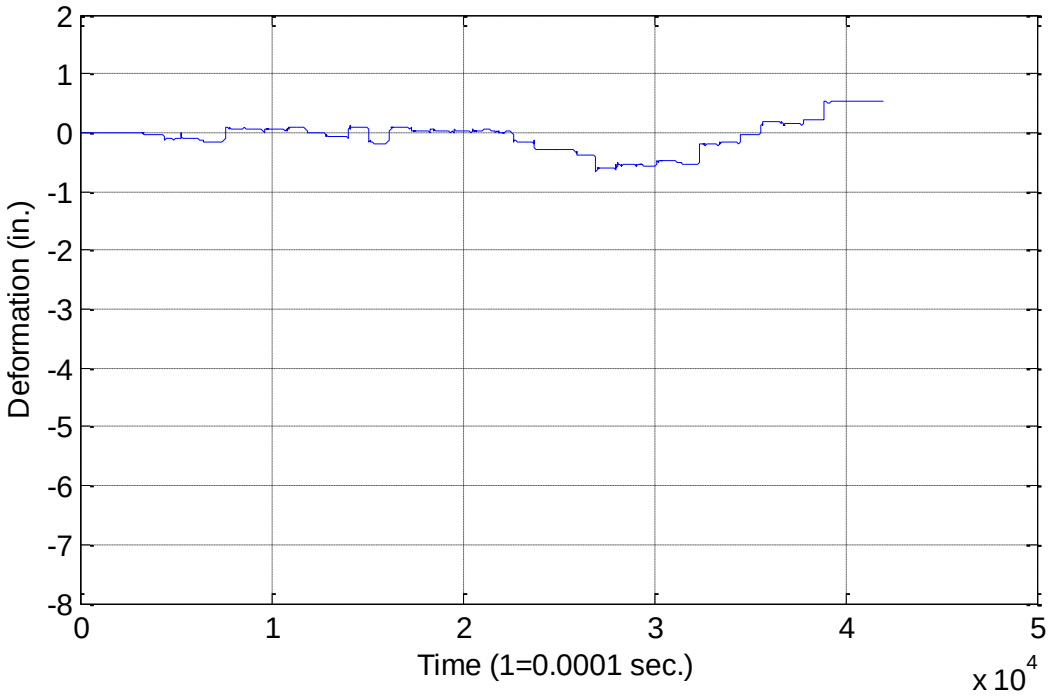


**Figure 325. Council Bluffs test 18 segment 3 acceleration analysis A**

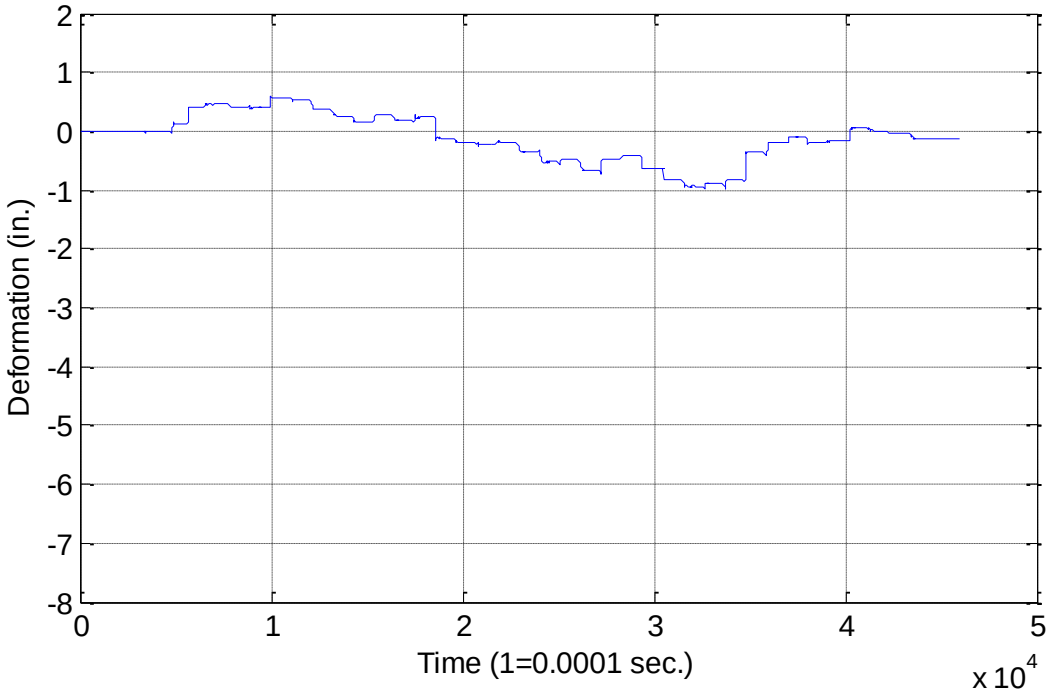


**Figure 326. Council Bluffs test 18 segment 4 acceleration analysis A**

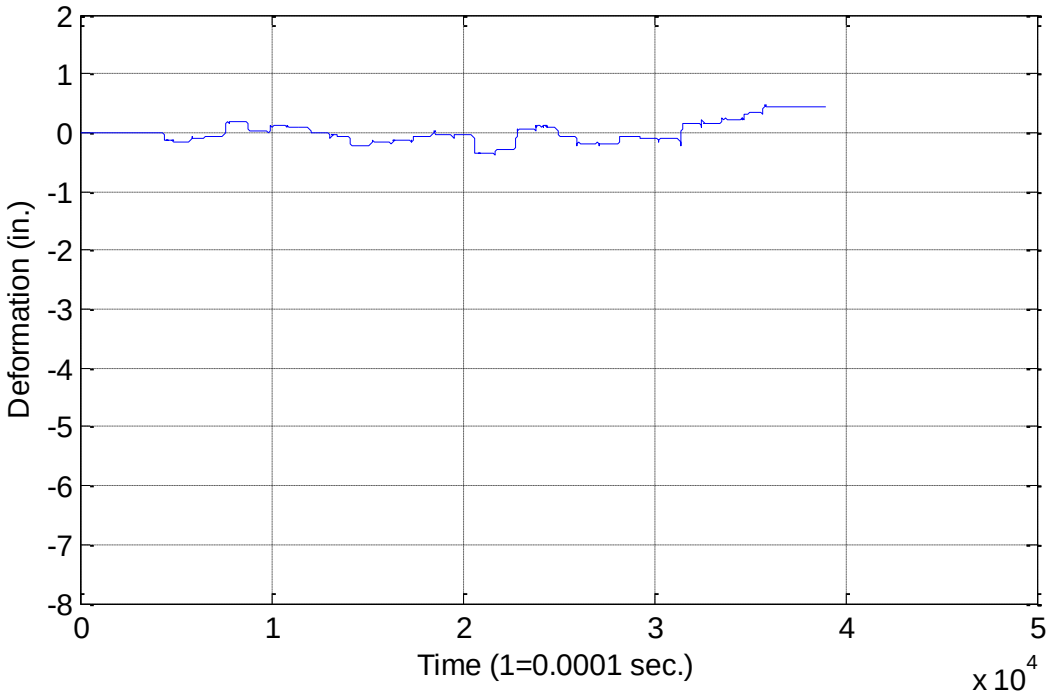


**Figure 327. Council Bluffs test 18 segment 5 acceleration analysis A**

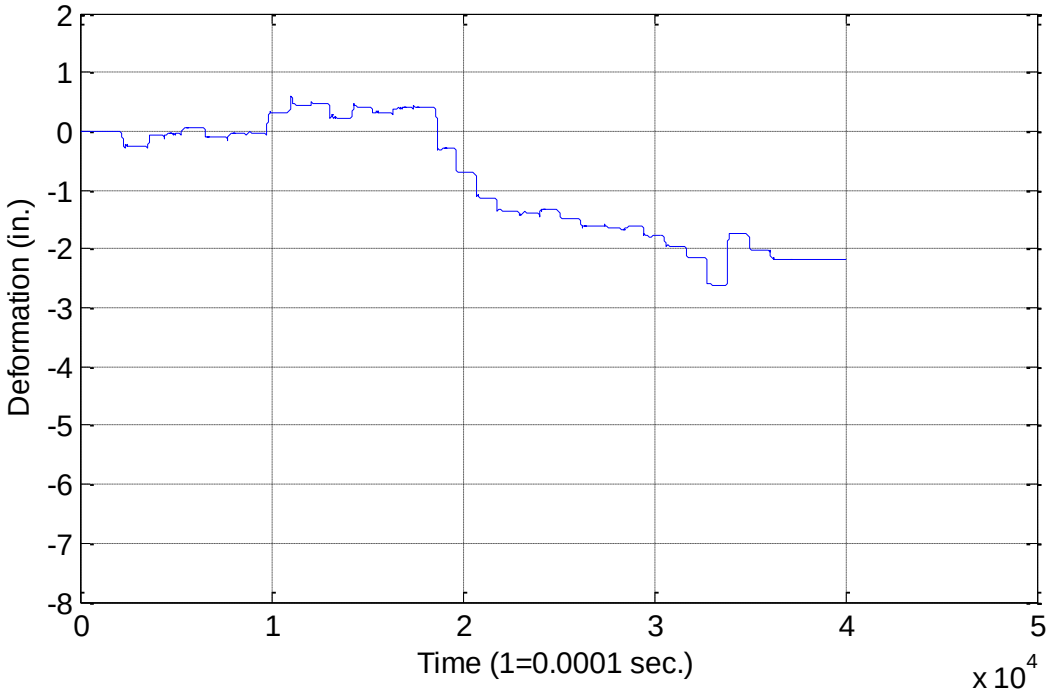


**Figure 328. Council Bluffs test 19 segment 1 acceleration analysis A**

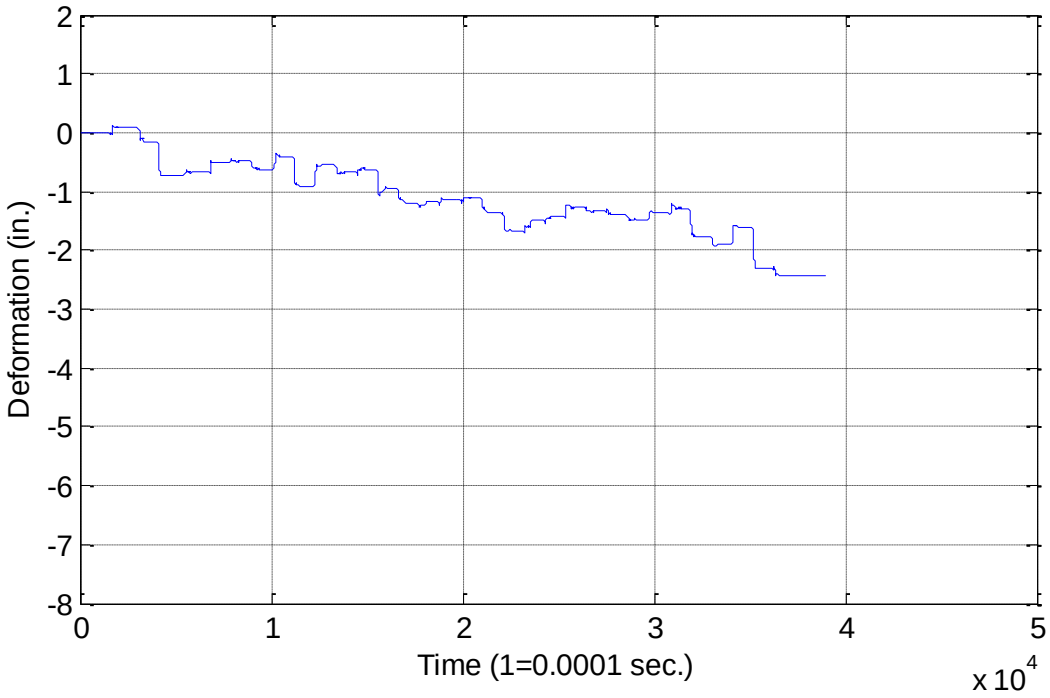


**Figure 329. Council Bluffs test 19 segment 2 acceleration analysis A**

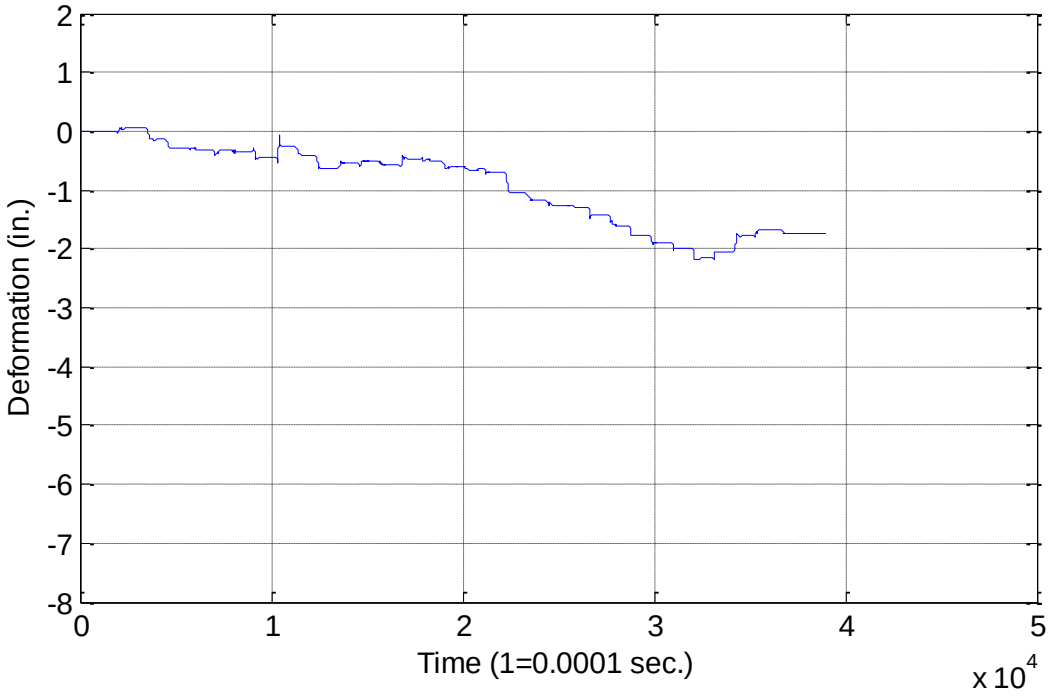


**Figure 330. Council Bluffs test 19 segment 3 acceleration analysis A**

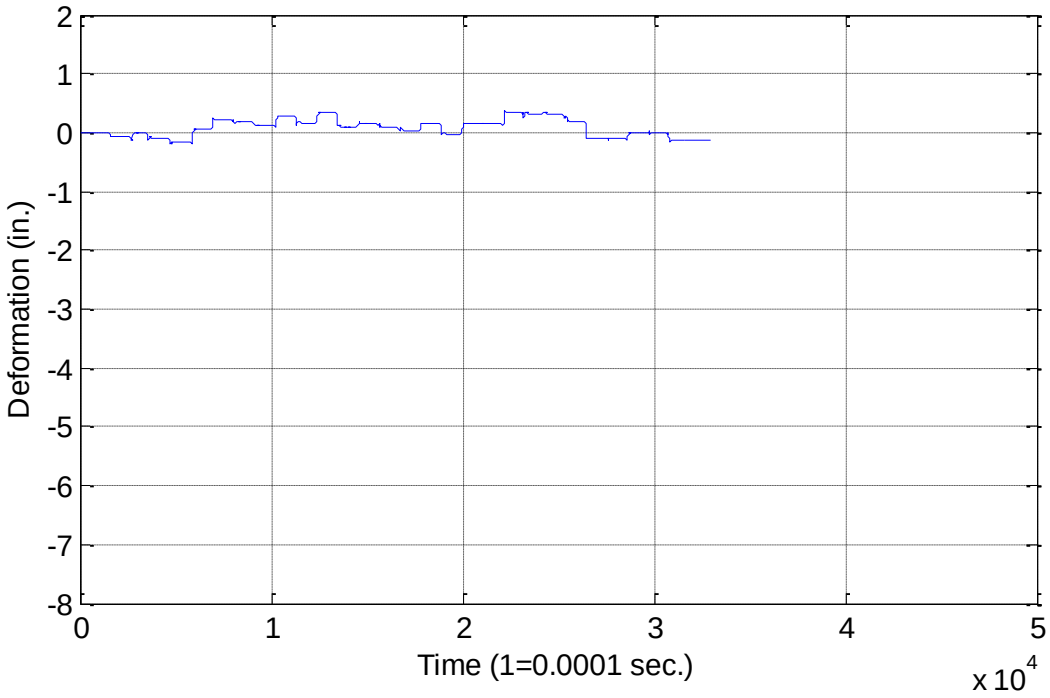


**Figure 331. Council Bluffs test 19 segment 4 acceleration analysis A**

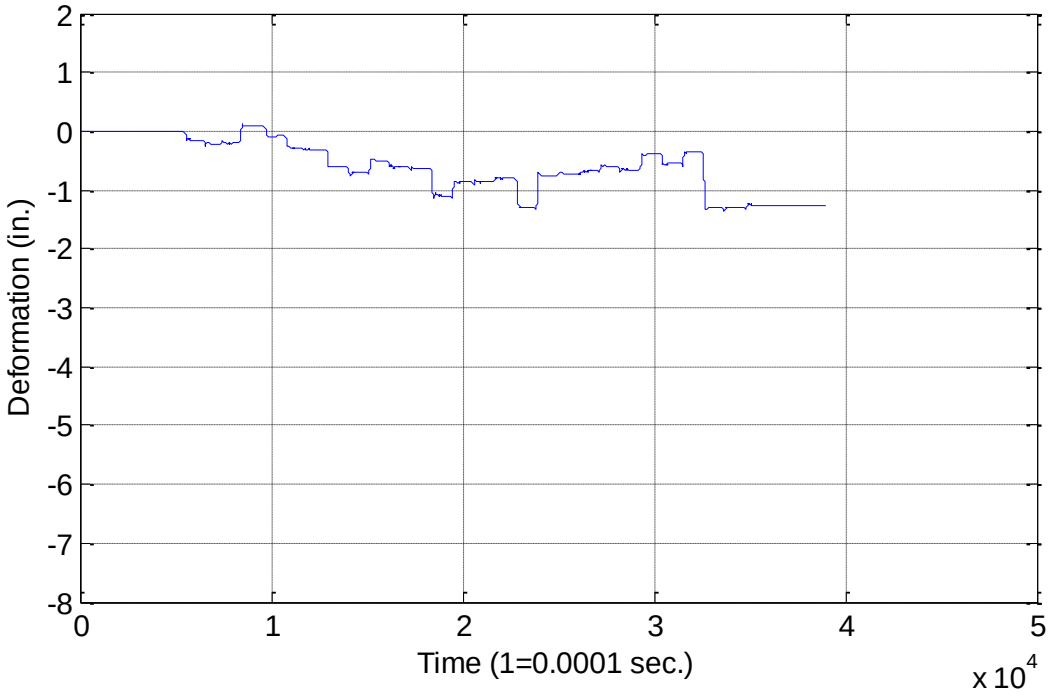


**Figure 332. Council Bluffs test 21 segment 1 acceleration analysis A**

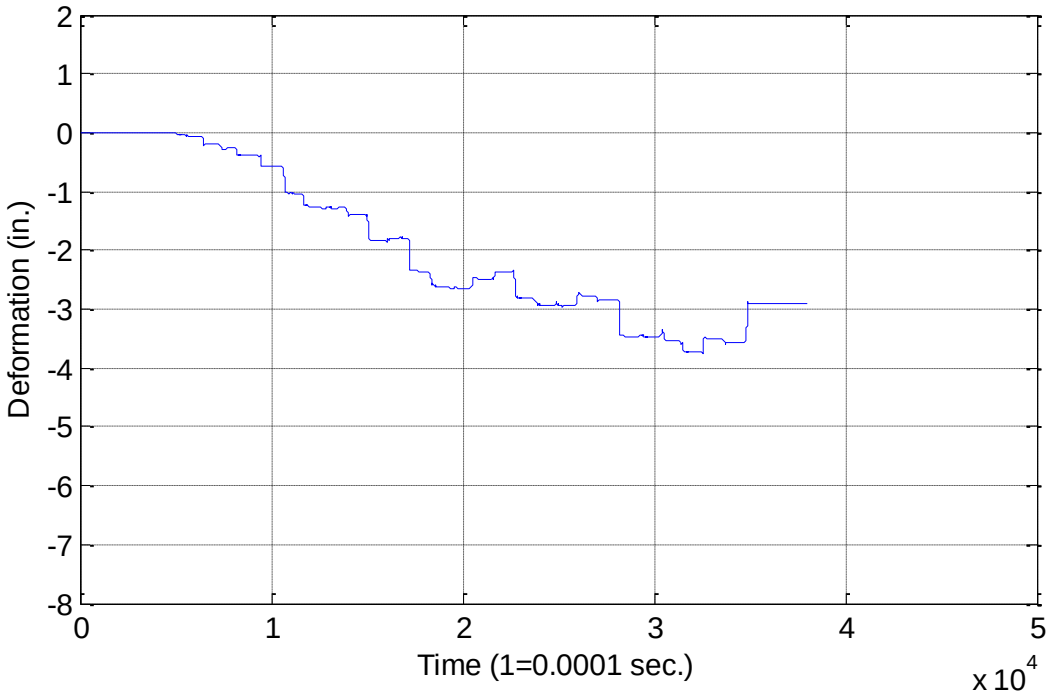


**Figure 333. Council Bluffs test 21 segment 2 acceleration analysis A**

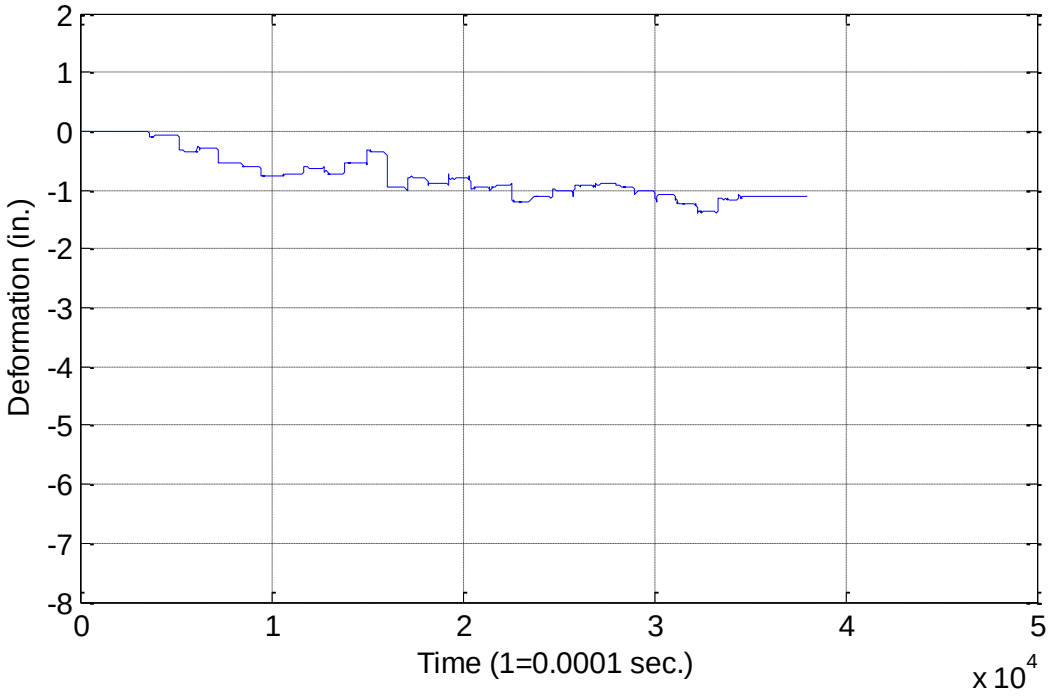


**Figure 334. Council Bluffs test 21 segment 3 acceleration analysis A**

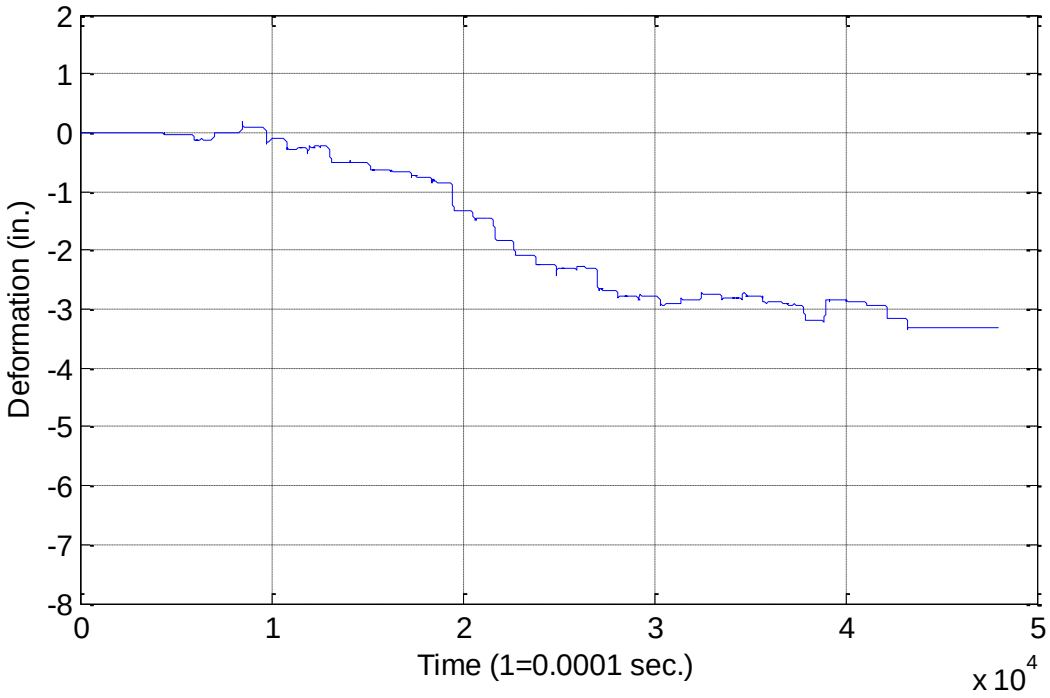


**Figure 335. Council Bluffs test 21 segment 4 acceleration analysis A**

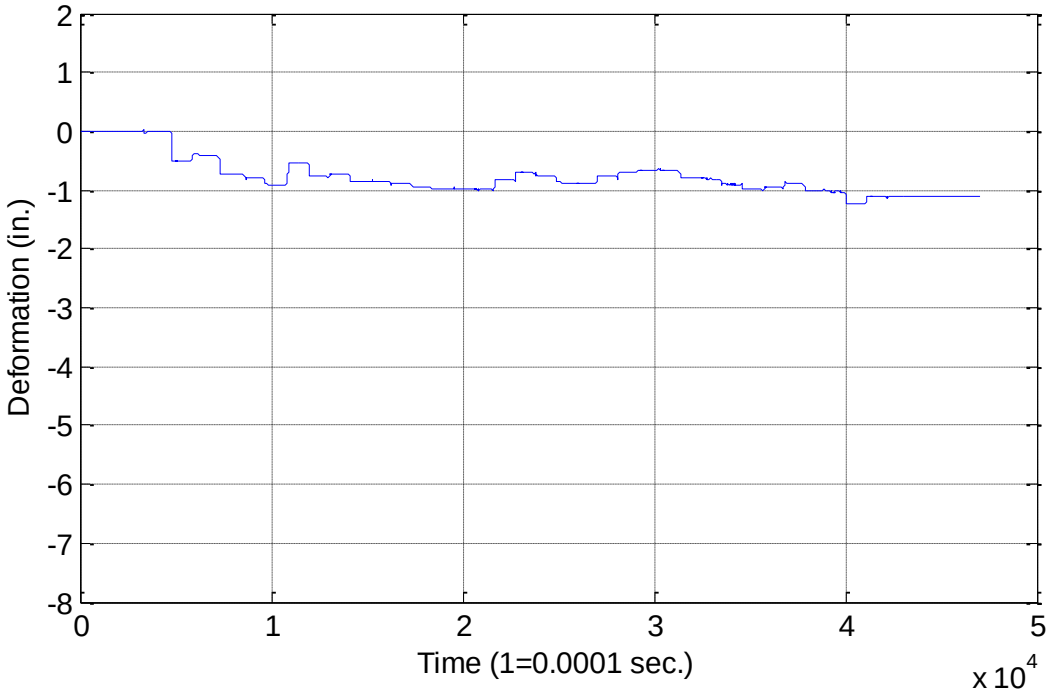


**Figure 336. Council Bluffs test 21 segment 5 acceleration analysis A**

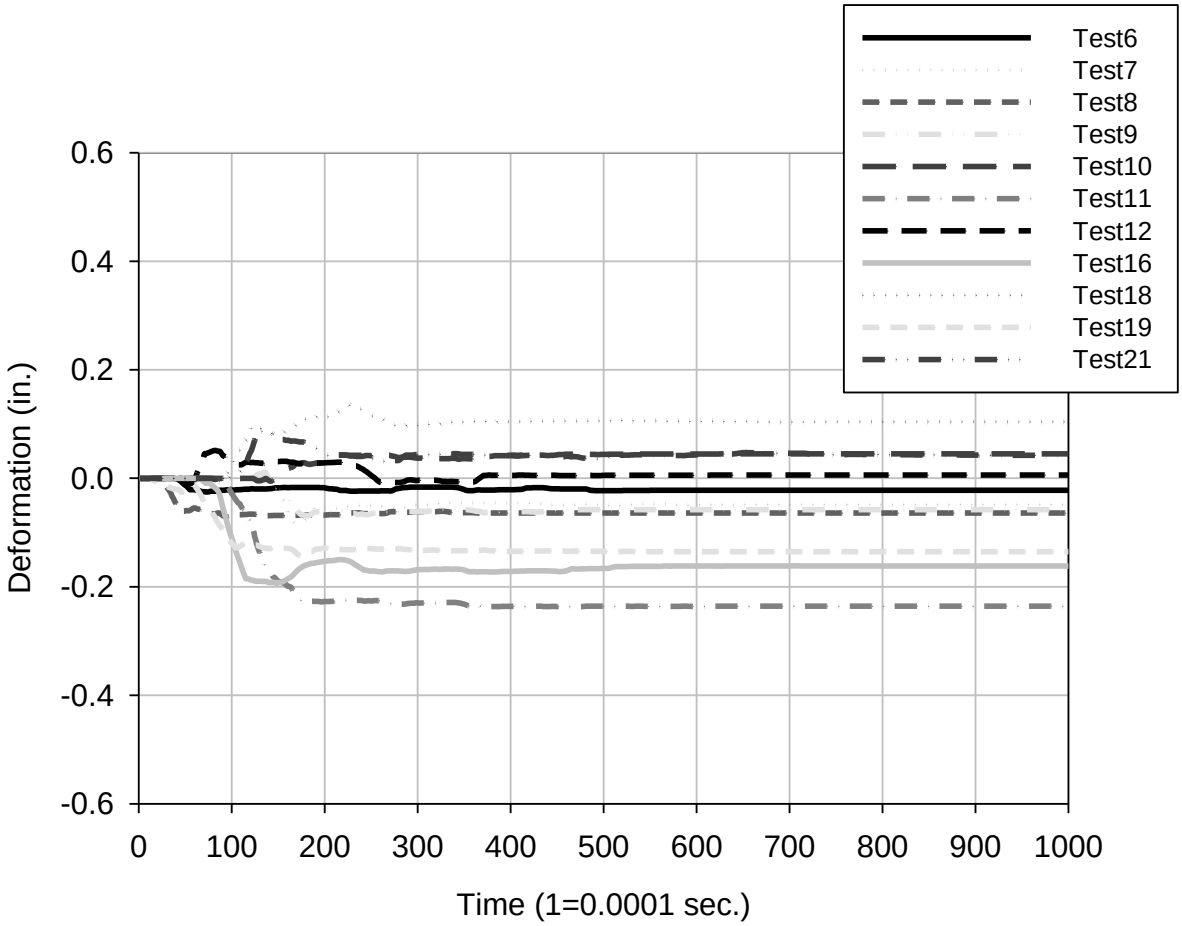


**Figure 337. Council Bluffs tests 6–21 acceleration analysis B**

**Oskaloosa**

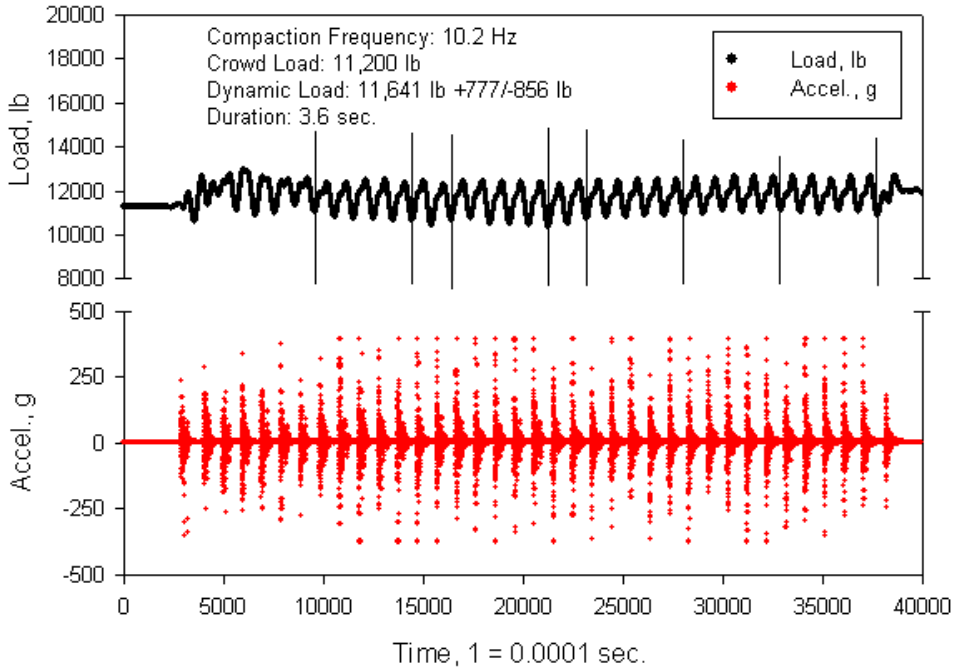


**Figure 338. Oskaloosa test 1 segment 1**

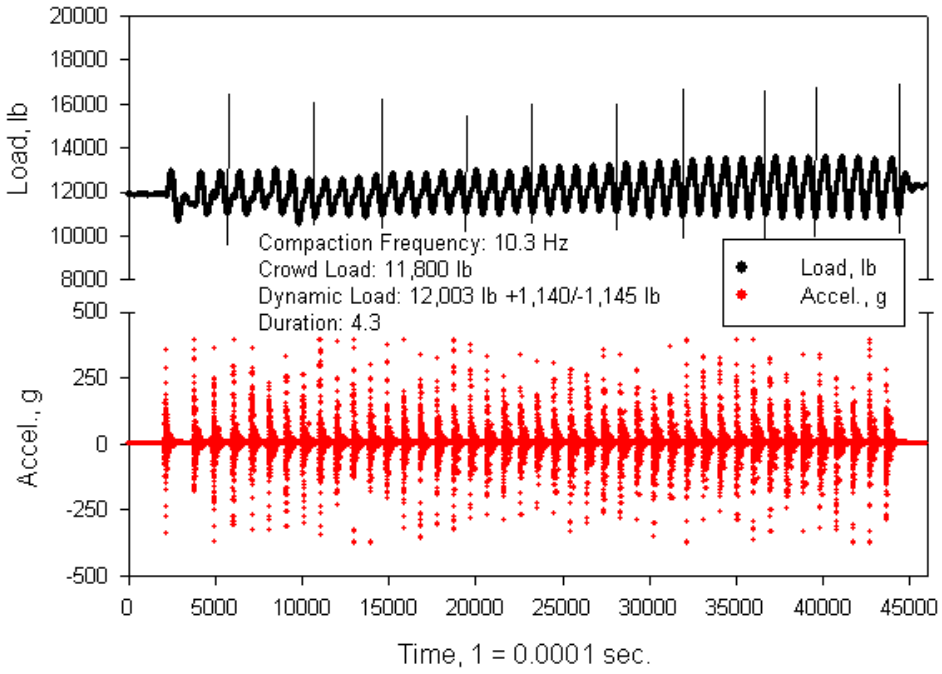


**Figure 339. Oskaloosa test 1 segment 2**

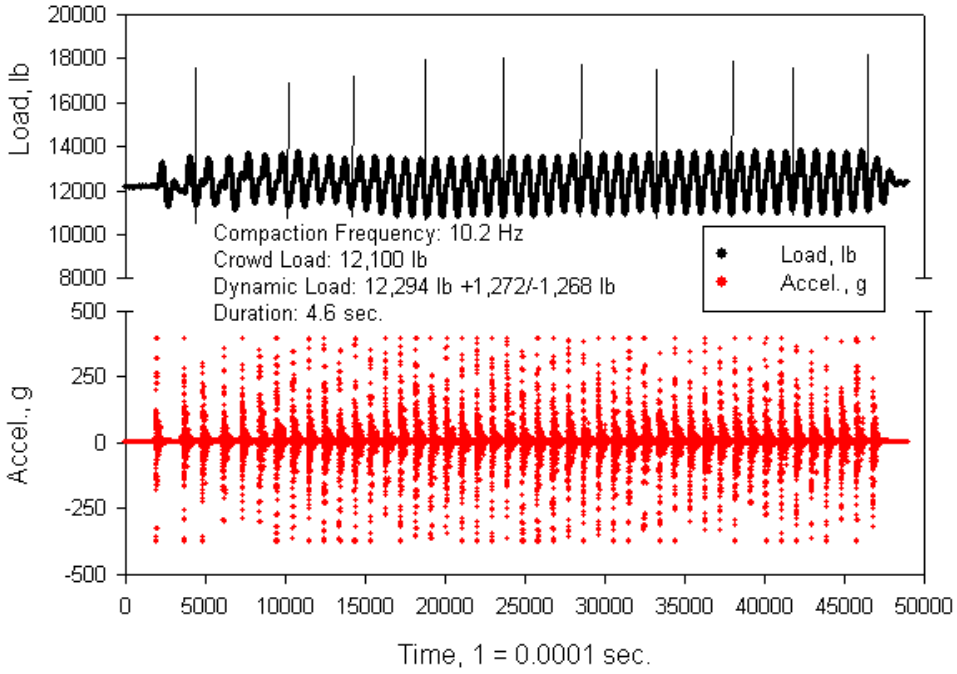


**Figure 340. Oskaloosa test 1 segment 3**

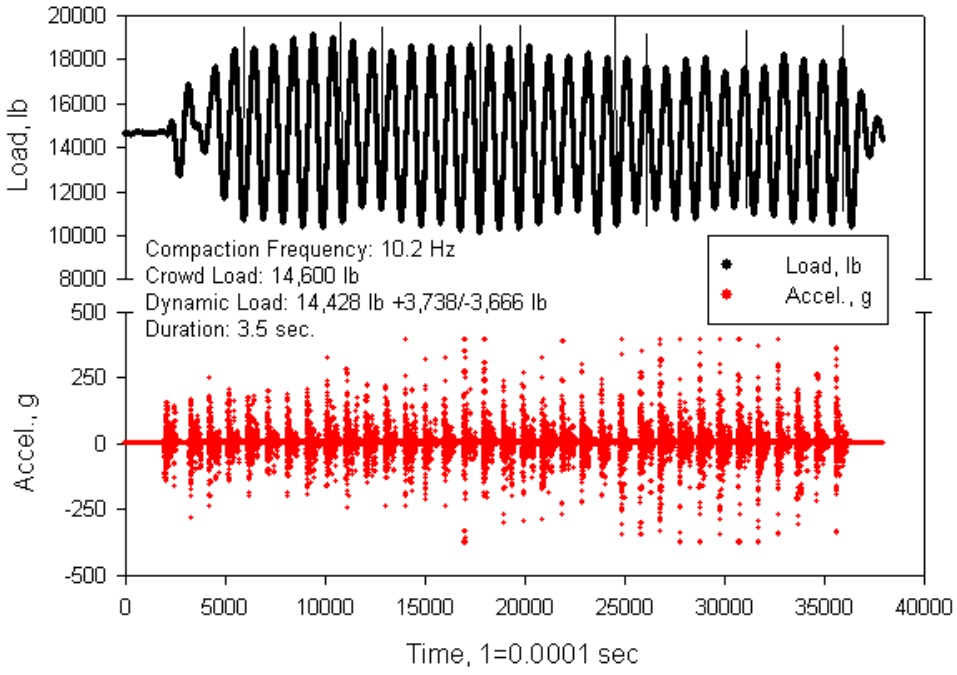


**Figure 341. Oskaloosa test 2 segment 1**

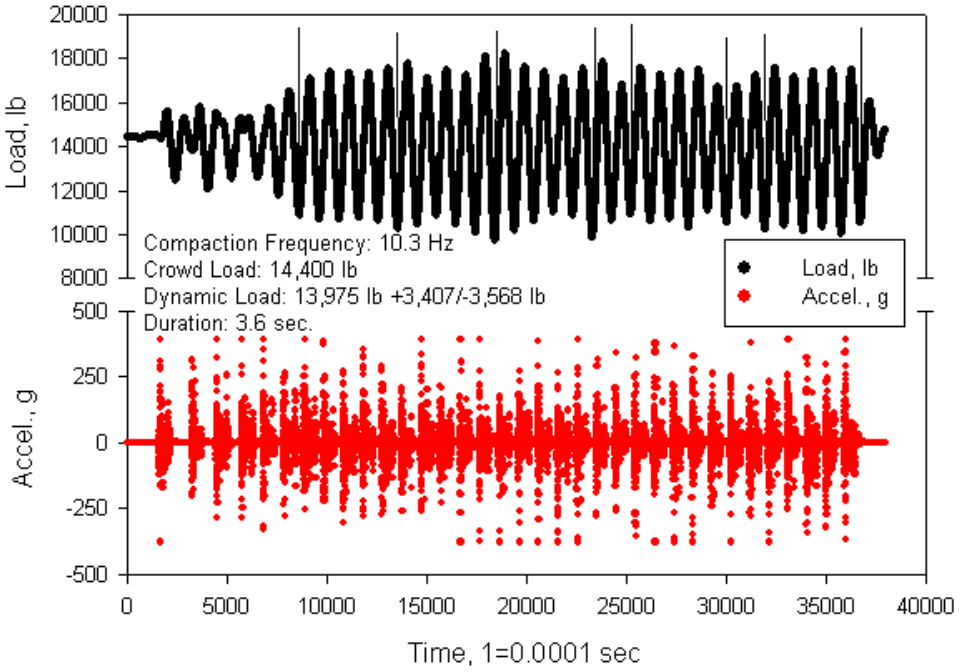


**Figure 342. Oskaloosa test 2 segment 2**

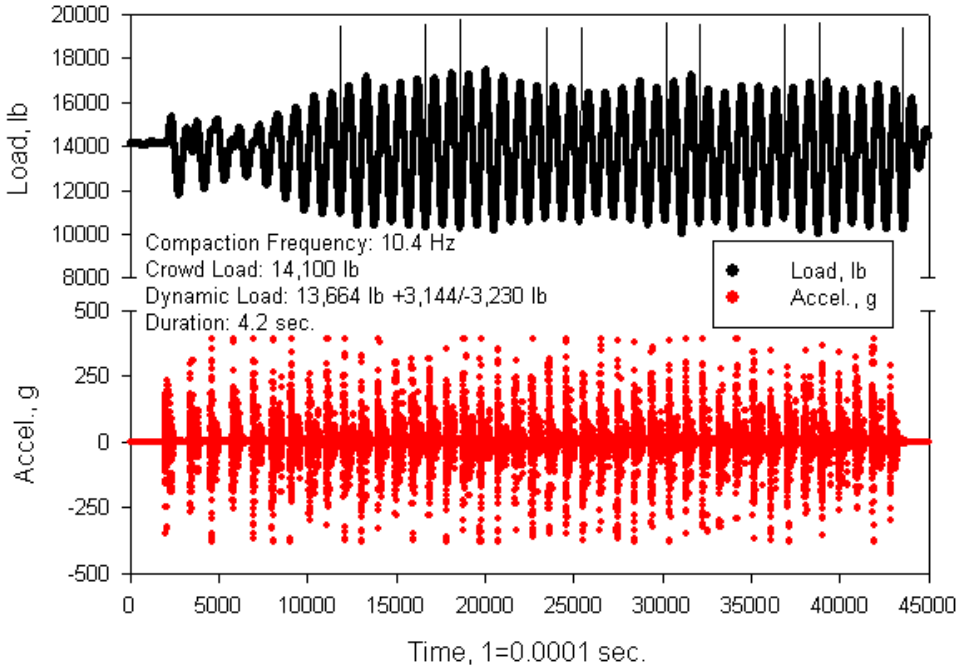


**Figure 343. Oskaloosa test 2 segment 3**

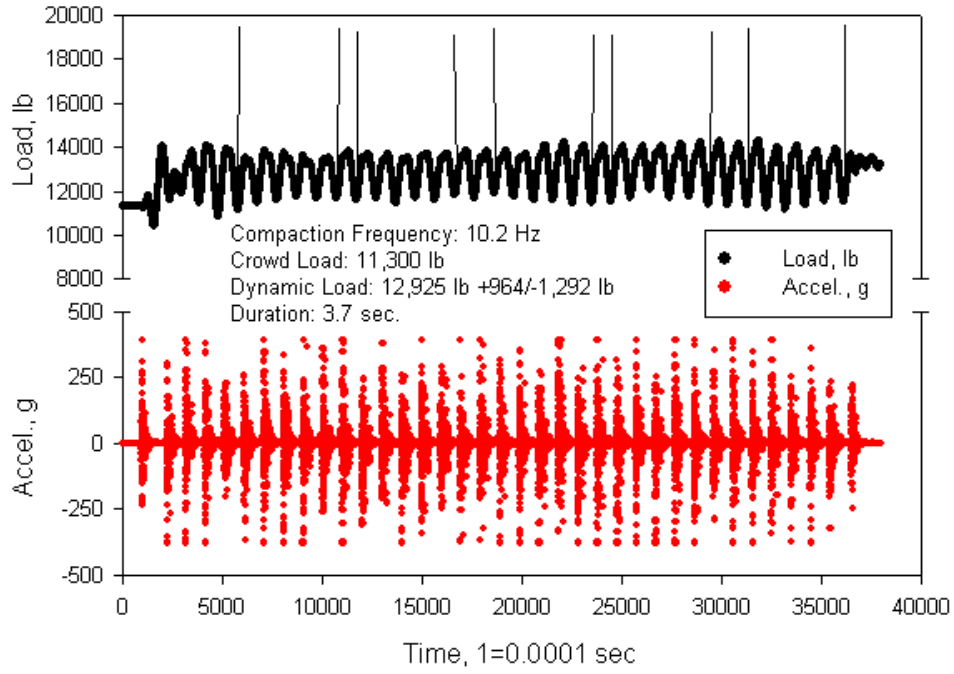


**Figure 344. Oskaloosa test 3 segment 1**

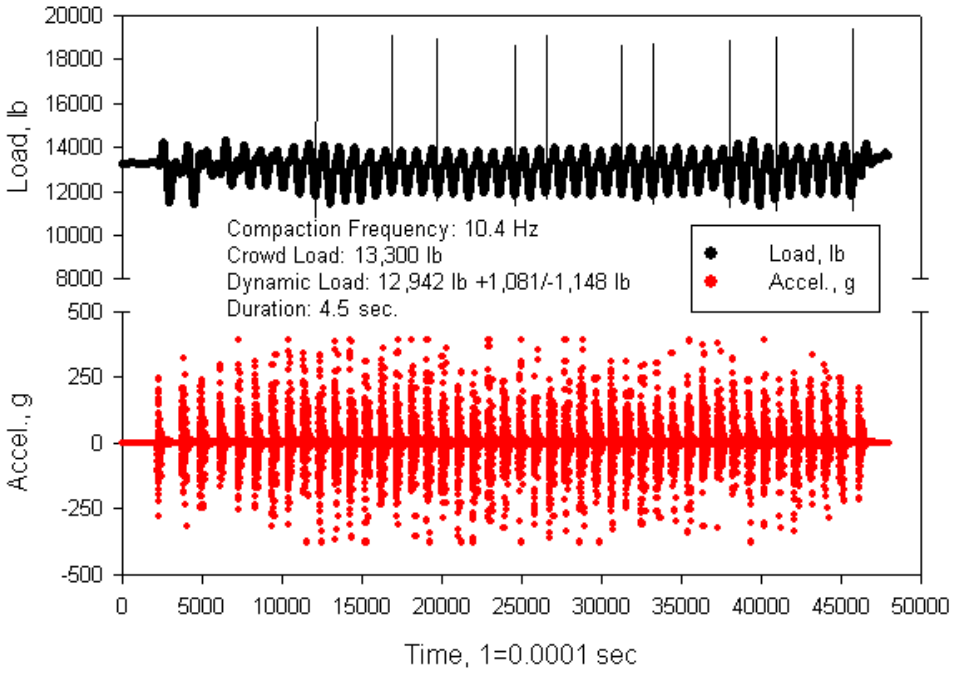


**Figure 345. Oskaloosa test 3 segment 2**

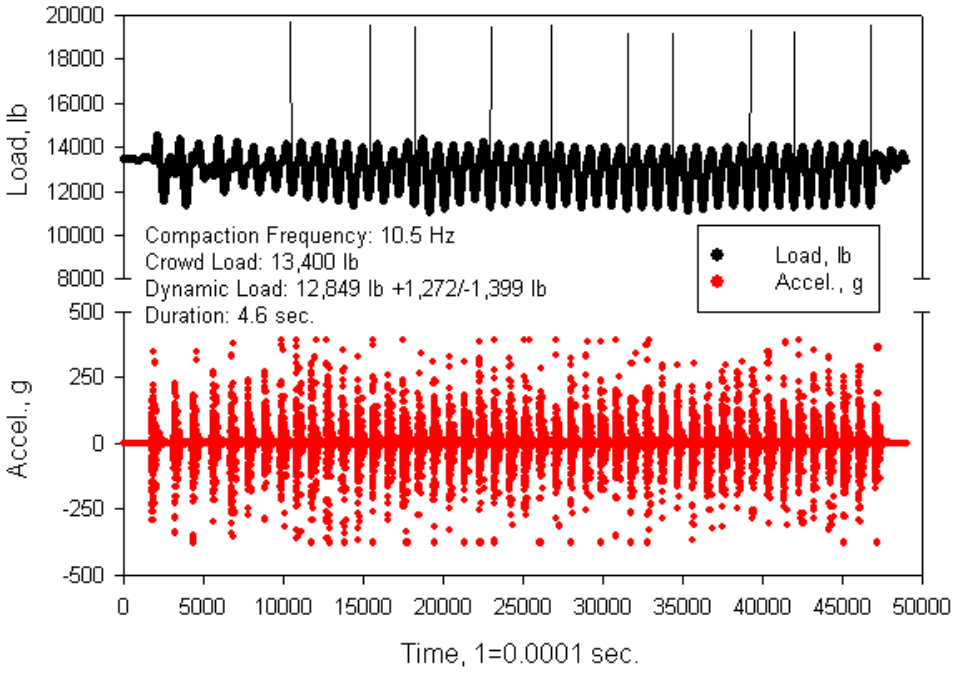


**Figure 346. Oskaloosa test 3 segment 3**

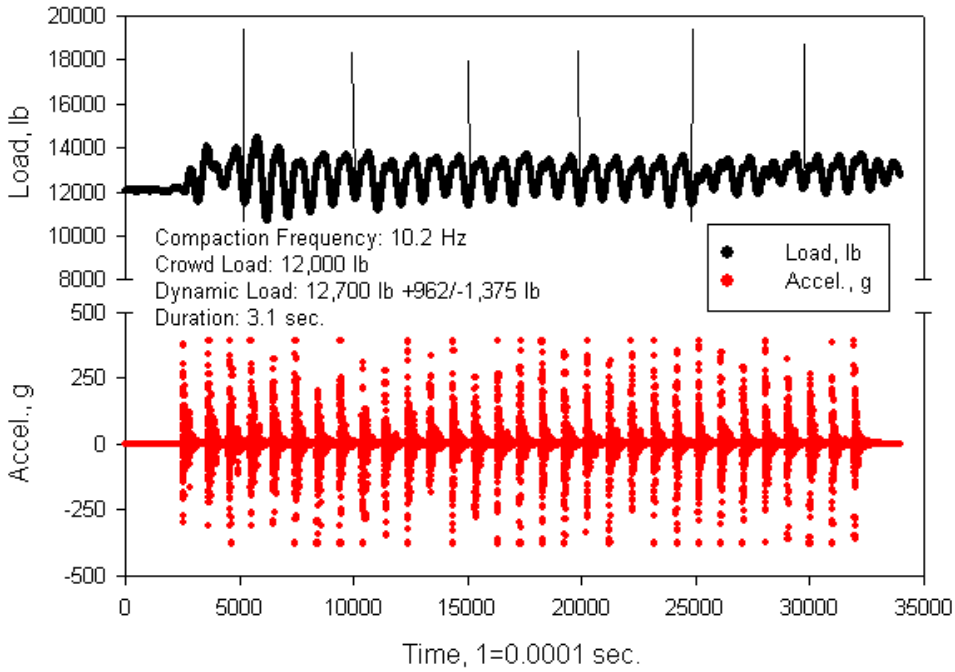


**Figure 347. Oskaloosa test 4 segment 1**

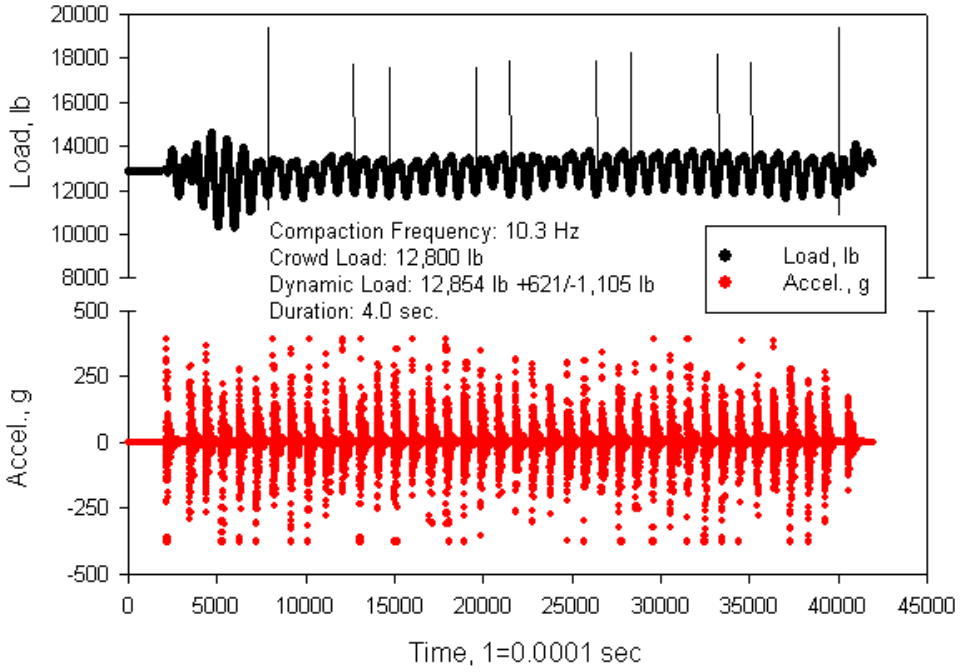


**Figure 348. Oskaloosa test 4 segment 2**

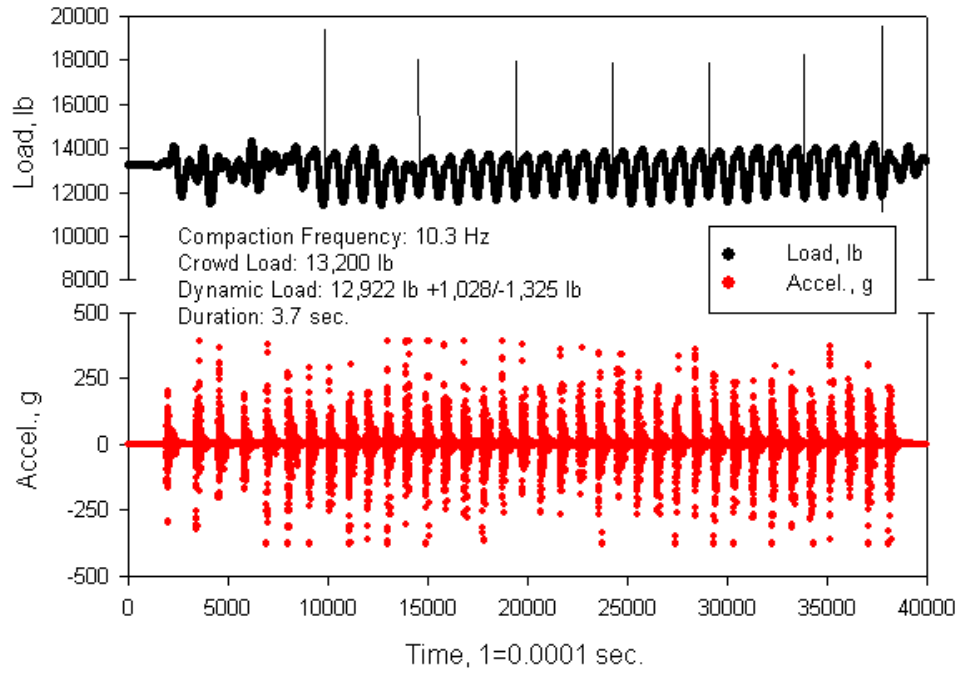


**Figure 349. Oskaloosa test 4 segment 3**

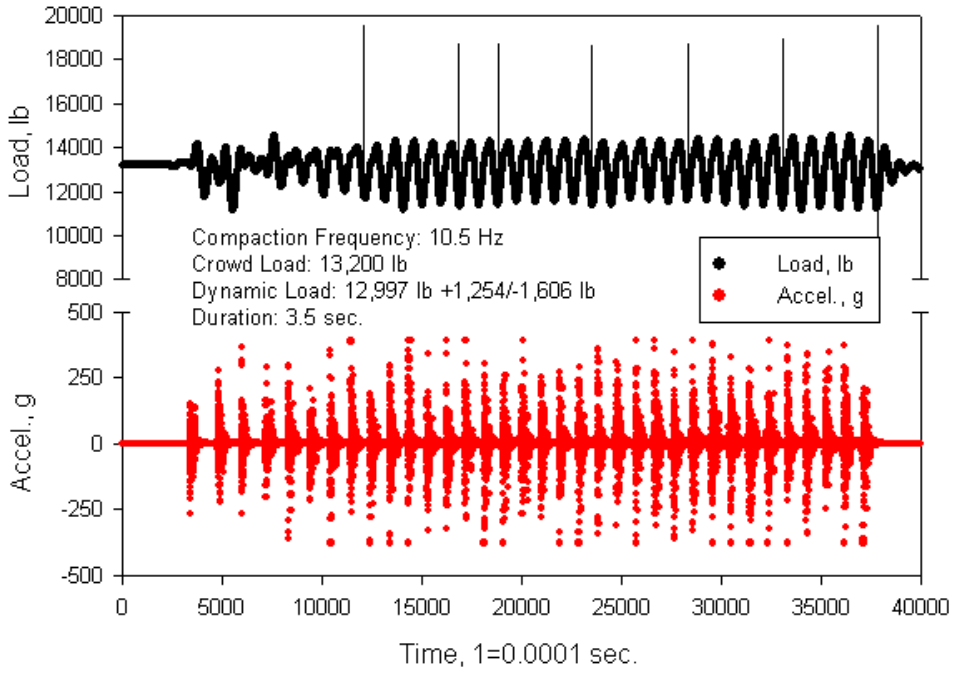


**Figure 350. Oskaloosa test 4 segment 4**

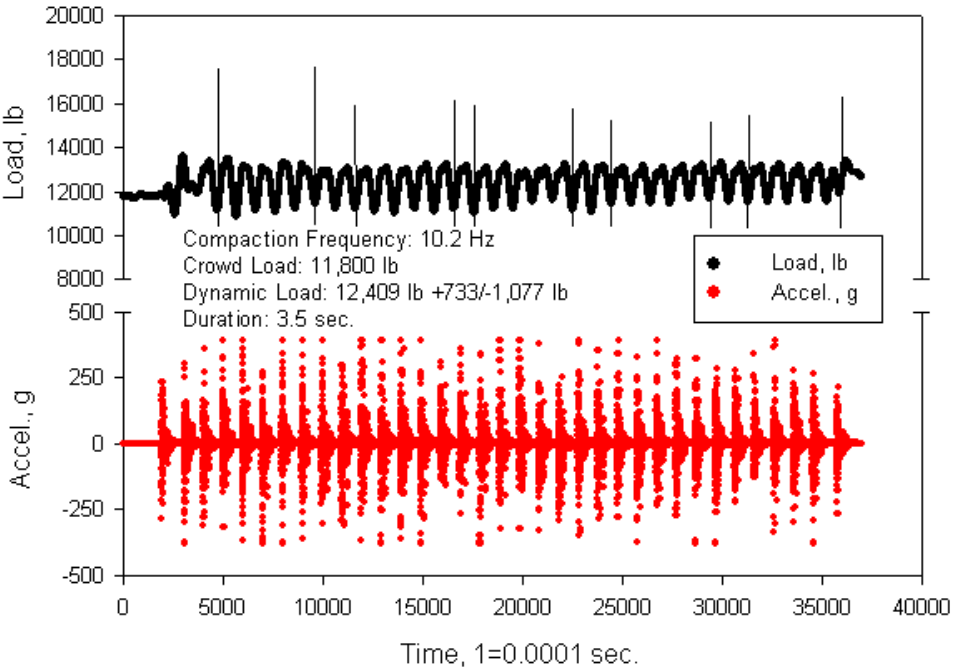


**Figure 351. Oskaloosa test 5 segment 1**

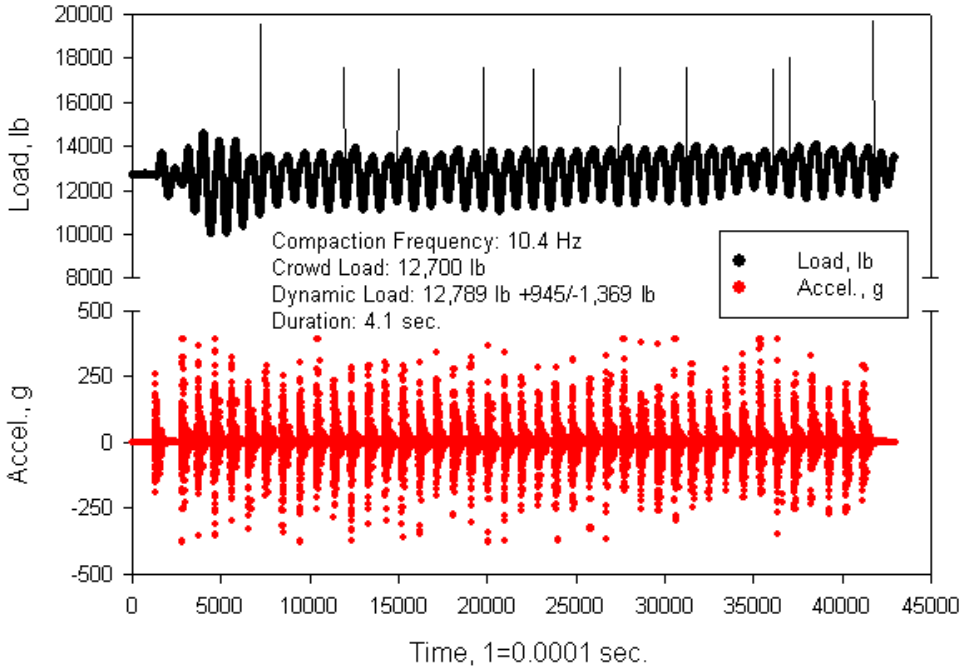


**Figure 352. Oskaloosa test 5 segment 2**

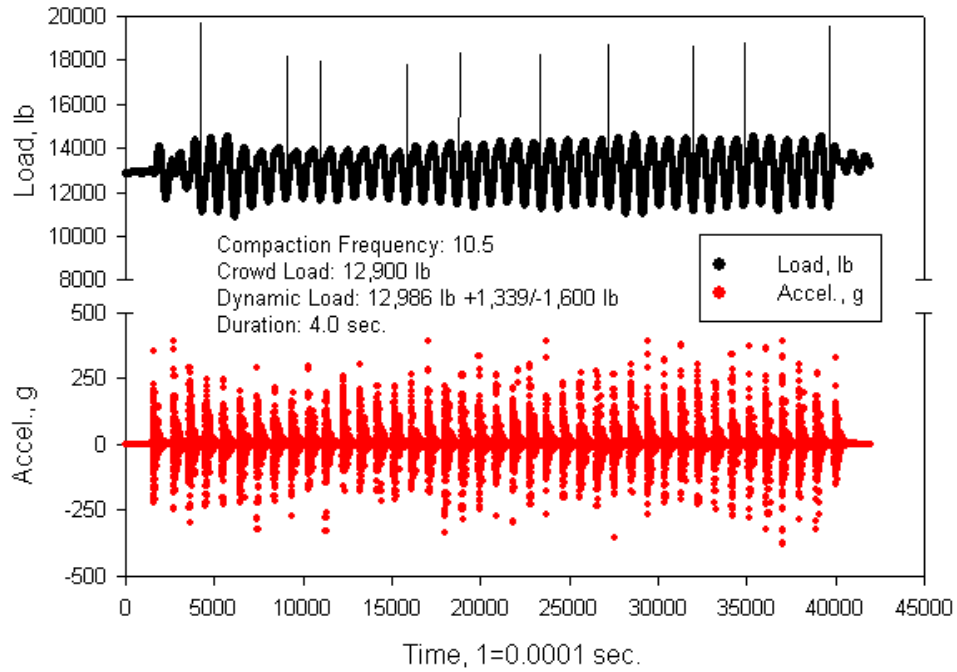


**Figure 353. Oskaloosa test 5 segment 3**

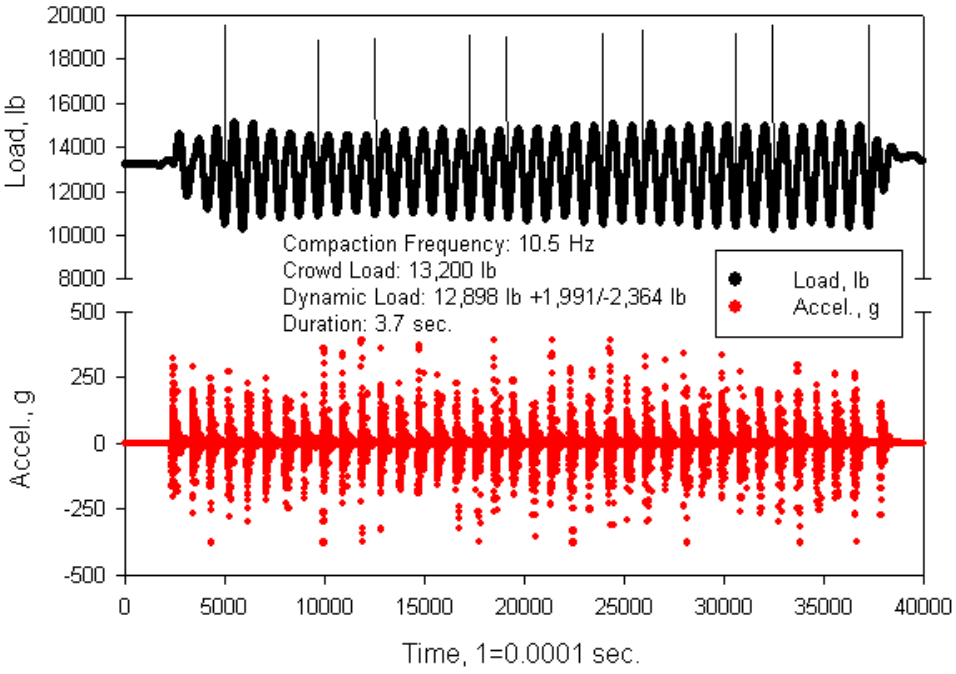


**Figure 354. Oskaloosa test 5 segment 4**

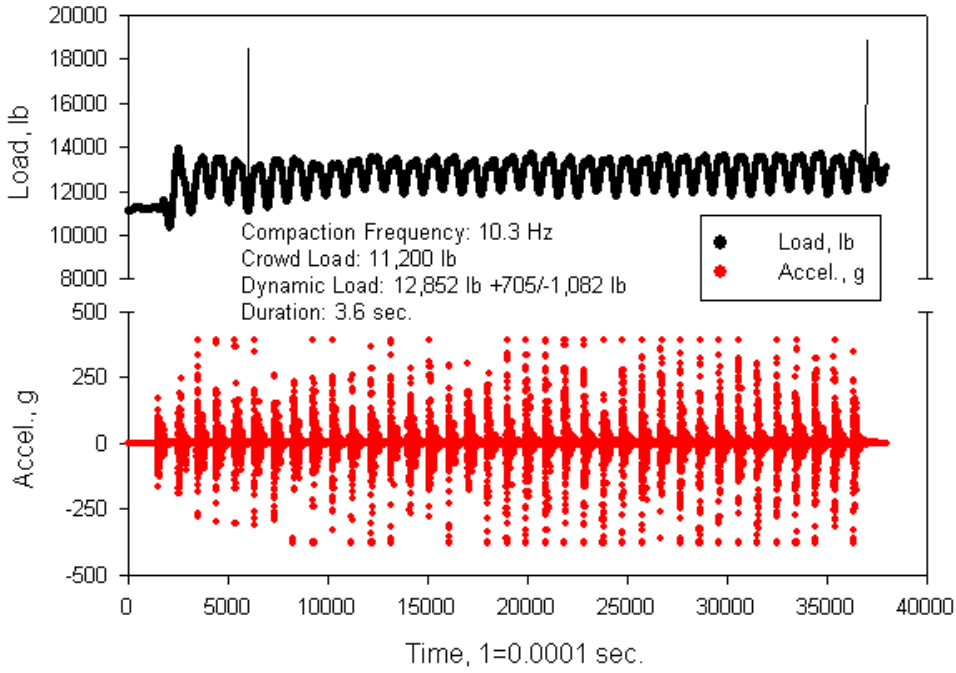


**Figure 355. Oskaloosa test 6 segment 1**

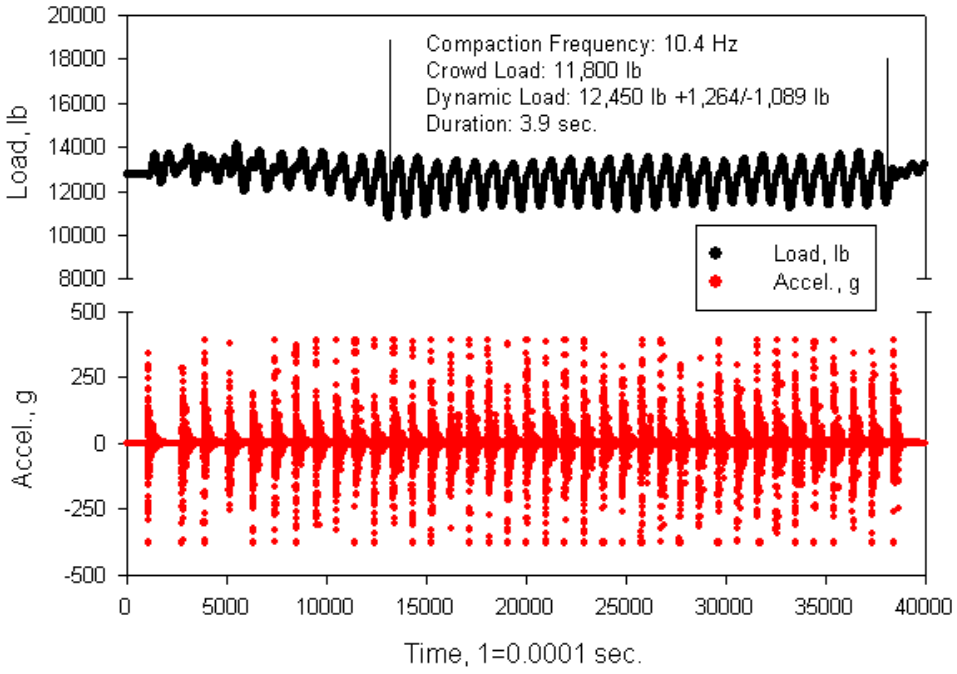


**Figure 356. Oskaloosa test 6 segment 2**

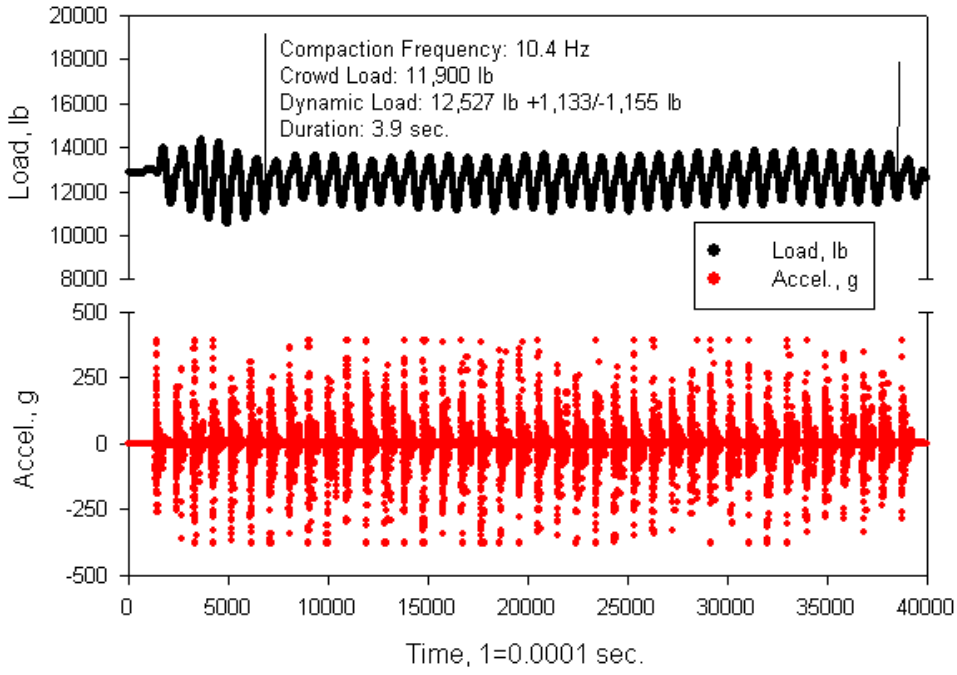


**Figure 357. Oskaloosa test 6 segment 3**

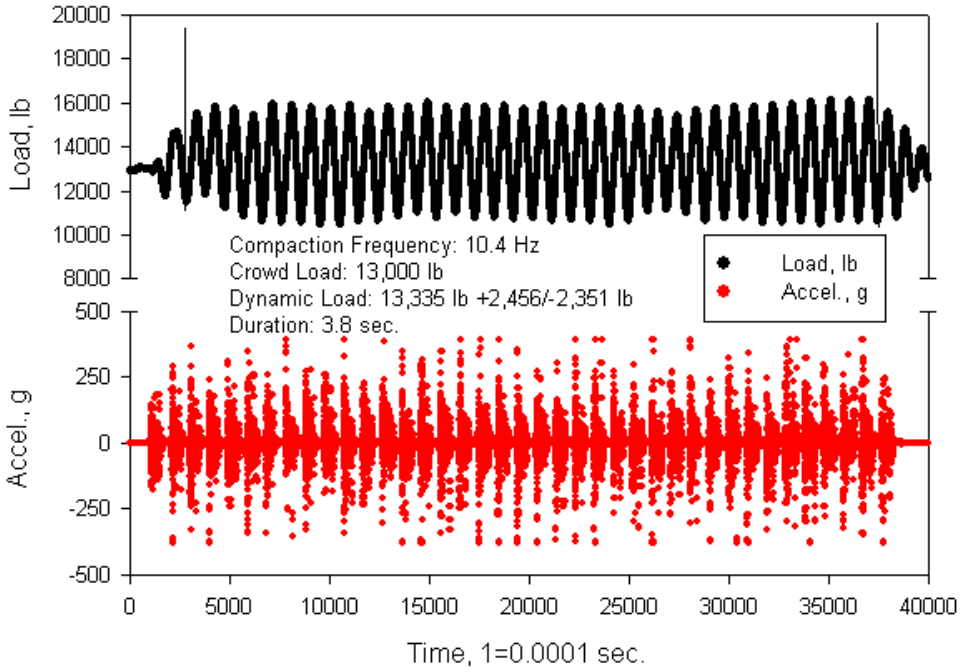


**Figure 358. Oskaloosa test 7 segment 1**

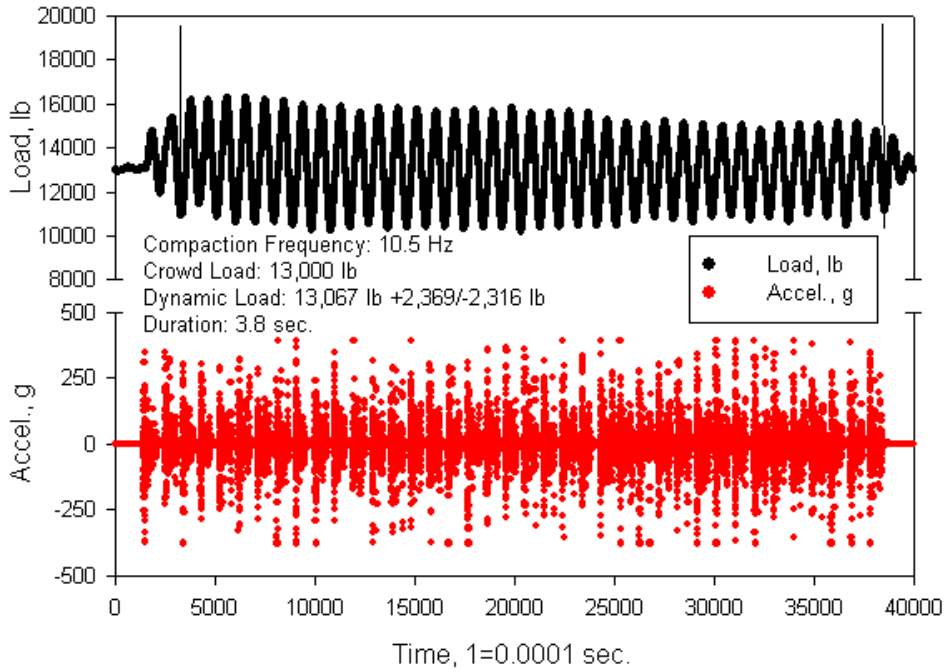


**Figure 359. Oskaloosa test 7 segment 2**

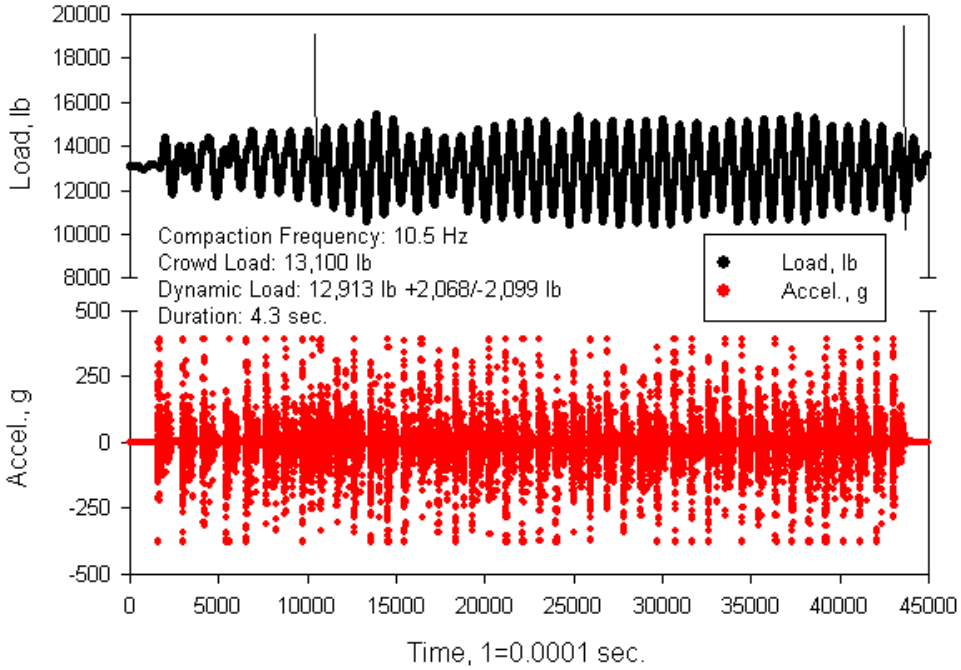


**Figure 360. Oskaloosa test 7 segment 3**

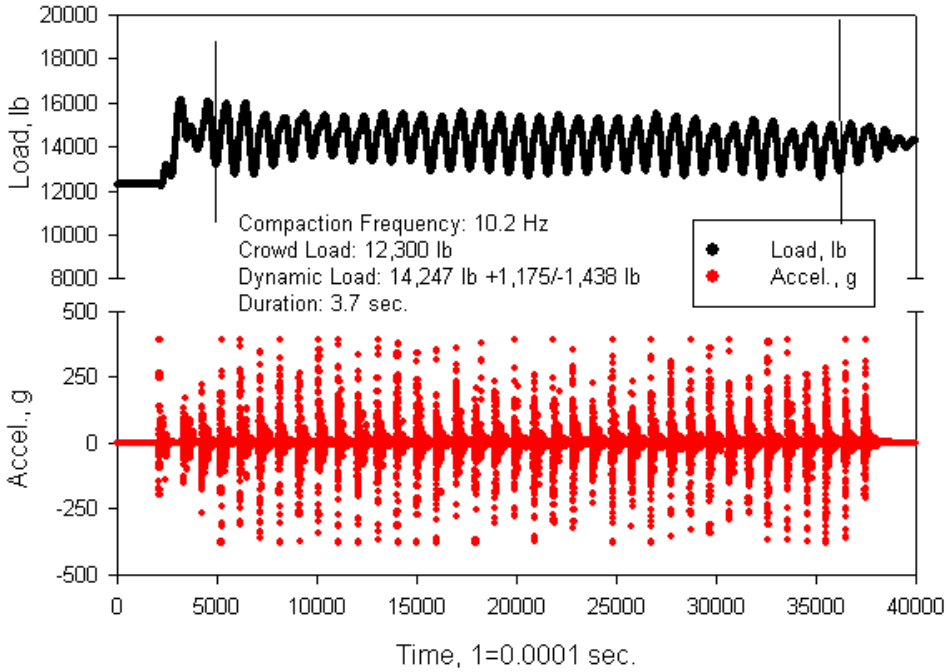


**Figure 361. Oskaloosa test 8 segment 1**

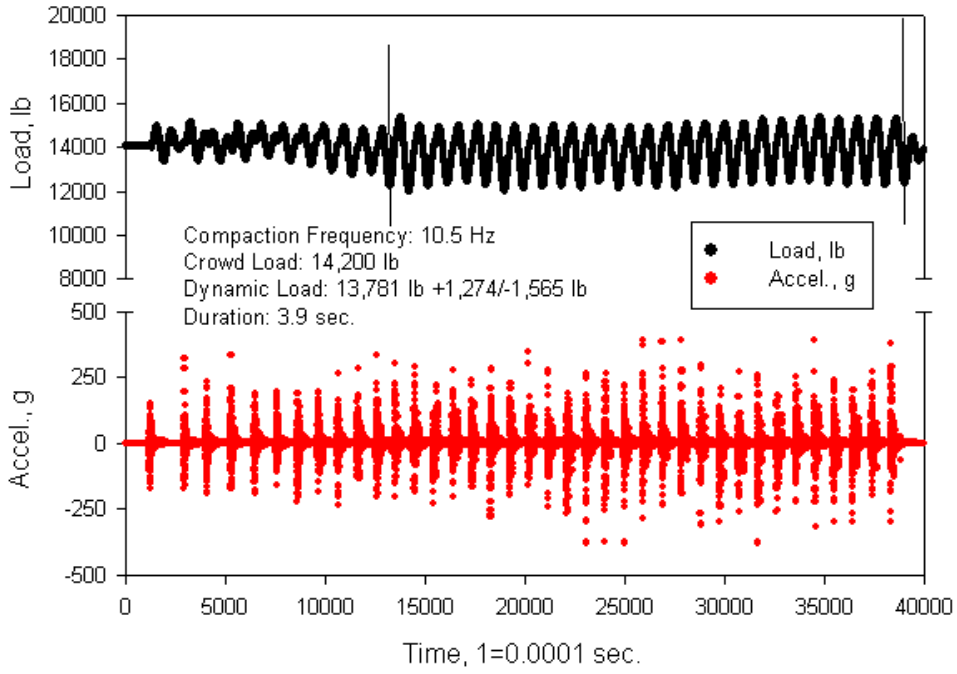


**Figure 362. Oskaloosa test 8 segment 2**

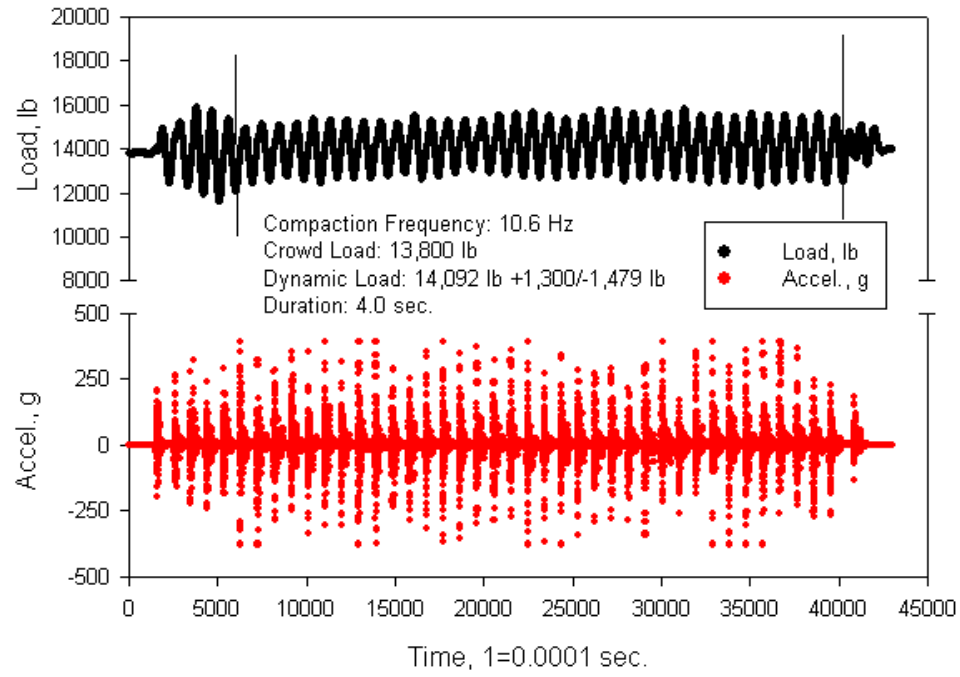


**Figure 363. Oskaloosa test 8 segment 3**

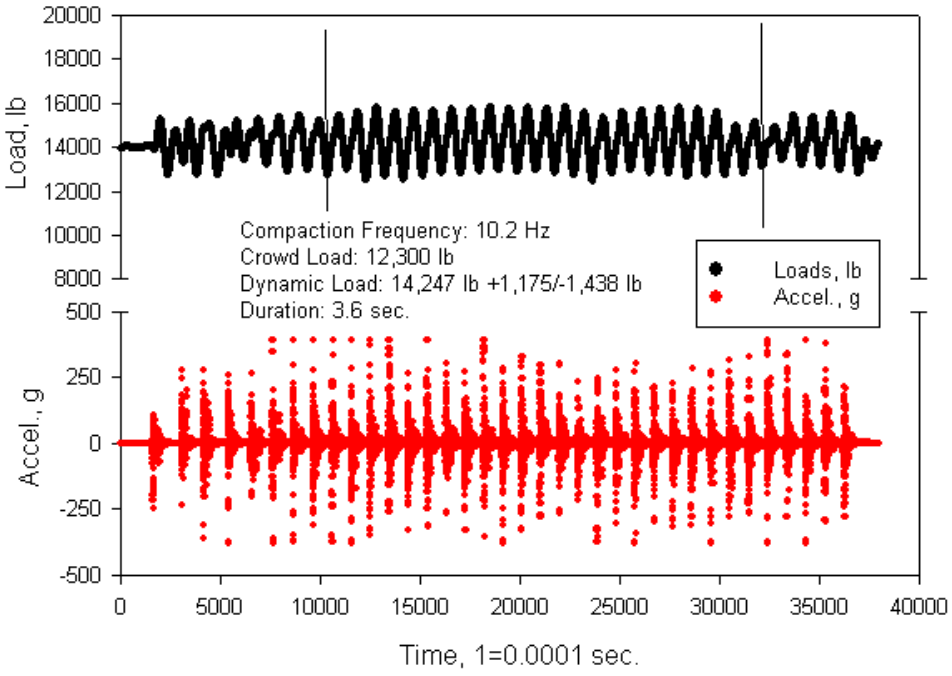


**Figure 364. Oskaloosa test 8 segment 4**

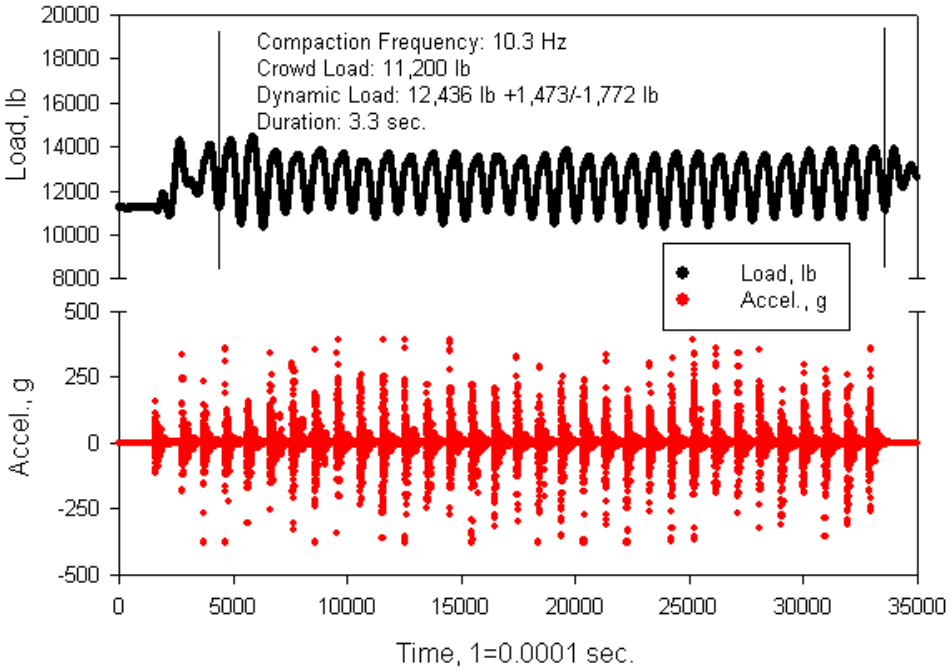


**Figure 365. Oskaloosa test 9 segment 1**

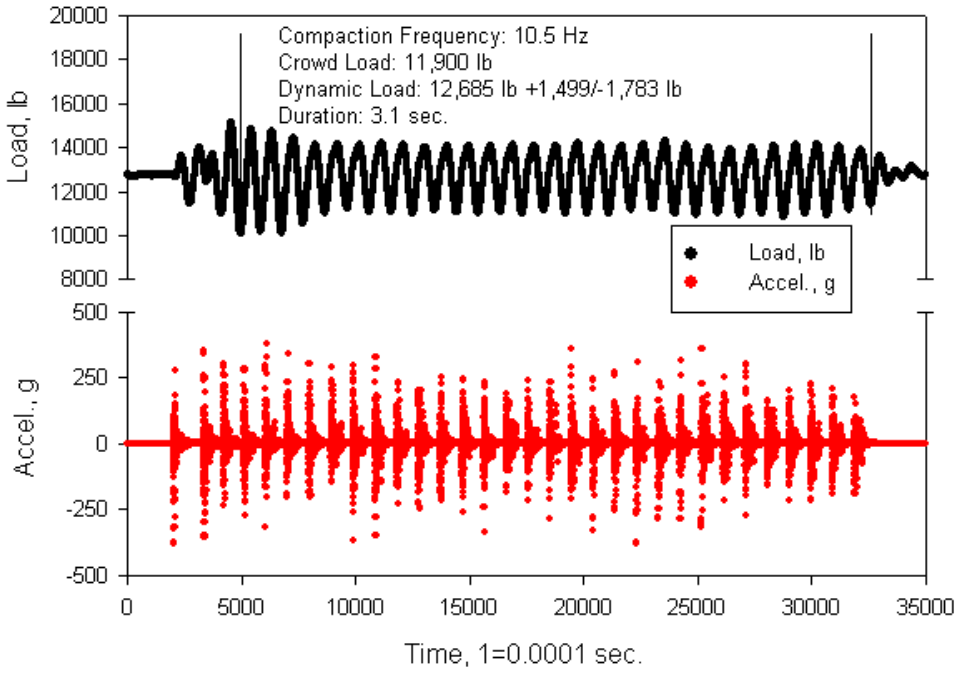


**Figure 366. Oskaloosa test 9 segment 2**

5

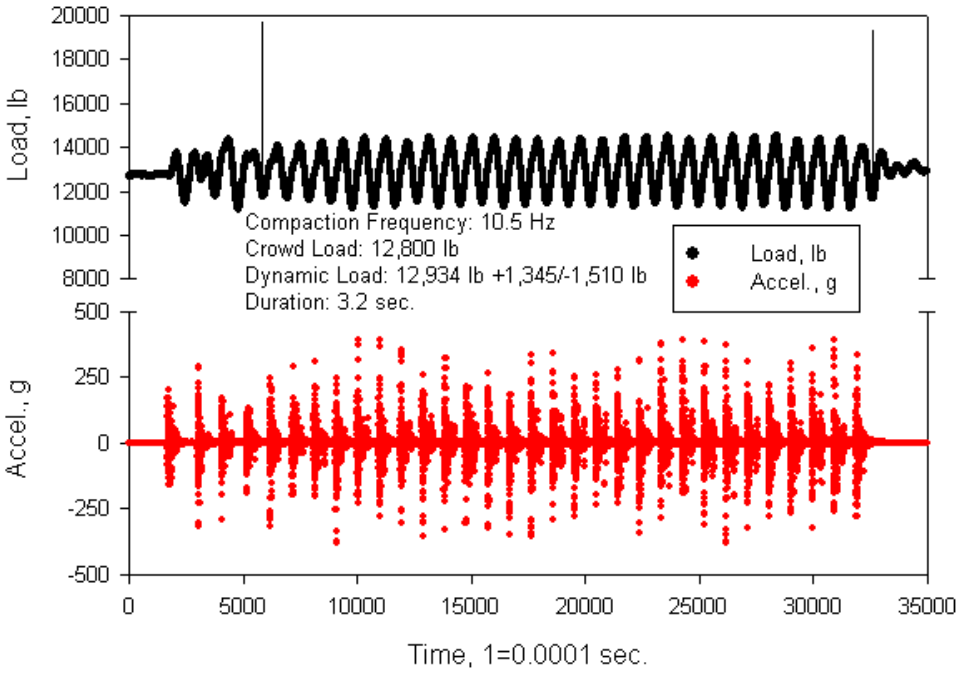


**Figure 367. Oskaloosa test 9 segment 3**

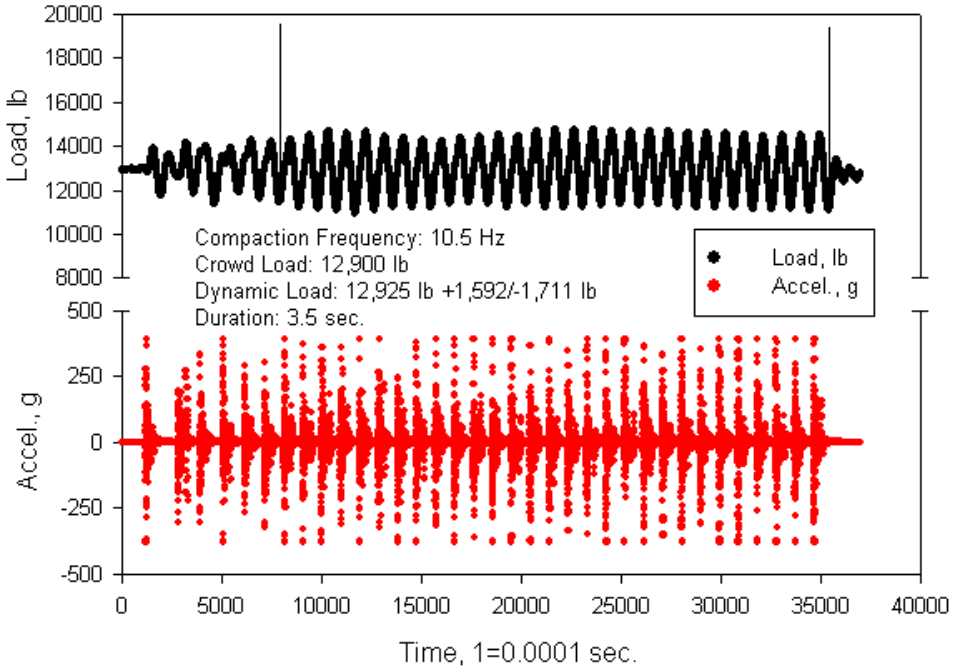


**Figure 368. Oskaloosa test 9 segment 4**

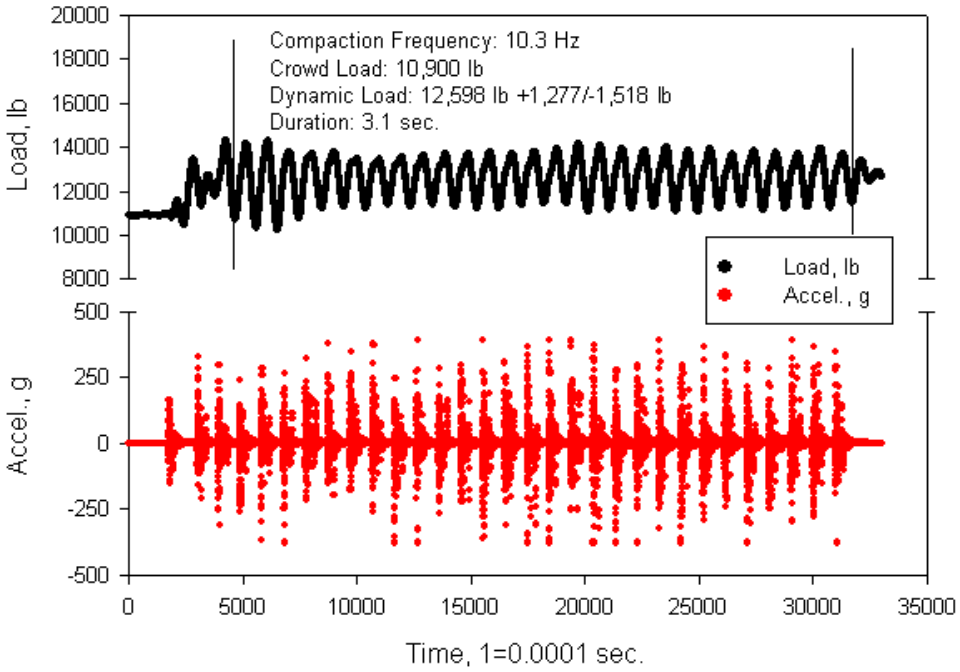


**Figure 369. Oskaloosa test 10 segment 1**

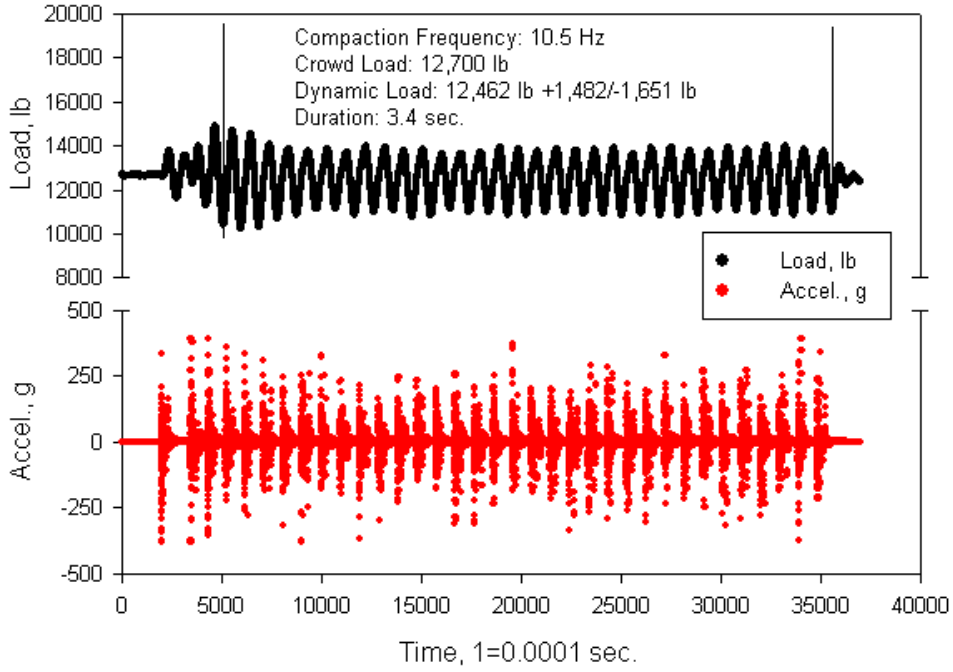


**Figure 370. Oskaloosa test 10 segment 2**

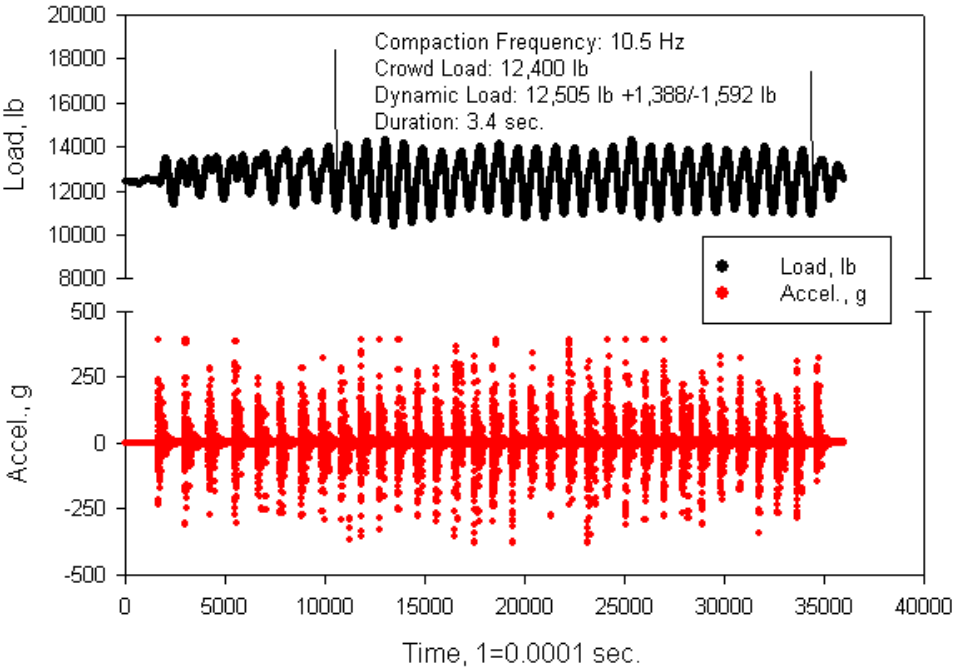


**Figure 371. Oskaloosa test 10 segment 3**

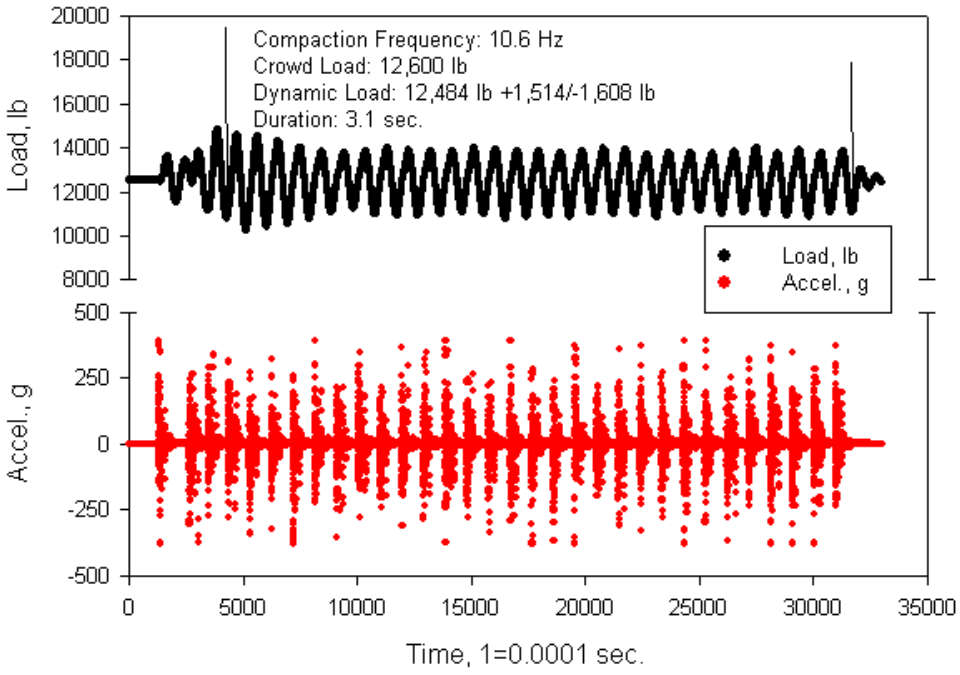


**Figure 372. Oskaloosa test 10 segment 4**

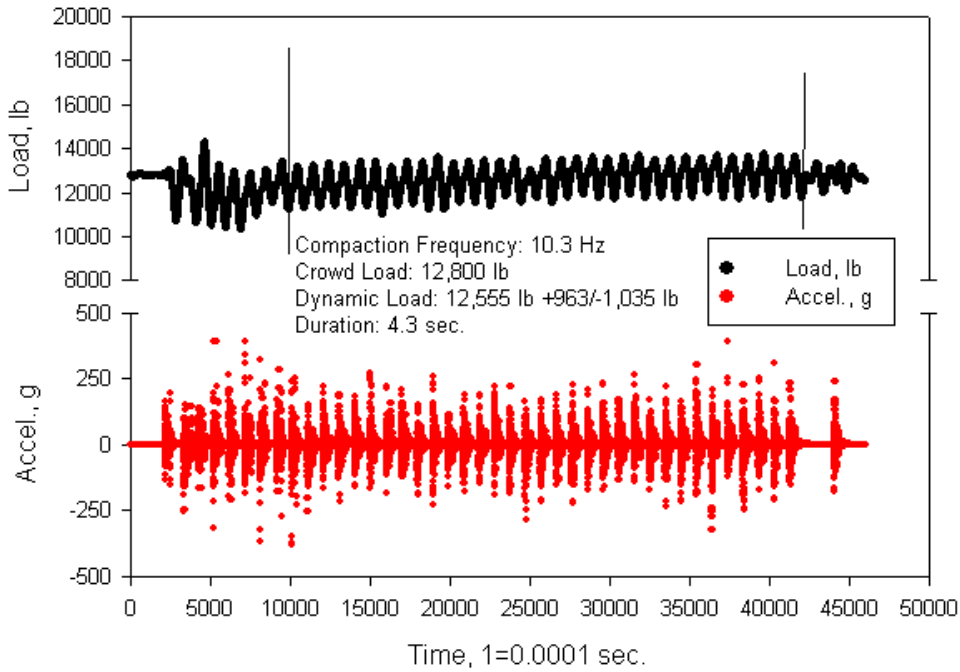


**Figure 373. Oskaloosa test 11 segment 1**

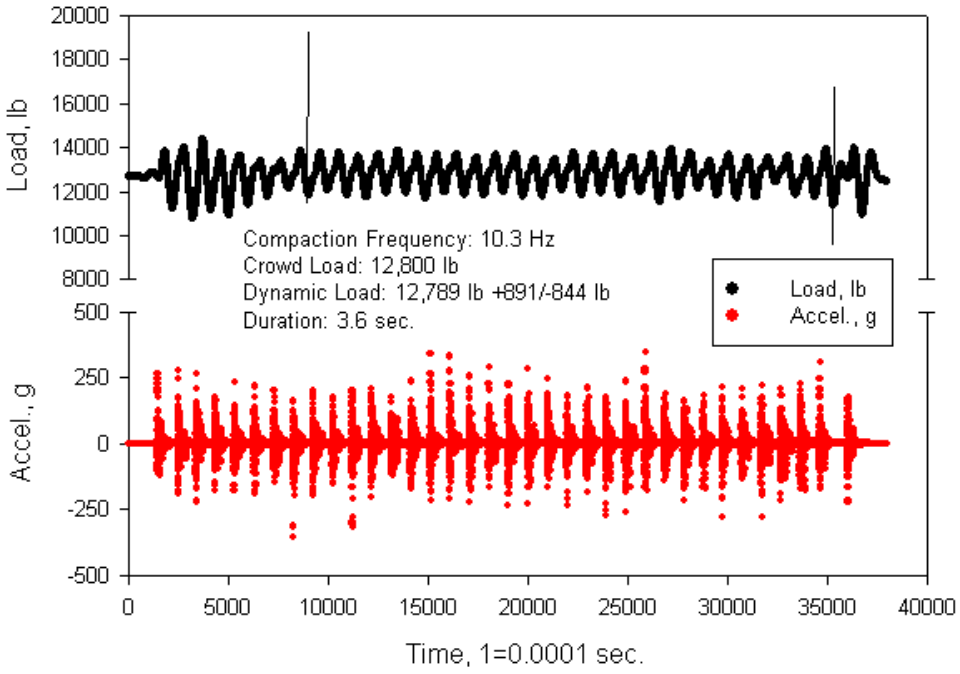


**Figure 374. Oskaloosa test 11 segment 2**

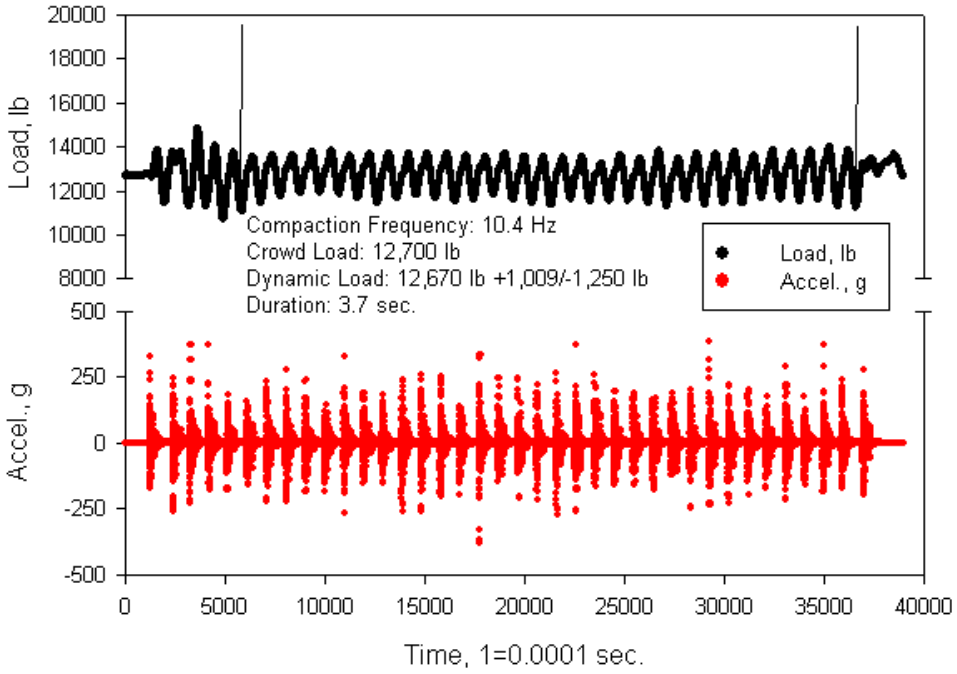


**Figure 375. Oskaloosa test 11 segment 3**

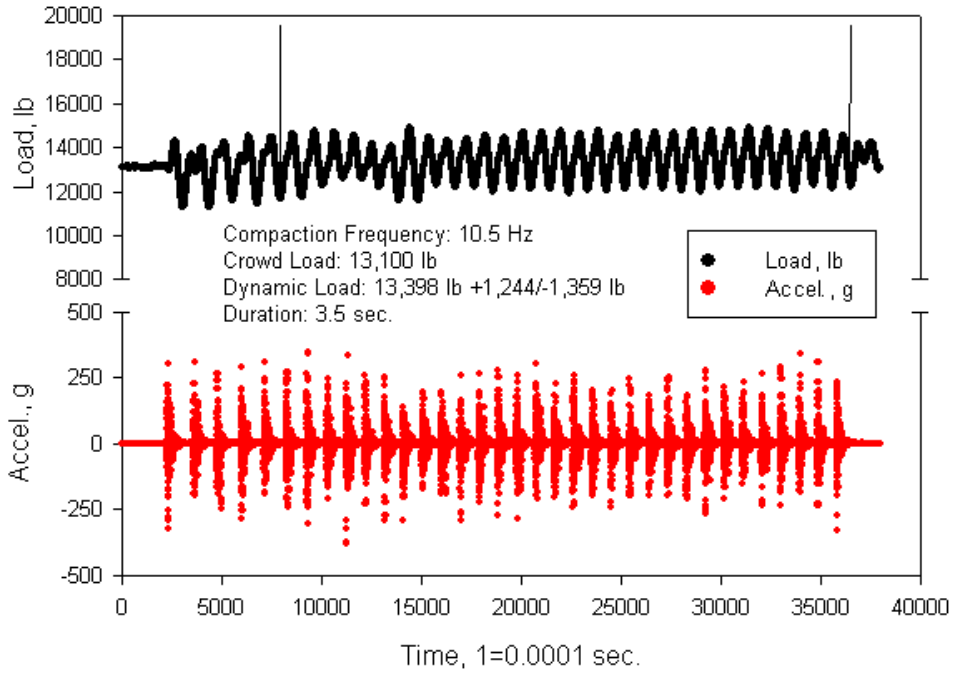


**Figure 376. Oskaloosa test 11 segment 4**

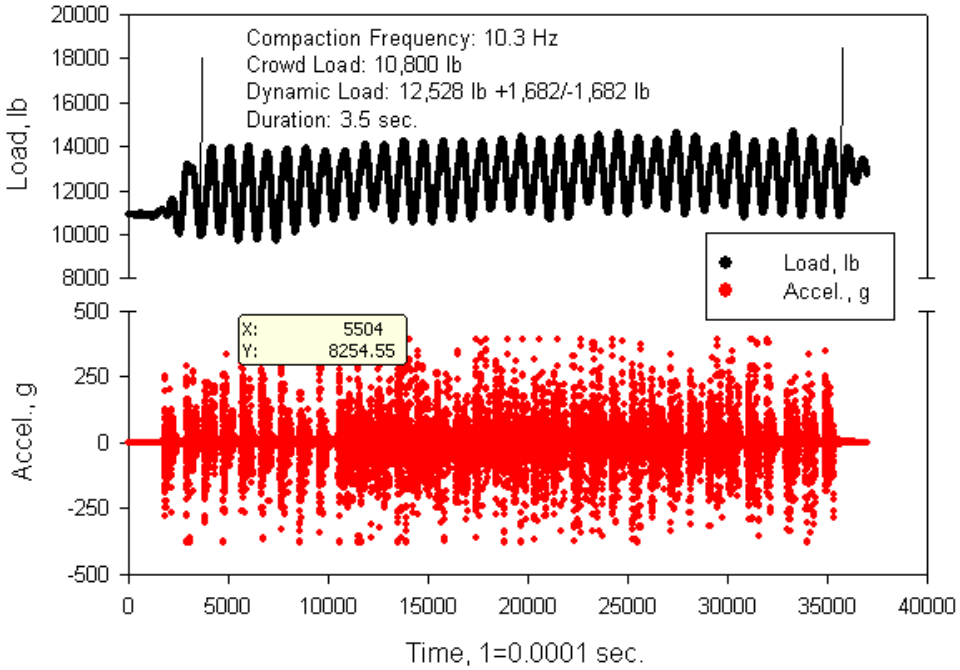


**Figure 377. Oskaloosa test 12 segment 1**

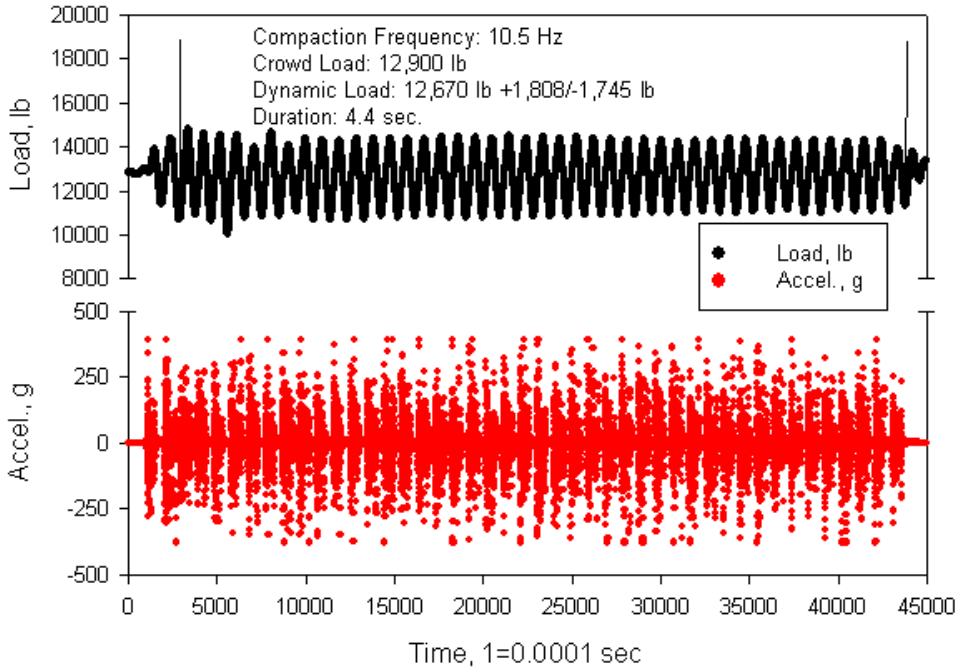


**Figure 378. Oskaloosa test 12 segment 2**

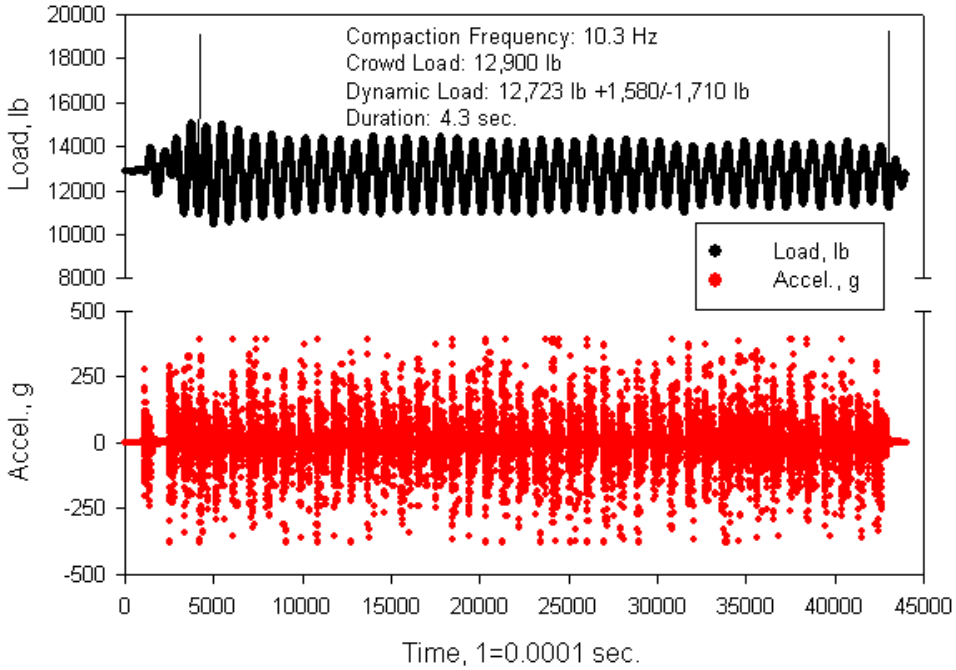


**Figure 379. Oskaloosa test 12 segment 3**

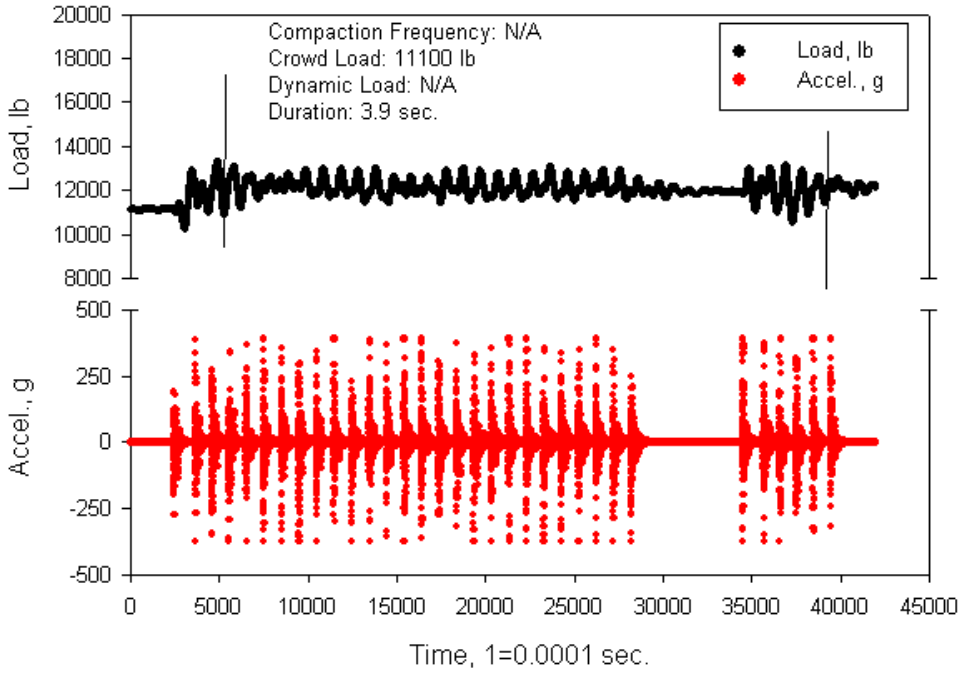


**Figure 380. Oskaloosa test 13 segment 1**

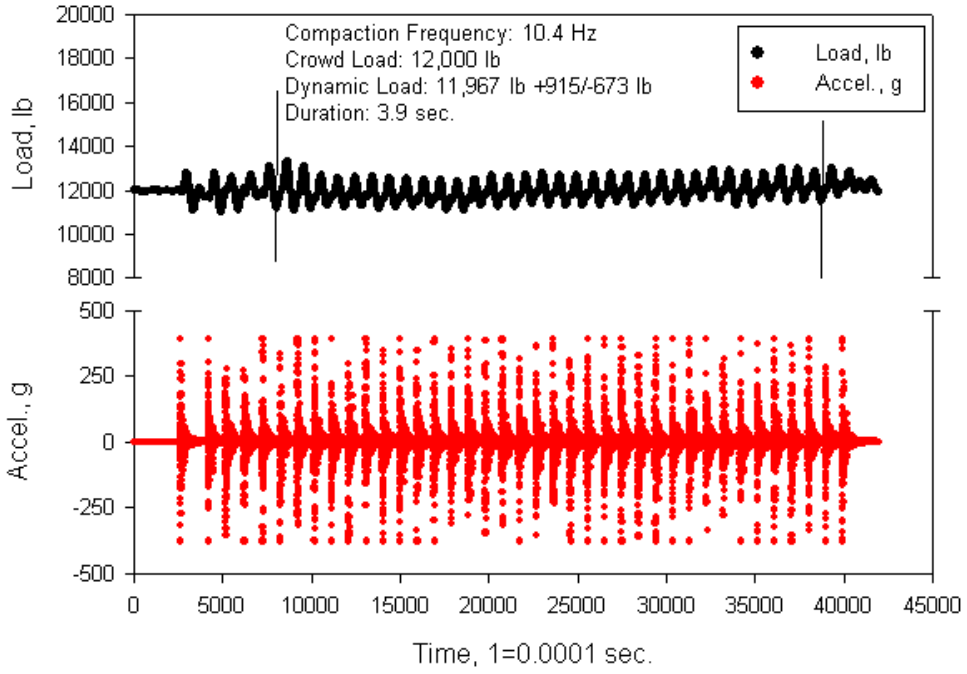


**Figure 381. Oskaloosa test 13 segment 2**

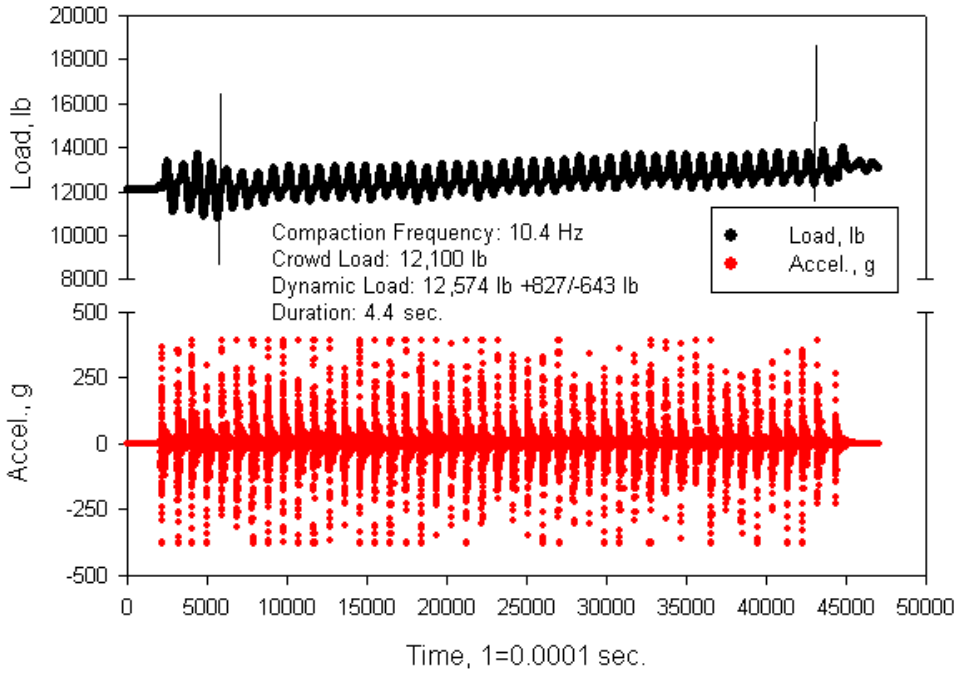


**Figure 382. Oskaloosa test 13 segment 3**

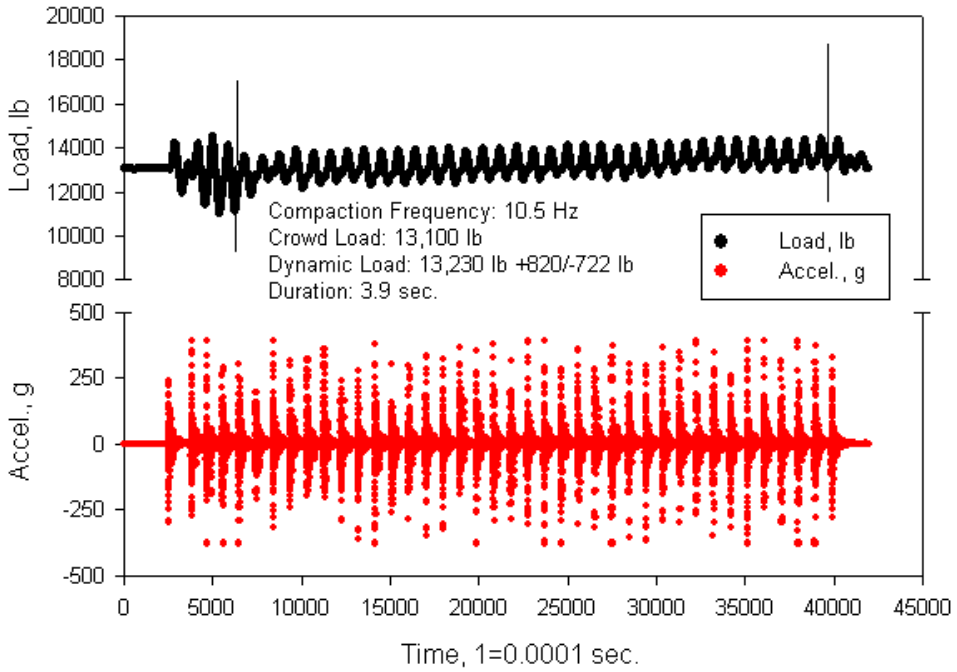


**Figure 383. Oskaloosa test 13 segment 4**

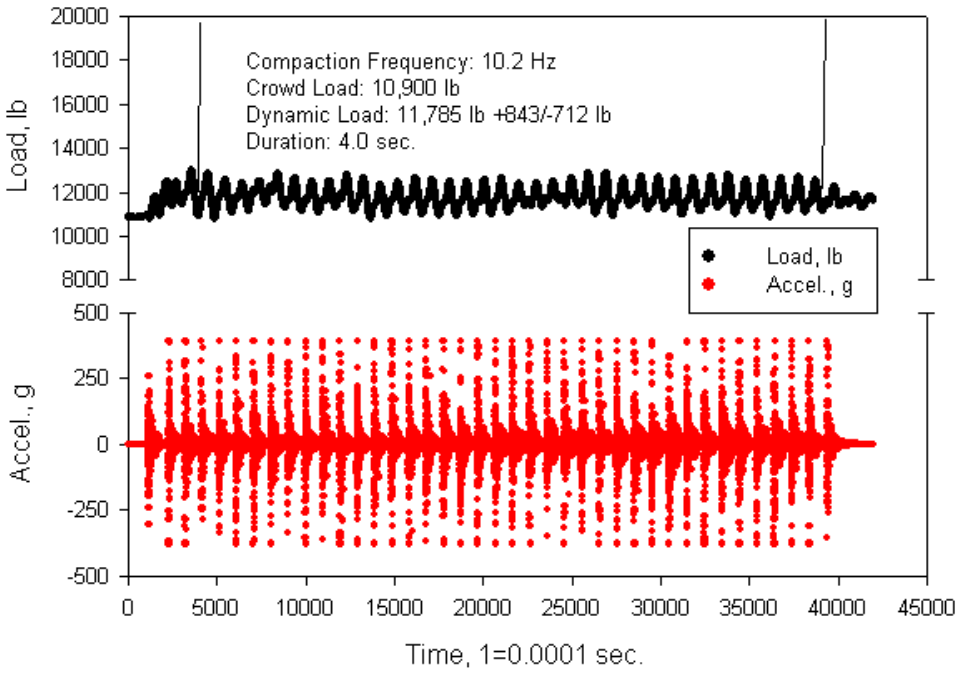


**Figure 384. Oskaloosa test 14 segment 1**

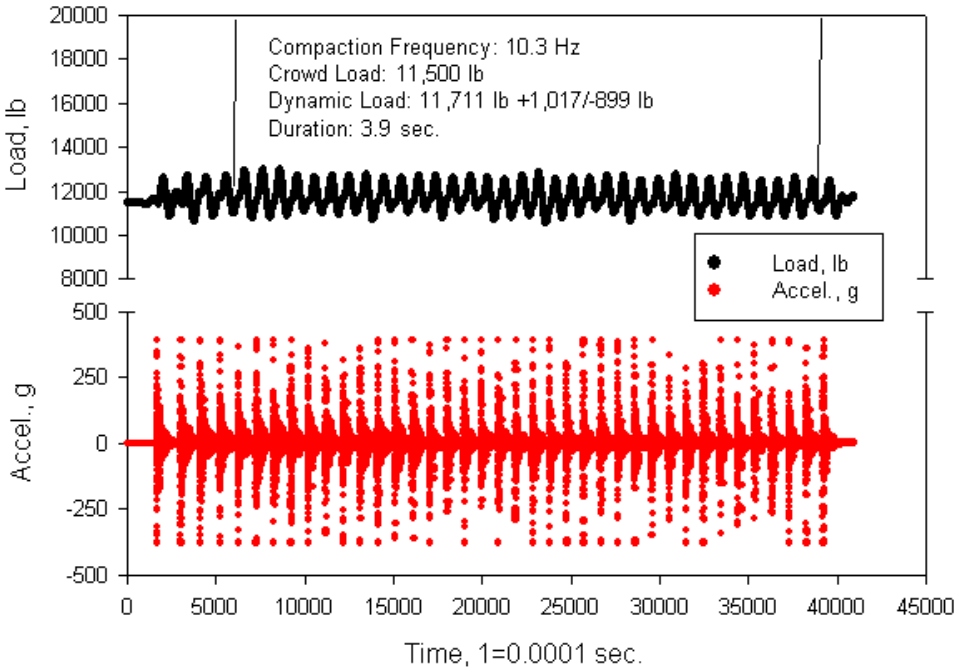


**Figure 385. Oskaloosa test 14 segment 2**

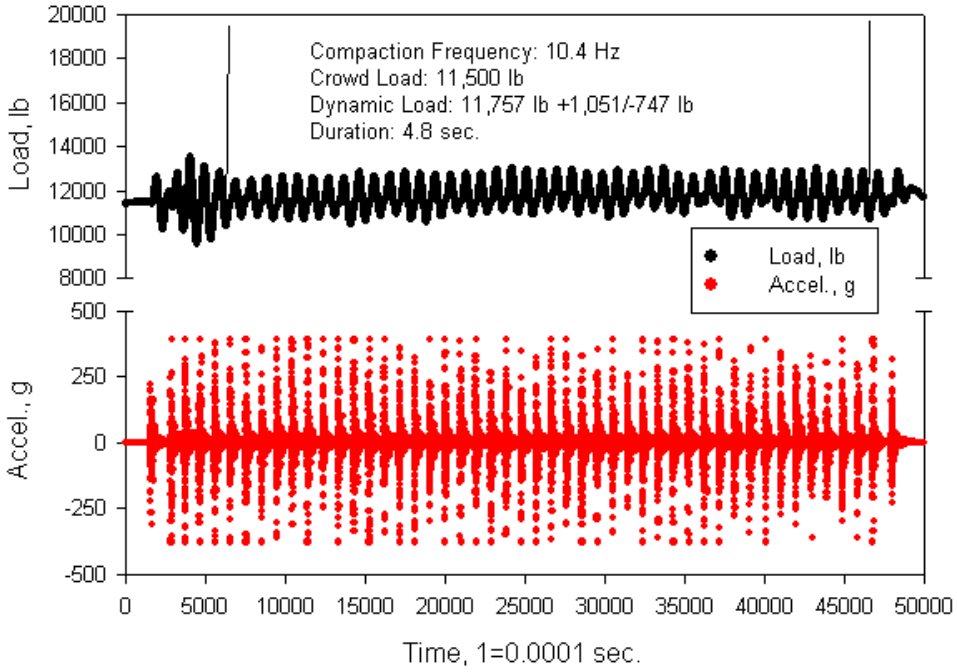


**Figure 386. Oskaloosa test 14 segment 3**

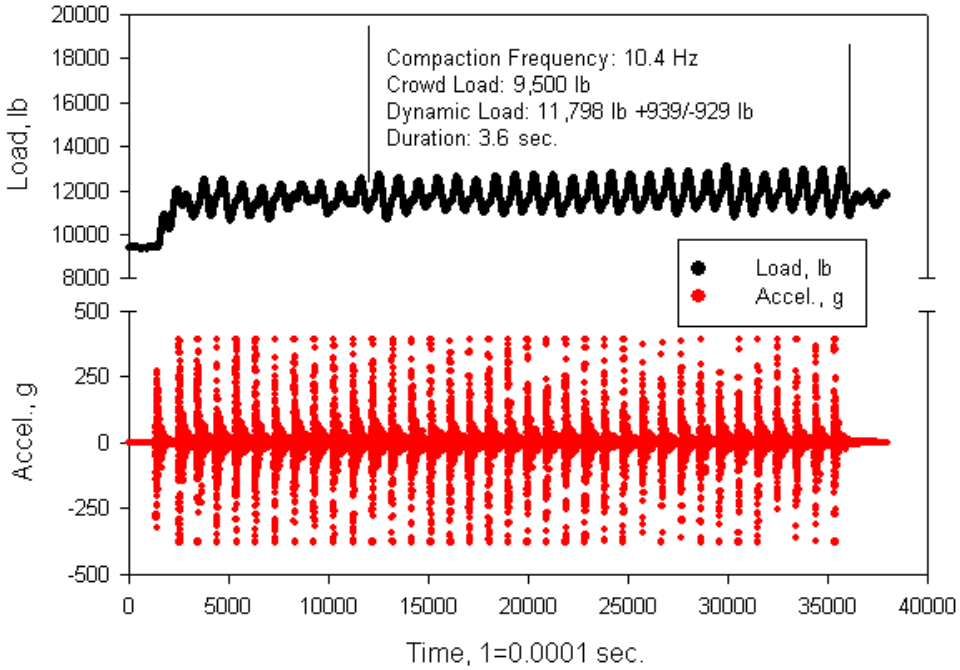


**Figure 387. Oskaloosa test 15 segment 1**

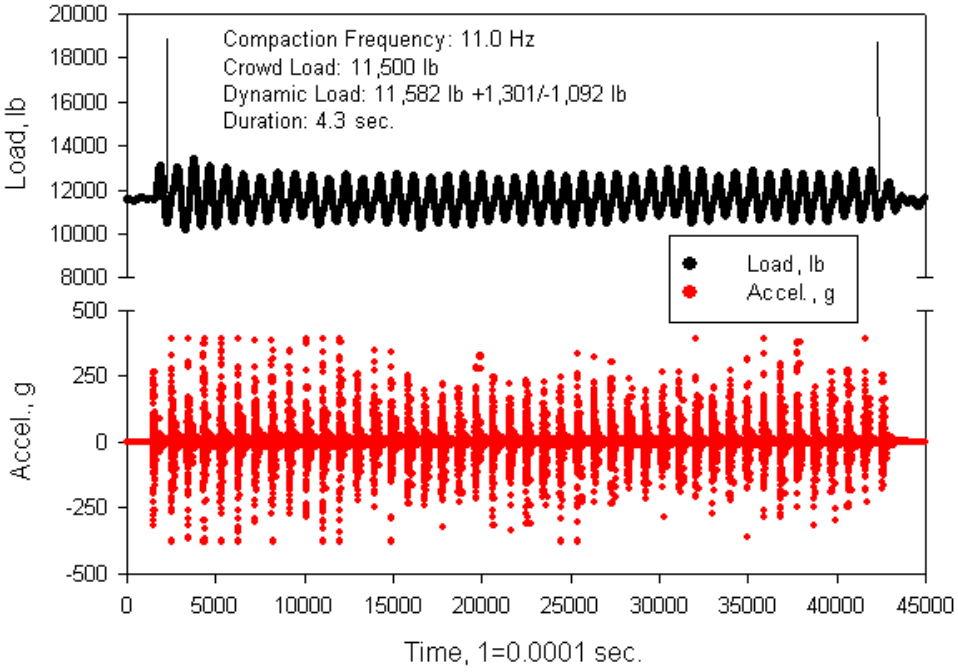


**Figure 388. Oskaloosa test 15 segment 2**

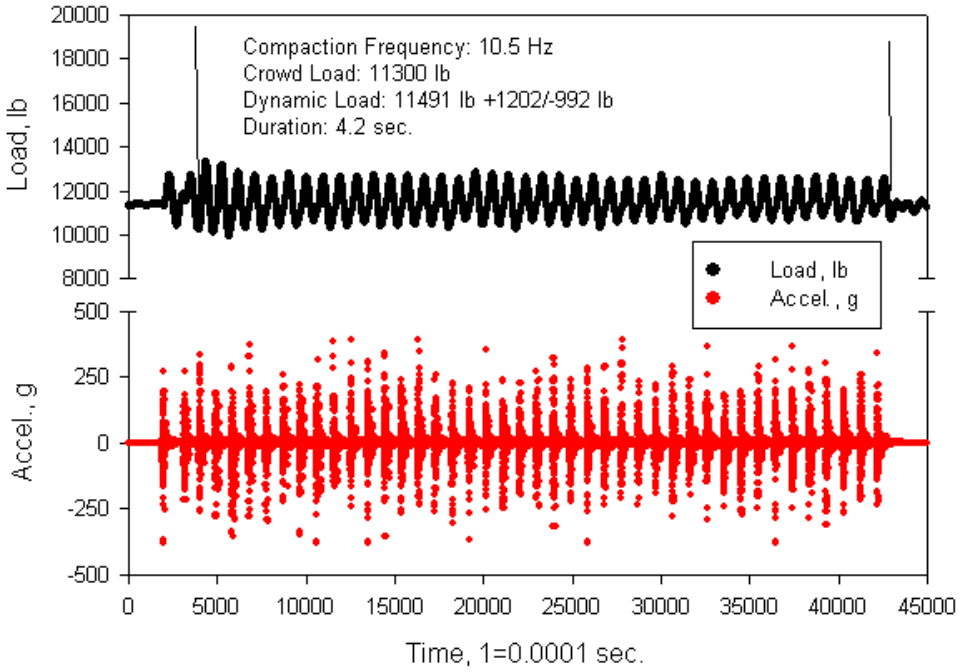


**Figure 389. Oskaloosa test 15 segment 3**

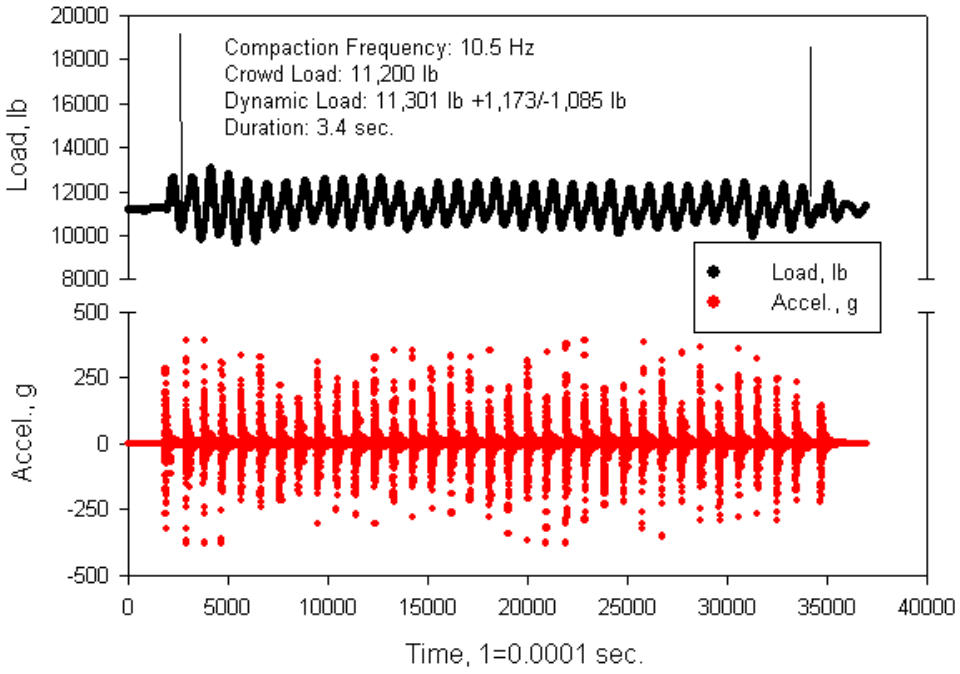


**Figure 390. Oskaloosa test 15 segment 4**

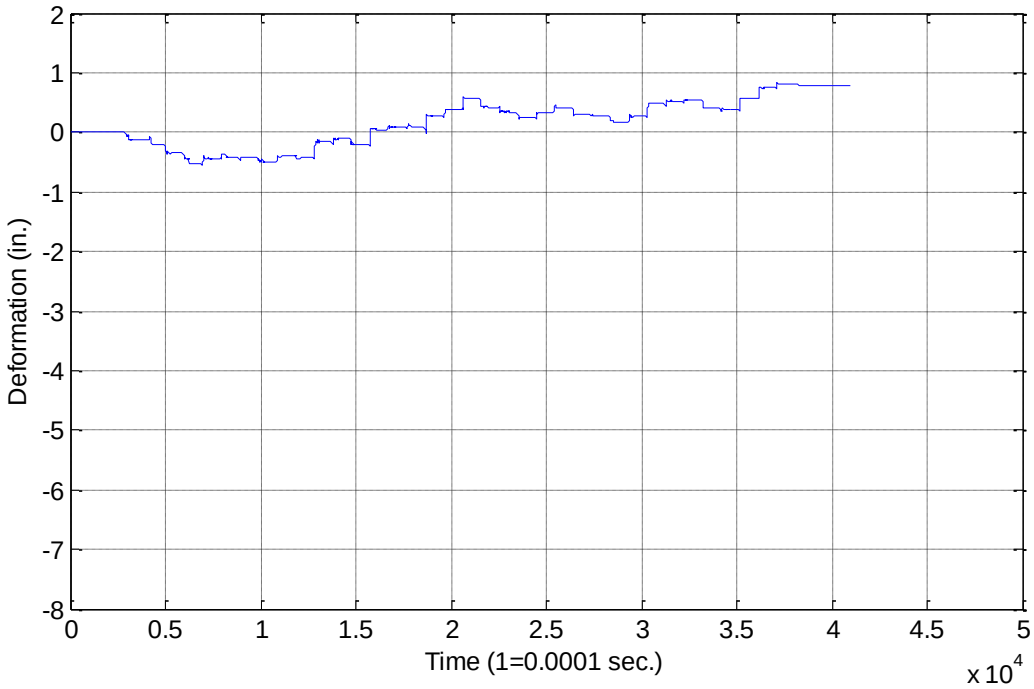


**Figure 391. Oskaloosa test 1 segment 1, 18 in. plate, acceleration analysis A**

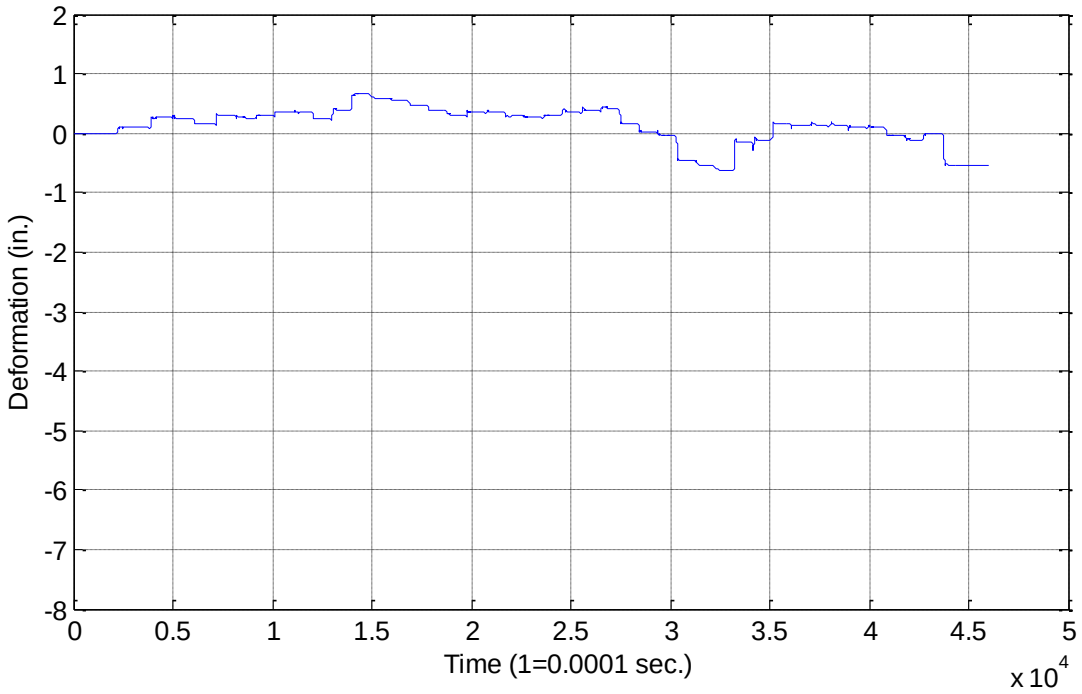


**Figure 392. Oskaloosa test 1 segment 2, 18 in. plate, acceleration analysis A**

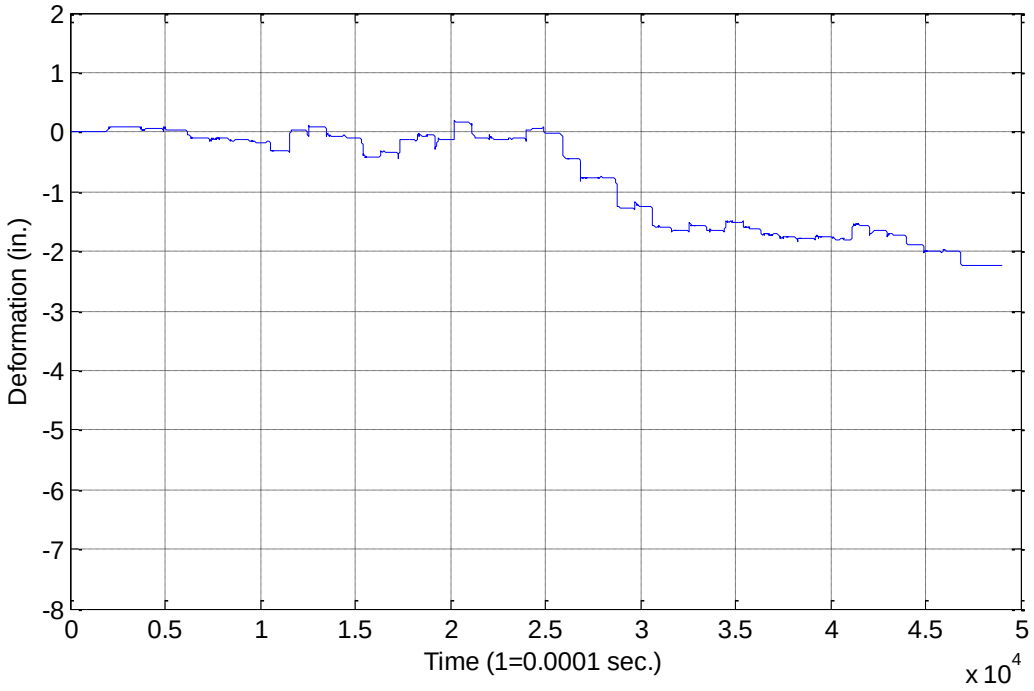


**Figure 393. Oskaloosa test 1 segment 3, 18 in. plate, acceleration analysis A**

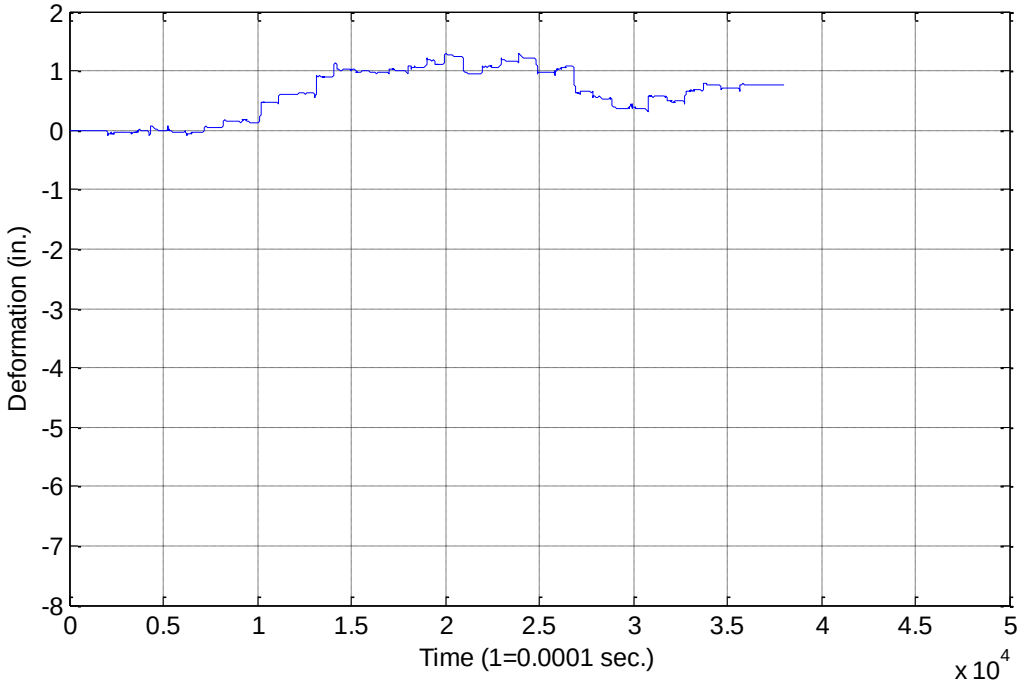


**Figure 394. Oskaloosa test 2 segment 1, 24 in. plate, acceleration analysis A**

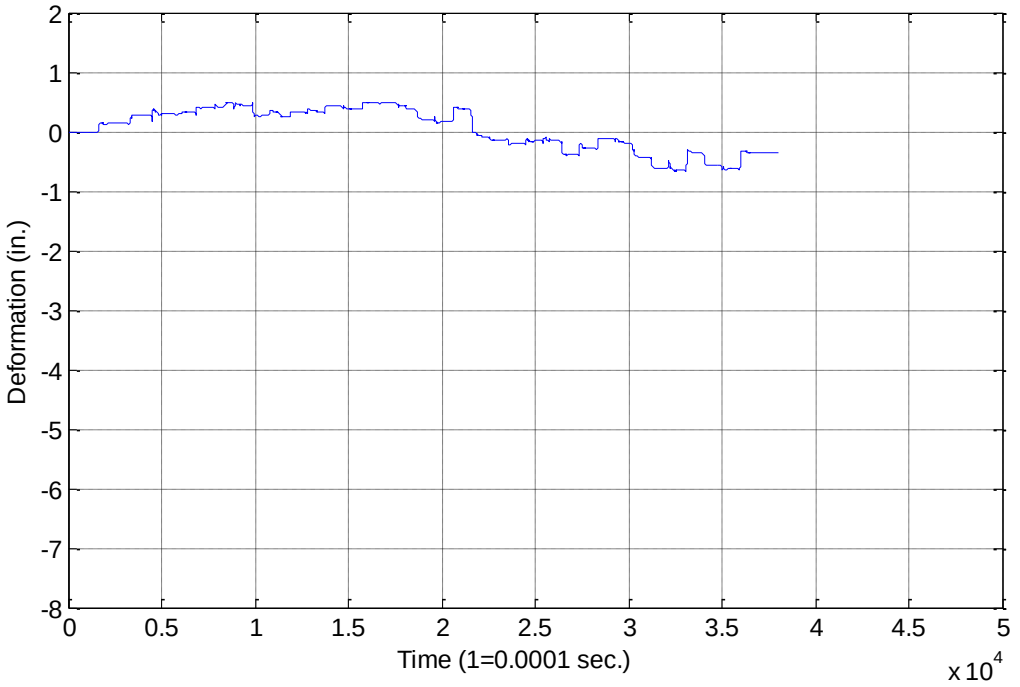


**Figure 395. Oskaloosa test 2 segment 2, 24 in. plate, acceleration analysis A**

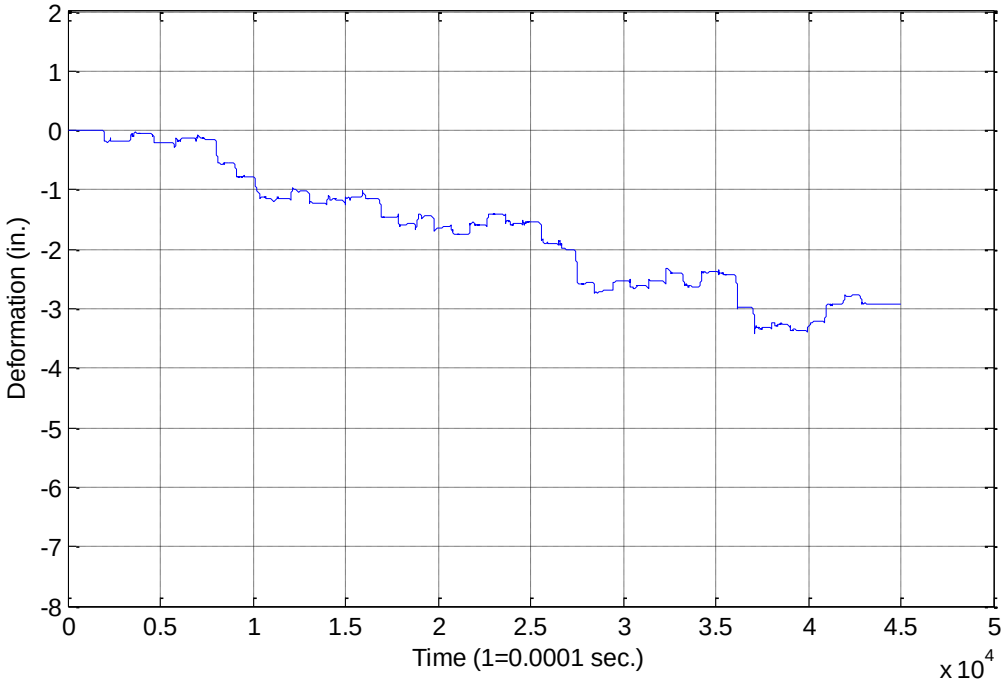


**Figure 396. Oskaloosa test 2 segment 3, 24 in. plate, acceleration analysis A**

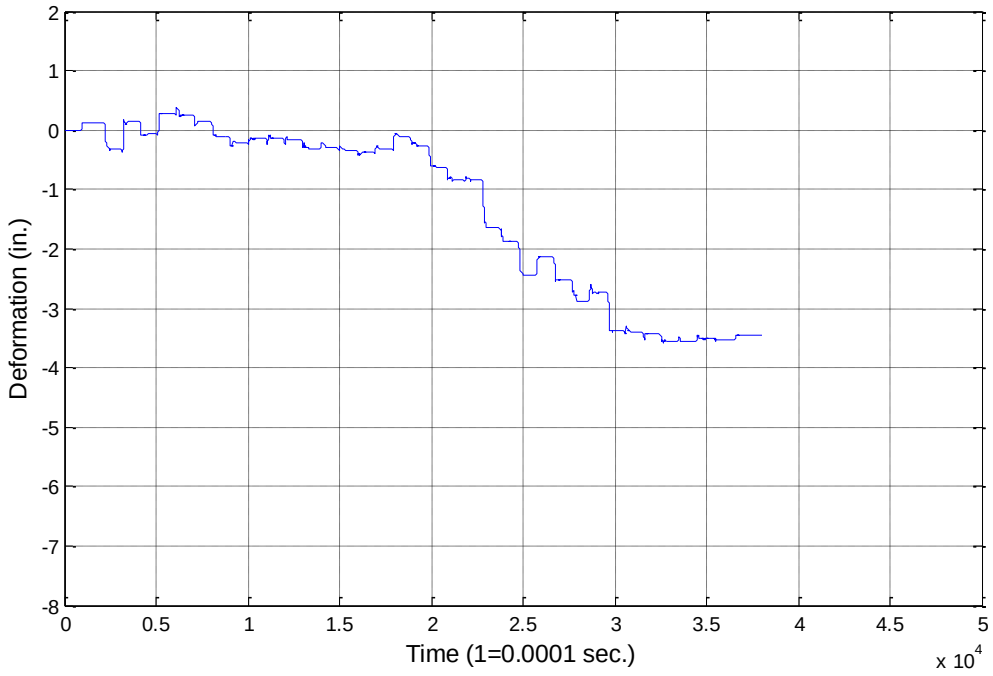


**Figure 397. Oskaloosa test 3 segment 1, 18 in. plate, acceleration analysis A**

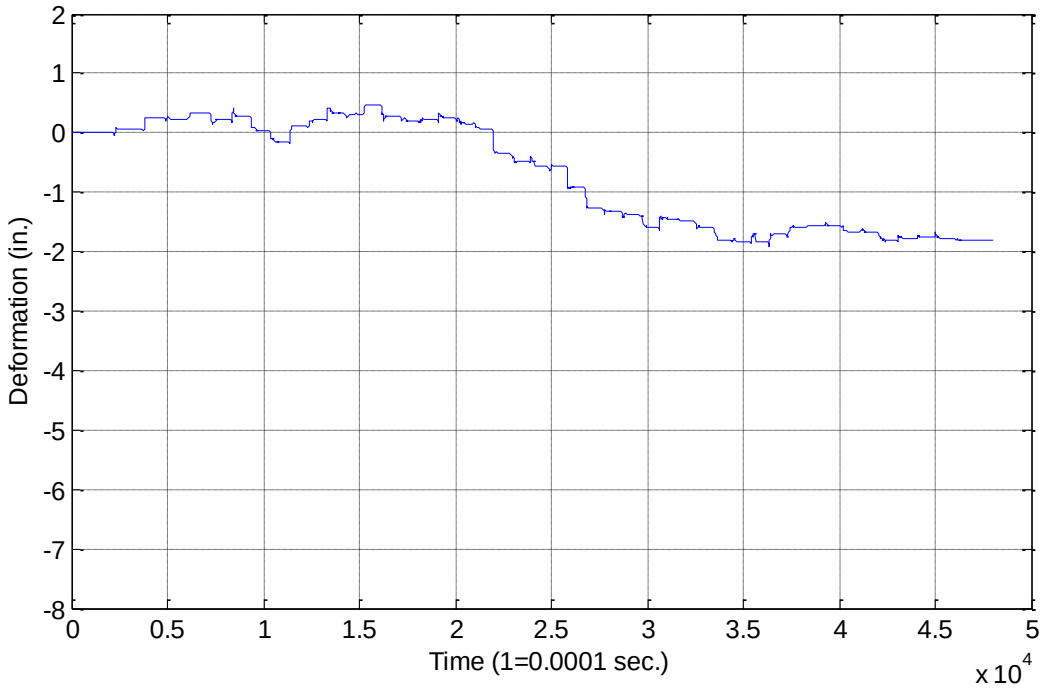


**Figure 398. Oskaloosa test 3 segment 2, 18 in. plate, acceleration analysis A**

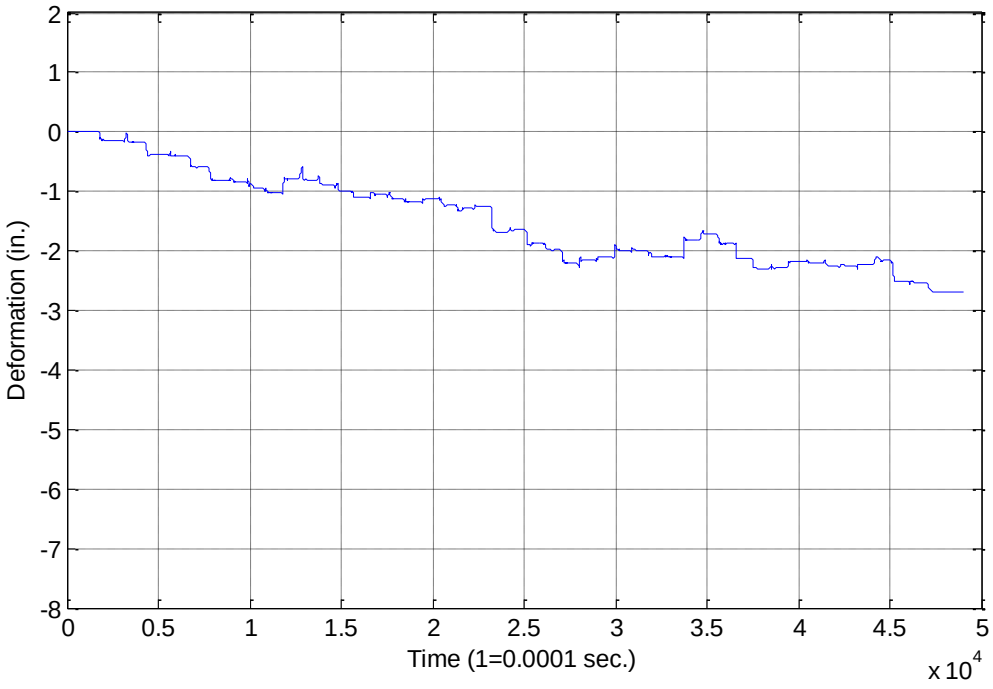


**Figure 399. Oskaloosa test 3 segment 3, 18 in. plate, acceleration analysis A**

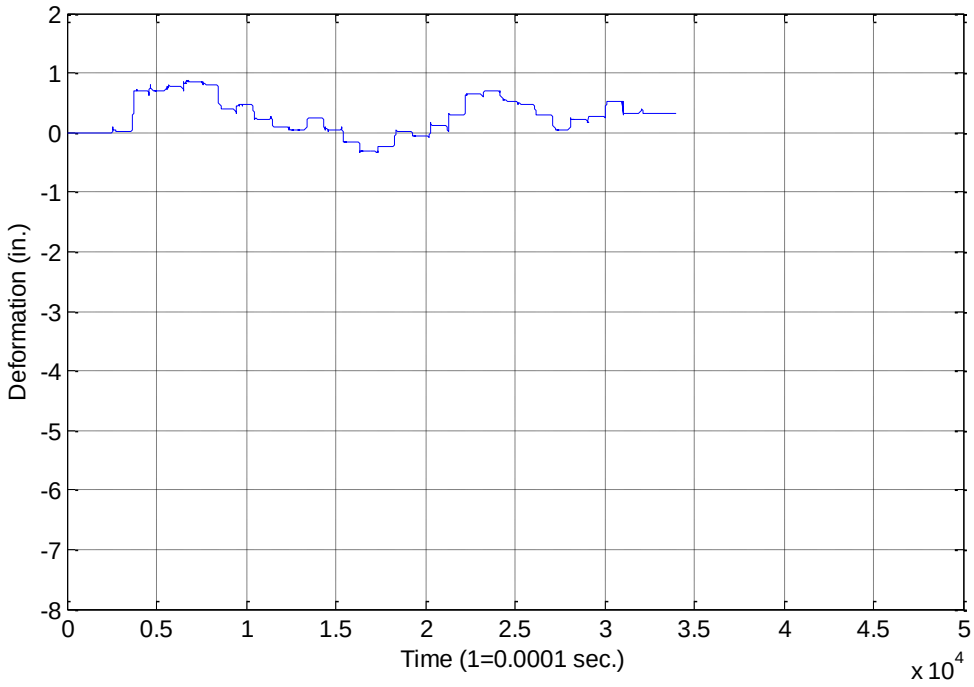


**Figure 400. Oskaloosa test 4 segment 1, 12 in. plate, acceleration analysis A**

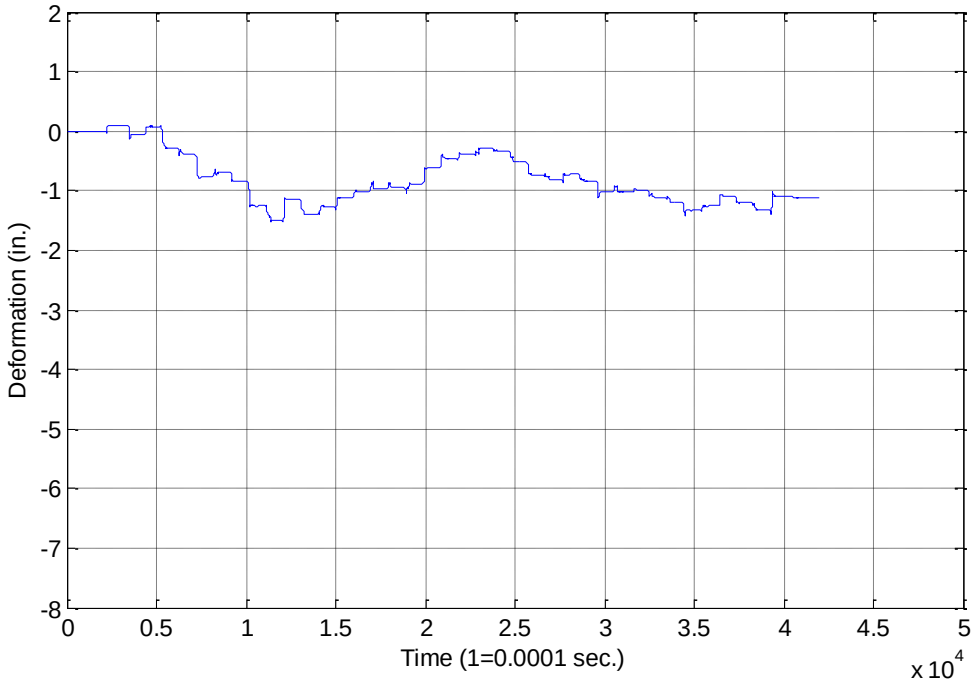


**Figure 401. Oskaloosa test 4 segment 2, 12 in. plate, acceleration analysis A**

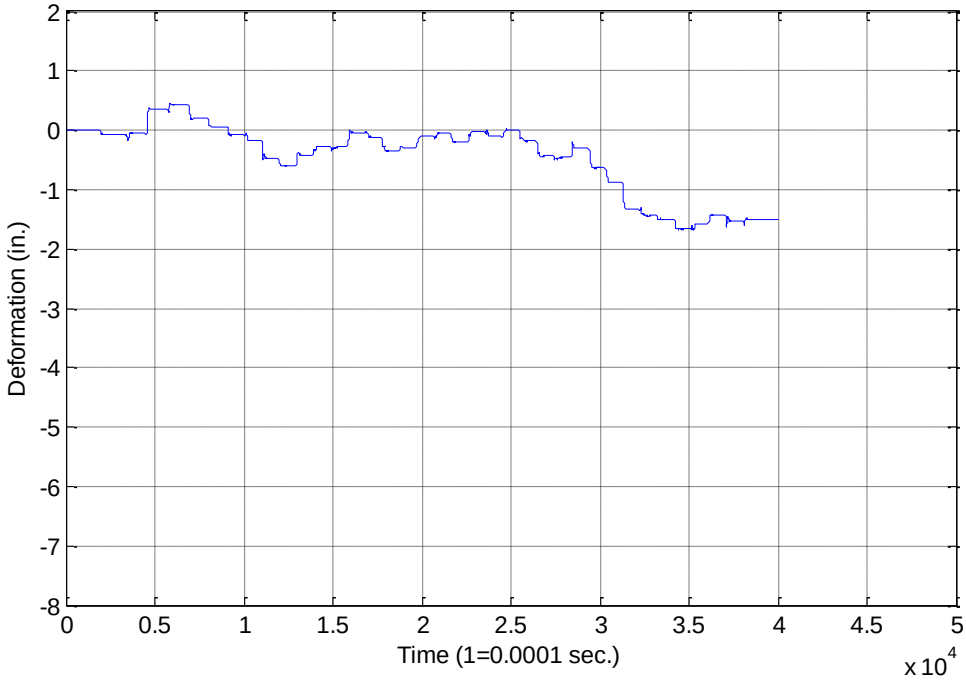


**Figure 402. Oskaloosa test 4 segment 3, 12 in. plate, acceleration analysis A**

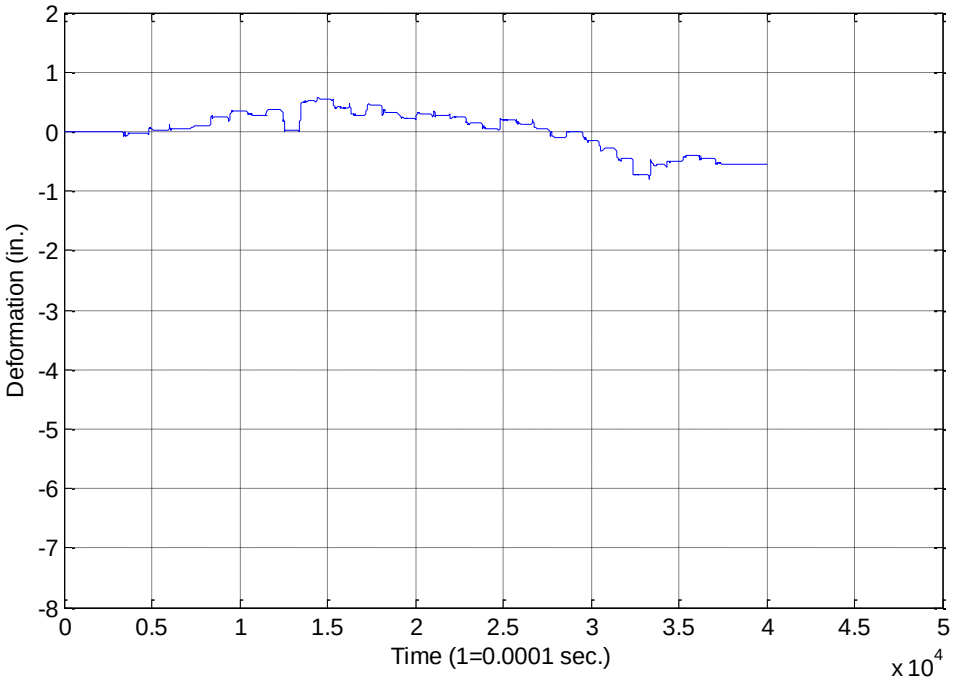


**Figure 403. Oskaloosa test 4 segment 4, 12 in. plate, acceleration analysis A**

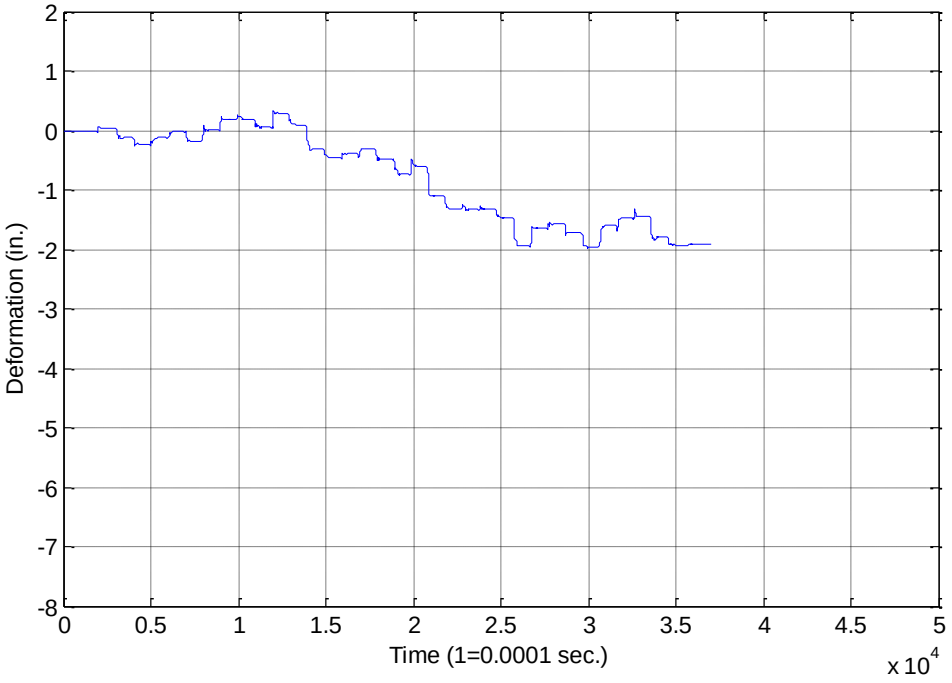


**Figure 404. Oskaloosa test 5 segment 1, 9 in. plate, acceleration analysis A**

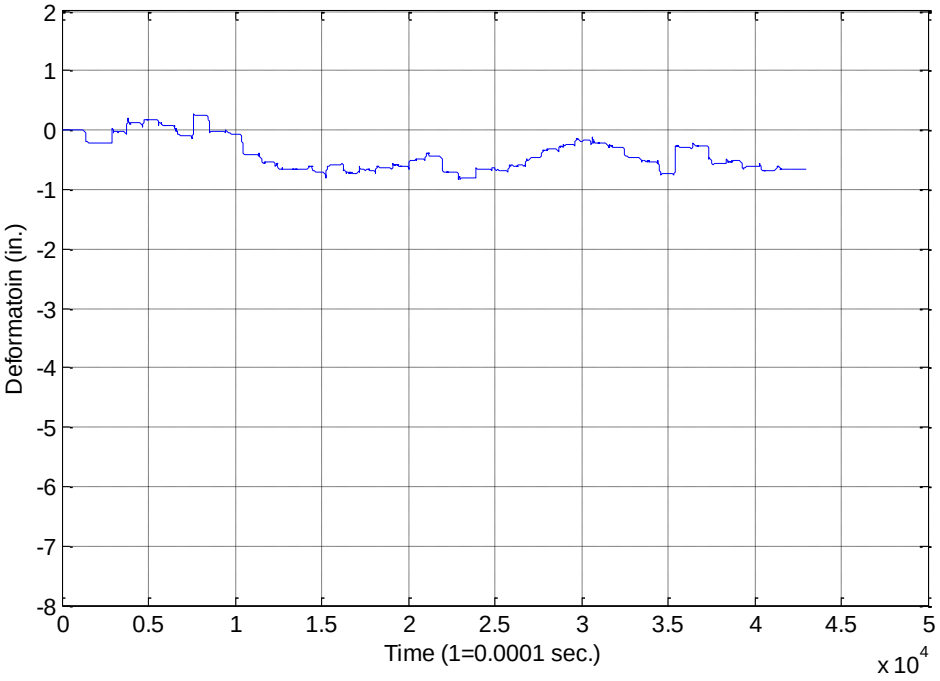


**Figure 405. Oskaloosa test 5 segment 2, 9 in. plate, acceleration analysis A**

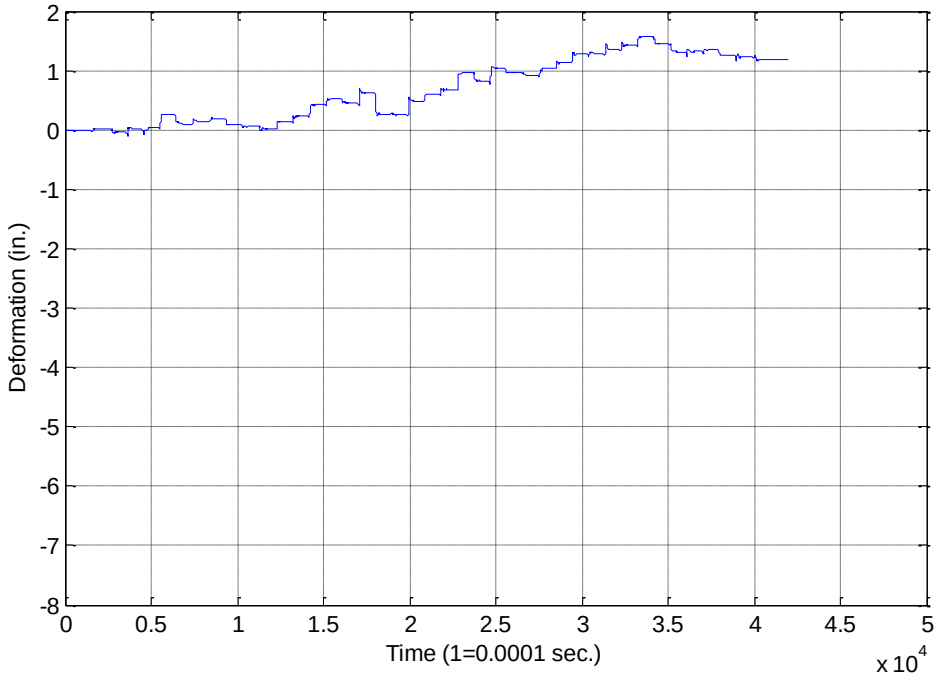


**Figure 406. Oskaloosa test 5 segment 3, 9 in. plate, acceleration analysis A**

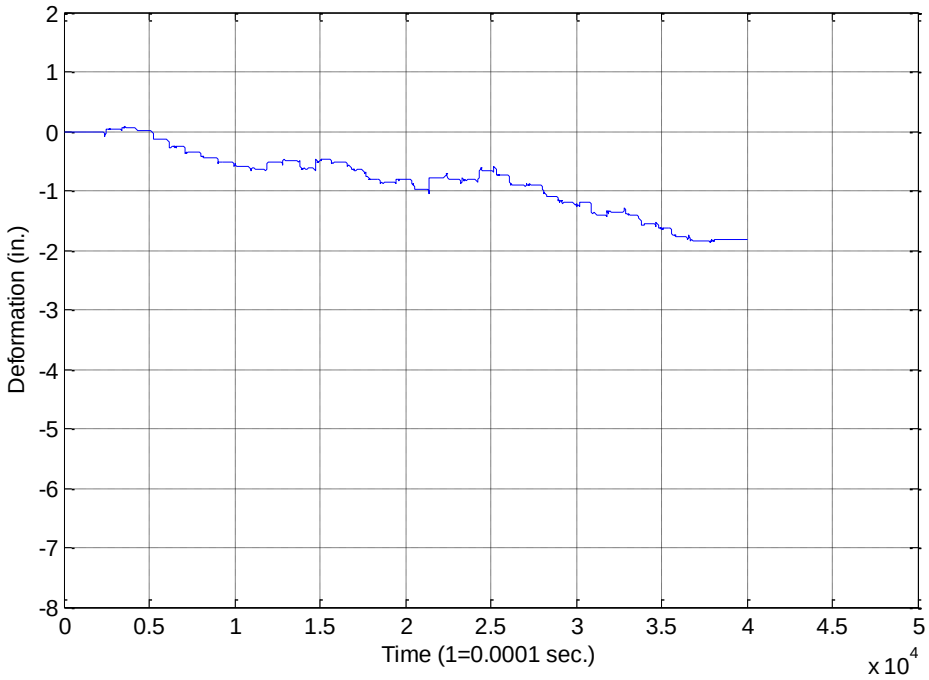


**Figure 407. Oskaloosa test 5 segment 4, 9 in. plate, acceleration analysis A**

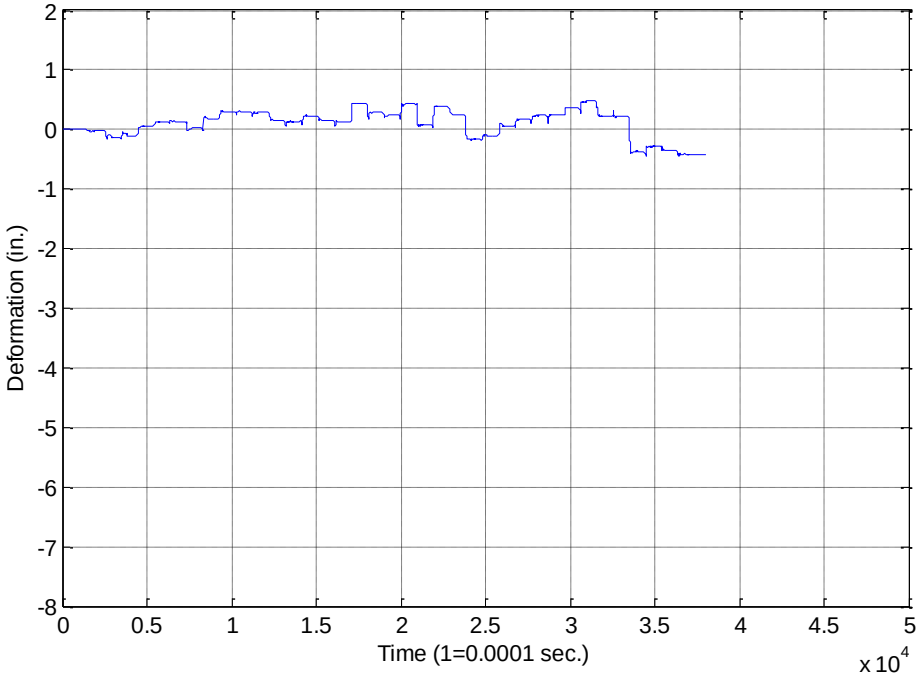


**Figure 408. Oskaloosa test 6 segment 1, 18 in. plate, acceleration analysis A**

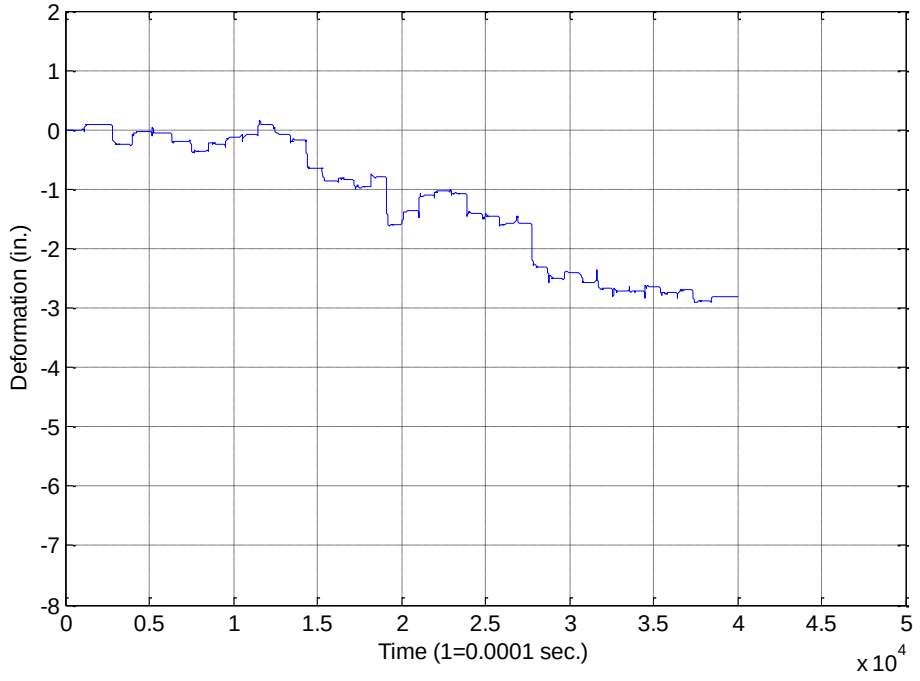


**Figure 409. Oskaloosa test 6 Segment 2, 18 in. plate, acceleration analysis A**

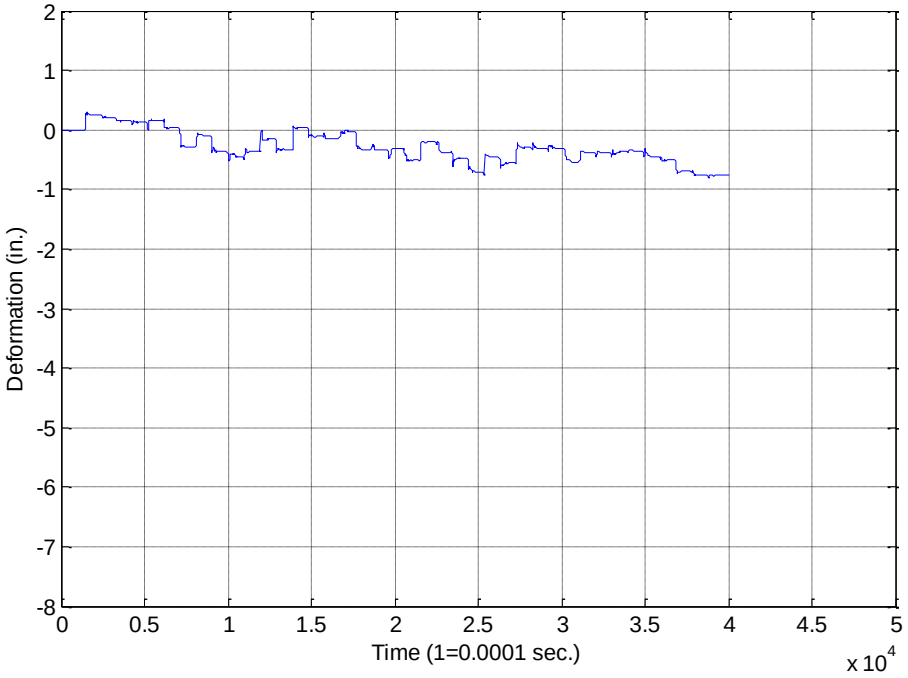


**Figure 410. Oskaloosa test 6 segment 3, 18 in. plate, acceleration analysis A**

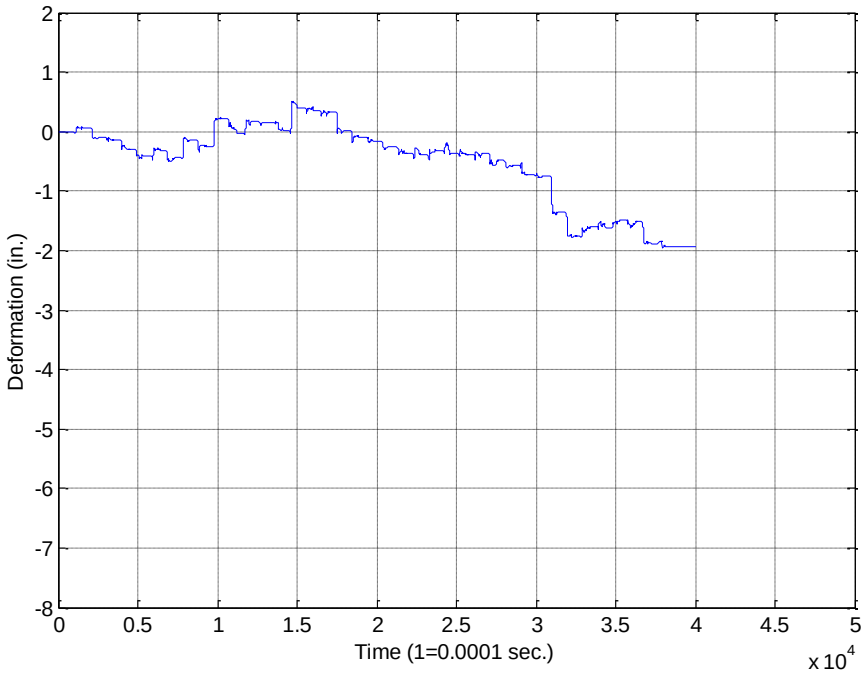


**Figure 411. Oskaloosa test 7 segment 1, 24 in. plate, acceleration analysis A**

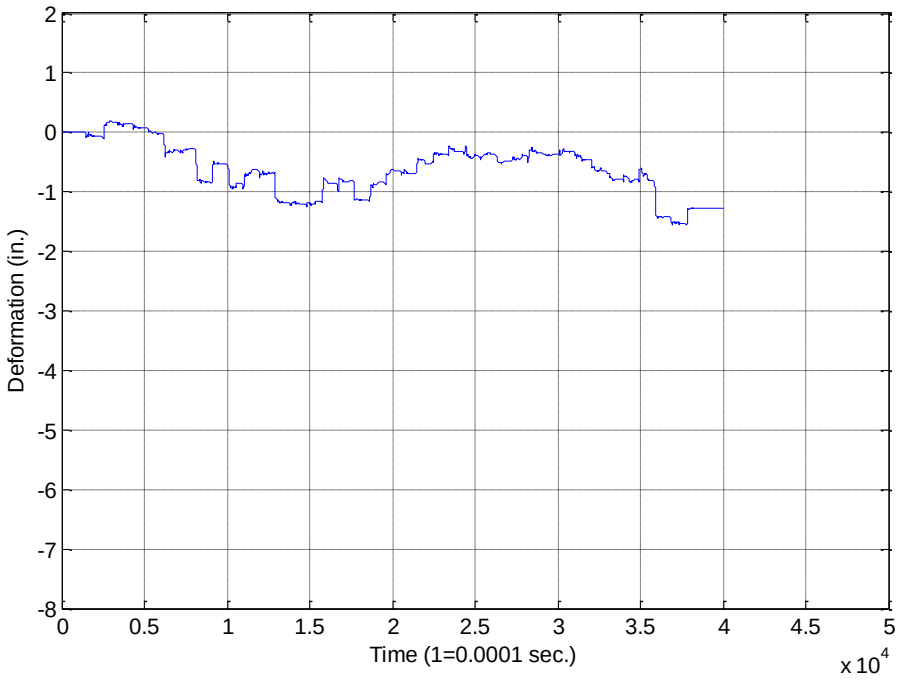


**Figure 412. Oskaloosa test 7 segment 2, 24 in. plate, acceleration analysis A**

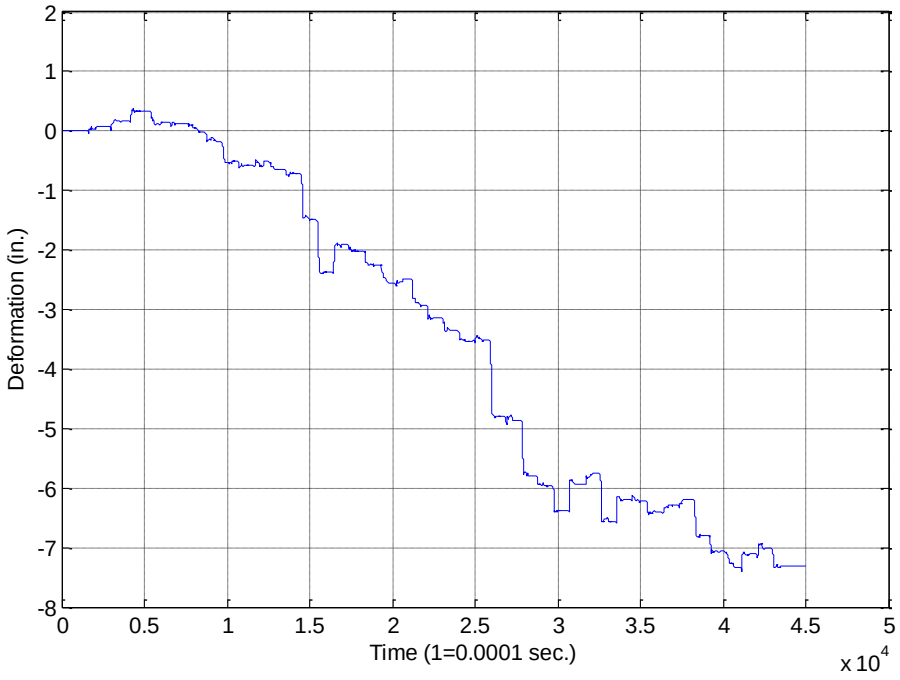


**Figure 413. Oskaloosa test 7 segment 3, 24 in. plate, acceleration analysis A**

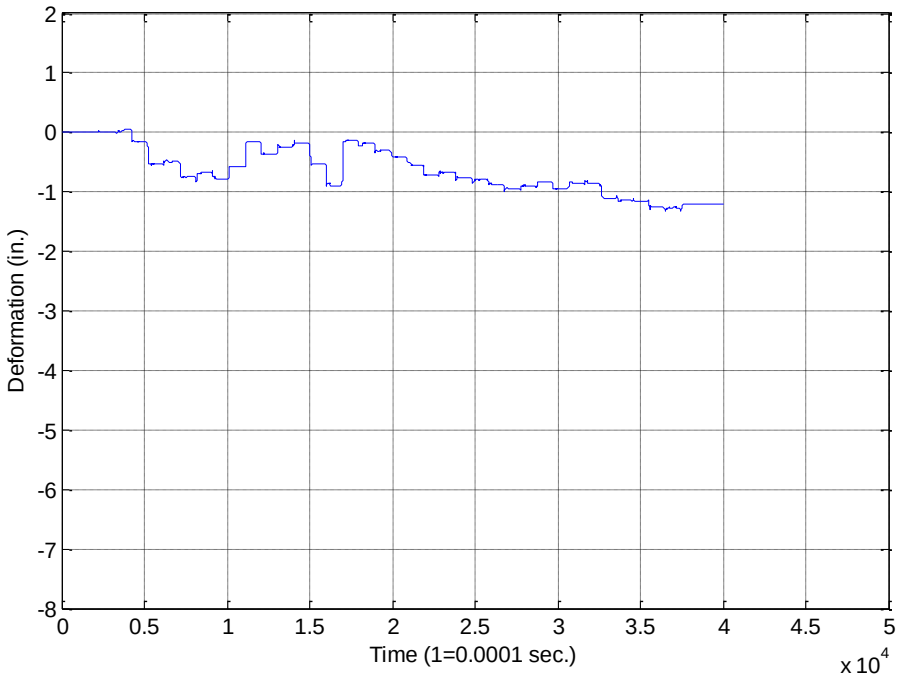


**Figure 414. Oskaloosa test 8 segment 1, 18 in. plate, acceleration analysis A**

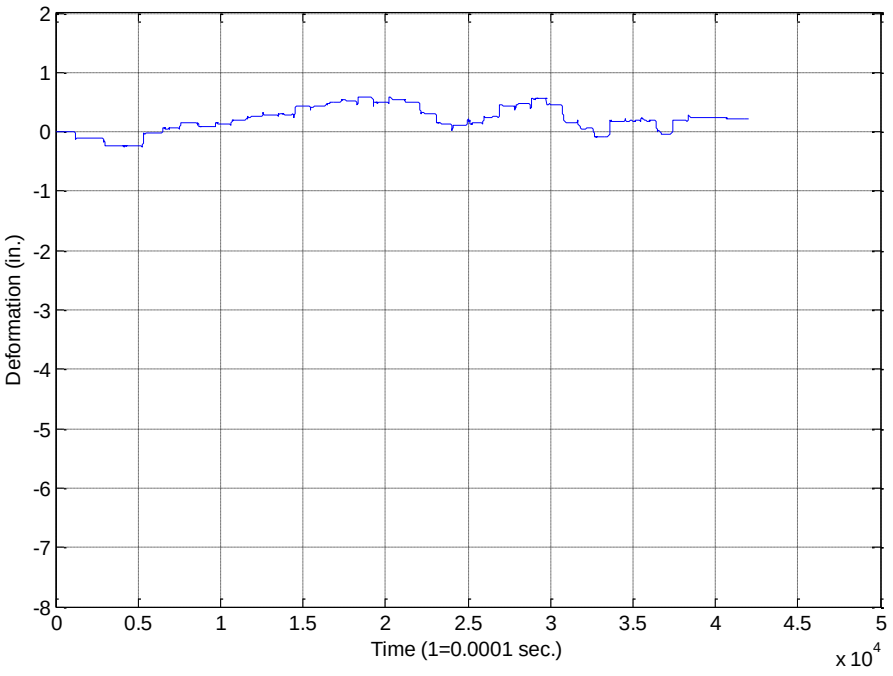


**Figure 415. Oskaloosa test 8 segment 2, 18 in. plate, acceleration analysis A**

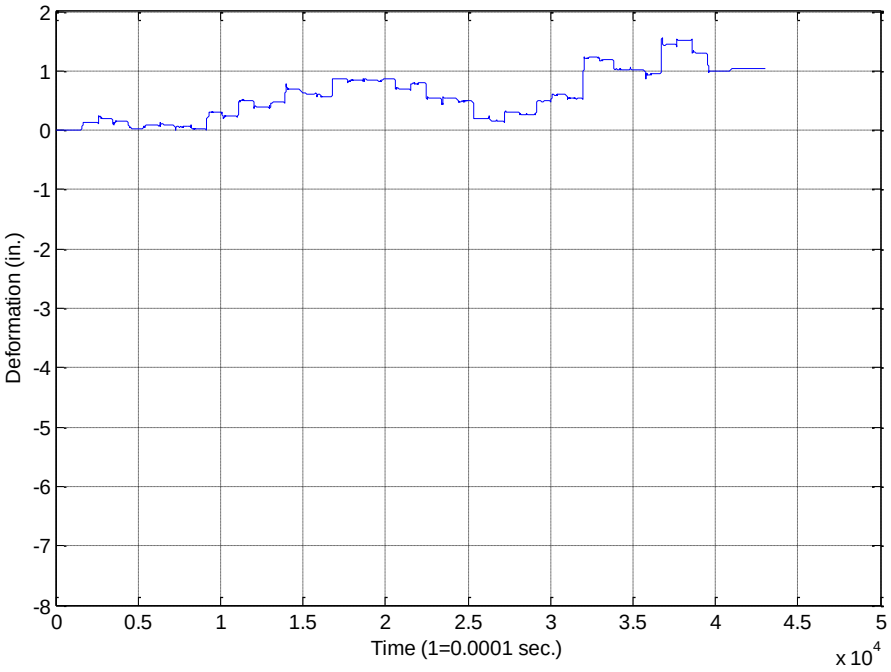


**Figure 416. Oskaloosa test 8 segment 3, 18 in. plate, acceleration analysis A**

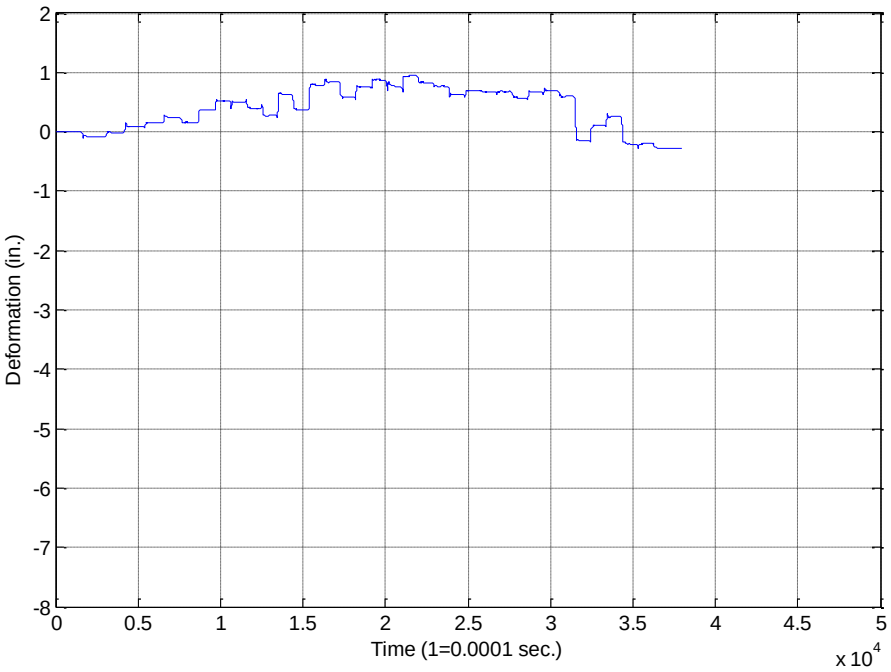


**Figure 417. Oskaloosa test 8 segment 4, 18 in. plate, acceleration analysis A**

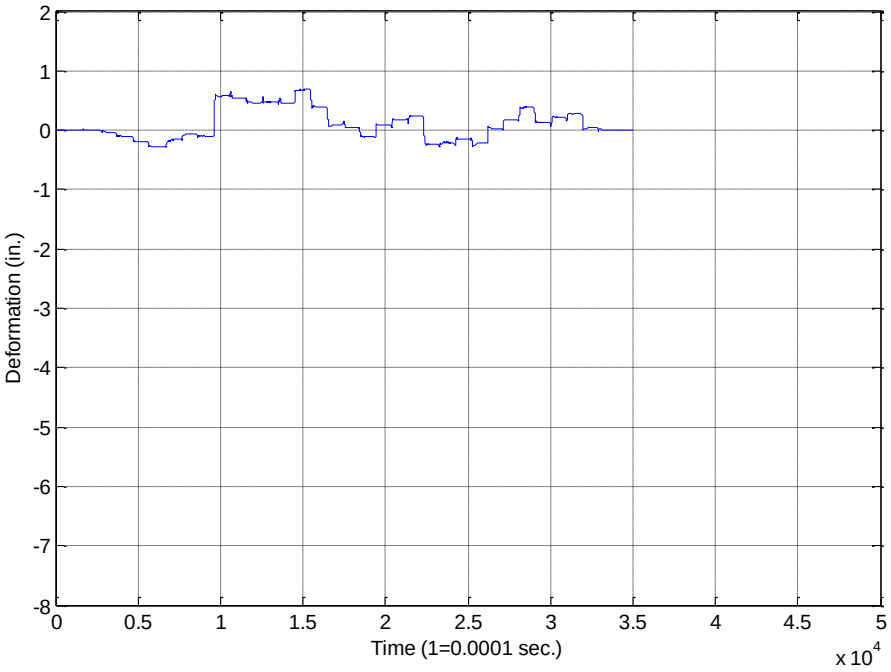


**Figure 418. Oskaloosa test 9 segment 1, 12 in. plate, acceleration analysis A**

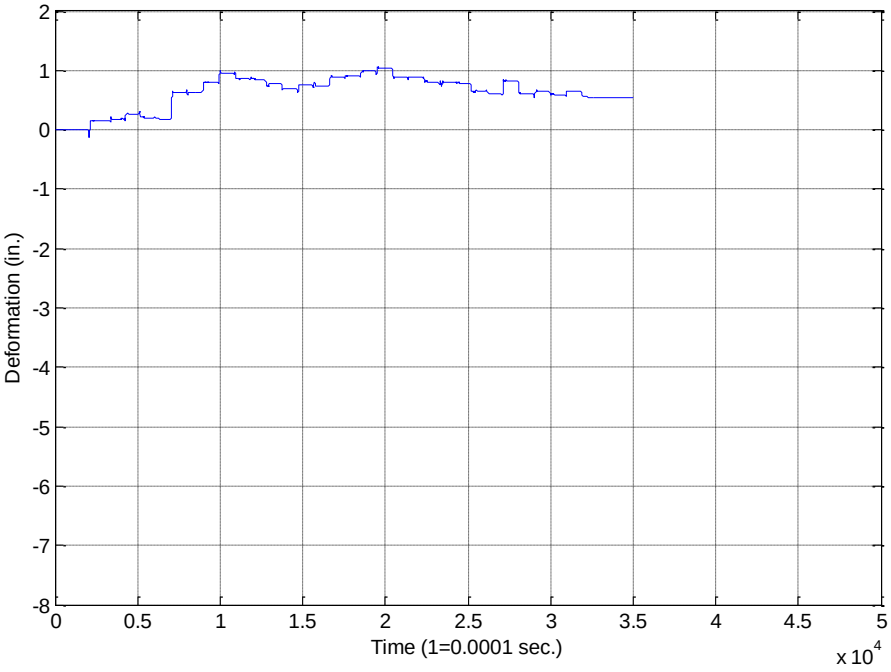


**Figure 419. Oskaloosa test 9 segment 2, 12 in. plate, acceleration analysis A**

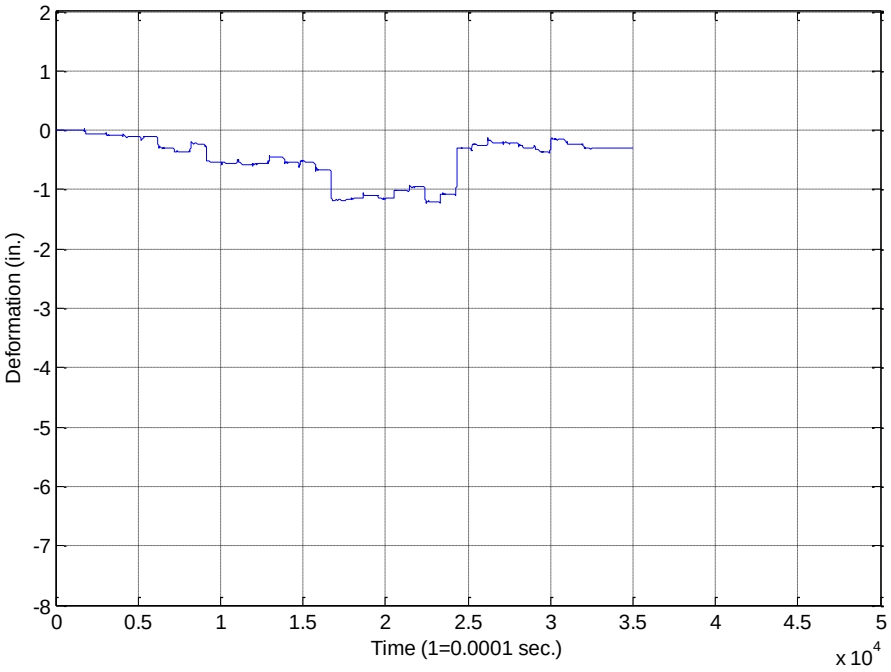


**Figure 420. Oskaloosa test 9 segment 3, 12 in. plate, acceleration analysis A**

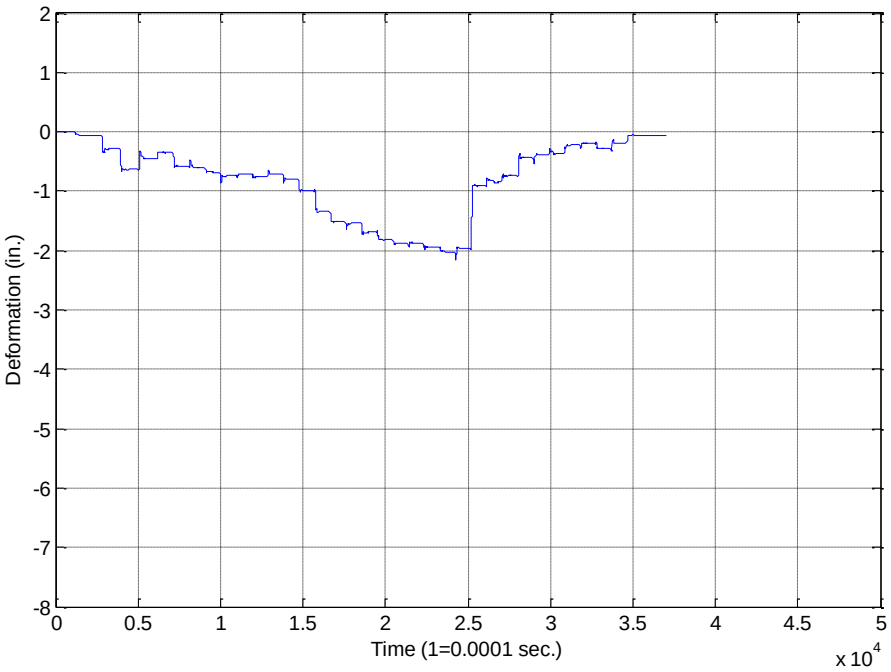


**Figure 421. Oskaloosa test 9 segment 4, 12 in. plate, acceleration analysis A**

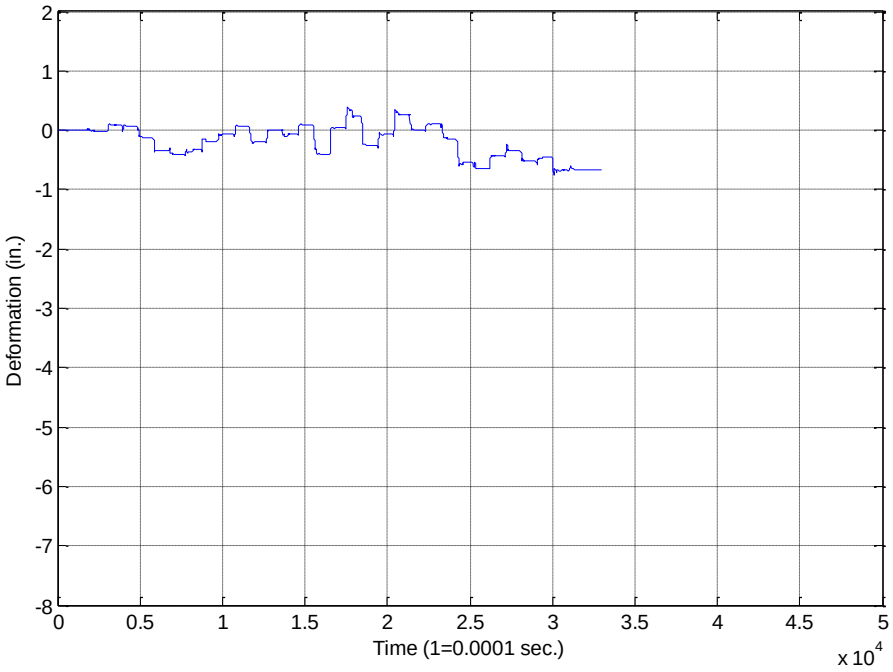


**Figure 422. Oskaloosa test 10 segment 1, 9 in. plate, acceleration analysis A**

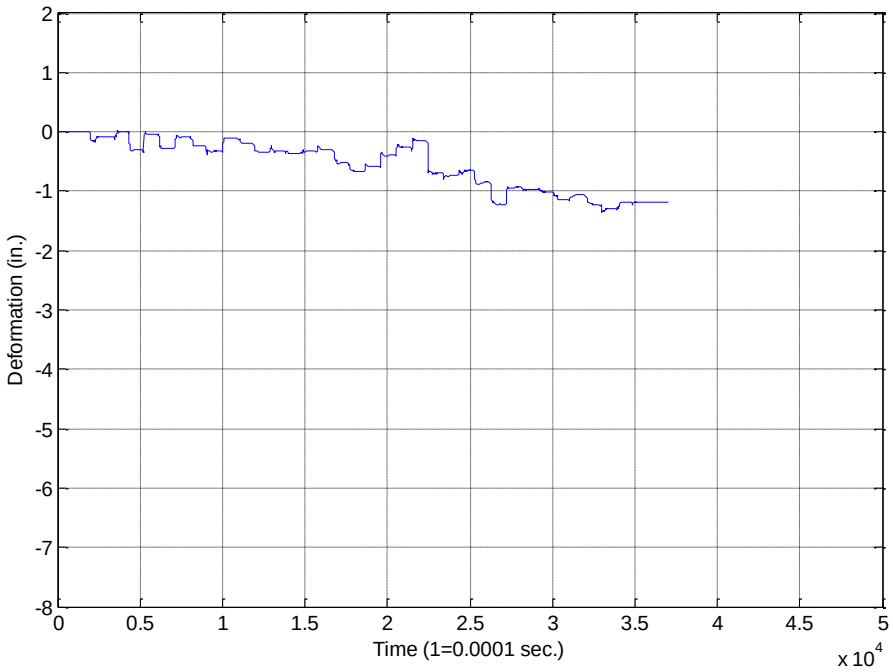


**Figure 423. Oskaloosa test 10 segment 2, 9 in. plate, acceleration analysis A**

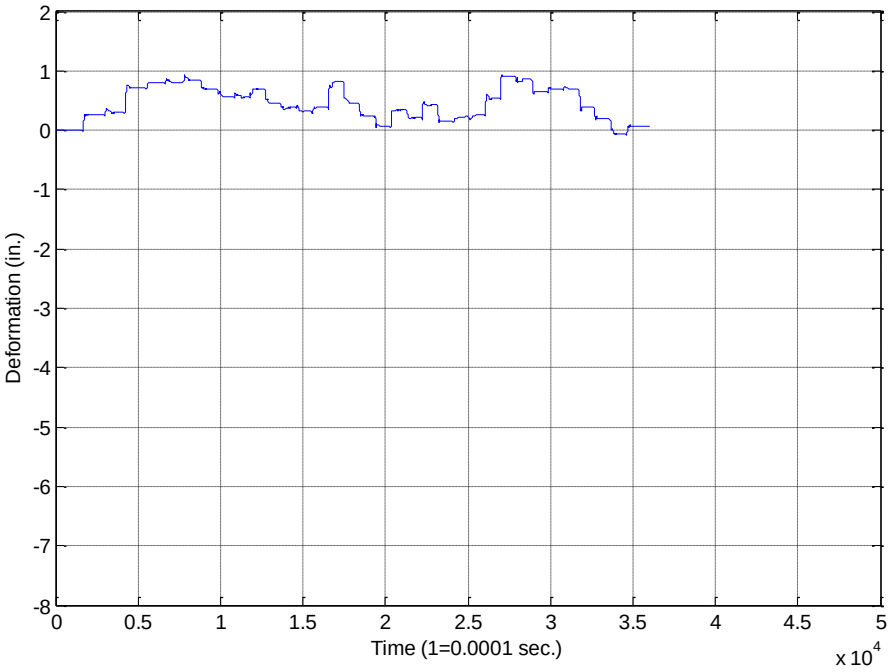


**Figure 424. Oskaloosa test 10 segment 3, 9 in. plate, acceleration analysis A**

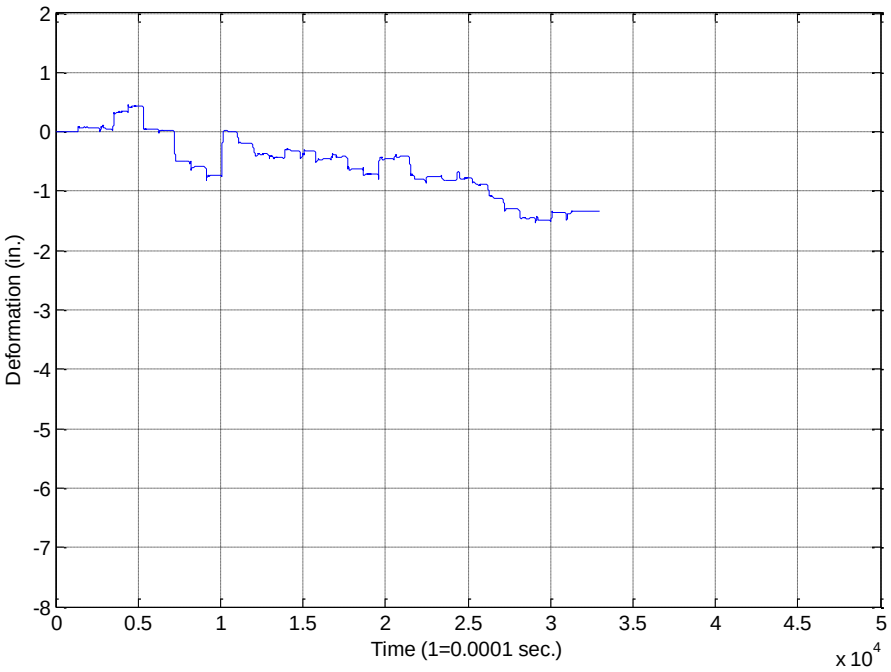


**Figure 425. Oskaloosa test 10 segment 4, 9 in. plate, acceleration analysis A**

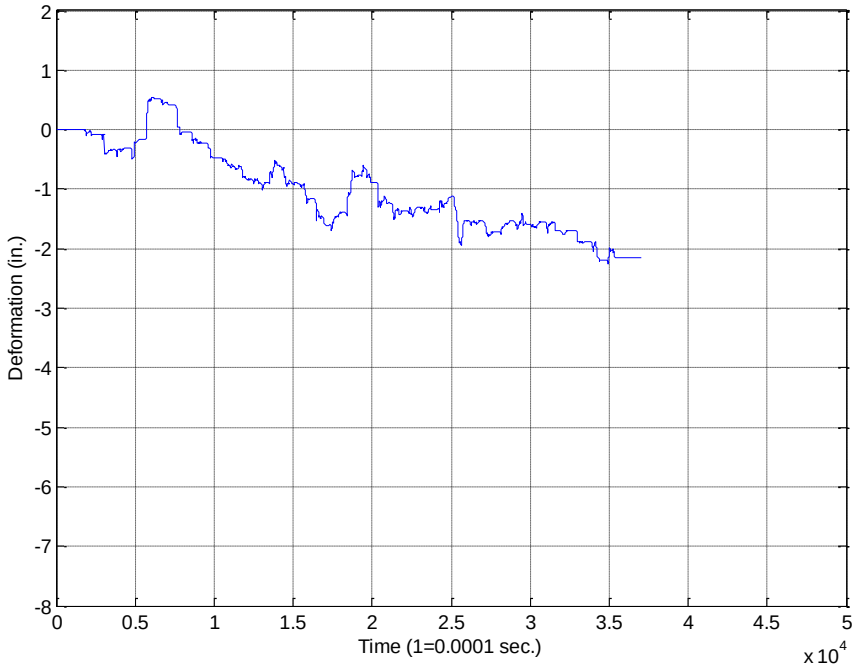


**Figure 426. Oskaloosa test 11 segment 1, 18 in. plate, acceleration analysis A**

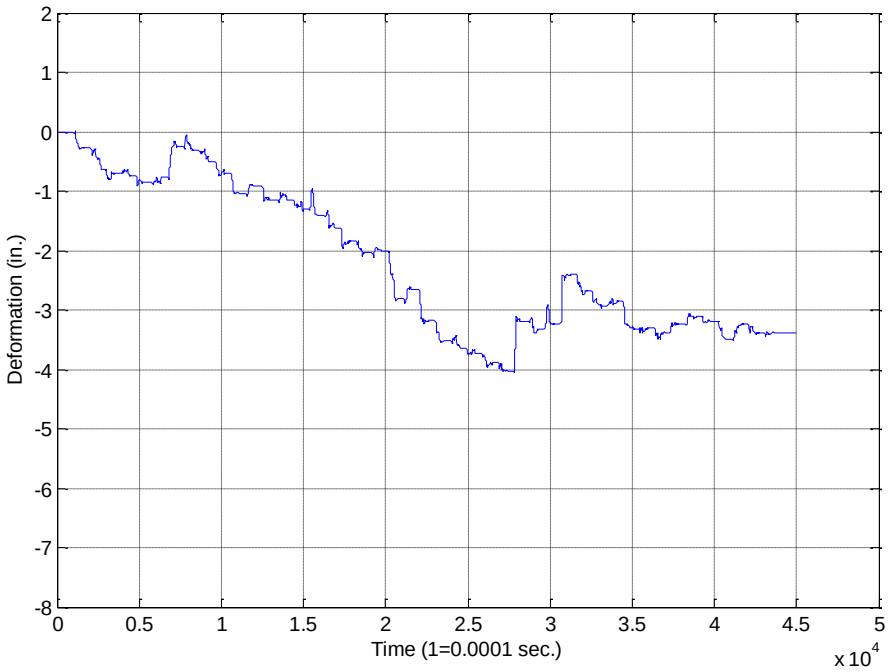


**Figure 427. Oskaloosa test 11 segment 2, 18 in. plate, acceleration analysis A**

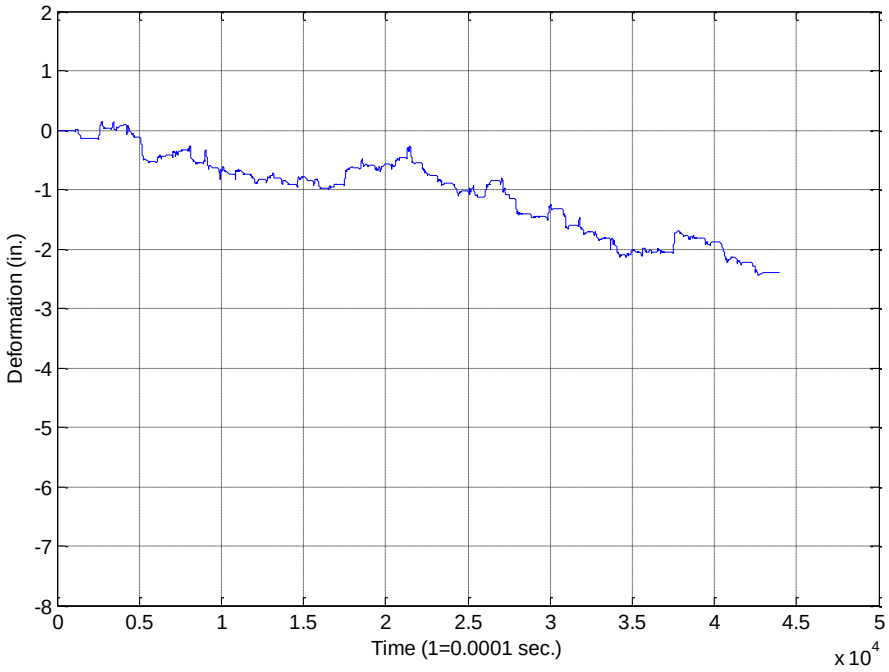


**Figure 428. Oskaloosa test 11 segment 3, 18 in. plate, acceleration analysis A**

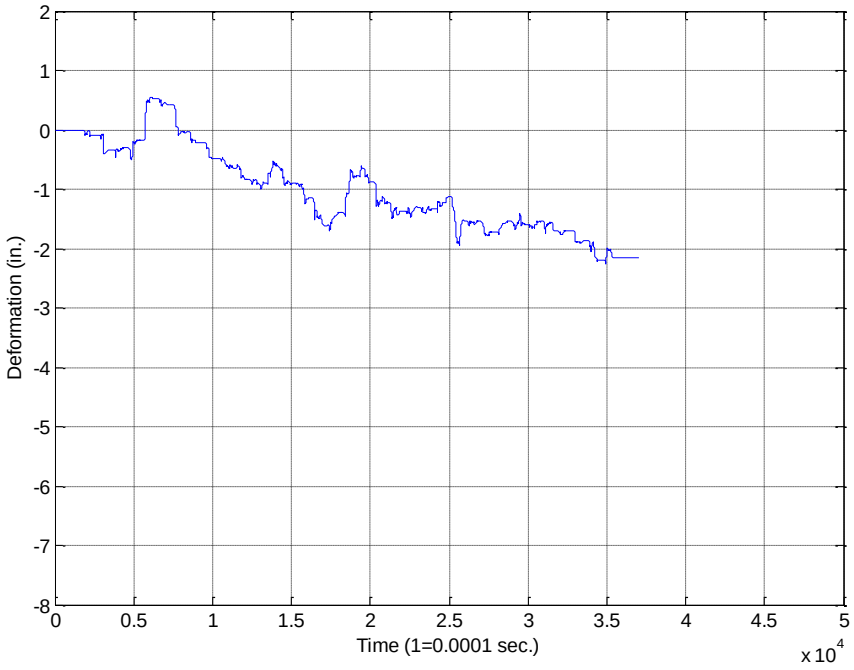


**Figure 429. Oskaloosa test 12 segment 1, 24 in. plate, acceleration analysis A**

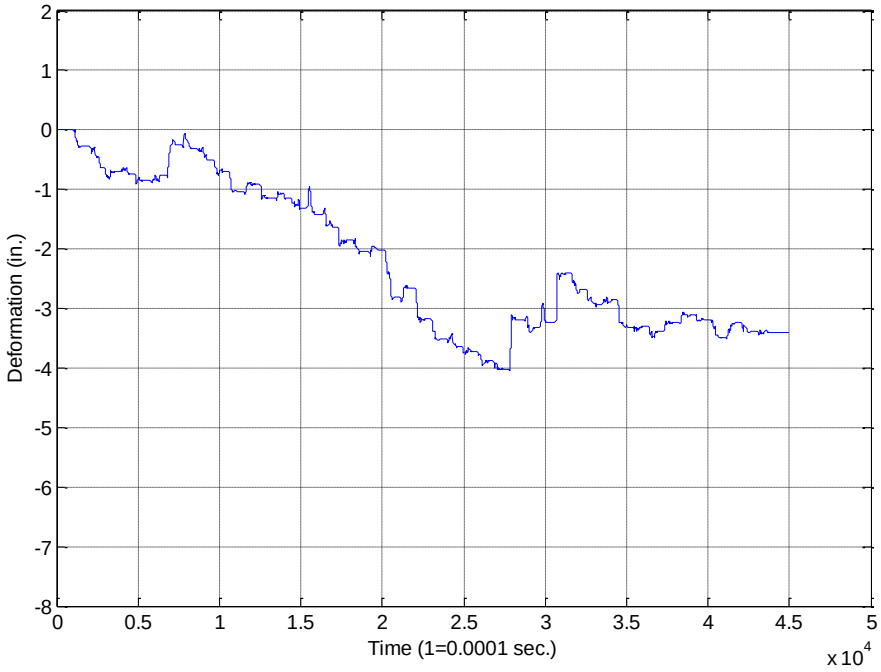


**Figure 430. Oskaloosa test 12 segment 2, 24 in. plate, acceleration analysis A**

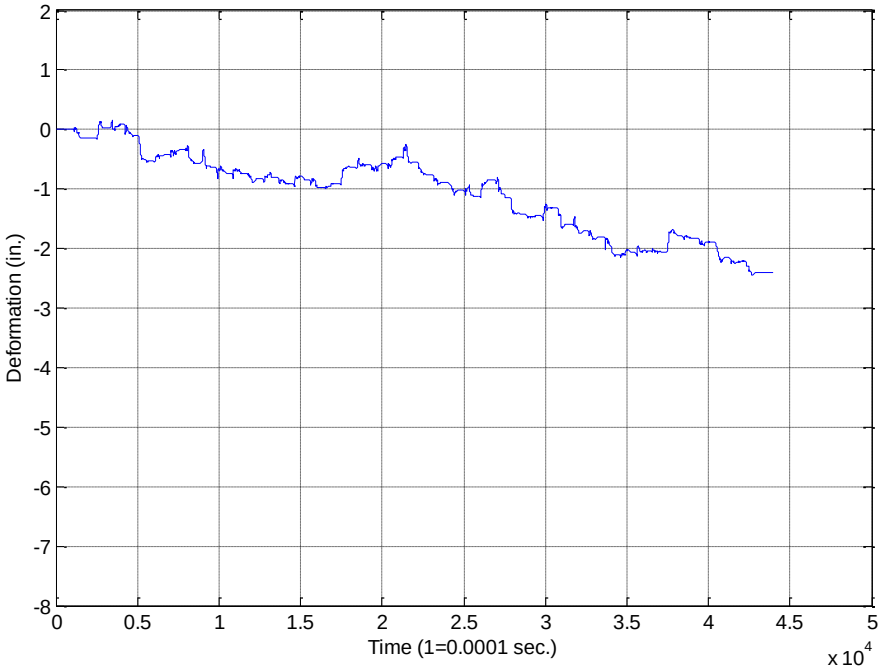


**Figure 431. Oskaloosa test 12 segment 3, 24 in. plate, acceleration analysis A**

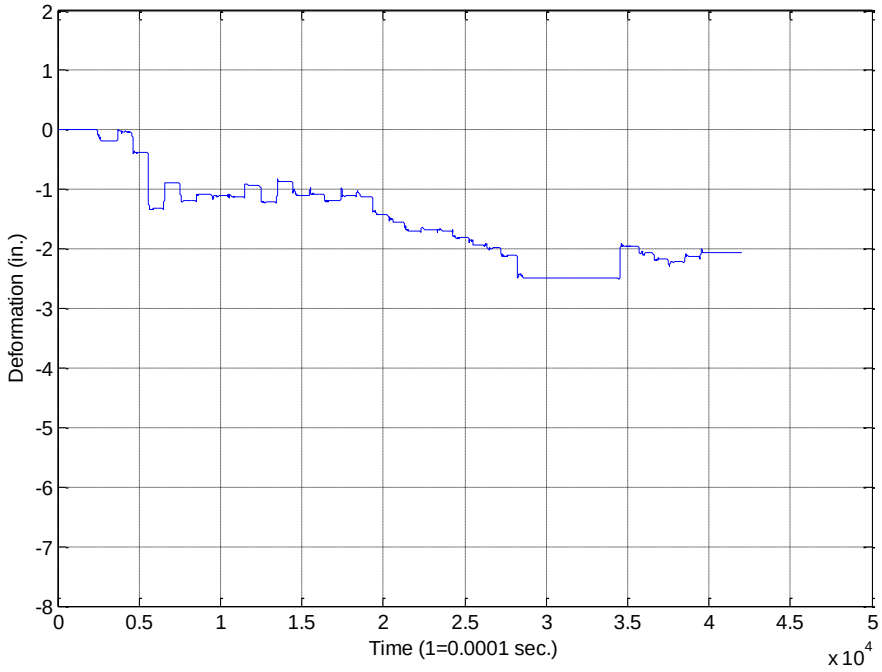


**Figure 432. Oskaloosa test 13 segment 1, 18 in. plate, acceleration analysis A**

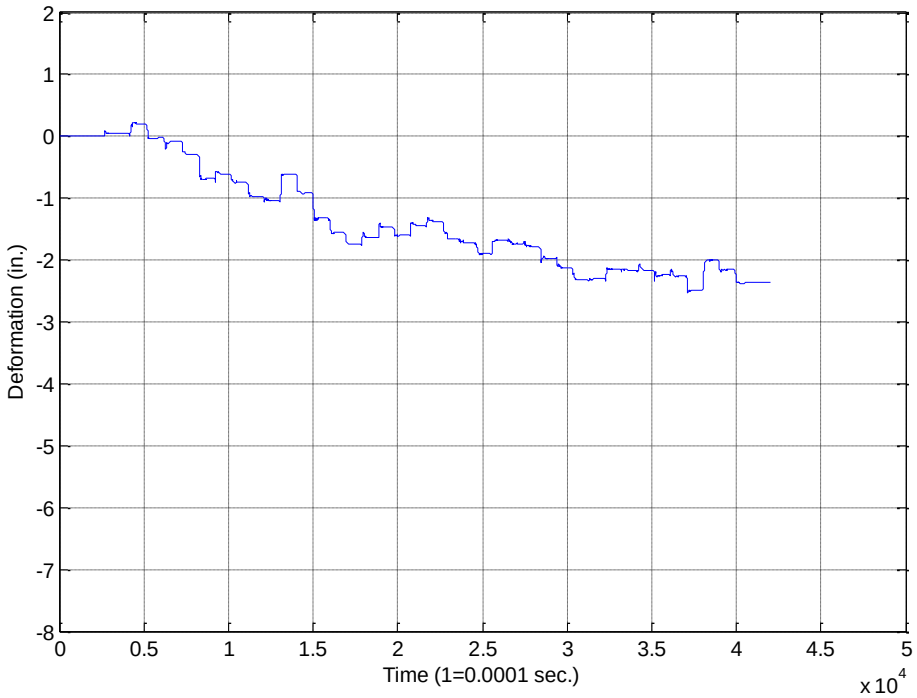


**Figure 433. Oskaloosa test 13 segment 2, 18 in. plate, acceleration analysis A**

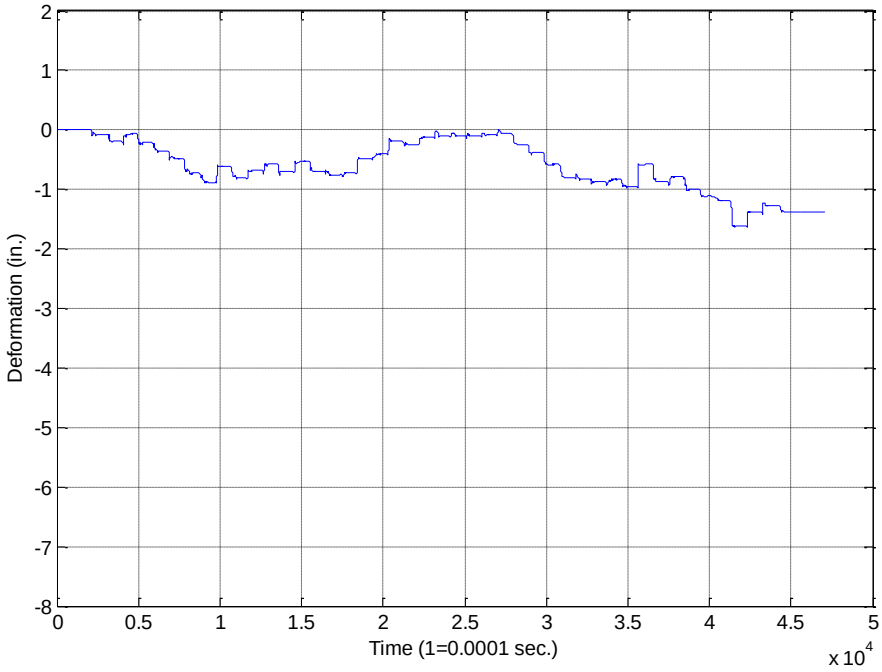


**Figure 434. Oskaloosa test 13 segment 3, 18 in. plate, acceleration analysis A**

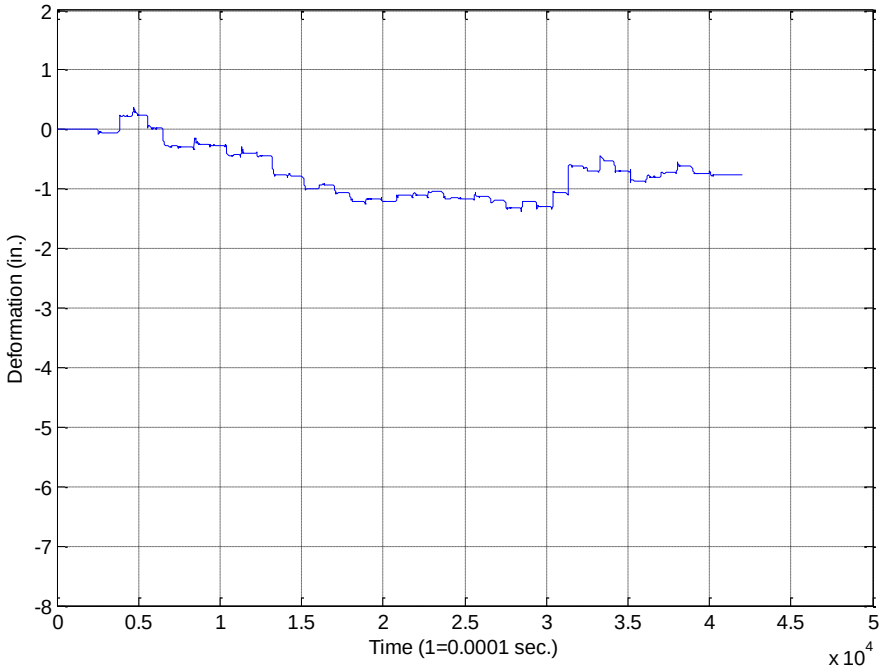


**Figure 435. Oskaloosa test 13 segment 4, 18 in. plate, acceleration analysis A**

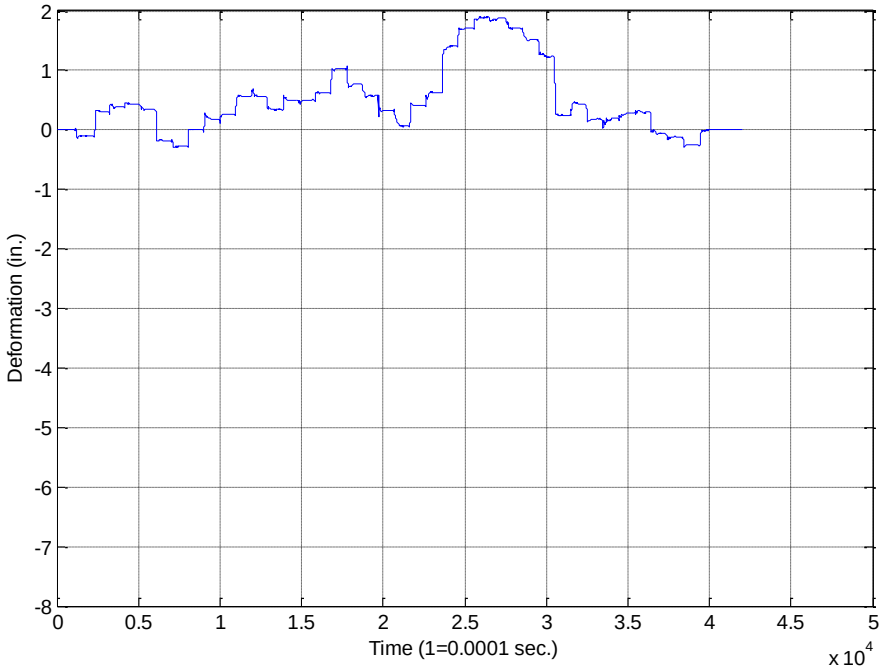


**Figure 436. Oskaloosa test 14 segment 1, 12 in. plate, acceleration analysis A**

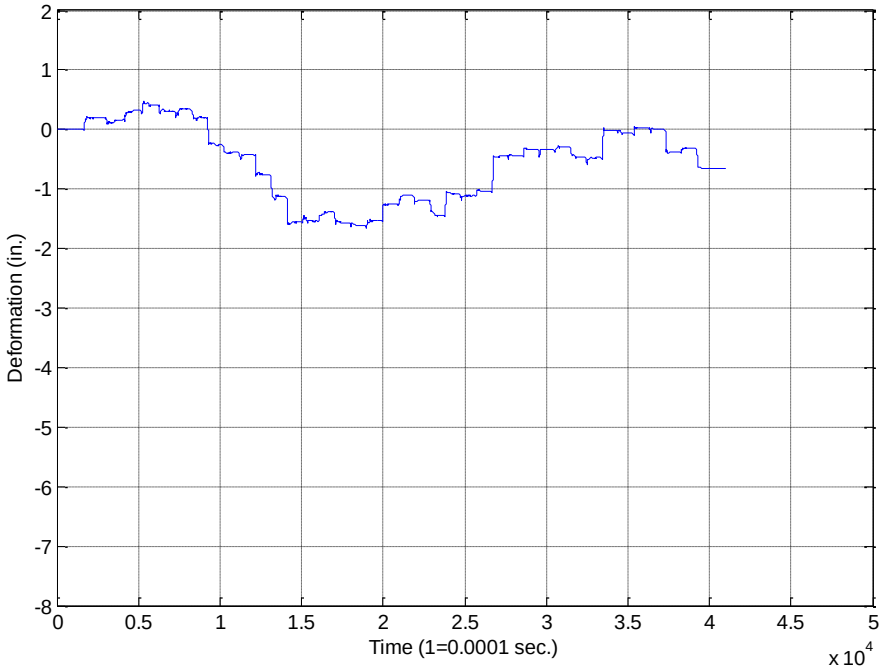


**Figure 437. Oskaloosa test 14 segment 2, 12 in. plate, acceleration analysis A**

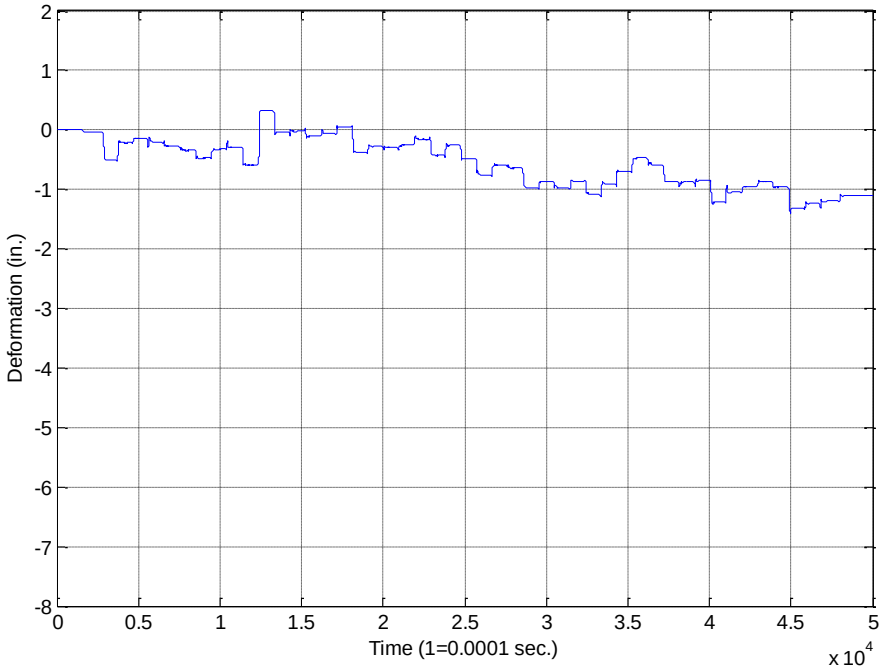


**Figure 438. Oskaloosa test 14 segment 3, 12 in. plate, acceleration analysis A**

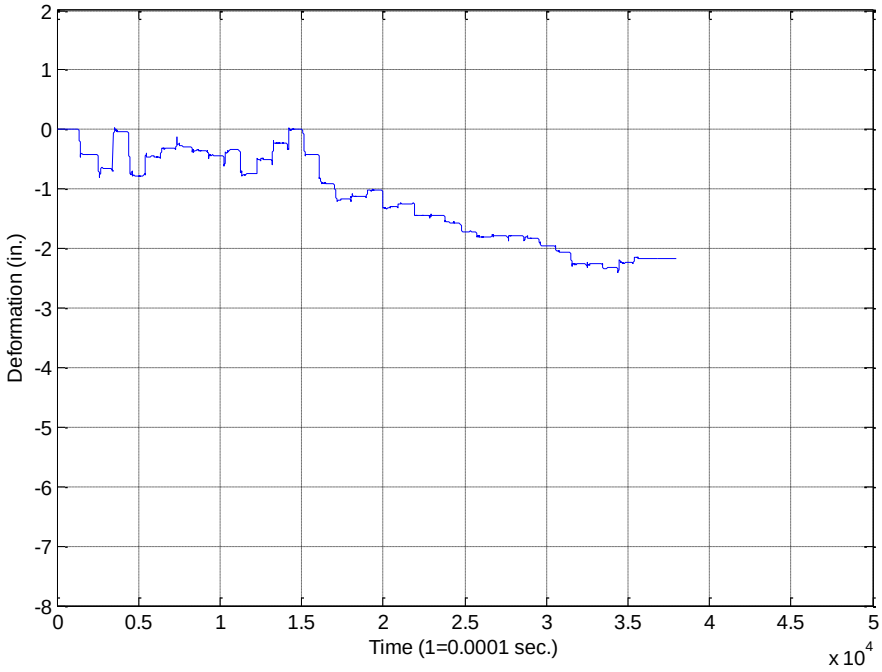


**Figure 439. Oskaloosa test 15 segment 1, 9 in. plate, acceleration analysis A**

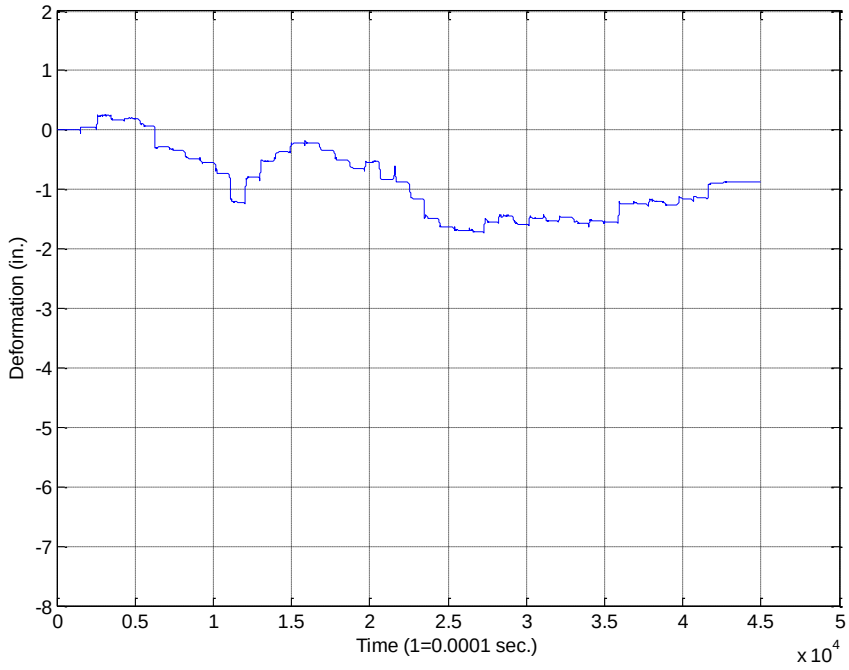


**Figure 440. Oskaloosa test 15 segment 2, 9 in. plate, acceleration analysis A**

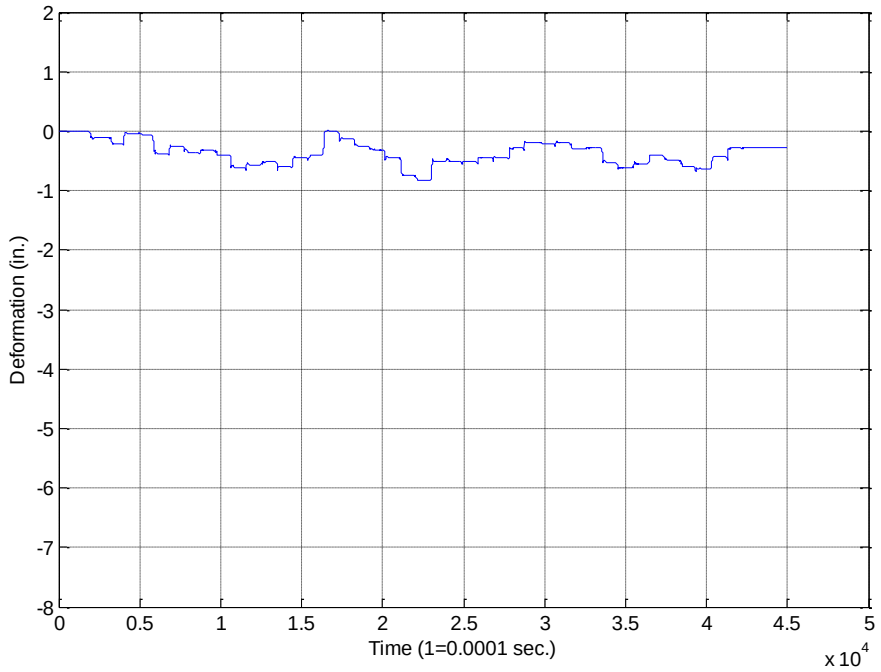


**Figure 441. Oskaloosa test 15 segment 3, 9 in. plate, acceleration analysis A**

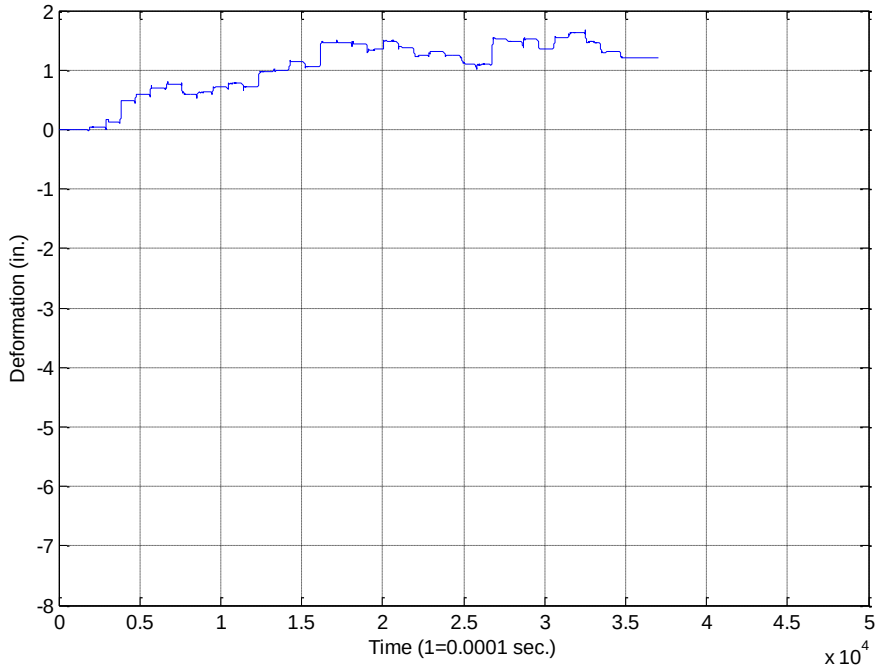


**Figure 442. Oskaloosa test 15 segment 4, 9 in. plate, acceleration analysis A**

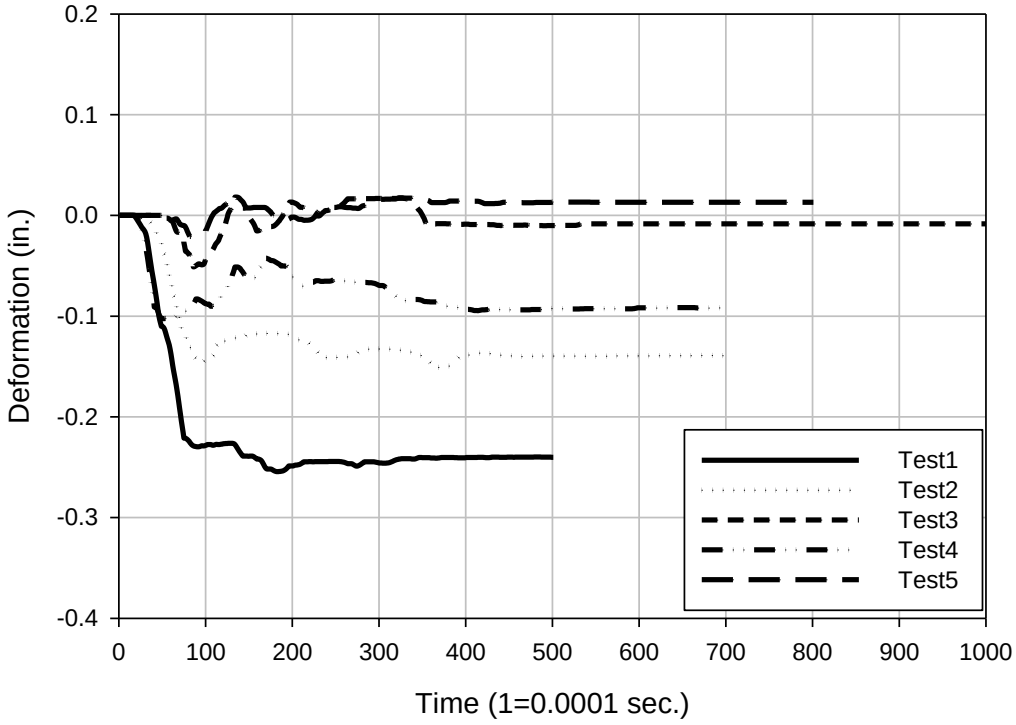


**Figure 443. Oskaloosa pier 1 acceleration analysis B**

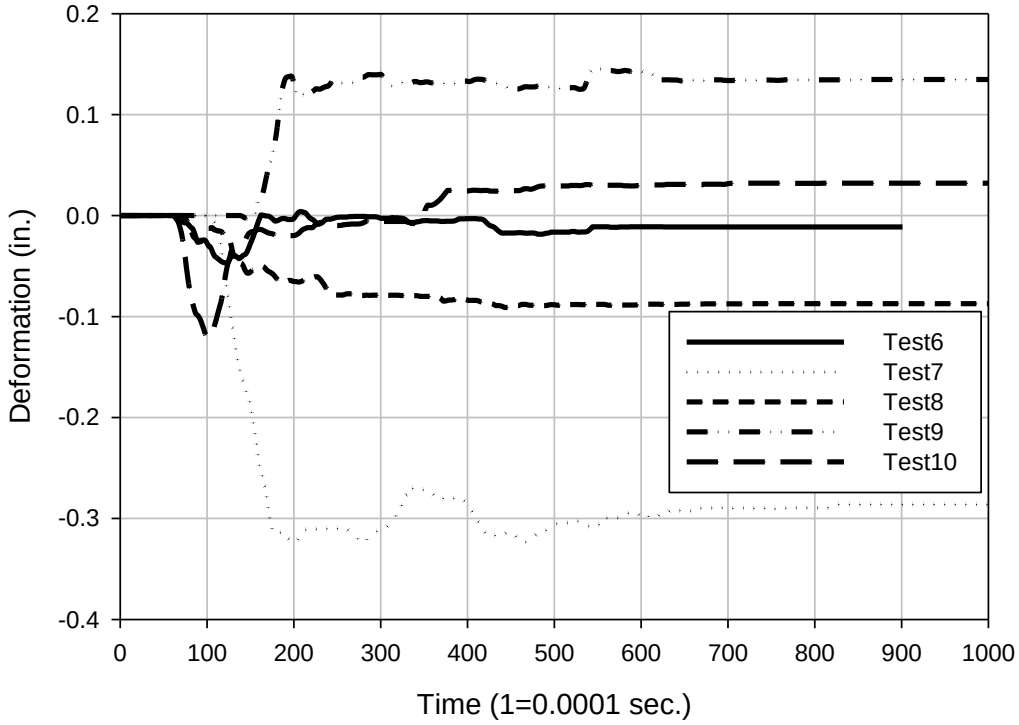


**Figure 444. Oskaloosa pier 2 acceleration analysis B**

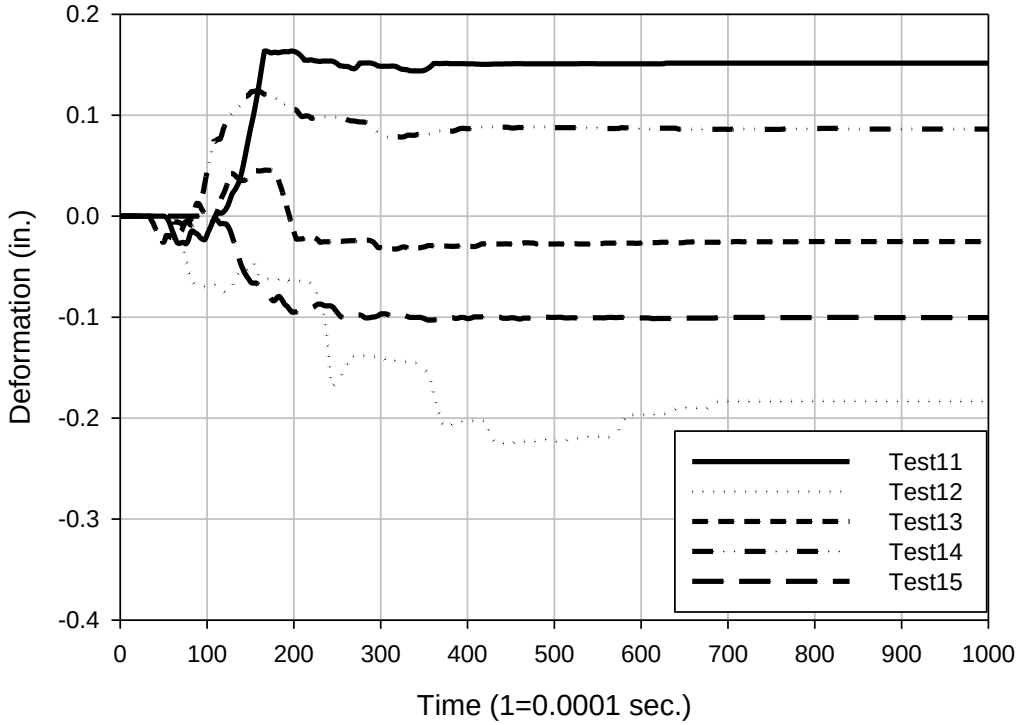


**Figure 445. Oskaloosa pier 3 acceleration analysis B**

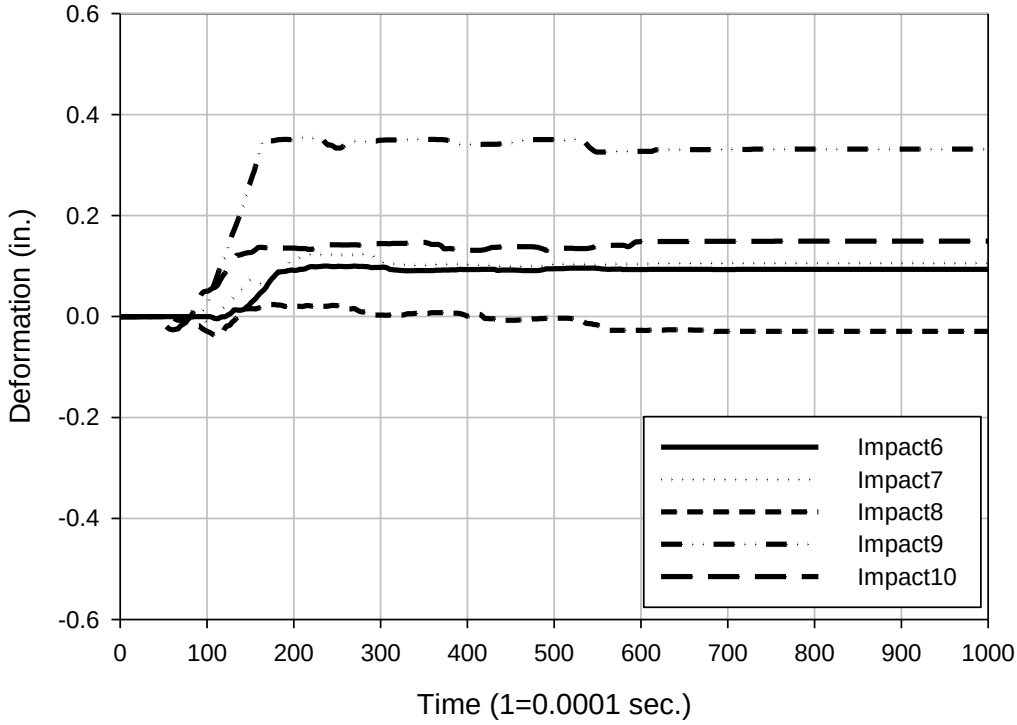


**Figure 446. Oskaloosa test 2 segment 1, 24 in. plate, acceleration analysis C**

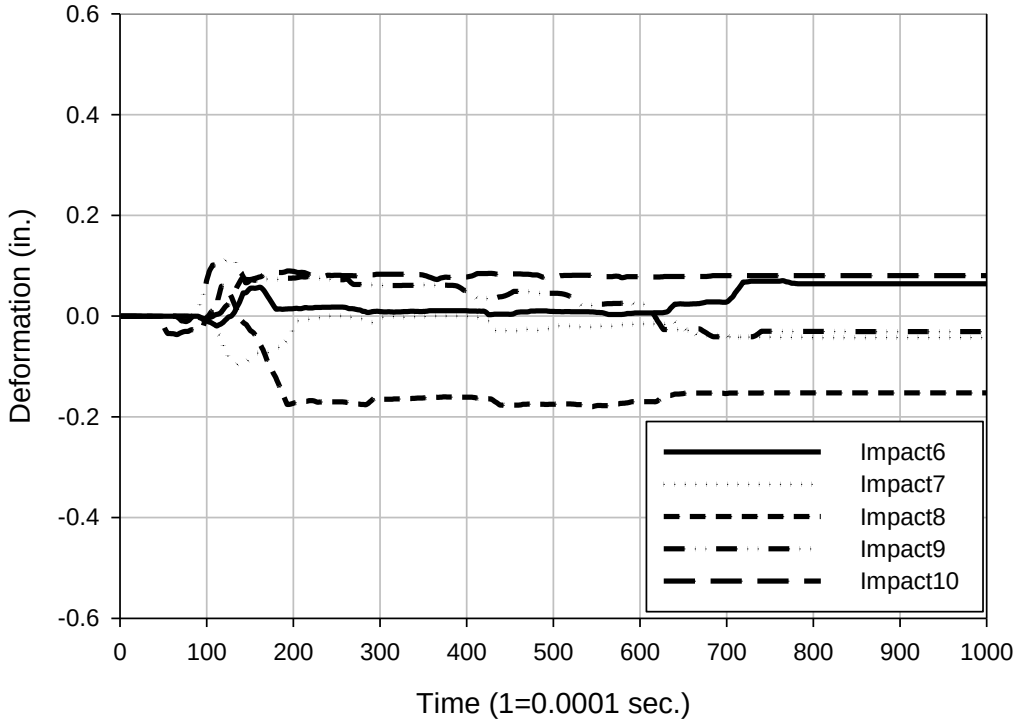


**Figure 447. Oskaloosa test 2 segment 2, 24 in. plate, acceleration analysis C**

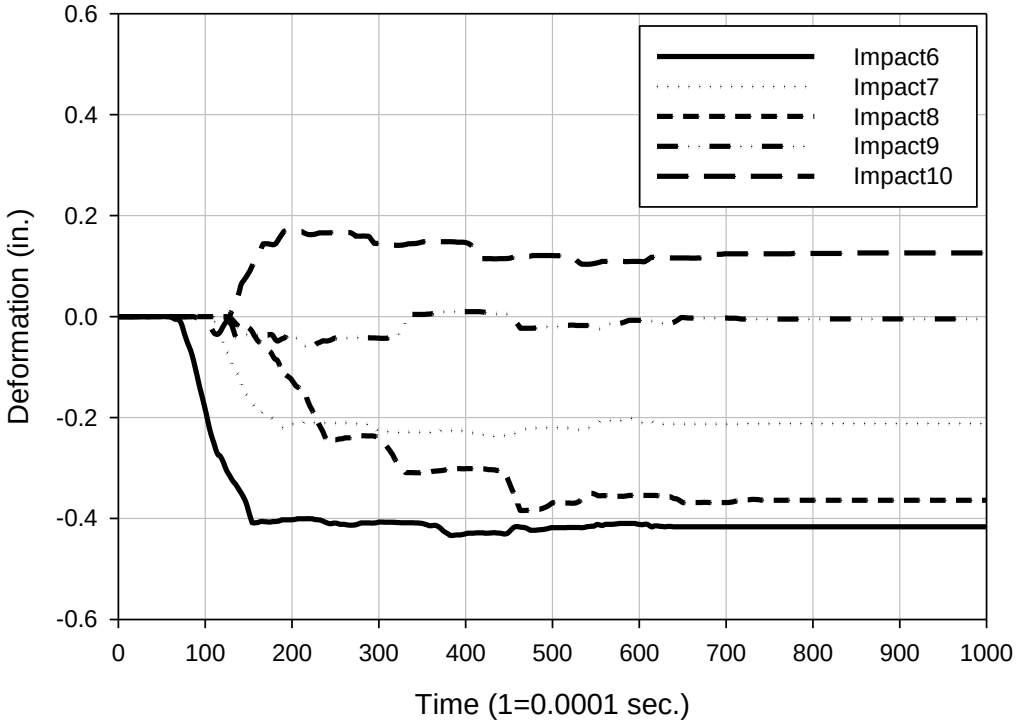


**Figure 448. Oskaloosa test 2 segment 3, 24 in. plate, acceleration analysis C**

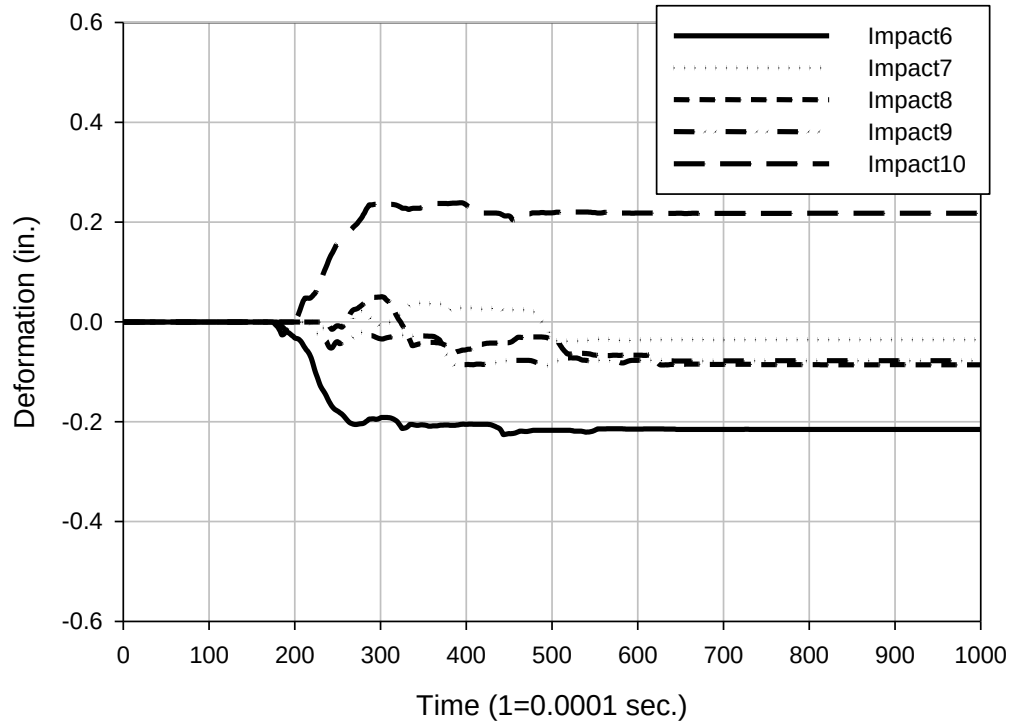


**Figure 449. Oskaloosa test 3 segment 3, 18 in. plate, acceleration analysis C**

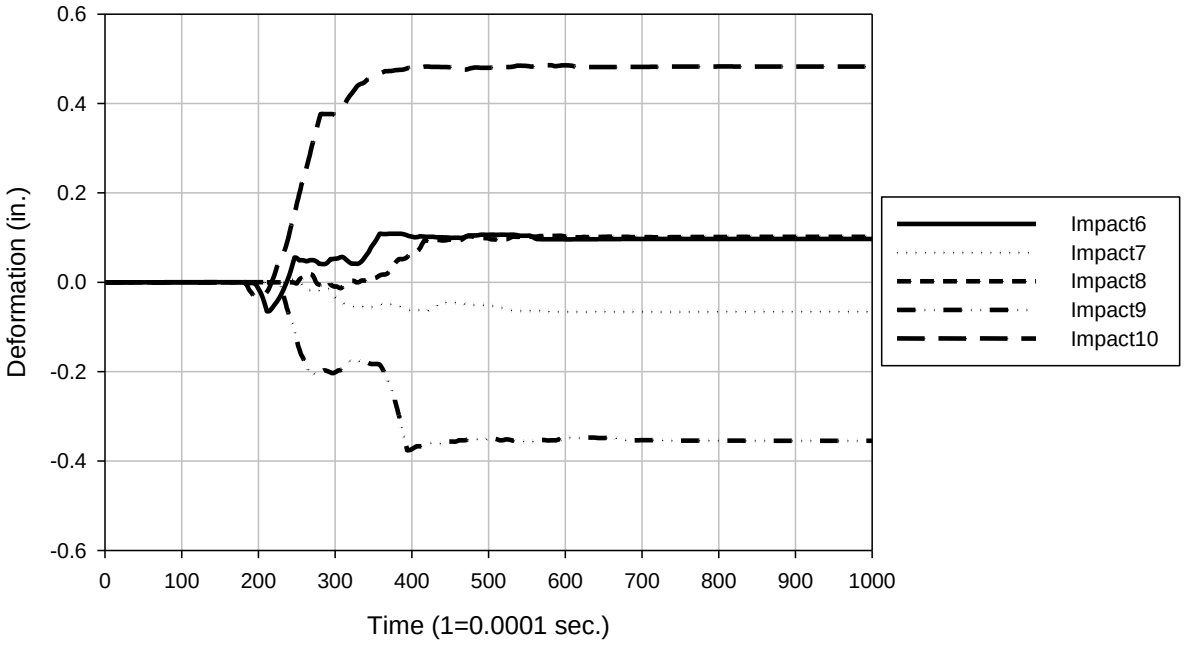


**Figure 450. Oskaloosa test 4 segment 4, 12 in. plate, acceleration analysis C**

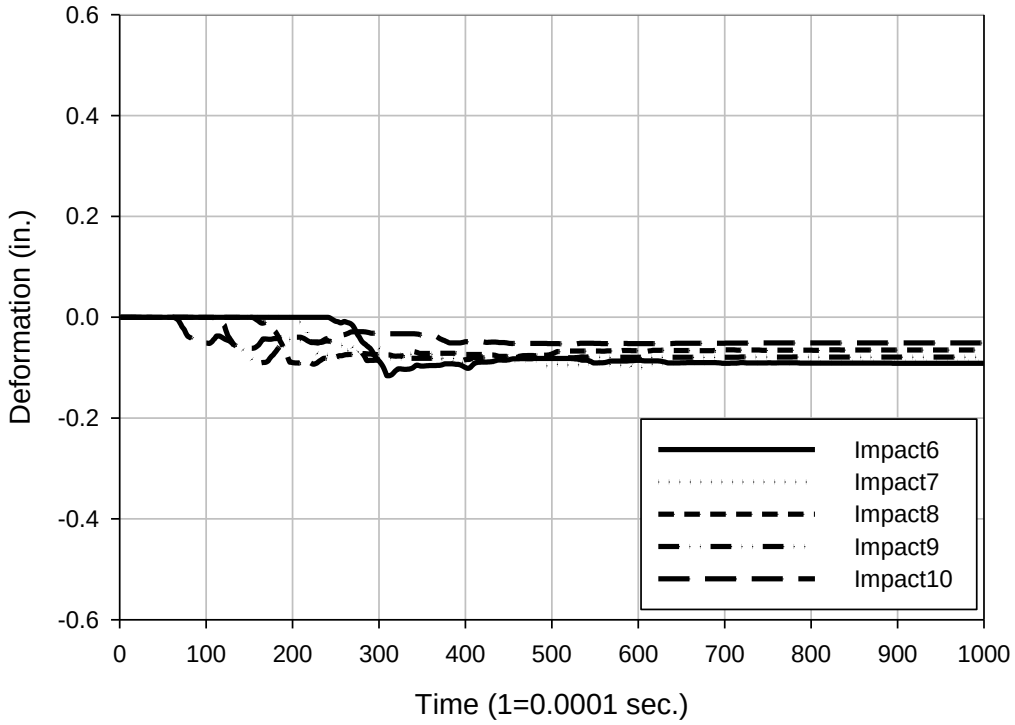


**Figure 451. Oskaloosa test 5 segment 4, 9 in. plate, acceleration analysis C**

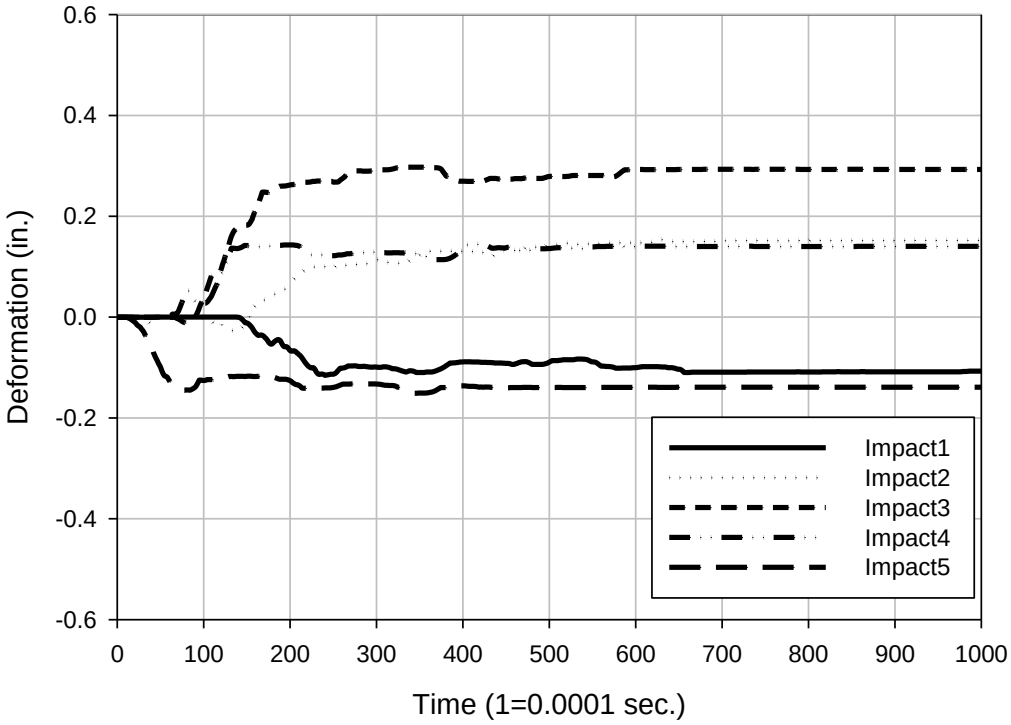


**Figure 452. Oskaloosa test 2 segment 3, 24 in. plate, acceleration analysis D**

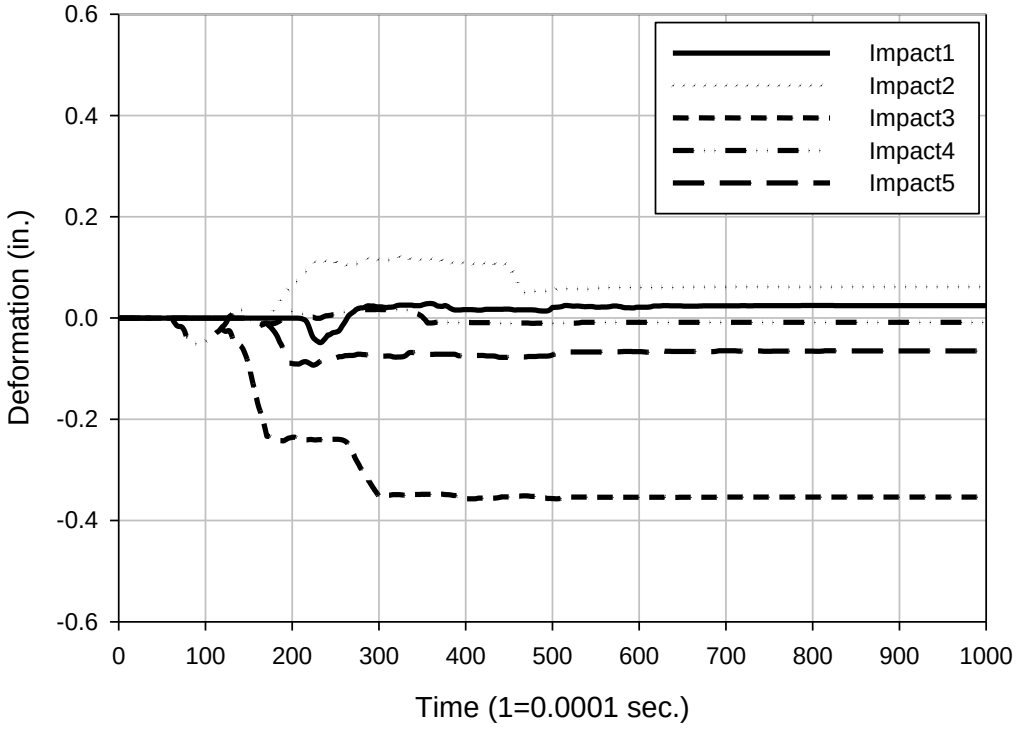


**Figure 453. Oskaloosa test 3 segment 3, 18 in. plate, acceleration analysis D**

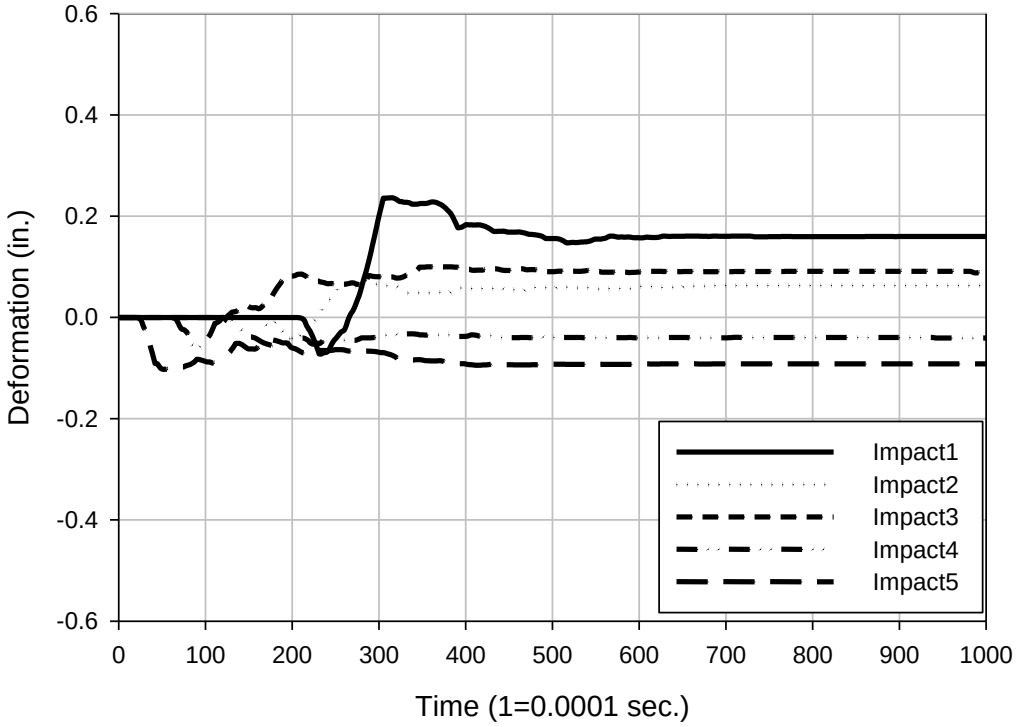


**Figure 454. Oskaloosa test 4 segment 4, 12 in. plate, acceleration analysis D**

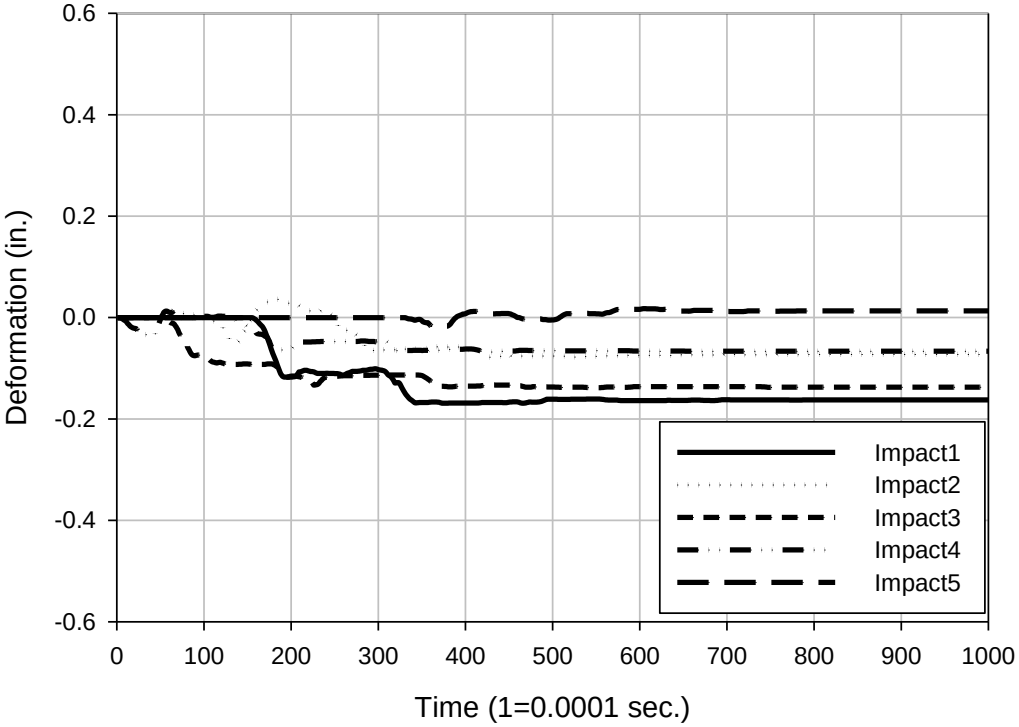


**Figure 455. Oskaloosa test 5 segment 4, 9 in. plate, acceleration analysis D**

## REFERENCES

ASTM. (2004). "Nonrepetitive Static Plate Load Tests of Soils and Flexible Pavement Components, for Use in Evaluation and Design of Airport and Highway Pavement." Annual book of ASTM standards, ASTM D1196, West Conshohocken, PA.

ASTM. (2004). "Repetitive Static Plate Load Tests of Soils and Flexible Pavement Components, for Use in Evaluation and Design of Airport and Highway Pavement." Annual book of ASTM standards, ASTM D1195, West Conshohocken, PA.

Carder, D.R. (1976). "Finite Element Analysis of the Performance of Rigid Plate Soil Pressure Cells." *Ground Engineering*, 9(8), 40–46.

Farrell Design-Build | Geopier California. Impact Pier Soil Densification for Liquefaction. Web. 31 Aug. 2010. http://www.farrellinc.com/impact-pier-california.htm.

Fleming, P. R., Frost, M. W., Lambert, J., P. "A Review of the Light Weight Deflectometer (LWD) for Routine In situ Assessment of Stiffness", In *Proceedings of the Transportation Research Board Conference* (TRB CD-ROM), Washington D.C, January 2007.

Fox, N. S., and Cowell, M. J. (1998) *Geopier Foundation and Soil Reinforcement Manual.* Scottsdale, Arizona.

Fox, N. S. and Lien, B. H. "Geopier® Soil Reinforcement Technology: An Overview." Proceedings, Asian Institute of Technology Conference. Bangkok, Thailand. November 2001.

Fugro (2011). O-cell® Testing – How it works. Loadtest, Gainesville, Florida. http://www.loadtest.co.uk/PDF/O-cell%20testing%20How%20it%20works.pdf (accessed March 17, 2011).

Liu, R., Chen, X., Li, J., Guo, L., and Yu, J. (2005). *Evaluate Innovative Sensors and Techniques for Measuring Traffic Loads*. Final report submitted to Research and Technology Implementation Office, Texas Depart of Transportation, Austin, TX.

LoadTest (2011). The Osterberg Cell: General Information. Loadtest, Gainesville, Florida. http://www.loadtest.co.uk/Loadtest%20Ltd/the%20osterberg%20cell_files/ocell.htm (accessed March 14, 2011).

Minks, Allen. "Geopier testing - La Port City, IA - Iowa State University." 2 Nov. 2009. E-mail.

Noori, P., Palmer, J., and Boomhower, D. (2005). Geotechnical Policies and Procedures Manual. Nevada Department of Transportation, Carson City, Nevada. http://www.nevadadot.com/uploadedFiles/Geo_PPM_Glossary.pdf (accessed March 14, 2011).

Paikowsky, Samuel G. Innovative Load Testing Systems. NCHRP Web Document, Issue 84, 2006, 675 p.

Plotkin, Marc. "Council Bluffs Modulus Tets." 11 Oct. 2010. E-mail.

Plotkin, Marc. "Geopier-RAM Test Oskaloosa, IA." 28 Feb. 2011. E-mail.

Stokoe II, K H; Bay, J A. Development and Preliminary Investigation of a Rolling Dynamic Deflectometer. Interim Report. University of Texas, Austin; Texas Department of Transportation; Federal Highway Administration, 1995, 72 p.

Uddin, W., and McCullough, F. (1989). “In Situ Material Properties from Dynamic Deflection Equipment.” presented at 1989 First International Symposium on Nondestructive Testing of Pavements and Backcalculation of Moduli conference, Baltimore, Maryland, June.

Vennapusa, Pavana K.R., and White, David J. (2009). “Comparison of Light Weight Defletometer Measurements for Pavement Foundation Materials.” Geotechnical Testing Journal, ASTM International, 32(3), 239-251.

Walter, Patrick L. "The History of the Accelerometer." *Sound and Vibration* 40 (2007): 84-92.

White, David J. “Geotechnical considerations for designing Geopier supported embankments”. Iowa State University Presentation. October 4, 2003.

Wilson, B. Never Guess Again: Intelligent Compaction Making Precision Commonplace at the Jobsite. Roads & Bridges, Volume 42, Issue 8, 2004, 22-25.

Zorn, Gerhard (2003) *Light Drop Weight Tester ZFG 2000 – Operating Manual*. Stendal, Germany.